Bacterial Evolution in Response to the Cancer Chemotherapeutic Drug Bleomycin

Erica Szewin Li

(BSc)

Thesis submitted in fulfilment of the requirement for the degree of Doctor of Philosophy

The University of East Anglia

Faculty of Medicine and Health Sciences

Date of submission: March 2022

University of East Anglia

Abstract

The threat of antibiotic resistance has stimulated research into the factors that lead to antibiotic resistance and the spread of antibiotic resistance genes. Recently, it has been shown that exposure to different drugs and disinfectants can select for antibiotic resistance, as many of these agents have antibacterial properties. This includes cancer chemotherapy drugs like bleomycin, used to treat some squamous cell carcinomas and lymphomas. Bleomycin has been shown to have antibacterial activity through damaging bacterial DNA. It has also been found that a bleomycin resistance gene in *Enterobacteriaceae* is located 3 bp downstream of bla_{NDM} β-lactamase variants that produce the NDM enzyme responsible for conferring resistance to the carbapenem antibiotics. The purpose of this project was to determine whether bleomycin could select for antibiotic resistance via three main mechanisms: identify whether *de novo* mutations in bacteria that arise after bleomycin exposure may alter bacterial sensitivity to antibiotics, determine whether the bleomycin resistance gene adjacent to the bla_{NDM} β-lactamase may confer a fitness advantage, and whether exposure to bleomycin promotes the movement of mobile genetic elements (MGEs, commonly associated with antibiotic resistance genes). We have found that exposure to bleomycin induces *de novo* mutations in *Escherichia coli* in genes that are involved in membrane transporters, biofilm formation and metabolism which may make them less susceptible to the action of antibiotics. Our results indicate that carriage of the bleomycin resistance gene may confer a fitness advantage to bacteria, which may explain its prevalence in existing genome databases and may also indicate its importance in clinical isolates. The movement of MGEs could be tracked using the Hi-C method and combining long-read sequencing can help to overcome the weaknesses associated with short-read sequencing.

List of Contents

List of Figures

List of Tables

List of Abbreviations

Abbreviation	Meaning
ABVD	Adriamycin (doxorubicin), Bleomycin, Vinblastine and Dacarbazine
AMP	Ampicillin
AMR	Antimicrobial resistance
B&W	Binding and washing (buffer)
BDL	Below the Detection Limit
BEACOPP	Bleomycin, Etoposide, Doxorubicin, Cyclophosphamide, Vincristine, Procarbazine and Prednisolone
Bm	Bleomycin
bp	Base pairs
BR	Broad range
BRP	Bleomycin-binding protein
bwa	Burrow-Wheeler Aligner
CFU	Colony forming unit
CHL	Chloramphenicol
CIDs	Chromosome interacting domains
CIP	Ciprofloxacin
DF	Dilution factor
DIN	DNA Integrity Number
DMSO	Dimethyl sulfoxide
dsDNA	Double-stranded DNA
DSG	Disuccinimidyl glutarate
ECM	Extracellular matrix
EDTA	Ethylenediaminetetraacetic acid
EMS	Ethyl methanesulfonate
EPS	Exopolysaccharide
EtBr	Ethidium bromide
EUCAST	European Committee on Antimicrobial Susceptibility Testing
FDA	Food and Drug Administration
FSC	Forward scatter
GenOMICC study	Genetics of Mortality in Critical Care study
GENT	Gentamicin
GISAID	Global Initiative on Sharing Avian Influenza Data
GM	Genetically modified
HGT	Horizontal gene transfer
Hi-C	High-throughput chromosomal conformation capture
HQ	High quality
HS	High sensitivity
MDR	Multi-drug resistant
MERO	Meropenem
MFS	Major facilitator superfamily
MGE	Mobile genetic element
MHA	Mueller-Hinton agar
MHB	Mueller-Hinton broth
MIC	Minimum inhibitory concentration
MMC	Mitomycin C
mRNA	Messenger RNA

MRSA	Methicillin-resistant *Staphylococcus aureus*
NA	Nalidixic acid
NDM	New Delhi metallo-β-lactamase
NEB	New England Biolabs
NICE	The National Institute for Health and Care Excellence
NIH	The National Institutes of Health
OD	Optical density
OIL-PCR	One-step isolation and lysis PCR
OMVs	Outer membrane vesicles
ONT	Oxford Nanopore Technologies
ORF	Open Reading Frame
PBS	Phosphate-buffered saline
PEG	Polyethylene glycol
PMBN	Polymyxin B nonapeptide
PUP	Peptide uptake permease
PVC	Polyvinyl chloride
QIB	Quadram Institute Biosciences
REs	Restriction enzymes
RPs	Read pairs
RT-PCR	Reverse transcription polymerase chain reaction
SDS	Sodium dodecyl sulfate
SEM	Standard error of the mean
SNP	Single nucleotide polymorphism
SOD	Superoxide dismutase
SPRI	Solid Phase Reversible Immobilisation
SSC	Side scatter
ssDNA	ssDNA
STD	Standard deviation of the mean
TADs	Topologically associated domains
TAE	Tris-acetate-EDTA (buffer)
TE	Tris-EDTA (buffer)
TET	Tetracycline
TLS	Translesion synthesis
UVD	UV damage
WHO	World Health Organisation

Acknowledgements

1.   Chapter 1 – Introduction

1.1.   Antibiotic resistance

Resistance to antibiotics is a major issue in the present day. It is estimated that 10 million lives a year could be lost by 2050 due to antibiotic resistance (O'Neill, 2016). A predictive model published by Murray *et al*. (2022), estimated that in 2019 4.95 million deaths were associated with bacterial antimicrobial resistance. These estimates indicate an underestimation of the antibiotic resistance issue. Antibiotics are crucial in our everyday lives for the treatment of infections and as a precautionary measure before complicated surgery or anti-cancer therapy (O'Neill, 2016). Bacteria that are of particular concern in a clinical setting are the ESKAPE pathogens. This group comprises *Enterococcus faecium, Staphylococcus aureus, Klebsiella pneumoniae, Acinetobacter baumannii, Pseudomonas aeruginosa* and *Enterobacter* species. The leading pathogens associated with death and antibiotic resistance were *Escherichia coli*, *S. aureus, K. pneumoniae, Streptococcus pneumoniae, A. baumannii* and *P. aeruginosa* in a estimate conducted by Murray *et al*. (2022) and were estimated to be responsible for 3.57 million deaths associated with AMR in 2019.

1.2.   Mechanisms of antibiotic resistance

There are many mechanisms that a bacterium can employ in order to resist the effects of an antimicrobial. There are many intrinsic mechanisms of resistance that are explored further in this section.

1.2.1.   Efflux pumps

Efflux pumps are proteins that are able to transport substances in and out of a bacterium, and in many cases contribute towards antibiotic resistance due to their broad substrate ranges (Blair *et al.,* 2015). Efflux pumps can vary in their structure but they all belong to the major facilitator superfamily (MFS) of transporters (Porse *et al*., 2020). To combat the action of antibiotics, bacteria may overproduce efflux pumps which can be done by mutating: a local repressor gene, a global regulatory gene, promoter region of a efflux pump gene or insertion elements upstream of the pump gene (Blair *et al*., 2015). Efflux pumps as a mechanism of antibiotic resistance is energetically costly to the cells, as energy is needed to move the antimicrobial from an area of low concentration to a more highly concentrated area- energy that could be used for the growth and reproduction of the cell (Herren and Baym, 2021).

1.2.2. Protein secretion/enzymes

One way in which bacteria can resist the effects of antibiotics is through the secretion of proteins and enzymes that interact and inactivate the antibiotic (Amanatidou *et al.*, 2019). Examples of this mechanism can be seen against tetracycline (TET) in *Escherichia coli* in the study by Gasparrini *et al.* (2020) where they noted that resistance mechanisms against TET typically involve efflux systems and ribosomal protection. In the study by Gasparrini *et al.* (2020) they found that Tet(X7) present in media allowed the growth of *E. coli* that were susceptible to the action of TET. A more common example of bacteria resisting the effects of antibiotics by secreting proteins that interfere with the antibiotic activity are the β-lactamases that allow bacteria to resist the effects of β-lactam antibiotics (Amanatidou *et al.*, 2019). The secretion of proteins that detoxify antibiotics confers protection for any bacteria in the local area that are unable to produce the protein and resist the effects of the antibiotic, and can be important in biofilms as a public good (Amanatidou *et al.*, 2019).

1.2.3. Charge repulsion

Bacterial surface membranes are negatively charged due to the presence of lipopolysaccharides and phospholipids like phosphatidylglycerol and cardiolipin (Dombach *et al.*, 2020; Spohn *et al.*, 2019). Antimicrobial peptides are cationic and are able to interact with bacterial membranes and disrupt the membrane enough to cause destabilisation of the membrane which can lead to pore formation (Hartmann *et al.*, 2010). Some bacteria are able to resist the effects of antimicrobial peptides through altering the surface charge of their membranes. In a study conducted by Spohn *et al.* (2019), they found that *E. coli* that had been grown in the presence of antimicrobial peptides had a reduction in their negative charge on their membrane compared to the untreated, wild-type strain and the strains that demonstrated a reduced charge had mutations in the BasR-BasS two-component system.

1.2.4. Biofilm formation

Biofilms are an aggregation of bacterial cells that are attached at a surface, encompassed by an extracellular matrix (ECM) (Lagendijk *et al.*, 2010). Many bacterial species have demonstrated the ability to grow in biofilms, and are often implicated in nosocomial infections, like *S. aureus*, *P. aeruginosa* and *A. baumannii* (Ma *et al.*, 2019; Tanner *et al.*, 2017). One way in which biofilms protect bacteria from the action of antibiotics is by providing an environment where cells are in close contact to each other and are able to transfer genes horizontally that may contain resistance determinants (Savage *et al.*, 2013). Biofilms also provide a barrier from the external environment for the bacteria where it makes it difficult for antibiotics to penetrate, but also

limits the effects of a host immune response in humans as immune cells aren't able to come into contact with the bacterial cells (Savage *et al.*, 2013). Bacterial cells within a biofilm can also be metabolically inactive or slow growing, so any antibiotics that do manage to penetrate the outer surface may not act on the bacterial cells to then kill them (Trampari *et al.*, 2021). As mentioned previously, biofilms are communities where there are shared public goods that benefit the bacteria there, for instance the secretion of a detoxifying enzyme can benefit cells within the biofilm that do not produce the enzyme when an antibiotic is encountered, or an energy source can be degraded and the subsequent metabolites can be used by other cells in the vicinity (Amanatidou *et al.*, 2019).

1.3.   Cross-resistance between antibiotics

Cross-resistance can occur between similar and different antibiotic classes where a similar mechanism is used to resist the effect of the antibiotic for instance, the activation of an efflux pump that can interact with a variety of antibiotics (Cherny *et al.*, 2021). A study conducted by Lázár *et al.* (2014) demonstrated using genome-wide analyses that cross-resistance that is seen between two antibiotics isn't dependent on whether the antibiotics are synergistic in effect when they are combined as a treatment.

1.4.   Prevalence of cancers

Globally, cancer is a major public health concern as it is becoming one of the most common diseases found in human populations. The most frequently used treatments for cancer involve surgery, radiotherapy and chemotherapy. In this review, the antibacterial properties of anti-cancer drugs will be explored, with particular focus on the use of bleomycin (Bm), including its mechanism of action and the nature of Bm resistance found in clinically important bacteria.

According to estimates generated by the GLOBOCAN project, in 2012 there were around 14.1 million new cancer cases and 8.2 million deaths from cancer or cancer-related illnesses, with this becoming more of an issue in developing countries as they currently account for 65% of cancer-related deaths worldwide (Ke and Shen, 2017). More than half of all cancer cases in 2009 were reported to occur in adults ≥65 years old (White *et al.*, 2014). As life expectancy is estimated to increase, especially in the US where the number of adults aged over 85 years old is projected to increase from 5.5 million to 19 million between 2010 and 2050, this problem will only grow (White *et al.*, 2014). There are many risk factors involved with cancer development, such as a sedentary lifestyle, poor diet and environmental factors. Alongside an increasingly large geriatric population, all of these can make cancer prevention and treatment complex tasks.

An aspect of concern is the risk of secondary bacterial infections associated with cancer treatment. A study conducted by Ashour and el-Sharif (2007), demonstrated that bacteria extracted from cancer patients from different areas of the body (for example, in the bloodstream or the respiratory tract) are shifting from being mainly Gram-negative to Gram-positive bacteria, where bacteria such as *S. aureus* are more dominant. There are many possible factors for this shift in dominance, for instance aggressive chemotherapy treatment may cause damage and weaken mucosal barriers, encouraging the translocation of Gram-positive flora from the gastrointestinal tract. The implantation of intravenous catheters that introduce skin colonising bacteria into the bloodstream and prophylactic drugs that act as a selective pressure against Gram-negative species are also possible causes for the shift in bacterial dominance (Ashour and el-Sharif, 2007). A study conducted by Wisplinghoff *et al.* (2003) demonstrated that 61% of all bloodstream infections in patients with haematological malignancies and solid neoplasms were caused by Gram-positive organisms compared to 27% by Gram-negative organisms in 2,340 cases. These bacteria are potentially able to cause secondary infections in the patient as they are already immunocompromised due to invasive, surgical procedures and aggressive chemotherapy (Ashour and el-Sharif, 2007). Similarly, in a study conducted by Abdollahi *et al*. (2016) on samples from patients with acute leukaemia, it was found that the most common bacterial isolates from both blood and urine cultures from patients were *E. coli* and in wound samples, *S. aureus* was most commonly isolated. These bacteria are able to cause complications in cancer treatment and lead to morbidity and mortality as the patient can be suffering from neutropenia and changes to their own defensive microbiota.

Studies have shown that bacteria such as *E. coli*, *Salmonella typhimurium* and *Listeria monocytogenes* can show increased motility towards the site of a tumour and also replicate there when introduced directly into tumour samples (Yu *et al*., 2004). As a result, it is suggested in the literature that it is possible for opportunistic infections to occur at tumour sites as a hypoxic environment can be found where competitive bacteria may struggle to survive. However, it is not clear how often opportunistic infections by bacteria occur at or near tumours.

Secondary bacterial infections in cancer patients present further issues as the administration of anti-cancer drugs can stimulate genetic changes that alter the phenotype of the bacteria, where the drug exposure can act as a selective pressure, resulting in mutation and adaptation to the therapies the patient is receiving (Dallo and Weitao, 2010). It was hypothesised by Dallo and

Weitao (2010) that mutations and adaptation to the administered drug would arise from activation of the bacterial SOS response.

1.5. Anti-cancer drugs

Conventional chemotherapeutics are the main focus of this project and can be divided into more specialist groups such as: alkylators, antibiotics, antimetabolites, topoisomerase inhibitors and mitosis inhibitors. A combination of anti-cancer drugs can be used to obtain the best possible outcome for the patient, which is largely lead by The National Institute for Health and Care Excellence (NICE) guidelines. The most frequently prescribed anti-cancer drugs according to a survey conducted in the north west of England in 2014 were capecitabine (a pro-drug of 5-fluorouracil), followed by cyclophosphamide, hydroxyurea, 5-fluorouracil, imatinib and gemcitabine (Booker *et al.*, 2014).

In response to the growing healthcare and drug resistance problems that cancer presents, many novel anti-cancer drugs have been developed in the last few decades. One example is phleomycin that causes double-strand breaks in the DNA of cancer cells which inhibits its replicative ability and allows the immune system to combat the cancerous cells (van Peer *et al.*, 2009). Tirapazamine is another drug currently in phase II/III clinical trials for a variety of different cancers in conjunction with cisplatin or with radiotherapy (Shah *et al*., 2013). Tirapazamine is a pro-drug that is bactericidal under aerobic and anaerobic conditions. It is believed that tirapazamine causes both single- and double-strand DNA breaks by free radical production, ultimately leading to cell death and could be a good candidate drug against multidrug resistant bacteria (Shah *et al*., 2013).

Doxorubicin is another commonly used chemotherapeutic that is used in a wide range of cancers including but not limited to: haematological malignancies, Kaposi's sarcoma, breast and bladder cancer (Auda, 2007). The mechanism of action of doxorubicin is through interactions with DNA, whether it be inducing DNA damage through the generation of free radicals or inhibiting the topoisomerase II enzyme which unwinds DNA for replication (Westman *et al*., 2012). Due to the interactions of doxorubicin and DNA, there are numerous side effects associated with the drug as well as toxicity as the drug is able to interact with the patient's own normal cells and any bacteria present.

In conclusion, there are a variety of drugs that are used in chemotherapy to treat cancer patients. Many of the mechanisms by which these drugs work is not clear, and the effects they can have on commensal bacteria present in the body are unknown. Unsurprisingly, these anti-cancer drugs act on or interact with DNA, and it is possible that these interactions with DNA-especially bacterial DNA-can cause sequence changes (mutations) that can affect the phenotype of the bacteria, which poses an issue in terms of treatment of cancer patients.

1.6. Anti-cancer drugs and antimicrobial resistance

In recent years, more work has been conducted that looks into the action of anti-cancer drugs in the development of associated antimicrobial resistance. It is known that cancer chemotherapy drugs can have antibiotic effects that can damage DNA and stimulate the SOS response and lead to changes in the bacterial mutation rate (Guðmundsdóttir *et al*., 2021; Meunier *et al*., 2019). A study conducted by Meunier *et al*. (2019) highlighted the issues associated with pathogenic bacteria and cancer chemotherapy. In this study, 39 chemotherapy drugs were analysed for their ability to induce the SOS response. They found that the drugs dacarbazine, azacitidine and streptoztocin were able to drive mutations in *S. aureus*, *P. aeruginosa* and *E. cloacae* that resulted in resistance to first-line antibiotics. Methotrexate is another drug that has been found to have an effect on antibiotic resistance. In a study conducted by Guðmundsdóttir *et al*. (2021) found that methotrexate (400 µg/mL) was able to select for trimethoprim resistance determinants in clinical strains of *E. coli*. A review article written by Papanicolas *et al*. (2018) also broaches the subject of anti-cancer drugs stimulating antibiotic resistance, with a particular focus on the human gut. They propose that the administration of anti-cancer chemotherapeutics can stimulate antibiotic resistance through increasing mutagenesis in bacteria which can then lead to outgrowth of bacteria and pathogens that can translocate out of the gut into the bloodstream.

In a study conducted by Auda (2007) they found that uropathogenic *E. coli* were able to develop resistance to the antibiotic ciprofloxacin when exposed to the anti-cancer agents cyclophosphamide and doxorubicin. Approximately 90% of their isolates (60 isolates) demonstrated resistance to antibiotics that the patients had received previously at the time of the administration of anti-cancer chemotherapies. They concluded that the resistance was due to the anti-cancer drugs having a mutagenic effect.

Bodet *et al*. (1985) highlighted that the action of antineoplastic drugs (for instance bleomycin, cisplatin, cyclophosphamide, methotrexate, vinblastine and vincristine) needs to be studied in more depth, especially when coupled with antibiotics that are given to cancer patients. The authors suggested that these drugs may be synergistic and affect patient outcomes as it is not

clear what concentrations of each drug are present in certain bodily environments e.g. the gastrointestinal tract and their effects on the human microflora.

Overall, it is clear that research surrounding the use of anti-cancer drugs and their potential mutagenic effects on bacteria has been experimented on, with a small number of instances where the use of anti-cancer agents is associated with antibiotic resistance. However, the link between anti-cancer drug usage and antibiotic resistance evolution has not been explored in enough depth.

1.7. Bleomycin, an anti-cancer drug

Bleomycin (Bm) is a Food and Drug Administration (FDA) approved anti-cancer drug that is naturally produced by *Streptomyces verticillus* and features on the World Health Organisation's (WHO) Model List of Essential Medicines (Danshiitsoodol *et al.*, 2006). There are different forms of the Bm molecule, but the two most common forms found in a clinical dose of Bm are the A_2 and B_2 forms (see Figure 1). Bm is classed as an anti-mitotic antibiotic as it acts by interacting with DNA and causing multiple single- and double-strand breaks, stopping cell division and ultimately leading to cell death (Dortet *et al.*, 2017). Although Bm is commonly used for its DNA damaging effects, Bm has also been found to degrade some RNA, usually in the form of tRNAs which may impact on both human and bacterial protein synthesis alike, although this interaction has not been well explored (Kawano *et al*., 2000).
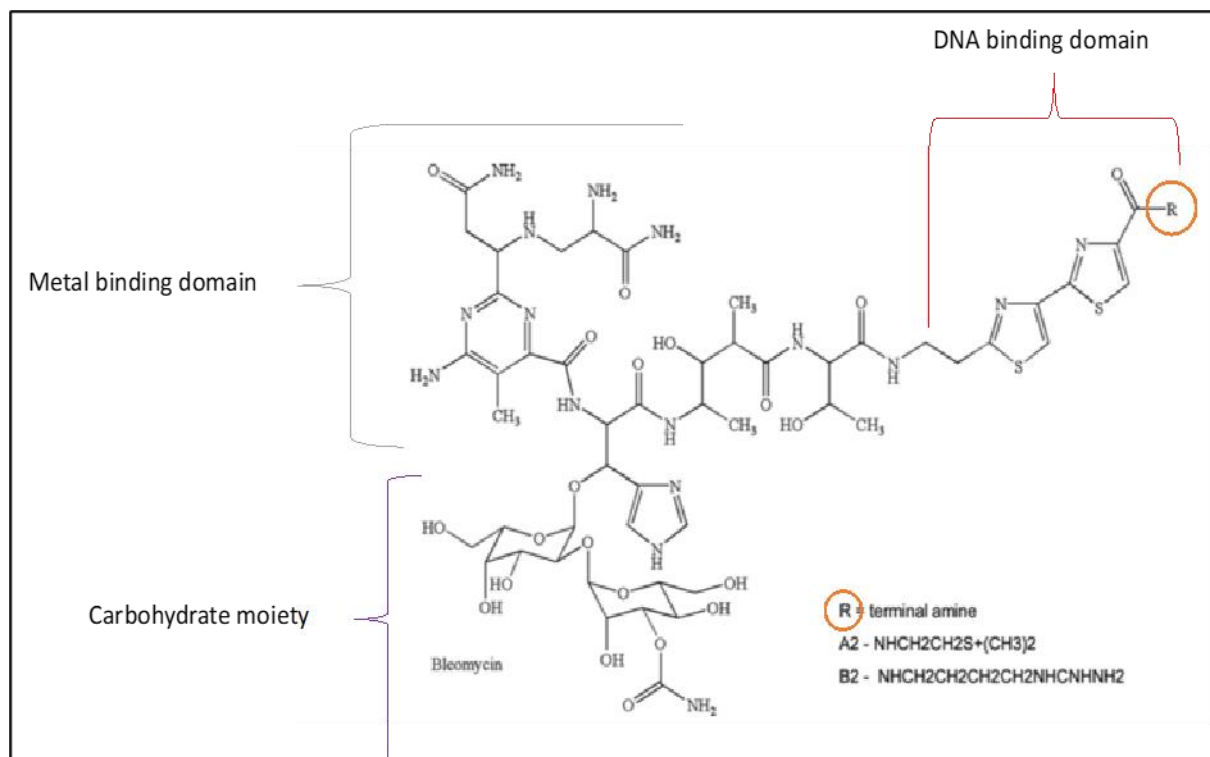
Figure 1: Diagram of the two main forms of bleomycin commonly used in cancer therapy, A2 and B2. The differences in the structures of the two forms of bleomycin are circled in orange, where the structure differs in terms of the terminal amine found in the DNA binding domain and carbohydrate moiety in the structures. Diagram adapted from Galba *et al*. (2014) and Holmes *et al*. (1996).

Bm is typically used in combination with other chemotherapeutic drugs for the treatment of some squamous cell carcinomas (in the head and neck) and the treatment of Hodgkin's and non-Hodgkin's lymphomas and tumours of the testes (Haidle *et al*., 1972a; NICE, 2021; Twentyman, 1983). Therefore, Bm is used in a variety of patients. It has been reported that head and neck squamous cell carcinoma mainly affects middle-aged men, but increased incidence has been seen in younger populations, especially women in developed areas of the world like the United States and in Europe (Chitapanarux *et al*., 2006; Shiboski *et al*., 2005).

Testicular cancer, in comparison to other types of cancer, is relatively rare but can be the most common cancer in the 15-40 years old age group of men, with its incidence increasing within the last 40 years (Chia *et al*., 2010). The incidence of Hodgkin's and non-Hodgkin's lymphomas have gradually seen an increase, with males being diagnosed earlier and at a younger age (Smith *et al*., 2015). Although Bm demonstrates little bone marrow toxicity, which could indicate some level of cell specificity, the possible resulting pulmonary fibrosis limits the dose that can be administered clinically to patients (Kimura *et al*., 1972).

Bm is used in a range of chemotherapy regimens. The current first line therapy for patients suffering from Hodgkin's lymphoma is a combination of doxorubicin (adriamycin), Bm, vinblastine and dacarbazine (ABVD). Another commonly used chemotherapy regimen is that of Bm, etoposide, doxorubicin, cyclophosphamide, vincristine, procarbazine and prednisolone (BEACOPP). These combinations of drugs have been found so far to be the most effective therapy for Hodgkin's lymphoma and highlights the use of Bm in the treatment of certain cancers (Jóna *et al.*, 2016). Bm is also part of the first line treatment for patients that are suffering from disseminated germ cell cancer and malignant germ cell tumour. It is used with other anti-cancer drugs such as etoposide and cisplatin due to its broad range activity and relatively low myelotoxicity (Kier *et al.*, 2017). The use of Bm, etoposide and cisplatin in combination has also been extended to ovarian granulosa cell tumours, where the addition of Bm appeared to have enhanced the response rate to the regimen when studied in a phase II trial (Pautier *et al.*, 2008).

1.8. Bleomycin mechanism of action

The way in which Bm causes DNA damage has not been fully elucidated, despite numerous studies that have investigated this. In a study by Kumagai *et al.* (1999), it was suggested that DNA cleavage followed a two-step process where a Bm and iron complex with oxygen (Fe(II)-Bm-O_2) and a reducing agent caused DNA cleavage in a sequence-specific way. The Bm complex is suggested to interact with DNA and degrade to form a Fe(III)-Bm complex along with a hydroxyl or superoxide radical that damages DNA and causes its cleavage (Kumagai *et al.*, 1999).

It has been found that Bm is able to form complexes with a variety of metal ions such as Cu(II), Zn(II) and Co(II) but these complexes are unable to degrade DNA (Grollman and Takeshita, 1980). However, the cobalt(III)-Bm complex is able to cause DNA strand breakage when UV light was applied. It is believed that the UV light causes photoreduction of cobalt to activate the cobalt-Bm complex (Subramanian and Meares, 1986). Upon Bm interaction with isolated DNA, it was discovered that DNA breakage led to the release of free bases from the structure, with thymidine being preferentially lost at a Bm dose of 0.1 mg/mL. However, at higher Bm concentrations (12-50 mg/mL) all four bases had the potential to be released from the DNA structure (Haidle *et al.*, 1972b). Upon further experimentation, Sausville *et al.* (1978) found that the effects of Bm on DNA degradation could be enhanced when a reducing agent was added, for instance 2-mercaptoethanol. Conversely, the ability of Bm to degrade DNA could be reduced or inhibited by using metal ions such as Cu(II) or by using a chelating agent such as

ethylenediaminetetraacetic acid (EDTA). Free radical DNA damage caused by Bm could also be inhibited by the addition of superoxide dismutase (SOD) as it is believed to scavenge the free radicals produced by the Bm complex to prevent damage to DNA. However, a study conducted by Galvan *et al.* (1981), suggested that SOD works by physically binding to DNA and either competing with Bm or interfering with Bm's interaction with DNA rather than scavenging the damaging free radicals.

In a study conducted by Heydari-Bafrooei *et al.* (2017), an electrochemical method was utilised to look at the effect of certain metal ions on the action of Bm. Using a modified electrode with DNA, they observed changes in the charge transfer resistance of the electrode and also looked for 8-Oxo guanine peaks in the solution as an indicator for DNA lesions and DNA damage. From their experiments, they confirmed that Bm cannot cause DNA damage independently as it doesn't interact with double-stranded DNA (dsDNA), but when Bm was combined with metal ions, DNA damage could be detected. When looking at the interactions of Bm complexed with metal ions in solution, they found that a buffer solution at pH 4 caused the greatest interaction between Bm and the DNA, theorised to be due to an increased positive charge of Bm complexes which allows for better interactions with the predominantly negatively charged DNA (Heydari-Bafrooei *et al.*, 2017).

Clearly the mechanism of action of Bm requires more comprehensive investigation. Studies have indicated that Bm only has an active effect when it is in an iron complex which then interacts with DNA and degrades to form free radicals that are believed to degrade DNA. DNA damage through the use of Bm could be enhanced with the addition of a reducing agent but could be reduced with the use of a free radical scavenger, such as SOD.

1.9. Known resistance genes to bleomycin

1.9.1. *Streptomyces verticillus* resistance

The natural producer of Bm, *S. verticillus* is resistant to the effects of Bm. *S. verticillus* has been estimated to resist the effects of over 400 μg/mL of Bm whereas the *E. coli* strain TG1 is susceptible to 10 μg/mL (Sugiyama *et al.*, 1994). It is not unlikely that *S. verticillus* is able to transfer the Bm resistance genes to other neighbouring bacteria that come into contact with it in the environment, especially in soil where *Streptomyces* species are typically found. A study conducted by Calcutt and Schmidt (1994) reported that a 7 kb nucleotide sequence held two resistance genes to Bm as well as a further five open reading frames within the *S. verticillus* DNA

structure. The two resistance genes found on the chromosomal DNA are *blmA* and *blmB*, where *blmA* codes for a protein that is 60% similar to the bleomycin-binding protein (BRP) from the gene Sh*ble* found in *Streptoalloteichus hindustanus* which naturally produces the antibiotic tallysomycin (Sugiyama *et al.*, 1994; Yuasa and Sugiyama, 1995). The BRP molecule has been found to be made from two identical folded half structures (dimers) where one dimer is able to bind to two molecules of antibiotic (Dumas *et al.*, 1994).

The action of the *blmA* protein (BLMA) is believed to be through the binding of the antibiotic and inhibiting it from interacting with DNA and thus, preventing its cleavage. The *blmB* protein on the other hand, codes for an acetyltransferase (BAT) that appears to interact with antibiotics and cause their inactivation through enzyme modifications (Sugiyama *et al.*, 1994). The action of BAT was demonstrated through the use of *S. verticillus* cell extracts incubated with acetyl coenzyme A that had been labelled with carbon-14 and it was observed that the [^{14}C]acetyl moiety was transferred to Bm, forming the inactive Bm acetate that demonstrates no antibacterial effect (Sugiyama *et al.*, 1994).

In a study conducted by Danshiitsoodol *et al.* (2006), they discovered that the binding of a mitomycin C (MMC) binding protein to MMC was similar to BLMA in structure when analysed using crystallography. It is believed that the MMC binding protein functions in a similar way to the BLMA protein, as they have two pockets within its structure for Bm or MMC to bind to. Each binding pocket in the structure of the BLMA protein has the ability to bind to two molecules of Bm which could explain why the presence of BLMA can demonstrate high resistance to Bm, as two molecules of Bm can be sequestered by one BLMA protein (Danshiitsoodol *et al.*, 2006).

1.9.2. Tn*5* transposon

A transposon is defined as DNA sequences that are able to move from one location on a genome to another. The Tn*5* transposon has been detected in Gram-negative bacteria like *E. coli,* is approximately 5,818 base pairs (bp) long and carries a resistance determinant against the antibiotic Bm (Figure 2). The gene *ble* is found located between genes that are determinants for resistance to other antibiotics such as kanamycin, neomycin and streptomycin (Genilloud *et al.*, 1984; Mazodier *et al.*, 1985). When the action of the Tn*5* transposon was investigated further by Blot *et al.* (1993), it was found that the Bm resistance protein required the activity of the *aidC* gene product and DNA polymerase (Pol) I in order to confer resistance to Bm, although it is not clear what the role of the gene *aidC* is in terms of alkyl-DNA repair as it is induced by the DNA-

alkylating agent *N*-methyl-*N*-nitro-*N*-nitrosguanidine. When the Tn*5* transposon was inserted into *E. coli*, it was found that Tn*5* positive *E. coli* had a fitness advantage over the wildtype *E. coli* cells. It was theorised that this advantage was a result of the increased action of repair in the DNA of *E. coli* when spontaneous lesions appeared. Another study by Enne *et al*. (2005) demonstrated that Tn*5* also conferred a selective advantage in *E. coli* as the *ble* gene was able to prevent DNA strand breakage, though the mechanism by which this happens is not understood.
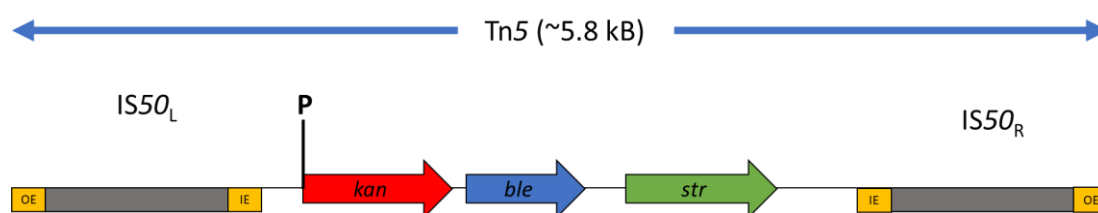
Figure 2*: Diagram of the Tn*5* transposon, outlining the IS*50* left (IS50$_L$) and IS*50* right (IS50$_R$) elements that flank the Tn*5* transposon, kanamycin (*kan*)-, bleomycin (*ble*)- and streptomycin (*str*)-resistance genes and inverted repeat recognition sequences found in the IS*50* elements: the outside end (OE) and the inside end (IE) (highlighted in yellow). Diagram adapted from Mazodier *et al*. (1985) and Jilk *et al*. (1996).

A study by Biel and Hartl (1983) demonstrated in chemostat experiments that when Tn*5* and non-Tn*5* strains of *E. coli* were competing for a limited carbon source, the Tn*5*-strains were able to grow at a more rapid rate than the non-Tn*5* strains and increase in frequency from 50% to 90% within the first 20 generations. It is possible that acquiring the Tn*5* transposon is important in natural environments and populations as bacteria are exposed to fluctuating access to nutrients, so having a faster growth rate is important when adapting to new conditions and the maintenance of their population.

When Tn*5*-mediated resistance to Bm was investigated in more depth in *E. coli*, it was found that sensitive strains were killed at concentrations <1 μg/mL whereas the resistant *E. coli* strains could withstand concentrations >500 μg/mL (Adam *et al.*, 1998). The same study found that the

resistance mechanism employed by the *ble* gene was not through enzymatic modification, as when the Bm or bleomycin/Ble-6His complex (where the *ble* gene was tagged with histidine) were treated with heat (100˚C), Bm was able to recover its ability to degrade DNA and Ble was sensitive to heat treatment (Adam *et al.*, 1998). This study also suggested that the *nrfG* gene is important in Bm resistance in *E. coli*, this gene is the last gene found in the formate-dependent periplasmic nitrite reductase *nrf* operon (composed of 7 genes in total) and when this gene was inactivated, Bm resistance was lost as well as the fitness advantage phenotype. It was then suggested that NrfG and Ble are part of a detoxification pathway for harmful activated oxygen or reduced iron-containing molecules that can damage DNA, and that Bm may be recognised by the cell as a haeme-like molecule that needs to be either removed from the cytoplasm or processed into a non-toxic compound to the cell.

Mobile genetic elements (MGEs) can pose an issue in organisms if they insert into genes that are essential for the organism, causing detrimental effects. In a study by Blot *et al*. (1993), they believed that when the Tn*5* transposon was inserted into non-essential genes, it was more advantageous to *E. coli* by enabling the organism to grow faster, compared to *E. coli* strains without the transposon-although the exact mechanism by which this improves the fitness of the organism has not been elucidated. The *ble* gene product from the transposon is believed to work by inhibiting the formation of damaging radicals by binding to Bm. In a study conducted by Kumagai *et al*. (1999), the minimum inhibitory concentration (MIC) of Bm needed to inhibit *E. coli* growth when the *ble* resistance gene was present was over 250 µg/mL whereas a mutant *ble* that had lost Bm resistance had an MIC of <4 µg/mL. However, many other advantages have been speculated to accompany the action of the *ble* gene product, for instance experiments conducted on the survival of *E. coli* carrying a mutant *ble* gene or a wildtype *ble* gene demonstrated that the presence of the gene itself could stimulate DNA repair in the host cells or provide resistance to other sources of DNA damage (Kumagai *et al*., 1999).

The Tn*5* transposon has also been found to confer resistance to other antibiotics such as phleomycins and tallysomycins that are related and damage DNA through single- and double-strand breaks, this work was demonstrated in *E. coli* and *S. typhimurium* (Collis and Hall, 1985). Phleomycin (and its derivatives, part of the Bm family of antibiotics) are typically used in research whereas tallysomycin in theory could be used as an anti-cancer agent once issues with its cell penetration capabilities are solved. Through amino acid identity comparisons, it was found that ShBle from *S. hindustanus* and Ble from the Tn*5* transposon share approximately 25% of their amino acid sequence alignment. This indicates that Ble may act in a similar way to ShBle

in terms of DNA repair (although this mechanism is not fully understood) and that they derive from a common ancestor (Bostock *et al.*, 2003). If resistance to both phleomycins and tallysomycins is mediated by the Tn*5* transposon, this may pose a problem in terms of the use of tallysomycin in cancer therapy if it passes clinical trials and the discovery of new drugs.

1.9.3. pUB110 plasmid

In *S. aureus*, the plasmid pUB110 was found to have a resistance gene for Bm (Semon *et al.*, 1987). In a study conducted by Gennimata *et al*. (1996) where clinical isolates of *S. aureus* were tested for Bm resistance, it was discovered that 197 of the samples out of 254 isolates were resistant to Bm with 33% of these isolates also being resistant to the antibiotic tobramycin (an aminoglycoside derived from *Streptomyces tenebrarius*). Out of the 197 Bm resistant isolates, 43 were found through DNA dot-blot hybridisation analysis using [^{32}P]-labelled probe to detect pUB110-like Bm resistance DNA sequences (Gennimata *et al.,* 1996). It has been found that *S. aureus* Bm resistance is widespread in the environment, and it may not be due to selection pressure from drugs used in hospitals. It is theorised that the resistance genes for Bm may be located on plasmids or bacterial chromosomes that can co-exist with tobramycin genes and is being transferred in the environment (Gennimata *et al.*, 1996).

Strains of methicillin-resistant *S. aureus* (MRSA) have been found to demonstrate resistance to Bm or have resistance genes to other antibiotics. For instance, in a study conducted by Sugiyama *et al.* (1995), the MRSA strain B-26 had a Bm resistance gene which was found in the chromosome, rather than originating from a plasmid. This resistance gene was also found to be associated in a cluster with a kanamycin resistance gene. When the nucleotide sequence of the Bm resistance gene was tested, it was found to be identical to the pUB110 plasmid. With the presence of part of the IS*431mec* insertion-like element (methicillin resistance-associated) sequence, the study hypothesised that the Bm resistance gene was integrated into the chromosome of MRSA B-26 from the plasmid pUB110 (Sugiyama *et al*., 1995). Similarly, in a study conducted by Rolain *et al.* (2009) on an MRSA strain found in Marseille, France (CF-Marseille) they found that the MGE SCC*mec* (the staphylococcal cassette chromosome mec, that carries a methicillin resistance-determinant) had integrated into the pUB110 plasmid. This was of particular concern as the CF-Marseille strain also had resistance to other antibiotics such as β-lactams, fluoroquinolones, kanamycin, tobramycin, erythromycin and TET that had origins from plasmids and MGEs. This demonstrates the ability of *S. aureus* to adapt and evolve at remarkable speeds and to specific niches which allows it to compete and survive changing conditions effectively, with antibiotic pressure seeming to be a driver of the emergence of new

strains (Rolain *et al.*, 2009). It is not clear whether MRSA and Bm resistance have a direct link, or how widespread the association is in the environment or in a clinical setting.

1.9.4. NDM-1 operon

Globally, in Gram-negative bacilli, the New Delhi metallo-β-lactamase 1 enzyme (NDM-1) is spreading. It has also come to attention that a gene conferring resistance to Bm, ble_{MBL}, is associated with the bla_{NDM-1} gene which encodes for NDM-1, as shown in Figure 3 (Dortet *et al.*, 2017). The NDM-1 enzyme is an issue in itself as it is able to hydrolyse and disrupt the action of β-lactam antibiotics like ampicillin, penicillin, cephalosporin and carbapenems (Jamal *et al.*, 2016). Bacteria that are NDM-1 positive have been detected in India in drinking and sewage water which raises health concerns as NDM-1 bacteria are already posing issues within hospitals, and it is not clear how widespread the bla_{NDM-1} gene is globally (Farhat and Khan, 2020; Guo *et al.*, 2011). Studies have indicated that it is possible that *Acinetobacter* species that are under selective pressure by antibiotics are aiding the spread of bla_{NDM-1} to *Enterobacteriaceae*, as well as through the action of horizontal gene transfer (HGT) and insertion elements (Liu *et al.*, 2015).

The ble_{MBL} gene encodes a BRP named BRP_{MBL} as it is co-expressed with bla_{NDM-1} under the action of the same promoter (Dortet *et al.*, 2012). It is concerning to see that many NDM producers have been found to have the ble_{MBL} gene, and organisms that produce BRP_{MBL} are better adapted to surviving in different environments as the BRP_{MBL} expressing strains are able to stabilise the genes associated with NDM and are less likely to be inactivated through deleterious mutations (Dortet *et al.,* 2012*)*. In an experiment conducted by Dortet *et al*. (2012) it was discovered that when BRP_{MBL} was produced in hypermutable *E. coli*, there was an approximate 2.4-fold reduction in the spontaneous mutation rate, as measured by the generation of rifampin-resistant mutants. It was theorised that BRP_{MBL} interfered with the defective DNA repair system of the hypermutable *E. coli* when the DNA was defective or damaged, therefore stabilising the NDM associated resistance and served as an advantage to the organisms as they are more likely to survive as disadvantageous mutations are less likely to occur randomly within genes, although the exact mechanism by which BRP_{MBL} does this is not clear.
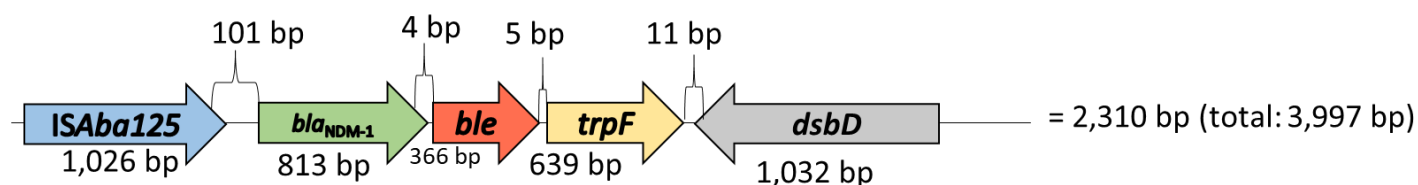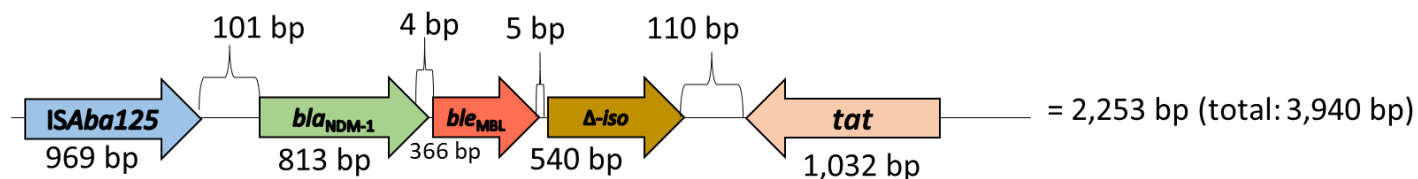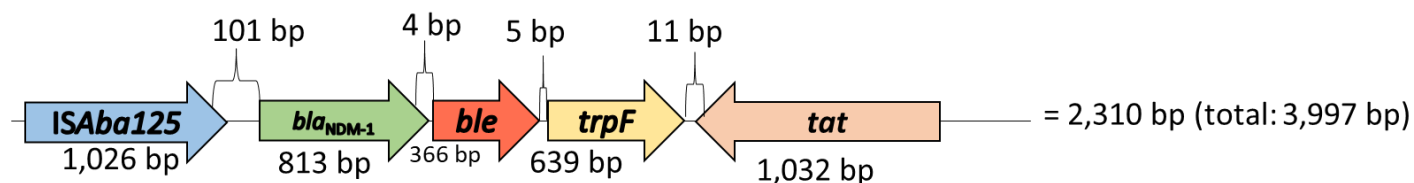
Figure 3: The NDM-1 operon local environment in *Acinetobacter baumannii* strains. Sequence order and base pair length was taken from GenBank (accession codes listed). Where **ISAba125** is an insertion sequence, **bla_NDM-1** is a gene encoding a metallo-β-lactamase (which confers resistance to β-lactam antibiotics), **ble/ble_MBL** is the gene encoding the bleomycin resistance protein, **trpF** encodes an N-(5'phosphoribosyl)anthranilate isomerase that is involved in the L-tryptophan from chorismite biosynthesis pathway, and **dsbD** encodes a thiol:disulphide interchange protein required to facilitate the formation of disulphide bonds in periplasmic proteins. The **Δ-iso** gene is the Δ-phosphoribosyl anthranilate isomerase-like gene, the product of which is involved in the tryptophan biosynthesis pathway, the **tat** gene encodes a twin-arginine translocation pathway signal protein.

It is interesting to note that in a study conducted in 2013, a *P. aeruginosa* isolate that was recovered from patient contained the *bla*_{NDM-1} gene which was adjacent to the IS*Aba*125 sequence and a truncated Bm resistance gene (Janvier *et al.*, 2013). The carriage of a Bm resistance gene (although it is truncated) is of particular concern as *P. aeruginosa* has been found to be intrinsically resistant to many antibiotics, and its ability to acquire new resistance genes is an issue. A study conducted by Murugan *et al.* (2016) found that a *P. aeruginosa* isolate from a keratitis patient exhibited multidrug resistance to β-lactams, aminoglycosides and quinolones. When the genome sequence was investigated, a Bm resistance protein was detected, which may then be used as a selective marker for other antibiotic resistance genes in the isolate.

Overall, the Tn*5* transposon, pUB110 plasmid and transposons carrying the NDM-1 operon indicate the potential for Bm to select for antibiotic resistance because it has been found that as well as carrying Bm resistance genes, these MGEs also contain resistance genes for other antibiotics such as ampicillin and carbapenems. This suggests that exposure to Bm will co-select for these antibiotic resistance genes in an organism, which may impact on cancer chemotherapeutic treatments where secondary bacterial infections are a threat to the patient.

1.9.5. Bleomycin hydrolases

Past studies have found that cancers are able to form resistance to anti-cancer drugs through methods such as drug inactivation, drug alteration, drug efflux pumps and cell death inhibition. Bm hydrolases are enzymes that are able to inactivate the antibiotic Bm (Jóna *et al.*, 2016). Bm hydrolases are more commonly associated with a range of eukaryotes to tolerate the toxic effects of Bm, for instance the Bm hydrolase enzyme has been found in mice, rabbits, humans and *Saccharomyces cerevisiae* when the expression of the Bm hydrolase mRNA was examined (Sebti *et al.*, 1989). Although it appears that the Bm hydrolase enzyme is ubiquitous and conserved in many species, it is not known what the role of the enzyme is *in vivo*, although it may have some importance in the normal function of the organism (Sebti *et al.*, 1989). It is also interesting to note that mammals are not typically exposed to Bm, the Bm hydrolase enzyme being conserved in mammals indicates that it may have some form of cellular function. When the enzyme was removed from mice, it was found that Bm hydrolase had importance in neonatal survival and the few mice that survived presented unusual scaling and shedding of skin from their body which was usually resolved after approximately 10 days but the tail still presented

abnormalities, including necrosis and autoamputation (O'Farrell *et al*., 1999; Schwartz *et al*., 1999).

In *S. cerevisiae*, the Bm hydrolase is encoded for by the *BLH1* gene. When Bm hydrolase deficient cells were produced, there appeared to be no impact on the yeast cell life and their differentiation, but upon exposure to Bm, cells died (Enenkel and Wolf, 1993). It is thought that *S. cerevisiae* utilises the Bm hydrolase in the natural environment for survival against bacteria that naturally produce and secrete antibiotics like Bm, although the concentrations of Bm in the environment and the exposure of environmental bacteria to naturally produced antibiotics like Bm is not known and therefore it is not known how essential Bm hydrolases are to such organisms (Enenkel and Wolf, 1993).

In humans, the Bm hydrolase gene is found within an open reading frame made up of 1,365 bp and shares 40% protein identity with the Bm hydrolase found in *S. cerevisiae* (Brömme *et al*., 1996). When the human Bm hydrolase from tissues and tumours were analysed by Northern blot, it was discovered that most organs expressed the protein in low to moderate levels, for instance in the spleen, heart, brain, prostate and ovary. In the lungs, expression of Bm hydrolase is poor, which could explain lung fibrosis in cancer patients treated with Bm (Crnovcic *et al*., 2018). Higher levels of Bm hydrolase expression was seen in the testis, pancreas and skeletal muscle (Brömme *et al*., 1996). What was interesting to note from this study was that the tumour cell lines used had higher levels of expression of the Bm hydrolase when compared to the human organs. This could reflect the use and efficacy of Bm, as the leukaemia cell lines expressed high levels of Bm hydrolase and previous studies have demonstrated that leukemic cancers don't respond well when treated with Bm (Brömme *et al.,* 1996).

Metabolic inactivation of Bm was explored in a study conducted in 1991, where they found that human Burkitt's lymphoma cells could resist the effects of Bm (Sebti *et al.*, 1991). In the study, they focused on the Bm hydrolase protein (a cysteine proteinase) and the cysteine proteinase inhibitor E-64 which blocked the effects of the Bm hydrolase. In their experimentation, they detected the amount of Bm (in the A_2 form) that hadn't been metabolised after incubation. They found that although Bm could inhibit the growth of the tumour cells, there was a greater effect on the inhibition of growth when the E-64 protein was added to the condition, working after 4 days as opposed to days 8 and 10 of treatment (Sebti *et al.*, 1991). When E-64 was added by itself without Bm, the growth of tumours was not inhibited; this could possibly be explored in

terms of cancer therapy for patients as the administration of Bm and E-64 could be more effective than if Bm was administered by itself (Sebti *et al.*, 1991).

Overall, it is clear that resistance to Bm can be present in different forms. From the natural producer of Bm, *S. verticillus* encodes the genes for the BLMA and BAT proteins, where the BLMA protein is similar to the Sh*ble* protein found in *S. hindustanus*. The transposon Tn*5* contains the Bm resistance gene *ble* and has been suggested to confer other advantages to an organism by stabilising DNA and reducing mutations from spontaneous mutations as well as being associated with resistance to other antibiotic drugs. Similar findings have been found in strains of *S. aureus*/MRSA where there has been the integration of the pUB110 plasmid. Another problem posed with resistance to Bm is the association of the NDM-1 operon with the BRP_{MBL} protein, and also resistance found in eukaryotes in the form of Bm hydrolases which interfere with the action of Bm in the treatment of cancers.

1.10. Causes of resistance evolution

There are numerous possible explanations for the rapid evolution of certain organisms to the action of Bm and other antibiotics. For instance, in patients it is believed that a tolerance to certain antibiotics can be a result of intermittent treatments with antibiotics that leaves a subpopulation of the pathogenic organism surviving. This tolerance can eventually lead to mutations that can contribute to persistence of the organism in a clinical setting and failure of a treatment program (Gefen *et al.*, 2017). It is also possible for bacteria to be exposed to differing antibiotic concentration gradients in the environment and within the human body. These concentrations can be non-lethal, sub-inhibitory concentrations that may stimulate changes in the bacteria. Genetic and phenotypic variability can be a consequence of exposure to antibiotics at sub-optimal levels. In a study conducted by Mahnik *et al.* (2007), they found that effluents from hospitals may be a source of anti-cancer agents that make it into the environment, as they are not treated specifically to inactivate or remove the drugs sufficiently, which presents an aspect of drug exposure to organisms living in the aquatic and surrounding environment. There are many theories on the mode and magnitude of selective pressures and the mechanisms by which organisms evolve and adapt after exposure to antibiotics in the wider environment.

1.10.1. Spontaneous genetic variability and genomic instability

There are common strategies for bacteria to generate genetic variability, for instance, small nucleotide sequence changes within the genome which can lead to an advantageous or

disadvantageous phenotype (Lopez *et al.*, 2007). Other strategies include re-shuffling of the genome and acquisition of new genes through HGT (Lopez *et al.*, 2007). Although spontaneous mutations can occur to cause bacterial diversity, it must be taken into consideration how other environmental factors can act as stimulants to alter the genome of bacterial organisms and how frequently spontaneous mutations occur to have an impact. Genomic instability can arise from point mutations or rearrangements in the genome such as amplifications, deletions, duplications, insertions, inversions or translocations. However, with specific reference to the effects of Bm, recombination was explored in this section of this report.

Recombination is where genetic material is rearranged and can lead to genetic diversity. In a study conducted on *S. cerevisiae*, it was found that administration of Bm caused recombination and had mutagenic effects on the genetic markers that were used in the study, these genetic markers were selected because there were no observable effects conferred on growth or sensitivity of cells to Bm (Moore, 1978). In this study, it showed that longer treatments with Bm led to increased recombinant survivors in the *S. cerevisiae* strains (treatment times varied depending on the *S. cerevisiae* strains used but ranged from 0-45 minutes, 0-60 minutes, and 0-20 minutes). In a different study conducted on the genetic effect of Bm on *S. cerevisiae*, it was found that Bm was also able to induce mitotic recombination at a high frequency, although when the effects of Bm were compared to positive controls such as UV, the mutagenic effect of Bm was low and more comparable to the effects of the positive control, gamma rays (Hannan and Nasim, 1978).

1.10.2. SOS response

It is thought that DNA damage can induce the SOS response in cells, which leads to the transcription of the *recA* gene and the production of RecA whilst removing the SOS transcriptional repressor, LexA (Lopez *et al.,* 2007). In *E. coli* cells, it was found that the genetic network that makes up the SOS response contains over 30 genes and altogether carry out different functions, for instance the repair of DNA, cell division arrest and homologous recombination (Friedman *et al.*, 2005).

The SOS response gene network is tightly controlled by the LexA repressor. The LexA repressor downregulates the expression of the SOS genes as well as itself, but upon DNA damage, RecA binds to single-stranded DNA (ssDNA) near where replication is arrested and encourages the

cleavage of the LexA repressor and the induction of the SOS genes by acting as a co-protease to cleave LexA, see Figure 4 below (Courcelle *et al.*, 2001; Friedman *et al*., 2005).
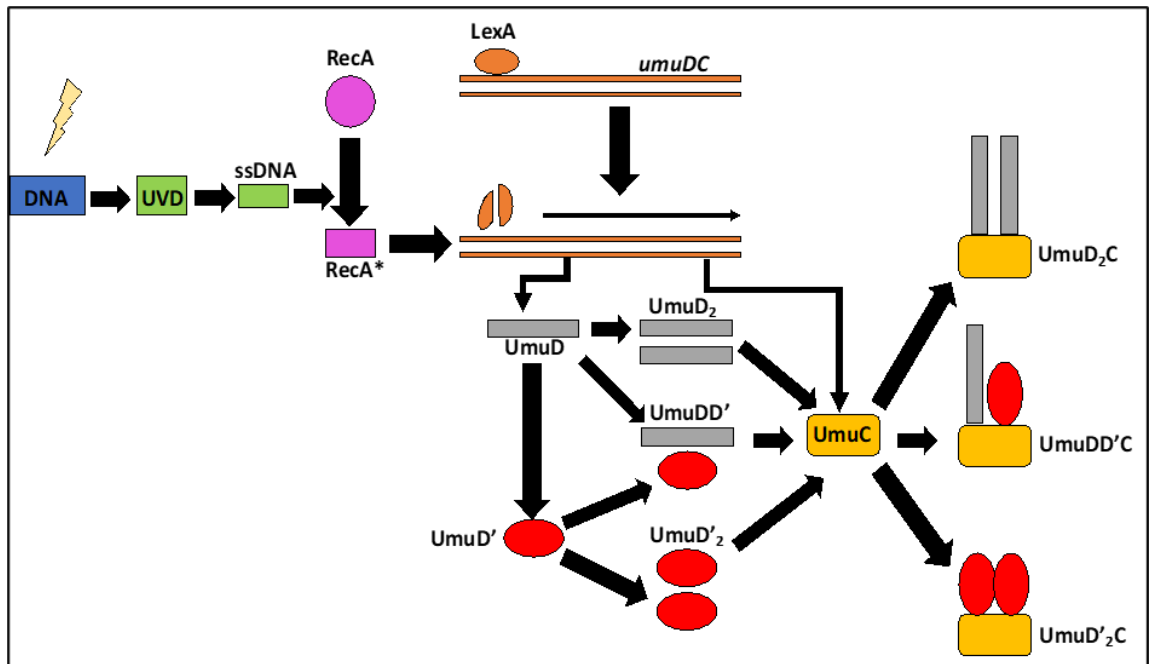
Figure 4: The SOS system in *Escherichia coli*. Diagram re-drawn from Belov *et al*. (2009). Damage occurs to the DNA, in this scenario it is UV damage (UVD, although this can be due to many things such as drug exposure). The emergence of single-stranded DNA (ssDNA) activates the SOS response, causing the activation of the RecA protein (RecA* is activated RecA). The RecA* is proteolytic and cleaves the LexA repressor protein. This leads to the de-repression of the SOS inducible genes *umuD* and *umuC*. Cleavage of the UmuD protein causes its activation (UmuD' form). The products UmuD$_2$, UmuDD' and UmuD'$_2$ form due to intermolecular reactions. All three are able to interact with the UmuC protein, due to an affinity to this protein, forming complexes UmuD$_2$C, UmuDD'C and UmuD'$_2$C (Pol V). UmuD$_2$C complex is involved in cell cycle regulation, stops DNA synthesis and allows the translesion synthesis repair process to begin and activation of other SOS response genes. The UmuDD'C complex is thought to inhibit SOS mutagenesis by suppressing UmuD' activity.

In *E. coli*, three DNA polymerases are induced in response to the SOS system being activated. These DNA polymerases are named Pol II (encoded by *polB*), Pol IV (encoded by *dinB*) and Pol V (encoded by *umuDC*) and have been implicated in mutagenesis through translesion synthesis (TLS) (Napolitano *et al*., 2000). TLS is less accurate than the process of normal DNA replication as the translesion DNA polymerases read through the damaged DNA template and can substitute bases and cause mutations in the strand that is newly synthesised.

In studies investigating the induction of the SOS pathway and the effect the pathway has on bacterial fitness, it has been found that the SOS response can give the bacteria an advantage when it comes to competitive ability with other organisms and mutagenesis induced by stress is a side effect of this ability (Torres-Barceló *et al.*, 2015). It is thought that the DNA polymerases

induced in response to stress increase the fitness of bacteria by protecting the cell against stress, for instance retaining the integrity of DNA and inhibiting replication arrest, allowing the bacteria to resist detrimental effects associated with stress (Torres-Barceló *et al*., 2015).

It is possible that as a DNA damaging agent, Bm exposure may activate the SOS response in an organism and induce repair of the damaged DNA through TLS, which may incorporate errors into the sequence and lead to *de novo* mutations that help reduce the susceptibility to certain antibiotics. If an organism is already carrying resistance to Bm and resists the DNA damaging effects, their genome is more stable in this regard and any antibiotic resistance genes remain in the population.

1.10.3. Horizontal gene transfer

Horizontal gene transfer (HGT, also known as lateral gene transfer) is the process by which bacteria can acquire genetic information from other species of bacteria, whether they are closely or distantly related. The most common mechanisms by which HGT occurs is through transformation (free, extracellular DNA), transduction (by bacteriophages) and conjugation (close, cell-to-cell contact). The transfer of MGEs and resistance genes can also be conducted through nanotubes and membrane vesicles (vesiduction) (Rodríguez-Beltrán *et al.*, 2021; Shin *et al*., 2016). In a study conducted by Jutkina *et al.* (2016), it was demonstrated that sub-optimal concentrations of the antibiotic TET (150 times below the MIC, where the MIC was 1.5 mg/L) encouraged HGT of antibiotic resistance genes whereas higher concentrations that impacted on bacterial growth reduced the amount of HGT events occurring. This study highlights the issue of the potential activity of antibiotics in the environment stimulating the exchange of resistance determinants between bacterial species, and the spread of antibiotic resistance. In the same study by Jutkina *et al.* (2016) in gnotobiotic rats, it was found that when bacteria in the gut of the rats were exposed to antibiotics, the mechanism of conjugative transfer of genes was increased.

The acquisition of resistance genes may not necessarily be beneficial to an organism and may come at a cost to the organism's competitive ability with other local bacteria- a fitness cost. It is also possible for the insertion of the new resistance genes to disrupt the function of normal, existing genes in the cell or disrupt the expression of other genes as they consume the resources available to the cell such as nucleic acids and proteins, impacting on the ability of the organism to grow (Suzuki *et al.*, 2016). In a study conducted by Suzuki *et al.* (2016), they found that when

resistant strains were created through evolution experiments, they had a reduced rate of growth when compared to normal strains when there was no drug administered. This suggested that acquiring the resistance genes involved a form of fitness cost. This demonstrates that the resistance genes may only provide a benefit to the organism when there is a selective pressure where the gene becomes useful for survival in the condition. This is important to note as bacteria may not be able to proliferate or be maintained if a resistance gene requires a high fitness cost unless the resistance gene is able to confer a benefit in an environment with no selective pressures.

In the case of *A. baumannii*, the *bla*$_{NDM-1}$ gene is found adjacent to the *ble* gene. If *A. baumannii* is exposed to carbapenem antibiotics, then the organism survives and proliferates, maintaining the *ble* gene. These genes can then be transferred horizontally to new organisms, and upon Bm exposure, allow the survival of the *bla*$_{NDM-1}$ gene. This could drive antibiotic resistance in organisms in the form of cross-resistance as the same resistance mechanisms can be employed to resist the effects of an antibiotic similar in structure or in its mode of action.

1.11. Persistence and drug tolerance

Drug tolerance and the term 'persistence' are usually used synonymously and are generally described as being the ability of bacteria to survive brief exposure to high concentrations of an antibiotic or agent. For the purposes of this project, 'tolerance' will be defined as the ability of bacteria to survive exposure to a high concentration of an antibiotic and remain metabolically active (this can be demonstrated by slow growth of the organism) (Brauner *et al*., 2016). Persisters are defined as a subset of the population that can phenotypically resist the action of an antibiotic that are metabolically dormant (Brauner *et al*., 2016; Trastoy *et al*., 2018). Persisters and tolerant bacteria that have been exposed to a harmful drug have the potential to mutate when the antibiotic is removed or present at a lower concentration. In the case of Bm, this subset of bacteria may activate their SOS response and undergo *de novo* mutations through TLS to resist the effects of Bm, which may also encourage cross-resistance to other antibiotics.

An aspect of administering drugs such as Bm that needs to be considered is the persistence or drug tolerance of organisms. It was theorised that although the bacterial cells with the ability to persist can lead to lower population fitness, they acted as a contingency plan when the whole population are presented with the challenge of antibiotics, allowing some cells to survive (Kussell *et al*., 2005). Persisters are an issue when treating a patient suffering from infection as

the cells that survive are able to replicate and continue the infection, regardless of the treatments administered (Kussell *et al.*, 2005).

1.12. Environmental exposure to antimicrobials

Microbial resistance to antibiotics is becoming a major issue in both the environment and clinical settings. Many sources of antibiotic resistance have been implicated in this issue, for instance, antibiotic prescriptions for patients that aren't followed strictly and the release of antibiotics into the environment through waste disposal. It is also not uncommon for drugs to pass through the human body unmetabolised and be released into the environment in its active form (Bound and Voulvoulis, 2005). As the concentrations of active antibiotics in effluents aren't well researched and quantified, it is difficult to determine the concentrations reaching the environment, although some small-scale studies have been attempted (Table 1). These concentrations can be intermittent and at sub-optimal levels to inhibit bacterial growth, but nevertheless lead to the evolution of antibiotic resistance or tolerance to the antibiotic (Levin-Reisman *et al.*, 2017). It is not clear either whether tolerance to antibiotics encourages the eventual resistance to the antibiotic or whether it delays resistance forming (Levin-Reisman *et al.*, 2017).

Table 1: A short collection of drugs (anti-cancer and antibiotics*) that have been detected in effluents and after wastewater treatment. Predicted concentrations have also been included. Data compiled from Ashton *et al.* (2004), Besse *et al.* (2012), Ferrando-Climent *et al.* (2014) and Quoc Tuc *et al.* (2017).

Substance	Mean Concentration (ng/L)	Location	Reference
Ofloxacin*	17900	Hospital, France	Quoc Tuc *et al.*, 2014
Norfloxacin*	12100	Hospital, France	Quoc Tuc *et al.*, 2014
Vancomycin*	3600	Hospital, France	Quoc Tuc *et al.*, 2014
Sulfamethoxazole*	2100	Hospital, France	Quoc Tuc *et al.*, 2014
Trimethoprim*	940	Hospital, France	Quoc Tuc *et al.*, 2014
Erythromycin*	800	Hospital, France	Quoc Tuc *et al.*, 2014
	159	Downstream sewage treatment works, UK	Ashton *et al.*, 2004
Capecitabine	117.24	(Predicted) Aquatic environment, France	Besse *et al.*, 2012
Amoxicillin*	110	Hospital, France	Quoc Tuc *et al.*, 2014
Ciprofloxacin*	103	Surface water value, after wastewater treatment, Spain	Ferrando-Climent *et al.*, 2014
Fluorouracil	39.57	(Predicted) Aquatic environment, France	Besse *et al.*, 2012
Tamoxifen	34	Surface water value, after wastewater treatment, Spain	Ferrando-Climent *et al.*, 2014
Imatinib	19.95	(Predicted) Aquatic environment, France	Besse *et al.*, 2012
Trimethoprim*	12	Downstream sewage treatment works, UK	Ashton *et al.*, 2004
Gemcitabine	8.66	(Predicted) Aquatic environment, France	Besse *et al.*, 2012
Cyclophosphamide	6.98	(Predicted) Aquatic environment, France	Besse *et al.*, 2012
Erlotinib	3.4	(Predicted) Aquatic environment, France	Besse *et al.*, 2012
Bevacizumab	1.99	(Predicted) Aquatic environment, France	Besse *et al.*, 2012
Methotrexate	1.71	(Predicted) Aquatic environment, France	Besse *et al.*, 2012
Irinotecan	1.06	(Predicted) Aquatic environment, France	Besse *et al.*, 2012
Etoposide	0.94	(Predicted) Aquatic environment, France	Besse *et al.*, 2012
Cisplatin	0.52	(Predicted) Aquatic environment, France	Besse *et al.*, 2012
Mitomycin C	0.07	(Predicted) Aquatic environment, France	Besse *et al.*, 2012
Bleomycin	0.02	(Predicted) Aquatic environment, France	Besse *et al.*, 2012
Daunorubicin	0.02	(Predicted) Aquatic environment, France	Besse *et al.*, 2012

Vinblastine	0.02	(Predicted) Aquatic environment, France	Besse *et al.,* 2012
Bortezomib	0.005	(Predicted) Aquatic environment, France	Besse *et al.,* 2012

In a study conducted by Kovacs *et al*. (2015), the anti-neoplastic drug 5-fluorouracil was tested for its toxicity in *Danio rerio* (zebrafish), as 5-fluorouracil is one of the most commonly used anti-cancer drugs. Residues of anti-neoplastic drugs have been detected as pollutants in the aquatic environment. From their study, there was no effect on the growth, survival or reproductive capacity of the zebrafish, but there were signs of tissue changes in liver and kidney samples at all of the concentrations of 5-fluorouracil tested (100 µg/L, 1.0 µg/L and 0.01 µg/L), as well as DNA damage in blood and liver cells, highlighting the possible dangers associated with anti-neoplastic drugs reaching the aquatic environment.

In the environment, resistance genes to Bm may be more widespread than initially thought. In a metagenomic study conducted by Mori *et al*. (2008), it was found that *ble* gene transfer in the non-clinical environment is mediated by MGEs such as the transposon Tn*5* and the pUB110 plasmid. When public databases are looked at, there appears to be numerous *ble* resistance genes. The study identified two novel *ble* resistance genes from activated sludge used to treat industrial wastewater. It would be interesting to investigate how common the *ble* genes are in the environment, whether organisms carrying the *ble* resistance genes have a competitive advantage over other environmental bacteria- perhaps in terms of cross-resistance to environmental antibiotics- and whether there is an advantage to carrying these genes that may incur a fitness cost when there is no exposure to Bm.

It is important to remember that although anti-cancer drugs may have mutagenic effects on bacteria, there may also be other synergistic effects within a patient's body or in the environment with other antibiotics or environmental molecules, which may lead to other unforeseen consequences (Hamilton-Miller, 1984). It is also important to note that not all areas of the body are exposed to the same concentration of an administered drug or antibiotic. It has been shown that low doses of antibiotics administered can lead to the long term generation of resistant mutants in laboratory experiments (McVicker *et al*., 2014). It has been found in previous studies that high concentrations and doses of antimicrobial therapies (particularly in cancer treatment), can cause an increase in the selection pressure on organisms in the environment (McVicker *et al*., 2014).

1.13. Bridging the gap between lab-based experiments and bioinformatics

As research and technology expand together, it is becoming increasingly important to combine the use of bioinformatics and laboratory experiments in order to help tackle and understand the

antibiotic resistance problem. In a study conducted by Brockhurst *et al.* (2019), they concluded that using both deep sequencing and culture-based sampling methods would allow for better ways to characterise the mechanisms that lead to antibiotic resistance in patients. This would also aid the development of new antibiotics and antimicrobial therapies. Using sequencing data and analysis of this data from studies of populations (like microbiome studies) will also help track the movement of MGEs, which is also important for monitoring antibiotic resistance spread (Brockhurst *et al*., 2019). Combining lab-based culture methods and sequencing also allows for the exploration of environments where the bacteria present are not so easily cultured. For instance, many studies have looked at the microbiota of rural and urban water systems. A study by McInnes *et al*. (2021) demonstrated that low- and middle-income countries have inadequate systems for treating wastewater and poor regulations of antibiotic use which allows the spread of antibiotic resistant bacteria. The McInnes *et al.* (2021) study in Bangladesh showed that antibiotic resistance genes were detected at high levels in urban areas and tended to be located on plasmids which can be shared horizontally with other bacteria.

Understanding the resistance genes present in a pathogenic bacterial species can be important when we attempt to re-purpose existing drugs or use multidrug strategies that exploit the collateral sensitivity effects that are associated with certain antibiotic resistance genes (Herencias *et al.*, 2021). The use of both laboratory work and sequencing data has allowed for the generation of antibiotic cross-resistance interaction networks that show the application of one antibiotic (and activation of the cell's resistance mechanism) can lead to a decreased sensitivity in other antibiotics, (Lázár *et al.*, 2014). Laboratory work and whole genome sequencing methods can also combine in another way for epidemiological studies and tracking infectious disease outbreaks, for instance, a study by Snitkin *et al*. (2013) was able to track the transmission of carbapenem-resistant *K. pneumoniae* in the US.

A more recent, notable example of the SARS-CoV-2 pandemic demonstrated how laboratory work and sequencing can work in tandem in order to control the spread of a virus. The SARS-CoV-2 virus was first identified in Wuhan, China in late 2019 and spread globally at a rapid rate (Wilkinson *et al*., 2021). Many teams were involved with the sharing of sequencing data and tools, with the Global Initiative on Sharing Avian Influenza Data (GISAID) at the head of this, contacting researchers to push the sharing of genomic data that could help scientists to understand the virus and its virulence and what measures could be put in place to limit its spread (Maxmen, 2021). The ability to sequence SARS-CoV-2 from positive patients also provided surveillance-based testing, where close contacts could isolate and environmental measures could be implemented such as disinfection protocols and the provision of personal protective equipment (Aggarwal *et al*., 2022). By the end of April 2021, more than 1.2 million coronavirus genomes had been uploaded and shared on the GISAID platform, with the UK in particular

sharing 379,510 sequences (Maxmen, 2021). From there, many other important projects were launched such as the GenOMICC study (Genetics of Mortality in Critical Care, international study that focused on extreme phenotypes associated with patients infected with SARS-CoV-2) and protocols that allowed the detection of SARS-CoV-2 in complex samples such as stool samples (Kousathanas *et al.*, 2022; Li *et al.*, 2021).

1.14. Hi-C uses and adaptations

Hi-C stands for high-throughput chromosomal conformation capture (Yaffe and Relman, 2020). Hi-C is a method used to quantify chromatin interactions and conformation on a larger, genome-wide scale using proximity-based ligation and next generation sequencing (Figure 5) (Davis *et al.*, 2021; Lieberman-Aiden *et al.*, 2009). In brief, the Hi-C method involves crosslinking the DNA using formaldehyde, quenching any excess formaldehyde with glycine, digesting the crosslinked DNA using REs that will leave 5'-overhangs that are subsequently filled with a biotinylated residue. The blunt-end DNA fragments are then ligated under dilute conditions so that fragments that are in close proximity in 3D space are joined together and marked with biotin where they join. The ligated DNA is then sheared and purified using streptavidin beads that bind to the biotin-labelled fragments. The final Hi-C library is then sequenced using paired-ends (Lieberman-Aiden *et al.*, 2009). To analyse the Hi-C data, a genome-wide contact matrix can be generated.
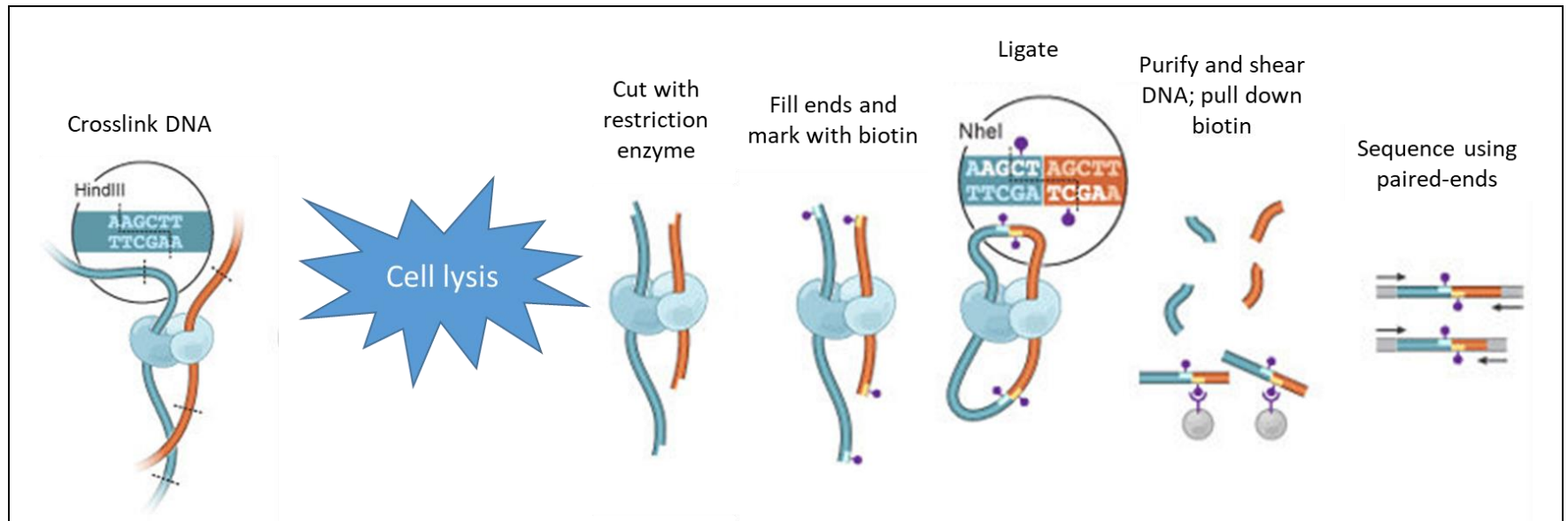
Figure 5: Hi-C method. The bacterial cells are treated with formaldehyde to crosslink DNA before cells are lysed. The crosslinked DNA is then cut using restriction enzymes and the ends are filled using biotin. The ends are then ligated together under dilute conditions before the DNA is purified further and sheared. The biotinylated fragments are then pulled down to create the Hi-C library that can then be sequenced. The figure is adapted from van Berkum *et al.*, (2010).

Understanding the chromosomal architecture inside bacterial cells is important as it can be used to determine how the chromosome can be re-organised during an infection and its role in pathogenicity through the regulation of gene expression and DNA repair (Davis *et al*., 2021). Although certain elements such as gene promoters don't appear to interact with other areas of the chromosome, the use of the Hi-C method can demonstrate that there is an association or interaction in 3D spatial proximity, also known as topologically associated domains (TADs) (Ulahannan *et al*., 2019; van Berkum *et al*., 2010). The use of Hi-C combined with next generation sequencing will be explored further in later sections of this thesis.

1.15. The bigger picture

It is of global concern that bacteria are becoming resistant to the antibiotics that we administer to patients suffering from infections. Bacteria are evolving different ways in order to combat antibiotics, and these methods can also lead to cross-resistance between similar antibiotics. As the human population grows, we are also seeing increasing cases of cancer which poses a different perspective of the same problem when many anti-cancer drugs we use also have antibiotic activity and can stimulate evolution that allows bacteria to grow in the presence of antibiotics. Cancer patients are also at a greater risk of secondary bacterial infections as they have a compromised immune system. The anti-cancer drug that will be the focus of this project is Bm, which has demonstrated antibacterial effects, but has been found in the literature to have resistance genes associated with it, which may be due to its environmental presence and use in a clinical setting. The effects of Bm on bacteria and its ability to stimulate evolution in the presence of the drug is not well elucidated.

1.16. Aims and Hypotheses

The purpose of this research project is to determine whether the anti-cancer drug Bm is able to stimulate antibiotic resistance and cross-resistance.

Our aims are as follows:

1. To determine how widespread the Bm resistance gene is amongst bacterial genomes in existing databases, and how conserved the bla_{NDM}-ble_{MBL} gene pairing is.
2. To determine whether carrying the bla_{NDM-1}-ble_{MBL} gene pairing in bacteria conferred a fitness advantage and whether this advantage changes under different growth conditions, for instance, in the presence of a drug or other external stressors.
3. To determine whether bacteria that are exposed to a sub-inhibitory concentration of Bm become less susceptible to the drug through the action of *de novo* mutations.

4. To determine whether the mutants that arise demonstrate an increased or decreased susceptibility to other antibiotics (cross-resistance).

5. To determine whether exposure to Bm alters the bacterial mutation rate.

6. To develop the existing Hi-C method to reduce the time taken to generate a Hi-C library.

7. To generate Hi-C libraries that are of a high quality and concentration that is suitable for long-read sequencing.

We hypothesise that the use of sub-minimum inhibitory concentrations of Bm can damage bacterial DNA which can lead to mutations that can change their susceptibility to different antibiotics. We also hypothesise that the Bm resistance gene (ble/ble_{MBL}) is common in bacteria and is associated with the bla_{NDM} gene variants. We also hypothesise that exposure to Bm can stimulate HGT, and we can detect and track the movement of MGEs through the combined use of the Hi-C method and long-read sequencing.

2.   Chapter 2- Fitness advantage of carrying the bleomycin resistance gene in bla_{NDM-1} bacteria

2.1.   Introduction

2.1.1.   Prevalence of bla_{NDM} genes

The bla_{NDM} gene encodes an enzyme (NDM) that hydrolyses β-lactam antibiotics, rendering them ineffective against bacteria (Guo *et al*., 2011). The rise of β-lactam resistance is a growing and major problem, where bacteria that produce NDM-1 have been found in 40 countries (Jamal *et al*., 2016). In a study conducted by Jamal *et al*. (2016), they found that *K. pneumoniae* was the dominant organism carrying the bla_{NDM-1} gene, followed by *E. coli* in Kuwait. All of the NDM-1-positive isolates (21 out of 61 isolates) that they found were resistant to a small panel of antibiotics, including: meropenem, ertapenem, cefotaxime, cefoxitin and ampicillin. bla_{NDM-1} carriage is commonly associated with *Pseudomonas*, *Acinetobacter* and *Salmonella* species and especially *Enterobacteriaceae*, with bacterial species such as *K. pneumoniae* and *E. coli* (Buser *et al.*, 2017; Poirel *et al*., 2010). NDM-producing bacteria have been detected in a variety of environments, from municipal wastewater, hospitals (more prominently from patients suffering from urinary tract infections) and animals (Bi *et al*., 2018; Liu *et al*., 2013; Mantilla-Calderon *et al*., 2016; Rahman *et al*., 2014; Wang *et al*., 2017).

2.1.2.   Different types of bla_{NDM} genes

Since the first identification of the bla_{NDM-1} gene in 2008, many variants of the gene have been discovered at a rapid rate (Bi *et al*., 2018). Many of these variants have been detected in mainland China and India, with some variants also being detected in Germany and Egypt (Ahmad *et al*., 2018; Bi *et al*., 2018; Göttig *et al.*, 2013; Rahman *et al*., 2014; Ramadan *et al*., 2020). Currently, there are 29 variants of the bla_{NDM} gene, found in a variety of different bacterial species with a small number of amino acid substitutions (Basu, 2020). It has been demonstrated in the past that different amino acid substitutions at 16 positions seen in the bla_{NDM} variants affects the activity of the NDM protein, where the action of the variants NDM-4, -5, -7, -9, -13, -14 and -17 have a higher hydrolytic ability than NDM-1 against carbapenem antibiotics (Rahman *et al.*, 2018).

2.1.3.   The association of the bla_{NDM} and the *ble* genes

In the literature to date, it has been seen that the bla_{NDM-1} is nearly always associated with the Bm resistance gene, often labelled on genetic structures as *ble* or ble_{MBL} (Ashcroft *et al*., 2020).

Further investigations into the genetic environment of the bla_{NDM} gene show that the IS*Aba125* insertion sequence is also present, either in a complete or truncated form (Ashcroft *et al.,* 2020). It is not yet clear why the Bm resistance gene is associated with the bla_{NDM} gene. In a study conducted by Wang *et al*. (2020), they discovered a single nucleotide polymorphism (SNP) in the *ble* gene from an *Acinetobacter towneri* strain AeBJ009 isolated from hospital sewage in China where there was a base change from cytosine to thymidine, which led to an amino acid substitution. It was not clear what the effect of this mutation was on the protein, but it was believed to have emerged from selection pressure of other antimicrobials detected in the sewage sample (Wang *et al*., 2020a).

2.1.4. Bacterial competition and fitness costs

Bacteria typically live in dense communities in a variety of different environments, where the ability to compete for resources and space is crucial for survival (Frost *et al*., 2018). The acquisition of advantageous genes (e.g. antibiotic resistance genes, virulence factors) can help an organism compete in an environment, but it is important to also note that the carriage of novel genes or plasmids can also impose a fitness cost on the bacteria, especially when the novel gene is not required for survival in the environment they are in (Frost *et al.,* 2018). The effects of a novel gene or plasmid on an organism can be ameliorated with compensatory mutations (Yang *et al.,* 2020). In a study conducted by Card *et al.* (2020), they investigated whether mutants resistant to TET were less fit than their parent strain in *E. coli*, in the absence of TET using competition experiments. From the study, they found that the resistant *E. coli* were less fit than their parents, but the reduction of fitness was not consistent with the level of resistance the mutants could achieve against TET. The authors hypothesised that even though the bacteria have the same resistance mutation, the fitness cost of the actual mutation and consequent resistance mechanism may be different depending on the genetic background of the organism (Card *et al.,* 2020). It is likely that in the wider environment, competitions between different organisms controls population levels, and can cause the gain and loss of new genes and lead to the exclusion and extinction of organisms that are unable to compete in the environment they are in, especially in stressful environments (Carvalho *et al.,* 2020).

2.2. Aims

This chapter had two aims:

1. To determine how widespread the Bm resistance gene is amongst bacterial genomes in existing databases, and how conserved the bla_{NDM}-ble_{MBL} gene pairing is.

2. To determine whether carrying the bla_{NDM-1}-ble_{MBL} gene pairing in bacteria conferred a fitness advantage and whether this advantage changes under different growth conditions, for instance, in the presence of a drug or other external stressors.

We hypothesise that bacterial strains that carry the bla_{NDM-1}-ble_{MBL} sequence would have a competitive fitness advantage over the strains that carry just the bla_{NDM-1} or ble_{MBL} gene, and it would be apparent under different growth conditions e.g. in the presence of an antibiotic that directly damages DNA as a mechanism of action. We also hypothesise that the bleomycin resistance gene is prevalent in bacterial genomes and is commonly associated with a bla_{NDM} variant.

2.3. Methods

2.3.1. Gene survey for the *ble* gene

A gene survey was conducted for the ble_{MBL} gene and its surrounding gene environment using Geneious Prime (v 2021.0.3). The nucleotide sequence from the NCBI database NZ_CM015668 was used as a reference for the ble_{MBL} gene in order to find identical or similar sequences. The NZ_CM015668 file was used as the query sequence for BLAST (BLAST+ v 2.12.0, accessed July 2021). For the BLAST parameters, we used the database nucleotide collection (nr/nt) and MegaBLAST. Results were presented as a hit table, and the option selected for retrieval was 'extended region with annotations', and the context size was limited to 1,000. The maximum number of hits was limited to 1,000 and all the other input settings and parameters were left as default (low complexity filter used, Max E-value of 0.05, scoring for Match mismatch was 1-2, word size 28 and gap cost (open extend) was set to linear)

2.3.2 Cloning/Transformation

2.3.2.1. pSTV 29 plasmid transformation for plasmid stock

The pSTV 29 plasmid from Takara Bio was first transformed into the *E. coli* 5-alpha strain from the Gibson Assembly kit (New England Biolabs, NEB). 10 µL of the chemically competent *E. coli* 5-alpha cells were mixed with 5 µL pSTV 29 plasmid and mixed gently by pipetting in a 1.5 mL Eppendorf tube. The competent cells and DNA mixture were incubated on ice for 5 minutes and then heat shocked at 42°C for 30 seconds. The cells were placed back on ice for 2 minutes. The cells were recovered by adding 1 mL of SOC outgrowth medium (from the Gibson Assembly kit, NEB), gently pipetted and then incubated at 37°C for 1 hour with 180 rpm shaking. After incubation, the cells were collected by centrifuging the Eppendorf tubes at 16,200 xg for 1 minute. The majority of the supernatant was discarded, but 50 µL was reserved to resuspend

the pellet. The mixture was then plated on 25 µg/mL chloramphenicol (≥98% HPLC, Fluka Analytics, Fisher Scientific) LB (Miller, Sigma Aldrich) plates. The plates were then incubated overnight at 37˚C. After overnight incubation, any transformants present were grown in a larger volume of LB broth and 25 µg/mL chloramphenicol (CHL) and saved using 700 µL of the overnight culture and 300 µL 80% glycerol, and frozen at -80˚C.

2.3.2.2. Plasmid preparation

The pSTV 29 plasmid was linearised using either the PvuI-HF (NEB) or a combination of BamHI-HF and KpnI-HF restriction enzymes (REs) (NEB), depending on the fluorescent protein that was being used in that construct. For ease, the PvuI-HF RE will be referred to for the rest of this chapter as PvuI, and the same applies to the BamHI-HF (BamHI) and KpnI-HF (KpnI) enzymes. 1 µg of the pSTV 29 plasmid was digested using 2.5 µL of the designated RE, 5 µL of CutSmart Buffer (NEB) and 40.5 µL sterile distilled water to make a total reaction volume of 50 µL. The digestion mixtures were incubated overnight at 37˚C. After incubation, the plasmids were purified by a standard ethanol precipitation method where 5 µL of 3 M sodium acetate trihydrate at pH 5.2 (Fisher BioReagents) was added to the digested plasmid with 100 µL of 100% ethanol. This was mixed by pipetting and then left at -20˚C overnight. After freezing, the digested plasmid mixture was centrifuged at full speed on a standard microcentrifuge at 4˚C for 30 minutes. The supernatant was discarded and the pellet was dried for 15 minutes with the cap of the tube open. The pellet was then gently resuspended in 50 µL of sterile distilled water. The digested plasmid DNA was quantified using the Invitrogen Qubit™ dsDNA High Sensitivity (HS) Assay kit (ThermoFisher Scientific) on a Qubit 4 fluorometer.

2.3.2.3. DNA strings synthesis and ligation into pSTV 29 plasmid

GeneArt Strings DNA Fragments (ThermoFisher Scientific) were used to synthetically create the genes mCherry, GFPuv, bla_{NDM-1}, ble_{MBL} and bla_{NDM-1}-ble_{MBL}. These genes were then inserted into the multiple cloning site in the low to medium copy number plasmid pSTV 29 in different combinations in order to generate different constructs to conduct competition experiments later.

2.3.2.4. Gibson Assembly to create plasmid constructs

Using the Gibson Assembly kit, different plasmid constructs were created where 30 ng of the desired synthetic gene was added to 10 ng of the linearised pSTV 29 plasmid. The reactions were performed on ice where the synthetic DNA and linearised pSTV 29 plasmid was added to a 1.5 mL Eppendorf tube with 10 µL of Gibson Assembly Master Mix (2X) so that the total volume in

the tube was 10 µL. The reactions were then incubated on a heat block for 1 hour at 50°C. The newly synthesised plasmids were purified by ethanol precipitation. The plasmids were placed on ice or in -20°C freezers for long term storage.

2.3.2.5. Heat shock transformation of constructed plasmids

Chemically competent *E. coli* 5-alpha cells were thawed on ice. To 1.5 mL Eppendorf tubes, 50 µL of the *E. coli* 5-alpha cells were added. Then, 5 µL of the desired plasmid construct was added to the Eppendorf tube. A positive control was set up using the pSTV 29 plasmid and 50 µL of *E. coli* 5-alpha cells and a negative control was set up with 50 µL of *E. coli* 5-alpha cells with no plasmid. The contents of the tube were gently mixed by pipetting. The tubes were then returned to ice for 5 minutes before they were heat shocked at 42°C for 30 seconds on a heat block. After heat shocking, the tubes were transferred to ice for 2 minutes. 1 mL of SOC outgrowth medium was then added to each tube and then incubated at 37°C for 1 hour with shaking at 180 rpm. LB plates containing 25 µg/mL CHL were pre-warmed at 37°C before use and 100 µL of the heat shocked cells were spread plated. The plates were then incubated overnight at 37°C.

2.3.2.6. Transformation of constructed plasmids using electroporation

There were issues with low transformation efficiency using the heat shock method of transformation. So, electrocompetent cells were created using *E. coli* DH5α cells which were provided by Dr. Emma Manners from the Wain group. This was done by taking an inoculating loop of the DH5α cells and growing them overnight in 10 mL LB broth in 50 mL Falcon tubes at 37°C. After incubation, a fresh 50 mL Falcon tube was prepared with 10 mL LB broth and 100 µL of the overnight culture after it had been diluted to optical density at 600 nm (OD_{600}) of 0.05. The cells were grown for 2-3 hours until an OD_{600} of 0.6-1.0 was reached. The cells were centrifuged for 5 minutes at 4,226 xg at 4°C and the supernatant was discarded. To the cell pellets, 10 mL of chilled 10% glycerol was added and used to resuspend the cell pellet. The cells were then centrifuged for 5 minutes at 4,226 xg and 4°C and the supernatant discarded. The cell washing steps were repeated a further three times before the cell pellet was resuspended in 100 µL of 10% glycerol and 10 aliquots were made and stored at -80°C.

For electroporation, the electrocompetent *E. coli* DH5α cells were defrosted on ice, the purpose of these experiments was to determine whether the cells were electrocompetent. A 0.1 cm electroporation cuvette was used per sample and these were pre-chilled on ice before use. The SOC outgrowth medium for recovery was also pre-warmed at 37°C. Different mixtures were set up to test: *E. coli* DH5α + GFPuv plasmid, *E. coli* DH5α + mCherry plasmid, DH5α + pSTV 29 plasmid and *E. coli* DH5α cells + pSTV 29 plasmid but with no shock. 1 µL of the desired plasmid

was added to the bottom of the electroporation cuvette and 50 μL of the electrocompetent cells was added to the cuvette on top of the plasmid. The cuvettes were then incubated for 30 minutes at room temperature before being put back onto ice. The cells were electroporated using the BTX ECM 630 Electro Cell Manipulator with the settings: 100 Ohm, 25 μF at 1.8 kV (with the exception of the no shock control). The sides and metal plates on the electroporation cuvettes were wiped before they were used. After electroporation, the cuvettes were immediately put back onto ice and resuspended in 1 mL of SOC outgrowth medium. After pipetting to mix the cells, the cells were transferred to a 1.5 mL Eppendorf tube and incubated at 37˚C with shaking at 180 rpm for 1 hour. The cells were then spread plated on 25 μg/mL CHL selective plates and incubated overnight at 37˚C.

2.3.2.7.   pSTV 29 plasmid extraction from 5-alpha cells

To determine whether methylation of the pSTV 29 plasmid will improve transformation efficiency, two cryovials of the pSTV 29 plasmid that was previously transformed into *E. coli* 5-alpha cells was extracted from a freezer stock in order to be inserted into *E. coli* DH5α. Plasmid extraction was done using the QIAprep Spin Miniprep kit (QIAGEN). Extraction was done in 1.5 mL LoBind Eppendorf tubes and according to manufacturer's instructions. After plasmid extraction, the plasmids were purified using ethanol precipitation before the samples were checked for contamination using a NanoDrop 2000 spectrophotometer (ThermoScientific) and quantified using a Qubit dsDNA HS kit.

2.3.2.8.   *E. coli* DH5α electroporation with plasmid controls

E. coli DH5α were prepared as described previously to make electrocompetent cells. Electroporation was attempted using *E. coli* DH5α cells with the pSTV 29 plasmid (shocked and no-shock) and then a pUC19 plasmid (shocked and no-shock, provided by Dr. Emma Manners from the Wain group). The pSTV 29 conditions were set up with 0.2 μL of the pSTV 29 plasmid and 100 μL of *E. coli* DH5α electrocompetent cells. The pUC19 plasmid conditions were set up with 1 μL of the pUC19 plasmid and 100 μL of the *E. coli* DH5α electrocompetent cells. All of the mixtures were prepared in 0.1 cm electroporation cuvettes and the shocked samples were done using the electroporation settings: 1.5 kV, 125 Ohm and 50 μF. The cells were then recovered in 1 mL of SOC outgrowth medium for 1 hour at 37˚C and 180 rpm shaking. After the recovery incubation, pSTV 29 shocked and no-shocked cells were plated on 10 μg/mL CHL LB plates and the pUC19 shocked and no-shocked cells were plated on 100 μg/mL ampicillin (sodium salt powder, Sigma Aldrich) LB plates and left to incubate overnight at 37˚C. Any colonies found on the pSTV 29 shocked cells plate were grown in 10 mL LB broth with 10 μg/mL CHL overnight before making glycerol stocks by adding 700 μL of the overnight culture and 300 μL of 80%

glycerol. Plasmids were then extracted using the QIAprep Spin Miniprep kit. Extracted plasmids were then tested on a NanoDrop, Qubit (dsDNA HS kit) and the TapeStation 2200 system (Agilent Technologies) using a Genomic DNA ScreenTape.

2.3.2.9. Gibson Assembly- Part 1

After determining that conditions were suitable for transformation, the desired constructs were created using Gibson Assembly. 50 ng of the pSTV 29 plasmid was digested with either PvuI or BamHI and KpnI depending on the target construct. The reaction to generate PvuI digested pSTV 29 plasmids was done by adding 5 µL of the Gibson Assembly master mix to 3.5 µL of plasmid DNA and 1.5 µL water to get a total volume of 10 µL. To generate plasmids that were digested with both BamHI and KpnI REs, the reaction was set up using 5 µL of the Gibson Assembly master mix and 6 µL of the pSTV 29 plasmid (approximately 3 µg of pSTV 29 plasmid DNA). Once the plasmids were digested, the synthesised desired genes were inserted into the pSTV 29 plasmid, construct designs are presented in Table 2. The reactions were incubated in 1.5 mL Eppendorf tubes at 50°C for 15 minutes. Completed reactions were stored long-term in -20°C freezers.

Table 2: Outline of constructs made in the first round of Gibson Assembly to create the desired constructs in the pSTV 29 plasmid.

Gibson Assembly step 1	Desired end construct in the pSTV 29 plasmid
PvuI digestion of pSTV 29 → + mCherry	mCherry
BamHI-KpnI digestion of pSTV 29 → + GFPuv	GFPuv
PvuI digestion of pSTV 29 → + mCherry	mCherry-bla_{NDM-1}
PvuI digestion of pSTV 29 → + mCherry	mCherry-ble_{MBL}
PvuI digestion of pSTV 29 → + mCherry	mCherry-bla_{NDM-1}-ble_{MBL}
BamHI-KpnI digestion of pSTV 29 → + bla_{NDM-1}	GFPuv-bla_{NDM-1}
BamHI-KpnI digestion of pSTV 29 → + ble_{MBL}	GFPuv-ble_{MBL}
BamHI-KpnI digestion of pSTV 29 → bla_{NDM-1}-ble_{MBL}	GFPuv-bla_{NDM-1}-ble_{MBL}

After the generation of the desired constructs, 6 electroporation reactions were set up for the desired constructs and 4 controls that consisted of the PvuI digested pSTV 29 plasmid which would be shocked or not with 0.2 µL pSTV 29 plasmid, and the BamHI-KpnI plasmid which would

also be shocked or not. Each sample was treated with 50 µL of electrocompetent *E. coli* DH5α cells and 2 µL of the desired plasmid. The electroporation settings used were 50 µF, 1.5 kV and 125 Ohm. After shocking, the cells were resuspended in 1 mL of SOC outgrowth medium and left to recover for 1 hour at 37˚C with 180 rpm shaking. After the recovery incubation, the cells were plated on LB agar that contained 10 µg/mL CHL. Colonies that grew on these plates were grown in 10 mL LB broth with 10 µg/mL CHL, where ~1 mL of culture was saved with 430 µL 80% glycerol, and the remaining 9 mL was used to extract the plasmids using the QIAprep Spin Miniprep kit. After plasmid extraction, the plasmids were run on the NanoDrop, Qubit (dsDNA HS) and TapeStation (TapeStation was conducted after the plasmids were digested using the RE HindIII).

2.3.2.10. Sanger sequencing

A selection of the extracted plasmids were sent for Sanger Sequencing with Source Bioscience, if they demonstrated good quality and concentration after NanoDrop and Qubit (dsDNA HS) testing. Approximately 10 µL of each plasmid was sent, and if the concentration of the plasmid after Qubit testing was less than 50 ng/µL, the sample also underwent template amplification before Sanger sequencing. Sanger sequencing was done to determine that the desired gene had been inserted and without the addition of any mutations to the sequence. For Sanger sequencing, the BamHI-KpnI pSTV 29 plasmids with either the GFPuv, bla_{NDM-1}, ble_{MBL} or bla_{NDM-1}-ble_{MBL} genes inserted used the Source Bioscience provided M13 forward and reverse primers. For the PvuI digested pSTV 29 plasmids with the mCherry gene inserted, our own primers were designed. The primers were PvuI_F (forward) primer: ATCATGATAAGCTCATTCG and PvuI_R (reverse) primer: TTACCCAACTTAATCGCCTT. After Sanger sequencing, the sequences were analysed using BLAST and 4Peaks and comparing to our target synthesised genes.

2.3.2.11. Functionality testing part 1- resistance genes

At this point, *E. coli* that have the resistance genes bla_{NDM-1}, ble_{MBL} or bla_{NDM-1}-ble_{MBL} in the pSTV 29 plasmid that have been transformed were tested for gene functionality. Resistance to carbapenems (as a result of bla_{NDM-1} expression) was tested using imipenem (Sigma Aldrich). An imipenem solution was made by dissolving 200 mg in 20 mL of 1 M MOPS buffer and then filtered using a 0.2 µM filter. To test Bm resistance (as a result of ble_{MBL} expression), 10 mg of bleomycin sulfate (Cayman Chemical) was dissolved in 1 mL dimethyl sulfoxide (DMSO) (Sigma Aldrich). MICs were tested in 96-well plates where the genetically modified (GM) *E. coli* were grown overnight in 10 mL LB broth with 10 µg/mL CHL to select for the pSTV 29 plasmid. The antibiotics (imipenem or Bm) were tested in a gradient ranging from 0-128 µg/mL with 2 columns left for the controls that either contained no organism or no antibiotic. The

concentration of DMSO present in each well was kept to levels that were low enough not to have an effect on cell survival, as demonstrated in section 3.4.1.2. The *E. coli* cells were then diluted to a 0.5 McFarland standard (OD_{600}: 0.08-0.1) and then further diluted 1:100. 100 µL of the standardised *E. coli* cells were then added to the appropriate wells. The 96-well plates were incubated overnight at 37˚C with 180 rpm shaking.

After overnight incubation, turbidity of each well was recorded before 20 µL of 0.01% resazurin sodium salt (Sigma Aldrich) was added to each well (resazurin sodium salt added at 10% of the well volume). The 96-well plates were then covered with foil and left to incubate at 37˚C for 30 minutes in the dark.

2.3.2.12.   Functionality testing part 1- fluorescent proteins

A summary of the Gibson Assembly and downstream functionality testing is shown in Figure 6. To determine whether the mCherry and GFPuv genes were functioning normally in the GM *E. coli*, fluorescence was tested using a FLUOstar Omega microplate reader (BMG LABTECH) and the Zeiss LSM 800 confocal microscope.

A FLUOstar Omega plate reader was set up using overnight cultures of the bacterial strains of interest with the fluorescent protein labels. To detect the presence of the GFPuv protein, absorbance was measured at 400-10/510 nm and to detect the presence of the mCherry protein, absorbance was measured at 584/620 nm with endpoint readings. One replicate of these strains were conducted where 200 µL of the cultures were added to the corresponding wells.

To prepare cells for confocal microscopy, the *E. coli* cells were grown overnight in 10 mL of LB broth. After overnight growth, 100 µL of the *E. coli* cells were used to inoculate 10 mL of fresh LB broth and left to grow at 37˚C with 180 rpm shaking until it reached the mid-log phase of growth (OD_{600}: 0.3-0.5). The cells were then pelleted by centrifuging at 7,197 *x*g for 20 minutes at 4˚C. The pelleted cells were then resuspended in 200 µL of phosphate buffered saline (PBS). Using the Mini PAP pen (ThermoFisher) a perimeter was drawn on Thermo Scientific Polysine Adhesion slides (Fisher Scientific) to mark out the area where the *E. coli* sample will be pipetted onto. 100 µL of the GM *E. coli* culture is pipetted gently to fill the slide. The slide was left to dry in the dark for approximately 1 hour. After incubating the slides in the dark, the slides are washed three times with PBS and then left to dry at 37˚C in the dark. One drop of Fluoromount Aqueous Mounting Medium (Sigma Aldrich) is then dotted onto the slide before a glass cover slip is placed on top. A pipette tip was used to push out any air bubbles under the cover slips.

The slides were then viewed using the Zeiss LSM 800 confocal microscope using water and a 63X objective lens.
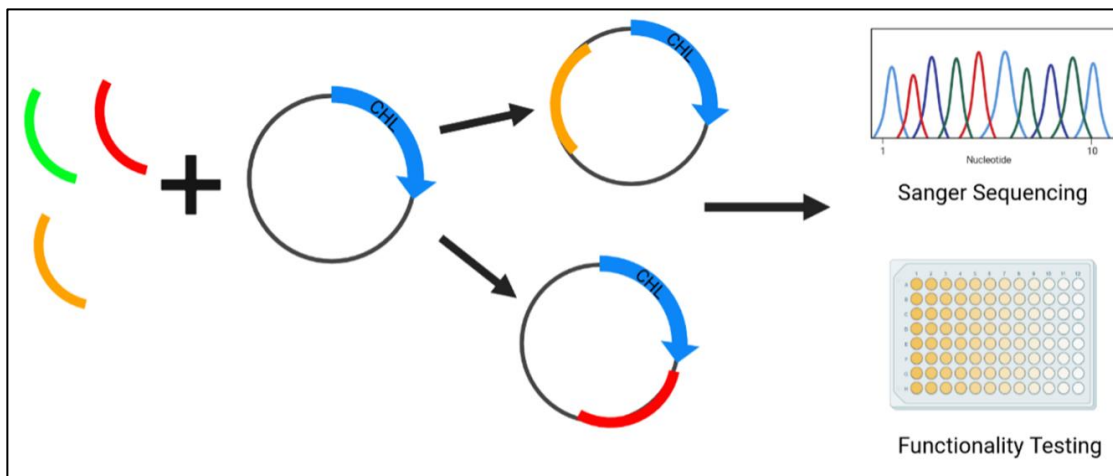
Figure 6: A summary of Gibson Assembly part one. The synthesised genes (red: mCherry, green: GFPuv and yellow: any variation of the target genes, e.g. ble_{MBL}, bla_{NDM-1} or bla_{NDM-1}-ble_{MBL}) are added to the pSTV 29 plasmid after the plasmid has been linearised. The pSTV 29 has a chloramphenicol (CHL) selectable marker. The constructs are then purified, Sanger sequenced and functionality testing was done after they were inserted into *E. coli* DH5α. Functionality testing involved MIC plates and viewing the fluorescence of the cells using a plate reader or confocal microscope. Diagram created using BioRender.

2.3.2.13. Gibson Assembly- Part 2

Using the plasmids generated in the first round of Gibson Assembly (containing either mCherry or GFPuv, bla_{NDM-1}, ble_{MBL} or bla_{NDM-1}-ble_{MBL}), the final desired genes were added to the pSTV 29 plasmid. The mCherry plasmids were digested using the both the BamHI and KpnI REs and the GFPuv, bla_{NDM-1}, ble_{MBL} and bla_{NDM-1}-ble_{MBL} plasmids were digested with PvuI. After the plasmids were digested, the concentration of plasmid DNA was determined by using Qubit (dsDNA HS). To create the final plasmid constructs, 30 ng of the digested pSTV 29 plasmid was added to a 1.5 mL Eppendorf tube with approximately 10 ng of the desired gene, 5 µL of the Gibson Assembly master mix and sterile distilled water to make a total reaction volume of 13 µL. Final constructs were created as demonstrated in Table 3. Plasmids were then stored at -20°C for long term storage. The issues seen previously with the bla_{NDM-1}-ble_{MBL} synthesised gene was rectified by ThermoFisher Scientific, where the wrong gene sequence was synthesised.

Table 3: Outline of the second part of Gibson Assembly to get the final, desired constructs in the pSTV 29 plasmid.

Gibson Assembly step 2	Desired end construct in the pSTV 29 plasmid
No changes made	mCherry
No changes made	GFPuv
BamHI-KpnI digestion of mCherry plasmid → + bla_{NDM-1}	mCherry-bla_{NDM-1}
BamHI-KpnI digestion of mCherry plasmid → + ble_{MBL}	mCherry-ble_{MBL}
BamHI-KpnI digestion of mCherry plasmid → + bla_{NDM-1}-ble_{MBL}	mCherry-bla_{NDM-1}-ble_{MBL}
PvuI digestion of bla_{NDM-1} plasmid → + GFPuv	GFPuv-bla_{NDM-1}
PvuI digestion of ble_{MBL} plasmid → + GFPuv	GFPuv-ble_{MBL}
PvuI digestion of bla_{NDM-1}-ble_{MBL} plasmid → + GFPuv	GFPuv-bla_{NDM-1}-ble_{MBL}

Electroporation to transform electrocompetent *E. coli* DH5α cells was conducted in the same way as before where 50 µL of cells were added to a 0.1 cm electroporation cuvette with 2 µL of the desired plasmid construct. Electroporation settings used on the BTX ECM 630 Electro Cell Manipulator were as follows: 50 µF, 1.5 kV and 125 Ohm. Cells were recovered in 1 mL SOC outgrowth medium and left to incubate for 1 hour at 37˚C before being plated on LB agar containing 10 µg/mL CHL.

Colonies that grew on the CHL plates were grown overnight in 10 mL LB broth with 10 µg/mL CHL. Glycerol freezer stocks were made with 1 mL of the overnight culture and 430 µL 80% glycerol, stored at -80˚C. The remaining 9 mL of culture was used in the QIAprep Spin Miniprep kit to extract the plasmids. Extracted plasmids were run on NanoDrop, Qubit (dsDNA HS) and TapeStation to determine quality, concentration and size of the plasmids.

2.3.2.14. Functionality testing of final plasmid constructs in *E. coli* 5-alpha cells

To test that the bla_{NDM-1} resistance gene was functioning normally in the *E. coli* cells, resistance testing was done in a plate screen with meropenem. Meropenem (Sigma Aldrich) was prepared by dissolving 10 mg in 1 mL of sterile distilled water. LB agar plates were made that contained either 10 µg/mL meropenem (MERO) or 2 µg/mL Bm for selection. 1 µL spots of the GM *E. coli* cultures were plated and left to dry before incubating overnight at 37˚C. Confocal microscopy

and the FLUOstar Omega plate reader were used again to determine visually if the fluorescent proteins were visually functional.

2.3.2.15. Sanger sequencing

The plasmids of the final constructs were extracted using the QIAprep Spin Miniprep kit and sent for Sanger Sequencing with Source Bioscience as before (section 2.3.1.10), after quality checking and quantification. Plasmids that had been digested using the BamHI-KpnI REs to insert bla_{NDM-1}, ble_{MBL} or bla_{NDM-1}-ble_{MBL} into the mCherry plasmids used the Source Bioscience provided M13 forward and reverse primers for Sanger sequencing. To sequence the pSTV 29 construct that had mCherry and the ble_{MBL} gene inserted, the primers Bam_F: TCCAGCTGAGATCTCCTAGG and Bam_R: GTGAATTCGAGCTCGGTACC were used. For the PvuI digested pSTV 29 plasmids containing either bla_{NDM-1}, ble_{MBL} or bla_{NDM-1}-ble_{MBL} and have the final fluorescent GFPuv inserted, our own primers were designed. The primers were PvuI_F (forward) primer: ATCATGATAAGCTCATTCG and PvuI_R (reverse) primer: TTACCCAACTTAATCGCCTT. After Sanger sequencing, the sequences were analysed using BLAST and 4Peaks and compared to the target synthesised genes.

To ensure all of the plasmid constructs were in the same *E. coli* background, any of the constructed plasmids in *E. coli* DH5α were extracted and then transformed into *E. coli* 5-alpha cells by electroporation, using the same settings as used previously on the electroporator. A summary diagram of part 2 of the Gibson Assembly is shown in Figure 7.
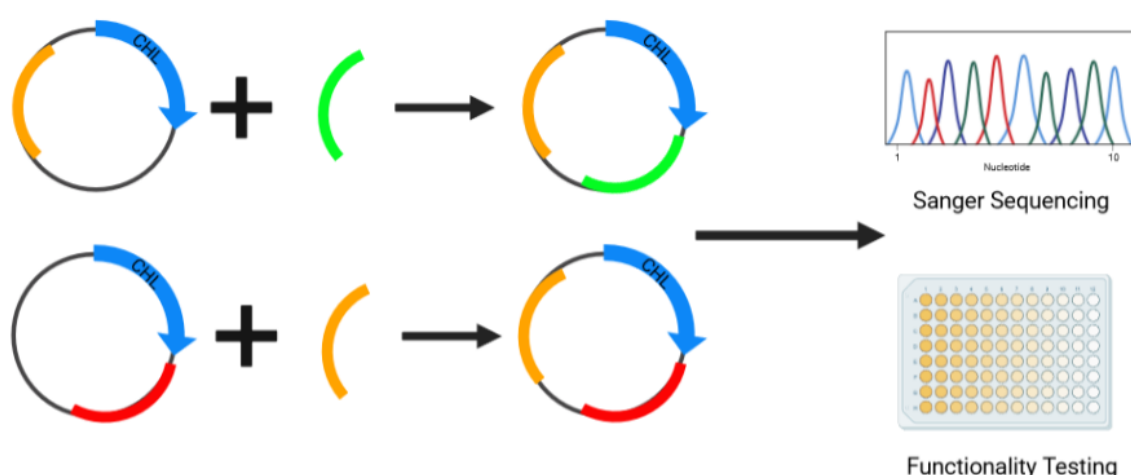
Figure 7: A summary of part 2 of the Gibson Assembly to generate the target constructs. The constructs made from part 1 of the Gibson Assembly were linearised and the next synthesised gene was inserted (red bands: mCherry, green bands: GFPuv and yellow bands: any variation of the target genes e.g. ble_{MBL}, bla_{NDM-1} or bla_{NDM-1}-ble_{MBL}). These constructs were then Sanger sequenced and inserted into *E. coli* 5-alpha for functionality testing by MIC plating or viewing

the fluorescent markers using a plate reader or confocal microscope. Diagram created using BioRender.

2.3.2.16. Passage to determine the stability of the inserted plasmids

To determine whether the inserted constructs were stable within *E. coli* 5-alpha, a colony of each construct was used to inoculate 10 mL of LB broth in 50 mL Falcon tubes with no CHL added (the selective agent for the inserted pSTV 29 plasmids). The tubes were then incubated for 24 hours at 37˚C with 180 rpm shaking. After 24 hours, 100 µL of the cultures was then used to inoculate fresh 10 mL LB broth in 50 mL Falcon tubes. These new cultures were then incubated for a further 24 hours at 37˚C with 180 rpm shaking. This process was repeated for 4 days. On the final day, 100 µL of the cultures were plated at dilutions ranging from 10^0-10^{-8} on both plain LB agar and 10 µg/mL CHL LB agar plates.

2.3.2.17. Growth curves of GM *E. coli* strains

All of the desired *E. coli* 5-alpha GM strains were grown overnight in 10 mL Mueller-Hinton broth (MHB, Oxoid, Fisher Scientific). After overnight growth, the cultures were diluted to a 0.5 McFarland standard (OD_{600}: 0.08-0.1) and then further diluted 1:100 to get approximately 1 x 10^6 CFU/mL. Then 20 µL of the diluted cultures were added to a 96-well plate with Bm at a sub-MIC concentration of 2 µg/mL and MHB to make the total volume in the wells 200 µL. Rows were also set up where no Bm were added to the strains and demonstrated normal growth. The plate was then loaded into the FLUOstar Omega plate reader for approximately 16 hours where absorbance readings (OD_{600}) were taken every 4 minutes with 65 cycles and a cycle time of 900 seconds. Shaking was used in orbital mode with a frequency of 100 rpm for 1 second after each cycle. Plate effects were considered, such as uneven heating in the plate reader that can lead to evaporation of liquids from the wells. A clear plate seal was used to ensure evaporation of the media from the wells was minimised, and post-incubation the wells were checked for equal volumes. Plate set up is demonstrated below in Table 4.

Table 4: An outline of the 96-well plate set up for growth curves using the FLUOstar Omega plate reader. Each construct in *E. coli* 5-alpha cells were grown in triplicate (*n* = 3), and Mueller-Hinton broth (MHB) (± sub-minimum inhibitory concentration (MIC)-Bleomycin (Bm) was used as blank controls. The growth curves were done under normal conditions (MHB) and also at 2 µg/mL bleomycin (Bm). Plate effects were taken into consideration, where it is possible that differences can arise in individual wells of the plate due to its position in the plate reader during incubation that can lead to variation in evaporation from the wells leading to unequal volumes which may affect the results of the experiment due to differences in mixing, aeration and concentration of nutrients present. Before and after incubation, all wells were checked for equal volumes and a plate seal was added to limit evaporation from the wells. Plate effects were also controlled for by normalising the construct absorbance readings against the average MHB blank control or average MHB + sub-MIC-Bm blank control, depending on the construct treatment.

	1	2	3	4	5	6	7	8	9	10	11	12
A	GFPuv replicates			mCherry replicates			bla_{NDM-1} replicates			ble_{MBL} replicates		
B	bla_{NDM-1}-ble_{MBL} replicates			mCherry-bla_{NDM-1} replicates			mCherry-ble_{MBL} replicates			mCherry-bla_{NDM-1}-ble_{MBL} replicates		
C	GFPuv-ble_{MBL} replicates			GFPuv-bla_{NDM-1} replicates			GFPuv-bla_{NDM-1}-ble_{MBL} replicates					
D	MHB replicates											
E										MHB + sub-MIC-Bm replicates		
F	GFPuv + sub-MIC-Bm replicates			mCherry + sub-MIC-Bm replicates			bla_{NDM-1} + sub-MIC-Bm replicates			ble_{MBL} + sub-MIC-Bm replicates		
G	bla_{NDM-1}-ble_{MBL} + sub-MIC-Bm replicates			mCherry-bla_{NDM-1} + sub-MIC-Bm replicates			mCherry-ble_{MBL} + sub-MIC-Bm replicates			mCherry-bla_{NDM-1}-ble_{MBL} + sub-MIC-Bm replicates		
H	GFPuv-ble_{MBL} + sub-MIC-Bm replicates			GFPuv-bla_{NDM-1} + sub-MIC-Bm replicates			GFPuv-bla_{NDM-1}-ble_{MBL} + sub-MIC-Bm replicates					

2.3.3. MIC testing of constructs

The MIC of all of the constructs was conducted in *E. coli* 5-alpha against a small panel of antibiotics, consisting of: Bm, MERO, ampicillin, CHL, ciprofloxacin (≥98.0% HPLC, Sigma), gentamicin (sulfate, Sigma Aldrich), nalidixic acid (99.5%, ACROS Organics, ThermoFisher) and TET (hydrochloride powder, Sigma Aldrich). MIC testing was conducted in triplicate in a 96-well plate format. An overnight culture of the constructs was grown from a single colony from a 10 μg/mL CHL selective plate at 37˚C with 180 rpm shaking. After incubation, the cultures were diluted to a 0.5 McFarland standard (equivalent to an OD_{600}: 0.08-0.1) and then further diluted 1:100 before 100 μL was added to each well. Controls were set up containing a 'no bacteria' control that also contained the lowest concentration of antibiotic and a 'no antibiotic' control which consisted of only the diluted bacteria. Concentration ranges of 0.0039-2 μg/mL or 1-512 μg/mL for Bm (depending on the construct being tested), 0.0039-2 μg/mL or 0.125-64 μg/mL for MERO (depending on the construct being tested), 0.0625-32 μg/mL for ampicillin (AMP), CHL, ciprofloxacin (CIP), gentamicin (GENT), nalidixic acid (NA) and TET were used. 100 μL of the antibiotic was used in the serial dilution. The plates were incubated overnight at 37˚C. After the incubation period, 20 μL resazurin sodium salt dissolved in water was added to each well at 0.01% and left to incubate in the dark for 30 minutes before any colour changes were recorded.

Statistical analyses were conducted on the MIC results to determine whether there was a significant difference between the constructs and the resulting susceptibility to the panel of antibiotics. A Kruskal-Wallis test and Dunn's pairwise tests were carried out, adjusted for multiple comparisons using the Bonferroni correction.

2.3.4. Competition/Fitness experiments

Competition experiments were set up in a similar way as the experiments outlined in Webber *et al.* (2015). Briefly, on the first day of the experiment the *E. coli* strains to be competed were grown overnight by taking one colony from an LB agar plate containing 10 μg/mL CHL and inoculating 10 mL LB broth in a 50 mL Falcon tube. An uninoculated 'blank' was also set up with just 10 mL LB broth in a 50 mL Falcon tube to test the media stock for potential contamination. The tubes were incubated for 24 hours at 37˚C with shaking at 180 rpm. After the first day of incubation, six 50 mL Falcon tubes were prepared for each *E. coli* strain that will be used in the competition experiment (total of twelve 50 mL Falcon tubes). 100 μL of the first *E. coli* strain culture was added to each of the six tubes that each contained 10 mL LB broth, and the same was done for the second *E. coli* strain in the competition experiment for the remaining six Falcon tubes. Each competition was done in triplicate. An uninoculated 'blank' was also set up with

these tubes to check for LB broth contamination. The tubes were then incubated for 24 hours at 37˚C with 180 rpm shaking. On the third day, the competition experiments began. The two strains were diluted 200-fold and then mixed together in a new 50 mL Falcon tube. 100 µL of the mixed culture was saved to dilute and plate on LB agar to count an approximate initial frequency of the two bacterial strains present at the start of the competition. 1 mL of the mixed culture was also saved in a 1.5 mL cryogenic vial with 313 µL of 80% glycerol and stored at -80˚C. The mixed cultures were then incubated for 24 hours at 37˚C with 180 rpm shaking. On the final day of the competition experiment, 1 mL of the mixed cultures (after 24 hours incubation) was saved in the -80˚C freezer with 313 µL 80% glycerol. The mixed cultures were then diluted and plated on LB agar in order to determine the final frequencies of each strain after competition.

Depending on the *E. coli* GM strains used in each competition experiment, 10 µg/mL CHL plates were set up for the initial and final counts of bacteria as well as the corresponding antibiotics, for example, if *E. coli* mCherry-*bla*$_{NDM-1}$ was competed against *E. coli* GFPuv-*ble*$_{MBL}$, then MERO and Bm selective plates were set up at a final concentration of 2 µg/mL. Competitions were also set up in the presence of other drugs and antibiotics that have or may have a DNA damaging effect on the bacterial cells. A full list of the competition experiments set up are outlined in Table 5.

Table 5: A summary of all the competition experiments conducted using the different *E. coli* 5-alpha strains that have the desired inserted plasmid. Competitions were conducted in different conditions, such as normal LB (no treatment), at the MIC or double the MIC of different drugs/antibiotics such as mitomycin C (MMC), bleomycin (Bm) and meropenem (MERO). Competitions that are marked with an asterisk (*) were only read using the BD LSRFortessa flow cytometer. Competitions were conducted in triplicate (*n* = 3).

Competition	Treatment
mCherry vs GFPuv	No treatment
	2xMIC MMC
mCherry-*bla*$_{NDM-1}$ vs GFPuv-*bla*$_{NDM-1}$	No treatment
mCherry-*ble*$_{MBL}$ vs GFPuv-*ble*$_{MBL}$	No treatment
mCherry-*bla*$_{NDM-1}$-*ble*$_{MBL}$ vs GFPuv-*bla*$_{NDM-1}$-*ble*$_{MBL}$	No treatment
mCherry-*ble*$_{MBL}$ vs GFPuv-*bla*$_{NDM-1}$	No treatment
mCherry-*bla*$_{NDM-1}$ vs GFPuv-*ble*$_{MBL}$	No treatment
	Sub-MIC MMC
	2xMIC MMC
mCherry-*bla*$_{NDM-1}$ vs GFPuv-*bla*$_{NDM-1}$-*ble*$_{MBL}$	No treatment
	Sub-MIC Bm
	Sub-MIC Mero
	MIC MMC*
mCherry-*ble*$_{MBL}$ vs GFPuv-*bla*$_{NDM-1}$-*ble*$_{MBL}$	No treatment
	Sub-MIC MMC
	2xMIC MMC
mCherry-*bla*$_{NDM-1}$-*ble*$_{MBL}$ vs GFPuv-*bla*$_{NDM-1}$	No treatment
	Sub-MIC Bm
	Sub-MIC Mero
	MIC MMC*

2.3.4.1. Calculating relative bacterial fitness

To determine the relative bacterial fitness of each strain in the competition experiments, the equation below was used (Wiser and Lenski, 2015).

$$Relative\ Fitness = \ln\left(\frac{StrainA_{Final}}{StrainA_{Initial}}\right) \div \ln\left(\frac{StrainB_{Final}}{StrainB_{Initial}}\right)$$

Where StrainA$_{Initial}$ was the initial number of colonies in the first population, StrainA$_{Final}$ was the final number of colonies present after the competition experiment. StrainB$_{Initial}$ was the initial

number of colonies in the second population, StrainB$_{Final}$ was the final number of colonies present after the competition and 'ln' is the natural logarithm. To account for the different fluorescent markers used having different effects on fitness of the bacteria (marker effect), the difference in the mean relative fitness value of GFPuv relative to the mCherry marker under normal LB conditions was subtracted from a of the relative fitness values generated in each competition.

2.3.4.2.   Statistical analysis

To determine whether there was a significant difference between the two strains used in each competition experiment performed on agar plates, Mann-Whitney U tests were used for the relative bacterial fitness values generated.

2.3.4.3.   Flow cytometry

To prepare the freezer stocks of the competition experiments for analysis using the flow cytometer, the cells were washed twice using glycerol, the method used was adapted from Ou *et al*. (2017). The samples were transferred to 1.5 mL Eppendorf tubes and the cells were harvested by centrifuging at 4,300 x*g* for 10 minutes at room temperature. The supernatant was removed before the cell pellet was resuspended in 1 mL of filtered phosphate-buffered saline (PBS). The cells were then washed twice in PBS by centrifuging at 4,300 x*g* for 10 minutes at room temperature and resuspended in 1 mL of filtered PBS. After the second PBS wash, the cells were resuspended in 1 mL PBS and transferred to 5 mL FACS tubes.

The BD LSRFortessa was used to analyse the samples. Initially, filtered PBS was run through the machine on 'high' and threshold set to 1,000 to determine any background debris that may be called as events. Other controls were run to determine the population and set gates for the detection of the GFPuv and mCherry fluorescence. The cultures were overnight cultures of the *E. coli* 5-alpha cells with the genes: GFPuv, mCherry, GFPuv-*bla*$_{NDM-1}$, GFPuv-*ble*$_{MBL}$, GFPuv-*bla*$_{NDM-1}$-*ble*$_{MBL}$, mCherry-*bla*$_{NDM-1}$, mCherry-*ble*$_{MBL}$ and mCherry-*bla*$_{NDM-1}$-*ble*$_{MBL}$. On the flow cytometer, the parameters that were set up included the detection of forward scatter (FSC), side scatter (SSC), PE-Texas Red and Alexa Fluor 488. Samples from the 'before' competition tubes were run on 'fast' mode for the sample flow rate and until 1,000 events had been reached, whereas samples from the 'after' competition tubes were run on 'medium' mode (sample flow rate) until 10,000 events had been reached.

After all the samples had been run, the counts from each experiment were analysed by working out a percentage of GFPuv- and mCherry-labelled cells from the total number of cells (GFPuv and mCherry cells detected). The relative fitness of each of the strains in the different

competition experiments was analysed as done previously in method section 2.3.3.1, and to account for the different fluorescent markers used having different effects on fitness of the bacteria (marker effect), the difference in the mean relative fitness value of mCherry relative to the GFPuv marker under normal LB conditions was subtracted from the relative fitness values generated in each competition.

2.3.4.4. Statistical analysis

To determine whether there was a significant difference between the two strains used in each competition experiment that were analysed using flow cytometry, Mann-Whitney U tests were used for the relative bacterial fitness values generated.

2.3.5. Mutation frequency

The *E. coli* 5-alpha strains that were tested were ones that contained the plasmids: pSTV 29 with no additional genes, pSTV 29 + bla_{NDM-1}, pSTV 29 + ble_{MBL}, pSTV 29 + bla_{NDM-1}-ble_{MBL}. The strains were grown overnight in 10 mL of MHB at 37°C. To ensure that the bacteria were free of pre-existing resistant mutants, 30 μL of the overnight cultures were spread plated on 50 μg/mL of rifampicin (Cayman Chemical Company) and incubated overnight at 37°C. The sample cultures were only used if no colonies grew on the rifampicin selection plates. The sample cultures were diluted to approximately 10^4 before 10 μL was used to inoculate 20 independent 1 mL MHB in 50 mL Falcon tubes. These cultures were then incubated overnight at 37°C with 180 rpm shaking. After incubation, a viable count was conducted on three of the overnight cultures by diluting the cultures $10°$-10^{-6} and plating 100 μL on plain Mueller-Hinton agar (MHA) plates. To determine the number of resistant mutants in the remaining 17 cultures, the cultures were transferred to 1.5 mL Eppendorf tubes before being centrifuged at 16,200 xg for 1 minute. Approximately 900 μL of the supernatant was removed before the cell pellets were resuspended and plated on 50 μg/mL rifampicin selection plates. All of the plates were then incubated overnight at 37°C. After incubation, the colonies present on the plates were counted and the mutation frequency was calculated using the average number of counts from the rifampicin selection plates and dividing by the average viable count from the plain MHA plates. The standard deviation for the mutation frequencies was also calculated alongside the 95% confidence interval.

2.3.5.1. Statistical analysis

To determine whether there was a significant difference in the mutation frequencies of the different *E. coli* constructs, a Kruskal-Wallis test was used.

2.4. Results

2.4.1. The *ble* gene is strongly associated with the *bla*_{NDM} gene

The purpose of the *ble* gene survey was to determine how prevalent the *ble* gene is in the wider environment, by looking at the data available on the NCBI database. A summary of the bla_{NDM} variants that has been found to be associated with the *ble* gene is displayed in Table 6. The *ble* nucleotide sequence used to BLAST against the NCBI database was from *E. coli* (accession number NZ_CM015668.1). Across the different genera from the initial search, the most common bla_{NDM} variants seen that were associated with the *ble* gene were bla_{NDM-1} and bla_{NDM-5}. In some cases, some of the sequences had no bla_{NDM} gene associated with the *ble* gene and some were not properly annotated in the database and were listed simply as a metallo-β-lactamase. From the 989 sequences that were kept for analysis, only 66 (6.67%) sequences had no metallo-β-lactamase present in the sequence.

Table 6: A summary of all NCBI entries that matched the NZ_CM015668.1 *ble* gene reference and the *bla*$_{NDM}$ gene variant found upstream of the *ble* gene. Some sequences had no NDM gene present ('None Annotated') and others had listed a metallo-β-lactamase but could not discern which *bla*$_{NDM}$ ('Unknown NDM').

				NDM															
Group	Total genomes found	None Annotated	Unknown	-1	-2	-3	-4	-5	-6	-7	-9	-12	-13	-14	-16	-17	-20	-21	-29
Acinetobacter	146	9	3	128	3	1	-	1	-	-	-	-	-	1	-	-	-	-	-
Citrobacter	28	-	5	20	-	-	-	3	-	-	-	-	-	-	-	-	-	-	-
Cronobacter	3	-	1	1	-	-	-	-	-	-	1	-	-	-	-	-	-	-	-
Enterobacter	68	2	6	50	-	-	2	6	-	2	-	-	-	-	-	-	-	-	-
Enterobacteriaceae	10	-	-	10	-	-	-	-	-	-	-	-	-	-	-	-	-	-	-
Escherichia	352	24	38	88	-	2	13	153	3	17	6	1	3	-	1	1	1	1	-
Klebsiella	277	23	50	145	-	2	3	42	3	5	3	-	-	-	-	-	-	-	1
Kluyvera	2	-	-	1	-	-	1	-	-	-	-	-	-	-	-	-	-	-	-
Leclerica	2	-	-	2	-	-	-	-	-	-	-	-	-	-	-	-	-	-	-
Morganella	5	-	-	3	-	-	-	2	-	-	-	-	-	-	-	-	-	-	-
Proteus	19	5	2	11	-	-	-	1	-	-	-	-	-	-	-	-	-	-	-
Providencia	31	2	2	27	-	-	-	-	-	-	-	-	-	-	-	-	-	-	-
Pseudomonas	13	-	-	11	-	-	-	2	-	-	-	-	-	-	-	-	-	-	-
Raoultella	9	-	1	7	-	-	-	1	-	-	-	-	-	-	-	-	-	-	-
Salmonella	11	1	-	8	-	-	-	1	-	-	1	-	-	-	-	-	-	-	-
Serratia	7	-	-	7	-	-	-	-	-	-	-	-	-	-	-	-	-	-	-
Stenotrophomonas	2	-	1	1	-	-	-	-	-	-	-	-	-	-	-	-	-	-	-
Vibrio	4	-	-	4	-	-	-	-	-	-	-	-	-	-	-	-	-	-	-

2.4.2. Fluorescent mCherry and GFPuv markers in *E. coli* DH5α are functional

Following confirmation by Sanger sequencing (Source Bioscience) that no sequence errors had been introduced during cloning, *E. coli* DH5α that had the resistance genes bla_{NDM-1}, ble_{MBL} or bla_{NDM-1}-ble_{MBL} inserted into the pSTV 29 plasmid were tested for resistance gene functionality. The results are outlined in Table 7 for imipenem susceptibility (as a result of bla_{NDM-1} gene expression) and Bm susceptibility (as a result of ble_{MBL} gene expression).

To test the functionality of the mCherry and GPuv inserted genes, fluorescence was detected using the FLUOstar plate reader and confocal microscope. From the FLUOstar Omega plate reader the endpoint readings demonstrated that the mCherry and GFPuv fluorescent proteins could be detected and differentiated from each other and also the media used in the experiments, demonstrated in Figure 8 and 9. The mCherry-marked cells produced a lower absorbance value at 584/620 nm than the GFPuv-marked cells at 400-10/510 nm.

Table 7: Tables demonstrating the MIC of the different constructs to imipenem and bleomycin. Two replicates were conducted for each construct (*n* = 2).

Construct (*n* = 2)	Imipenem MIC (range) µg/mL
bla $_{NDM-1}$	64 (32-64)
bla $_{NDM-1}$-*ble* $_{MBL}$	64
pSTV 29 control	0.125
DH5α control	0.125
Construct (*n* =2)	Bleomycin MIC µg/mL
ble $_{MBL}$	>64
bla $_{NDM-1}$-*ble* $_{MBL}$	>64
pSTV 29 control	0.5
DH5α control	0.5
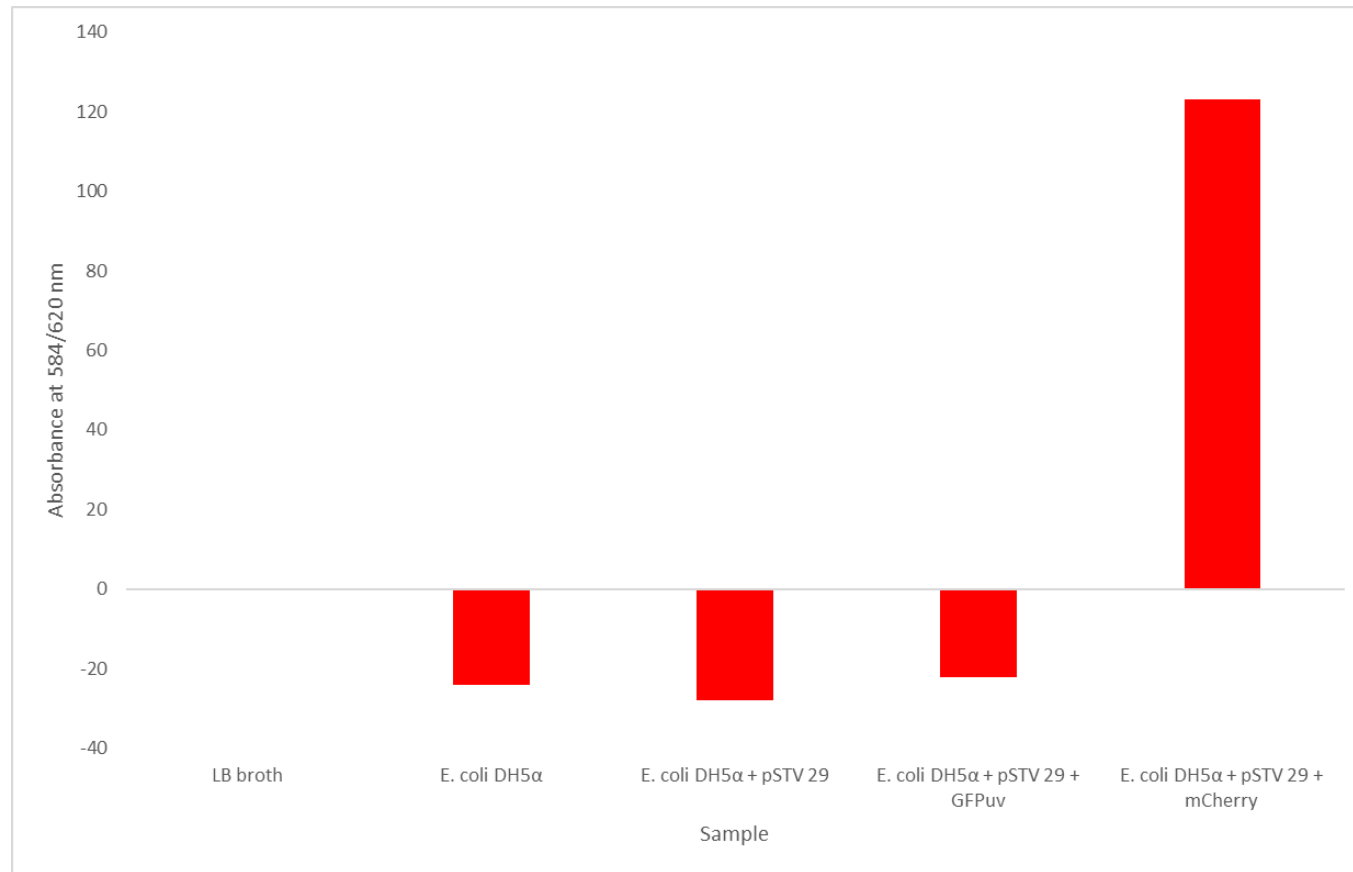
Figure 8: Absorbance of the different *E. coli* DH5α strains to detect the fluorescent protein mCherry (584/620 nm) using the FLUOstar Omega plate reader. LB broth was used as a negative control, as well as the *E. coli* DH5α cells with no pSTV 29 plasmid and *E. coli* DH5α with the pSTV 29 plasmid without fluorescent markers. One replicate was conducted for each strain (*n* = 1).
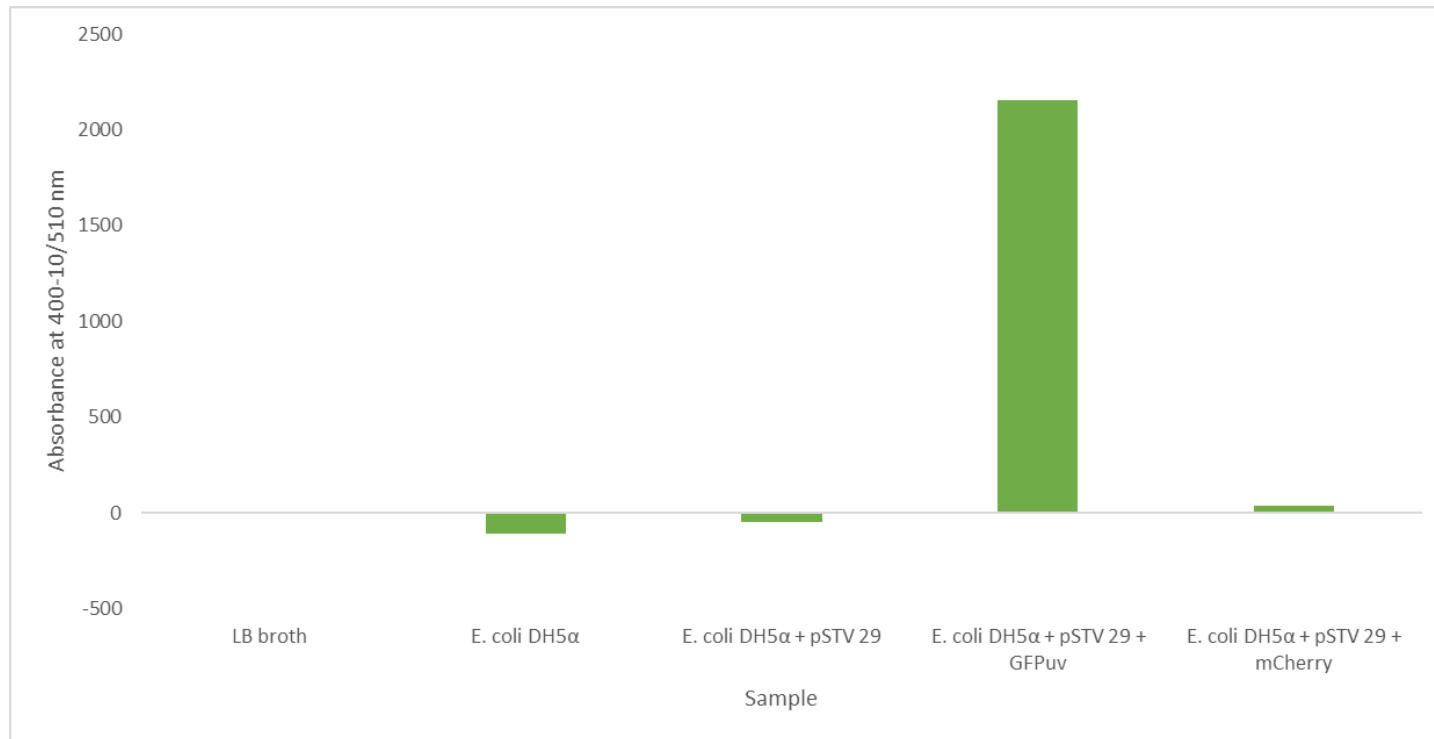
Figure 9: Absorbance of the different *E. coli* DH5α strains to detect the fluorescent protein GFPuv (400-10/510 nm) using the FLUOstar Omega plate reader. LB broth was used as a negative control, as well as the *E. coli* DH5α cells with no pSTV 29 plasmid and *E. coli* DH5α with the pSTV 29 plasmid without fluorescent markers. One replicate was conducted for each strain (n = 1).

56

Using confocal microscopy, slides containing *E. coli* DH5α with either the mCherry or GFPuv fluorescent protein were viewed to confirm that the proteins were functional, displayed in Figure 10. When the cells were viewed using a confocal microscope, there appeared to be no real difference (visually) in the fluorescent brightness of the cells regardless of whether they were marked with mCherry or GFPuv.
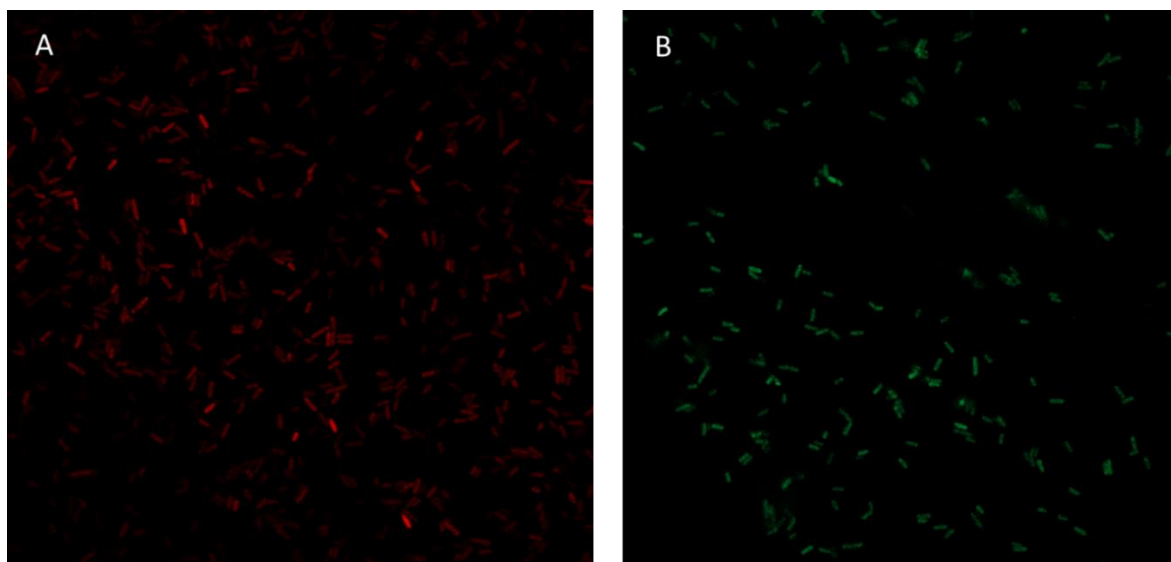
Figure 10: Images from the Zeiss LSM 800 confocal microscope using the 63X water lens. Picture A demonstrates the *E. coli* DH5α cells that contain the pSTV 29 plasmid with the mCherry gene inserted. Picture B demonstrates the *E. coli* DH5α cells that contain the pSTV 29 plasmid with the GFPuv gene inserted.

2.4.3. Functional *E. coli* DH5α with the desired *bla*$_{NDM-1}$, *ble*$_{MBL}$ or *bla*$_{NDM-1}$-*ble*$_{MBL}$ inserted

In the second round of gene cloning and Gibson Assembly, the GFPuv gene was inserted into the pSTV 29 plasmids containing either the *bla*$_{NDM-1}$, *ble*$_{MBL}$ or *bla*$_{NDM-1}$-*ble*$_{MBL}$ gene. The previous mCherry constructs described above were digested before the insertion of the *bla*$_{NDM-1}$, *ble*$_{MBL}$ and *bla*$_{NDM-1}$-*ble*$_{MBL}$ genes. All transformants were tested for functionality of the resistance genes and the results of the screen are demonstrated in Table 8. The results of the functionality testing demonstrated that on MERO agar plates, the inserted genes were not expressing the desired functional protein as expected. This was demonstrated by the mCherry-*bla*$_{NDM-1}$ and mCherry-*bla*$_{NDM-1}$-*ble*$_{MBL}$ constructs in *E. coli* showing no growth on 10 µg/mL MERO agar. Only one of the mCherry-*ble*$_{MBL}$ constructs in *E. coli* demonstrated growth on 2 µg/mL Bm agar. The GFPuv-labelled constructs in *E. coli* performed as expected on the selective agar plates, where the

GFPuv-bla_{NDM-1} constructs in *E. coli* grew on 10 µg/mL MERO and the GFPuv-ble_{MBL} constructs in *E. coli* grew on 2 µg/mL Bm.

Table 8: Functionality of the inserted desired genes into the pSTV 29 plasmid transformed into *E. coli* DH5α cells. Functionality of the bla_{NDM-1} gene was determined by growth on an agar plate containing 10 µg/mL meropenem (MERO) and functionality of the ble_{MBL} gene was determined by growth on an agar plate containing 2 µg/mL bleomycin (Bm). *E. coli* DH5α was used as a no growth control, as well as *E. coli* containing either the bla_{NDM-1} or ble_{MBL} inserted gene (positive controls) (n = 3).

Construct in *E. coli* DH5α	Growth on 10 µg/mL MERO	Growth on 2 µg/mL Bm
DH5α control	No growth	No growth
bla_{NDM-1} (positive) control	Growth	No growth
ble_{MBL} (positive) control	No growth	Growth
mCherry-bla_{NDM-1} replicate 1	No growth	Growth
mCherry-bla_{NDM-1} replicate 2	No growth	Growth
mCherry-bla_{NDM-1} replicate 3	No growth	No growth
mCherry-ble_{MBL} replicate 1	No growth	No growth
mCherry-ble_{MBL} replicate 2	No growth	Growth
mCherry-ble_{MBL} replicate 3	No growth	No growth
mCherry-bla_{NDM-1}-ble_{MBL} replicate 1	No growth	No growth
mCherry-bla_{NDM-1}-ble_{MBL} replicate 2	No growth	No growth
mCherry-bla_{NDM-1}-ble_{MBL} replicate 3	No growth	No growth
GFPuv-bla_{NDM-1} replicate 1	Growth	No growth
GFPuv-bla_{NDM-1} replicate 2	Growth	No growth
GFPuv-bla_{NDM-1} replicate 3	Growth	No growth
GFPuv-ble_{MBL} replicate 1	No growth	Growth
GFPuv-ble_{MBL} replicate 2	No growth	Growth

2.4.3.1. *E. coli* **DH5α strains fluorescence viewed by confocal microscopy and microplate reader**

After functionality testing, it was decided that there were issues with the synthesised bla_{NDM-1}-ble_{MBL} gene string, rather than issues with bacterial transformation, as the other constructs were being generated and were producing functional proteins as expected. The issues seen with the bla_{NDM-1}-ble_{MBL} gene sequence were ultimately due to manufacturer's error, and once the correct synthesised gene was sent and used, there were no further issues found with the functionality of the bla_{NDM-1}-ble_{MBL} synthesised gene string.

Sanger sequencing confirmed that the final constructs that were inserted into the *E. coli* had no mutations in the gene sequences and were true to the gene sequences that were synthesised. The final constructs generated are displayed in Figure 11a and Figure 11b. The final constructs were tested to determine whether the inserted resistance genes were functioning normally in the *E. coli* 5-alpha cells. For ease of testing the resistance genes (ble_{MBL} and/or bla_{NDM-1}), the final constructs were dot plated on MHA plates supplemented with either 2 µg/mL Bm or 10 µg/mL MERO. Colonies that demonstrated growth at these selective concentrations were used in the final competition experiments. The final *E. coli* DH5α strains containing the desired genes on the pSTV 29 plasmid were viewed again using the Zeiss LSM 800 confocal microscope and also viewed in a 96-well plate in the FLUOstar Omega microplate reader (Figure 12 and 13). This confirmed all strains were still expressing either the mCherry or GFPuv marker genes.

pSTV29
2999 bp

pSTV 29-mCherry-blaNDM-1
4863 bp

pSTV 29-mCherry-bleMBL
4580 bp

pSTV 29-mCherry-blaNDM-1-bleMBL
5396 bp
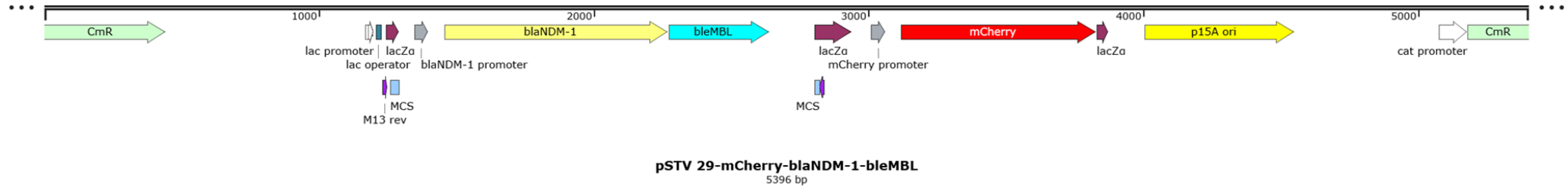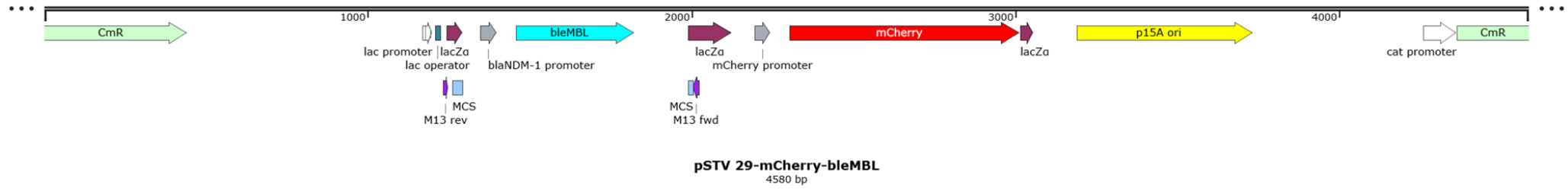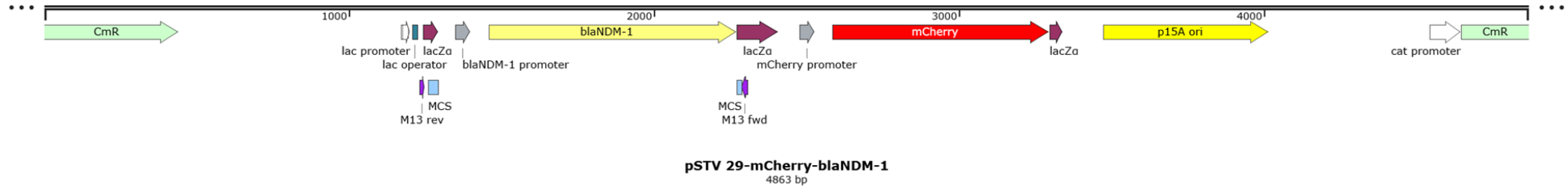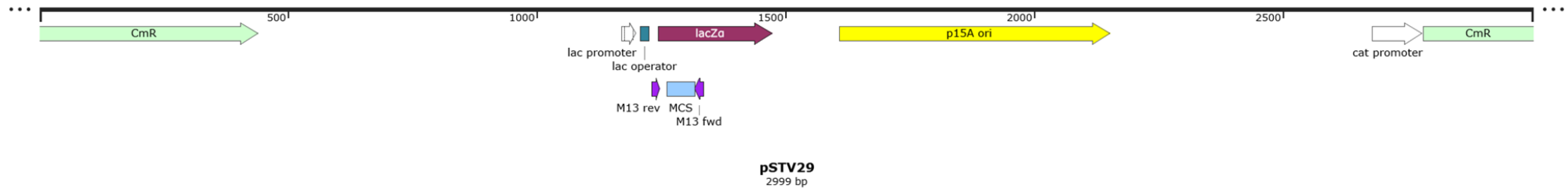
Figure 11a: The final mCherry constructs generated. The top sequence demonstrates the empty pSTV 29 plasmid used. The desired genes were inserted into the pSTV 29 plasmid and then transformed into *E. coli* 5-alpha strain. For each strain, the mCherry fluorescent marker was inserted, and then a combination of either the bla_{NDM-1}, the ble_{MBL} gene or both. Figure created using SnapGenev6.1.1. The distance between bla_{NDM-1} promoter and the bla_{NDM-1} gene is 62 bp. When the ble_{MBL} gene is associated with the bla_{NDM-1} gene, the distance between the bla_{NDM-1} promoter and ble_{MBL} is 878 bp, when ble_{MBL} is not associated with bla_{NDM-1} the distance between the bla_{NDM-1} promoter and ble_{MBL} is 62 bp. The distance between the bla_{NDM-1} promoter and the mCherry gene varies depending on the construct and is 1,189 bp (mCherry-bla_{NDM-1} construct), 906 bp (mCherry-ble_{MBL} construct) and 1,722 bp (mCherry-bla_{NDM-1}-ble_{MBL} construct). The distance between the mCherry promoter and the mCherry gene is always 60 bp. The distance between the mCherry promoter and the bla_{NDM-1} gene is 3,796 bp(mCherry-bla_{NDM-1} construct and mCherry-bla_{NDM-1}-ble_{MBL} construct). The distance between the mCherry promoter and the ble_{MBL} gene varies depending on the construct, where it is 3,796 bp (mCherry-ble_{MBL}) and 4,612 bp (mCherry-bla_{NDM-1}-ble_{MBL}). The bla_{NDM-1} and mCherry promoters are not fully characterised but they were identified using the Berkeley Drosophila Genome Project, Neural Network Promoter Prediction (Reese, 2001).
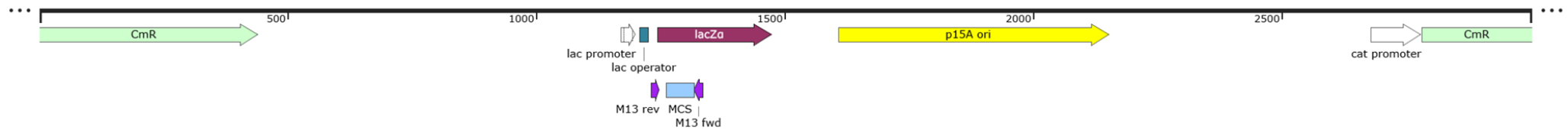
pSTV29
2999 bp
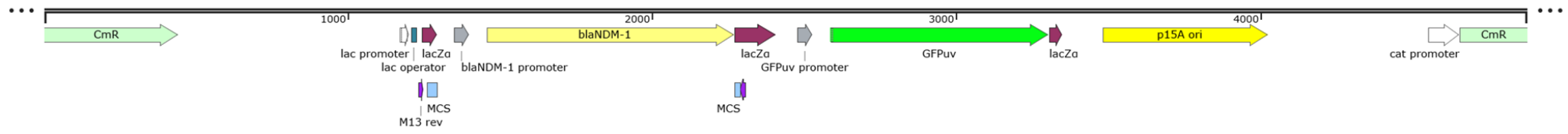
pSTV 29-GFPuv-blaNDM-1
4872 bp
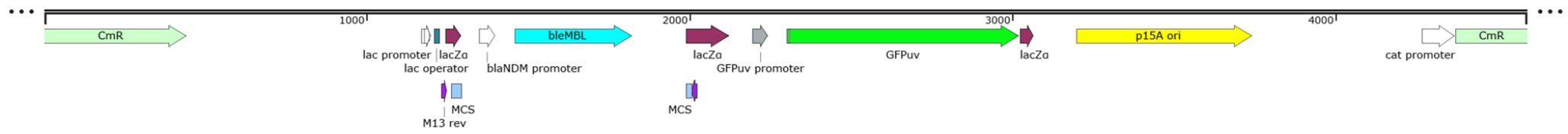
pSTV 29-GFPuv-bleMBL
4589 bp
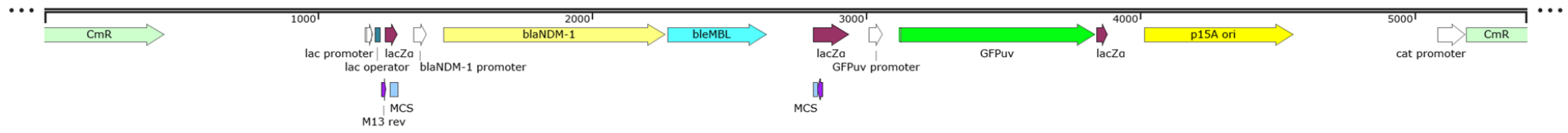
pSTV 29-GFPuv-blaNDM-1-bleMBL
5405 bp

Figure 11b: The final GFPuv constructs generated. The top sequence demonstrates the empty pSTV 29 plasmid used. The desired genes were inserted into the pSTV 29 plasmid and then transformed into *E. coli* 5-alpha strain. For each strain, the GFPuv fluorescent marker was inserted, and then a combination of either the bla_{NDM-1}, the ble_{MBL} gene or both. Figure created using SnapGene v6.1.1. The distance between the bla_{NDM-1} promoter and the bla_{NDM-1} gene is 62 bp. When the ble_{MBL} gene is associated with the bla_{NDM-1} gene, the distance between the bla_{NDM-1} promoter and the ble_{MBL} gene is 878 bp, when ble_{MBL} is not associated with bla_{NDM-1}, the distance from the bla_{NDM-1} promoter to ble_{MBL} is 62 bp. The distance between the bla_{NDM-1} promoter and the GFPuv gene varies depending on the construct: 1,189 bp (GFPuv-bla_{NDM-1}), 906 bp (GFPuv-ble_{MBL}) and 1,722 bp (GFPuv-bla_{NDM-1}-ble_{MBL}). The distance between the GFPuv promoter and the GFPuv gene is always 60 bp. The distance between the GFPuv promoter and the bla_{NDM-1} gene is 3,805 bp (for both GFPuv-bla_{NDM-1} and GFPuv-bla_{NDM-1}-ble_{MBL} constructs). The distance between the GFPuv promoter and the ble_{MBL} gene varies depending on the construct: 3,805 bp (GFPuv-ble_{MBL} construct) and 4,621 bp (GFPuv-bla_{NDM-1}-ble_{MBL} construct). The bla_{NDM-1} and GFPuv promoters are not fully characterised but they were identified using the Berkeley Drosophila Genome Project, Neural Network Promoter Prediction (Reese, 2001).
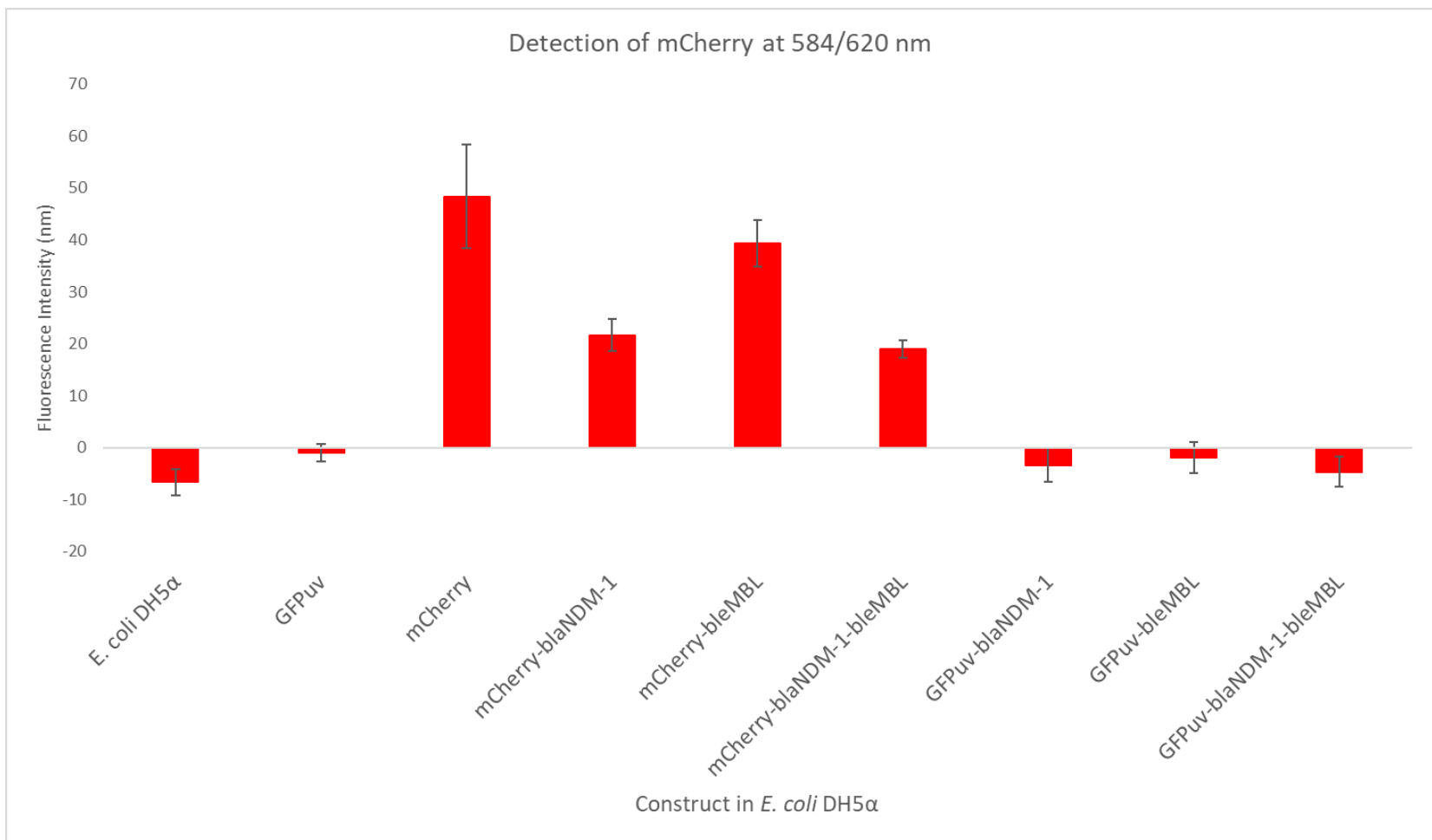
Figure 12: Fluorescence of the different *E. coli* DH5α strains with the pSTV 29 plasmid containing different desired synthesised genes. Fluorescence intensity was detected at 584/620 nm for mCherry detection. Standard deviation error bars are plotted (*n* = 3).
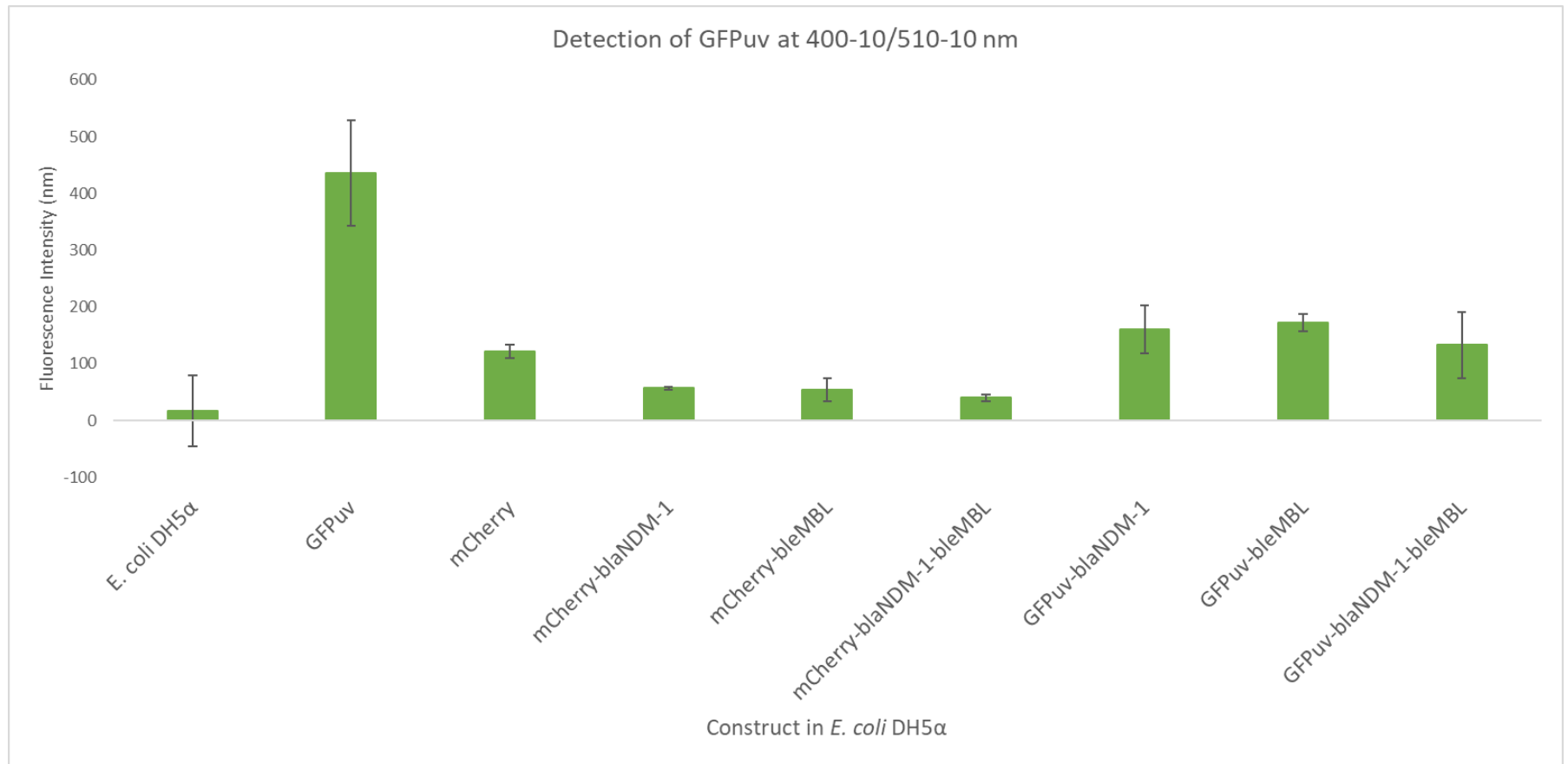
Figure 13: Fluorescence of the different *E. coli* DH5α strains with the pSTV 29 plasmid containing different desired synthesised genes. Fluorescence intensity was detected at 400-10/510-10 nm for GFPuv detection. Standard deviation error bars are plotted (*n* = 3)

2.4.3.2. Stability of genetically modified *E. coli* 5-alpha strains

The final constructs were all transformed into *E. coli* 5-alpha to ensure that the plasmids were being expressed in the same *E. coli* host. The different *E. coli* 5-alpha strains containing a marker gene (either mCherry or GFPuv) and any combination of the bla_{NDM-1} and ble_{MBL} gene were passaged over 4 days with no selective antibiotic to determine whether the plasmids were stable in the bacterial host. All of the strains (mCherry, GFPuv, mCherry-bla_{NDM-1}, mCherry-ble_{MBL}, mCherry-bla_{NDM-1}-ble_{MBL}, GFPuv-bla_{NDM-1}, GFPuv-ble_{MBL} and GFPuv-bla_{NDM-1}-ble_{MBL}) showed growth on 10 µg/mL CHL plates after 4 days of passage in LB media with no selection agent, demonstrating that the pSTV 29 plasmid is stably maintained.

2.4.4. Growth of the *E. coli* 5-alpha strains

Each of the constructed strains in *E. coli* 5-alpha were grown in MHB and also in the presence of Bm. The strains were grown in MHB in order to determine what normal growth looked like for each of the strains when there was no external stressor. The strains were also grown in sub-MIC Bm in order to determine whether the growth of the strains was affected by Bm, and whether the genes inserted (bla_{NDM-1}, ble_{MBL} or bla_{NDM-1}-ble_{MBL}) altered the growth of the organism in the presence of Bm. When comparing all of the constructs that contained the mCherry marker gene, there appeared to be no difference between the growth rate of all of the strains, but it did appear that the mCherry-ble_{MBL} *E. coli* 5-alpha strain had a slightly slower growth rate than the other mCherry strains. However, due to the variability between the strains, it is difficult to say for certain (Figure 14). For the GFPuv marker gene, there appeared to be no difference between the growth rate of all the strains, but there was a lot of variability when the GFPuv-marked *E. coli* 5-alpha strain was grown on its own. The GFPuv-ble_{MBL} *E. coli* 5-alpha strain also demonstrated slightly slower growth, but due to the variability between the three replicates, it is difficult to determine for certain (Figure 15). For ease of viewing, the GFPuv only marked *E. coli* 5-alpha strain has been removed from the growth curve graph due to the high variation seen between the replicates (Figure 16). When the mCherry constructs were exposed to a sub-MIC concentration of Bm, only those carrying the ble_{MBL} grew (Figure 17). The same was true with the GFPuv constructs except that the GFPuv-bla_{NDM-1}-ble_{MBL} *E. coli* 5-alpha strain had a lower maximum OD_{600} absorbance value (Figure 18).
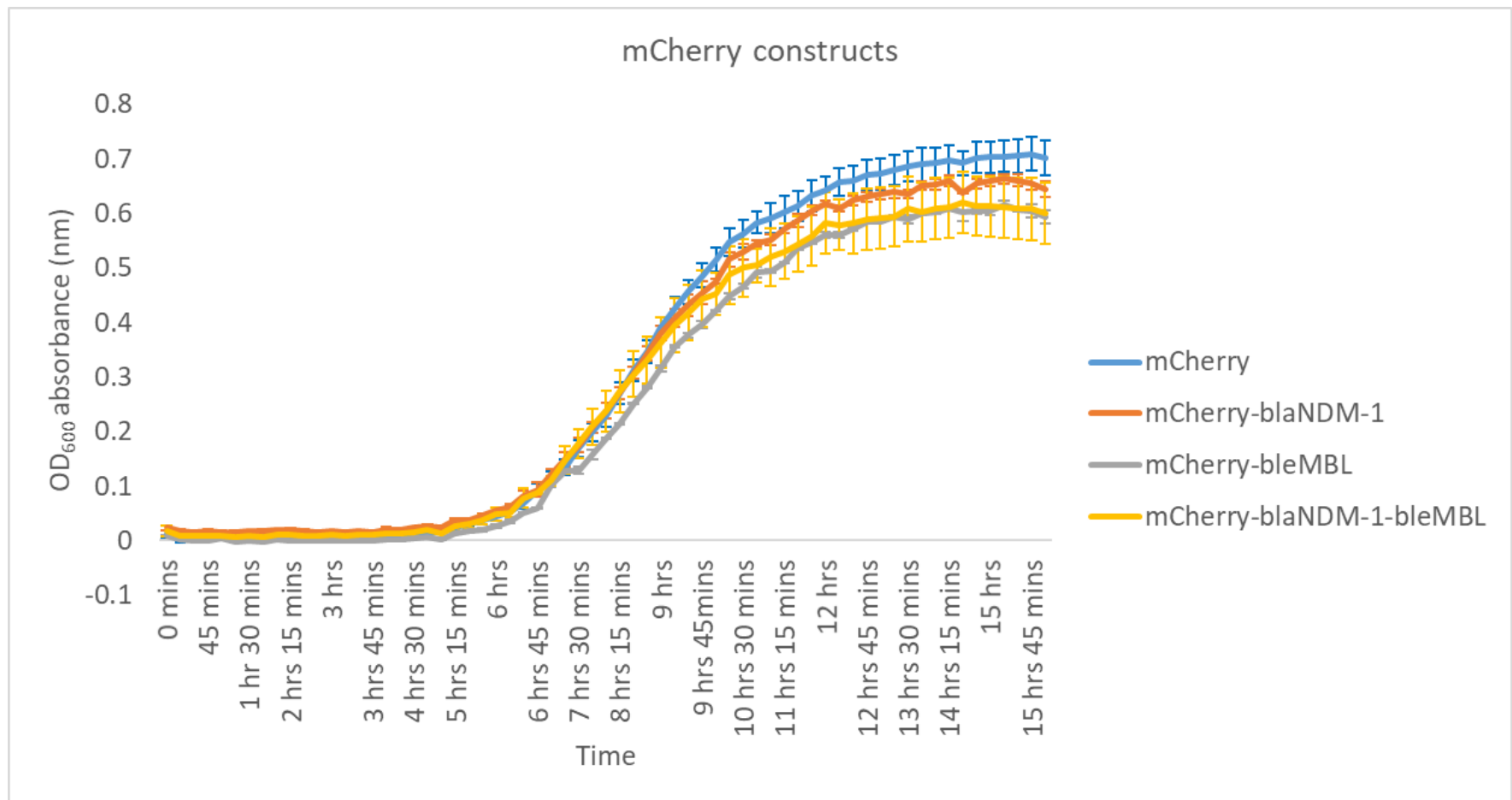
Figure 14: Growth curve of *E. coli* 5-alpha strains with the desired genes inserted with the mCherry fluorescent marker. Absorbance was read at an optical density (OD) of 600 nm and the growth curve was recorded over 16 hours. Standard error of the mean (SEM) bars are plotted (*n* = 3).
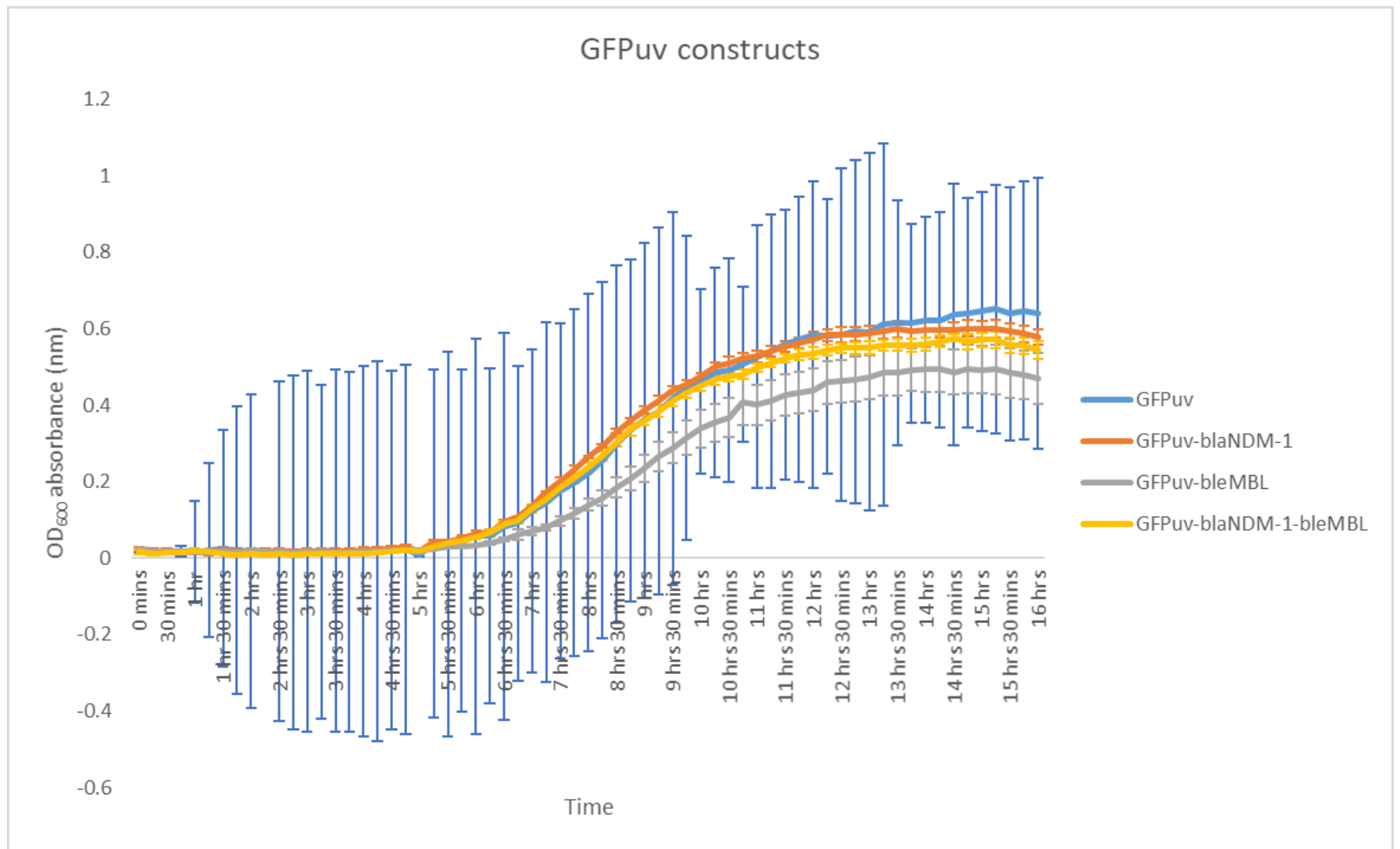
Figure 15: Growth curves of the *E. coli* 5-alpha strains that are marked with GFPuv fluorescent gene and the desired genes inserted into the pSTV 29 plasmid. Absorbance was recorded at an optical density (OD) at 600 nm and the growth curves were measured over 16 hours. Standard error of the mean (SEM) bars are plotted (*n* = 3).
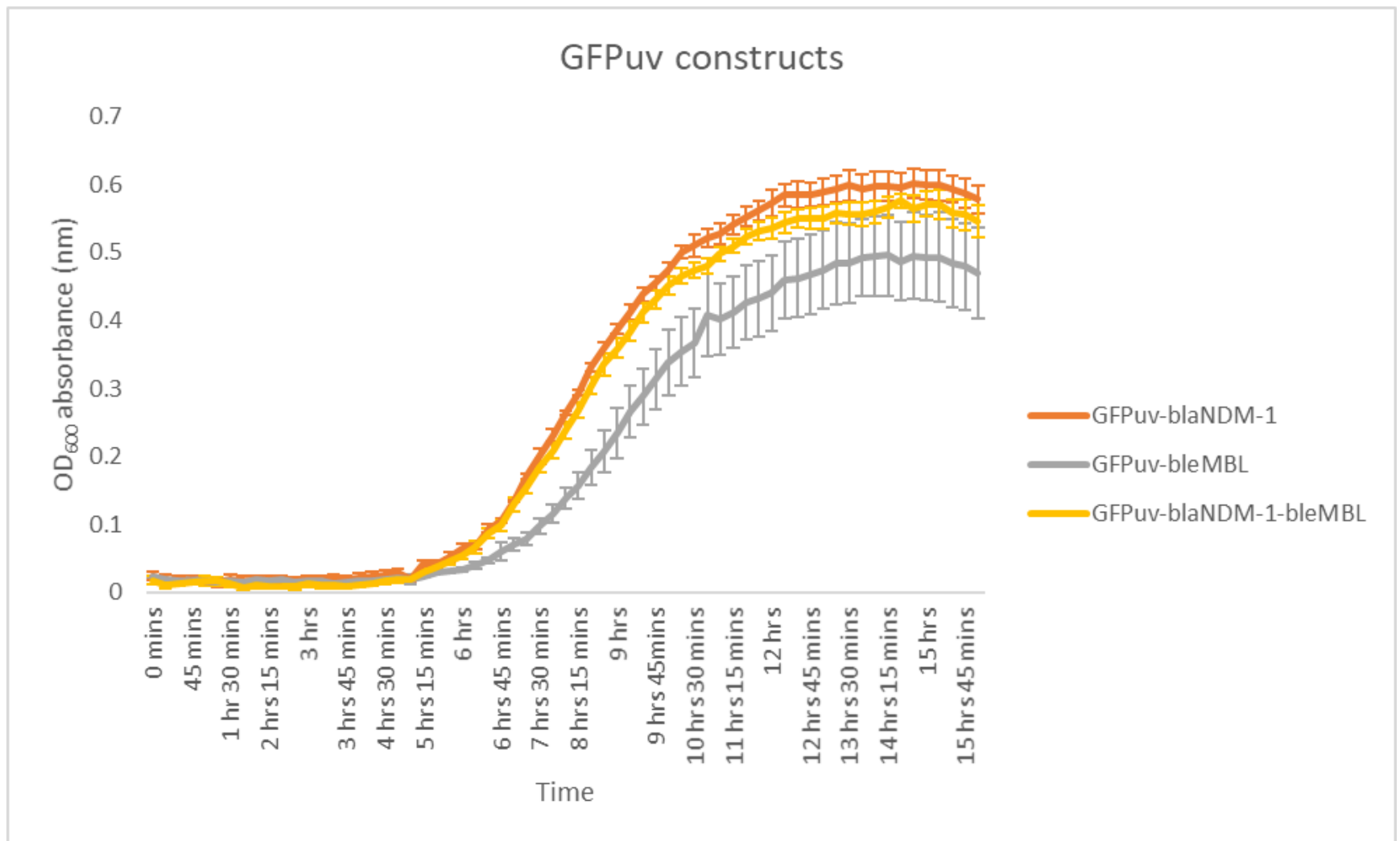
Figure 16: Growth curves of the *E. coli* 5-alpha strains that are marked with the GFPuv fluorescent gene and the desired genes inserted into the pSTV 29 plasmid. The GFPuv control *E. coli* 5-alpha strain was removed due to the high variability between replicates. Absorbance was recorded at an optical density (OD) of 600 nm over 16 hours. Standard error of the mean (SEM) bars are plotted (*n* = 3).
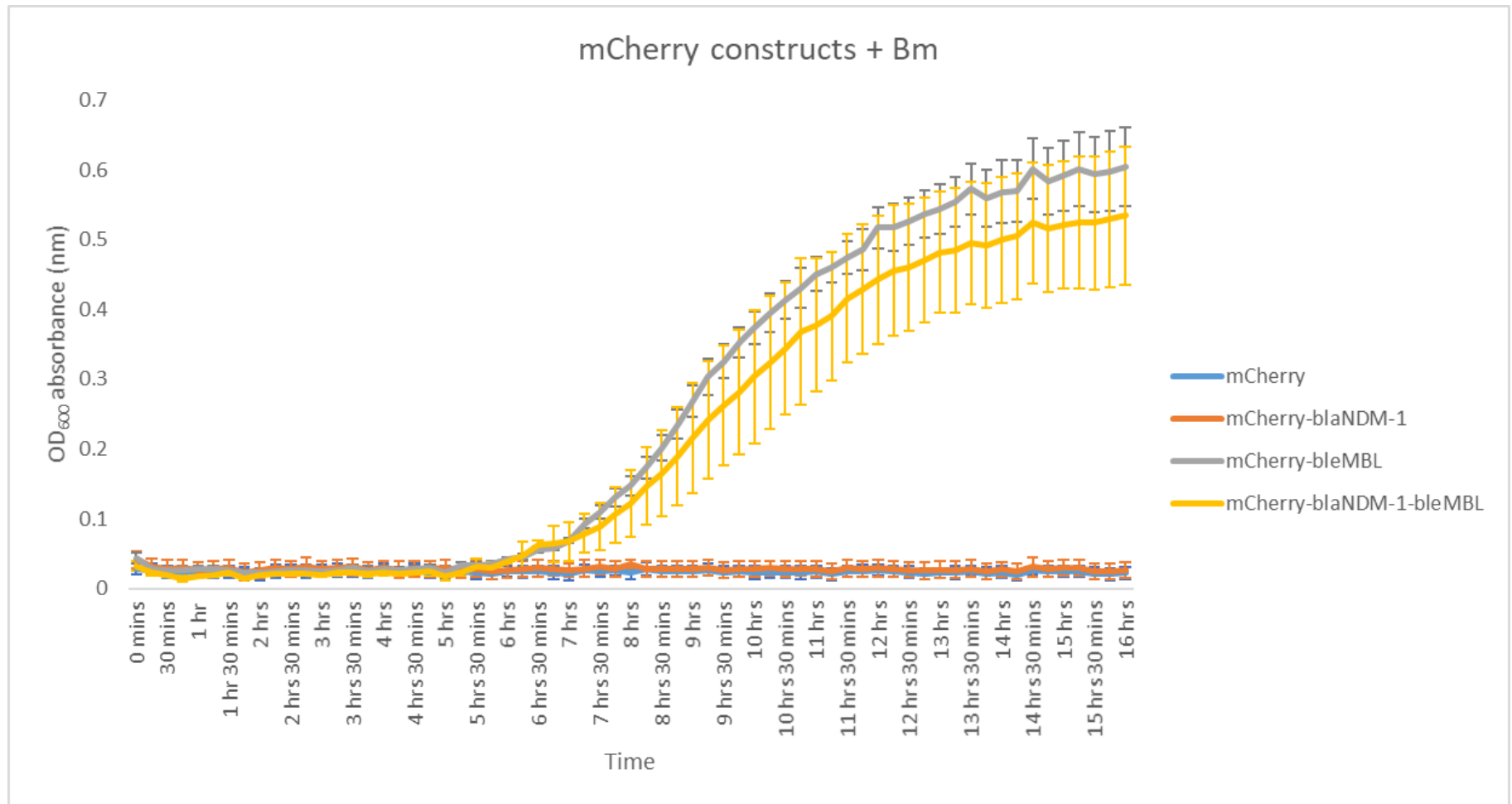
Figure 17: Growth curves of the mCherry labelled *E. coli* 5-alpha strains with different desired genes inserted into the pSTV 29 plasmid in the presence of 2 μg/mL bleomycin (Bm). Absorbance was recorded using an optical density (OD) of 600 nm over 16 hours. Standard error of the mean bars are plotted (*n* = 3).
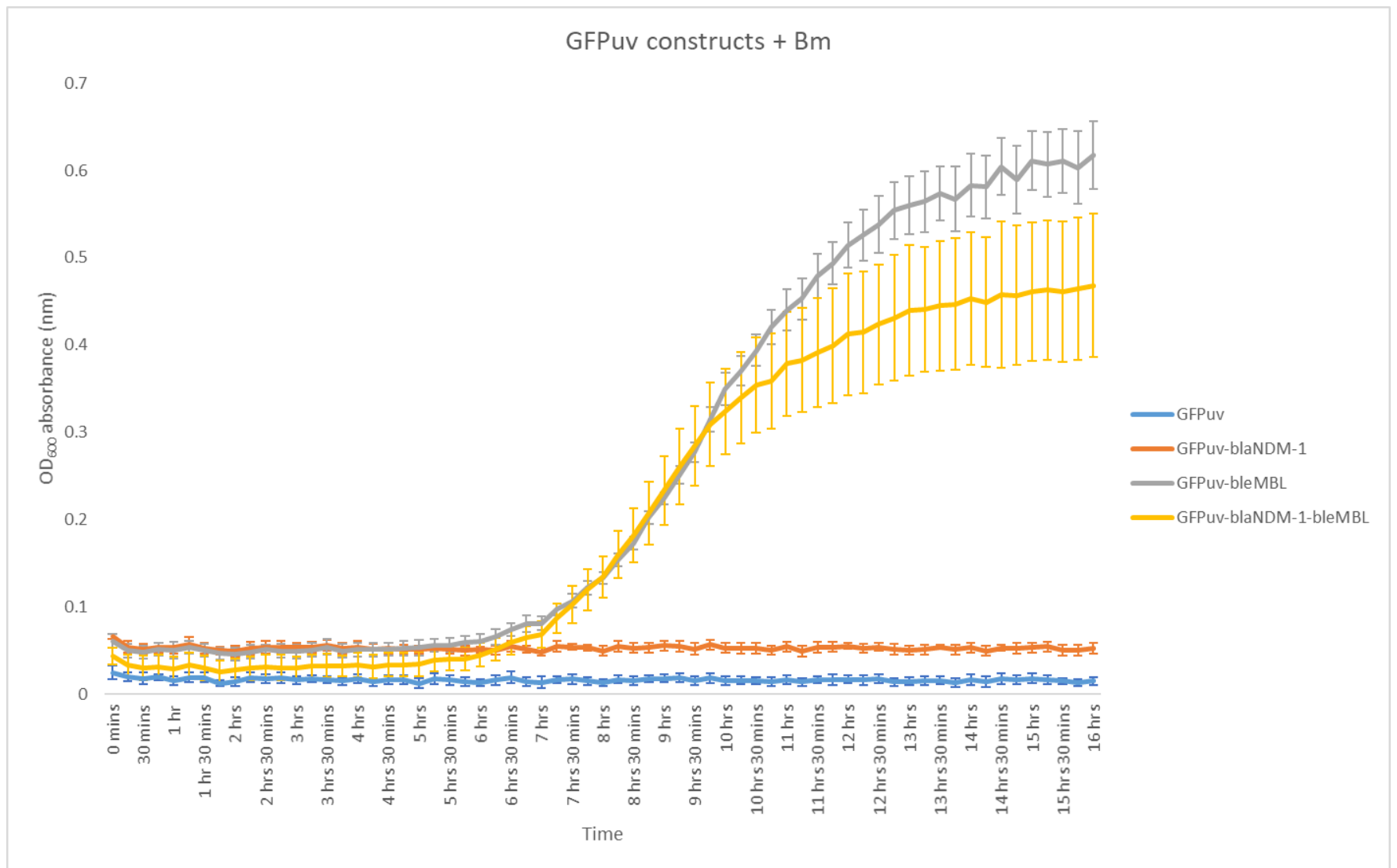
Figure 18: Growth curves of the GFPuv-labelled *E. coli* 5-alpha strains with the different desired genes inserted into the pSTV 29 plasmid. Absorbance values were recorded using an optical density (OD) of 600 nm over 16 hours. Standard error of the mean (SEM) bars are plotted (*n* = 3).

Overall, these experiments have demonstrated that the *E. coli* 5-alpha strains generated with the different combinations of marker gene (mCherry or GFPuv) and the desired antibiotic resistance genes (bla_{NDM-1} and ble_{MBL}) are being expressed and produce functional proteins. These experiments have also demonstrated that the inserted pSTV 29 plasmid is stable in *E. coli* 5-alpha, regardless of the genes we inserted on the plasmid. Under normal MHB conditions, the different *E. coli* 5-alpha strains showed little difference in their ability to grow, whereas when the cells were treated with sub-MIC Bm it looked as if the cells that carry bla_{NDM-1}-ble_{MBL} (with either mCherry or GFPuv as the fluorescent marker) had more difficulty growing than the cells that carry just the ble_{MBL} gene.

2.4.5. Antibiotic susceptibility of the *E. coli* 5-alpha strains

The different constructs were tested for their antibiotic susceptibilities to a small panel of drugs (Bm, MERO, AMP, CHL, CIP, GENT, NA and TET) (Table 9). All of the constructs showed similar antibiotic susceptibility profiles, except against Bm, MERO and AMP. The purpose of these experiments was to determine whether the expression of the bla_{NDM-1} and ble_{MBL} genes provided the *E. coli* 5-alpha strain with a reduced susceptibility to different classes of antibiotics. From the antibiotic susceptibility testing of the *E. coli* 5-alpha strains that were created, we can see that against the antibiotic Bm, the strains that have the ble_{MBL} resistance gene have a higher MIC than the normal 5-alpha *E. coli* host. However, there is a slight difference between the strains that have been transformed with just the ble_{MBL} gene or have the bla_{NDM-1} gene associated with it, where the bla_{NDM-1}-ble_{MBL} strain has an MIC of 64 µg/mL and the ble_{MBL} only strains have an MIC that is above the tested range of 512 µg/mL of Bm.

When the strains were tested against the antibiotic MERO, we don't see a huge exaggeration in the difference between solely having the bla_{NDM-1} gene or bla_{NDM-1}-ble_{MBL}. What is interesting to note, is that the mCherry-bla_{NDM-1} 5-alpha strain has an MIC of 1 µg/mL, whereas the mCherry-bla_{NDM-1}-ble_{MBL} and GFPuv-bla_{NDM-1} 5-alpha strains had an MIC of 4 µg/mL, and the GFPuv-bla_{NDM-1}-ble_{MBL} 5-alpha strain had an MIC of 8 µg/mL against MERO. MIC values against the antibiotic CHL were as expected, as the plasmid used in this study (pSTV 29) had a CHL selective marker on the plasmid.

Table 9: The minimum inhibitory concentration (MIC) of the different *E. coli* 5-alpha strains using different antibiotics. The *E. coli* 5-alpha strains have different marker genes inserted (mCherry or GFPuv) and different desired genes (bla_{NDM-1}, ble_{MBL} and bla_{NDM-1}-ble_{MBL}). Antibiotics marked with 'N/A' were not conducted for that strain (n = 3).

Strain	MIC (µg/mL)							
	Bleomycin	Meropenem	Ampicillin	Chloramphenicol	Ciprofloxacin	Gentamicin	Nalidixic Acid	Tetracycline
E. coli 5-alpha	0.0625	0.0156	4	2	<0.0625	0.5	32	0.5
E. coli 5-alpha + GFPuv	N/A	N/A	4	>64	<0.0625	0.5	32	0.5
E. coli 5-alpha + mCherry	N/A	N/A	4	>64	<0.0625	0.5	32	0.5
E. coli 5-alpha + mCherry-*bla* $_{NDM-1}$	0.0625	1	>64	>64	<0.0625	0.5	32	0.5
E. coli 5-alpha + mCherry-*ble* $_{MBL}$	>512	0.0156	4	>64	<0.0625	0.5	32	0.25
E. coli 5-alpha + mCherry-*bla* $_{NDM-1}$-*ble* $_{MBL}$	64	4	>64	>64	2	0.5	32	0.25
E. coli 5-alpha + GFPuv-*bla* $_{NDM-1}$	0.0625	4	>64	>64	1	0.5	32	0.25
E. coli 5-alpha + GFPuv-*ble* $_{MBL}$	>512	0.0156	4	>64	2	0.5	32	0.25
E. coli 5-alpha + GFPuv-*bla* $_{NDM-1}$-*ble* $_{MBL}$	64	8	>64	>64	<0.0625	0.5	32	0.25

2.4.6. Competition experiments

Competition experiments were conducted to determine whether the carriage of the ble_{MBL} gene with the bla_{NDM-1} gene conferred a fitness advantage to the *E. coli* 5-alpha strain, under normal conditions and also chemotherapeutic stress. In these experiments, sub-MIC Bm, sub-MIC MERO and MMC were used as stressors. MMC was included for its ability to cause ssDNA breaks, and past literature have hypothesised that the presence of the ble_{MBL} gene or the expressed protein is able to reduce damage to the DNA, which may explain its high prevalence in *Enterobacteriaceae*. The following competitions were conducted on agar plates in *E. coli* 5-alpha cells: mCherry vs GFPuv in LB broth and 2xMIC of MMC, mCherry-bla_{NDM-1} vs GFPuv-bla_{NDM-1} in LB, mCherry-ble_{MBL} vs GFPuv-ble_{MBL} in LB, mCherry-bla_{NDM-1}-ble_{MBL} vs GFPuv-bla_{NDM-1}-ble_{MBL} in LB, mCherry-bla_{NDM-1} vs GFPuv-bla_{NDM-1}-ble_{MBL} (in LB, sub-MIC Bm and sub-MIC MERO), mCherry-ble_{MBL} vs GFPuv-bla_{NDM-1}-ble_{MBL} (in LB, sub-MIC MMC and 2xMIC MMC) and mCherry-bla_{NDM-1}-ble_{MBL} vs GFPuv-bla_{NDM-1} (in LB, sub-MIC Bm and sub-MIC MERO).

In the bar charts generated from the competition experiments that were conducted using plate counts, it looks as if certain competitions have one strain that is more fit than the other when we look at the plotted average relative fitness values (Figures 19-36). However, when the relative fitness values were statistically analysed, all of the competition experiments showed no significant difference when the exact significance value was calculated ($P > 0.05$) (Table 10).
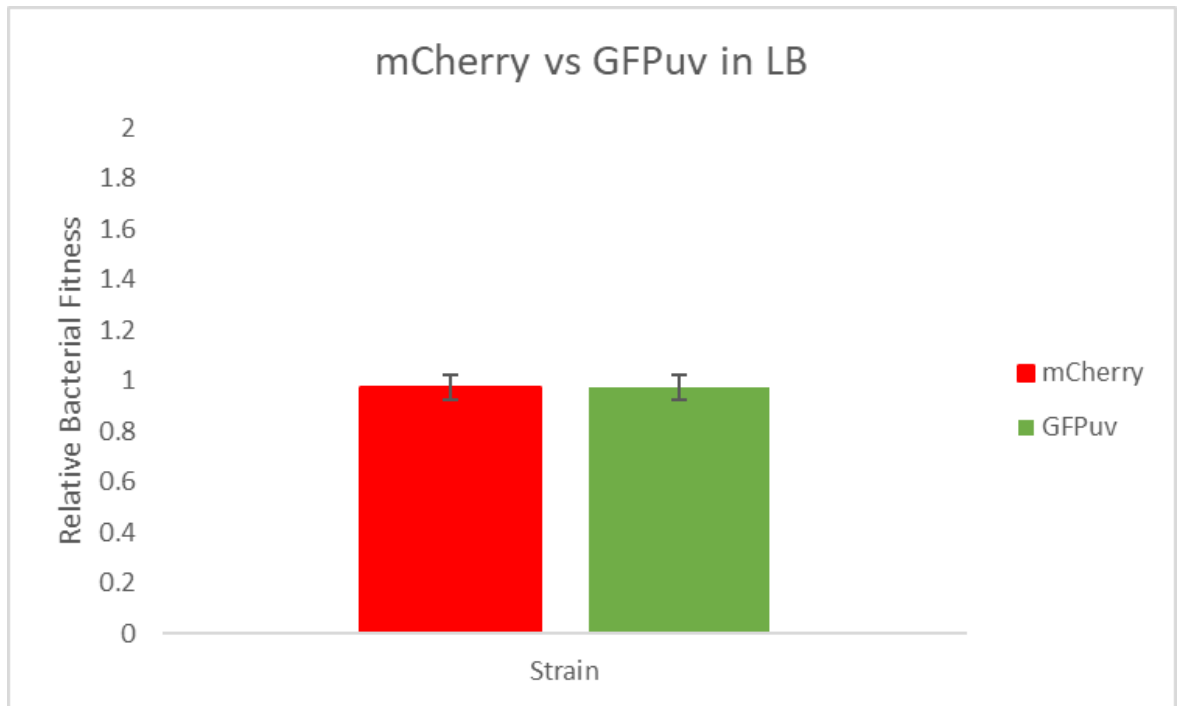
Figure 19: The relative bacterial fitness of the *E. coli* 5-alpha strain marked with either the mCherry (red) or GFPuv (green) fluorescent protein in normal LB. The 95% confidence interval is plotted for each strain (*n* = 3).
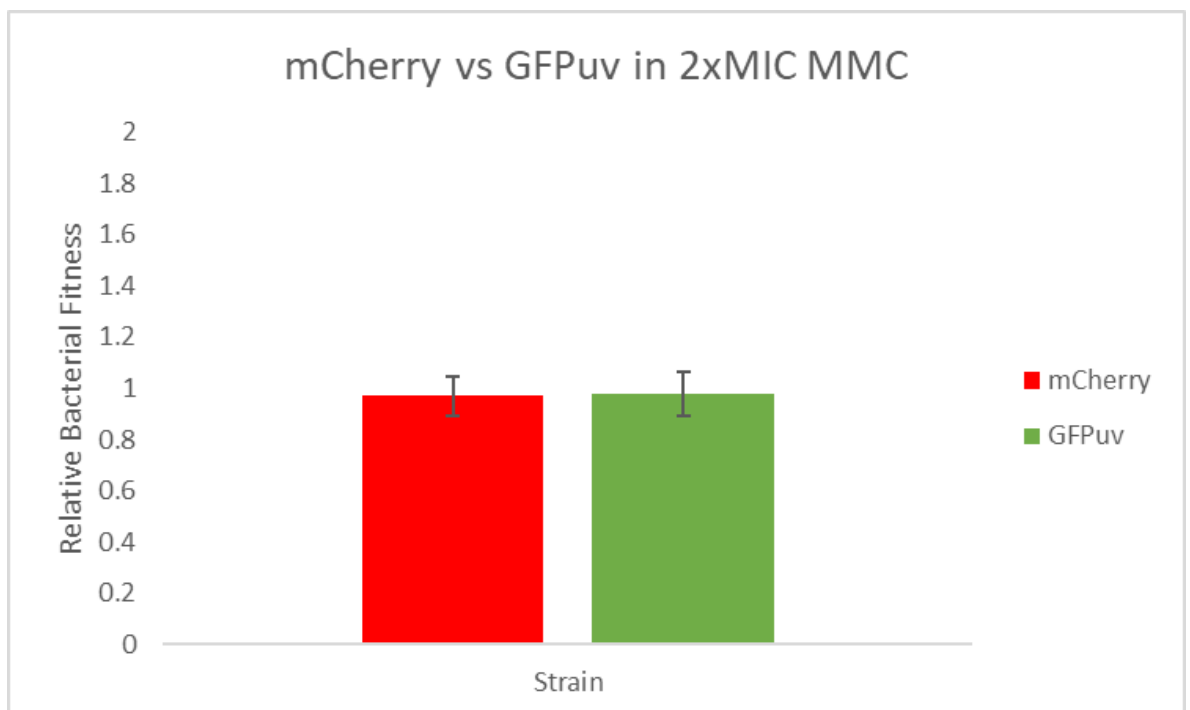
Figure 20: The relative bacterial fitness of the *E. coli* 5-alpha strain marked with either the mCherry (red) or GFPuv (green) fluorescent protein in 2xMIC mitomycin C (MMC). The 95% confidence interval is plotted for each strain (*n* = 3).
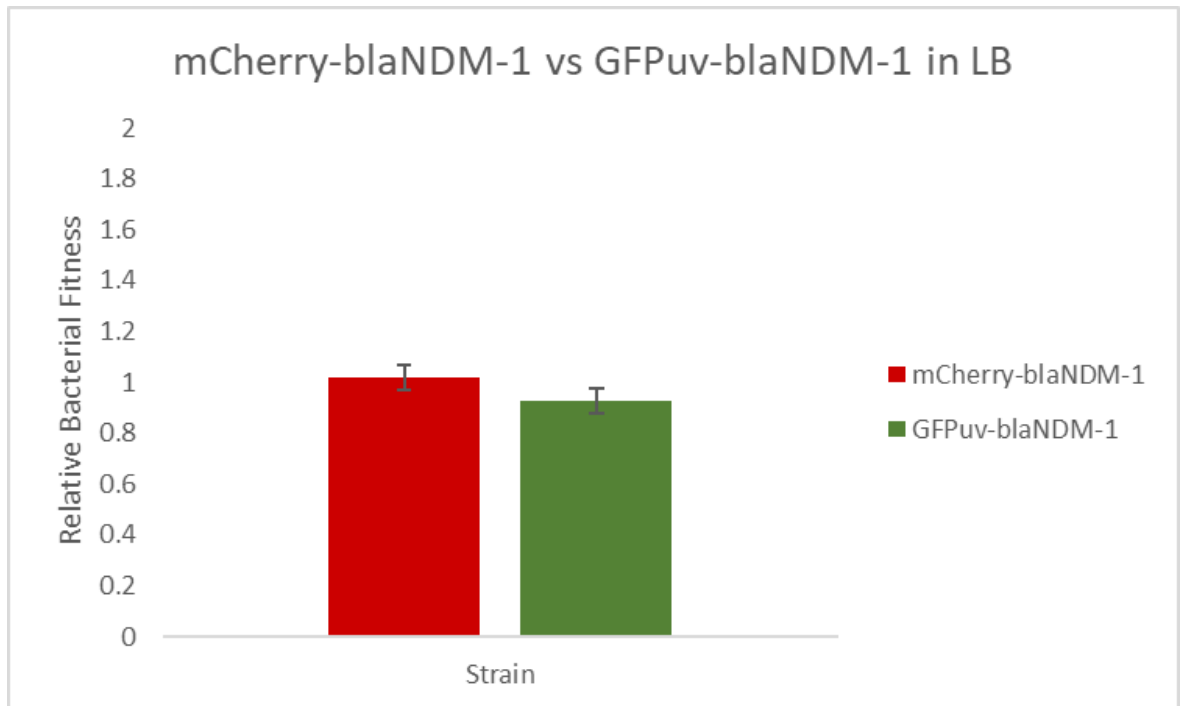
Figure 21: The relative bacterial fitness of the *E. coli* 5-alpha mCherry-*bla*NDM-1 strain and 5-alpha GFPuv-*bla*NDM-1 strain in normal LB. The 95% confidence interval is plotted for each strain (*n* = 3).
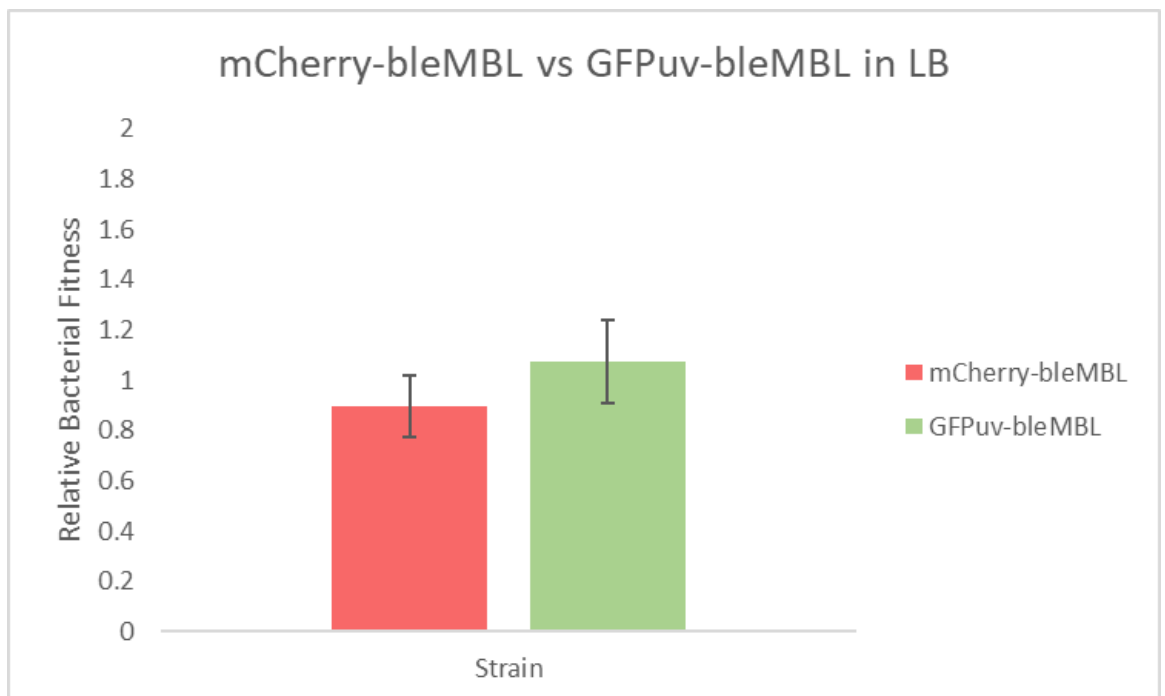
Figure 22: The relative bacterial fitness of the *E. coli* 5-alpha mCherry-*ble*MBL strain and 5-alpha GFPuv-*ble*MBL strain in normal LB. The 95% confidence interval is plotted for each strain (*n* = 3).
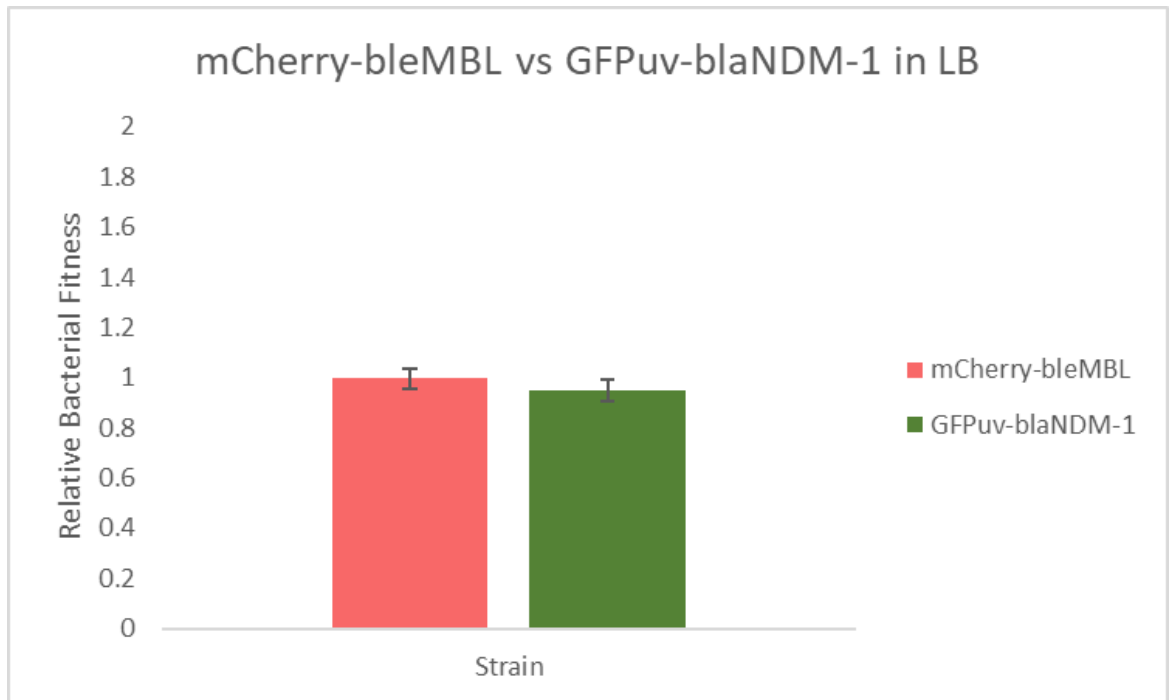
Figure 23: The relative bacterial fitness of the *E. coli* 5-alpha mCherry-*ble*_{MBL} strain and 5-alpha GFPuv-*bla*_{NDM-1} strain in normal LB. The 95% confidence interval is plotted for each strain ($n = 3$).
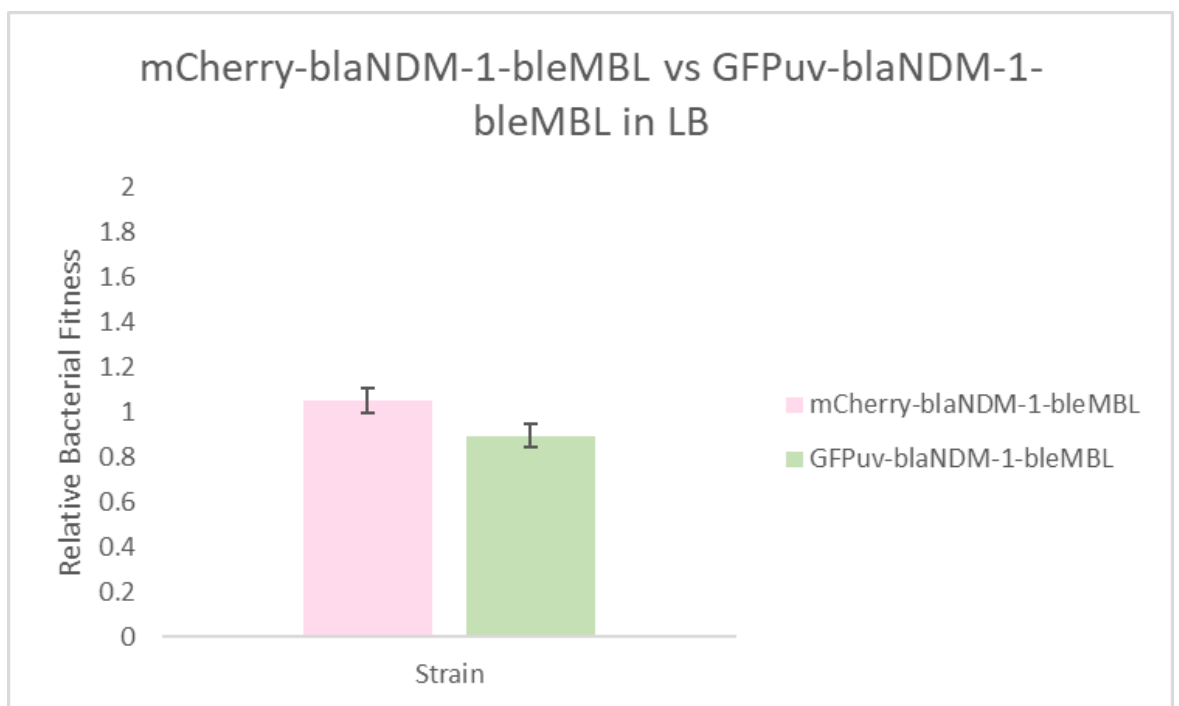
Figure 24: The relative bacterial fitness of the *E. coli* 5-alpha mCherry-*bla*_{NDM-1}-*ble*_{MBL} strain and 5-alpha GFPuv-*bla*_{NDM-1}-*ble*_{MBL} strain in normal LB. The 95% confidence interval is plotted for each strain ($n = 3$).
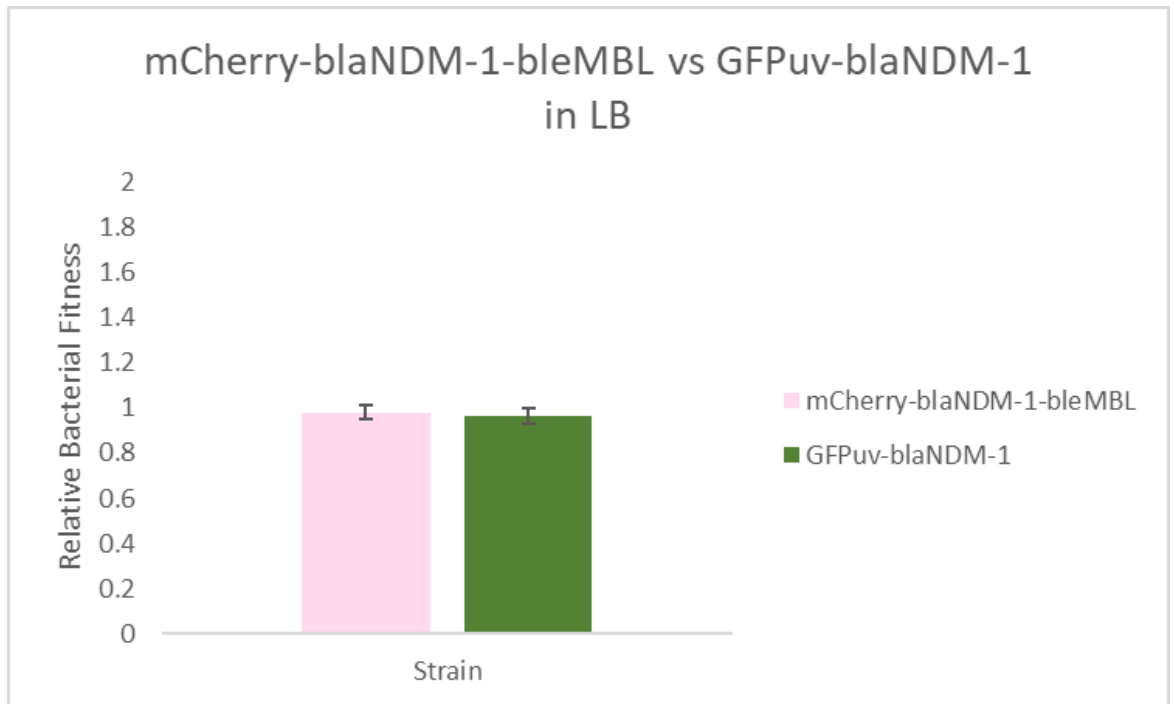
Figure 25: The relative bacterial fitness of the *E. coli* 5-alpha mCherry-*bla*$_{NDM-1}$-*ble*$_{MBL}$ strain and 5-alpha GFPuv-*bla*$_{NDM-1}$ strain in normal LB. The 95% confidence interval is plotted for each strain (*n* = 6).
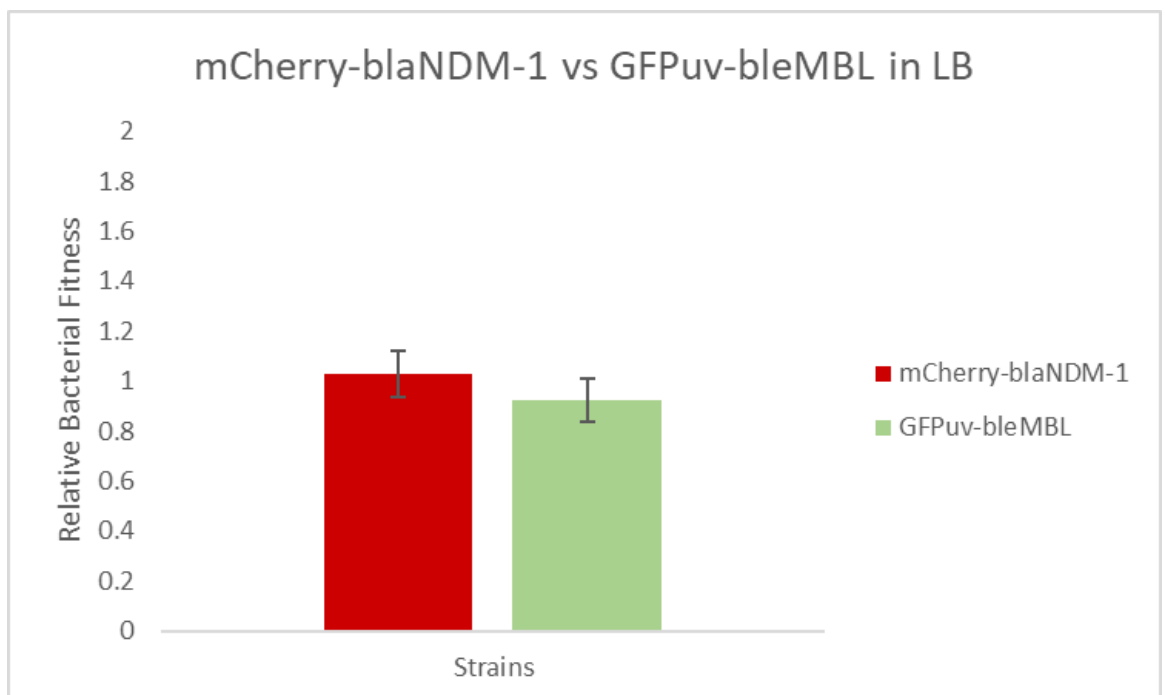
Figure 26: The relative bacterial fitness of the *E. coli* 5-alpha mCherry-*bla*$_{NDM-1}$ strain and 5-alpha GFPuv-*ble*$_{MBL}$ strain in normal LB. The 95% confidence interval is plotted for each strain (*n* = 3).
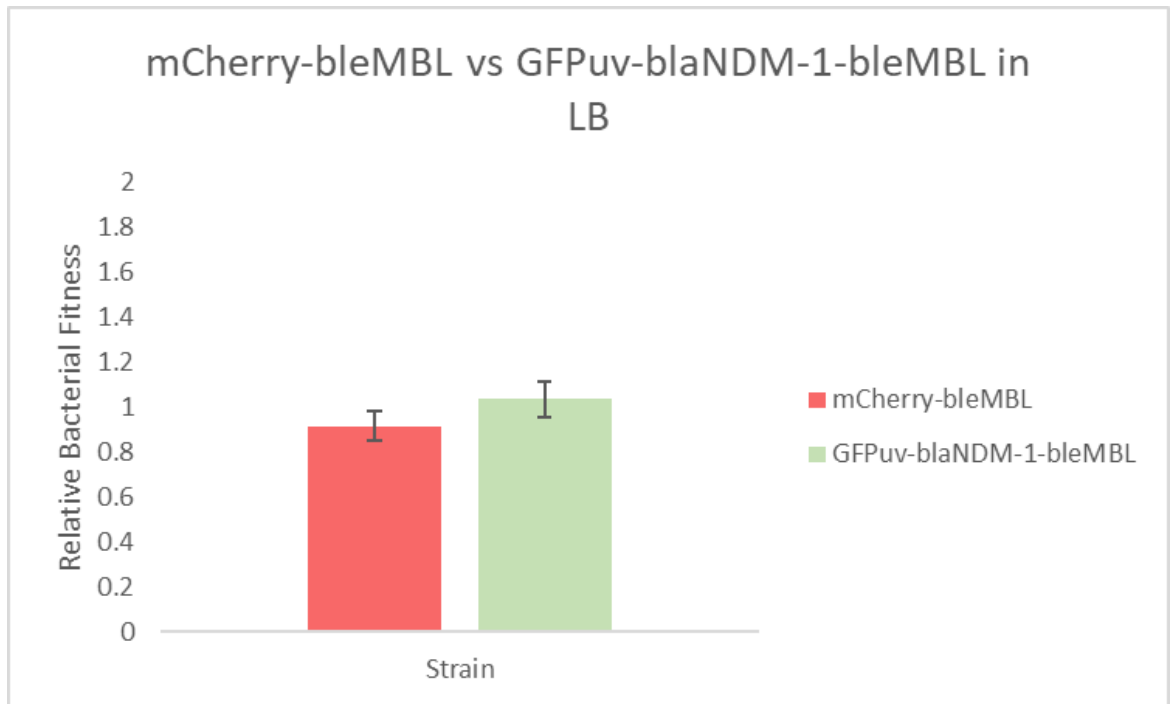
Figure 27: The relative bacterial fitness of the *E. coli* 5-alpha mCherry-*ble*MBL strain and 5-alpha GFPuv-*bla*NDM-1-*ble*MBL strain in normal LB. The 95% confidence interval is plotted for each strain ($n = 3$).
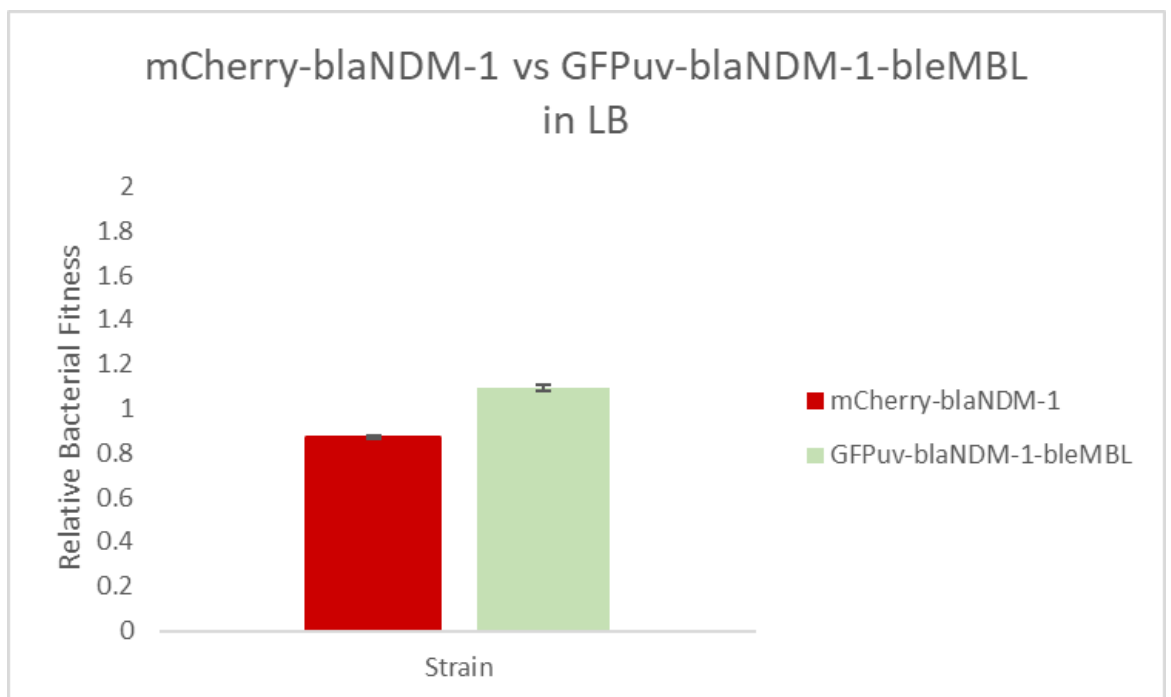
Figure 28: The relative bacterial fitness of the *E. coli* 5-alpha mCherry-*bla*NDM-1 strain and 5-alpha GFPuv-*bla*NDM-1-*ble*MBL strain in normal LB. The 95% confidence interval is plotted for each strain ($n = 3$).
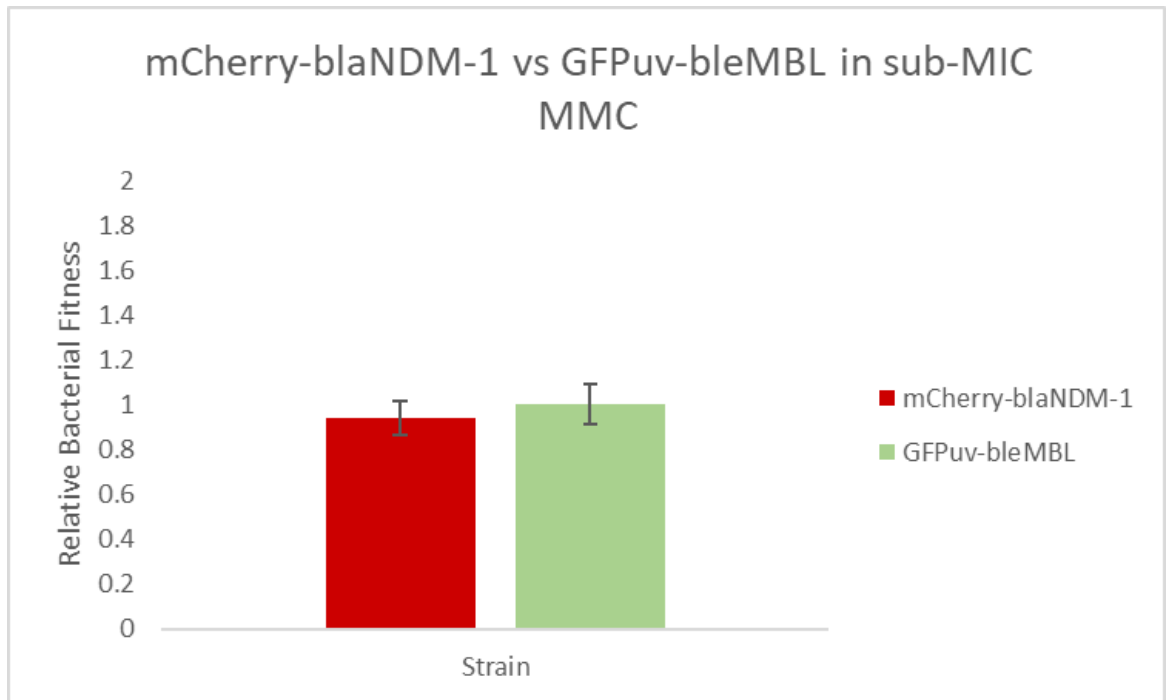
Figure 29: The relative bacterial fitness of the *E. coli* 5-alpha mCherry-*bla*NDM-1 strain and 5-alpha GFPuv-*ble*MBL strain in sub-MIC mitomycin C (MMC). The 95% confidence interval is plotted for each strain (*n* = 3).
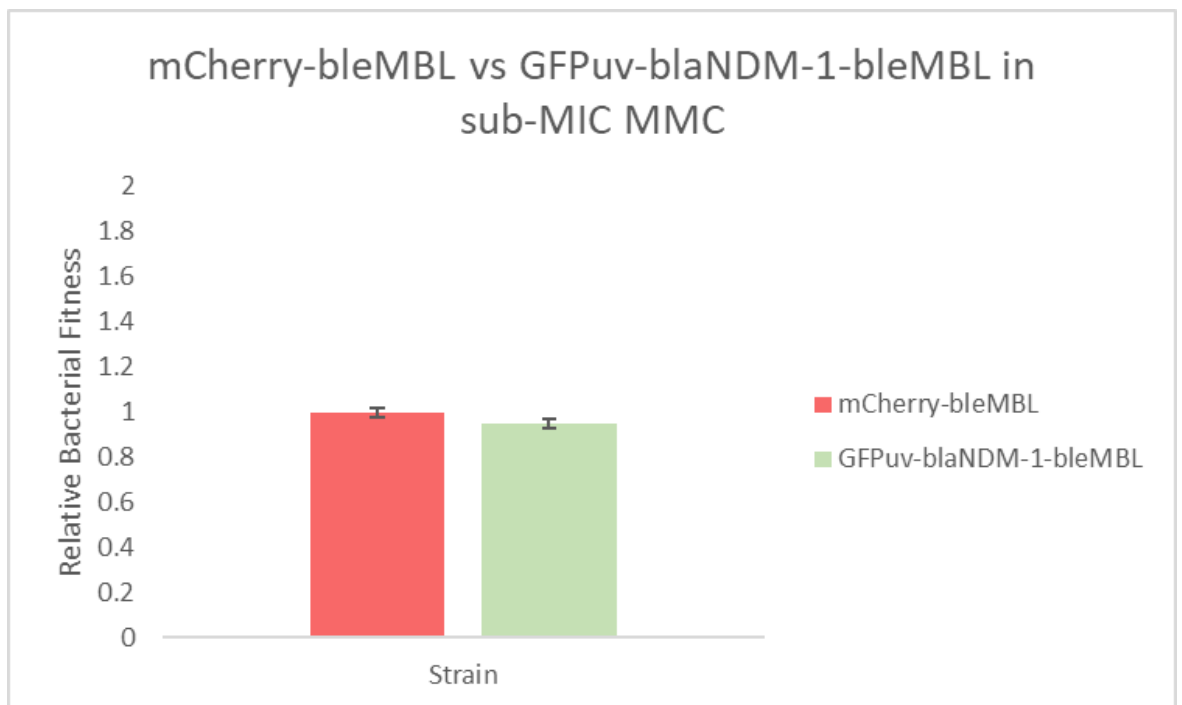
Figure 30: The relative bacterial fitness of the *E. coli* 5-alpha mCherry-*ble*MBL strain and 5-alpha GFPuv-*bla*NDM-1-*ble*MBL strain in sub-MIC mitomycin C (MMC). The 95% confidence interval is plotted for each strain (*n* = 3).
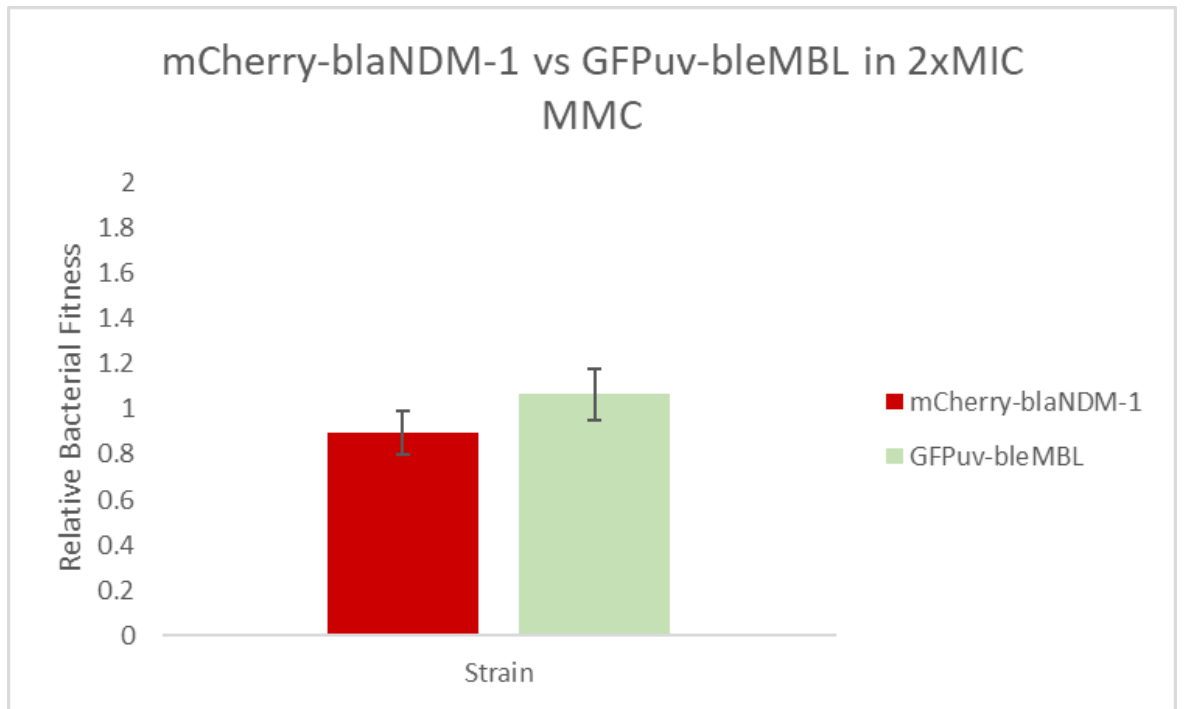
Figure 31: The relative bacterial fitness of the *E. coli* 5-alpha mCherry-*bla*NDM-1 strain and 5-alpha GFPuv-*ble*MBL strain in 2xMIC mitomycin C (MMC). The 95% confidence interval is plotted for each strain (*n* = 3).
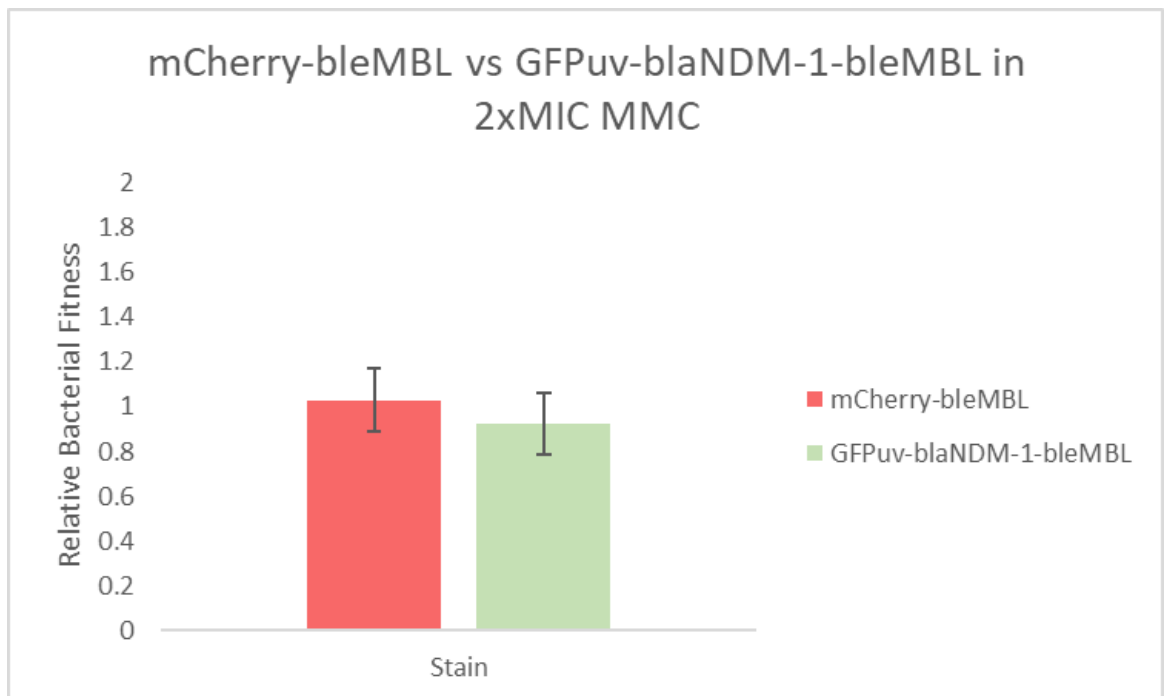
Figure 32: The relative bacterial fitness of the *E. coli* 5-alpha mCherry-*ble*MBL strain and 5-alpha GFPuv-*bla*NDM-1-*ble*MBL strain in 2xMIC mitomycin C (MMC). The 95% confidence interval is plotted for each strain (*n* = 3).
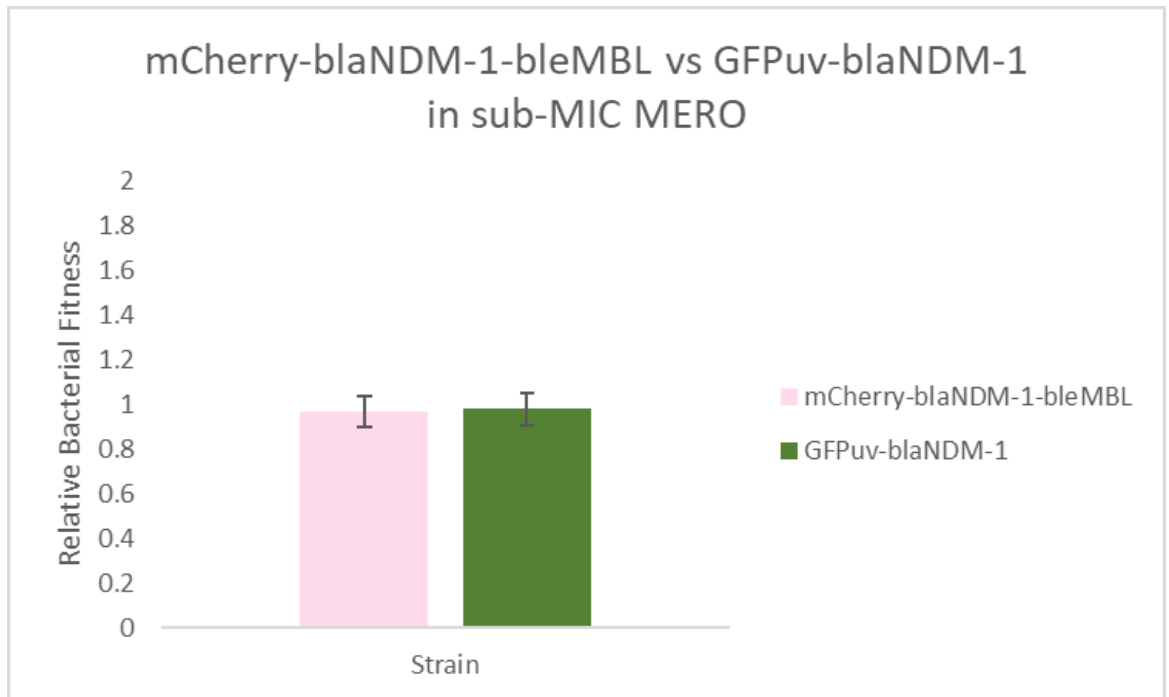
Figure 33: The relative bacterial fitness of the *E. coli* 5-alpha mCherry-*bla*$_{NDM-1}$-*ble*$_{MBL}$ strain and 5-alpha GFPuv-*bla*$_{NDM-1}$ strain in sub-MIC meropenem (MERO). The 95% confidence interval is plotted for each strain (*n* = 3).
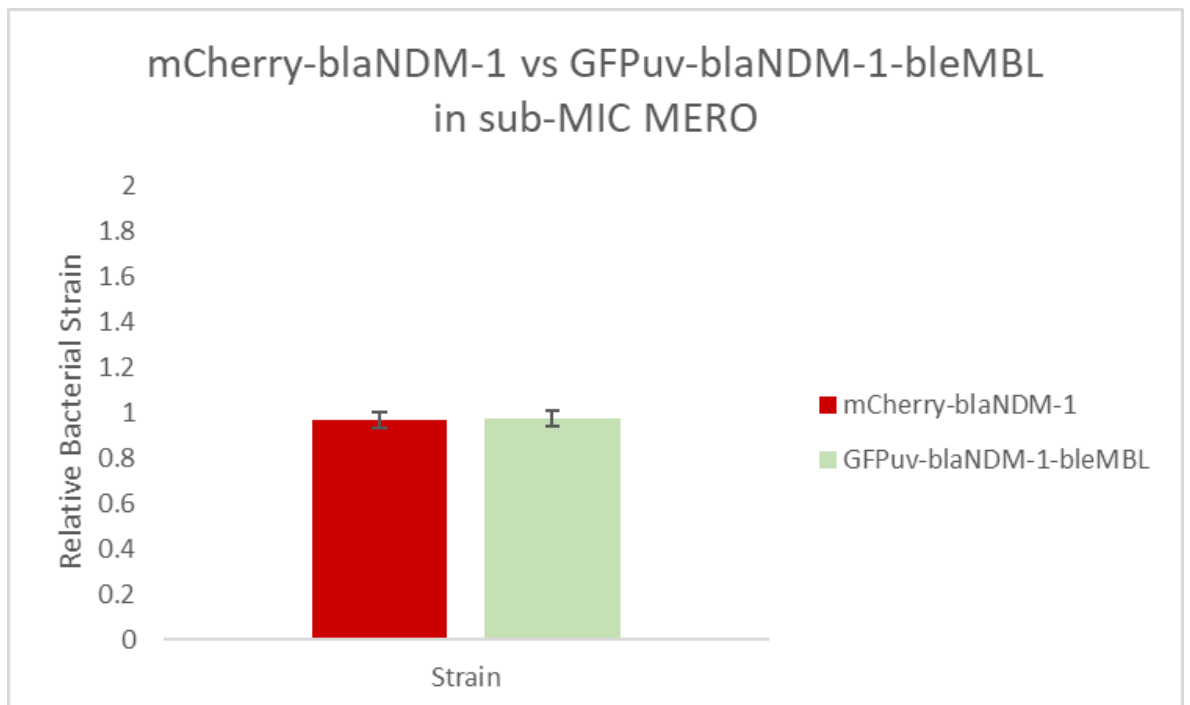
Figure 34: The relative bacterial fitness of the *E. coli* 5-alpha mCherry-*bla*$_{NDM-1}$ strain and 5-alpha GFPuv-*bla*$_{NDM-1}$-*ble*$_{MBL}$ strain in sub-MIC meropenem (MERO). The 95% confidence interval is plotted for each strain (*n* = 3).
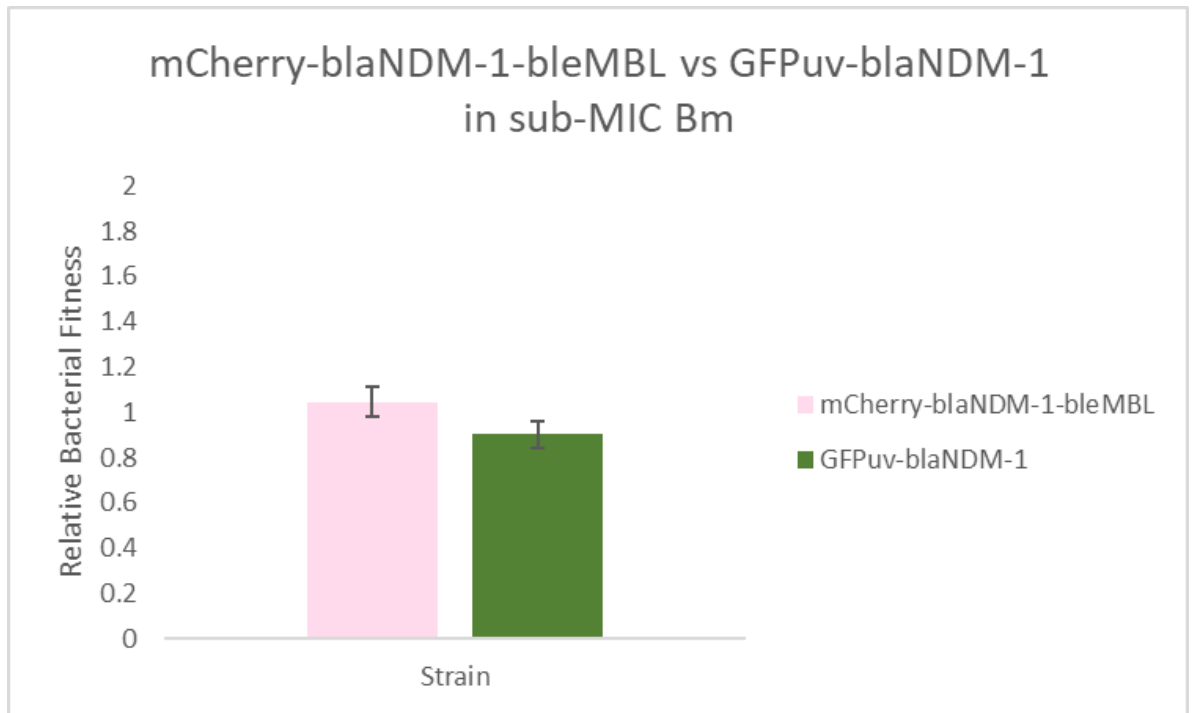
Figure 35: The relative bacterial fitness of the *E. coli* 5-alpha mCherry-*bla*$_{NDM-1}$-*ble*$_{MBL}$ strain and 5-alpha GFPuv-*bla*$_{NDM-1}$ strain in sub-MIC bleomycin (Bm). The 95% confidence interval is plotted for each strain (*n* = 3).
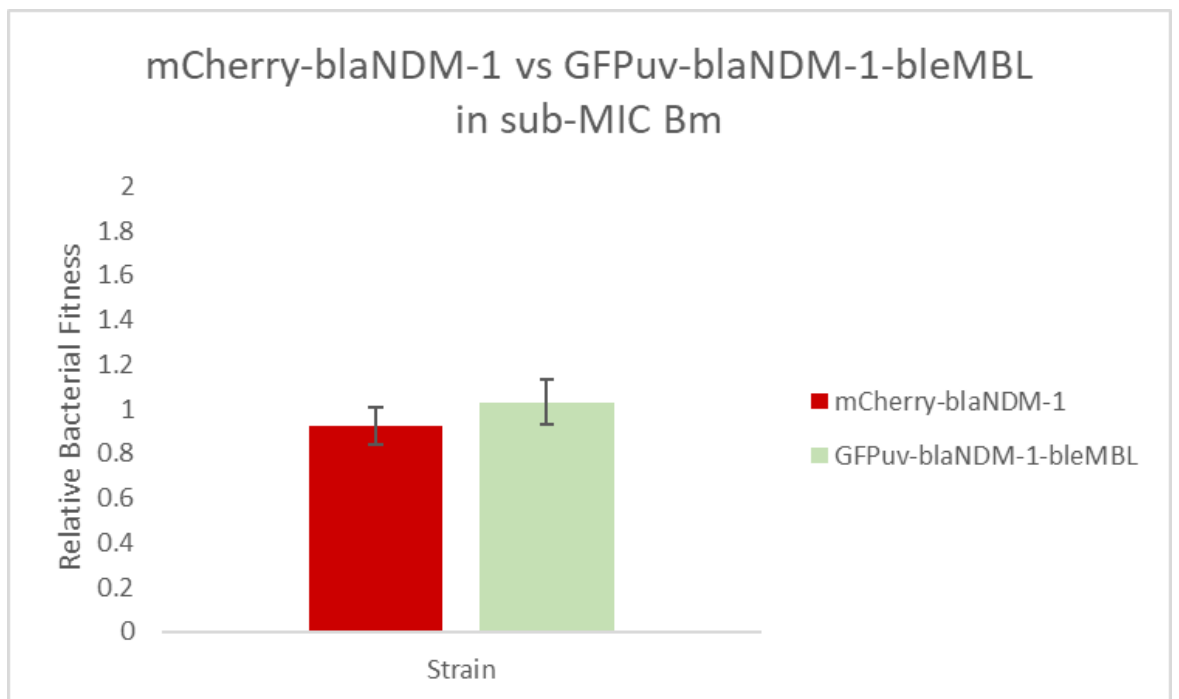
Figure 36: The relative bacterial fitness of the *E. coli* 5-alpha mCherry-*bla*$_{NDM-1}$ strain and 5-alpha GFPuv-*bla*$_{NDM-1}$-*ble*$_{MBL}$ strain in sub-MIC bleomycin (Bm) . The 95% confidence interval is plotted for each strain (*n* = 3).

Table 10: Competition experiments conducted with different strains of *E. coli* 5-alpha containing either the mCherry or GFPuv fluorescent marker and either the bla_{NDM-1}, ble_{MBL} or bla_{NDM-1}-ble_{MBL} genes. The competition experiments were also conducted in the presence of different drugs at different concentrations: meropenem (MERO), bleomycin (Bm), mitomycin C (MMC) and no drug/normal conditions (LB). The relative bacterial fitness for each strain was calculated and Mann-Whitney U tests were conducted to determine the statistical significance (significance cut-off $P < 0.05$). The exact significance value of each competition is presented. All of the tests had $n = 3$, with the exception of the competitions marked with an asterisk (*) that had an $n = 6$. Associated figures from this thesis are presented in the final column.

Competition	Condition	Mann-Whitney U value	Exact Significance value	Associated Figure
mCherry vs GFPuv	LB	4.00	1.00	19
	2xMIC MMC	4.00	1.00	20
mCherry-*bla* $_{NDM-1}$ vs GFPuv-*bla* $_{NDM-1}$	LB	0.00	0.10	21
mCherry-*ble* $_{MBL}$ vs GFPuv-*ble* $_{MBL}$	LB	1.00	0.20	22
mCherry-*ble* $_{MBL}$ vs GFPuv-*bla* $_{NDM-1}$	LB*	9.00	0.18	23
mCherry-*bla* $_{NDM-1}$-*ble* $_{MBL}$ vs GFPuv-*bla* $_{NDM-1}$-*ble* $_{MBL}$	LB	0.00	0.10	24
mCherry-*bla* $_{NDM-1}$-*ble* $_{MBL}$ vs GFPuv-*bla* $_{NDM-1}$	LB*	16.00	0.82	25
	Sub-MIC MERO	4.00	1.00	33
	Sub-MIC Bm	0.00	0.10	35
mCherry-*bla* $_{NDM-1}$ vs GFPuv-*ble* $_{MBL}$	LB	0.00	0.10	26
	Sub-MIC MMC	3.00	0.70	29
	2xMIC MMC	1.00	0.20	31
mCherry-*ble* $_{MBL}$ vs GFPuv-*bla* $_{NDM-1}$-*ble* $_{MBL}$	LB	0.00	0.10	27
	Sub-MIC MMC	0.00	0.10	30
	2xMIC MMC	1.00	0.20	32
mCherry-*bla* $_{NDM-1}$ vs GFPuv-*bla* $_{NDM-1}$-*ble* $_{MBL}$	LB	0.00	0.10	28
	Sub-MIC MERO	4.00	1.00	34
	Sub-MIC Bm	1.00	0.20	36

2.4.6.1.1. Flow cytometry

To count the population in a more sensitive way, a small amount of the competitions that were conducted on plates was saved to run through the BD LSRFortessa flow cytometer. Due to the higher sensitivity of the flow cytometer, samples that were more dilute (due to the drug condition they were exposed to) could be analysed that couldn't be done on the agar plates: mCherry-bla_{NDM-1} vs GFPuv-ble_{MBL} in MIC MMC and mCherry-bla_{NDM-1}-ble_{MBL} vs GFPuv-bla_{NDM-1} in MIC MMC.

In the bar charts generated from the competition experiments that were analysed using the flow cytometer, it appears as if certain competitions have one strain that was more fit than the other when we look at the plotted average relative fitness values (Figures 37-56). However, when the relative fitness values were statistically analysed, all of the competition experiments except one showed no significant difference when you look at the significance level of 0.05 ($P > 0.05$) (Table 11). The competition between mCherry-bla_{NDM-1}-ble_{MBL} vs GFPuv-bla_{NDM-1} in LB showed a significant difference in the relative bacterial fitness where mCherry-bla_{NDM-1}-ble_{MBL} had a higher fitness value than the GFPuv-bla_{NDM-1} strain.
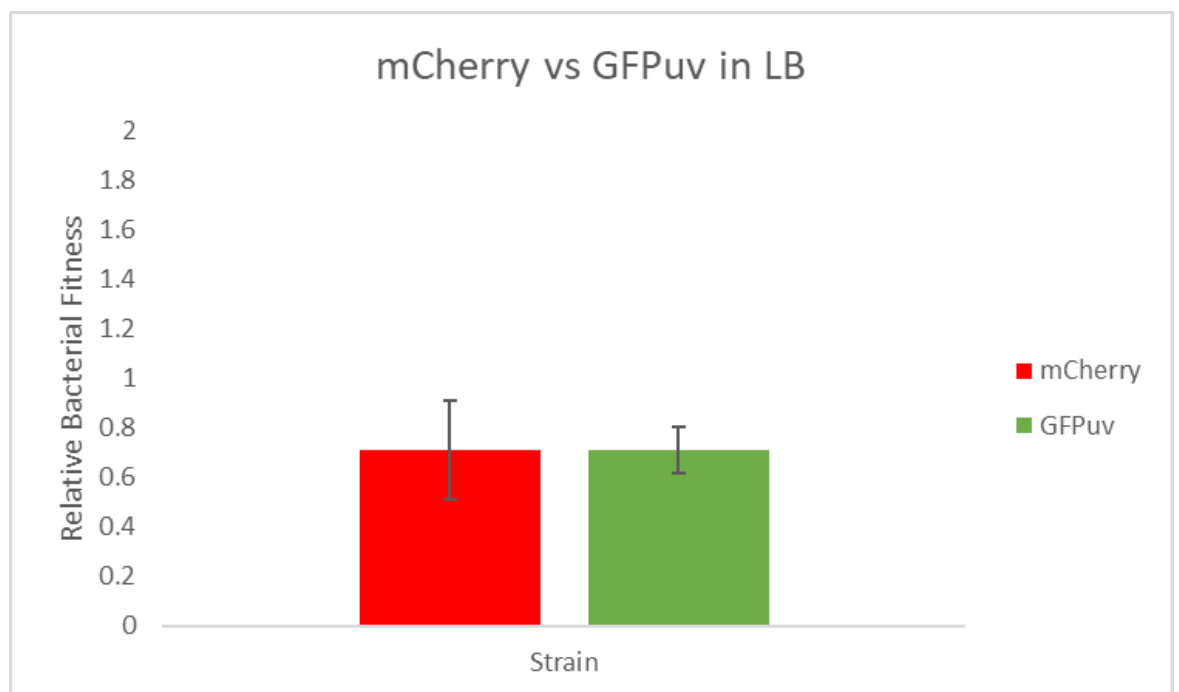
Figure 37: The relative bacterial fitness of the *E. coli* 5-alpha mCherry strain and 5-alpha GFPuv strain in normal LB media. The 95% confidence interval is plotted for each strain (*n* = 3).
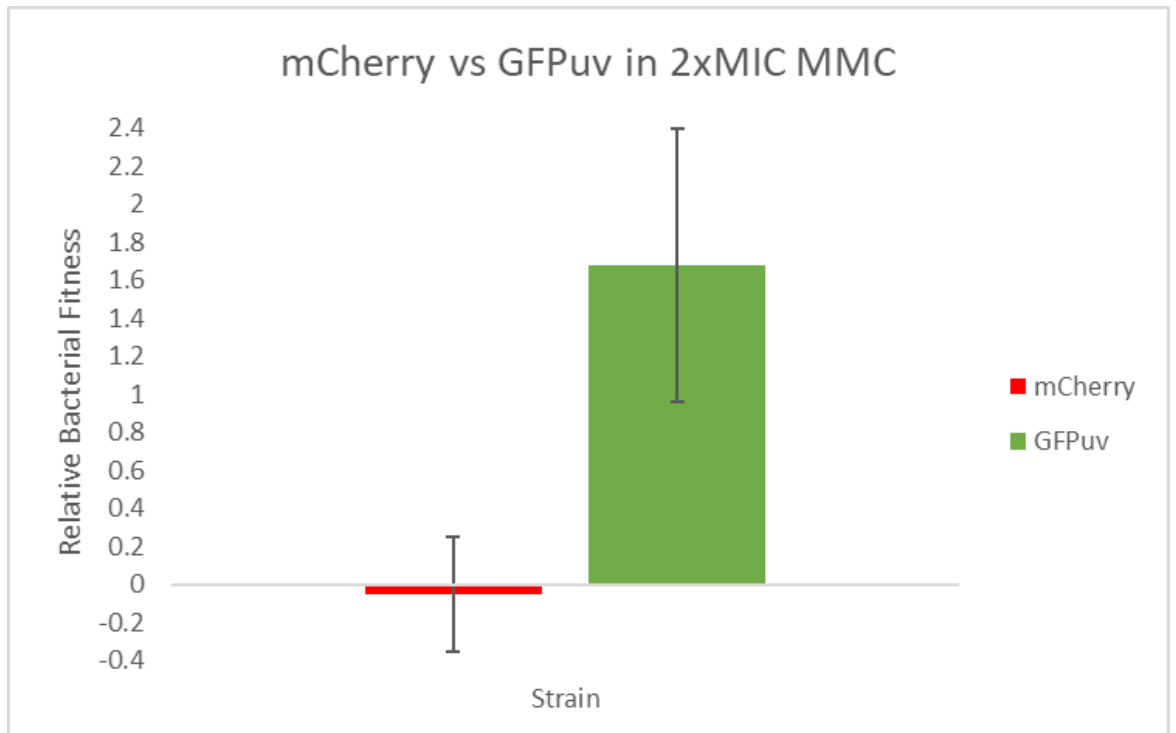
Figure 38: The relative bacterial fitness of the *E. coli* 5-alpha mCherry strain and 5-alpha GFPuv strain in 2xMIC mitomycin C (MMC). The 95% confidence interval is plotted for each strain (*n* = 3).
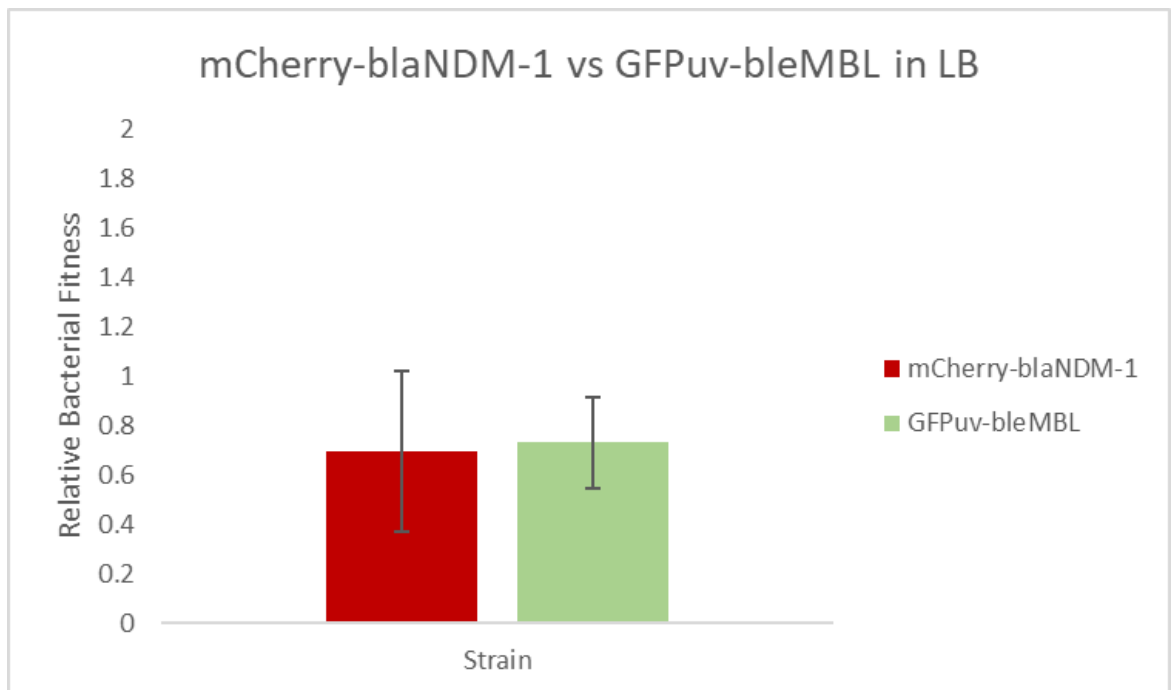
Figure 39: The relative bacterial fitness of the *E. coli* 5-alpha mCherry-*bla*$_{NDM-1}$ strain and 5-alpha GFPuv-*ble*$_{MBL}$ strain in normal LB media. The 95% confidence interval is plotted for each strain (*n* = 3).
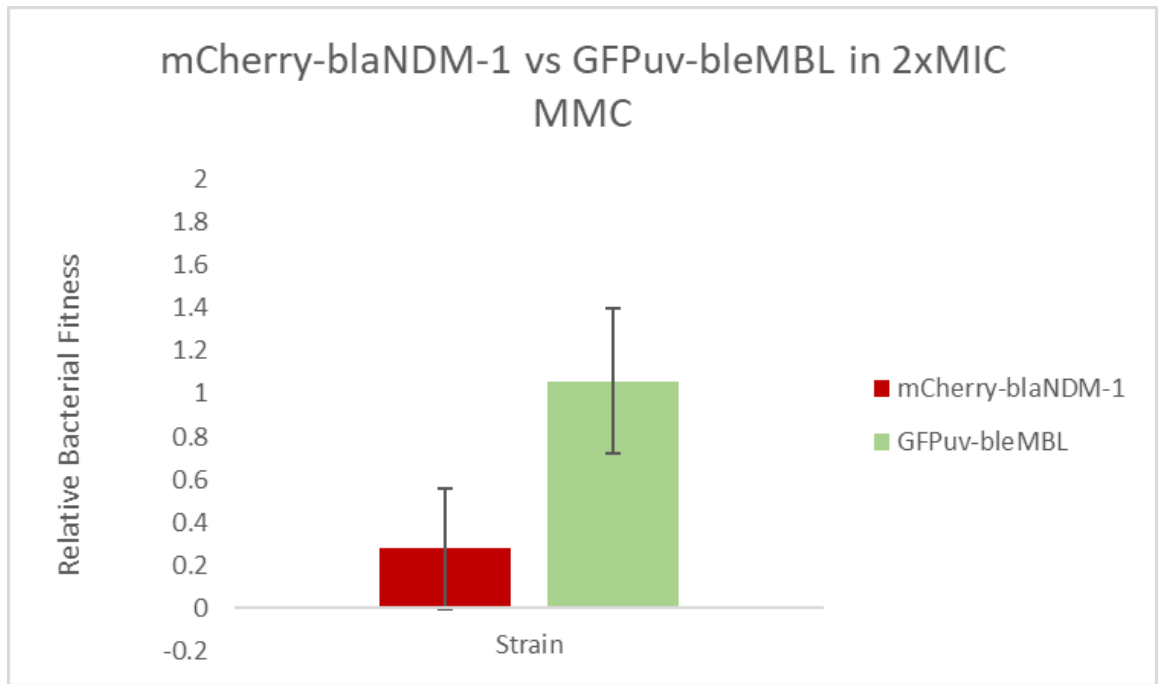
Figure 40: The relative bacterial fitness of the *E. coli* 5-alpha mCherry-*bla*$_{NDM-1}$ strain and 5-alpha GFPuv-*ble*$_{MBL}$ strain in 2xMIC mitomycin C (MMC). The 95% confidence interval is plotted for each strain (*n* = 3).
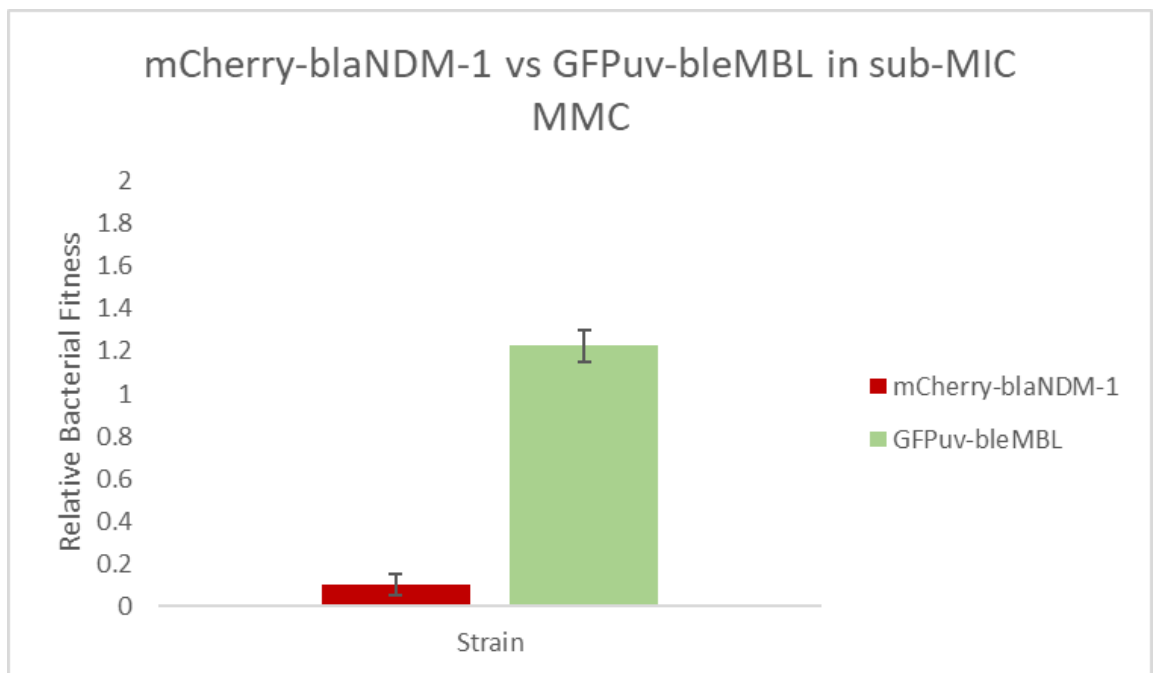
Figure 41: The relative bacterial fitness of the *E. coli* 5-alpha mCherry-*bla*$_{NDM-1}$ strain and 5-alpha GFPuv-*ble*$_{MBL}$ strain in sub-MIC bleomycin (Bm). The 95% confidence interval is plotted for each strain (*n* = 2).
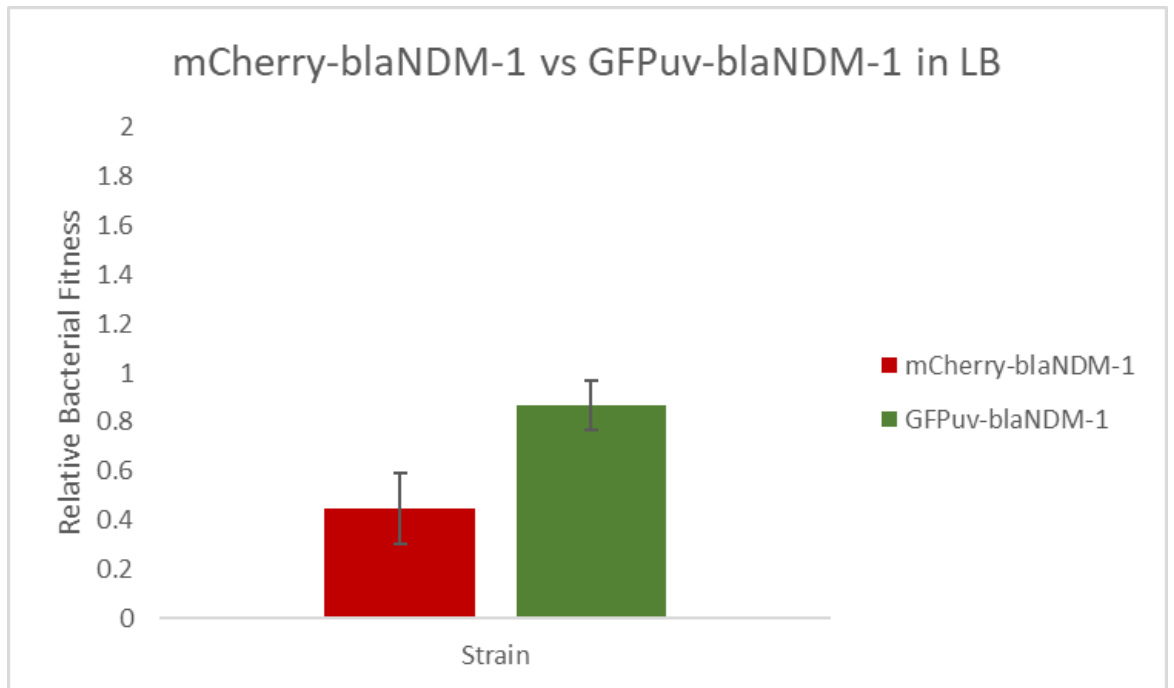
Figure 42: The relative bacterial fitness of the *E. coli* 5-alpha mCherry-*bla*NDM-1 strain and 5-alpha GFPuv-*bla*NDM-1strain in normal LB. The 95% confidence interval is plotted for each strain (*n* = 3).
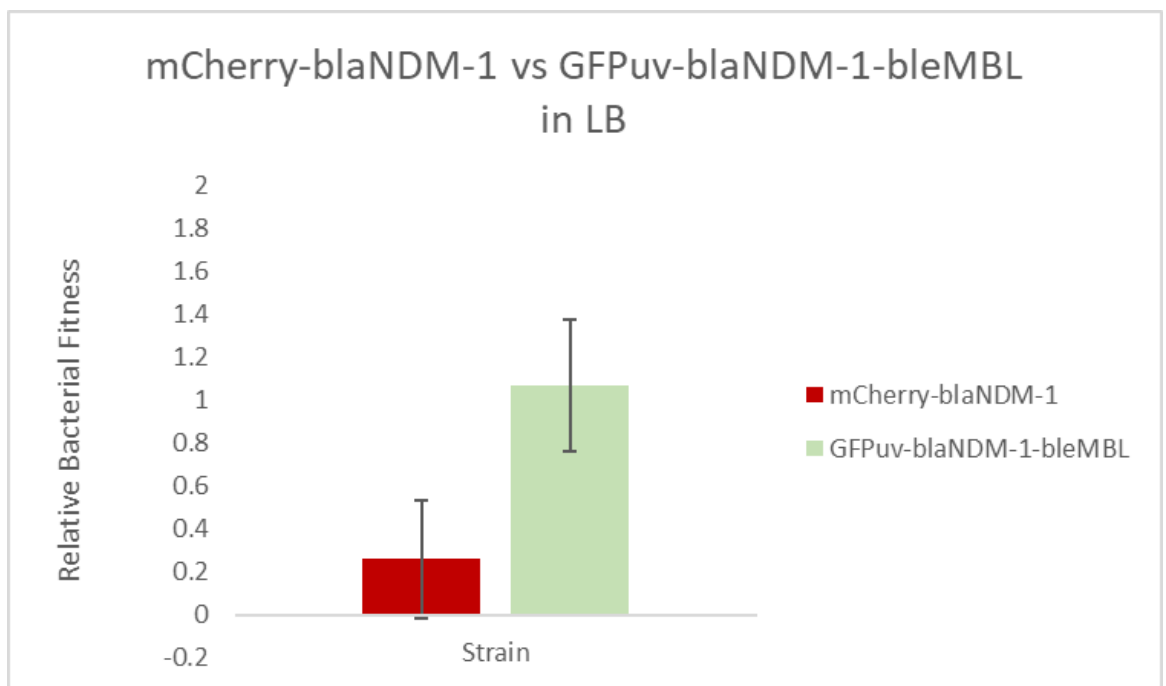
Figure 43: The relative bacterial fitness of the *E. coli* 5-alpha mCherry-*bla*NDM-1 strain and 5-alpha GFPuv-*bla*NDM-1-*ble*MBL strain in normal LB. The 95% confidence interval is plotted for each strain (*n* = 3).
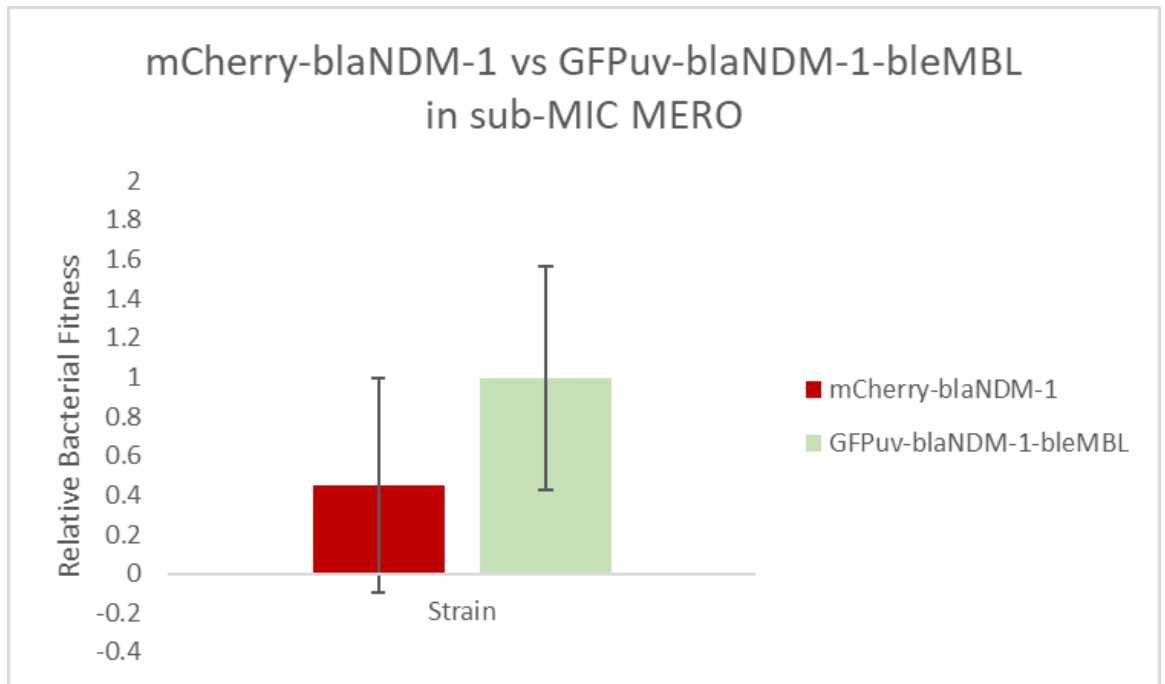
Figure 44: The relative bacterial fitness of the *E. coli* 5-alpha mCherry-*bla*NDM-1 strain and 5-alpha GFPuv-*bla*NDM-1-*ble*MBL strain in sub-MIC meropenem (MERO). The 95% confidence interval is plotted for each strain (*n* = 3).
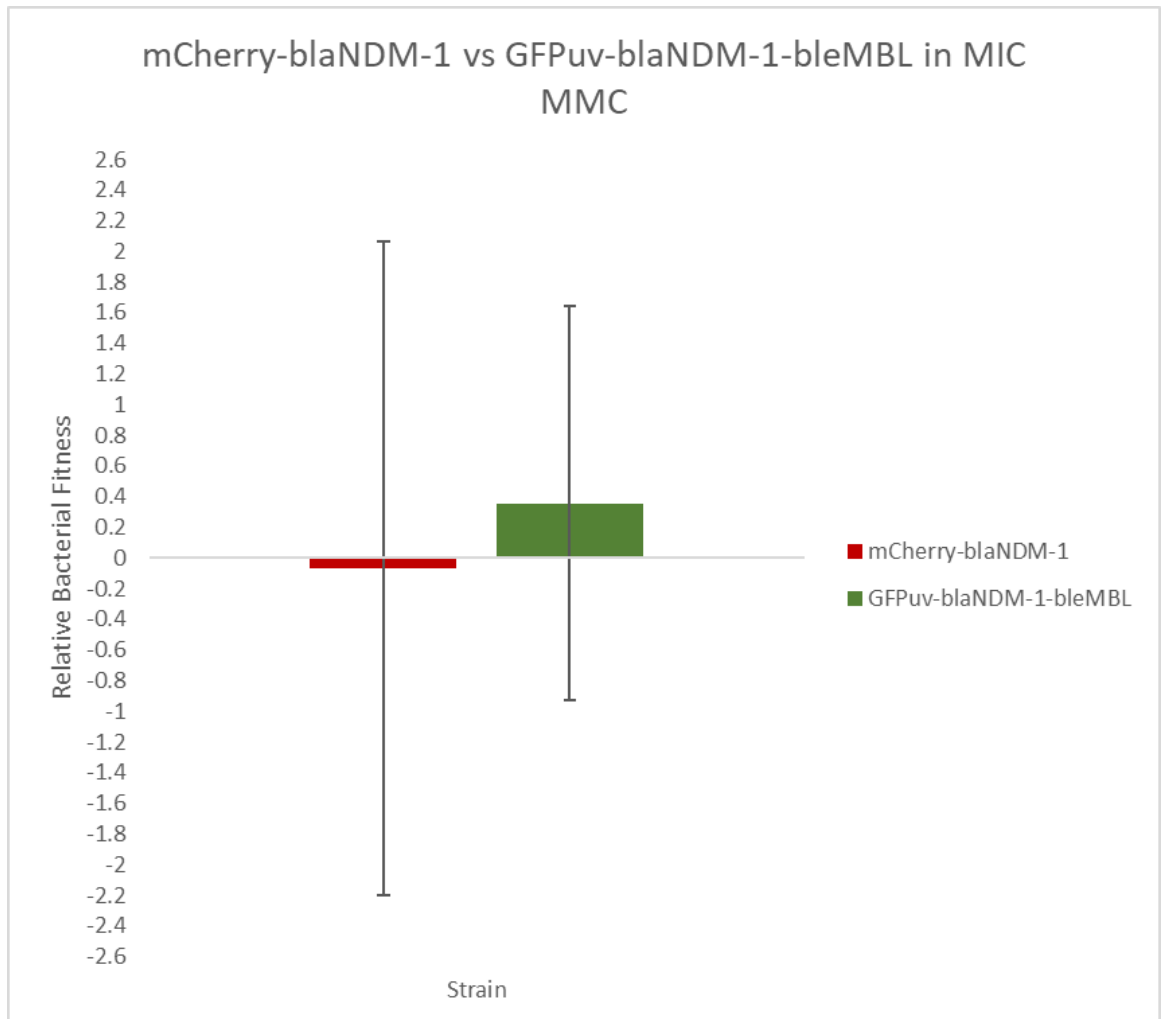
Figure 45: The relative bacterial fitness of the *E. coli* 5-alpha mCherry-*bla*NDM-1 strain and 5-alpha GFPuv-*bla*NDM-1-*ble*MBL strain in mitomycin C (MMC) at the MIC. The 95% confidence interval is plotted for each strain (*n* = 3).
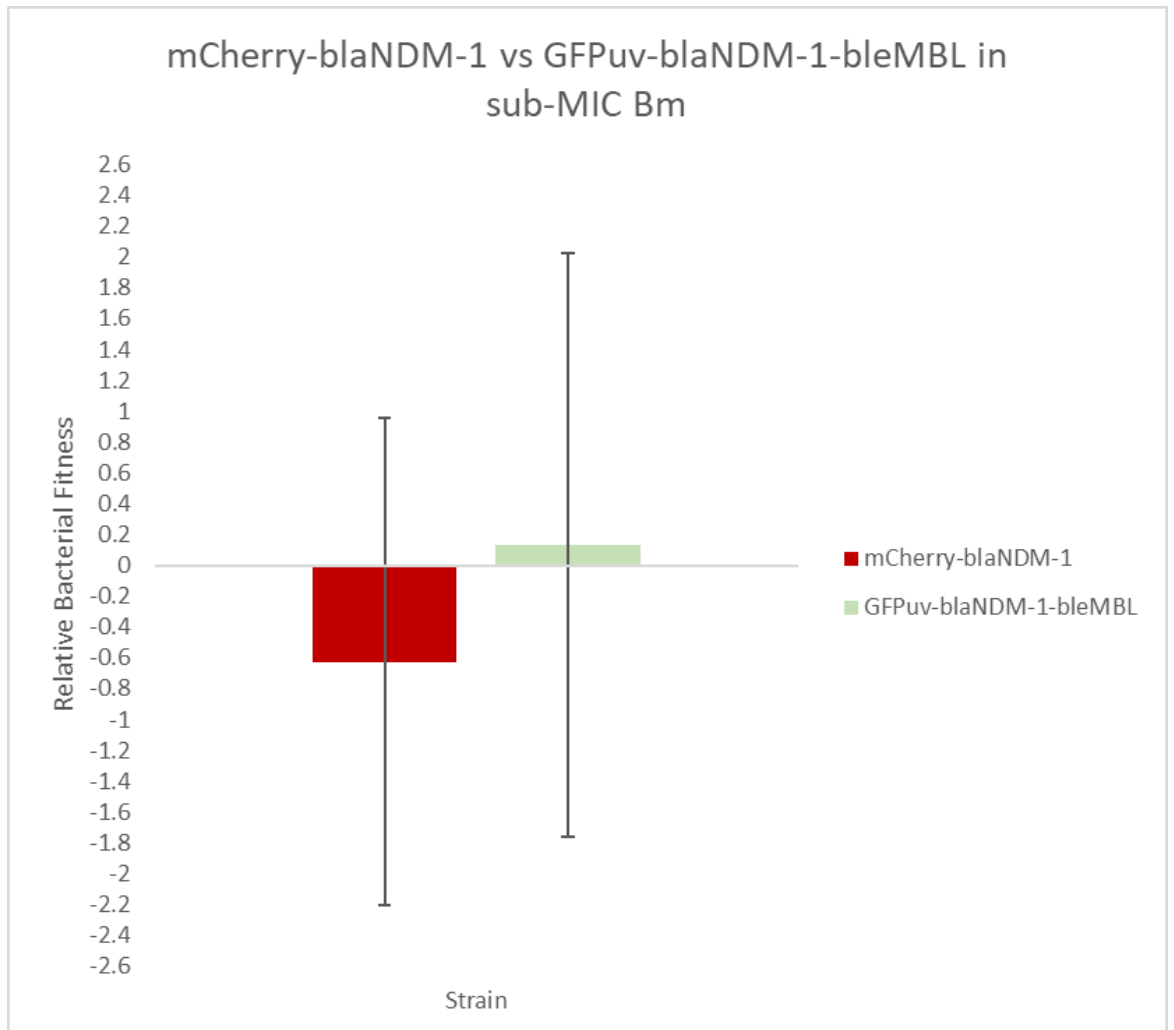
Figure 46: The relative bacterial fitness of the *E. coli* 5-alpha mCherry-*bla*_{NDM-1} strain and 5-alpha GFPuv-*bla*_{NDM-1}-*ble*_{MBL} strain in sub-MIC bleomycin (Bm). The 95% confidence interval is plotted for each strain (*n* = 6).
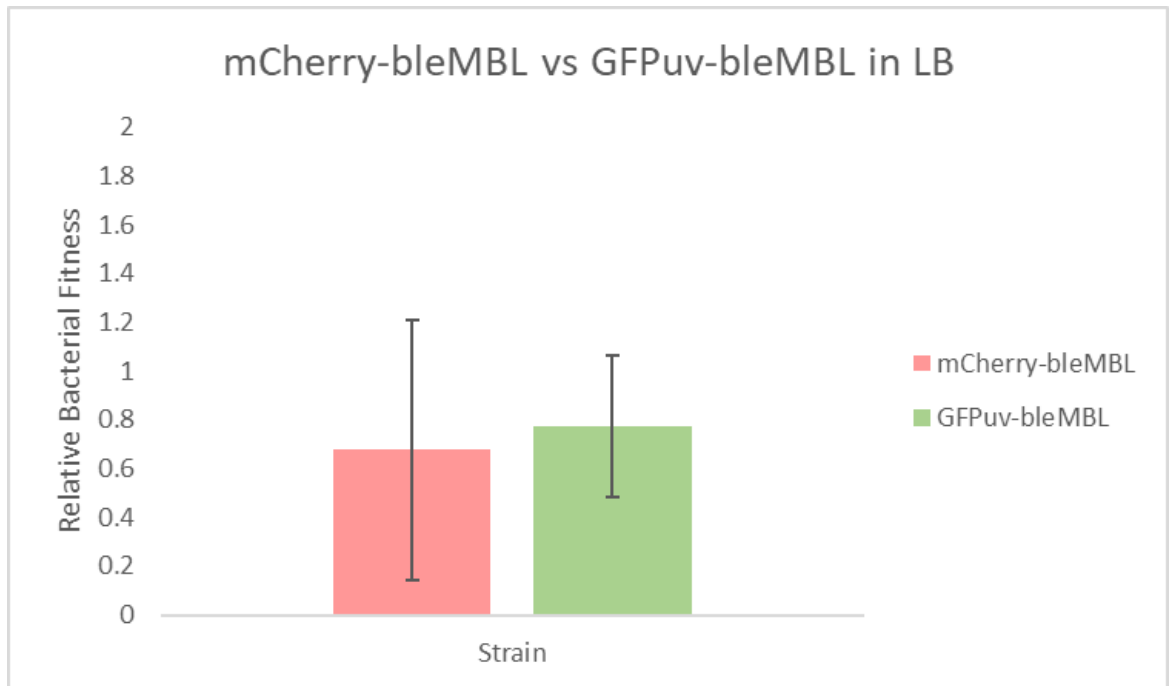
Figure 47: The relative bacterial fitness of the *E. coli* 5-alpha mCherry-*ble*MBL strain and 5-alpha GFPuv-*ble*MBL strain in normal LB. The 95% confidence interval is plotted for each strain (n = 3).
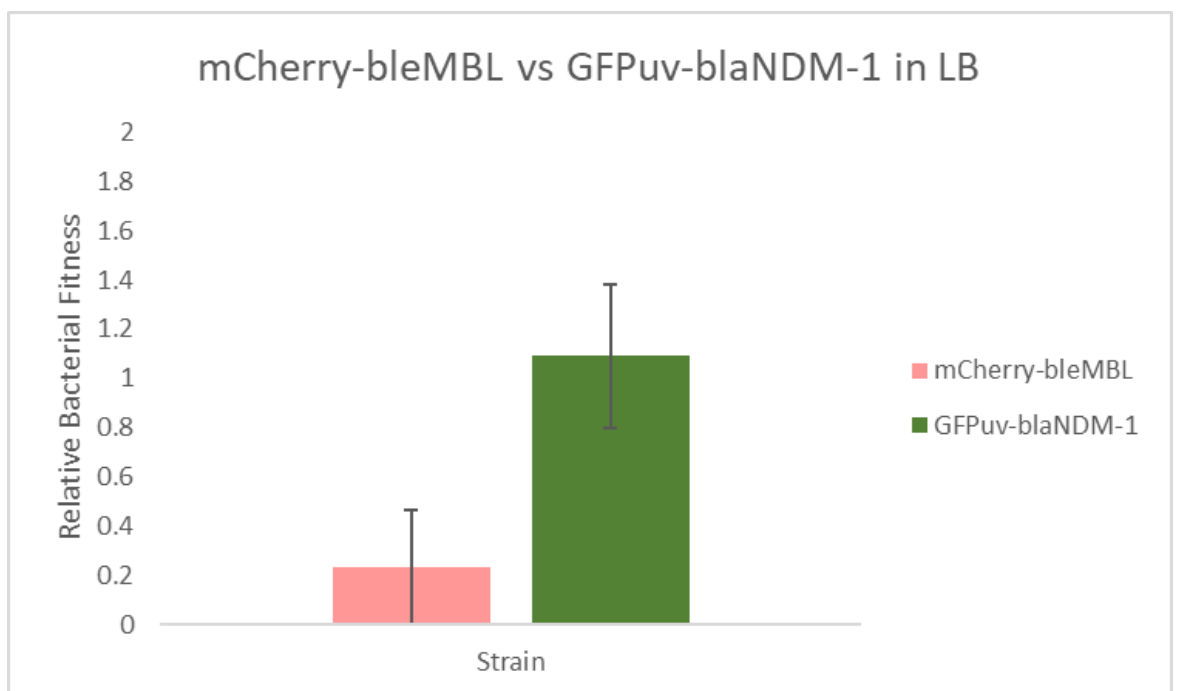
Figure 48: The relative bacterial fitness of the *E. coli* 5-alpha mCherry-*ble*MBL strain and 5-alpha GFPuv-*bla*NDM-1 strain in in normal LB. The 95% confidence interval is plotted for each strain (n = 3).
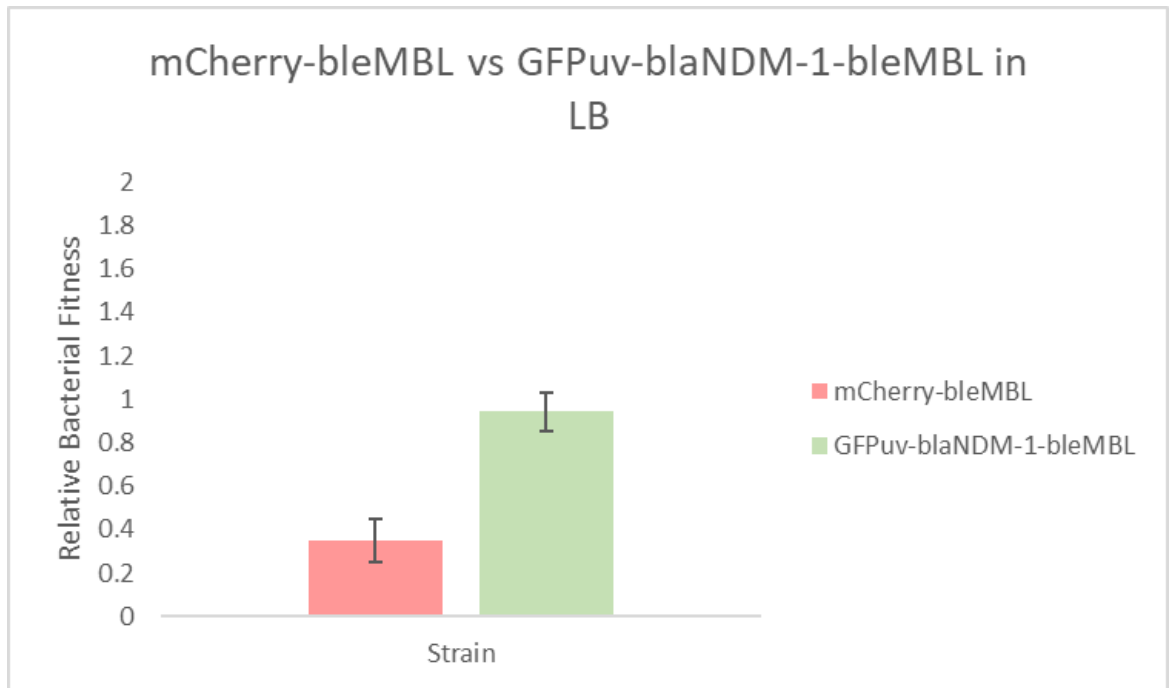
Figure 49: The relative bacterial fitness of the *E. coli* 5-alpha mCherry-*ble*MBL strain and 5-alpha GFPuv-*bla*NDM-1-*ble*MBL strain in normal LB. The 95% confidence interval is plotted for each strain (*n* = 2).
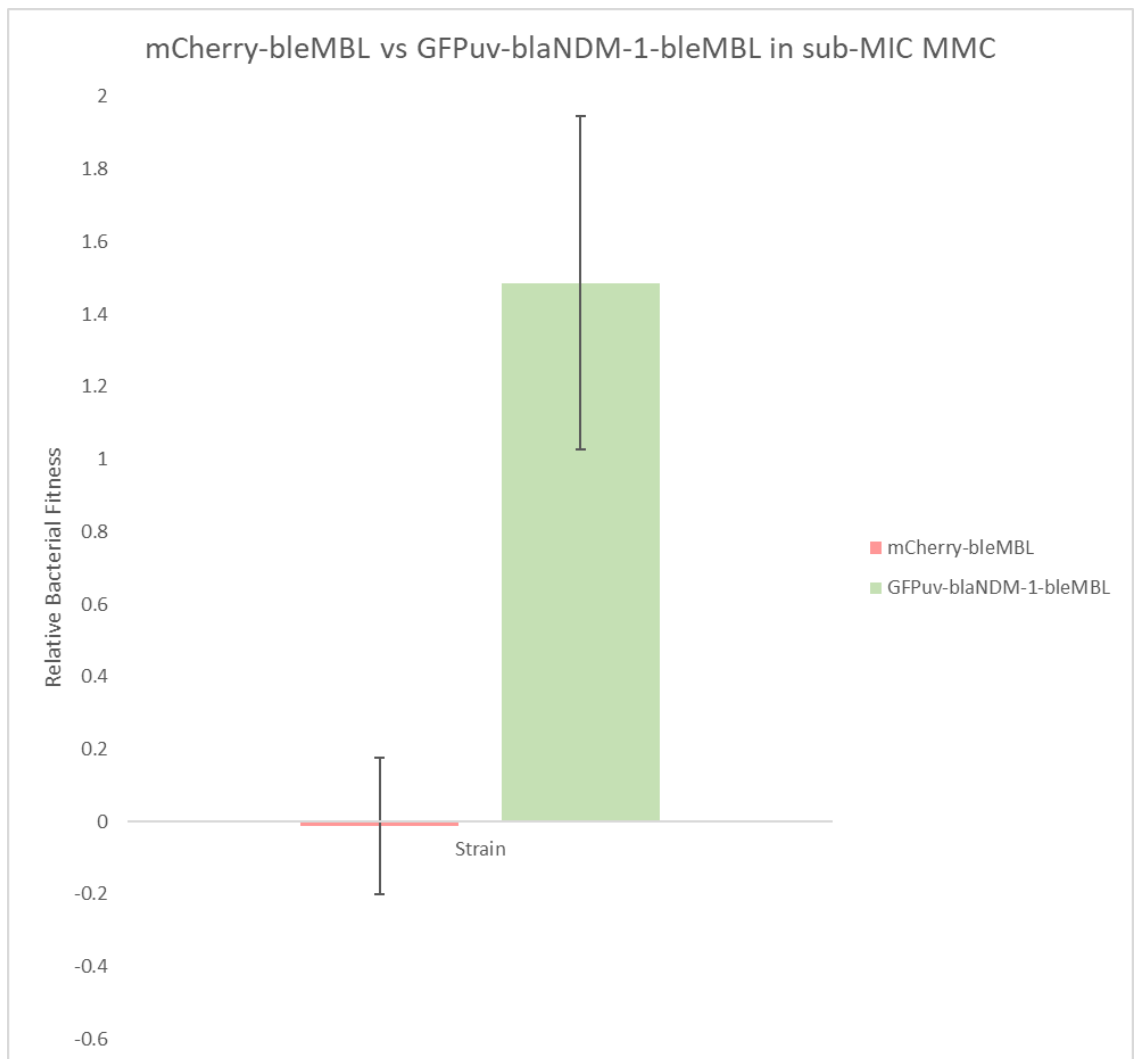
Figure 50: The relative bacterial fitness of the *E. coli* 5-alpha mCherry-*ble*MBL strain and 5-alpha GFPuv-*bla*NDM-1-*ble*MBL strain in sub-MIC mitomycin C (MMC). The 95% confidence interval is plotted for each strain (*n* = 3).
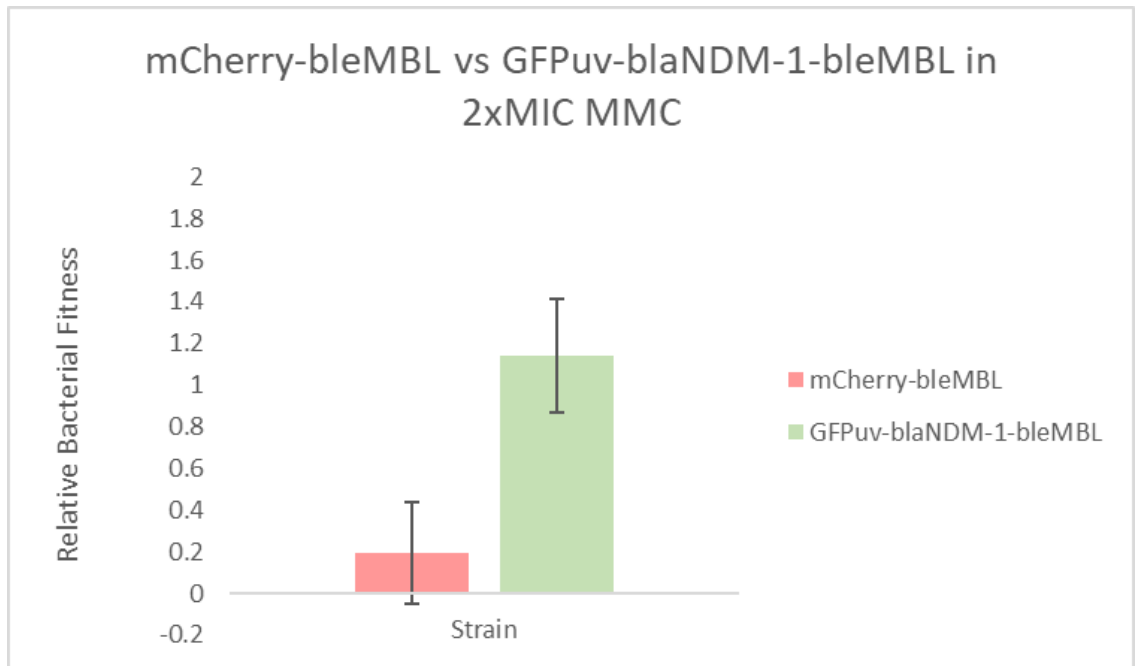
Figure 51: The relative bacterial fitness of the *E. coli* 5-alpha mCherry-*ble*MBL strain and 5-alpha GFPuv-*bla*NDM-1-*ble*MBL strain in 2xMIC mitomycin C (MMC). The 95% confidence interval is plotted for each strain (*n* = 3).
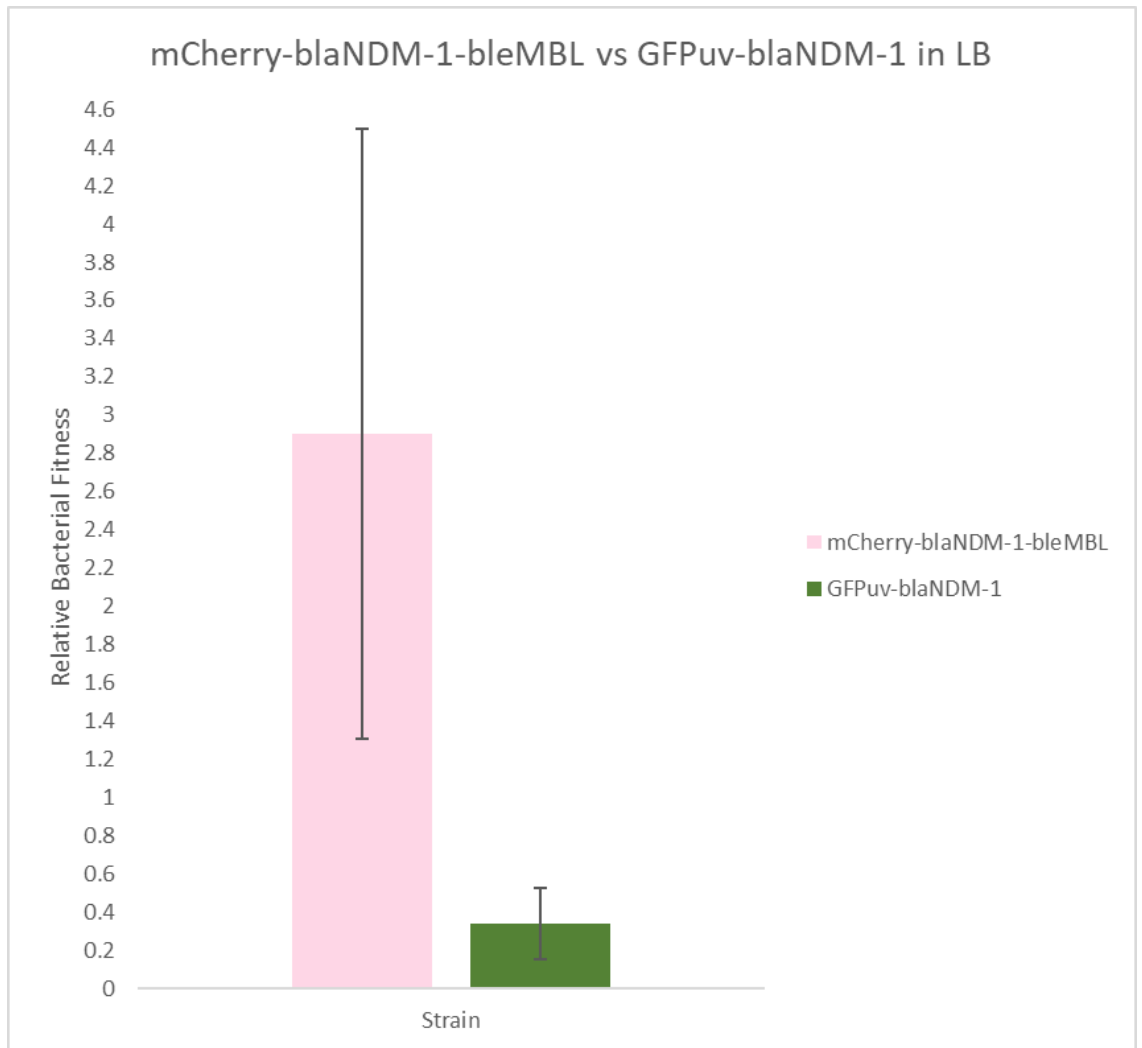
Figure 52: The relative bacterial fitness of the *E. coli* 5-alpha mCherry-*bla*$_{NDM-1}$-*ble*$_{MBL}$ strain and 5-alpha GFPuv-*bla*$_{NDM-1}$ strain in normal LB. The 95% confidence interval is plotted for each strain (*n* = 4).
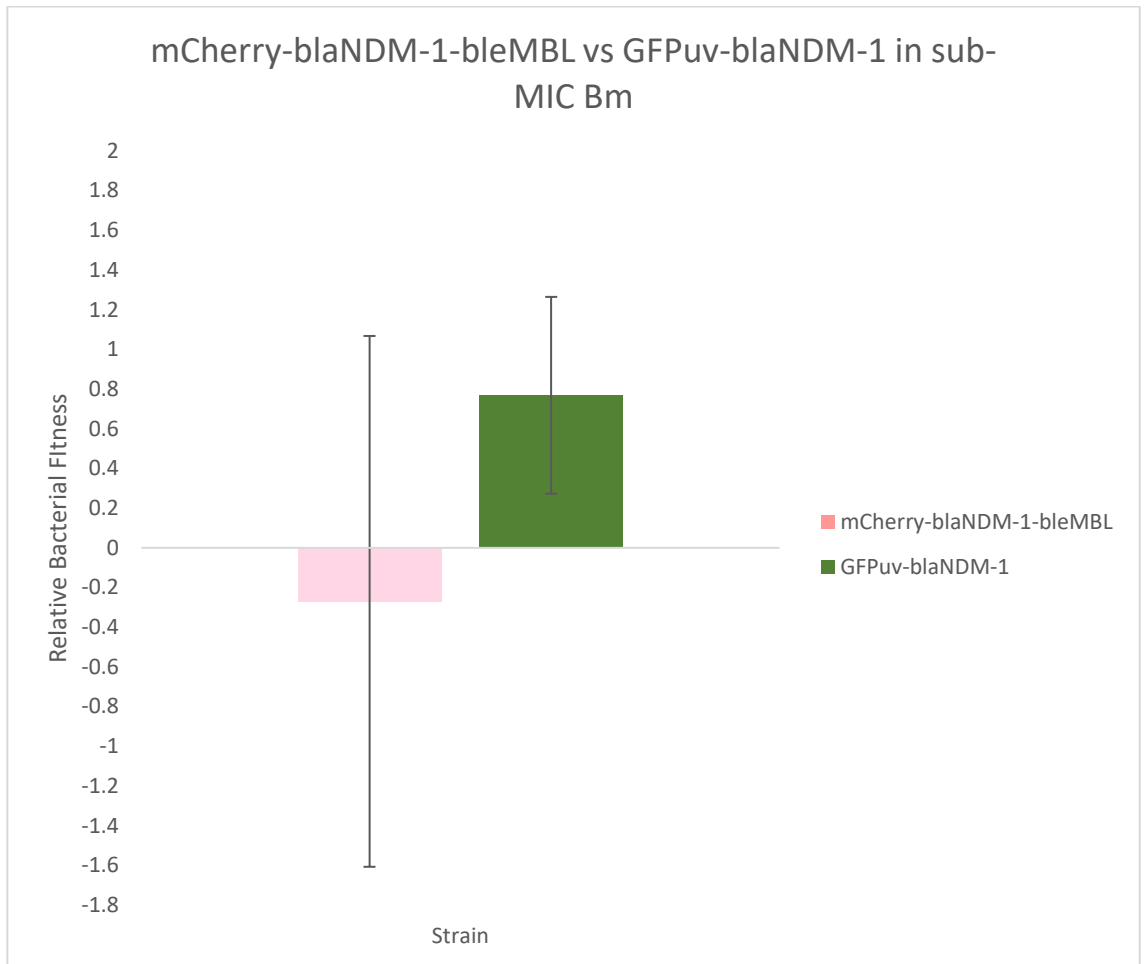
Figure 53: The relative bacterial fitness of the *E. coli* 5-alpha mCherry-*bla*$_{NDM-1}$-*ble*$_{MBL}$ strain and 5-alpha GFPuv-*bla*$_{NDM-1}$ strain in sub-MIC bleomycin (Bm). The 95% confidence interval is plotted for each strain (*n* = 6).
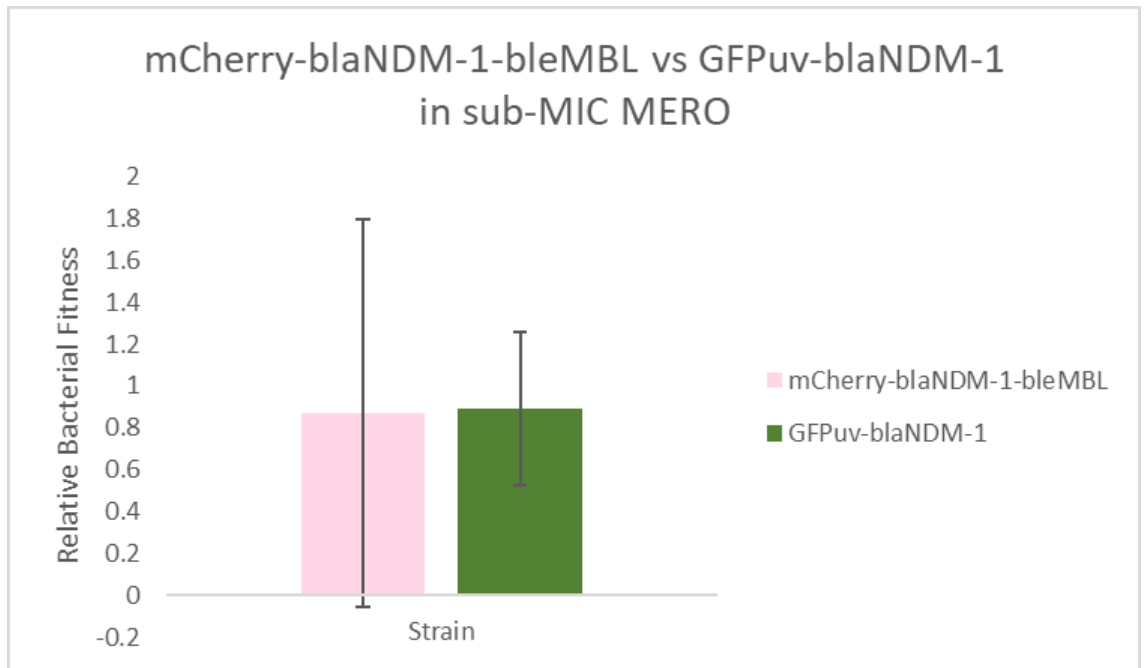
Figure 54: The relative bacterial fitness of the *E. coli* 5-alpha mCherry-*bla*NDM-1-*ble*MBL strain and 5-alpha GFPuv-*bla*NDM-1 strain in sub-MIC meropenem (MERO). The 95% confidence interval is plotted for each strain (*n* = 6).
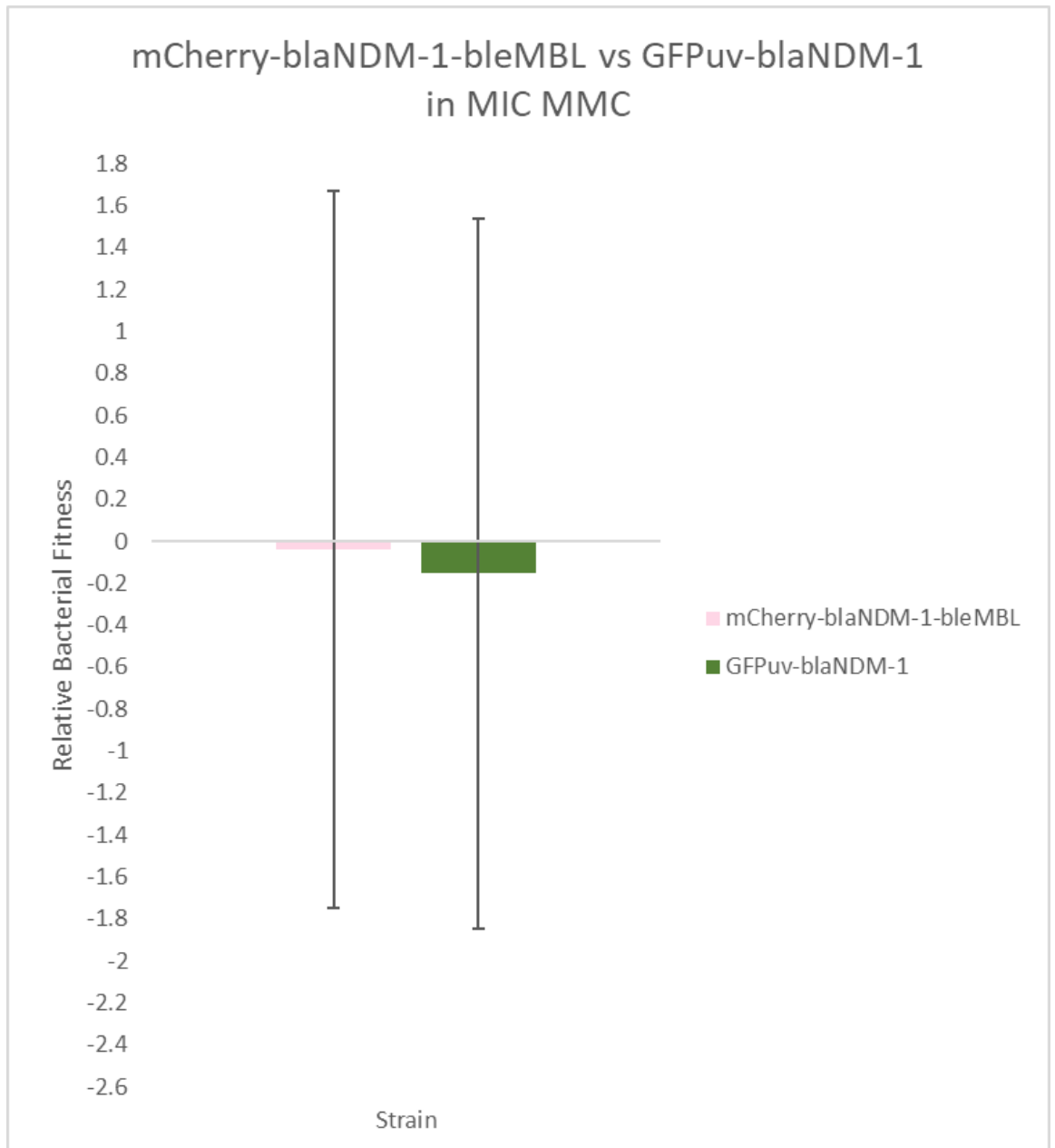
Figure 55: The relative bacterial fitness of the *E. coli* 5-alpha mCherry-*bla*$_{NDM-1}$-*ble*$_{MBL}$ strain and 5-alpha GFPuv-*bla*$_{NDM-1}$ strain in mitomycin C (MMC) at MIC. The 95% confidence interval is plotted for each strain (*n* = 5).
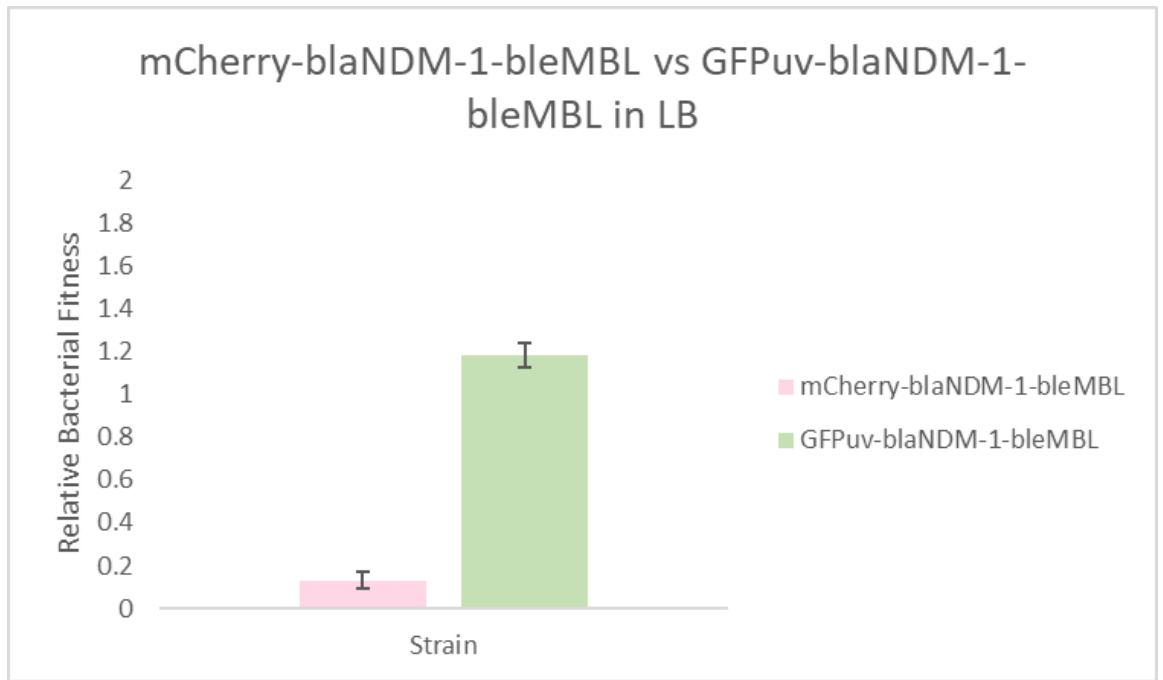
Figure 56: The relative bacterial fitness of the *E. coli* 5-alpha mCherry-*bla*NDM-1-*ble*MBL strain and 5-alpha GFPuv-*bla*NDM-1-*ble*MBL strain in normal LB. The 95% confidence interval is plotted for each strain (*n* = 2).

Table 11: Competition experiments conducted with different strains of *E. coli* 5-alpha containing either the mCherry or GFPuv fluorescent marker and either the bla_{NDM-1}, ble_{MBL} or bla_{NDM-1}-ble_{MBL} genes. The competition experiments were also conducted in the presence of different drugs at different concentrations: meropenem (MERO), bleomycin (Bm), mitomycin C (MMC) and no drug/normal conditions (LB). To count the number of bacterial cells present before and after the competition experiment, flow cytometry was used. The relative bacterial fitness for each strain was calculated and Mann-Whitney U tests were conducted to determine the statistical significance (significance cut-off $P < 0.05$). The exact significance value of each competition is presented, as well as replicates per competition. Associated figures from this thesis are presented in the final column.

Competition	Replicates (*n*)	Condition	Mann-Whitney U value	Exact Significance value	Associated Figure
mCherry vs GFPuv	3	LB	4.00	1.00	37
	3	2xMIC MMC	0.00	0.10	38
mCherry-bla_{NDM-1} vs GFPuv-bla_{NDM-1}	3	LB	0.00	0.10	42
mCherry-ble_{MBL} vs GFPuv-ble_{MBL}	3	LB	4.00	1.00	47
mCherry-ble_{MBL} vs GFPuv-bla_{NDM-1}	3	LB	0.00	0.10	48
mCherry-bla_{NDM-1}-ble_{MBL} vs GFPuv-bla_{NDM-1}-ble_{MBL}	2	LB	0.00	0.33	56
mCherry-bla_{NDM-1}-ble_{MBL} vs GFPuv-bla_{NDM-1}	4	LB	0.00	0.03*	52
	6	Sub-MIC Bm	8.00	0.13	53
	6	Sub-MIC MERO	14.00	0.59	54
	5	MIC MMC	12.00	1.00	55
mCherry-bla_{NDM-1} vs GFPuv-ble_{MBL}	3	LB	0.00	1.00	39
	3	2xMIC MMC	0.00	0.10	40
	2	Sub-MIC MMC	0.00	0.33	41
mCherry-ble_{MBL} vs GFPuv-bla_{NDM-1}-ble_{MBL}	2	LB	0.00	0.33	49
	3	Sub-MIC MMC	0.00	0.10	50
	3	2xMIC MMC	0.00	0.10	51
mCherry-bla_{NDM-1} vs GFPuv-bla_{NDM-1}-ble_{MBL}	3	LB	0.00	0.10	43
	3	Sub-MIC MERO	2.00	0.40	44
	3	MIC MMC	4.00	1.00	45
	6	Sub-MIC Bm	13.00	0.49	46

*$P < 0.05$

2.4.7. Mutation frequency is not affected by the presence of the *bla*_{NDM-1}, *ble*_{MBL} or *bla*_{NDM-1}-*ble*_{MBL} genes

Mutation frequency experiments on rifampicin selective plates was conducted to determine whether the presence of the *ble*$_{MBL}$ gene impacted the rate of mutation in the *E. coli* 5-alpha strains. The average mutation frequency of each strain is presented in Table 12. It was found that there was no significant difference between the mutation frequencies of the *E. coli* 5-alpha strains (χ^2(3) = 6.75, *P*= 0.08). This means that the presence of the *bla*$_{NDM-1}$, *ble*$_{MBL}$ or *bla*$_{NDM-1}$-*ble*$_{MBL}$ genes had no effect on the mutation frequency of *E. coli* 5-alpha. This indicates that the *ble*$_{MBL}$ gene has no effect on the integrity of the DNA, and doesn't stabilise the DNA against damage, as speculated in the paper written by Dortet *et al*. (2012). However, in the strains tested, the *E. coli* 5-alpha strain that had the *bla*$_{NDM-1}$-*ble*$_{MBL}$ had the lowest average mutation frequency.

Table 12: Average mutation frequency of the different *E. coli* 5-alpha strains. *E. coli* 5-alpha with either an empty pSTV 29 plasmid, the *bla*$_{NDM-1}$ gene, *ble*$_{MBL}$ or *bla*$_{NDM-1}$-*ble*$_{MBL}$ gene inserted were exposed to rifampicin selective plates to determine the mutation frequency of each strain. The 95% confidence interval for each strain is also presented (*n* = 17).

Inserted into *E. coli* 5-alpha + pSTV 29 plasmid	Average Mutation Frequency	95% Confidence Interval
Empty pSTV 29	6.61×10^{-8}	2.79×10^{-8} - 1.04×10^{-7}
bla$_{NDM-1}$	3.35×10^{-8}	-1.20×10^{-9} - 6.82×10^{-8}
ble$_{MBL}$	5.59×10^{-8}	1.07×10^{-8} - 1.01×10^{-7}
bla$_{NDM-1}$-*ble*$_{MBL}$	2.35×10^{-8}	1.33×10^{-8} - 3.37×10^{-8}

2.5. Discussion

2.5.1. The association between the bla_{NDM} gene and *ble* gene is prevalent

From the *ble* gene survey, it is clear that many organisms that host the bla_{NDM} gene also have the *ble* gene. From the limited search done in this current study, it was found that the most common bla_{NDM} variants associated with the *ble* gene were bla_{NDM-1} and bla_{NDM-5}. It may not be unusual that the *ble* gene is commonly associated with the bla_{NDM-1} and bla_{NDM-5} variants as they are the variants most commonly mentioned in the literature. For instance, a study conducted by Bi *et al*. (2018) found that out of the 53 carbapenem-resistant *E. coli* isolates from different hospitals in China, 58.5% were the bla_{NDM-5} variant and 26.4% were the bla_{NDM-1} variant. In a different study conducted by Rahman *et al*. (2014), they showed that even across different organisms such as *K. pneumoniae*, *E. coli, Citrobacter* species, *Enterobacter* species and *Providencia* species, bla_{NDM-1} was the most common NDM variant found in a tertiary hospital in India. In another study, Rahman *et al.* (2018) found that in clinical carbapenem-resistant *E. coli* isolates from a south Indian hospital, the most common NDM variant was the NDM-1 variant. It would be interesting to look in depth at the hydrolytic ability of the NDM variants found in the gene survey and whether the presence of the *ble* gene changes that ability and could account for the reason why we see such a high prevalence of the *ble* gene in the NCBI database. It is important to note that other bla_{NDM} variants may be associated with the *ble* gene, but poor gene annotations and the limitations of the NCBI database limit the scope of this study.

Another element that needs to be considered when looking at the data present in the NCBI database is the disparity and biases that exist between high income and low to middle income countries. It is likely that many of the sequences that have been uploaded to the NCBI database are from isolates of clinical significance found in high income countries. Many of our interests in bacteria stem from understanding these bacteria in a more clinical setting, to overcome infections and the issue of antibiotic resistance, rather than looking at all of the bacteria present in an environment (Kwong *et al.*, 2015). Low to middle income countries are less likely to contribute towards genomic projects due to a lack of funding which renders them unable to afford the laboratory infrastructures as well as equipment and reagents that are associated with genome sequencing projects (Acharya and Pathak, 2019; Hetu *et al.*, 2019). Low to middle income countries are more likely to use their limited resources to address immediate issues such as controlling infection and disease and improving quality of life, rather than sequencing efforts which may lead to under-representation of global bacterial strains (Acharya and Pathak, 2019).

2.5.2. Cloned pSTV 29 plasmid stability

The *E. coli* 5-alpha strains that were constructed with the different combinations of genes of interest were stable after passaging the cells over 4 days with no selective antibiotic. This gives us the confidence in any downstream experiments that any daughter cells from the original host cells will inherit the marked plasmids and will not be randomly lost during experiments, especially during competition experiments as we are selecting for a gene that is present on the constructed plasmid (Wein *et al.*, 2019). For the purposes of this experiment, we ensured that all of the competing strains contained the desired constructed plasmid and that the plasmid was maintained in the host. However, it is important to note that in a realistic environment, plasmids can be lost or stabilised depending on a range of different factors and stressors. In a paper by Wein *et al*. (2019), they looked specifically at plasmid stability in two different growth temperatures (37˚C to mimic the optimal growth temperature of *E. coli* and 20˚C, a colder temperature which is stress inducing). In the study conducted by Wein *et al*. (2019) they found that the host bacteria grown at 37˚C lost the plasmid faster than their counterparts grown in 20˚C with no selective pressure. In order to expand this research further, the evolution and maintenance of our plasmids should be viewed in a larger context and also take into account other bacteria that may compete for resources that can affect plasmid stability.

2.5.3. Variable growth curves

In the mCherry-marked strains there appeared to be no significant difference in the growth of the strains except in the strain that carried the ble_{MBL} gene under normal MHB conditions which grew slower than the other strains. This is not illogical as any genes that are not required under normal growth conditions e.g. antibiotic resistance genes, would be expected to be an energy burden to maintain because they may affect important biological functions in the cell (Melnyk *et al*., 2015). Due to the variability of the data, it is difficult to determine whether we see the same reduced growth in the mCherry-bla_{NDM-1}-ble_{MBL}. It would be expected that the mCherry-bla_{NDM-1}-ble_{MBL} strain grows in a similar way to the mCherry-ble_{MBL} strain, if not worse due to the energy burden of two resistance genes, unless the presence of the bla_{NDM-1} ameliorates this. In contrast, when the mCherry-marked strains were exposed to 2 µg/mL Bm, the mCherry-ble_{MBL} grew better than the mCherry-bla_{NDM-1}-ble_{MBL} strain. It could be possible that the bla_{NDM-1} gene incurs a fitness cost and the ble_{MBL} gene confers a small fitness cost, or even incur no fitness cost that can be detected under laboratory conditions (Melnyk *et al*., 2015).

In the GFPuv-marked *E. coli* strains, it is not clear why there is such diversity in the GFPuv-only strain, as three replicates were performed simultaneously and it is difficult to pinpoint the odd OD readings to one of the replicates to exclude that data. Under normal conditions, it appears

as if the GFPuv-*ble*$_{MBL}$ strain struggled to grow normally, compared to the other GFPuv-marked strains. It is clearer to see in Figure 9, that the GFPuv-*bla*$_{NDM-1}$ strain grew better than the other GFPuv-marked strains (*ble*$_{MBL}$ and *bla*$_{NDM-1}$-*ble*$_{MBL}$), and this may again be due to a reduced energy burden under normal conditions. In contrast, when the GFPuv-marked strains were exposed to 2 µg/mL Bm, the GFPuv-*ble*$_{MBL}$ grew better than the GFPuv-*bla*$_{NDM-1}$-*ble*$_{MBL.}$

2.5.4. MIC testing of constructed strains

It is possible that having the fluorescent markers in the strain may have some small effects on the ability to resist the effects of antibiotics, which may be the result of an energy cost that the cell cannot cope with. In this situation it appears that the mCherry gene may be more costly than the GFPuv gene, as summarised in Table 9 (section 2.4.5). However, it is not clear why the *bla*$_{NDM-1}$-*ble*$_{MBL}$ genes are able to resist the effects of MERO more than the GFPuv-*bla*$_{NDM-1}$ gene as it would be expected that the extra gene present in the *bla*$_{NDM-1}$-*ble*$_{MBL}$ in the strain would be more costly than having just one of the genes present.

The CIP MIC testing shows a variety of results (see Table 9, section 2.4.5), depending on the genes that are inserted into the pSTV 29 plasmid. Many of the strains were killed at the lowest concentration of CIP tested (0.0625 µg/mL), but the GFPuv-*bla*$_{NDM-1}$ strain showed an MIC of 1 µg/mL. The 5-alpha strains mCherry-*bla*$_{NDM-1}$-*ble*$_{MBL}$ and GFPuv-*ble*$_{MBL}$ had MIC values of 2 µg/mL. It appears as if no particular gene combination is linked to an increase or decrease in CIP MIC. At first glance, it appears as if the presence of the *ble*$_{MBL}$ could be responsible for the higher MIC values, however if this were true, a higher MIC value would also be expected in the strains mCherry-*ble*$_{MBL}$ and GFPuv-*bla*$_{NDM-1}$-*ble*$_{MBL}$, which is not the case. The MICs we see could be due to the presence of the *ble*$_{MBL}$ gene in combination with the fluorescent marker (mCherry or GFPuv).

When we tested the *E. coli* 5-alpha strains against GENT and NA, we observed no differences between the MIC values with different gene inserts. At the time of writing, there appears to be no instances in the literature where the presence of certain genes or mutations cause a decrease in the susceptibility of bacteria to CIP but show no change in the MIC when we test NA. Past studies have demonstrated that mutations that lead to a lower susceptibility to NA either have no effect on CIP resistance or also lower the susceptibility of the bacteria to CIP, for instance in *Campylobacter coli* and *Campylobacter jejuni* that were isolated from animals where two mutations in *gyrA* were responsible for the change in the resistance profile (Jesse *et al.*, 2006).

When the strains were tested against the antibiotic TET, there was a slight difference in the MIC values, where the control strains (5-alpha, mCherry-marked, GFPuv-marked) had an MIC of 0.5 µg/mL and the strains that had genes inserted into the pSTV 29 plasmid had an MIC of 0.25 µg/mL, with the exception of the strain carrying mCherry-bla_{NDM-1} which had an MIC value of 0.5 µg/mL. However, this difference is within the range of error for this technique.

In a study conducted by Wang *et al*. (2020a), an extensively-drug resistant *E. coli* W60 strain was isolated from a bladder tumour patient and was found to be resistant to many antibiotics – including β-lactam and β-lactamase inhibitor combinations. This *E. coli* isolate was determined to be highly resistant to several antibiotics due to the presence of multidrug resistance plasmids and the presence of bla_{NDM-5}. In addition, bla_{NDM-5} was thought to be enhanced by the presence of the co-expressed ble_{MBL} gene. The authors tested the impact of the ble_{MBL} gene on the bla_{NDM-5} gene by cloning into a pBCKS plasmid, transforming the plasmid into *E. coli* DH5α and comparing their resistance profiles. In the strains that contained the ble_{MBL} gene, increased resistance was seen for AMP, ceftazidime and cefoxitin (Wang *et al*., 2020b). In our study, when comparing the bla_{NDM-1} against bla_{NDM-1}-ble_{MBL} strains, we saw an increase in the MIC values across three replicates against MERO. The mCherry-bla_{NDM-1} *E. coli* 5-alpha cells had an MIC of 1 µg/mL against MERO, whereas the mCherry-bla_{NDM-1}-ble_{MBL} *E. coli* 5-alpha strain had an MIC of 4 µg/mL. When we look at the GFPuv-labelled *E. coli* 5-alpha strains, the GFPuv-bla_{NDM-1} strain had an MIC of 4 µg/mL and the GFPuv-bla_{NDM-1}-ble_{MBL} strain had an MIC of 8 µg/mL against MERO. In our study, we also tested the susceptibility of our cloned strains against the antibiotic AMP, but all of the strains we generated grew up to the upper limit of the concentrations we tested, and we did not go above 64 µg/mL.

For future work, it would be interesting to see if there are changes in the MIC between the bla_{NDM-1} and the bla_{NDM-1}-ble_{MBL} labelled *E. coli* strains, and if they are in agreement with the results seen in the Wang *et al*. (2020b) study for AMP-derived antibiotic treatments such as amoxicillin-clavulanate, ceftazidime-avibactam and piperacillin-tazobactam. In the Wang *et al.* (2020b) study, the bla_{NDM-5} gene in *E. coli* DH5α gave an MIC value of 64 µg/mL and the bla_{NDM-5}-ble_{MBL} cloned *E. coli* had an MIC of 128 µg/mL when AMP was used, but the ble_{MBL} gene on its own in *E. coli* DH5α was not tested for its susceptibility to AMP. Further investigation of the strains is also needed against the antibiotic CIP, as we can see that the bla_{NDM-1} gene and the ble_{MBL} gene alone have an MIC of <0.0625 µg/mL but when the strains were labelled with the mCherry fluorescent marker, the MIC increased to 2 µg/mL. In contrast, when the strains were labelled with GFPuv, the ble_{MBL} construct had an MIC of 2 µg/mL, whereas bla_{NDM-1} had an MIC of 1 µg/mL and the bla_{NDM-1}-ble_{MBL} construct had the lowest MIC of <0.0625 µg/mL. From these results, it is possible that exposing bacteria to Bm in cancer therapy could select for bacterial strains that carry the ble_{MBL} gene which in turn may select strains that also carry a bla_{NDM} gene.

Selecting for bacterial strains that carry NDM genes in cancer patients can be dangerous as they are already immunocompromised and susceptible to secondary bacterial infections, especially infections caused by *A. baumannii*, a notorious nosocomial pathogen that the WHO have classified as a critical priority for human health, and is found to be resistant to many carbapenem antibiotics (Imai *et al.*, 2019; Tran *et al.*, 2018).

2.5.5. Competition/Fitness experiments

From the competition experiments conducted in liquid broth and then plated onto agar plates, we found no significant difference when different strains were competed against each other and in different antibiotic conditions. In terms of the control strains that were tested to determine whether there could be biases due to the marker the strain carried, no significant effect (as determined by Mann-Whitney U tests) was found. It could be possible that the colony counts before and after the competitions were limited by the size of the agar plates. This means that cultures were diluted in order to be plated, and because the samples were diluted we were unable to get finer, more accurate counts. We attempted to resolve this issue by using the BD LSRFortessa flow cytometer to count our bacterial cells that can be differentiated by their fluorescent marker present.

Similarly to the plate count method above, when the samples before and after competition were analysed with the BD LSRFortessa, no significant difference in the competition was found when tested using the Mann-Whitney U tests, with the exception of one competition. In the competition between mCherry-bla_{NDM-1}-ble_{MBL} and GFPuv-bla_{NDM-1}, there was a significant difference between the relative fitness values when the two strains were competed in plain, LB broth ($U = 0.00$, $P < 0.05$), with the mCherry-marked strain having a higher average relative fitness value than the GFPuv-marked strain. Under different antibiotic conditions (sub-MIC Bm, sub-MIC MERO and MIC MMC), there was no significant difference between the mCherry-bla_{NDM-1}-ble_{MBL} and GFPuv-bla_{NDM-1} strains. These experiments demonstrate that having the ble_{MBL} gene may confer a fitness advantage to the *E. coli* strains when it is coupled with the bla_{NDM-1} gene under normal, stress-free conditions. It is not clear however, why the complementary experiment with GFPuv-bla_{NDM-1}-ble_{MBL} and mCherry-bla_{NDM-1} did not demonstrate the same difference in fitness. It could be that these experiments need more replicates to reduce variability in the results and to confirm a difference between the marked strains. It appears that even though the bla_{NDM-1}-ble_{MBL} genes are beneficial under normal conditions, the advantage is not through stabilising the *E. coli* genome, as suggested by the Dortet *et al*. (2012) study, and protect against DNA damage or, the advantage is too costly in stress conditions to maintain. There are other experiments that need to be considered here, that should be done in future

research. For instance, other abiotic conditions such as temperature, could be manipulated to determine whether carriage of the ble_{MBL} resistance gene confers a benefit for survival under different stressors (Wein *et al.*, 2019).

It is puzzling that when we look at the growth curve data that we can see differences in the growth between the different strains, but when the competition experiments are conducted, we don't see these differences. It is possible, that as NDM-1 is secreted from bacteria in outer membrane vesicles (OMVs) as a public good, that the Bm resistance protein is also exported out of the cells with NDM-1 (González *et al.*, 2016). As the secreted OMVs are a public good, the benefits of the contents may also benefit the bacteria that are in close proximity (López *et al.*, 2021). In the case of the competition experiments, we don't see any differences between the strains as the strains that don't produce NDM-1 or the Bm resistance protein themselves still reap the benefits of the producer strain. In the future, competition experiments should be conducted in a different condition where the non-producer is less likely to benefit from the contents of the OMVs, for instance conducting the competition experiments on agar plates where it is more difficult for the OMVs to diffuse in the environment.

Another aspect of the competition experiments that could be improved in this study would be to use specific bead counting kits or using a combination of antibodies and viability markers in order to give accurate counts of all of the cells in the sample (absolute counts). ThermoFisher have beads available for this purpose such as the CountBright and CountBright Plus Absolute Counting Beads that have a specific concentration of microspheres in solution that can be run on the flow cytometer to calculate the number of microsphere events. Another element that could be added to the competition experiments that were run on the flow cytometer would be the use of live/dead staining (for instance, the ThermoFisher LIVE/DEAD *Bac*Light™ Bacterial Viability and Counting Kit, for flow cytometry) to determine whether the cells present in our sample are alive or dead, and the number of these relative to the overall population (whether they are labelled with mCherry or GFPuv). This would also help the sensitivity of the experiments as it would be easier than to remove any cell debris that could be falsely counted as events when running the samples through the flow cytometer.

In the competition experiments, we controlled for any fitness costs associated with the addition of the GFPuv or mCherry fluorescent marker to ensure that carrying the specific gene and the expression of the protein wasn't to the detriment of the *E. coli* strain. However, it may have also been prudent to compete the unlabelled *E. coli* 5-alpha strain against each of the strains that contained either the GFPuv or mCherry gene. Conducting control experiments in this way would allow us to see the overall effects of the fluorescent genes on the 'normal' ancestor strain and

would be easier to compare the action of each marker gene. In a study by Wendling *et al.* (2021), the authors examined whether the carriage of prophages with and without antibiotic resistance genes affected the fitness of bacteria. In their study, the competing strains of *E. coli* K-12 MG1655 that is susceptible to the phages and antibiotics they were testing was labelled with yellow-super-fluorescent protein marker. To account for fitness effects as a result of the fluorescent marker, they subtracted the difference in the relative fitness of the wildtype strain and the labelled wildtype strain from the lysogen (prophage that has integrated into the bacterial chromosome) relative fitness value in the different environments they were testing. By conducting controls in this way, we can generate relative fitness values that demonstrate the actual cost of the *E. coli* cells that have a plasmid with a fluorescent marker gene.

In the future, further experiments such as qPCR need to be conducted in order to confirm that there are no differences in expression levels for our genes of interest (mCherry, GFPuv, bla_{NDM-1} and ble_{MBL}) that may be having an effect on the competition experiments. As there is no terminator sequence downstream of the bla_{NDM-1}, ble_{MBL} or bla_{NDM-1}-ble_{MBL} genes, it is possible that single transcripts were produced that contained the open reading frames (ORFs) coding for both the genes of interest (bla_{NDM-1}, ble_{MBL} and bla_{NDM-1}-ble_{MBL}) and the fluorescent proteins (mCherry and GFPuv). However, this would not result in fusion proteins, as even if the stop codons were read through by ribosomes, the mRNA sequence between the ORFs is not a continuous sequence of in-frame codons, and so translation would be terminated. It is possible that some of the differences in the data, for instance the MIC data, may be due to different transcript lengths. As transcription and translation are closely linked (transcription-translation coupling), messenger RNA (mRNA) can be translated as soon as DNA has been transcribed in the same cellular compartment (Blaha and Wade, 2022). We would expect shorter transcripts to therefore be translated and expressed quicker, and provide a competitive advantage. However, the exact dynamic within the bacterial cell is not clear, as our bla_{NDM-1} is in the same operon as the ble_{MBL} gene but translation of an ORF can impact transcription and terminate the transcription of downstream genes (Blaha and Wade, 2022). What is also important to note is that the mRNA produced after transcription can form secondary and tertiary structures that may affect translation efficiency, which from this study we have not determined whether the individual or joint transcripts can form structures that impact mRNA translation (Gingold and Pilpel, 2011).

From our data, the shorter bla_{NDM-1} and ble_{MBL} transcripts result in lower and higher MICs respectively than the longer joint (bla_{NDM-1}-ble_{MBL}) transcript. It is possible that expression of ble_{MBL} when it is not associated with bla_{NDM-1} is higher, as the ble_{MBL} transcript is shorter than the bla_{NDM-1} transcript and may take less time to transcribe which may be reflected in the MIC data, where the constructs with the fluorescent marker and ble_{MBL} resulted in an MIC of >512 µg/mL

when exposed to bleomycin whereas the bla_{NDM-1}-ble_{MBL} constructs had an MIC of 64 µg/mL. When we look at our competition experiments, the only experiment that was statistically significant ($P<0.05$) was between mCherry-bla_{MBL}-ble_{MBL} and GFPuv-bla_{NDM-1} where the mCherry strain was more fit in LB. In this scenario, the distance between the bla_{NDM-1} promoter and the bla_{NDM-1} gene is the same in both strains and we would expect similar expression levels and would not expect a competitive advantage due to the way the genes were cloned into the plasmids. However, by conducting qPCR, we would be able to determine if the levels of gene expression are unequal and how this may affect competition between bacterial strains.

2.5.6. Mutation frequency

Initially from the mutation frequency experiments it appears as if the pSTV 29 plasmid on its own with no inserted genes had the highest mutation frequency of 6.61 x 10^{-8} (compared to the bla_{NDM-1}, ble_{MBL} and bla_{NDM-1}-ble_{MBL} inserted plasmids). The bla_{NDM-1}-ble_{MBL} gene cassette in the pSTV 29 plasmid had the lowest mutation frequency of 2.35 x 10^{-8}. When a Kruskal-Wallis test was used, there was no significant difference between the strains in terms of their mutation frequencies. This indicates that the presence of the different inserted genes had no effect on the mutation frequency of *E. coli* 5-alpha. It is possible that the large variability between the 17 replicates for each strain impacted the average mutation frequency which then impacted the statistical analyses. In order to resolve this in the future, more replicates should be conducted. The mutation frequency experiments were also conducted in the presence of the antibiotic rifampicin, but it is possible that the mutation frequencies for each strain will change depending on the antibiotic the strains are exposed to, and also the environmental conditions they are in. In a study conducted by Blot *et al*. (1991), it was discovered that the *E. coli* K-12 strains that expressed the Bm resistance gene product were more fit than the wildtype ancestor and appeared to protect against DNA damaging agents such as ethyl methanesulfonate (EMS). What is important to note in this study is that the Bm resistance gene studied was present on the Tn*5* transposon, it is not clear whether the different forms of the Bm resistance gene impact bacterial phenotype and fitness equally. In a different study conducted by Dortet *et al*. (2012), it was found that the expression of the ble_{MBL} gene (associated with the bla_{NDM-1} gene) reduced mutation frequency by approximately 2.4-fold compared to the reference strain used in the study that had no plasmid present but had a defective DNA repair system which presented as a hypermutable phenotype. The strains in this study were exposed to rifampin (rifampicin). It is difficult to understand without further investigation why the strains used in this our study demonstrated no difference in the mutation frequency whereas the hypermutator strain used in the Dortet *et al.* (2012) study was able to compensate for the defective DNA repair system and even resist mutagenesis when expressing the ble_{MBL}. If the experiment was repeated on a

larger scale with more replicates, it is possible that we would be able to see a significant difference between the different *E. coli* 5-alpha strains.

It is important to note that in this study, we studied whether carrying both the bla_{NDM-1} and the ble_{MBL} gene conferred a fitness advantage to *E. coli* 5-alpha. However, as mentioned previously, there are other Bm resistance genes that have been found and annotated in genome sequences on databases such as NCBI. It could be that other genes are needed in order for a bacterial strain to demonstrate the benefits of carrying both the bla_{NDM-1} and ble_{MBL} gene. For instance, other genes and elements that have been found associated with these two genes include insertion sequences IS*Ec33*, IS*Sen4* and a (truncated) phosphoribosyl anthronilate isomerase (*trpF*) (Dortet *et al.*, 2012). In the initial *ble* gene survey conducted, across many of the bacterial species looked at, many genes appeared on multiple occasions. For instance, *folP* (dihydropteroate synthase), *manA* (mannose-6-phosphate isomerase), *tnpA* (transposase from transposon Tn*3*), *tat* (twin-arginine translocation pathway signal proteins) and *dsbC* (thiol:disulfide interchange protein). It is not clear how these genes interact throughout the cell, and it is possible that the bla_{NDM-1} and ble_{MBL} genes are only beneficial and may confer a fitness advantage in the presence of these other genes and may even benefit from compensatory mutations that we have not investigated in this study. It should also be noted that we looked at the bla_{NDM-1} gene in this study, but the *ble* gene was found downstream of various bla_{NDM} genes in our *ble* gene survey, such as NDM-2, -4, -5, -7, -9, -13, -17, -20. It would be interesting in future studies to determine whether the *ble* gene is the same across all of the NDM variants, as it may impact on the resistance phenotypes we see.

The Bm resistance gene can also be found on different MGEs, such as the pUB110 plasmid and the Tn*5* transposon. In a study by Blot *et al*. (1994), they demonstrated that on the Tn*5* transposon, the ble_{MBL} gene reduces the rate of death in *E. coli* cells when they were in the stationary phase of growth and appears to enhance the DNA repair of the cells. They also concluded that the ble_{MBL} gene improved the fitness of the host in the competition experiments they conducted, and that the benefits seen from the Tn*5* containing strains was dependent on a functioning *aidC* gene. Further research into the fitness associated costs and benefits of carrying a ble_{MBL} gene should be investigated in other instances where it is found in bacteria, for instance on the pUB110 plasmid and on the Tn*5* transposon.

3.   Chapter 3 – *de novo* mutations in response to bleomycin exposure

3.1. Introduction

3.1.1. Antibiotic resistance and cross-resistance

Cross-resistance occurs when a resistance gene can confer protection against other antimicrobials (Cheng *et al*., 2019). Cross-resistance is thought to occur with antimicrobials that are part of the same family or share a similar structure that can be recognised by the resistance mechanisms employed by the bacteria (Cherny *et al*., 2021). In a study conducted by Hines *et al*. (2019), they highlighted cross-resistance that could be seen between glycopeptides, lipopeptides and lipoglycopeptides that are commonly used to treat multidrug-resistant *S. aureus* infections. The cross-resistance seen to the antimicrobials was concluded to be a result of a changing membrane lipid composition (Hines *et al*., 2019). Cross-resistance can be driven by exposure to sub-lethal concentrations of antimicrobials. In a study by Ching and Zaman (2020), it was found that when *E. coli* were exposed to a range of CIP concentrations (from 0% to 110% of the MIC), there were a variety of mutations that allowed resistance to different classes of antibiotics. The phenotype of the *E. coli* was a result of mutations seen in efflux systems, for example the *acrR* efflux regulator that represses the transcription of the *acrB* gene (which encodes a multidrug efflux pump) (Ching and Zaman, 2020). Although the low-level resistance seen in this study is not of statistical significance, it demonstrated that events like this can stimulate problems of a larger scale in terms of the antibiotic resistance problem where a reduced susceptibility to other antibiotic classes can be seen (Figure 57).
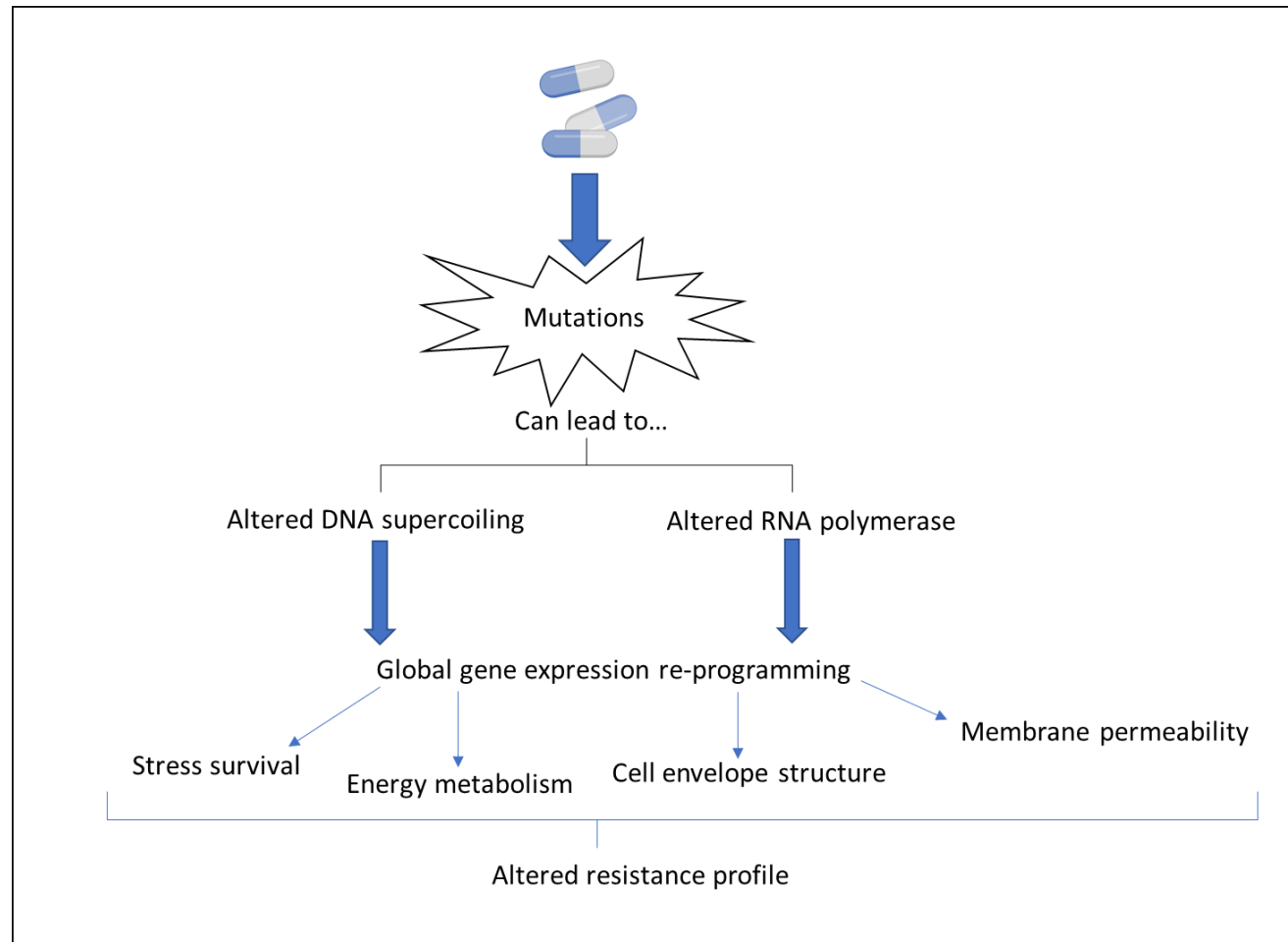
Figure 57: Changing bacterial resistance profiles in response to drug exposure. Diagram modified from Pál *et al.* (2015), made using BioRender. An antibiotic can be available at a low concentration that can lead to genetic mutations in bacteria that may impact DNA or RNA polymerase which can then in turn affect the global gene expression. Changes to global gene expression can then have an impact on the cell envelope structure, energy metabolism, membrane permeability and stress survival. These changes can lead to an altered resistance profile of the bacteria present.

Cross-resistance has strong ties to the antibiotic resistance problem, but it has also been shown that adaptation to an antimicrobial can impose its own cost on the bacteria (Trampari *et al.*, 2021). In a study by Trampari *et al.* (2021), *S.* Typhimurium exposed to azithromycin at sub-inhibitory concentrations were able to evolve resistance to the antibiotic they were subsequently exposed to, but at the detriment of biofilm formation and the virulence of the strain. The ability of *S.* Typhimurium to resist the effects of the antibiotics was determined to be mainly due to a SNP seen in the *acrB* gene, a multidrug efflux pump (Trampari *et al*., 2021). In a similar study conducted by Wardell *et al*. (2019), *P. aeruginosa* PAO1 was exposed separately to three different antibiotics (CIP, MERO and tobramycin) to generate mutants that were highly resistant to the antibiotics they were challenged with. The mutants that arose from the study were whole genome sequenced to identify the mutations that led to the resistance phenotype and tested for cross-resistance to antibiotics from different classes. When *P. aeruginosa* were exposed to tobramycin, the mutants that were generated were less susceptible to the action of the carbapenem antibiotics tested, with a particularly high resistance to the carbapenem imipenem. Although cross-resistance was seen in this study, collateral sensitivity was also seen where they saw an increase in the susceptibility of the mutants to certain antibiotics (Wardell *et al.*, 2019). When *P. aeruginosa* PAO1 was exposed to CIP and mutants were generated, collateral sensitivity was seen where the cells were more sensitive to carbapenems or aminoglycosides (Wardell *et al.*, 2019). It is worth noting that although the mutants generated in the study were able to resist the effects of a range of antibiotics, in the absence of a selective pressure in the form of an antibiotic, the mutants were unable to grow as well as the parental *P. aeruginosa* PAO1 strain and were deemed less fit and reflected the cost of gaining antibiotic resistance (Wardell *et al*., 2019).

3.1.2. SOS response and translesion synthesis

As mentioned previously in section 1.10.2, the SOS response is triggered when the bacterial cells are under stress conditions and can provide an advantage when exposed to antibiotics and the bacterial DNA is damaged (Torres-Barceló *et al.*, 2015). The induction of the SOS response is dependent on the magnitude of the DNA damage, whether it be through the direct action of an antibiotic on DNA or an indirect action on DNA, for instance through the generation of reactive oxygen species (Dörr *et al*., 2009; Jara *et al*., 2015). It has also been seen in the literature, that the activation of the SOS pathway after exposure to certain antibiotics (e.g. AMP and kanamycin) and agents leads to an increase in mutation rate of bacteria (Kohanski *et al.*, 2010; Torres-Barceló *et al*., 2015).

During the SOS response, many genes are induced in order to repair DNA, including genes involved in TLS (Norton *et al.*, 2013). It has been demonstrated in a variety of bacteria, including *A. baumannii* that the activity of error-prone DNA polymerases that are activated during the SOS response to conduct TLS encourages the evolution of the organism to resist the action of antimicrobials or other environmental stressors by the misrepair of DNA lesions (Norton *et al.*, 2013).

Theoretically, the anti-cancer drug Bm that induces double-strand DNA breaks in both human and bacterial cells may invoke the SOS response and result in erroneously repaired DNA through the use of DNA polymerases activated in TLS. The inaccurate repair of the DNA may lead to the introduction of SNPs that may affect the ability of the organism to resist the effects of different classes of antibiotics or stressors.

3.2. Aims
The aim of this project was three-fold:

1) to determine whether bacteria that are exposed to a sub-inhibitory concentration of Bm become less susceptible to the drug through the action of *de novo* mutations
2) to determine whether the mutants that arise demonstrate an increased or decreased susceptibility to other antibiotics (cross-resistance)
3) to determine whether exposure to Bm alters the bacterial mutation rate.

We hypothesise that exposure to a sub-inhibitory concentration of bleomycin would lead to a lower susceptibility to bleomycin in our bacterial strains. We hypothesise that the mutations that lead to a lower susceptibility to bleomycin would provide cross-resistance to other antibiotics. We also hypothesise that exposure to bleomycin will increase the mutation rate of the bacterial strains.

3.3. Methods

3.3.1. Minimum inhibitory concentration testing
Bacterial organisms that were selected to use in this study included: *E. coli* ATCC 25922, *E. coli* NCTC 10418, *S. aureus* ATCC 25923, *S. aureus* NCTC 6571, *P. aeruginosa* ATCC 27853, *P. aeruginosa* NCTC 10662, *Enterococcus faecium* ATCC 7171 and an *E. faecium vanB*-positive clinical isolate. The panel of antibiotics used through MIC testing consisted of AMP, CHL, CIP, GENT, NA and TET (as described in Chapter 2, section 2.3.2). The ranges of antibiotic

concentrations that were used against the bacteria were determined using the European Committee on Antimicrobial Susceptibility Testing (EUCAST) guidelines for interpreting breakpoint values. MICs were determined as described in Chapter 2, section 2.3.2. To determine the inhibitory properties of the solvent DMSO, a concentration range of 0-4% DMSO was used as well as a 50% and 100% DMSO treatment for MIC testing. The concentrations of Bm that were tested ranged from 0.125-64 µg/mL. When adding Bm dissolved in DMSO to the 96-well plates, less than 0.1% of DMSO was calculated to be administered to each well.

3.3.2. Testing the solubility of bleomycin in water

The Bm used in this study was dissolved in the solvent DMSO. The purpose of this experiment was to see whether Bm could be diluted in water for experiments, rather than DMSO which would increase the volume of DMSO being used. DMSO has been shown at high concentrations to have effects on the cell and can cause cell death. Bm that had been initially solubilised in DMSO was used at a concentration of 1000 µg/mL as a stock solution. The Bm stock solution was then diluted to the concentrations 10, 20, 30, 40, 50, 60 and 70 µg/mL using sterile distilled water in Eppendorf tubes. After dilution, these tubes were vortexed for 30 seconds to see whether Bm came out of solution. These tubes were then left in the -20˚C freezer to see whether Bm came out of solution after it was defrosted.

3.3.3. Bleomycin MIC on agar plates

MHA plates were set up with final concentrations of Bm ranging from 0.125-64 µg/mL, and in parallel DMSO controls were set up, as well as plain MHA plates for normal growth controls. Each of the organisms was standardised to a McFarland 0.5 standard (OD$_{600}$: 0.08-0.1) before being inoculated on the plates using a multipoint inoculator. The plates were then incubated overnight at 37˚C before being read.

3.3.4. Mutation induction experiments on agar plates

The method used in this experiment was adapted from Auda (2007). The purpose of this experiment was to determine whether Bm can encourage mutations that lead to reduced susceptibility to the antibiotics tested. The bacterial organisms used previously were grown overnight in 10 mL of MHB. Before pouring agar plates, the MIC of the chosen antibiotic was added into the molten MHA (Table 13). The tube containing the MHA and antibiotic is gently inverted before pouring into a plate and left to set. Bm drug discs were prepared by adding Bm at peak plasma concentration (2 µg/mL) to paper discs and then left to dry. The overnight culture of the chosen organism was then standardised to a 0.5 McFarland standard (OD$_{600}$: 0.08-0.1)

before being swabbed onto the corresponding agar plate and left to dry. The dry Bm disc was then applied to the agar plate, with a control disc containing 5 µL DMSO placed on the other half of the plate. The plates were then incubated for 18 hours at 37°C. An organism control plate was also set up where the organism was swabbed onto a plain MHA plate and left to incubate overnight at 37˚C. Each experiment was replicated in triplicate for each antibiotic tested.

Table 13: Antibiotic concentrations used to make minimum inhibitory concentration (MIC) plates for the mutation induction experiments on Mueller-Hinton agar (MHA) plates. The mode average was used for each antibiotic. Values with a (*) are mean averages (*n*= 4). Values with a (**) are median averages (*n*=4).

Organism tested	Antibiotic	Concentration of antibiotic in the MHA plate µg/mL
E. coli ATCC 25922	AMP	4
E. coli NCTC 10418		2
S. aureus ATCC 25923		0.03
S. aureus NCTC 6571		0.03
E. faecium ATCC 7171		1
E. coli ATCC 25922	CHL	4
E. coli NCTC 10418		2
S. aureus ATCC 25923		8
S. aureus NCTC 6571		6^{*}
E. faecium ATCC 7171		8
E. faecium vanB clinical isolate		8
S. aureus ATCC 25923	CIP	0.125
S. aureus NCTC 6571		0.125
P. aeruginosa ATCC 27853		0.125
P. aeruginosa NCTC 10662		0.125
E. faecium ATCC 7171		4
E. faecium vanB clinical isolate		2
E. coli ATCC 25922	GENT	1
E. coli NCTC 10418		1
S. aureus ATCC 25923		0.5
S. aureus NCTC 6571		1
P. aeruginosa ATCC 27853		1
P. aeruginosa NCTC 10662		0.5
E. faecium vanB clinical isolate		1
E. coli ATCC 25922	NA	2^{**}
E. coli NCTC 10418		1^{**}
E. coli ATCC 25922	TET	1
E. coli NCTC 10418		1

S. aureus ATCC 25923	1
S. aureus NCTC 6571	1
E. faecium ATCC 7171	0.5
E. faecium vanB clinical isolate	0.5

3.3.5. Mutation induction experiments in liquid broth

The method used in this experiment was adapted from Auda (2007). The purpose of this experiment was to see whether exposure to Bm and an antibiotic at sub-MIC would lead to a reduced susceptibility of the bacteria to a small panel of different antibiotics. The cells were exposed to the agents over a longer time period, as mutations that could lead to antibiotic resistance can arise after long exposure to sub-optimal concentrations of antibiotic.

In labelled universal tubes, Bm was added at peak plasma concentration (2 µg/mL) to MHB and the chosen antibiotic at half of the MIC value, and the organism being tested following standardisation to a 0.5 McFarland standard (OD_{600}: 0.08-0.1). A control tube was set up in the same way, with DMSO used as the solvent control. The total volume in each tube was 10 mL. The tubes were incubated for 24 hours at 37˚C, with shaking at 180 rpm. Then 500 µL of the incubated culture was then diluted again to a 0.5 McFarland standard (OD_{600}: 0.08-0.1) and subjected to the disc diffusion test for antibiotic susceptibility (see below, section 3.3.6). The remainder of the culture was used to set up the next serial culture, where the antibiotic being tested was added at half the MIC (see Table 14 below of antibiotics and concentrations used) and 100 µL of the previous culture were added to reach a total volume of 10 mL. This was incubated for a further 24 hours (48 hours in total). This process was then repeated again for another 24 hours (72 hours total). A -80°C stock was also made with 300 µL of 80% glycerol and 700 µL of the incubated cells at each serial transfer time point. The bacterial strains used in this experiment were *E. coli* ATCC 25922, *E. coli* NCTC 10418, *S. aureus* ATCC 25923 and *S. aureus* NCTC 6571. These strains were selected as models for Gram-negative and Gram-positive bacteria, respectively, as well as having a low MIC against the panel of antibiotics that were being used (AMP, CHL, CIP, GENT, NA, TET). Statistical analyses were conducted using the Mann-Whitney U test.

Table 14: A summary of the bacterial strains tested in the mutation induction experiments conducted in liquid broth and the concentration of the background antibiotic used (µg/mL). The two antibiotics ciprofloxacin (CIP) and nalidixic acid (NA) were used at a concentration that was half of the minimum inhibitory concentration (MIC) (n = 3). Strains that were marked as '-' were not conducted as MIC values were not previously determined.

Strain	Antibiotic concentration used µg/mL	
	CIP	NA
E. coli ATCC 25922	-	1
E. coli NCTC 10418	-	0.5
S. aureus ATCC 25923	0.0625	-
S. aureus NCTC 6571	0.0625	16

3.3.6. Disc diffusion test for antibiotic susceptibility

MHA plates were produced, each with 25 mL of agar in a Petri dish. The test organism was diluted to a 0.5 McFarland standard (OD_{600}: 0.08-0.1). The plates were inoculated by dipping a sterile swab into the inoculum and streaked onto the surface of the agar plate. It was then left to dry at room temperature with the lid on. The chosen antibiotic discs were then added to the plate using sterile forceps. The selected concentrations of antibiotics used were according to EUCAST guidelines for testing antibiotic susceptibility. Plates were then incubated at 37°C overnight. To gather the results, the diameter of the zones of inhibition were measured in millimetres (mm) and recorded.

3.3.7. Growth curves of test *E. coli* in normal media and sub-MIC bleomycin

E. coli were grown overnight in 10 mL MHB. As the Bm MIC for *E. coli* ATCC 25922 was 1 µg/mL, 0.5 µg/mL Bm was used in wells of a 96-well plate. *E. coli* NCTC 10418 had a Bm MIC of 0.5 µg/mL so 0.25 µg/mL of Bm was used in wells of a 96-well plate. The overnight cultures of bacteria were diluted to a 0.5 McFarland standard, and then a 1:100 dilution was made to get ~1 x 10^6 CFU/mL. 20 µL of the diluted bacterial culture was then added to the corresponding well. A solvent control was set up in the exact same way, but instead of adding Bm, DMSO was added in the equivalent volume. A sterile control was also set up in the same way as the test control, but with bacteria and Bm replaced with water and DMSO, respectively. Another separate sterile control was set up in the same way as the experimental control, but with bacteria being replaced with sterile distilled water. And finally, a growth control was set up where the wells contained MHB, bacteria and water. Triplicates for each strain and test condition were set up on the same plate. The 96-well plate was then sealed with a plate seal and lid before being loaded into a FLUOstar Omega plate reader, incubating at 37°C for 16 hours, with OD_{600} readings taken approximately every 4 minutes.

3.3.8. Generation times of test *E. coli*

Overnight cultures of *E. coli* ATCC 25922 and *E. coli* NCTC 10418 were diluted to a 0.5 McFarland standard (OD$_{600}$: 0.08-0.1) and then further diluted 1:100 to get approximately 1 x 10^6 cells. To inoculate the MHB, 100 µL of the diluted bacterial cultures used. A sample of this inoculated MHB was plated at 10^0-10^{-5} dilutions for a '0 hours' time point on MHA. These plates were then incubated at 37°C overnight. The inoculated MHB were incubated at 37°C with shaking at 180 rpm for 15 hours, according to the preliminary growth curve data where early stationary phase was reached around 15 hours of incubation. After 15 hours of incubation, the cultures were serially diluted from 10^0-10^{-11} and plated on MHA and left to incubate overnight. Colonies from the 0 hours plates and 15 hours plates were counted. Generation time was then calculated using the equation re-arranged from Tempest (1978):

$$\text{Number of generations} = (\log_{\text{end cells}}) - (\log_{\text{start cells}})/0.301$$

Where the number of generations can be calculated by using the log of the cells at the end of the experiment (log$_{\text{end cells}}$), the log of the cells at the start of the experiment (log$_{\text{start cells}}$) and dividing by the log base of 2 (which is equal to 0.301, for exponential growth of the bacteria). The test *E. coli* strains were also grown in sub-MIC Bm conditions. The cultures were prepared in the same way where an overnight culture was set up and then diluted to a 0.5 McFarland standard (OD$_{600}$: 0.08-0.1) and then diluted 1:100. 100 µL of the diluted cultures were then used to inoculate MHB, with the addition of Bm at sub-MIC concentrations, depending on the strain being used. *E. coli* ATCC 25922 was grown in 0.5 µg/mL Bm in a total volume of 10 mL in 50 mL Falcon tubes. *E. coli* NCTC 10418 was grown in 0.25 µg/mL Bm. Controls were set up in the same way but Bm was substituted with sterile distilled water or DMSO (the solvent used to dissolve the bleomycin sulfate powder). These cultures were set up in triplicate for each *E. coli* strain. Once the cultures were set up, dilutions were made ranging from 10^0-10^{-5} and 20 µL of each dilution was plated onto a segment of MHA for a 0 hours time point. The MHA plates were incubated overnight at 37˚C and the cultures were incubated for 15 hours at 37˚C with 180 rpm shaking. After 15 hours, the cultures were again serially diluted in the range of 10^0-10^{-11} and 20 µL plated onto MHA and incubated overnight at 37˚C.

Controls were set up in growth curve experiments, where the method outlined above was used. A solvent control (containing DMSO) and negative and positive controls were set up.

The data generated from the growth curves was used to calculate the bacterial cell division time using the equation presented by Frost *et al*. (2018):

$$Cell\ divisions = \log_2(\frac{Cells\ final}{Cells\ initial})$$

Once the bacterial cell division time was calculated (also known as the generation time), a Kruskal-Wallis statistical test was conducted to determine if there was a difference in generation time when the *E. coli* strains were exposed to either Bm, water, DMSO or MHB.

3.3.9. Mutation induction

The method used in these experiments was adapted from the paper by Webber *et al*. (2015) and is summarised in Figure 58. Overnight cultures of the desired organism were grown in 10 mL MHB at 37°C with shaking at 180 rpm in a 50 mL Falcon tube. A freezer stock of the overnight culture was made by freezing 1 mL of culture with 313 µL 80% glycerol. MHB was then pre-warmed at 37°C approximately 20 minutes before use. The overnight cultures of *E. coli* were then standardised to a 0.5 McFarland standard (OD$_{600}$: 0.08-0.1), with 100 µL of this standardised culture used to inoculate the experimental tubes. The experimental conditions were made up to a final volume of 10 mL, with Bm added to each strain culture that was sub-MIC, so the tubes set up with *E. coli* ATCC 25922 had a final concentration of 0.5 µg/mL Bm and *E. coli* NCTC 10418 had a final concentration of 0.25 µg/mL Bm. Each experimental condition was set up with six replicates, along with six replicates of DMSO controls set up containing equivalent volumes of DMSO. Before these tubes were incubated at 37°C with shaking at 180 rpm for 24 hours, a freezer stock was made with 1 mL of culture and 313 µL 80% glycerol. After 24 hours of growth, 1 ml of each sample tube was added to 313 µL 80% glycerol and stored at -80°C. 100 µL of each sample tube was then used to inoculate a new 50 mL Falcon tube which contained fresh MHB which had been pre-warmed at 37°C at least 20 minutes before use. Each tube was set up in the same way as the start of the experiment, where experimental tubes had a final volume of 10 mL and a sub-MIC concentration of Bm (0.5 µg/mL for *E. coli* ATCC 25922 and 0.25 µg/mL *E. coli* NCTC 10418) with DMSO controls containing the same volumes as the experimental conditions but with Bm replaced with DMSO. Bacterial cultures were repeatedly sub-cultured over 12 days (total of 12 sub-cultures), with 1 mL of sample stored in at -80°C with 313 µL 80% glycerol. On the last day of the sub-culturing series, 100 µL from each of the tubes (experimental and controls) were plated on Mueller-Hinton Bm plates at ½ MIC, MIC value and 2xMIC value to determine whether mutants to Bm had arisen. These plates were incubated overnight at 37°C.
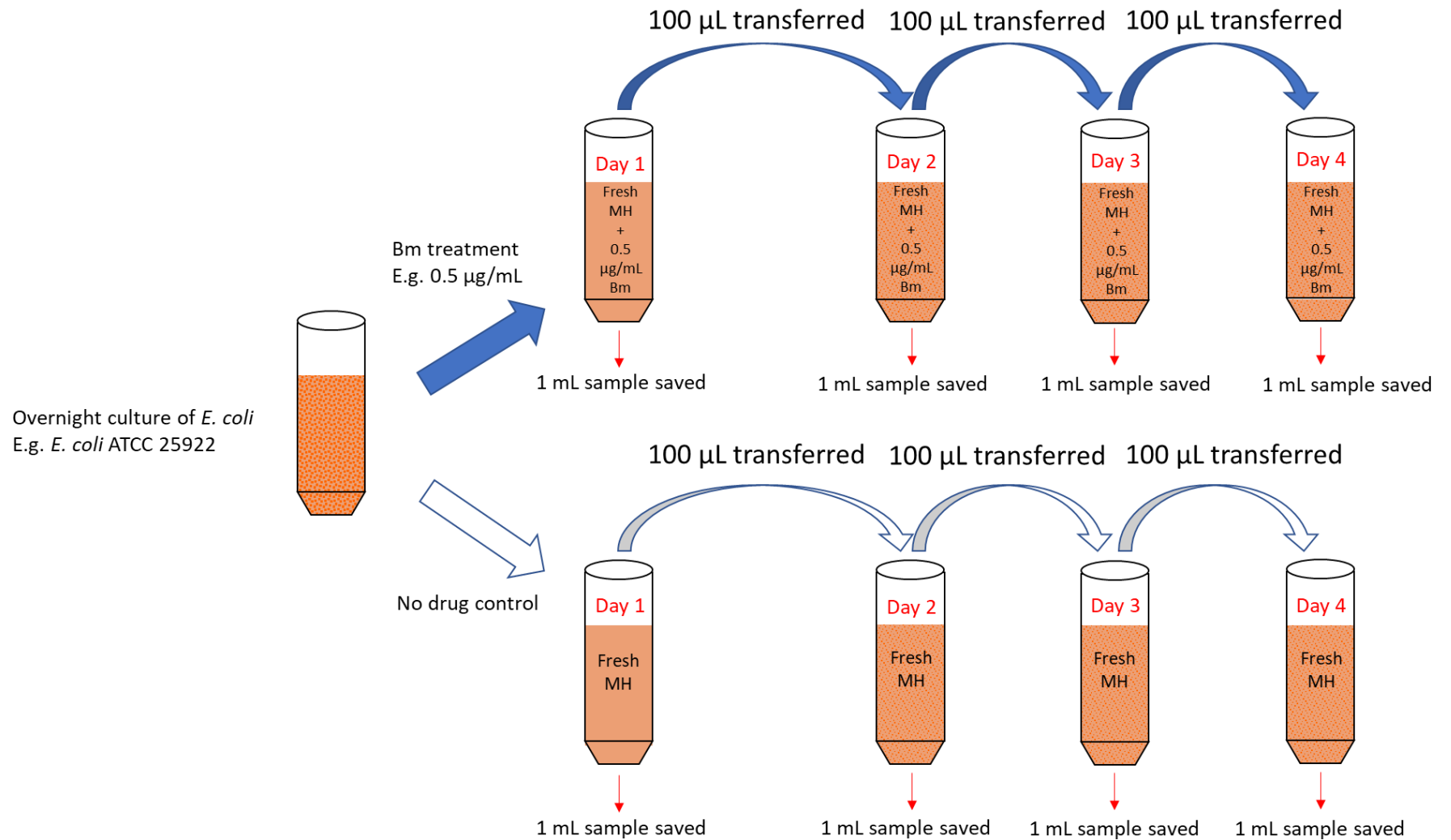
Figure 58: Mutation induction method. An overnight culture of the desired *Escherichia coli* strain (ATCC 25922 or NCTC 10418) is grown, before it is diluted and added to Mueller-Hinton (MH) broth with either bleomycin (Bm) at sub-MIC concentrations or an equal volume of DMSO (no drug control). After the cultures were incubated overnight at 37˚C with 180 rpm shaking, 1 mL of the sample was saved in a glycerol stock and 100 µL was transferred to a freshly prepared tube with either Bm or DMSO. This continued for the duration of 12 days (*n* = 6).

3.3.9.1. Determining experiment stopping point

To determine whether we have a suitable stopping point for the experiments, we theoretically want to give each base pair the opportunity to mutate at least once.

Initially, approximately 1 x 10^7 bacterial cells were transferred from an overnight *E. coli* culture. This was based on the assumption that *E. coli* cultures grown in normal media overnight contain 1 x10^9 cells in 10 mL of media, and in every transfer event 100 μL of the overnight culture is transferred into a new 10 mL volume. Each *E. coli* strain (ATCC 25922 and NCTC 10418) was grown in MHB with water (instead of Bm) over 24 hours. At the end of the 24 hours, *E. coli* ATCC 25922 had 2 x 10^{12} cells and *E. coli* NCTC 10418 had 1.9 x 10^{12} cells, this was calculated by conducting serial dilutions on agar and counting colonies. The equation (below) for determining mutation rate from Pope *et al*. (2008) was rearranged to determine how many mutants were to be expected after 24 hours of growth. We assumed that the *E. coli* strains had an average mutation rate of 1 x 10^{-3}, as determined in a study conducted by Lee *et al*. (2012).

$$\mu = [(r_2/N_2) - (r_1/N_1)] \times \ln(N_2/N_1)$$

Where μ is the mutation rate, r_1 is the number of mutants present at time point 1, r_2 is the number of mutants seen at time point 2, and N_1 and N_2 are the number of cells present at time points 1 and 2. For ease of calculations, we assumed for these calculations that the *E. coli* genomes were approximately 4,000,000 bp, as the *E. coli* genome can vary in size and has been previously estimated to be between 3.98-5.86 Mbp depending on the strain (Kurylo *et al*., 2016).

3.3.9.2. Passage for stable mutants

The mutants identified from the Bm selective plates at the end of the mutation induction experiment (section 3.3.9) were passaged in plain MHB for 10 days in order to determine whether the mutations in the bacteria were stable. From the Day 12 freezer stocks, an inoculating loop was used to streak the Bm treated mutants and DMSO control cultures onto Bm and plain MHA, respectively. *E. coli* ATCC 25922 mutants were plated on 4 μg/mL Bm plates and *E. coli* NCTC 10418 mutants were plated on 2 μg/mL Bm plates. The corresponding DMSO controls were plated on plain MHA. After 10 days, 10 μL of each culture was plated on MHA that contained Bm in the range of 0.25-64 μg/mL Bm.

3.3.9.3. Antibiotic susceptibility tests for mutants

Antibiotic susceptibility testing was conducted as described in Chapter 2, section 2.3.2. Antibiotic agents that were tested included Bm, MERO, AMP, CHL, GENT, NA, CIP and TET. A

Mann-Whitney U test was conducted to determine if there was a difference in antibiotic MICs between the strains treated with sub-MIC Bm and no drug (DMSO control), followed by a Wilcoxon Signed-Rank test to determine if there was a significant difference in the antibiotic MICs between the 0 days and 12 days samples. Finally, a Mann-Whitney U test was used to determine if there was a significant difference in the antibiotic MICs between the two *E. coli* strains (*E. coli* ATCC 25922 and *E. coli* NCTC 10418) used in the study.

3.3.9.4. Sequencing of mutants and analysis

The six replicates of each *E. coli* strain (ATCC 25922 and NCTC 10418) that evolved resistance to Bm after 12 days, their 0 days ancestors and DMSO control counterparts were grown overnight in 10 mL MHB, the colonies were taken from the Bm selective agar plates. For the ease of identification of the different strains, the abbreviations are listed below in Table 15. DNA from the mutants and ancestors were extracted using the Promega Wizard® Genomic DNA Purification kit. DNA was solubilised using sterile distilled water. After the DNA was extracted, it was quantified using the Invitrogen Qubit™ dsDNA HS Assay kit. DNA was standardised to 0.5 ng/μL (acceptable range: 0.25-1.25 ng/μL) and sequenced at the Quadram Institute Biosciences (QIB) using the Illumina NextSeq 500 with approximately 60X coverage. Sequences were then trimmed using Trimmomatic (v 0.36). Sequences were trimmed using the following settings: NexteraPE-PE.fa:2:30:10, HEADCROP:20, LEADING:20, TRAILING:20, SLIDINGWINDOW:4:20 and MINLEN:36. The resulting trimmed sequences were quality checked with FastQC (v 0.11.5). After quality checking the sequences, the reads were assembled using SPAdes (v 3.13.0) using the parameters -k 21,33,55,77,99,127 and –careful. The assembled reads were then annotated using Prokka (v 1.14.5) with a minimum contig length of 200 and –compliant. The resulting annotated assembly was analysed using snippy (v 3.2). The no treatment parental control was used as the reference for snippy. Coverage and viewing of the sequencing data was done using ACT: the Artemis Comparison Tool (Carver *et al.*, 2005).

Table 15: Mutation induction strain abbreviations. *Escherichia coli* was used in this study, specifically the two lab strains ATCC 25922 and NCTC 10418. The strains were either exposed to sub-MIC bleomycin or an equal volume of DMSO (as a control). After each day, samples of the cultures were saved for 12 days. For the purpose of analysis, we focussed on samples from day

0 and day 12. From selective bleomycin plates, 6 replicates were taken for each condition. To easily refer to these strains in the rest of this thesis, a strain name abbreviation has been created.

Organism	Strain	Experimental condition	Day	Replicate number	Strain Abbreviation
Escherichia coli	ATCC 25922	Bleomycin	0	1	ATCC.Bm.0.1
				2	ATCC.Bm.0.2
				3	ATCC.Bm.0.3
				4	ATCC.Bm.0.4
				5	ATCC.Bm.0.5
				6	ATCC.Bm.0.6
			12	1	ATCC.Bm.12.1
				2	ATCC.Bm.12.2
				3	ATCC.Bm.12.3
				4	ATCC.Bm.12.4
				5	ATCC.Bm.12.5
				6	ATCC.Bm.12.6
		DMSO control	0	1	ATCC.DO.0.1
				2	ATCC.DO.0.2
				3	ATCC.DO.0.3
				4	ATCC.DO.0.4
				5	ATCC.DO.0.5
				6	ATCC.DO.0.6
			12	1	ATCC.DO.12.1
				2	ATCC.DO.12.2
				3	ATCC.DO.12.3
				4	ATCC.DO.12.4
				5	ATCC.DO.12.5
				6	ATCC.DO.12.6
	NCTC 10418	Bleomycin	0	1	NCTC.Bm.0.1
				2	NCTC.Bm.0.2
				3	NCTC.Bm.0.3
				4	NCTC.Bm.0.4
				5	NCTC.Bm.0.5
				6	NCTC.Bm.0.6
			12	1	NCTC.Bm.12.1
				2	NCTC.Bm.12.2
				3	NCTC.Bm.12.3
				4	NCTC.Bm.12.4
				5	NCTC.Bm.12.5
				6	NCTC.Bm.12.6
		DMSO control	0	1	NCTC.DO.0.1
				2	NCTC.DO.0.2
				3	NCTC.DO.0.3
				4	NCTC.DO.0.4
				5	NCTC.DO.0.5
				6	NCTC.DO.0.6
			12	1	NCTC.DO.12.1
				2	NCTC.DO.12.2
				3	NCTC.DO.12.3
				4	NCTC.DO.12.4
				5	NCTC.DO.12.5
				6	NCTC.DO.12.6

3.3.9.5.   Mutation frequencies

From the *E. coli* ATCC 25922 mutants, a subset was tested for their differences in mutation frequency using the antibiotic rifampicin. The method used here was adapted from Björkholm *et al*. (2001). The *E. coli* ATCC 25922 replicates 1, 3 and 4 were used as during MIC testing in an interest of time, these replicates were found to have noticeable changes in their susceptibility to different antibiotics. The *E. coli* mutant strains: ATCC.Bm.12.1, ATCC.Bm.12.3, ATCC.Bm.12.4, ATCC.DO.0.1, ATCC.DO.0.3, ATCC.DO.0.4, ATCC.DO.12.1, ATCC.DO.12.3 and ATCC.DO.12.4 were tested.

The strains were grown overnight in 10 mL MHB at 37˚C with 180 rpm shaking. To ensure that the bacterial strains that were grown were free of pre-existing mutants that were resistant to rifampicin, 30 µL of the overnight cultures were spread onto 50 µg/mL rifampicin plates (Krašovec *et al*., 2014). The plates were then incubated overnight at 37˚C. Simultaneously, 20 independent cultures were set up for each strain and conditions in 5 mL universal tubes with 1 mL of MHB. The overnight cultures were diluted to 10^4 in MHB and 10 µL of this diluted culture was used to inoculate the 20 tubes. The cultures were then grown overnight at 37˚C with 180 rpm shaking. If no spontaneous mutants were found on the first 50 µg/mL rifampicin plates set up the previous day, the following cultures that were set up could be used. After incubation, 3 of the 20 tubes were used to conduct a viable count on plain MHA for each strain. To determine the number of resistant mutants, the whole volume of the rest of the 17 tubes were centrifuged on a tabletop centrifuge at 16,200 *x*g for 1 minute and 900 µL of broth was removed before the pellet was resuspended and spread plated on a selective 50 µg/mL rifampicin plate. The plates were then incubated overnight at 37˚C before the plates were counted for colonies. The mutation frequency was calculated by using the median number of mutants divided by the viable count generated from the median from the plain MHA plates.

3.3.9.6.   Statistical analysis

To determine whether there was a significant difference in the mutation frequencies of the strains after exposure to sub-MIC Bm or DMSO and if there was a difference between the 0 days and 12 days exposure times, Kruskal-Wallis tests were used.

3.4. Results

3.4.1. Initial drug sensitivity of strains

3.4.1.1. Against a panel of antibiotics

MIC testing was conducted on the lab strains to determine their antibiotic susceptibility profile before mutation induction experiments were conducted on the strains. Knowing the antibiotic susceptibility profiles of the lab strains also allowed us to remove any strains that were already resistant or less susceptible to the panel of antibiotics we had chosen. A summary of the MIC results is presented in the table below (Table 16). For *E. coli* ATCC 25922, the MIC fell into the expected range as outlined in the EUCAST guidelines for AMP, CHL, GENT, TET and NA. *E. coli* ATCC 25922 was susceptible to all concentrations of CIP tested. *E. coli* NCTC 10418 had similar MIC results to ATCC 25922. For the two *S. aureus* strains tested, MIC results were broadly similar except for NA where ATCC 25923 demonstrated an MIC of >128 μg/mL whereas strain NCTC 6571 demonstrated an MIC of 32 μg/mL. The MIC results for both of the *P. aeruginosa* strains were broadly similar. The MIC values for the two *E. faecium* strains differed for AMP and GENT but were similar for the other drugs tested.

Table 16: A summary of the minimum inhibitory concentrations (MICs) of 6 antibiotics against 8 bacterial strains. The antibiotics tested were: ampicillin (AMP), chloramphenicol (CHL), ciprofloxacin (CIP), gentamicin (GENT), nalidixic acid (NA) and tetracycline (TET). Where the tested concentration range of antibiotics was too high or too low, and so the MIC value couldn't be determined, a '<' or '>' is indicated beside the lowest or highest concentration tested.

n= 3	Average MIC (µg/mL)					
Organism strains	AMP	CHL	CIP	GENT	NA	TET
E. coli **ATCC 25922**	4	4	<0.125	1	2	1
E. coli **NCTC 10418**	2	2	<0.125	1	1	1
S. aureus **ATCC 25923**	0.03	8	0.125	0.5	>64	1
S. aureus **NCTC 6571**	0.03	6	0.125	1	32	1
P. aeruginosa **ATCC 27853**	>64	>128	0.125	1	>64	16
P. aeruginosa **NCTC 10662**	>64	128	0.125	0.5	64	16
E. faecium **ATCC 7171**	1	8	4	>64	>64	0.5
E. faecium vanB **clinical isolate**	>64	8	2	1	>64	0.5

3.4.1.2. DMSO MIC

In the literature it has been found that DMSO at high concentrations has the ability to disrupt cell membranes and potentially lyse the cells, so to ensure that the DMSO solvent wasn't impacting the antibiotics we were testing, we conducted MIC tests using DMSO to determine

what concentration would impact cell viability and a suitable concentration to use going forward with experiments (Gurtovenko and Anwar, 2007). All of the bacterial strains (*E. coli* ATCC 25922, NCTC 10418, *S. aureus* ATCC 25923, NCTC 6571, *P. aeruginosa* ATCC 27853, NCTC 10662, *E. faecium* ATCC 7171 and the *vanB*-positive clinical isolate) showed normal growth between the DMSO concentrations at 0-4% and then no growth when DMSO was added at 50% and 100%. It was therefore determined that a concentration of 4% DMSO (v/v) could be used in future experiments without impacting bacterial growth.

3.4.1.3. Bleomycin MIC with low DMSO solvent

MIC testing was conducted using Bm to determine at what concentration the bacterial strains were unable to survive and what concentration would be used in the mutation induction experiments. After exposure to Bm with less than 0.1% DMSO in the suspension, only the two *E. coli* strains were susceptible to low concentrations of Bm, with all the other strains demonstrated MICs of >32 µg/mL in both broth and agar (Table 17). We therefore ruled out the *P. aeruginosa* strains (ATCC 27853 and NCTC 10662) and the *E. faecium* strains (ATCC 7171 and the *vanB* clinical isolate) and only included the *E. coli* strains (ATCC 25922 and NCTC 10418) for future experiments, and the *S. aureus* ATCC 25923 and NCTC 6571 strains if we wanted to investigate Gram-positive bacteria.

Table 17: A summary of the MIC of bleomycin for each of the bacterial strains. Where the tested concentrations of bleomycin were too high and a MIC value couldn't be determined, a '>' is indicated next to the highest concentration tested (*n* = 3).

Organism	Modal MIC (µg/mL)
E. coli ATCC 25922	1
E. coli NCTC 10418	0.5
S. aureus ATCC 25923	32
S. aureus NCTC 6571	64
P. aeruginosa ATCC 27853	>128
P. aeruginosa NCTC 10662	>128
E. faecium ATCC 7171	>128
E. faecium vanB clinical isolate	>128

3.4.2. Mutation induction experiment on agar plates

Mutation induction experiments were conducted to determine whether exposure to sub-MIC concentrations of Bm would alter the antibiotic susceptibility profile of the strains tested. Auda (2007) had previously attempted mutation induction on agar plates, and it was attempted here. For all strains and antibiotic combinations tested, only *E. coli* NCTC 10418 showed any impact of Bm on surviving antibiotic challenge. When *E. coli* NCTC 10418 was plated on 1 µg/mL GENT, for the first replicate there was no growth seen on the DMSO side of the plate, but three small colonies were seen on the Bm positive side of the plate. For the second replicate, 9 small colonies were seen on the Bm treated side of the plate. This indicates that the presence of Bm enabled a small number of *E. coli* to grow in the presence of GENT. No other strains had visible colonies growing near the Bm disc.

3.4.3. Mutation induction experiment in liquid broth

3.4.3.1. Simultaneous exposure to NA and Bm

Another mutation induction method that was mentioned in Auda (2007) utilises liquid broth in order to grow the strains for longer, exposed to Bm for longer and in the presence of one of the antibiotics from our small panel.

Growth in sub-MIC NA plus Bm appears to visually have a significant impact upon the ability of *E. coli* to survive exposure to various antibiotics, while no effect was seen for *S. aureus* (Figures 59-64). Compared with exposure to sub-MIC NA alone, the presence of Bm increased the ability of *E. coli* to survive exposure to AMP, CHL, GENT and TET. However, interestingly there was no benefit to survival against NA with the addition of Bm, despite this being the antibiotic they were initially exposed to. Statistical analyses were conducted to compare the Bm treated strains to their control (DMSO) treated counterparts using the Mann-Whitney U test. From these analyses, none of the Bm treated strains were significantly different ($P<0.05$) from the control strains. In the statistical analyses conducted, in six instances a replicate was removed as there was no bacterial growth anywhere on the plate so it could not be determined if any changes were due to Bm treatment or just because no cells were plated. Strains that only had two replicates for the analysis were from the 48 hours time point: *E. coli* NCTC NA + Bm against GENT, NA and TET, *S. aureus* ATCC with NA + Bm treatment against AMP, CHL, and CIP.
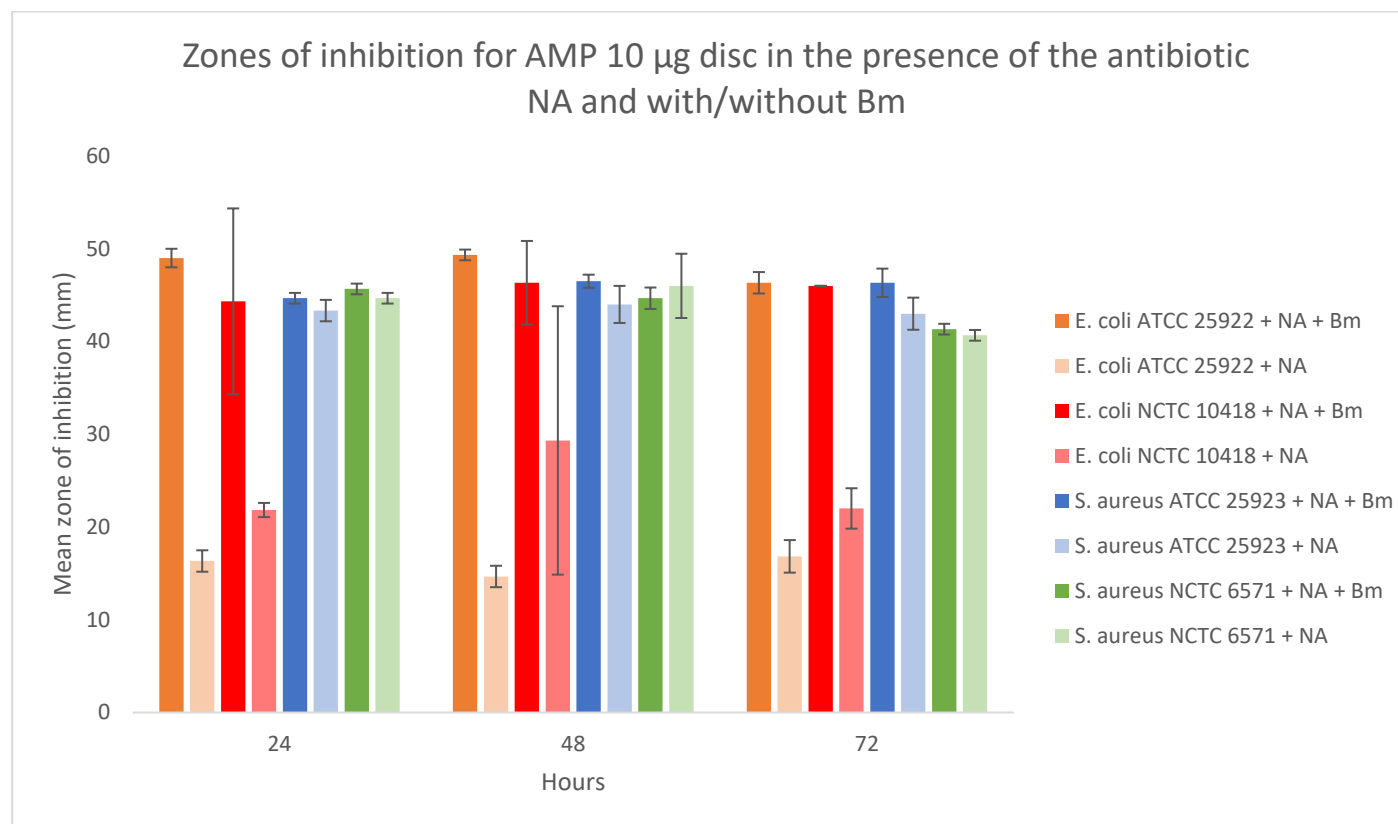
Figure 59: *Escherichia coli* and *Staphylococcus aureus* antibiotic susceptibility to ampicillin after exposure to nalidixic acid and bleomycin. A bar chart demonstrating the zones of inhibition (mm) for the *E. coli* strains ATCC 25922 and NCTC 10418 and the *S. aureus* strains ATCC 25923 and NCTC 6571 when they were treated initially with Bleomycin (Bm) or DMSO (control) in combination with nalidixic acid (NA) and then tested for their susceptibility against an ampicillin (AMP) 10 µg disc. Zones of inhibition were read after 24, 48 and 72 hours, and are shown as the mean with standard deviation bars plotted for 3 replicates (*n* = 3), the only exception here is the *S. aureus* ATCC 25923 strain treated with NA + Bm at 48 hours which had two replicates (*n* = 2).
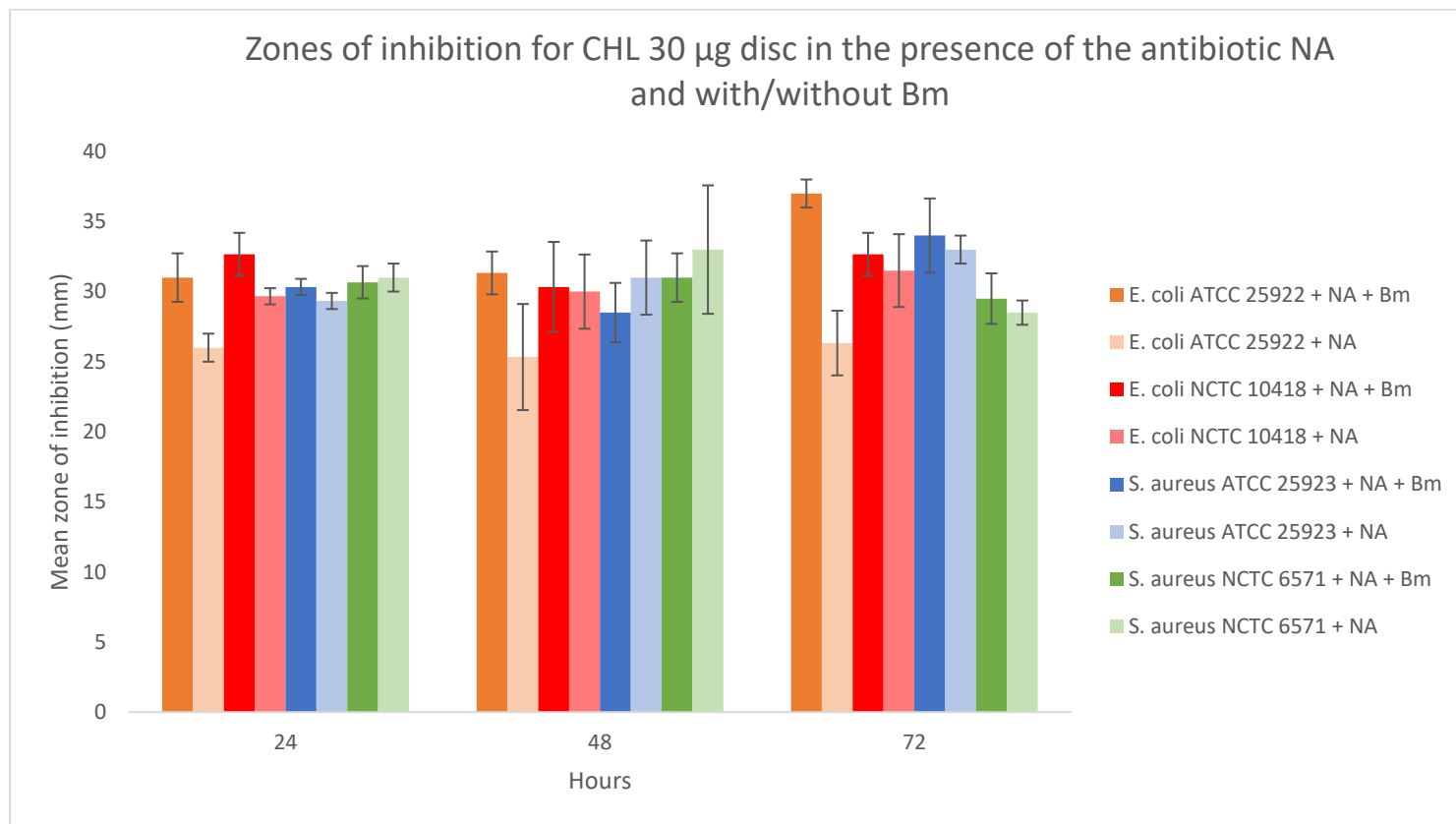
Figure 60: *Escherichia coli* and *Staphylococcus aureus* antibiotic susceptibility to chloramphenicol after exposure to nalidixic acid and bleomycin. A bar chart demonstrating the zones of inhibition (mm) for the *E. coli* strains ATCC 25922 and NCTC 10418 and the *S. aureus* strains ATCC 25923 and NCTC 6571 when they were treated initially with Bleomycin (Bm) or DMSO (control) in combination with nalidixic acid (NA) and then tested for their susceptibility against a chloramphenicol (CHL) 30 μg disc. Zones of inhibition were read after 24, 48 and 72 hours, with standard deviation bars plotted for 3 replicates (*n* = 3), the only exception here is the *S. aureus* ATCC 25923 strain treated with NA + Bm at 48 hours which had two replicates (*n* = 2).

Figure 61: *Escherichia coli* and *Staphylococcus aureus* antibiotic susceptibility to ciprofloxacin after exposure to nalidixic acid and bleomycin. A bar chart demonstrating the zones of inhibition (mm) for the *E. coli* strains ATCC 25922 and NCTC 10418 and the *S. aureus* strains ATCC 25923 and NCTC 6571 when they were treated initially with Bleomycin (Bm) or DMSO (control) in combination with nalidixic acid (NA) and then tested for their susceptibility against a ciprofloxacin (CIP) 5 µg disc. Zones of inhibition were read after 24, 48 and 72 hours, with standard deviation bars plotted for 3 replicates ($n = 3$), the only exception here is the *S. aureus* ATCC 25923 strain treated with NA + Bm at 48 hours which had two replicates ($n = 2$).
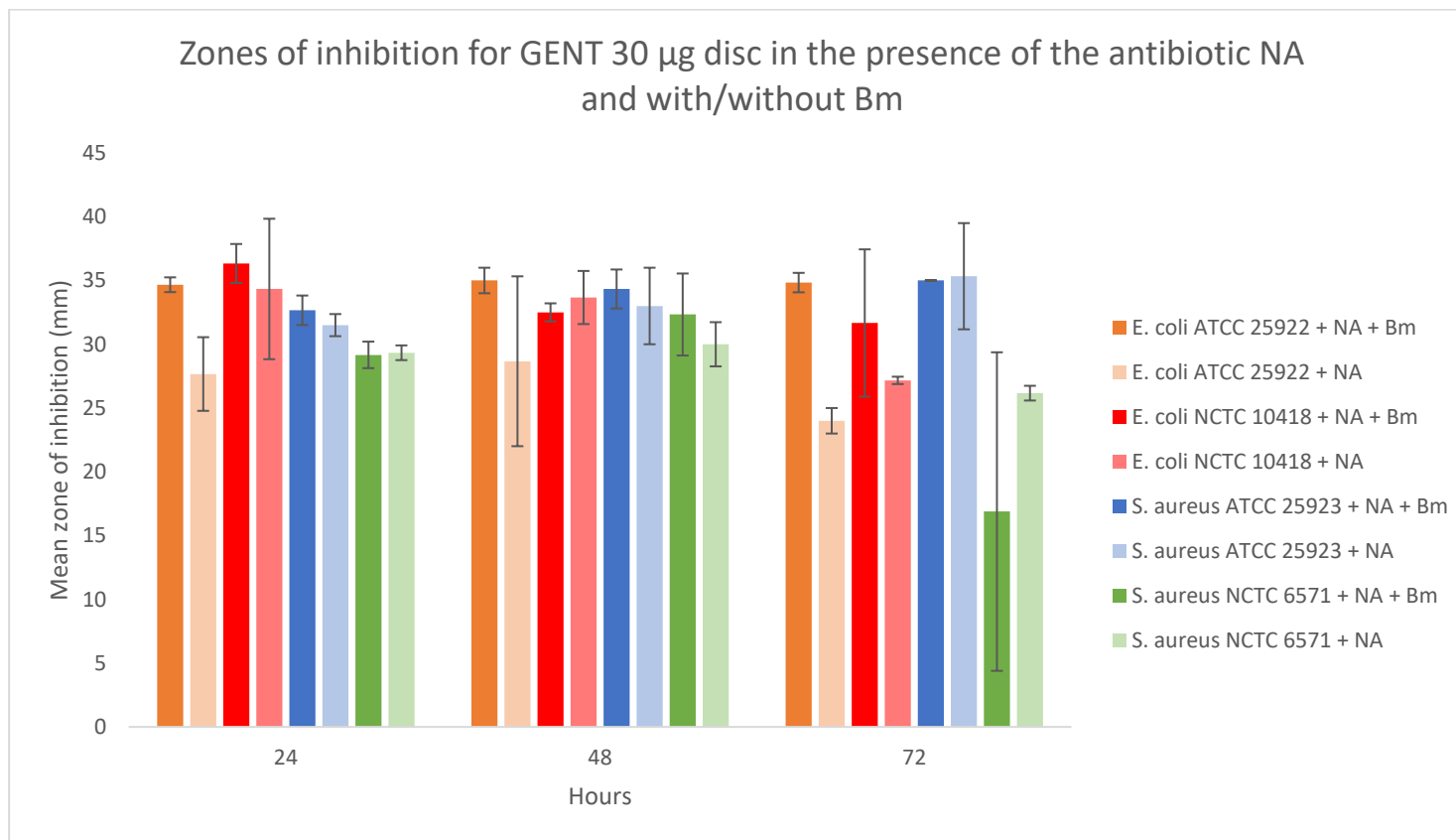
Figure 62: *Escherichia coli* and *Staphylococcus aureus* antibiotic susceptibility to gentamicin after exposure to nalidixic acid and bleomycin. A bar chart demonstrating the zones of inhibition (mm) for the *E. coli* strains ATCC 25922 and NCTC 10418 and the *S. aureus* strains ATCC 25923 and NCTC 6571 when they were treated initially with Bleomycin (Bm) or DMSO (control) in combination with nalidixic acid (NA) and then tested for their susceptibility against a gentamicin (GENT) 30 µg disc. Zones of inhibition were read after 24, 48 and 72 hours, with standard deviation bars plotted for 3 replicates (n = 3), the only exception here is the *E. coli* NCTC 10418 strain treated with NA + Bm at 48 hours which had two replicates (n = 2).

Figure 63: *Escherichia coli* and *Staphylococcus aureus* antibiotic susceptibility to nalidixic acid after exposure to nalidixic acid and bleomycin. A bar chart demonstrating the zones of inhibition (mm) for the *E. coli* strains ATCC 25922 and NCTC 10418 and the *S. aureus* strains ATCC 25923 and NCTC 6571 when they were treated initially with Bleomycin (Bm) or DMSO (control) in combination with nalidixic acid (NA) and then tested for their susceptibility against an NA 30 µg disc. Zones of inhibition were read after 24, 48 and 72 hours, with standard deviation bars plotted for 3 replicates (*n* = 3), the only exception here is the *E. coli* NCTC 10418 strain treated with NA + Bm at 48 hours which had two replicates (*n* = 2).
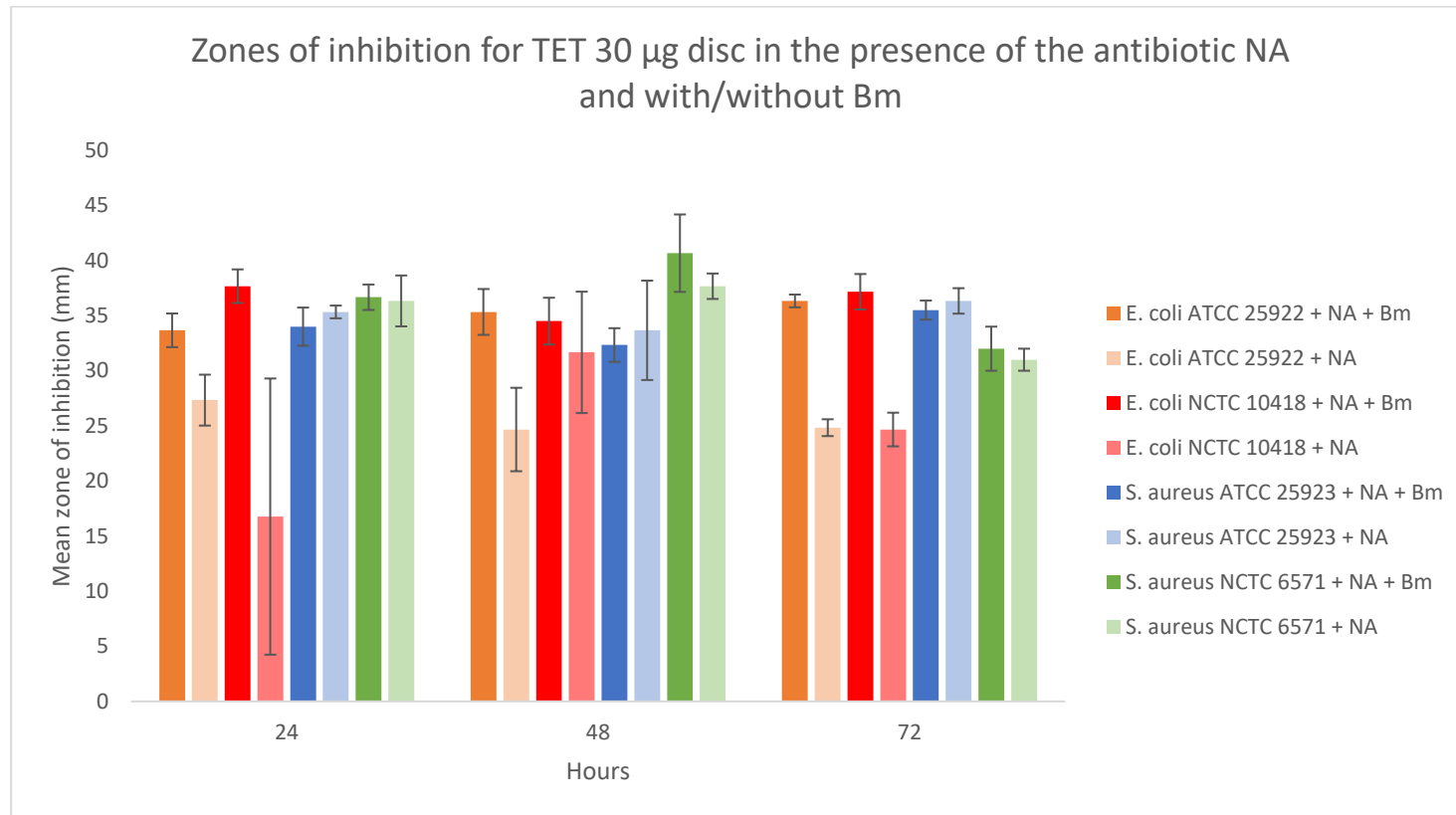
Figure 64: *Escherichia coli* and *Staphylococcus aureus* antibiotic susceptibility to tetracycline after exposure to nalidixic acid and bleomycin. A bar chart demonstrating the zones of inhibition (mm) for the *E. coli* strains ATCC 25922 and NCTC 10418 and the *S. aureus* strains ATCC 25923 and NCTC 6571 when they were treated initially with Bleomycin (Bm) or DMSO (control) in combination with nalidixic acid (NA) and then tested for their susceptibility against a tetracycline (TET) 30 µg disc. Zones of inhibition were read after 24, 48 and 72 hours, with standard deviation bars plotted for 3 replicates (n = 3), the only exception here is the *E. coli* NCTC 10418 strain treated with NA + Bm at 48 hours which had two replicates (n =2).

3.4.3.2.   Simultaneous exposure to CIP and Bm

When the *S. aureus* strains are compared for their antibiotic susceptibility profiles after exposure to sub-MIC CIP and Bm or just sub-MIC CIP, we visually see no significant difference between the two conditions when the data is plotted in a bar chart (Figure 65-70). After conducting statistical analyses using the Mann-Whitney U tests, it was confirmed that there was no significant difference between the sub-MIC CIP and Bm or just sub-MIC CIP treated cells in terms of their susceptibilities to a small panel of antibiotics.
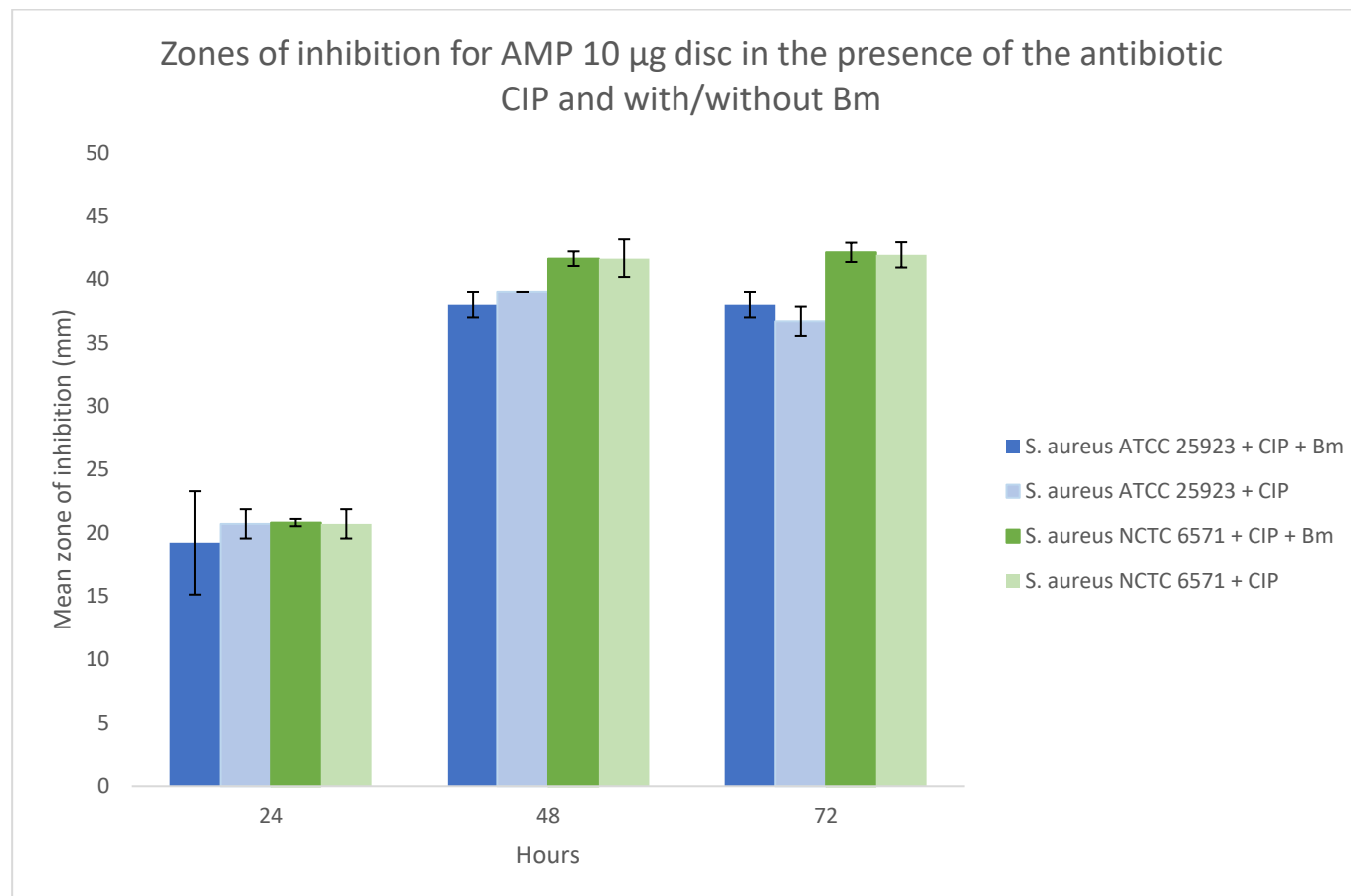
Figure 65: *Staphylococcus aureus* antibiotic susceptibility to ampicillin after exposure to ciprofloxacin and bleomycin. A bar chart demonstrating the zones of inhibition (mm) for the *S. aureus* strains ATCC 25923 and NCTC 6571 when they were treated initially with Bleomycin (Bm) or DMSO (control) in combination with ciprofloxacin (CIP) and then tested for their susceptibility against an ampicillin (AMP) 10 µg disc. Zones of inhibition were read after 24, 48, and 72 hours, with standard deviation bars plotted for 3 replicates (*n* = 3).
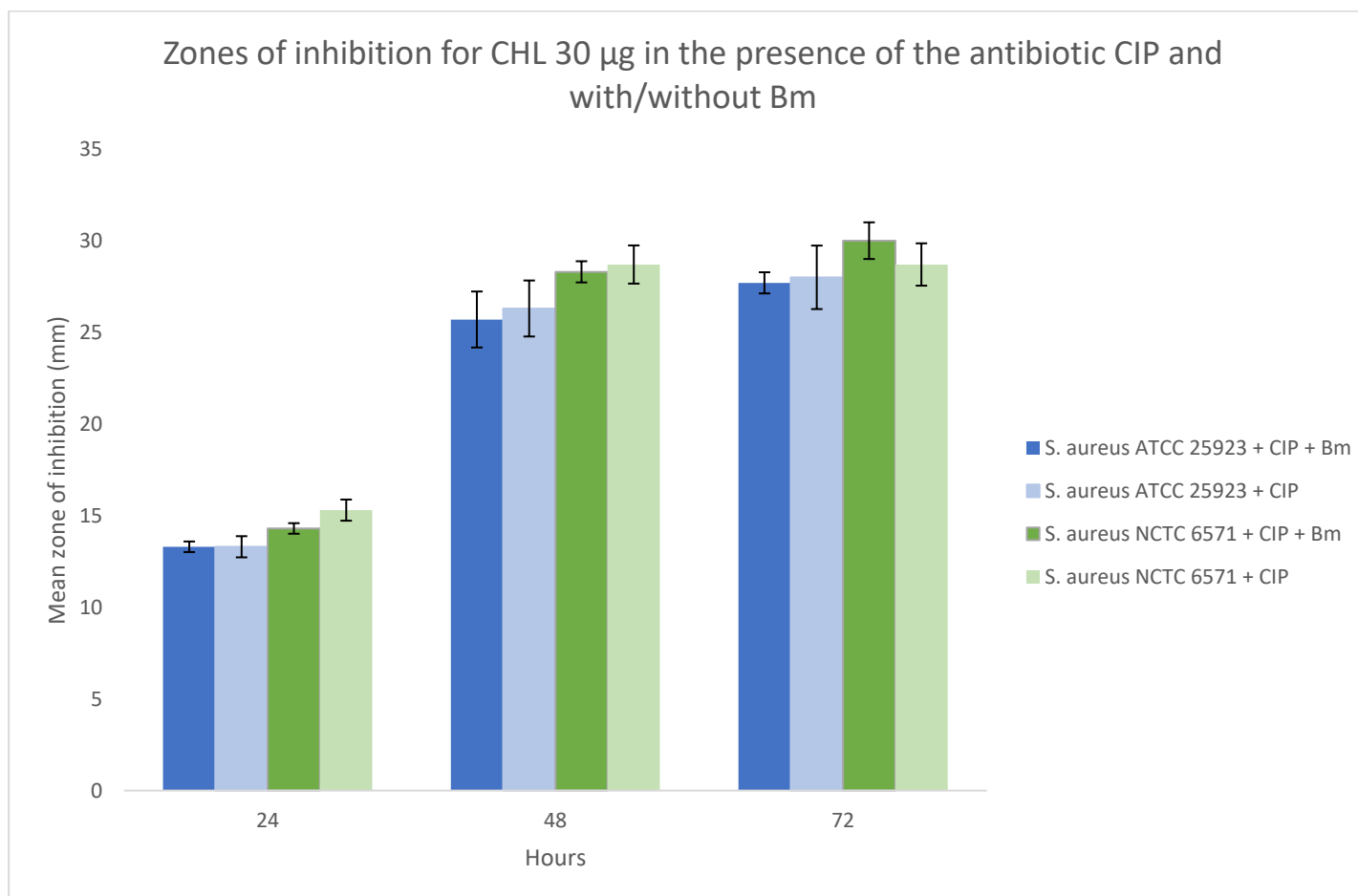
Figure 66: *Staphylococcus aureus* antibiotic susceptibility to chloramphenicol after exposure to ciprofloxacin and bleomycin. A bar chart demonstrating the zones of inhibition (mm) for the *S. aureus* strains ATCC 25923 and NCTC 6571 when they were treated initially with Bleomycin (Bm) or DMSO (control) in combination with ciprofloxacin (CIP) and then tested for their susceptibility against a chloramphenicol (CHL) 30 µg disc. Zones of inhibition were read after 24, 48, 72 and 96 hours, with standard deviation bars plotted for 3 replicates (n = 3).
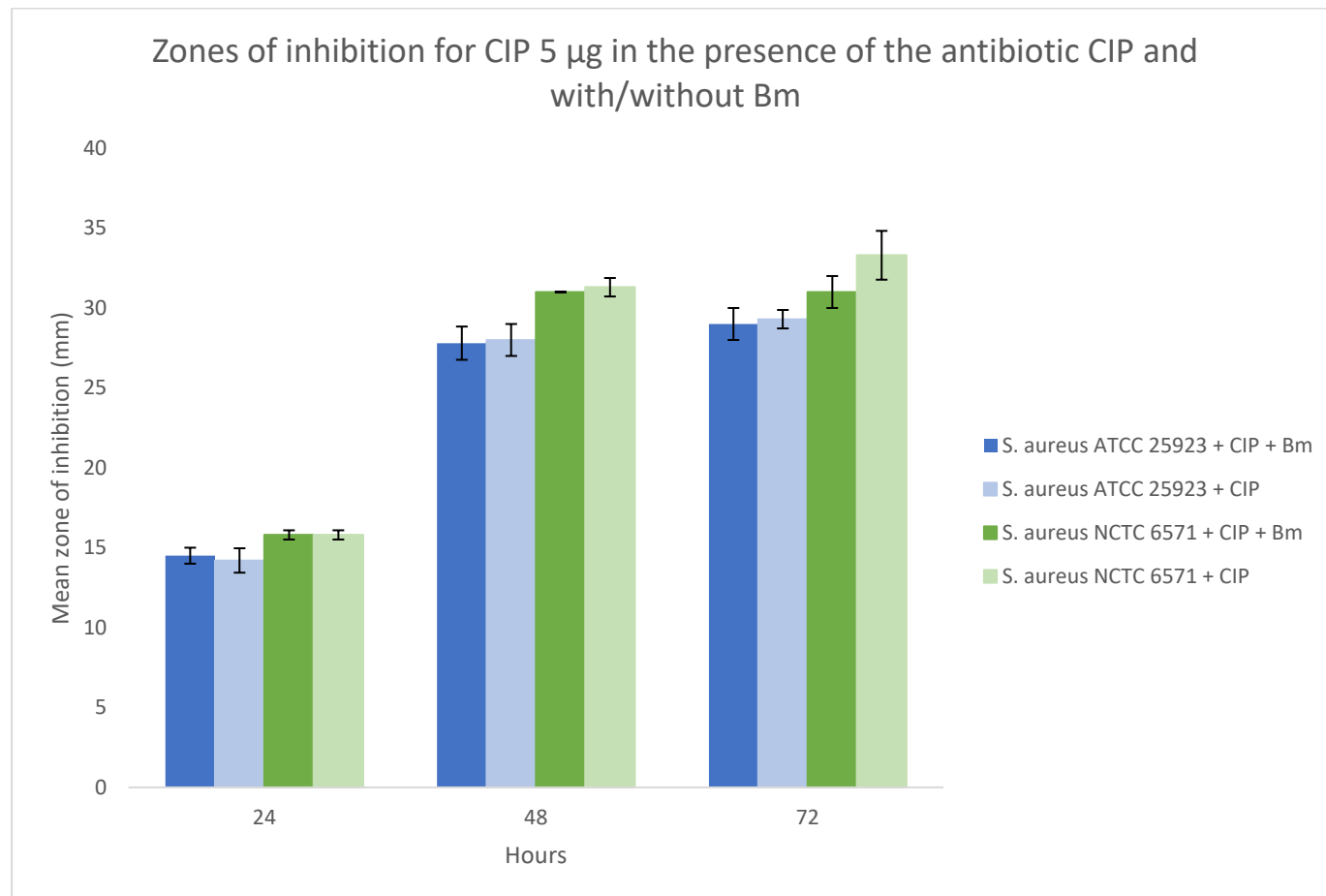
Figure 67: *Staphylococcus aureus* antibiotic susceptibility to ciprofloxacin after exposure to ciprofloxacin and bleomycin. A bar chart demonstrating the zones of inhibition (mm) for the *S. aureus* strains ATCC 25923 and NCTC 6571 when they were treated initially with Bleomycin (Bm) or DMSO (control) in combination with ciprofloxacin (CIP) and then tested for their susceptibility against CIP 5 μg disc. Zones of inhibition were read after 24, 48, 72 and 96 hours, with standard deviation bars plotted for 3 replicates (*n* = 3).
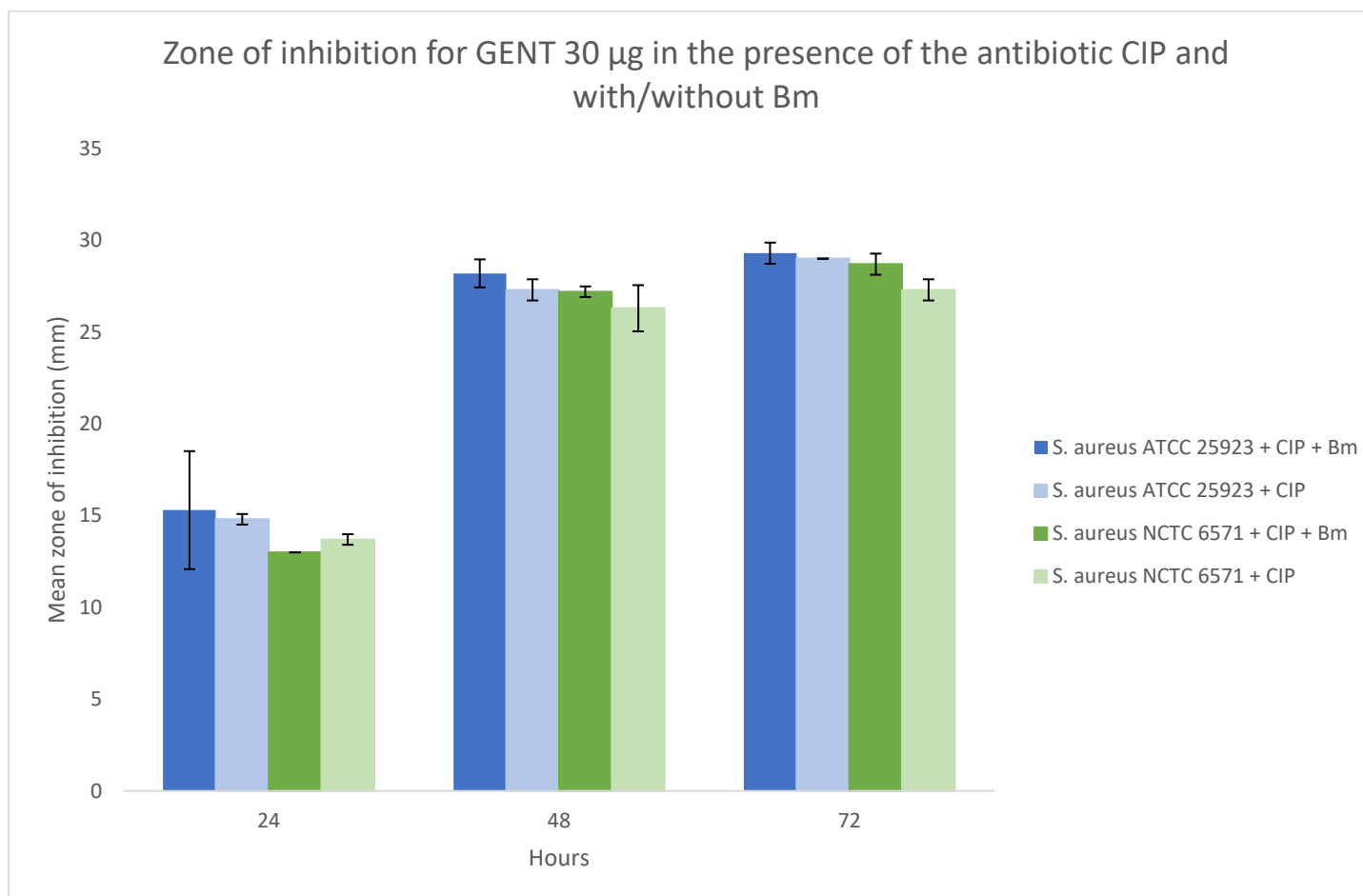
Figure 68: *Staphylococcus aureus* antibiotic susceptibility to gentamicin after exposure to ciprofloxacin and bleomycin. A bar chart demonstrating the zones of inhibition (mm) for the *S. aureus* strains ATCC 25923 and NCTC 6571 when they were treated initially with Bleomycin (Bm) or DMSO (control) in combination with ciprofloxacin (CIP) and then tested for their susceptibility against a gentamicin (GENT) 30 μg disc. Zones of inhibition were read after 24, 48, 72 and 96 hours, with standard deviation bars plotted for 3 replicates (*n* = 3).
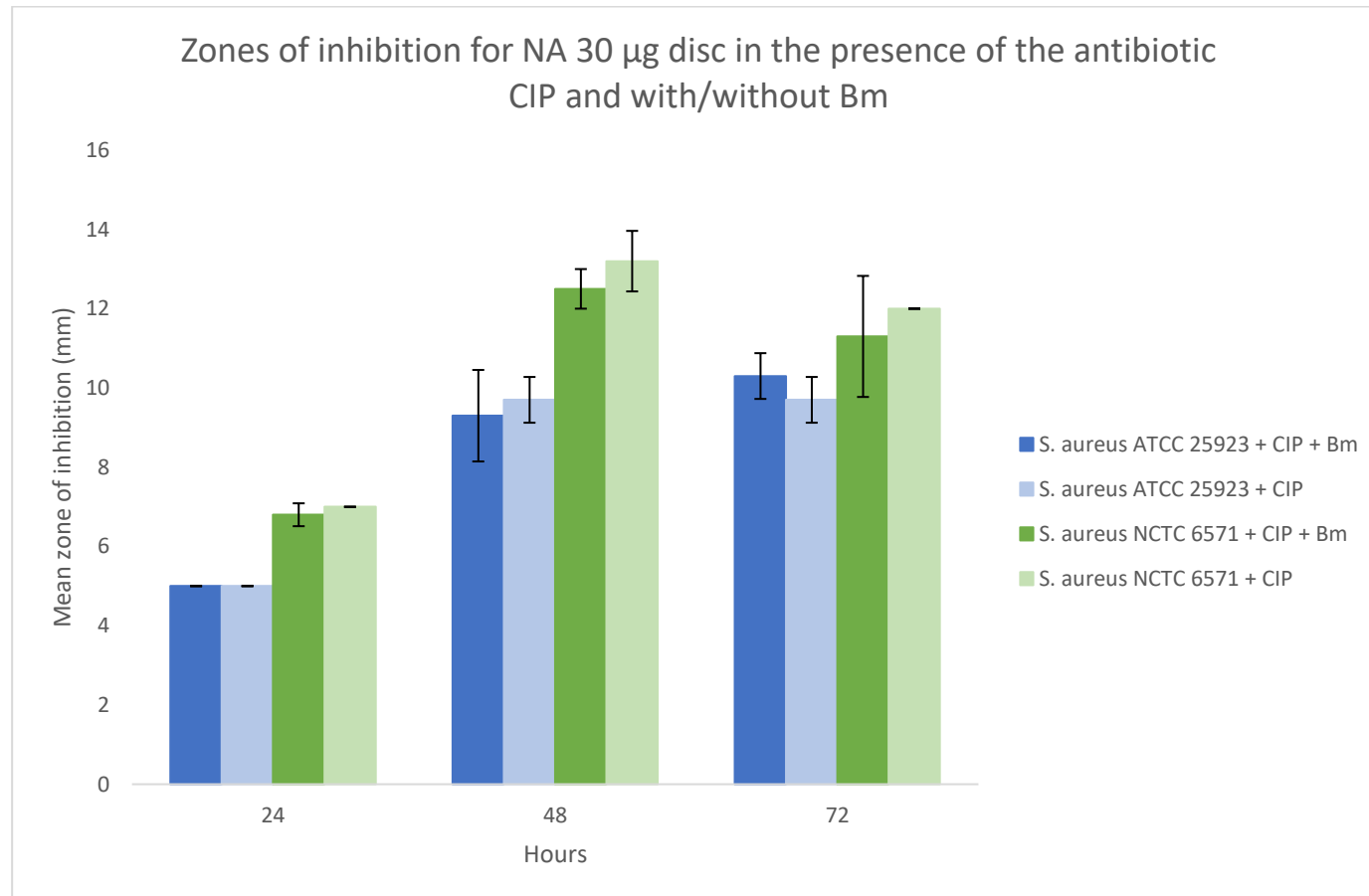
Figure 69: *Staphylococcus aureus* antibiotic susceptibility to nalidixic acid after exposure to ciprofloxacin and bleomycin. A bar chart demonstrating the zones of inhibition (mm) for the *S. aureus* strains ATCC 25923 and NCTC 6571 when they were treated initially with Bleomycin (Bm) or DMSO (control) in combination with ciprofloxacin (CIP) and then tested for their susceptibility against a nalidixic acid (NA) 30 µg disc. Zones of inhibition were read after 24, 48, 72 and 96 hours, with standard deviation bars plotted for 3 replicates (*n* = 3).
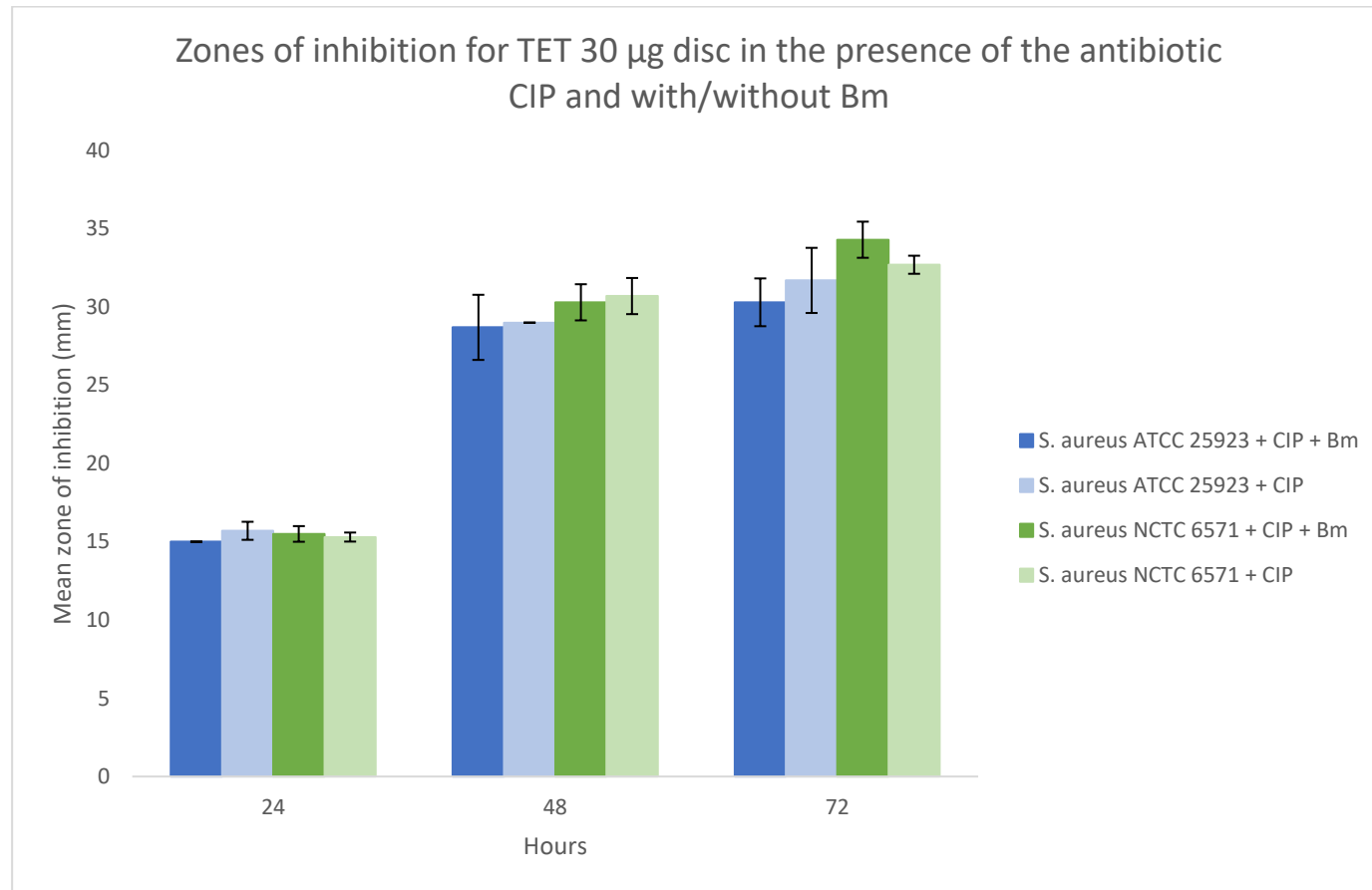
Figure 70: *Staphylococcus aureus* antibiotic susceptibility to tetracycline after exposure to ciprofloxacin and bleomycin. A bar chart demonstrating the zones of inhibition (mm) for the *S. aureus* strains ATCC 25923 and NCTC 6571 when they were treated initially with Bleomycin (Bm) or DMSO (control) in combination with ciprofloxacin (CIP) and then tested for their susceptibility against a tetracycline (TET) 30 µg disc. Zones of inhibition were read after 24, 48, 72 and 96 hours, with standard deviation bars plotted for 3 replicates (*n* = 3).

3.4.4. Growth curves of test *E. coli* in normal media and sub-MIC bleomycin

Growth curves were conducted in order to determine whether the addition of sub-MIC Bm impacted on the growth of the lab strains *E. coli* ATCC 25922 and *E. coli* NCTC 10418. The *E. coli* ATCC 25922 strain grown in sub-MIC Bm had a slower rate of growth than when the strain was grown in normal MHB (Figure 71). The DMSO treated culture showed a similar growth curve to the culture grown in normal MHB, demonstrating that the differences displayed between the different treatment conditions is due to the action of Bm. The controls of just media and media with DMSO were as expected with no readings detected by optical density at 600 nm (OD$_{600}$).

The *E. coli* NCTC 10418 strain showed similar results to the *E. coli* ATCC 25922 strain, where the Bm treated culture had a slower rate of growth than the culture that was grown in normal MHB (Figure 72). The growth of the culture in the DMSO treated control appears to be similar to the cultures grown in the MHB as normal. The negative containing MHB, DMSO and water, but no bacteria or Bm, showed no growth. From these results, we see that the addition of Bm at sub-MIC reduced the growth rate of the *E. coli* strains, and the addition of DMSO (which was the solvent control) had no detectable difference in growth when compared to the cultures grown in MHB.
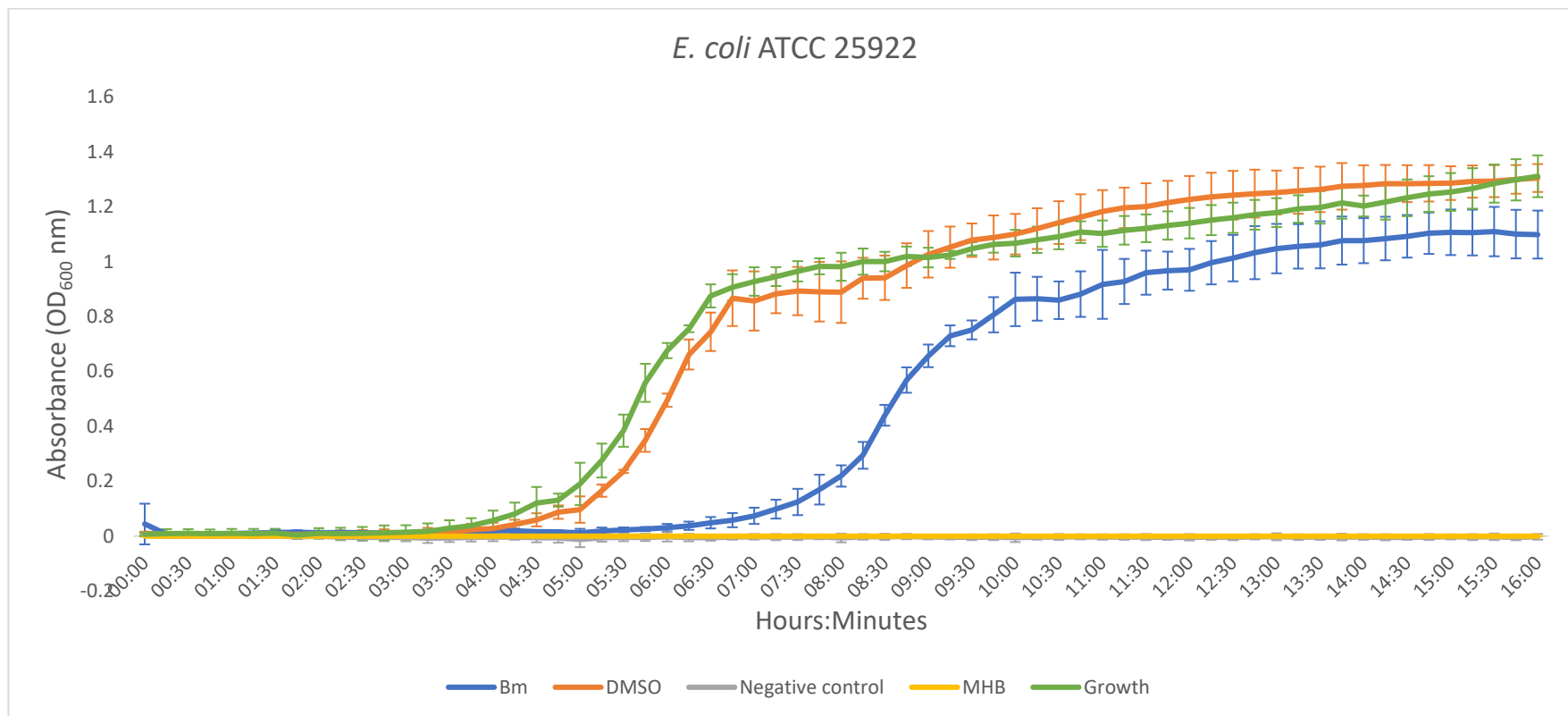
Figure 71: Growth curves of the *E. coli* ATCC 25922 strain under different conditions. In the presence of sub-MIC bleomycin (Bm) at a concentration of 0.5 µg/mL is shown in blue, in the presence of a equivalent volume of DMSO (solvent control) is demonstrated in orange. Shown in grey is the negative control that contains Mueller-Hinton broth, DMSO and water instead of the bacterial cells. Shown in yellow is the standard Mueller-Hinton broth (MHB) that was used as a blank in the FLUOstar Omega plate reader. Shown in green is the normal growth of the bacterial strain in MHB. All absorbance values were taken at an optical density (OD) of 600 nm. The standard deviation of the mean is plotted as bars ($n = 3$).
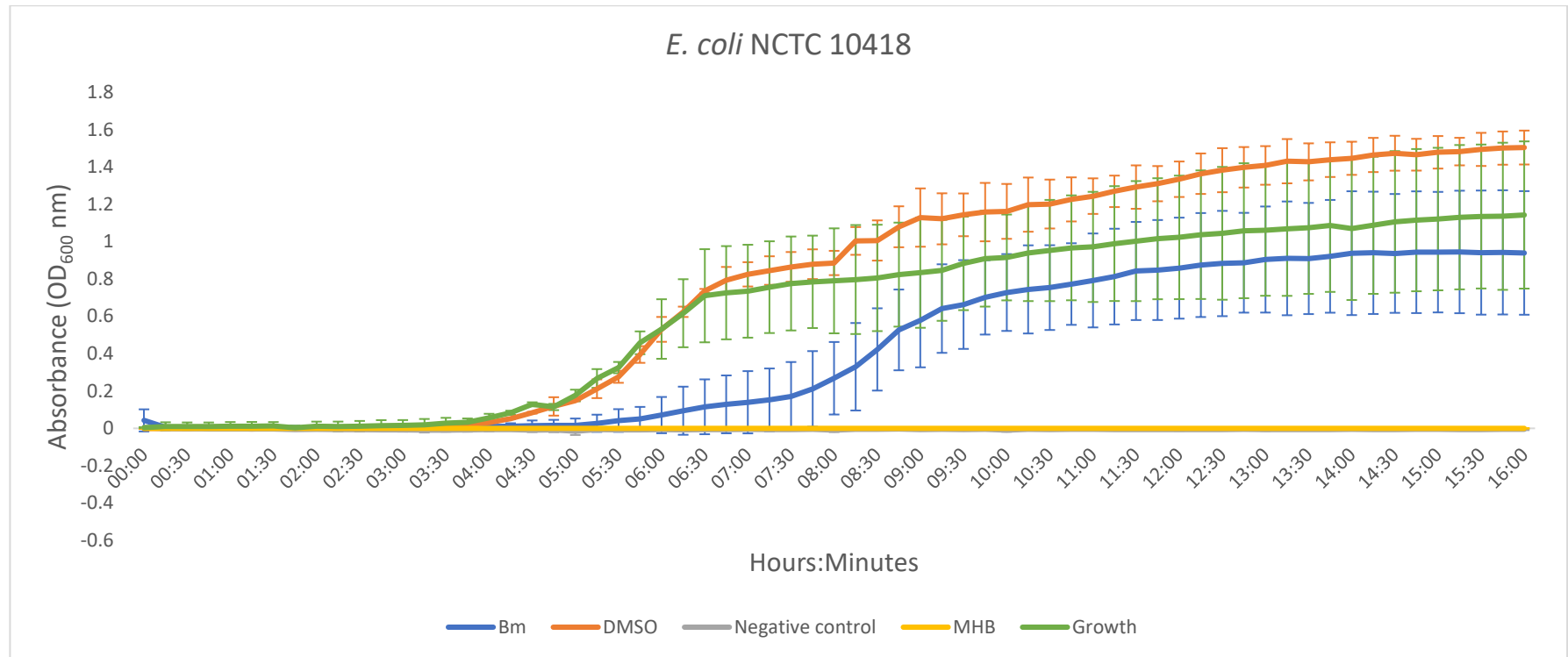
Figure 72: Growth curves of the *E. coli* NCTC 10418 strain under different conditions. In the presence of sub-MIC bleomycin (Bm) at a concentration of 0.5 µg/mL is shown in blue, in the presence of an equivalent volume of DMSO (solvent control) is demonstrated in orange. Shown in grey is the negative control that contains Mueller-Hinton broth (MHB), DMSO and water instead of the bacterial cells. Shown in yellow is the standard Mueller-Hinton broth (MHB) that was used as a blank in the FLUOstar Omega plate reader. Shown in green is the normal growth of the bacterial strain in MHB. All absorbance values were taken at an optical density (OD) of 600 nm. The standard deviation of the mean is plotted as bars (*n* = 3).

3.4.5. Generation time of *E. coli* strains

Generation time calculations were conducted for the *E. coli* strains under different conditions to determine the impact of sub-MIC concentrations of Bm on growth. From the growth curve data, we calculated a rough estimate of the generation times (in minutes) of the different strains when they were grown in the presence of Bm, DMSO, MHB or sterile distilled water, using the end point number of cells and the initial number of cells at the start of the growth curve over a 15 hour time course. The generation time for each *E. coli* strain (ATCC 25922 and NCTC 10418) in different conditions is listed below in Table 18. When a Kruskal-Wallis test was conducted to determine if there was a difference in the generation time for each *E. coli* strain when exposed to either Bm, water, DMSO or MHB, there was no significant difference at a significance level of 0.05 between any of the treatments for *E. coli* ATCC 25922 (χ^2(3) = 1.51, *P*= 0.679) and *E. coli* NCTC 10418 (χ^2(3) = 7.21, *P*= 0.066).

Using the cell division calculation from the Frost *et al*. (2018) paper (mentioned in method section 3.3.8), we calculated the cell division for each strain under the four conditions tested (Table 19).

Table 18: Generation time of the *Escherichia coli* strains ATCC 25922 and NCTC 10418 under different experimental conditions: sub-MIC bleomycin (Bm), sterile distilled water, DMSO and Mueller-Hinton broth (MHB). Generation time is presented in minutes (n = 3).

Strain	+ Bm	+ Sterile distilled water	+ DMSO	+ MHB
E. coli ATCC 25922	82.57	81.37	78.95	75.69
E. coli NCTC 10418	124.31	82.34	82.34	75.00

Table 19: Cell division of the *Escherichia coli* strains ATCC 25922 and NCTC 10418 under different experimental conditions: sub-MIC bleomycin (Bm), sterile distilled water, DMSO and Mueller-Hinton broth (MHB) (n = 3). The cell division calculation used was from the paper by Frost *et al.* (2018).

	Cells final	Cells start	Cell division
Bm			
E. coli ATCC 25922	32,666,667	17,000	10.90
E. coli NCTC 10418	1,666,667	11,000	7.24
Sterile distilled water			
E. coli ATCC 25922	26,666,667	12,667	11.04
E. coli NCTC 10418	14,666,667	7,667	10.90
DMSO			
E. coli ATCC 25922	48,666,667	18,000	11.40
E. coli NCTC 10418	27,333,333	14,000	10.93
MHB			
E. coli ATCC 25922	160,000,000	43,333	11.85
E. coli NCTC 10418	93,333,333	23,333	11.97

3.4.6. Evolution of bleomycin-resistant mutants

3.4.6.1.   Determining experiment stopping point

The equation from the Lee *et al*. (2012) paper used to calculate an experimental stopping point was:

$$\mu = [(r_2/N_2) - (r_1/N_1)] \times \ln (N_2/N_1)$$

Where μ is the mutation rate, r_1 is the number of mutants present at time point 1, r_2 is the number of mutants seen at time point 2, and N_1 and N_2 are the number of cells present at time points 1 and 2. In the example of *E. coli* ATCC 25922, we re-arranged the calculation to find r_2 which is the number of mutants we would expect to see after a set amount of time. If we use our generation time for this strain that was calculated earlier when water was added to the media, which was 17.70 generations after 24 hours we would expect to see 2.13 x 10^{12} cells present. Our starting culture had approximately 1 x 10^7 cells, and we assume that *E. coli* have an average mutation rate of 1 x 10^{-3}. So, the equation re-arranged with our values included:

$$\frac{r2}{2 \; x \; 10^{12}} = \frac{1 \; x \; 10^{-3}}{12.21}$$

We determined that the *E. coli* ATCC 25922 strain has approximately 164,000,000 mutants after 24 hours of growth. If we assume that the *E. coli* genome is 4,000,000 bp then we would expect there to be 41 mutations per base pair. After 12 days, we then expect that each base pair would have the opportunity to be mutated 492 times. The *E. coli* NCTC 10418 strain has approximately 156,400,000 mutants after 24 hours of growth. If we assume again that the *E. coli* genome is 4,000,000 bp then we would expect there to be 39 mutations per base pair. After 12 days, we then expect that each base pair would have the opportunity to be mutated 469 times.

3.4.6.2. Antibiotic susceptibility tests for mutants

After mutation induction, one colony from the Bm selective plate for each mutant was cultured in a larger volume of MHB broth and used for antibiotic susceptibility testing. This was done for each replicate, where each strain (*E. coli* ATCC 25922 or NCTC 10418) and condition (sub-MIC Bm or DMSO) had 6 replicates. The MIC results for the different *E. coli* strain mutants vary between the 6 replicates, displayed in Table 20 is the range of MICs across the 6 replicates and the panel of antibiotics the strains were tested against. For both of the *E. coli* strains (ATCC 25922 and NCTC 10418) we can see that the MIC for CHL and Bm is higher when the strains were treated with Bm than DMSO (the control).

Table 20: The MIC range of the *Escherichia* coli strains ATCC 25922 and NCTC 10418 after mutation induction with either sub-minimum inhibitory concentration (MIC) bleomycin (Bm) or DMSO (negative control) against the panel of antibiotics: ampicillin (AMP), chloramphenicol (CHL), ciprofloxacin (CIP), gentamicin (GENT), nalidixic acid (NA), tetracycline (TET), Bm and meropenem (MERO). These results are the ranges across the six replicate cultures, with the MICs replicated 3 times as technical replicates.

E. coli strain	Treatment	Days	Antibiotic MIC* (µg/mL)							
			AMP	CHL	CIP	GENT	NA	TET	Bm	MERO
ATCC 25922	Bm	0	2-4	4-8	0.00781->0.0625	2-4	2	0.5	0.5	0.0156
		12	2-4	4-8	0.00781-0.0156	2-4	2	0.5-1	16-32	0.0156
	DMSO	0	2-4	4	0.0039->0.0625	2-4	2	0.5	0.5	0.0156-0.0313
		12	4	2-4	0.00781-0.0039	2-4	2	0.5	0-0.5	0.0156
NCTC 10418	Bm	0	1	2-4	0.0039->0.0625	1-2	1	0.5	<0.25	0.0156-0.0313
		12	1-2	2-4	0.0039-0.00781	1-2	1-2	0.5	2-8	0.0156
	DMSO	0	1	2	0.0039->0.0625	1-2	0.5-1	0.5	<0.25	0.0156-0.0313
		12	1	2	0.0039	1-2	1	0.5	<0.25	0.0156-0.0313

*Range across the 6 replicates averaged for 3 technical repeats

3.4.6.3. Passage for stable mutants

The *E. coli* strains ATCC 25922 and NCTC 10418 were passaged in plain MHB after being treated with sub-MIC Bm or DMSO in order to determine whether the mutations induced were stable in the bacteria after the mutation induction experiment. The mutant strains generated after exposure to sub-MIC Bm were passaged in plain MHB for 10 days and then dot plated on agar plates with different concentrations of Bm (Figure 73). The result of this MIC test is displayed in Table 21. For the *E. coli* ATCC 25922 strain, there was at least a 4-fold difference in the MIC when the cells were treated with either sub-MIC Bm or DMSO. For the *E. coli* NCTC 19418 strain, there was at least a 16-fold difference in the MIC when the cells were treated with either sub-MIC Bm or DMSO. The results show that the induced mutations were stable in the mutant strains generated.
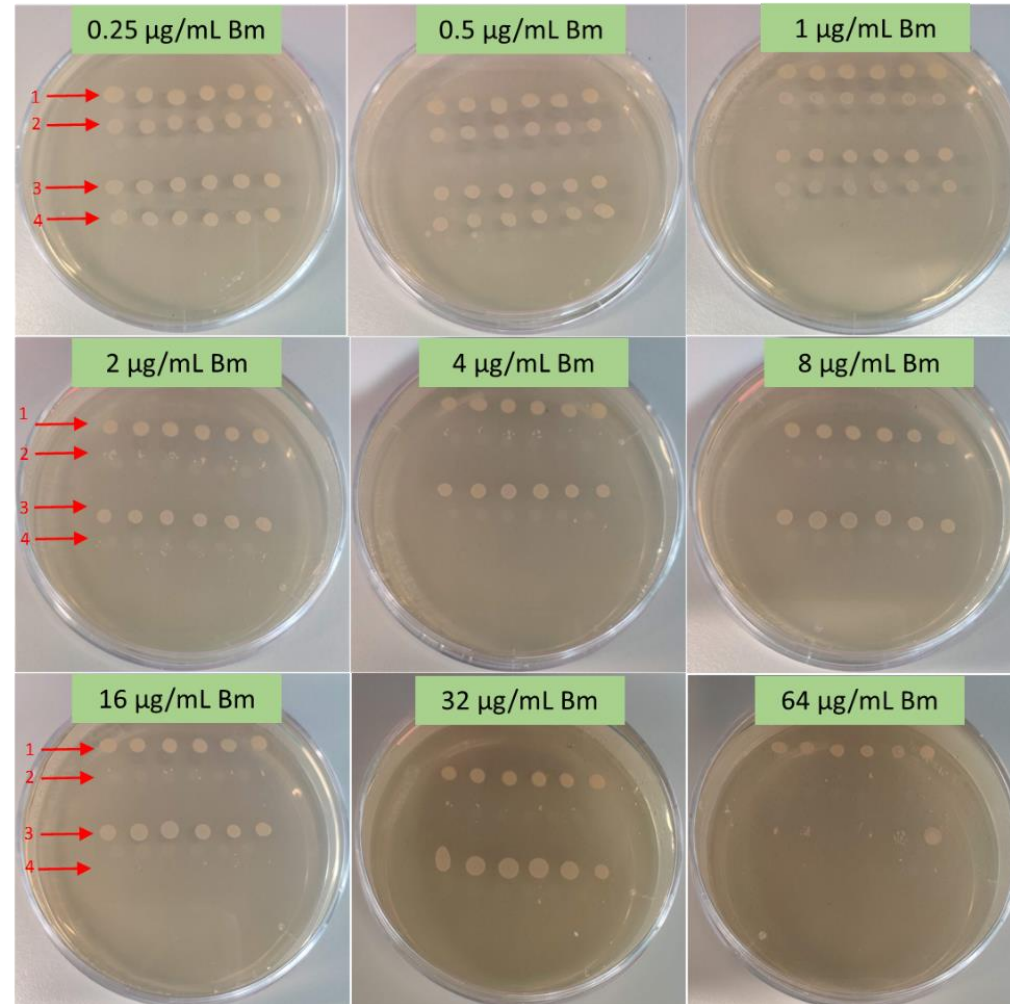
Figure 73: MIC plate results for the *Escherichia coli* ATCC 25922 and NCTC 10418 mutant strains after passaging for 10 days. The plate concentrations ranged from 0.25-64 µg/mL. Row 1 are the 6 replicates of *E. coli* ATCC 25922 cells treated with sub-MIC Bm, row 2 are the 6 replicates of *E. coli* ATCC 25922 cells treated with DMSO (negative control), row 3 are the 6 replicates of *E. coli* NCTC 10418 treated with sub-MIC Bm, and row 4 are the 6 replicates of *E. coli* NCTC 10418 treated with DMSO (negative control).

Table 21: Passaging the *Escherichia coli* mutants. The MIC for the *E. coli* strains ATCC 25922 and NCTC 10418 mutants (and their control counterparts) after passaging for 10 days in plain Mueller-Hinton broth (*n* = 3).

Strain	Treatment before passage	Bm MIC (µg/mL)
E. coli ATCC 25922	sub-MIC Bm	>64
	DMSO	16
E. coli NCTC 10418	sub-MIC Bm	>64
	DMSO	4

Using the data generated and statistical analyses, three questions were asked:

1) Is there a significant difference in the antibiotic MICs between the *E. coli* strains when they were treated with sub-MIC Bm and when they weren't treated with a drug?

2) Is there a significant difference in the antibiotic MICs when you compare the treatments after 0 days and 12 days?

3) Is there a significant difference in the antibiotic MICs between the two *E. coli* strains, *E. coli* ATCC 25922 and NCTC 10418?

To address the first question on whether there is a significant difference in the antibiotic MICs between the *E. coli* strains when they were treated with either sub-MIC Bm or not after 12 days of exposure, Mann-Whitney U tests were used. There was a significant increase in the *E. coli* ATCC 25922 MICs when the strains were treated with Bm in terms of their resulting susceptibility to CHL (U= 157.5, P <0.05), CIP (U= 468, P= 0.023) and Bm (U= 253.5, P <0.05). There was also a significant increase in MIC when *E. coli* NCTC 10418 was treated with Bm or not in terms of its resulting susceptibility to the antibiotics CHL (U= 463.5, P <0.05), NA (U= 436, P <0.05) and Bm (U= 324, P <0.05).

To address the second question of whether there is a significant difference between the antibiotic MICs when you compare treatment days 0 and 12, a Wilcoxon Signed Ranks test was used. In the *E. coli* ATCC 25922 samples treated with sub-MIC Bm, there was a significant increase in MIC of CHL (Z= -2.209, P <0.05), AMP (Z= -2.530, P= 0.011) and Bm (Z= -3.765, P <0.05) after 12 days. There was no significant difference between 0 days and 12 days for the other drugs tested: GENT (Z= -0.632, P= 0.527), CIP (Z= -1.451, P= 0.147), TET (Z= -0.378, P= 0.705), NA (Z= -1.414, P= 0.157) and MERO (Z= -0.710, P= 0.478). With the exception of three antibiotics (CHL, AMP and Bm), it appears as if the antibiotic susceptibility of the *E. coli* ATCC 25922 strain after sub-Bm treatment doesn't vary when the duration of treatment changes.

In the *E. coli* ATCC 25922 negative controls, there was no significant difference in MIC between the 0 days and 12 days isolates for any drug: AMP (Z= -0.816, P= 0.414), CHL (Z= -1.134, P= 0.257), CIP (Z= -0.187, P= 0.851), NA (Z= -0.816, P= 0.414), TET (Z= -0.849, P= 0.396), Bm (Z= -1.239, P= 0.215) and MERO (Z= -1.273, P= 0.203). This demonstrates that throughout the duration of the experiment (0-12 days), the antibiotic susceptibility profiles did not change significantly in the *E. coli* ATCC 25922 controls.

In the *E. coli* NCTC 10418 samples treated with sub-MIC Bm, there was a significant increase in MIC between the 0 days and 12 days isolates for AMP (Z= -2.058, P <0.05), NA (Z= -2.887, P

<0.05), and Bm (Z= -3.826, P<0.05), where the MIC was higher after 12 days. There was no significant difference for GENT (Z= -1.134, P= 0.257), CIP (Z= -0.949, P= 0.343), TET (Z= -1.00, P= 0.317) and MERO (Z= -0.965, P= 0.335). With the exception of three antibiotics (AMP, NA and Bm), there was no significant difference in the antibiotic susceptibility profiles of the *E. coli* NCTC 10418 strain after 0 or 12 days treatment with sub-MIC Bm.

In the *E. coli* NCTC 10418 negative controls, there was a significant increase in MIC between the 0 days and 12 isolates for CIP (Z= -2.640, P<0.050), where the MIC was lower after 12 days. There was no significant difference in MIC for the other drugs tested: AMP (Z= -0.333, P= 0.739), CHL (Z= -1.732, P= 0.083), GENT (Z= 0.00, P= 1.00), NA (Z= -0.913, P= 0.361), TET (Z= -1.00, P= 0.317), Bm (Z= 0.00, P= 1.00) and MERO (Z= -1.717, P= 0.086).

To address the third question on whether there was a significant difference in the MICs between the *E. coli* ATCC 25922 strain and the *E. coli* NCTC 10418 strain, Mann-Whitney U tests were used. There was a significant difference in MICs between the Bm treated *E. coli* strains for CHL (U= 128.5, P<0.05), GENT (U= 130, P<0.05), AMP (U= 32, P<0.05), CIP (U= 394, P<0.05), TET (U= 507.5, P<0.05), NA (U= 204, P<0.05), and Bm (U= 367.5, P<0.05). The MICs of all drugs were higher for *E. coli* ATCC 25922 than for *E. coli* NCTC 10418 with the exception of MERO (U= 570, P= 0.314). In the negative controls, there was a significant difference in MICs between *E. coli* ATCC 25922 and *E. coli* NCTC 10418 for CHL (U= 324, P<0.05), GENT (U= 144, P<0.05), AMP (U= 5, P<0.05), NA (U= 64, P<0.05), Bm (U= 216, P<0.05) and MERO (U= 480.5, P<0.05). The MICs for the antibiotics tested were generally higher in *E. coli* ATCC 25922 than *E. coli* NCTC 10418. However, there was no significant difference in MIC between *E. coli* ATCC 25922 and *E. coli* NCTC 10418 controls for CIP (U= 624, P= 0.727) and TET (U= 611.5, P= 0.391).

To summarise, the antibiotic susceptibility profile of the *E. coli* ATCC 25922 strain was significantly different to *E. coli* NCTC 10418 when treated with sub-MIC Bm, where *E. coli* ATCC 25922 was less susceptible to the action of all of the antibiotics with the exception of MERO. In the control condition, *E. coli* ATCC 25922 was significantly different to *E. coli* NCTC 10418, where *E. coli* ATCC 25922 was less susceptible to the action of all of the antibiotics with the exception of CIP and TET.

3.4.7. Identifying mutations associated with reduced susceptibility to bleomycin

Following sequencing of the isolates with reduced susceptibility to Bm, SNPs were separated into non-synonymous and synonymous mutations, summarised in Tables 22-25. A synonymous mutation is defined as a change in the DNA sequence that does not change the encoded amino acid (Chu and Wei, 2019). A non-synonymous mutation is a change in the DNA sequence that

does change the subsequent encoded amino acid (Chu and Wei, 2019). Other types of mutations include frameshifts (the addition or deletion of a base pair that shifts the position of the reading frame for translation), missense (a mutation that results in a different encoded amino acid) and stop codon gain or loss mutations A nonsense mutation is a term that can also be used to describe the premature gain of a stop codon (Chu and Wei, 2019).

In the *E. coli* ATCC 25922 strain treated with sub-MIC Bm, frameshift mutations were seen in 2 of the 6 replicates, in three different genes. In replicate 1 there was a deletion in *bcsA* (which codes for the catalytic subunit of cellulose synthase) and a deletion in *sbmA* (which codes for the peptide antibiotic transporter SbmA), both leading to frameshift mutations. These SNPs may impact the ability of *E. coli* to synthesise cellulose and import antibiotics, allowing the bacteria to resist the effects of Bm treatment. In replicate 6 of the *E. coli* ATCC 25922, a SNP was introduced in *sbmA* that resulted in a stop codon. In replicate 2 there was an insertion in *bglB* (this gene codes for the protein 6-phospho-beta-glucosidase, BglB) that led to a frameshift mutation which may affect the ability of the bacteria to access different energy sources and aid in cell survival under stress conditions. There was also a stop codon introduction in replicate 3 in *yfiR*. YfiR is a putative HTH-type transcriptional regulator. In 4 of 6 replicates there were SNPs in *ompX*, part of the outer membrane protein X. Replicate 1, 2, 4 and 6 all had mutations at nucleotide position 350 (mutation reflected in amino acid position 117), which may not have a significant impact on the structure of the protein as a valine to alanine mutation is seen (alanine to valine in replicate 2, the two amino acids have hydrophobic side chains). Replicate 1, 4 and 6 all had mutations at nucleotide position 119 (mutation reflected in amino acid position 119) that may have a significant impact on the structure of the resulting protein as a valine is mutated to a methionine which is a change from an amino acid with a hydrophobic side chain to methionine which has a sulphur containing side chain that may change protein function. In 4 of 6 replicates for *E. coli* ATCC 25922, mutations in *pduV*, which codes for the propanediol utilization protein PduV, involved in propanediol utilization were seen. All four mutations occurred at the same position (nucleotide position 46, reflected in amino acid position 16). In replicates 2 and 3 there were missense mutations in the same position in the *hokC* gene, that codes for the toxic protein HokC.

In *E. coli* NCTC 10418 treated with sub-MIC Bm, all six replicates had mutations in *sbmA*, which codes for a protein involved in a peptide antibiotic transporter. Of the six mutations, four were frameshift mutations, one resulted in a premature stop codon, and only one was missense. In all of the replicates, there were multiple missense mutations in the *flu* gene which affects the Antigen 43 protein found on the surface of *E. coli* thought to be involved with autoaggregation.

In comparison, in the *E. coli* ATCC 25922 negative control, there were missense mutations in these genes: *agaS* (gene for a putative D-galactosamine-6-phosphate deaminase) (3 of 6 replicates), *garD* (the gene for galactarate dehydratase) (2 of 6 replicates), *hokC* (3 of 6 replicates), *ompX* (2 of 6 replicates) and the *srlR* (gene that codes for a DNA-binding transcriptional repressor) (2 of 6 replicates). In the *E. coli* NCTC 10418 strain that was treated with DMSO as a control, there were missense mutations in the *flu* gene (labelled as *flu_1*, *flu_2* and *flu_3*) (5/6 replicates). Missense mutations were detected in the *hokA* gene (which produces the protein HokA that is the toxic component of a type I toxin-antitoxin system) (5 of 6 replicates). Missense mutations were also detected in the *rhsC* gene (function of the RhsC protein is not fully elucidated) (1 of 6 replicates). Missense mutations were found in the *rhsD* gene (which codes for the RhsD protein, the function is not fully elucidated) (1 of 6 replicates). And finally, missense mutations were present in the *ygcB* gene which codes for a CRISPR-associated endonuclease/helicase Cas 3 (6 of 6 replicates).

The mutations that are attributed to the exposure of the *E. coli* strains to sub-MIC Bm appear to be involved in biofilm formation (*bcsA* and *yfiR*), metabolism/energy use (*bglB* and *pduV*) and transporters/porins (*sbmA*). Mutations that encourage biofilm formation and the activity of transporters or porins could reduce the ability of antibiotics to interact with the bacteria and allow the antibiotics to be exported from cells. Mutations that change the metabolic activity and the energy sources the bacteria can use would also be beneficial as resisting the effects of antibiotics, especially through the use of transporters and porins, can deplete the energy available to the cells.

Table 22: A summary of mutations altering the final protein found in the mutated *Escherichia coli* strain ATCC 25922 after exposure to sub-minimum inhibitory concentration of bleomycin (Bm) for 12 days, Illumina sequencing and analysis using the program snippy. Shown in red are the inserted DNA bases in the sequence.

E. coli ATCC 25922 replicate	Type		Amino Acid Position	Effect	Amino Acid Change	Gene	Product
1	Deletion	CGC > CC	196/872	Frameshift		*bcsA*	Cellulose synthase catalytic subunit (UDP-forming)
1	Deletion	GCG > GG	40/406	Frameshift		*sbmA*	Peptide antibiotic transporter SbmA
1	SNP	T > C	117/199	Missense	Val117Ala	*ompX_3*	Outer membrane protein X
1	SNP	G > A	119/199	Missense	Val119Met	*ompX_3*	Outer membrane protein X
2	Insertion	GCA > GCCA	130/133	Frameshift		*bglB_1*	6-phospho-beta-glucosidase BglB
2	SNP	C > T	117/199	Missense	Ala117Val	*ompX_2*	Outer membrane protein X
2	SNP	G > A	16/118	Missense	Arg16Cys	*pduV_2*	Propanediol utilization protein PduV
2	SNP	A > G	20/51	Missense	Met20Val	*hokC_2*	Toxic protein HokC
3	SNP	G > A	16/118	Missense	Arg16Cys	*pduV_2*	Propanediol utilization protein PduV
3	SNP	T > C	20/51	Missense	Met20Val	*hokC_2*	Toxic protein HokC
3	SNP	G > T	148/188	Stop gained		*yfiR*	Putative HTH-type transcriptional regulator YfiR
4	SNP	T > C	117/199	Missense	Val117Ala	*ompX_3*	Outer membrane protein X
4	SNP	G > A	119/199	Missense	Val119Met	*ompX_3*	Outer membrane protein X
4	SNP	C > T	16/118	Missense	Arg16Cys	*pduV_2*	Propanediol utilization protein PduV
6	SNP	G > A	99/406	Stop gained		*sbmA*	Peptide antibiotic transporter SbmA
6	SNP	C > T	119/199	Missense	Val119Met	*ompX_3*	Outer membrane protein X
6	SNP	A > G	117/199	Missense	Val117Ala	*ompX_3*	Outer membrane protein X
6	SNP	C > T	16/118	Missense	Arg16Cys	*pduV_2*	Propanediol utilization protein PduV

Table 23: A summary of mutations altering the final protein found in the mutated *Escherichia coli* strain NCTC 10418 after exposure to sub-minimum inhibitory concentration of bleomycin (Bm), Illumina sequencing and analysis using the program snippy. Shown in red are the inserted DNA bases in the sequence.

E. coli NCTC 10418 replicate	Type			Effect	Amino Acid Change	Gene	Product
1	SNP	G > A	648/949	Missense	Ser648Asn	*flu_3*	Antigen 43
1	Complex	GGACA > **T**GAC**G**	881/949	Missense	Met883Val	*flu_3*	Antigen 43
1	Complex	ACA > **CC**G	899/949	Missense	Gln900Arg	*flu_3*	Antigen 43
1	SNP	T > A	102/406	Missense	Val102Glu	*sbmA*	Peptide antibiotic transporter SbmA
2	SNP	A > G	738/1039	Missense	Asn738Ser	*flu_2*	Antigen 43
2	Complex	TGACG > **G**GAC**A**	971/1039	Missense	Val973Met	*flu_2*	Antigen 43
2	Complex	CCG > **A**C**A**	989/1039	Missense	Arg990Gln	*flu_2*	Antigen 43
2	Deletion	ATG > AG	112/406	Frameshift		*sbmA*	Peptide antibiotic transporter SbmA
3	Complex	TGT > **C**G**G**	900/949	Missense	Gln900Arg	*flu_3*	Antigen 43
3	SNP	C > T	648/949	Missense	Ser648Asn	*flu_3*	Antigen 43
3	Deletion	CAAAAAG > CAAAAG	70/406	Frameshift		*sbmA*	Peptide antibiotic transporter SbmA
4	SNP	G > A	648/949	Missense	Ser648Asn	*flu_3*	Antigen 43
4	Complex	GGACA > **T**GAC**G**	881/949	Missense	Met883Val	*flu_3*	Antigen 43
4	Complex	ACA > **CC**G	899/949	Missense	Gln900Arg	*flu_3*	Antigen 43
4	SNP	C > T	111/406	Stop gained		*sbmA*	Peptide antibiotic transporter SbmA
5	Complex	CGG > **T**G**T**	990/1039	Missense	Arg990Gln	*flu_1*	Antigen 43

5	Complex	CGTCA > **T**GTC**C**	973/1039	Missense	Val973Met	*flu_1*	Antigen 43
5	SNP	G > A	648/949	Missense	Ser648Asn	*flu_3*	Antigen 43
5	Insertion	ATA > A**T**TA	128/406	Frameshift		*sbmA*	Peptide antibiotic transporter SbmA
6	Complex	TGT > **C**G**G**	900/949	Missense	Gln900Arg	*flu_3*	Antigen 43
6	Complex	TGTCC > **C**GTC**A**	883/949	Missense	Met883Val	*flu_3*	Antigen 43
6	SNP	C > T	648/949	Missense	Ser648Asn	*flu_3*	Antigen 43
6	Deletion	TGA > TA	108/406	Frameshift		*sbmA*	Peptide antibiotic transporter SbmA

Table 24: A summary of the synonymous mutations found in the mutated *Escherichia coli* strain ATCC 25922 after exposure to sub-minimum inhibitory concentration of bleomycin (Bm), Illumina sequencing and analysis using the program snippy. Shown in red are the inserted DNA bases in the sequence.

E. coli ATCC 25922 Replicate	Type		Amino Acid Position	Gene	Product
1	SNP	T > A	198/329	*iolS_2*	Aldo-keto reductase IolS
1	SNP	C > T	783/1347	*ftsK*	DNA translocase FtsK
1	Complex	TAA > **CA**G	131/245		Hypothetical protein
1	SNP	G > A	185/351	*phoE*	Outer membrane pore protein E
1	SNP	A > G	105/199	*ompX_3*	Outer membrane protein X
2	SNP	A > G	115/245		Hypothetical protein
2	Complex	TGTT > **C**GT**C**	126/245		Hypothetical protein
2	Complex	TTA > **CT**G	131/245		Hypothetical protein
2	SNP	G > A	105/199	*ompX_2*	Outer membrane protein X
2	SNP	C > T	1553/2166	*tycC*	Tyrocidine synthase 3
3	SNP	A > G	278/308	*menA*	1,4-dihydroxy-2-naphthoate octaprenyltransferase
3	SNP	C > T	337/377		Hypothetical protein
3	Complex	TAA > **CA**G	131/245		Hypothetical protein
3	Complex	AACA > **G**AC**G**	126/245		Hypothetical protein
3	SNP	T > C	115/245		Hypothetical protein
3	SNP	A > G	64/377		Hypothetical protein
4	SNP	G > A	115/245		Hypothetical protein
4	Complex	CGTC > **T**GT**T**	126/245		Hypothetical protein
4	Complex	CTG > **TT**A	131/245		Hypothetical protein
4	SNP	G > A	1553/2166	*tycC*	Tyrocidine synthase 3
5	SNP	G > A	1553/2166	*tycC*	Tyrocidine synthase 3
6	SNP	A > G	128/250	*bcsQ*	Cellulose biosynthesis protein BcsQ
6	SNP	T > C	155/493		Hypothetical protein
6	SNP	T > C	155/493		Hypothetical protein
6	SNP	G > A	63/90		Hypothetical protein
6	SNP	C > T	337/377		Hypothetical protein
6	Complex	GGTTCCG > **C**GT**CCCA**	11/72		Hypothetical protein
6	SNP	A > G	115/245		Hypothetical protein
6	Complex	TGTT > **C**GT**C**	126/245		Hypothetical protein

6	Complex	TTA > **CTG**	131/245		Hypothetical protein
6	SNP	T > C	105/199	*ompX_3*	Outer membrane protein X
6	SNP	T > C	1267/2154	*mbtB*	Phenyloxazoline synthase MbtB

Table 25: A summary of the synonymous mutations found in the mutated *Escherichia coli* strain NCTC 10418 after exposure to sub-minimum inhibitory concentration of bleomycin (Bm), Illumina sequencing and analysis using the program snippy.

E. coli NCTC 10418 replicate	Type		Amino Acid Position	Gene	Product
1	SNP	A > G	674/949	*flu_3*	Antigen 43
1	SNP	C > A	879/949	*flu_3*	Antigen 43
1	SNP	T > C	902/949	*flu_3*	Antigen 43
1	SNP	A > G	20/520	*casA*	CRISPR system Cascade subunit CasA
1	SNP	G > A	23/520	*casA*	CRISPR system Cascade subunit CasA
1	SNP	A > G	17/29		Hypothetical protein
1	SNP	G > A	13/29		Hypothetical protein
1	SNP	T > G	126/272		Hypothetical protein
1	SNP	T > C	75/104		Hypothetical protein
1	SNP	C > T	131/199		Hypothetical protein
1	Complex	TGGT > CGGC	144/199		Hypothetical protein
1	Complex	CTA > TTG	150/199		Hypothetical protein
1	SNP	C > T	163/199	*ompX_3*	Outer membrane protein X
1	SNP	A > G	170/199	*ompX_3*	Outer membrane protein X
1	SNP	G > A	15/50	*hokA_1*	Protein HokA
1	SNP	A > G	17/50	*hokA_1*	Protein HokA
1	Complex	AGAC > GGAT	25/50	*hokA_1*	Protein HokA
1	SNP	T > C	351/748	*rhsD_6*	Protein RhsD
1	SNP	G > A	340/748	*rhsD_6*	Protein RhsD
1	Complex	GCCA > ACCG	330/748	*rhsD_6*	Protein RhsD
1	SNP	C > T	176/214	*ybdM_2*	Putative protein YbdM
2	SNP	G > A	764/1039	*flu_2*	Antigen 43
2	SNP	A > C	969/1039	*flu_2*	Antigen 43
2	SNP	C > T	992/1039	*flu_2*	Antigen 43
2	SNP	A > G	17/29		Hypothetical protein
2	SNP	G > A	13/29		Hypothetical protein
2	SNP	T > C	75/104		Hypothetical protein
2	SNP	T > C	170/199	*ompX_4*	Outer membrane protein X
2	SNP	G > A	163/199	*ompX_4*	Outer membrane protein X
2	SNP	A > G	15/50	*hokA_2*	Protein HokA
2	SNP	G > A	17/50	*hokA_2*	Protein HokA
2	SNP	T > C	351/748	*rhsD_6*	Protein RhsD

2	SNP	G > A	340/748	*rhsD_6*	Protein RhsD
2	Complex	GCCA > ACCG	330/748	*rhsD_6*	Protein RhsD
2	SNP	T > C	174/212	*ybdM_3*	Putative protein YbdM
3	SNP	C > T	764/1039	*flu_2*	Antigen 43
3	SNP	A > G	902/949	*flu_3*	Antigen 43
3	SNP	G > T	879/949	*flu_3*	Antigen 43
3	SNP	C > T	23/520	*casA*	CRISPR system Cascade subunit CasA
3	SNP	T > C	20/520	*casA*	CRISPR system Cascade subunit CasA
3	SNP	T > C	75/104		Hypothetical protein
3	SNP	G > A	15/50	*hokA_1*	Protein HokA
3	SNP	A > G	17/50	*hokA_1*	Protein HokA
3	Complex	AGAC > GGAT	25/50	*hokA_1*	Protein HokA
3	Complex	TGGC > CGGT	329/748	*rhsD_6*	Protein RhsD
3	SNP	C > T	340/748	*rhsD_6*	Protein RhsD
3	SNP	A > G	351/748	*rhsD_6*	Protein RhsD
3	SNP	T > C	174/212	*ybdM_4*	Putative protein YbdM
3	SNP	T > C	21/35	*ldrA_2*	Small toxic polypeptide LdrA
4	SNP	A > G	674/949	*flu_3*	Antigen 43
4	SNP	A > G	20/520	*casA*	CRISPR system Cascade subunit CasA
4	SNP	G > A	23/520	*casA*	CRISPR system Cascade subunit CasA
4	SNP	C > T	163/199	*ompX_3*	Outer membrane protein X
4	SNP	A > G	170/199	*ompX_3*	Outer membrane protein X
4	SNP	T > C	17/50	*hokA_2*	Protein HokA
4	SNP	C > T	15/50	*hokA_2*	Protein HokA
4	SNP	T > C	351/748	*rhsD_6*	Protein RhsD
4	SNP	G > A	340/748	*rhsD_6*	Protein RhsD
4	Complex	GCCA > ACCG	330/748	*rhsD_6*	Protein RhsD
4	SNP	C > T	176/214	*ybdM_3*	Putative protein YbdM
5	SNP	G > A	992/1039	*flu_1*	Antigen 43
5	SNP	T > G	969/1039	*flu_1*	Antigen 43
5	SNP	C > T	764/1039	*flu_1*	Antigen 43
5	SNP	A > G	75/104		Hypothetical protein
5	SNP	C > T	163/199	*ompX_4*	Outer membrane protein X
5	SNP	A > G	170/199	*ompX_4*	Outer membrane protein X
5	Complex	GTCT > ATCC	26/50	*hokA_2*	Protein HokA
5	SNP	T > C	351/748	*rhsD_5*	Protein RhsD
5	SNP	G > A	340/748	*rhsD_5*	Protein RhsD
5	Complex	GCCA > ACCG	330/748	*rhsD_5*	Protein RhsD
5	SNP	G > A	176/214	*ybdM_3*	Putative protein YbdM
6	SNP	A > G	20/520	*casA*	CRISPR system Cascade subunit CasA

					CRISPR system Cascade
6	SNP	G > A	23/520	*casA*	subunit CasA
6	SNP	T > C	75/104		Hypothetical protein
6	SNP	T > C	163/199	*ompX_1*	Outer membrane protein X
6	SNP	G > A	170/199	*ompX_1*	Outer membrane protein X
6	Complex	ATCC > GTCT	26/50	*hokA_1*	Protein HokA
6	SNP	C > T	17/50	*hokA_1*	Protein HokA
6	SNP	T > C	15/50	*hokA_1*	Protein HokA
6	Complex	TGGC > CGGT	329/748	*rhsD_5*	Protein RhsD
6	SNP	C > T	340/748	*rhsD_5*	Protein RhsD
6	SNP	A > G	351/748	*rhsD_5*	Protein RhsD
6	SNP	G > A	176/214	*ybdM_2*	Putative protein YbdM

Table 26 and 27 inserted below summarise the mutations altering the final protein and synonymous mutations seen in the two *E. coli* strains (ATCC 25922 and NCTC 10418) when they were treated with sub-MIC Bm or the equivalent volume of DMSO.

Table 26: A summary of the mutations altering the final protein found in the *E. coli* strains ATCC 25922 and NCTC 10418 when a sub-inhibitory concentration of bleomycin (Bm) or the equivalent volume of DMSO was added in the *in vitro de novo* mutations experiment. The frequency of the SNPs is presented with the number of replicates in brackets describing how many of the replicates displayed a mutation in the corresponding gene. For each condition, 6 replicates were conducted ($n = 6$).

| Gene | Number of SNPs detected (presence in replicates) | | | |
	E. coli ATCC 25922 + Bm	*E. coli* ATCC 25922 + DMSO	*E. coli* NCTC 10418 + Bm	*E. coli* NCTC 10418 + DMSO
agaS		3 (3/6 replicates)		
bcsA	1 (1/6 replicates)			
bglB	1 (1/6 replicates)			
flu			13 (5/6 replicates)	11 (5/6 replicates)
garD		2 (2/6 replicates)		
hokA			10 (5/6 replicates)	9 (5/6 replicates)
hokC	2 (2/6 replicates)	3 (3/6 replicates)		
mdoH			2 (2/6 replicates)	
ompX	8 (4/6 replicates)	4 (2/6 replicates)		
pduV	4 (4/6 replicates)			
rhsC				3 (1/6 replicates)
rhsD			12 (6/6 replicates)	1 (1/6 replicates)
sbmA	2 (2/6 replicates)		6 (6/6 replicates)	
srlR		4 (2/6 replicates)		
ybdM			5 (5/6 replicates)	
yfiR	2 (2/6 replicates)			
ygcB			8 (6/6 replicates)	9 (6/6 replicates)

Table 27: A summary of the synonymous mutations found in the *E. coli* strains ATCC 25922 and NCTC 10418 when a sub-inhibitory concentration of bleomycin (Bm) or the equivalent volume of DMSO was added in the *in vitro de novo* mutations experiment. The frequency of the SNPs is presented with the number of replicates in brackets describing how many of the replicates displayed a mutation in the corresponding gene. For each condition, 6 replicates were conducted (n = 6).

| Gene | Number of SNPs detected (presence in replicates) | | | |
	E. coli ATCC 25922 + Bm	*E. coli* ATCC 25922 + DMSO	*E. coli* NCTC 10418 + Bm	*E. coli* NCTC 10418 + DMSO
bcsQ	1 (1/6 replicates)			
casA			8 (4/6 replicates)	10 (5/6 replicates)
era		5 (2/6 replicates)		1 (1/6 replicates)
flu			13 (5/6 replicates)	12 (5/6 replicates)
ftsK	1 (1/6 replicates)			
garD		2 (2/6 replicates)		
hokA			14 (6/6 replicates)	11 (5/6 replicates)
iolS	1 (1/6 replicates)			
ldrA			1 (1/6 replicates)	
mbtB	1 (1/6 replicates)	4 (4/6 replicates)		
menA	1 (1/6 replicates)			
ompD		1 (1/6 replicates)		
ompX	3 (3/6 replicates)	4 (4/6 replicates)	10 (5/6 replicates)	5 (3/6 replicates)
phoE	1 (1/6 replicates)			
rhsD			18 (6/6 replicates)	11 (5/6 replicates)
srlR		12 (4/6 replicates)		
tycC	3 (3/6 replicates)	2 (2/6 replicates)		
upaG		2 (2/6 replicates)		
ybdM			6 (6/6 replicates)	1 (1/6 replicates)
ycbX		1 (1/6 replicates)		

3.4.8. The impact of bleomycin on mutation frequency

Mutation frequency experiments were conducted on 3 strains from the mutation induction experiments: *E. coli* ATCC 25922 replicate 1 exposed to sub-MIC Bm for 12 days (ATCC.Bm.12.1) and DMSO (control) for both 0 days (ATCC.DO.0.1) and 12 days (ATCC.DO.12.1). The same conditions and day duration samples were also used for *E. coli* ATCC 25922 replicate 3 and 4 (ATCC.Bm.12.3, ATCC.DO.0.3, ATCC.DO.12.3, ATCC.Bm.12.4, ATCC.DO.0.4, ATCC.DO.12.4). The average mutation frequencies are presented in Table 28 below. A significant difference was found in the mutation frequency between the Bm treated strain and the control strain at 12 days (U= 46, P<0.05) for *E. coli* ATCC 25922 replicate 1 where the negative control (DMSO solvent only) had a higher mutation frequency than the cells treated with Bm. There was no significant difference in the mutation frequency after exposure to either 0 days or 12 days DMSO (U= 107, P= 0.205), demonstrating that the DMSO used as a solvent control was not responsible for the change in mutation frequency after 12 days exposure. For the *E. coli* ATCC 25922 strain replicate 3, there was no significant difference between the Bm treated strain and the controls in *E. coli* ATCC 25922 replicate 3 after 12 days (U= 93, P= 0.127) and no significant difference in the mutation frequency of the control after 0 days or 12 days of DMSO (U= 120, P= 0.581). For the *E. coli* ATCC 25922 replicate 4 strain, a Mann-Whitney U test determined that there was no significant difference in the mutation frequency when you compare the Bm treated and control strains (U= 105, P= 0.276) but there was a significant difference when you compare the control strains after 0 days exposure and 12 days (U= 60, P<0.05). Out of the three strains examined here (*E. coli* ATCC 25922 replicates 1, 3 and 4), only one of the strains had a lower mutation frequency when compared to the DMSO control strain.

Table 28: Average mutation frequency of the *Escherichia coli* ATCC 25922 strains generated in the mutation induction experiments. The strains were labelled according to the original wildtype strains (ATCC), treatment condition (Bm or DMSO (control, DO)), the duration of treatment (0 or 12 days) and then replicate number (*n* = 3).

E. coli strain	Average Mutation Frequency
ATCC.Bm.12.1	2.86×10^{-8}
ATCC.DO.0.1	2.64×10^{-7}
ATCC.DO.12.1	1.53×10^{-7}
ATCC.Bm.12.3	2.79×10^{-7}
ATCC.DO.0.3	1.43×10^{-7}
ATCC.DO.12.3	2.12×10^{-7}
ATCC.Bm.12.4	2.33×10^{-7}
ATCC.DO.0.4	2.05×10^{-7}
ATCC.DO.12.4	1.48×10^{-7}

3.5. Discussion

3.5.1. Bleomycin can select for reduced antibiotic susceptibility

When the antibiotic susceptibility was tested after mutation induction on agar plates using the method from the Auda (2007) paper we did not see any mutants grow that could be attributed to the action of bleomycin. It is possible that the organisms tested were growing on the antibiotic plates when there should have been no growth because the MIC of the organism for the antibiotic being tested was on the boundary of the MIC range tested. To resolve this issue in the future, MIC testing should be done using a finer, more precise range with more replicates. This method of mutation induction and subsequent antibiotic susceptibility testing was also discontinued because it was possible that the bacteria were failing to mutate as the stress of Bm exposure, as well as exposure to a secondary antibiotic depleted a lot of energy and the bacteria were unable to grow. A more likely explanation is that exposure to Bm and a secondary antibiotic works in a similar way to antibiotic combination therapy. There are a variety of theories as to why combination therapies are more effective against pathogenic bacteria. They can act in different ways, for instance by one drug increasing the activity of the other; by sequestering an inhibitor for one of the antibiotics; or by targeting different pathways (Sullivan *et al.*, 2020). Throughout the literature, we can see the action of combination therapies succeeding together

rather than given individually. For instance, trimethoprim and sulfamethoxazole act synergistically together by targeting different steps in a biosynthetic pathway for tetrahydrofolate, which is an important component in energy metabolism which is important for cell survival and growth (Minato *et al.*, 2018).

It is also possible that only a few resistant colonies (that were detected when the cells were exposed to the antibiotic GENT) were identified using this method as the bacterial strains we used were normal laboratory strains that have been grown under controlled conditions and may not react to the conditions in the same way that wildtype bacteria do. It has been commented on in the literature that many of the laboratory strains we use, differ from strains that we see in different environments and clinical infections as scientists create an environment that encourages bacterial growth (Bollenbach *et al.*, 2009). This brings attention to the idea that the laboratory strains that we use as models and the results we see may not apply to 'real-world' bacterial strains, especially as bacteria can live in communities where the behaviour of one species can affect the behaviour of another (Palkova, 2004). The difference between strains from a clinical setting and the laboratory was also demonstrated in a study by Bundy *et al.* (2005), where the genomic DNA of both commonly used laboratory strains and clinical strains was examined for any toxin genes that could be used as candidate genes to distinguish between the two different groups. Although the study found no potential candidate genes, they showed that through analysing the metabolomics of the two groups, they were able to distinguish between the laboratory and clinical strains, which indicates that although the strains are similar in terms of their genomic content, they may behave differently in the same environment (Bundy *et al.*, 2005).

3.5.2. Antibiotic susceptibility tests for mutants induced by bleomycin

When *E. coli* ATCC 25922 was tested for its susceptibility against CHL, CIP and Bm after being previously exposed to Bm or the control, there was a significant difference in the MIC values, where cells that were treated with sub-MIC Bm were more susceptible to the antibiotics than the controls. When *E. coli* NCTC 10418 was tested for its susceptibility against CHL, NA and Bm, there was a significant difference between cells treated with Bm and the control, where the sub-MIC Bm treated cells were less susceptible. When the *E. coli* ATCC 25922 were treated with Bm on 0 days and 12 days incubation, there was a difference in the MIC against the antibiotics CHL, AMP and Bm, where the MIC was greater after 12 days exposure to Bm. When *E. coli* NCTC 10418 was treated with Bm, there was a significant difference in the strain's MIC against AMP, NA and Bm but not to GENT, CIP, TET and MERO after the 12 days exposure. For the control, there was a significant difference between the 0 and 12 days treated samples in the MIC against

CIP, where the MIC was lower after 12 days. When we look at the antibiotic susceptibility profiles of the *E. coli* mutants, we see that although there are changes that are concerning, they MICs are not at clinically significant levels. It is important to note that we determined the stopping point of these evolution experiments using a conservative experimental design that allowed for multiple substitutions per site. We assumed the average *E. coli* genome to be 4 Mbp which indicated that after 24 hours the *E. coli* ATCC 25922 would have 41 mutations per base pair and *E. coli* NCTC 10418 would have 39 mutations per base pair. If we were to use an estimate at the upper end of known genome sizes for *E. coli* of 6 Mbp, the *E. coli* ATCC 25922 strain would have 27 mutations per base pair after 24 hours and *E. coli* NCTC 10418 would have 26 mutations per base pair. As the study was run over 12 days, we would expect *E. coli* ATCC 25922 to have 328 mutations per base pair over 12 days, and *E. coli* NCTC 10418 to have 313 mutations per base pair. This does not affect our results or our experimental stopping point, as we have still given enough time and opportunity for a mutation to arise in every base pair of the genome over the course of the experiment in each *E. coli* strain.

The differences that we can see in the susceptibility profiles of the *E. coli* strains could be attributed to the effects of cross-resistance. Cross-resistance usually entails resistance to multiple antibiotics through one molecular mechanism. Examples for such mechanisms include how the antibiotics enter the cell, interaction with the same targets or involvement in the same cellular pathway that can be important for cell growth (Colclough *et al*., 2019). A study by Chuanchuen *et al*. (2001) demonstrated that when *P. aeruginosa* was exposed to triclosan (an antiseptic commonly used in household cleaners), efflux systems such as MexAB-OprM, MexCD-OprJ and MexEF-OprN were important for its removal from the cell. For a *P. aeruginosa* PAO1 strain that was expressing MexAB-OprM, the MIC of antibiotics such as TET, trimethoprim and erythromycin were much higher than the *P. aeruginosa* PAO200 strain that does not express any efflux proteins.

A study conducted by Sutherland *et al.* (1964), demonstrated that *in vitro* studies where *Salmonella paratyphi* B was repeatedly sub-cultured in the presence of antibiotics, there was cross-resistance between antibiotics such as penicillins (AMP and benzyl-penicillin), CHL, TET and streptomycin when the cells were cultured with AMP. These differences were also seen when the cells were treated with the antibiotics benzyl-penicillin, CHL and TET, but not streptomycin. It is difficult to determine why cross-resistance is seen with these antibiotics, especially in our study where the susceptibilities for the antibiotics CHL, CIP, NA and AMP are significantly different to the control group, as these antibiotics have different mechanisms of action.

3.5.3. Mechanisms responsible for resistance

It is not unusual to see SNPs when the bacteria are exposed to DMSO, as DMSO (and other organic solvents) can affect the cell membrane to an extent that ultimately leads to cell death at certain concentrations that accumulate in the membrane (Dyrda *et al.*, 2019). As living organisms, bacteria will try to adapt to a changing environment or stressor. This is why any mutations that were seen in the DMSO controls and the sub-MIC Bm treated cells were disregarded, as they are thought to be as a result of the solvent rather than the action of Bm.

A mutation in *bcsA* resulting in a frameshift mutation was seen in a single isolate that had evolved reduced susceptibility to Bm. The *bcsA* gene is involved in the synthesis of cellulose, specifically making up the cellulose synthase (Omadjela *et al.*, 2013). Cellulose produced by bacteria can be used as a component in the ECM, commonly involved in biofilm formation (Salgado *et al.*, 2019). In a study conducted by Salgado *et al.* (2019), they found that mutations in the BcsA protein conferred resistance to pellicin in the organism *Komagataeibacter xylinus* through the formation of a pellicle. A previous study conducted by Ochoa *et al.* (2016) highlighted the importance of the *bcsA* gene in uropathogenic *E. coli* strains, as the expression of the *bcsA* gene is associated with the operon *csg*, which encodes for curli fimbriae. It is possible that mutations in the *bcsA* gene reduce the motility of the bacteria and encourages aggregation and adhesion to surfaces to enable the formation of biofilms that may confer general protection to antimicrobials. In order to determine the effect of the mutations seen in the *bcsA* gene on the phenotype of the *E. coli* cells seen in this study, more work needs to be conducted to monitor the motility and adhesion of the cells and also the ability of the cells to form biofilms. Simple experiments could be conducted to determine whether the cells are forming biofilms, for instance growing the cells on a slide or in plate wells and staining with crystal violet and measuring its absorbance. These slides could then be viewed using microscopes to determine whether the cells were attached and forming biofilms. A microtiter plate assay with different materials/surfaces (e.g. polyvinyl chloride, PVC) could also be used as an indirect way of determining biofilm formation (Djordjevic *et al.*, 2002).

Mutations in *sbmA* were seen across many mutants with reduced susceptibility to Bm in the present study. Previous studies have demonstrated that the SbmA transporter (in the peptide uptake permease (PUP) family and similar in the transmembrane domain to ABC transporters) interacts with Bm and other proline-rich peptides and imports these molecules into the cell, with mutations in the SbmA protein conferring an increased resistance to Bm (Mattiuzzo *et al.*, 2007; Narayanan *et al.*, 2014). It is not fully elucidated what the role of the SbmA transporter is in bacteria, but *in vitro* studies have demonstrated that the SbmA protein is not essential for cell

survival (Narayanan *et al*., 2014). In a study conducted by Vallejos *et al*. (2011), they found that when the function of the SbmA and TolC proteins were disrupted, *E. coli* cells were more susceptible to heat damage but more resistant to the effects of peptide antibiotics (including Bm). Vallejos *et al*. (2011) hypothesised that sensitivity to heat in SbmA and TolC mutants may be as a result of peptides or metabolites building up in the cell that the cell is unable to remove due to the inactivation of the transporters. It is possible that as SbmA has been previously shown to uptake antimicrobials such as Bm, mutations to the *sbmA* gene that potentially inactivate the gene, renders the Bm unable to access the cell and interact with DNA to inflict damage. The study conducted by Vallejos *et al*. (2011) also suggested that the *sbmA* transporter may also function as an exporter under certain conditions e.g. under stress, rather than acting as just an importer of molecules.

In the present study, a single mutant with reduced Bm susceptibility had a mutation resulting in a frameshift in *bglB*. The *bglB* gene is part of the *bgl* operon involved in the cell's ability to utilise β-glucosides as an energy source but is silent in wild-type strains of *E. coli* (Madan *et al*., 2005). Specifically, the *bglB* gene codes for a phosphor-β-glucosidase that hydrolyses the glycosides salicin and arbutin when they are in their phosphorylated forms (Harwani *et al*., 2012). In a study conducted by Madan *et al*. (2005), they found that expression of the *bgl* operon increased bacterial fitness in the stationary phase of growth and provided a competitive advantage when it was coupled with the *rpoS819* allele. It is possible that mutations in the *bgl* operon, specifically the *bglB* gene allows the bacterial cells to utilise a wider range of energy sources for metabolism. As the *bgl* operon is silent under normal conditions in wildtype *E. coli*, it is possible that in this study, mutations to the operon and the *bglB* gene allows the activation and expression of the operon to confer a fitness advantage in an environment challenged with antibiotics. One way to determine whether mutations to the *bgl* operon-specifically the *bglB* gene- affected the fitness of bacteria, experiments could be conducted where the same mutation is introduced to the normal wildtype *E. coli* strain and then tested for its susceptibility to a small panel of antibiotics. Other methods that could be employed here are gene expression experiments to determine whether strains with the mutation or the normal wildtype have the same *bglB* gene expression profiles using microarrays or reverse transcription polymerase chain reaction (RT-PCR). As wildtype *E. coli* typically are unable to grow on arbutin and salicin, a simple way of determining whether the *bgl* operon is activated as a result of mutations in the *bglB* gene, the *de novo* mutants generated in the mutation induction experiments could be grown on salicin and/or arbutin plates, with the ancestors and control strains as controls.

A single isolate with reduced susceptibility to Bm contained a mutation in the *yfiR* gene, which is part of the *yfiBNR* operon involved in the regulation of c-di-GMP levels in *P. aeruginosa.* The operon *yfiBNR* is thought to play a part in small colony variants seen in *P. aeruginosa* populations (Malone *et al.*, 2010). In a study conducted by Malone *et al*. (2010), *yfiR* transposon mutants were generated and also mutants without the *yfiR* gene showed an increased ability to attach to surfaces, with a reduction in motility compared to the wildtype *P. aeruginosa* ancestor PAO1 strain. A reduction in motility, an increase in cell adhesion to surfaces and a reduced surface size could be beneficial when the bacterial cells are resisting the action of antimicrobials when the *yfiR* gene is mutated. A study conducted by Raterman *et al*. (2013) also demonstrated the importance of the *yfiR* gene, where disruption of this gene led to the increased production of cellulose and curli fimbriae in the *E. coli* strain CFT073. When the mutated *yfiR E. coli* strain was compared to the wild-type strain *in vivo*, they found that the mutant was detected at a lower bacterial load in the bladder and the kidneys of a murine model, indicating a potential attenuation of the strain as a consequence of mutating (Raterman *et al*., 2013). A full deletion of the *yfiR* gene also impacted the motility of the *E. coli* CFT073 strain, and deletion of the genes *csgD* (involved in curli fimbriae formation) and *bcsA* (involved in cellulose production) brought the mutant *yfiR E. coli* CFT073 strain back to the same colonisation ability as the wild-type strain (Raterman *et al*., 2013). Coupled with *bcsA* mutations, cells may be accumulating and behaving in a more biofilm-like manner that allows survival of the cells and reduces the penetration of certain antibiotics that are detrimental to the cells. In *E. coli*, a deletion of the *yfiR* gene leads to defects in the cell's ability to be motile, and an increase in cellulose production can be observed (Li *et al*., 2015). In the literature, there is an indication that cellulose production is important in antimicrobial resistance, as the main components of the extracellular matrix (ECM, also referred to as exopolysaccharide, EPS) in biofilms are cellulose and curli fimbriae (Dieltjens *et al*., 2020). Biofilms are of particular concern when we look at the antimicrobial resistance (AMR) crisis as many studies have demonstrated the ability of biofilms to resist the effects of antibiotics. For instance, a study conducted by Cepas *et al*. (2019) found that *E. coli* biofilms were able to resist the effects of the antibiotic GENT. Santos-Lopez *et al*. (2019) highlighted that as biofilms are huge players in terms of the AMR crisis, understanding how antibiotic resistance can evolve in biofilms is also important to note in laboratories, as opposed to solely just focusing on planktonic cells in *in vitro* models. Their study found that *A. baumannii* ATCC 17978 in biofilms were less resistant to the antibiotics tested than their planktonic counterparts but were generally more fit when the antibiotic was removed (Santos-Lopez *et al.*, 2019). What was also interesting to note from their study was the appearance of collateral sensitivity to cephalosporin antibiotics in the biofilm populations, which with further research could be exploited to tackle the issues biofilms present in clinical infections (Santos-Lopez *et al*., 2019).

The *de novo* mutants generated from Bm exposure were found to have mutations in the *ompX* gene. The OmpX protein is found on the outer membrane of cells. In the organism *Enterobacter aerogenes*, overexpression of the *ompX* gene appears to be associated with the reduced expression of Omp36, a major porin (Dupont *et al.*, 2007; Viveiros *et al.*, 2007). It has been found in the past literature that expression of *ompX* increases when bacterial cells are exposed to antimicrobial agents or stress and may have an important role in membrane permeability and controlling any antibiotics that may penetrate the outer membrane (Dupont *et al.*, 2007). In *E. coli* cells, deletion of *ompX* causes increased cell surface contact in fimbriated cells, and the opposite in non-fimbriated cells on abiotic surfaces (Otto and Hermansson, 2004). In a study conducted by Otto and Hermansson (2004), they found that deleting the *ompX* gene led to changes in the cell surface hydrophobicity and the surface charge. It is possible that mutations in the *ompX* gene allows the *E. coli* mutants to resist the effects of antibiotics by reducing entry into the cell (by reducing surface porins), but also altering the cell surface properties (hydrophobicity and charge). In the case of this specific study, it is not clear what the effect of the specific SNPs we see have on the phenotype of the mutants. What adds to this complexity are the numbers of SNPs we see in parts of the genome that are not well annotated, where we may be losing important information that may indicate any changes to the regulation of certain genes that may be important for antibiotic resistance. To determine if there is a difference between the wild-type strain and the *de novo* mutants that we suspect to have SNPs that alter the function of efflux pumps, efflux assays could be conducted using ethidium bromide and detecting the fluorescence when the cells are treated with Bm and supplemented with glucose and analysing the fluorescence over time at excitation/emissions at 520/590 nm (Pal *et al.*, 2020).

Mutations were also seen in the *pduV* gene, the function of which is not currently known for certain, but it is believed to have a role in 1,2-propanediol degradation (Cheng *et al.*, 2008). Faber *et al.* (2017) demonstrated the ability of *Salmonella enterica* serovar Typhimurium to use 1,2-propanediol and suggested that the *pdu* genes conferred a competitive advantage by allowing the organism to use another carbon source (1,2-propanediol) for respiration. However, in order to use 1,2-propanediol in a mouse model, *S.* Typhimurium also required the presence of other saccharolytic bacteria such as *Bacteroides thetaiotaomicron* and *Bacteroides fragilis* in order to degrade carbohydrates to fucose and rhamnose which is fermented to produce 1,2-propanediol (Faber *et al.*, 2017). Another study by Mangalappalli-Illathu and Korber (2006) found that when *Salmonella enterica* serovar Enteritidis ATCC 4931 biofilms were exposed to benzalkonium chloride (a quaternary ammonium compound used a disinfectant), many proteins were upregulated, including the proteins PduJ and PduA which are involved in 1,2-propanediol

degradation. This may indicate the importance of utilising different carbon sources when bacteria are faced with an antimicrobial agent. Mutations in the *hokC* gene poses an enigma as to why a bacterial cell may benefit from changes to this gene.

The *flu* gene was found to have mutated in the *E. coli* NCTC 10418 strain. The *flu* gene codes for Antigen 43 (Ag43) which is an autotransporter protein found on the surface of the cell that enhances autoaggregation of the cells and binding to inert surfaces (Hasman *et al*., 1999; Schembri *et al*., 2003). It is possible that coupled with the other mutations seen in the *E. coli* strain that mutation in the *flu* gene may also promote biofilm formation or a change in the external surface of the cell that encourages a barrier to antimicrobials. In a study conducted by Beloin *et al.* (2006), they found that in *E. coli* K-12 and a uropathogenic *E. coli* strain the deletion of the gene *rfaH* (transcription anti-terminator) increased the expression of the *flu* gene. The authors did not comment on whether or not this impacted the ability of the strains to form biofilms in terms of how quickly they developed or the density of the biofilm. However, the authors did find that in a uropathogenic *E. coli* strain, deletion of *rfaH* led to the cells in the biofilm packing together more tightly than the wildtype, although the impact of this on the ability to withstand the action of antibiotics is not clear (Beloin *et al.,* 2006). A different study by Schembri *et al*. (2003) looked at the global expression of genes in *E. coli* biofilms and found that the expression of the *flu* gene was significantly higher when the cells were in a biofilm than when they were growing as planktonic cells, indicating the crucial role of the *flu* gene in biofilm formation.

For all of the mutations that we have detected in the *E. coli* strains after Bm treatment, it is difficult to determine whether any specific mutation is responsible for a reduced susceptibility to a specific antibiotic, as many of strain replicates have mutations in the same genes. In order to unravel the effect of bleomycin exposure on antibiotic resistance evolution, more experiments need to be conducted to determine the effects mutations have on the phenotype of the bacteria. Future studies should probe into whether it is the action of a few key mutations or a consequence of all the mutations that we see in response to bleomycin exposure that leads to changes in antibiotic susceptibility.

3.5.4. The impact of bleomycin exposure on mutation frequency

From the mutation induction experiments, a small selection of *E. coli* ATCC 25922 mutants was selected in order to determine whether there was a change in mutation frequency after exposure to Bm. No overall pattern in changes to mutation frequency was observed.

Many studies in the past have demonstrated that the exposure of bacteria to antimicrobials can lead to spontaneous point mutations especially antimicrobials that interact with or damage DNA (Belov *et al*., 2009). In a study by Baharoglu and Mazel (2011), demonstrated that *Vibrio cholerae* strains showed an increased rate of mutation (a higher mutation frequency) after exposure to the antibiotics CHL and tobramycin which is suggested to be as a result of the induction of the SOS response. A study conducted by Miller *et al.* (2002) suggests that the elevated mutation rates seen in bacteria, and hypermutator strains are beneficial to the bacteria when they are challenged by antibiotics, allowing them to resist the effects or allow for a greater opportunity for compensatory mutations to arise that can ameliorate the fitness costs associated with acquired resistance plasmids. This makes logical sense and may apply in this study when the *E. coli* cells are exposed to sub-MIC concentrations of Bm, as it is a DNA damaging agent, which makes it unusual that from our experiments we didn't see any significant differences in mutation rates of the *de novo* mutants. It is possible that for these experiments, not enough replicates were conducted in order to capture the differences between the mutants compared to their parent strain. It is also possible that DMSO may have small effects on the bacterial genome and impact the SNPs we see, although we have accounted for this through the use of our solvent treated control strains.

4. <u>Chapter 4- Hi-C and long-read sequencing</u>

4.1. Introduction

4.1.1. Mobile genetic elements

Mobile genetic elements (MGEs) are pieces of DNA/genetic material that are able to move within a genome or between genomes of different bacteria. Examples of MGEs include plasmids, transposons, and insertion sequences (Carr *et al*., 2020). MGEs commonly have other genes associated with them, such as antibiotic resistance genes, and the movement of these genes can be altered by environmental stressors.

4.1.2. Horizontal gene transfer

Horizontal gene transfer (HGT) is the process by which bacteria transfer MGEs and has been found to be one of the main drivers of bacterial evolution (Vielva *et al.*, 2017). There are many different ways that bacteria can transfer MGEs like plasmids, the most common mechanisms being through transformation, conjugation, transduction (Baquero and Levin, 2020). Other mechanisms by which bacteria share genetic information are through conduction (non-mobilisable plasmids can be moved through co-integration with a mobilisable or conjugative plasmid) and vesiduction (the use of vesicles to aid in the transfer of the plasmid) (Baquero and Levin, 2020). Under certain conditions, HGT can be stimulated, for instance during inflammation of the gut in humans (Stecher *et al*., 2012). In a disease state, Stecher *et al*. (2012) suggested that HGT through conjugation can be triggered by pathogens and can lead to the shuffling of genetic material that can enhance virulence but also stimulate the evolution of any commensal organisms in the vicinity.

In biofilms, HGT occurs at a higher frequency. Which may be one component of how biofilms are able to resist the action of many antibiotics, as they are acquiring new genetic material that may provide a new phenotype (Penesyan *et al.*, 2020). This is of particular concern as The National Institutes of Health (NIH) estimates that 80% of infections in the body are caused by pathogens that are able to form biofilms and have an innate tolerance to antibiotics (Penesyan *et al.*, 2020; Trampari *et al*., 2021). Biofilms are also able to respond rapidly to new environments, and this is further exacerbated under antibiotic pressure (Trampari *et al*., 2021).

It is of particular concern that antibiotics used in health and biocides used in agriculture are detected at low concentrations in the wider environment, and that low level concentrations are able to stimulate HGT between different bacteria, as well as provide a selective pressure for genes that provide an advantage to persist (Jutkina *et al*., 2018).

Multiple roles have been proposed for HGT and the movement of MGEs in bacterial evolution. It has been suggested that HGT allows for the acquisition of new, beneficial genes and the sharing of these genes between different bacterial populations (Carvalho *et al*., 2020). Another suggestion has been made that HGT allows MGEs that are parasitic to be removed from the genome and stabilise it (Carvalho *et al*., 2020). In stochastic environments, bacterial cells that are able to uptake new DNA/MGEs are able to compete better in the environment than cells that are less competent/transformable (Carvalho *et al*., 2020). However, uptake of these MGEs and antibiotic resistance genes that are beneficial to the organism under certain stress conditions, impose a fitness cost on the bacteria and can be detrimental to maintain. Uptake of any extracellular DNA is also risky to cells as new MGEs have the potential to be toxic and detrimental to the organism (Carvalho *et al.*, 2020).

4.1.3. Advantages and disadvantages of short-read and long-read sequencing

Short-read sequencing technologies are limited to short sequences that are typically between 75 to 400 bp long (Adewale, 2020). Of the short-read sequencing (next generation sequencing) technologies, Illumina is the most robust and affordable. However, due to the short-read lengths used in short-read sequencing where DNA is fragmented and amplified, there isn't sufficient overlap in the reads to build a consensus sequence (Adewale, 2020). Small nucleotide level changes, insertions and deletions are identified well using short-read sequencing, however it struggles to detect larger scale sequence changes, such as inversion and translocation events. Current analysis tools and pipelines are more widely in place for short-read sequencing which is more attractive to researchers for their ease of use and availability (Amarasinghe *et al*., 2020).

Long-read sequencing (third-generation sequencing technologies) are typically capable of between 5,000 and 30,000 bp sequences which allows for better assemblies as more reasonable overlaps in the sequences are possible (Adewale, 2020). Long-read sequencing technologies also benefit from sequencing a single molecule of DNA and removes the need for amplification steps (Adewale, 2020). A major advance in technology was the release of the MinION by Oxford Nanopore Technologies (ONT) for long-read sequencing. On a standard MinION flowcell, there are 512 channels with 4 pores per channel where sequencing can be performed (Xu and Seki, 2019). The appeal of long-read sequencing is the ability to resolve DNA assemblies, especially sequences that can be repetitive in nature (Bertrand *et al*., 2019). Although long-read sequencing technologies can overcome issues with assembly associated with repetitive sequences, the error rate is higher than short-read sequencing technologies at around 5% as opposed to 0.1% (Adewale, 2020).

4.1.4. Hybrid assemblies

Through a combination of short-read sequencing and long-read sequencing to form hybrid assemblies, it is possible to utilise the strengths of both sequencing methods in order to achieve accurate and complete genomes (Bertrand *et al*., 2019). In studies that look at the microbiome and biofilms in antibiotic resistance where there is a mixture of bacterial organisms present, hybrid assemblies are particularly useful in discerning between different species (metagenomes) (Brown *et al*., 2021). An added advantage of the ONT MinION is the development of the ONT wash kit that enables the multiple use of a flow cell for multiple libraries that are run for a short time. This will reduce the costs of long-read sequencing using a MinION device (Lipworth *et al.*, 2020). In a paper by Ashton *et al*. (2015), hybrid assembly using MinION and the Illumina HiSeq platform was used to identify an antibiotic resistance island found in *Salmonella* Typhi which had not been previously characterised. The use of hybrid assemblies in the Lipworth *et al*. (2020) paper allowed the full resolution of MGEs by demonstrating the usefulness of hybrid assemblies where the low error read of Illumina reads and improved structural resolution of ONT sequencing were combined.

4.1.5. Hi-C and environmental samples

As mentioned previously in section 1.14, the Hi-C method is an interesting technique that can be used to explore DNA further in order to better understand the interactions of DNA in 3D space inside a cell. The Hi-C method has been used in wastewater samples to determine the associations between bacterial hosts and antibiotic resistance genes. In a study conducted by Stalder *et al*. (2019), they found that antibiotic resistance genes were more commonly found in γ- and β-*proteobacteria* in wastewater collected from Idaho (USA) in 2017. Resistance genes that were detected confer TET, β-lactam and macrolide resistance. The authors of the paper noted that determining the bacterial species a plasmid or MGE came from is difficult due to the low resolution of contigs, especially between closely related species.

4.1.6. Hi-C and microbiome studies

The Hi-C method has been shown to be very useful in microbiome studies to track the movement of antibiotic resistance genes, especially in the human gut microbiome. In a study by Kent *et al*. (2020), they demonstrated that MGEs were transferred within an individual's gut microbiome and transfer of these elements were higher in neutropenic patients. What was interesting to note in this study was that they observed novel antibiotic resistance genes in enteric pathogens in their patient samples. This poses a serious problem as neutropenic patients are more susceptible to infections and sepsis. Understanding where resistance genes and other virulence

genes come from and how frequently they are shared between different bacteria is important in controlling the spread of these genes and understanding how to treat patients in an appropriate manner that does not exacerbate the problem. It has been recorded that treating patients with antibiotics can stimulate more HGT events. A study by Kent *et al*. (2020) demonstrated that the Hi-C method has limitations in microbiome studies, where the origin of a MGE can only be determined if the bacterial host sequence data can be assembled and annotated. It is also emphasised that assembly of these sequences can be difficult as MGEs can undergo frequent recombination events and rearrange the genome order. It is the hope that by combining the Hi-C method with long-read sequencing and hybrid assemblies, the issues with assembly and annotation will be overcome.

4.1.7. Amplification and methylation patterns of DNA

The structure of chromosomes within a cell is dynamic and can be more or less easily accessible depending on the chromosome conformation at any given time (Wang *et al.*, 2019). Methylation patterns and sites on bacterial DNA are usually associated with the ability of the cell to distinguish between self and non-self DNA, but in recent years, more focus has been placed on the epigenetic effects of methylated DNA (Bart *et al.*, 2005). However, methylation patterns of DNA can be lost when the DNA is subcloned or PCR amplified (Bart *et al*., 2005). An advantage of using long-read sequencing methods, such as the ONT platform, allows the direct sequencing of DNA without the need for amplification. This can allow the downstream analysis of DNA methylation patterns that may be useful in studies looking at gene expression and the effect of external stressors on both the chromosome conformation and expression of genes (Wang *et al.*, 2019). A study conducted by Lee *et al.* (2018) used long-read sequencing on the ONT platform to investigate CpG methylation in human cell lines and the accessibility of chromatin by developing a method called nanoNOMe.

4.2. Aims and Objectives

The aim of this project is to develop the Hi-C method so that preparation of a Hi-C library can be done in a shorter time frame and also produce sufficient concentrations and quality of DNA to be used for long-read sequencing on a MinION device. This is so plasmid DNA/MGEs can be linked to their host bacteria and the movement of these elements within a population can be tracked. In the original Hi-C method by Lieberman-Aiden *et al.* (2009), conducting the whole method takes approximately 60 hours from having a cell pellet to creating a Hi-C library ready for sequencing, including quality checks. After the development of a more streamlined Hi-C method combined with long-read sequencing, the method will be tested on a known single bacterial culture, a known mixed bacterial culture and a clinical sample. In the analysis of the Hi-

C libraries, we want to determine whether it is possible to view the conformation of the chromosome and determine where antibiotic resistance genes are located in 3D space, and whether this structure changes under stress conditions.

We hypothesise that streamlining the Hi-C method is achievable and can be coupled with long-read sequencing in order to link mobile genetic elements that contain antibiotic resistance genes to their host bacteria to track their movement within a population. We hypothesise that exposure to antimicrobial agents such as bleomycin will alter the 3D chromosome conformation and therefore, affect the expression of genes involved in resisting the action of the agent.

4.3. Methods

4.3.1. Phase Genomics kit for Hi-C

The Phase Genomics ProxiMeta Hi-C kit was used (version 1.0). An overnight culture of a MDR *E. coli* was grown in 10 mL MHB (Oxoid, Fisher Scientific). The MDR *E. coli* strain that was used throughout this study is described in a paper written by Schmidt *et al*., (2017) and is referred to in their study as MDR *E. coli* H141480453. The protocol calls for a 50 µL bacterial pellet which was equivalent to the 10 mL overnight culture. Bacterial cells were pelleted by centrifuging 1 mL at a time in a 1.5 mL Eppendorf tube at 16,200 xg for 1 minute and the supernatant was discarded. The protocol was then followed as normal for the crosslinking, cell lysis, fragmentation, proximity ligation and DNA purification steps. After the DNA was purified, the sample was split in half and the DNA concentration was determined using the Invitrogen Qubit™ dsDNA HS Assay kit (ThermoFisher Scientific) and the DNA size was estimated using the TapeStation 2200 system (Agilent Technologies). The rest of the Phase Genomics protocol was followed for the sample that was sequenced on the Illumina NextSeq 500 platform.

4.3.1.1. Phase Genomics Hi-C kit for Illumina sequencing

The Phase Genomics ProxiMeta kit was used to extract DNA for sequencing on the Illumina NextSeq 500 platform with the MDR *E. coli* strain. When the DNA concentration was tested, the supernatants from each step was saved to test where DNA was lost in the protocol. DNA concentration and size was tested after each step using Qubit (HS) and TapeStation. Illumina sequencing was conducted by David Baker and Steven Rudder at the QIB on the Illumina NextSeq 500 platform.

4.3.1.2. Phase Genomics Hi-C kit for MinION sequencing

For the sample that was sequenced on the ONT MinION, the low input PCR MinION DNA preparation kit was used to prepare the Hi-C library for sequencing. Sequencing on the MinION device was conducted by Alex Trotter at the QIB. After sequencing, the ONT Epi2Me WIMP sequence analysis workflow was used.

4.3.1.3. Bioinformatics analysis

Analysis of the sequence data generated was performed by Dr. Lisa Crossman. A reference scaffold (created from both our short- and long-read sequencing of the MDR *E. coli* strain) was restriction digested computationally with the enzymes MluCI and Sau3AI were used in the Phase Genomics ProxiMeta kit in order to see where the Hi-C kit enzymes cut in a sequence and how the genome is broken down and digested. The MinION sequences were assembled using the Flye assembler (v 2.9) and visualised using a Bandage assembly graph. The Illumina generated reads were assembled using SPAdes (v 3.12.0) but using the MinION reference scaffold created from our long-read sequencing of the MDR *E. coli* strain. The program's pairtools (*GitHub-Open2c/Pairtools: CLI Tools to Process Mapped Hi-C Data* https://github.com/open2c/pairtools) and HiC-Pro (Servant *et al*., 2015) were used, coupled with ICE normalisation. A workflow was in development for the analysis of Hi-C data generated using long-read and short-read sequencing methods. Programs that were tested included GoTHiC, Calfea and pyHICCUPS but these were discarded for further use. Programs that were tested and kept included HiC-Pro, Fit-Hi-C (Ay *et al*., 2014), Pore-C (Ulahannan *et al*., 2019), HiGlass (Kerpedjiev *et al*., 2018) and pairtools.

Chromosome tests were conducted to identify if the plasmid would assemble with the chromosome when the plasmid was supplied at various proportions and whether the plasmid was supplied separately or artificially joined. To do this, different random percentages of *S. aureus* plasmid sequence and an *E. coli* K12 chromosomal DNA was used. Bandage graphs were used again to visualise and determine the outcome of these tests. To assess the quality of the sequenced Hi-C library, the Phase Genomics analysis platform was used to generate a Hi-C library QC report.

The MinION reads were also aligned to the MinION assembly to generate a 25K resolution contact map using Pore-C where the reads were mapped using bwa (Burrow-Wheeler Aligner) and default ONT parameters.

4.3.2. ProxiMeta Hi-C protocol with reagents substituted

The Phase Genomics ProxiMeta Hi-C kit method was used but with the reagents substituted in with reagents commonly used in the literature that aligned with the ProxiMeta method. This was done in order to utilise the method used in the kit but not the actual kit reagents due to expense and difficulty in acquiring the kit. The ProxiMeta Hi-C kit method was also used as it is a more streamlined method compared to the traditional Hi-C method used in the Lieberman-Aiden *et al.* (2009) paper and an objective of this project was to streamline the Hi-C method.

An overnight culture of a MDR *E. coli* strain was grown in 10 mL MHB. The overnight culture was then centrifuged in a tabletop centrifuge at 16,200 *x*g for 1 minute, using 1 mL of culture at a time and the supernatant discarded. 1 mL of fresh MHB was used to resuspend the cells. 48.78 μL formaldehyde (37-41%, Fisher Scientific) was added to the bacterial pellet to get a final concentration of 2% and resuspend the pellet. The Eppendorf tube was then incubated for 20 minutes at room temperature with occasional mixing by inversion. 52.44 μL of 2.5 M glycine was added to get a final concentration of 0.125 M. The Eppendorf tube was left to incubate for another 20 minutes at room temperature with occasional mixing. The tubes were then centrifuged at 17,000 *x*g for 5 minutes. The supernatant was saved separately to quantify any DNA present. The bacterial pellet was then resuspended in 200 μL of MHB. 5 μL of the sample was saved for later testing. The DNA from the bacterial cells was then extracted using the MagNA Pure Compact system (Roche Molecular Systems). The DNA was eluted in 50 μL, and 5 μL of this was saved for later testing. The DNA was then fragmented using the REs MluCI and Sau3AI. The restriction reaction was set up by adding to the DNA sample 0.5 μL of each enzyme (MluCI and Sau3AI) and 5 μL of NEBuffer 1.1. The tube was then incubated at 37°C for 1 hour. After incubation, the tube was centrifuged on a tabletop centrifuge at 16,200 *x*g for 1 minute. The supernatant was removed and saved for later testing. The DNA pellet was then resuspended in 500 μL of deionised water and DNA concentration was quantified using the HS dsDNA Qubit kit. The sample was then transferred to a 1.5 mL Falcon tube for proximity ligation. Proximity ligation of the DNA was then conducted by adding 2 μL of 10X T4 DNA Ligase buffer (ThermoFisher Scientific), 2 μL of 50% polyethylene glycol (PEG) (ThermoFisher Scientific), 1 μL DNA ligase (5 U/μL, ThermoFisher Scientific) and deionised water to a final volume of 8 mL. The tube was then incubated at 22°C for 1 hour and occasional mixing. After incubation, the crosslinks in the DNA were reversed by centrifuging the Falcon tube at 17,000 *x*g for 5 minutes. 1.5 mL of the supernatant was removed and saved for later testing, leaving 500 μL of solution and DNA pellet. 20 μL of proteinase K (20 mg/mL, QIAGEN) was added and the DNA pellet was resuspended, before incubation for 1 hour at 60°C. After incubation, proteinase K was heat inactivated by heating at 95°C for 10 minutes. Around 5 μL of the sample was then saved for use at a later date. The DNA was then purified by using the Promega Wizard® Genomic DNA Purification kit, the

protocol for isolating genomic DNA from Gram-positive and Gram-negative bacteria was used from step 13 where the DNA sample is added to a 1.5 mL Eppendorf tube with 600 μL of room temperature isopropanol. The DNA was eluted using 100 μL of the DNA Rehydration Solution. The purified DNA was then run on Qubit using the Broad Range (BR) kit for dsDNA and TapeStation to assess DNA concentration and size.

4.3.3. Testing DNase treatment in the Hi-C method

The effect of DNase treatment on the samples during the Hi-C method was tested to see if it negatively impacted the Hi-C method. Our initial tests of the Hi-C method showed that DNA was detected before the cell lysis step, and we want to make sure that any DNA we were analysing were from viable whole cells, rather than any extracellular DNA. Four overnight cultures of MDR *E. coli* were set up where 10 mL of overnight culture was treated with DNase, 10 mL of overnight culture treated with water as a control, 1 mL of overnight culture treated with DNase and 1 mL of overnight culture was treated with water as a control. To begin, the desired volume of MDR *E. coli* overnight culture was added to the corresponding tube. The bacterial cells were pelleted at 7197 *x*g for 5 minutes. The bacterial pellets were then resuspended in 1 mL of MHB before 48.78 μL of 37-41% formaldehyde was added to the tubes. The tubes were then incubated for 20 minutes at room temperature with occasional mixing by inversion. After incubation, 52.44 μL of 2.5 M glycine was added to the samples (final concentration 0.125 M) and incubated for 20 minutes at room temperature with occasional mixing by inversion. The samples were then centrifuged at 17,000 *xg* for 5 minutes. The supernatant was then saved for later testing. The bacterial pellet was then resuspended in 200 μL of MHB. Approximately 5 μL of the samples were saved for later testing. The cells were then lysed using the MagNA Pure Compact Instrument (Roche). All of the saved samples (and final sample) were run on the Invitrogen Qubit™ dsDNA BR Assay kit, TapeStation and NanoDrop 2000 to determine DNA concentration, size and quality.

4.3.4. Testing different DNA extraction methods

The purpose of these experiments was to determine which DNA extraction kit would provide enough DNA for MinION sequencing and also the longest DNA for long-read sequencing, after the initial treatments with formaldehyde and glycine. The kits that were trialled were the Fire Monkey kit from RevoluGen, Promega Wizard® Genomic DNA kit, QIAGEN DNeasy Blood and Tissue kit and a bead beating method. The tests were conducted using 1 mL of the MDR *E. coli* overnight cultures and the same formaldehyde and glycine treatments as used previously (section 4.3.2) and then the protocols from each kit was used. In the bead beating method, the MDR *E. coli* cells were pelleted and resuspended in 600 μL of the MagNA Pure bacterial lysis

buffer (Roche Life Science) and transferred to MP Biomedicals Lysing Matrix E tubes. The sample was shaken with a frequency of 50 oscillations per second for 3 minutes using the QIAGEN TissueLyser II. The tubes were then centrifuged for 1 minute at 16,200 xg and the resulting supernatant was transferred into a clean 1.5 mL Eppendorf tube. The Promega Wizard® Genomic DNA kit was used for purification from step 7 of the 'Isolating Genomic DNA from Gram-positive and Gram-negative bacteria' protocol where the cells are lysed at 80˚C for 5 minutes and cooled to room temperature. DNA extraction was also tested using the MagNA Pure extraction system. The MDR *E. coli* strain was treated in the same way as before until DNA extraction, when the cells were centrifuged at 16,200 xg for 1 minute and the bacterial pellet was resuspended in 200 µL MHB and the MagNA Pure protocol was followed but without the enzymatic digestion steps with lysozyme and lysostaphin and eluted into 50 µL.

When each kit was tested, 6 different conditions were set up: 1A (DNase initial treatment and reversal of DNA crosslinks post-extraction), 1B (DNase initial treatment and DNA crosslinks present and then reversed post-extraction), 1C (DNA crosslinked and then reversed post-extraction), 2A (DNase initial treatment), 2B (DNase initial treatment and DNA crosslinked), 2C (DNA crosslinked). A Kruskal-Wallis test and Dunn's pairwise tests with Bonferroni correction for multiple tests were then conducted to determine the statistical difference between DNA extraction kits used and the DNA extracted per colony forming unit, the effect of crosslinks on DNA extraction and the initial DNase treatment on DNA yield.

4.3.5. Hi-C DNA Extraction using the MagNA Pure Extraction System

Freezer stocks of the MDR *E. coli* were used where 1 mL of the culture had an average of 3.5 x 10^9 CFU/mL. Three tubes were set up where: A) positive control (DNase treatment, will not be crosslinked), B) test sample (will be treated with DNase and will be crosslinked) and C) negative control (won't be treated with DNase but will be crosslinked). A summary of these sample conditions is presented below (Table 29).

Table 29: A summary of the sample tube conditions used to test the impact of formaldehyde crosslinking, DNase treatment and reversal of the crosslinks using proteinase K on the MagNA Pure DNA extraction system. The samples were treated according to the condition used where the samples are: A) DNase treated, B) DNase treated and crosslinked, C) crosslinked, 1) samples were treated with proteinase K to reverse crosslinks and 2) samples were treated with sterile distilled water (control, instead of proteinase K).

	Sample					
Treatment	1A	1B	1C	2A	2B	2C
Formaldehyde (crosslinking)	No	Yes	Yes	No	Yes	Yes
Glycine	No	Yes	Yes	No	Yes	Yes
TURBO DNase	Yes	Yes	No	Yes	Yes	No
EDTA	Yes	Yes	No	Yes	Yes	No
Proteinase K (reverse crosslinks)	Yes	Yes	Yes	No	No	No

To tubes B and C, 48.78 µL of 37-41% formaldehyde was added and the same volume of water was added to tube A. All tubes were incubated for 20 minutes at room temperature with occasional mixing by gentle inversion. Then, to tubes B and C, 52.44 µL of 2.5 M glycine was added, and an equal volume of water was added to tube A. All tubes were incubated at room temperature for 20 minutes with occasional mixing by gentle inversion. To tubes A and B, 110.12 µL of 10X TURBO DNase Buffer was added and 24 µL of TURBO DNase. To tube C, 134.12 µL of sterile distilled water was added. All three tubes were then incubated at 37°C for 30 minutes. To tubes A and B, 37.1 µL of 0.5 M ethylenediaminetetraacetic acid (EDTA) was added, and an equivalent volume of sterile distilled water was added to tube C. All of the samples were then incubated at 75°C for 10 minutes. The tubes were centrifuged at 16,200 xg for 1 minute and the supernatant was disposed of. The pellet was resuspended in 200 µL MHB. The protocol for MagNA Pure DNA extraction for bacterial cells was followed, but the enzymatic digestion step with lysozyme and lysostaphin was not conducted. The proteinase K digestion was done following the normal protocol before the samples were loaded into the MagNA Pure Compact system. The DNA was eluted into 50 µL. After extraction, the samples were split equally into two sets of microcentrifuge tubes (A1 and A2, B1 and B2, C1 and C2). To set one of the tubes (A1, B1 and C1), 20 µL of proteinase K was added, whilst in set 2 20 µL of sterile distilled water was added. All tubes from both sets were then incubated at 60°C for one hour and then incubated at 95°C for 10 minutes to inactivate the proteinase K. All of the samples were then tested on the NanoDrop and the DNA was quantified using the Qubit dsDNA HS and BR kits. The results were then analysed using a Kruskal-Wallis statistical test, alongside the DNA extraction kits and methods previously used to determine how effective this extraction system was in comparison.

4.3.6. Optimised Hi-C method trials

4.3.6.1. Hi-C DNA digestion inside cells

The purpose of these experiments was to see whether the *E. coli* DNA could be digested inside the crosslinked cells without lysing the cells, and whether permeabilising the membrane helped with DNA digestion. To permeabilise the membrane, we explored the use of polymyxin B nonapeptide (PMBN). Overnight cultures of *E. coli* ATCC 25922 and *S. aureus* ATCC 25923 were grown at 37˚C at 180 rpm shaking. After incubation, the cells were fixed with formaldehyde by using 48.78 μL of 37-41% formaldehyde for 20 minutes with occasional mixing at room temperature. The samples were then quenched with 52.4 μL of 2.5 M glycine, which was again incubated at room temperature for 20 minutes with occasional mixing. The cells were then pelleted at 16,200 *x*g for 1 minute and four treatments were set up for each bacterial strain: A) Just bacteria, where the cells were resuspended in 400 μL MHB and then the DNA was extracted using the MagNA Pure extraction system, B) Bacteria and REs (Sau3AI and MluCI), where the samples were treated with the REs and incubated at 37˚C for 1 hour before the REs were heat inactivated by heating at 65˚C for 20 minutes and the sample was processed through the MagNA Pure extraction system, C) Bacteria, REs and PMBN where 20 μg/mL of PMBN was added and incubated for 1 hour at 37˚C with the REs (Sau3AI and MluCI) before being run through the MagNA Pure extraction system, D) Crude DNA extraction and REs, where the sample was run through the MagNA Pure extraction system before the REs (Sau3AI and MluCI) were added and incubated for 1 hour at 37˚C. The extracted DNA was then quantified using the Qubit dsDNA HS kit and run on the TapeStation.

4.3.6.2. Polymyxin B nonapeptide permeabilisation

A different approach was used in order to streamline the traditional Hi-C method by Lieberman-Aiden *et al.* (2009), and this was through the use of polymyxin B nonapeptide (PMBN) which is able to permeabilise the membrane of bacterial cells. The purpose of these experiments was to see whether the DNA could be digested in the cells once the DNA was crosslinked through permeabilising the membrane and remove the need for a cell lysis and purification step earlier in the method. The *E. coli* strain ATCC 25922 was used. An overnight culture was grown of *E. coli* ATCC 25922 in MHB. A cell counting experiment for the approximate DNA concentration of the cells was set up where the *E. coli* ATCC 25922 strain was grown overnight in triplicate before being serially diluted in the range of 10^0-10^{-8}. Once diluted, the cell density was read using a spectrophotometer at OD_{600}. To determine the colony forming units in each diluted sample, plate counting was conducted where 20 μL of the culture was dropped onto a MHA plate and incubated overnight at 37˚C. After incubation, the calculation to determine colony forming unit (CFU) per millilitre was used:

$$Average\ colony\ count\ x\ DF = CFU/mL$$

Where the colony forming unit per mL (CFU/mL) was calculated by multiplying the average colony count by the dilution factor (DF). Alongside this information, to get approximately 1 μg of DNA that would be used in all the conditions, the following calculation was used for *E. coli* ATCC 25922:

$$\frac{1\ \mu g}{5.014\ x\ 10^{-9}\mu g}\ (DNA\ in\ one\ cell) = number\ of\ cells\ needed\ for\ 1\ \mu g\ of\ DNA$$

The calculation for DNA concentration in one cell uses the assumption that the *E. coli* genome is approximately 4.6 Mb and that 1 Mb is equivalent to 1.09 fg. So, 1.09 fg x 4.6 Mb = 5.014 fg in one cell. For *E. coli* ATCC 25922, $2.0\ x\ 10^8$ cells are needed for 1 μg of DNA. The bacterial cells were pelleted by centrifuging at 16,200 *x*g for 1 minute and the supernatant was discarded before it was stored at -20˚C. The cells were then resuspended in 1 mL of MHB and 133.3 μL of this was used to get approximately 1 μg of DNA from the cells and MHB was added to get a final volume of 1 mL. The cells were then fixed using 48.78 μL of 37-41% formaldehyde and incubated at room temperature for 20 minutes with occasional mixing by gentle inversion. Formaldehyde was then quenched by adding 52.4 μL of 2.5 M glycine for a final concentration of 0.125 M. The samples were then centrifuged at 17,000 *x*g for 5 minutes. The supernatant was then discarded. Eight treatments were then set up where the tubes contained: A) just bacteria, B) bacteria treated with REs, C-G) bacteria treated with REs and PMBN at 5 different concentrations (20, 40, 60, 80 and 100 μg/mL) and finally, H) a crude DNA extraction which was then treated with REs. In the 'just bacteria' treatment, after formaldehyde fixation and quenching, the DNA was extracted using the MagNA Pure extraction system and eluted into 50 μL.

In the bacteria and REs treatment, the bacterial cells were treated with formaldehyde and quenched before being treated with 0.5 μL MluCI and 0.5 μL Sau3AI, 5 μL NEBuffer 1.1 and 44 μL MHB and incubated for 1 hour at 37˚C. After incubation, the DNA was extracted by using the MagNA Pure extraction system.

For the samples treated with the REs and PMBN, the cells were fixed with formaldehyde and quenched as before. Then to the samples, 0.5 μL of MluCI and 0.5 μl Sau3AI was added with 5 μl NEBuffer 1.1 and PMBN to the desired concentration. The final volume was made up to 50 μL by adding MHB. The sample was incubated for 1 hour at 37˚C before the DNA was extracted using the MagNA Pure extraction system.

For the crude DNA extraction and RE control, after formaldehyde fixation and quenching, DNA was extracted using the MagNA Pure extraction system. Once the DNA was extracted, 44 µL of the DNA was used and restriction digestion was carried out by adding 0.5 µL of MluCI and 0.5 µL Sau3AI and 5 µL of NEBuffer 1.1. The sample was then incubated for an hour at 37˚C.

To extract the DNA from the samples using the MagNA Pure Compact system, the MagNA Pure Compact Nucleic Acid Isolation kit I was used. MHB was added to the sample to a total volume of 200 µL. Then, 180 µL of the MagNA Pure Bacteria Lysis Buffer (Roche Life Science) was added. The sample was then pipetted gently to mix. 20 µL of proteinase K was added and mixed before incubating at 65˚C for 10 minutes. When the samples were loaded onto the MagNA Pure machine, 400 µL of the sample is transferred to MagNA Pure tubes and the 'DNA Bacteria' protocol was used.

All of the samples were then analysed using Qubit dsDNA HS kit assay and TapeStation.

4.3.6.3. Agarose gels

To determine the length of the DNA that was extracted using the MagNA Pure system, a 1.5% agarose gel was run. The gel was set up by weighing out 4.5 agarose powder and adding it to 300 mL 1X TAE (Tris-acetate-EDTA) buffer and heating until the powder dissolved. When the agarose solution had cooled slightly, 20 µL ethidium bromide (EtBr) was added and shaken gently to mix. When the gel was placed in the gel tank, 20 µL of EtBr was added to the reservoir (filled with 1X TAE buffer). To load the gel, 5 µL of the DNA sample and 5 µL of loading dye was added to the well. The ladder used was the CHEF DNA Size Standards 8-48 kB (Bio-Rad). The gel was run for 1 hour at 100 V. A separate gel was also set up in the same way but was run for 4 hours instead of 1 hour at 100 V.

The DNA samples were also run on a 0.8% agarose gel, which was made using 2.4 g agarose and adding 300 mL 1X TAE buffer. Loading the DNA was done the same as before. The gel was run for 4 hours at 100 V with the CHEF DNA Size Standards 8-48 kB.

4.3.6.4. DNA extraction using phenol-chloroform

MDR *E. coli* cultures were grown overnight in MHB to approximately mid- to late-log phase (OD$_{600}$: 0.5-0.8). To three 1.5 mL microcentrifuge tubes, 1 mL of the overnight culture was added. Each tube was labelled as: A) the positive control (where the sample was not crosslinked), B) the test sample (which followed the normal Hi-C protocol) and C) the DNase negative sample. These samples were set up in triplicate (for a total of 9 tubes). To tubes B and C, 48.78 µL of 37-41% formaldehyde was added. An equal volume of sterile distilled water was added to tube A. All of the tubes were then incubated for 20 minutes at room temperature and occasional mixing by

inversion. After incubation, 52.44 µL of 2.5 M glycine was added to tubes B and C, while an equal volume of sterile distilled water was added to tube A. All of the tubes were then incubated for 20 minutes at room temperature with occasional mixing by inversion. To tubes A and B, 110.12 µL of 10X TURBO DNase buffer was added and 24 µL of TURBO DNase. To tube C, 134.12 µL of sterile distilled water was added. All of the tubes were then incubated at 37˚C for 30 minutes. Then, to tubes A and B, 37.1 µL of 0.5 M EDTA was added, and an equivalent volume of sterile distilled water was added to tube C. All of the tubes were then incubated at 75˚C for 10 minutes. All of the tubes were then centrifuged at 16,200 xg for 1 minute. The supernatant was then discarded and the cells were resuspended in 600 µL Tris-EDTA (TE) buffer before 20 µL of 10 mg/mL lysozyme (Sigma Aldrich) was added and 20 µL of 10 mg/mL RNase A (ThermoFisher Scientific) and mixed by gentle pipetting. Then, 40 µL of 10% sodium dodecyl sulfate (SDS) was added and mixed well before incubating the solution for 1 hour at 37˚C. The mixture was then further incubated for 1 hour at 50˚C. After incubation, 200 µL of 5 M NaCl was added to the samples and mixed well by pipetting. In a fume hood, 500 µL of chloroform:isoamyl alcohol (24:1) was added to the sample and mixed thoroughly by shaking so that the aqueous and organic phases combined. The samples were then placed on ice for 30 minutes. The tubes were then centrifuged at 16,200 xg for 10 minutes. In a fume hood, the top aqueous phase was transferred to a fresh tube. 500 µL phenol:chloroform:isoamyl alcohol (25:24:1) was added to the aqueous phase sample and mixed so that the aqueous and organic phases could combine. The new solution was then centrifuged at 16,200 xg for 10 minutes. The supernatant was discarded and the DNA pellet was washed with 500 µL of fresh 70% ethanol. The sample was then centrifuged at 16,200 xg for 5 minutes before the ethanol was removed and the DNA pellet air dried for 5-10 minutes. The DNA pellet was then resuspended in 30 µL TE buffer. All of the DNA extraction eluates were then split into two sets of microcentrifuge tubes (e.g. tubes A1 and A2, B1 and B2, C1 and C2), conducted in triplicate. 20 µL of proteinase K (20 mg/mL) was added to set 1 tubes (A1, B1 and C1) and set 2 (A2, B2 and C2) had 20 µL of sterile distilled water added. All of the tubes were then incubated at 60˚C for one hour. After incubation at 60˚C, the tubes were then incubated at 95˚C for 10 minutes to inactivate the proteinase K. Measurements of the DNA samples were then taken using Qubit.

4.3.6.5.   Zymo HMW bead extraction

The Zymo Research *Quick*-DNA HMW MagBead Kit was used to determine whether it could be used to extract long DNA from the MDR *E. coli* strain after it had been through Hi-C treatment. Testing of this DNA extraction method was done in the same way as presented before where the MDR *E. coli* cells were grown overnight in MHB and then 1 mL was used for each of the three treatments (A: positive control, B: the test sample and, C: DNase negative sample).

Formaldehyde was added to a final concentration of 2% to crosslink DNA in the test and DNase negative sample. Glycine was added to the samples to quench the formaldehyde at a final concentration of 0.125 M. In the positive control and test sample, DNase was added before it was inactivated using EDTA to a final concentration of 15 mM. The tubes were then used in the *Quick*-DNA HMW MagBead kit following the microbial lysis protocol with the optional RNase treatment done. Each of the three samples were then split in half to create a 'set 1' and a 'set 2', where set 1 had the crosslinks reversed in the DNA using proteinase K. Measurements of the DNA quality, concentration and size was done using the NanoDrop, Qubit (HS) and TapeStation machines, respectively.

4.3.6.6.   Plasmid extraction and detection of MDR *E. coli*

The purpose of this experiment was to ensure that there was a plasmid present in the MDR *E. coli* and that it hadn't been lost in the repeated culturing of the strain. Plasmid extraction for the MDR *E. coli* strain was done using a 10 mL overnight culture grown in MHB and the QIAGEN QIAprep Spin Miniprep kit. The plasmid DNA was then quantified using Qubit (BR) kit, and DNA size was determined using TapeStation. Genome extraction of the MDR *E. coli* strain was conducted using the Promega Wizard® Genomic DNA Purification kit and sent for sequencing on the Illumina NextSeq 500, the resulting raw sequences were trimmed and assembled before being run with the default settings on ARIBA.

4.3.6.7.   Partial digestion of DNA

To improve the Hi-C method and the final DNA fragment length suitable for long-read sequencing, partial digestion of the DNA was tested in order to determine the optimal conditions for DNA fragmentation. This was done by using MDR *E. coli* DNA that was extracted using the Fire Monkey Kit following the kit protocol. MDR *E. coli* DNA was mixed with 1X NEBuffer 2.1 (NEB) RE buffer to make a total volume of a 100 μL reaction mixture. 20 μL of the reaction mixture was added to a 1.5 mL Eppendorf tube and then 10 μL of the reaction mixture was added to 8 additional Eppendorfs and placed on ice. 1 μL of the HindIII enzyme (20,000 units/mL) was added to the first tube containing 20 μL of the reaction mixture and mixed before being placed back on ice. 10 μL of the solution from the first tube was then serially diluted into the remaining 8 tubes by transferring 10 μL each time and mixing in between transfers and returning them to ice. All of the tubes were then incubated for 15 minutes at 37˚C. After incubation, the HindIII enzyme was heat inactivated by incubating for 20 minutes at 65˚C. The samples were then run on a 2% agarose gel for 1 hour at 100 V with a 8-48 kb ladder (CHEF DNA size standards 8-48 kb, Bio-Rad). The samples were also run on a 2% agarose gel for 2 hours at 100 V with a 1 kb ladder (Quick-Load Purple 1 kb DNA ladder from NEB).

4.3.6.8.   Hi-C method with wash step and Fire Monkey DNA extraction

The purpose of this experiment was to determine whether the difficulties with DNA extraction with the Fire Monkey kit was due to kit incompatibility or whether the spin column was proving to be a physical barrier to the crosslinked DNA/chromatin generated in the initial steps of the Hi-C method. Briefly, MDR *E. coli* was grown overnight in MHB. 1 mL of the overnight culture was transferred to a 1.5 mL microcentrifuge tube and conducted in duplicate. A positive control was set up that would not have the DNA crosslinked. A DNase negative sample was also set up. Formaldehyde was added to the test and the DNase negative sample at a final concentration of 2% to crosslink the DNA. Sterile distilled water was added to the positive control. All of the samples were then incubated for 20 minutes at room temperature with occasional mixing by gentle inversion. After incubation, glycine was added to a final concentration of 0.125 M to quench the formaldehyde in the test and DNase negative sample. An equal volume of sterile distilled water was added to the positive control. All of the samples were incubated for 20 minutes at room temperature with occasional mixing by gentle inversion. In the positive control and the test sample, 24 µL TURBO DNase (2 U) was added with 110.12 µL 10X TURBO DNase buffer. The DNase negative control had the equivalent 134.12 µL of sterile distilled water added to it. All of the sample were then incubated at 37˚C for 30 minutes. After incubation, the TURBO DNase was inactivated by adding 37.1 µL of 0.5 M EDTA to the test tube and DNase positive control tube. An equivalent volume of sterile distilled water was added to the DNase negative control tube and all of the samples were incubated at 75˚C for 10 minutes.

Before the samples were transferred to the Fire Monkey kit for DNA extraction, the samples were washed by pelleting the cells at 16,200 *x*g for 1 minute and the supernatant was removed. The cells were then resuspended in 1 mL Tris-buffered saline. The cells were centrifuged again at 16,200 *x*g for 1 minute and the supernatant removed. The Fire Monkey kit was followed as per the manufacturer's guidance. After DNA extraction, the samples were split into two sets (set A and set B), and the crosslinks were reversed in set B by adding 20 µL of proteinase K, mixed by pipetting and incubated at 60˚C for one hour. Proteinase K was inactivated by incubating at 95˚C for 10 minutes. Measurements were then taken on the Nanodrop, Qubit (HS) and TapeStation.

4.3.6.9.   Substituted Reagents Hi-C test with DNA Loss

This method follows the Phase Genomics ProxiMeta Hi-C protocol, but the reagents were substituted for our own laboratory reagents. The equivalent of a 50 µL pellet of the MDR *E. coli* strain was used, this amounted to 10 mL of an overnight culture of MDR *E. coli* grown in MHB at 37˚C. Centrifugation was done at 16,200 *x*g for 1 minute, the supernatant was saved for later

DNA quantification. The MDR *E. coli* pellet was resuspended in 1 mL of MHB before the addition of 48.78 µL of 37-41% formaldehyde and incubated for 20 minutes at room temperature with occasional mixing by inversion. The formaldehyde was then quenched using 52.44 µL of 2.5 M glycine and incubated for 20 minutes at room temperature with occasional mixing. After incubation, the sample was centrifuged at 17,000 x*g* for 5 minutes and the supernatant was removed and discarded. The pellet was resuspended in 200 µL of MagNA Pure Bacterial Lysis Buffer. A Qubit and TapeStation reading were then taken. For the cell lysis steps, the MagNA Pure Compact Nucleic Acid Isolation Kit I protocol was followed for the extraction of bacterial DNA and the DNA was eluted in 50 µL. A Qubit and TapeStation reading was taken.

For the fragmentation steps, a restriction digestion was set up using 0.5 µL of Sau3AI and 0.5 µL of MluCI enzymes, 5 µL of 10X NEBuffer 1.1, the equivalent of 1 µg of DNA to a total reaction volume of 50 µL. This mixture was incubated for 1 hour at 37˚C. The sample was centrifuged at 16,200 x*g* for 5 minutes and the resulting supernatant was saved to be DNA quantified later. The samples were run on Qubit and TapeStation. For the proximity ligation steps, the pellet was resuspended in 500 µL of sterile distilled water and the DNA was quantified using Qubit and size of the DNA was determined using TapeStation. To the sample, 2 µL of 10X T4 DNA Ligase buffer, 2 µL pf 50% PEG, 1 µL of T4 DNA Ligase and sterile distilled water was added to bring the final volume to 8 mL (this is different to the Hi-C kit method). The sample was then incubated for 4 hours at room temperature with occasional mixing. To reverse the crosslinks, the sample was centrifuged at 7,200 x*g* for 5 minutes and 1.5 mL of the supernatant was removed and saved separately. 20 µL of proteinase K (20 mg/mL) was added and the pellet was resuspended. The sample was then incubated for an hour at 60˚C. The sample was then run on TapeStation and quantified using Qubit. The DNA was then purified using the Promega Wizard® Genomic Purification Kit, but as the DNA at this point was already extracted, the kit protocol was followed from step 13 where ethanol precipitation was done. The final extracted DNA (Hi-C library) was then quantified using Qubit and DNA size determined using TapeStation.

4.3.6.10. Hi-C method with Fire Monkey extraction and bead purification

A similar method was employed as before to prepare a Hi-C library (section 4.3.6.8), but rather than using the spin columns provided in the Fire Monkey kit, AMPure XP (Beckman Coulter) bead washes for purification was used instead. The experiment was conducted on the *A. baumannii* strain A21 and MDR *E. coli* in triplicate. The Hi-C method was followed as normal with the addition of formaldehyde, addition of glycine to quench the formaldehyde and TURBO DNase treatment. The Fire Monkey kit was followed as normal for DNA extraction, but the proteinase K treatment and associated incubation step was removed. For the AMPure bead wash, the beads

were allowed to reach room temperature before use and 200 µL was added, mixed by gentle pipetting before incubating with rotation on a Stuart SB3 rotator at 20 rpm for 15 minutes. To purify the DNA, 70% ethanol washes were done by adding 500 µL of freshly prepared 70% ethanol was added to the beads for 30 seconds on the magnetic rack before the ethanol was removed. This was repeated before the beads were left to air dry for up to 10 minutes at room temperature. After the beads were washed and dried, the DNA was eluted in 50 µL MinION buffer (recipe: 100 µL 1 M Tris-HCl, 100 µL 5 M NaCl and 9.8 mL sterile distilled water). The DNA concentration was determined using the Qubit dsDNA HS kit.

4.3.6.11. Hi-C method run through with bead purification and centrifugation steps

Overnight cultures of the MDR *E. coli* strain and *A. baumannii* strain A21 were grown in 10 mL MHB, three cultures were made for each strain for replicates. 1 mL of each overnight culture was transferred to 1.5 mL Eppendorf tubes. To these cultures, the same method as outlined above under 'Substituted reagents Hi-C test with DNA Loss' (section 4.3.6.9) was followed for the formaldehyde crosslinking step, quenching of the formaldehyde using glycine, the DNase treatment, lysozyme and RNase treatment. To conduct the restriction digestion part of the Hi-C method, 5 µL of 10X NEBuffer 2.1 (NEB) was added to each tube with 1 µL HindIII RE (NEB) and water to reach a total volume of 50 µL. The mixtures were then incubated for 1 hour at 37˚C. After restriction digestion, the HindIII enzyme was heat inactivated by heating at 80˚C for 20 minutes. Another small volume of each sample was saved for later examination by Qubit and TapeStation.

To carry out the ligation steps, the samples were centrifuged for 5 minutes at 16,200 *x*g and the supernatant was discarded. The pellets were then resuspended in 500 µL deionised water before the addition of 1.5 µL 10 mM of dATP, dGTP and dTTP (Invitrogen, ThermoFisher Scientific), 37.5 µL 0.4 mM biotin-14-dCTP (Invitrogen, ThermoFisher Scientific), 10 µL 5 U/ µL Klenow fragment (ThermoFisher Scientific), 1 µL T4 DNA Ligase (NEB) and T4 DNA Ligase Buffer to bring the final total volume to 1.5 mL. The samples were then incubated for 4 hours at room temperature with occasional mixing on a Stuart rotator SB3 at the maximum speed of 20 rpm. After incubation, enzymes were inactivated by heating at 65˚C for 10 minutes. A small volume of each sample was saved for examination by Qubit and TapeStation. The DNA in the sample tubes then had the crosslinks reversed by first centrifuging the ligated sample at 16,200 *x*g for 5 minutes. Approximately 1.5 mL of the supernatant was removed and leaving 500 µL. 20 µL of proteinase K was added and the pellet was resuspended. The samples were then incubated at 60˚C for at least one hour. After incubation, biotin purification was conducted. Dynabeads MyOne Streptavidin C1 beads (ThermoFisher Scientific) were prepared according to manufacturer's

instructions. 12 µL of the beads were used initially and after 3 wash steps and resuspension in the 2X Binding and Washing (B&W) buffer (10 mM Tris-HCl pH 7.5, 1 mM EDTA and 2 M NaCl), 24 µL of the final washed bead mixture was added to the samples. The samples were then incubated at room temperature for 15 minutes with rotation at 20 rpm. The samples were then added to a magnetic rack for 3 minutes at room temperature and the supernatant removed. The beads were then washed 3 times using 1X B&W buffer. The beads were then resuspended in 400 µL 1X B&W buffer before they were placed on a magnetic rack for 3 minutes and the supernatant removed. The beads were resuspended in 50 µL of MinION buffer and incubated at 65˚C with 10 mM EDTA, pH 8.2. The sample was then added to the magnetic rack for 3 minutes and the supernatant transferred to a new 1.5 mL Eppendorf tube. A small volume of the samples was then saved for later examination. This experiment was run twice. In the first run, when the biotin ligation was conducted, the sample was incubated overnight at 37˚C instead of at room temperature. In the second run through of this experiment, an *A. baumannii* A21 strain was also run alongside the MDR *E. coli* strain and the biotin ligation step was conducted overnight at room temperature.

4.3.6.12. Whole method run through with bead purification and no centrifugation steps

The method above was followed (section 4.3.6.11) but with additional bead purification steps and the test strains used were MDR *E. coli* and *A. baumannii* A21. After biotin purification, a 2.5X bead wash was conducted using 112.5 µL AMPure XP beads, and the samples were mixed for 5 minutes at room temperature at 20 rpm on a Stuart SB3 rotator. The samples were then briefly vortexed to resuspend the solution and beads before they were placed on a magnetic rack for 5 minutes and the supernatant removed. After the supernatant was removed, 500 µL of fresh 70% ethanol was added and left for 30 seconds before it was removed. The ethanol wash was then repeated. After the ethanol wash, the beads were air dried on the magnetic rack for up to 10 minutes, making sure that the beads did not crack. The samples were then removed from the magnetic rack and the beads were resuspended in 50 µL MinION buffer and left to incubate for 5 minutes at room temperature. The samples were added to a magnetic rack and left for 5 minutes before the eluate was transferred to a new 1.5 mL Eppendorf tube.

After the 2.5X bead wash, a further wash to remove smaller DNA fragments was done using a 1X bead wash. To the DNA samples, 50 µL of AMPure beads were added and mixed for 5 minutes at room temperature at 20 rpm on the Stuart SB3 rotator. The samples were then briefly vortexed to resuspend the beads before they were transferred to a magnetic rack and left for 5 minutes. The supernatant was then removed before two ethanol washes were done where 500 µL of fresh 70% ethanol was added, left for 30 seconds and then removed with the samples on

a magnetic rack. After the ethanol washes, the beads were air dried on a magnetic rack for up to 10 minutes at room temperature. The beads were then resuspended in 50 μL MinION buffer and left to incubate for 5 minutes, not on the magnetic rack. The samples were then added to the magnetic rack and left for 5 minutes, before the eluate was removed and transferred to a new 1.5 mL Eppendorf tube. When biotin pulldown was conducted with the Dynabeads MyOne Streptavidin C1 beads, 100 μL of the beads were added for the MDR *E. coli* samples and 5 μL of beads was used for the *A. baumannii* samples. Throughout many steps of this method, samples were taken for Qubit and TapeStation analysis. Any steps that required supernatants to be discarded were also kept to determine where DNA was being lost in the method.

For references, the MDR *E. coli* and *A. baumannii* A21 DNA was extracted using the Fire Monkey kit and sequenced on a MinION device. The samples for MinION sequencing were prepared using the MinION Rapid Sequencing kit (ONT) and run by Dr. Emma Ainsworth at the QIB. The DNA was also extracted from the MDR *E. coli* strain using the Promega Wizard® Genomic DNA Purification kit and then sequenced at the QIB by David Baker and Steven Rudder.

4.3.7. Conjugation experiments

4.3.7.1.   MIC testing

The *E. coli* strain J53 was used as a recipient for the conjugation experiments and the strains *E. coli* EC1 and EC4 (isolates from Kuwait, both contain resistance determinants for CTX-M-15 and NDM-4) and *K. pneumoniae* K9 (clinical isolate from Kuwait-Amiri Hospital, which has the resistance determinant for NDM-1) were tested for their susceptibility to MERO and Bm for their use as NDM donors. Susceptibility to MMC was also tested after dissolving the powder in DMSO. Susceptibility testing was done on MHA plates. Overnight cultures were grown in 10 mL MHB from a single colony of the strain. The cultures were then standardised by diluting with MHB to a 0.5 McFarland standard (OD$_{600}$: 0.08-0.1) and then further diluted 1:100. The diluted samples were then spot plated on Bm and MERO plates ranging from 0-64 μg/mL using 2 μL of diluted culture. Plates were then incubated overnight at 37˚C. A narrower range of the antibiotics were used, ranging from 0-0.25 μg/mL for MERO and 0-0.55 μg/mL for Bm.

The ability of the strains to grow on sodium azide was also simultaneously tested to determine whether it could be used as a selectable marker for just the recipient strain, *E. coli* J53, which is resistant to sodium azide. MHA plates were made with 100 μg/mL sodium azide (ACROS organics) and diluted in sterile distilled water. The diluted overnight cultures of the strains were spot plated again with 2 μL.

4.3.7.2.   Growth curves

Overnight cultures of the strains were set up in 10 mL LB broth at 37˚C and 180 rpm shaking. These cultures were set up in triplicate for each strain. A dilution series for these cultures were set up from 10^0-10^{-14}. Each dilution had an OD reading taken and was plated on plain LB agar plates. The agar plates were incubated overnight at 37˚C.

4.3.7.3.   Conjugation

The conjugation method used in these experiments was adapted from Sana *et al*. (2014). The donor and recipient strains were grown separately overnight in 10 mL of LB broth at 37˚C. The cells were then pelleted at 1,057 *x*g for 5 minutes before re-suspending in fresh LB broth. 1 mL of the cultures were saved in 100 µL 80% glycerol as a freezer stock. The cells were then diluted to get approximately a 1:1 ratio of the cells (approximately 10^7 cells). Plain LB agar plates were prepared and separated into 4 sections. In the first section, 30 µL of the donor was added. In the second section, 30 µL of the *E. coli* J53 recipient was added, in the third section 30 µL of LB broth was added. In the final section, 30 µL of the donor and 30 µL of the recipient were mixed and spot plated. The plates were left to dry before incubating overnight at 37˚C. The conjugation experiments were also conducted in the presence of sub-MIC Bm, sub-MIC MERO and sub-MIC MMC in the LB agar plates.

After incubating, the recipient and donor strain mix from section 4 were scraped off and resuspended in 1 mL LB broth in a 1.5 mL Eppendorf tube and mixed gently. The tubes were then centrifuged at 1,057 *x*g for 5 minutes, the supernatant was removed before re-suspending in 1 mL LB broth. Then, 100 µL of culture was spread plated on selective plates containing MERO (at 1 µg/mL) and sodium azide (at 100 µg/mL). A recipient cell plate count was done by plating 100 µL of the culture onto a 100 µg/mL sodium azide plate. Plates were then incubated overnight at 37˚C. 1 mL of the cultures were saved in an 80% glycerol stock with MERO (1 µg/mL).

Colonies that appeared on the MERO and sodium azide selective plates were grown in 10 mL LB broth and 80% glycerol stocks were made. Colony counts were also conducted for the plates that contained either just sodium azide or MERO and sodium azide for selection. An independent-samples Kruskal-Wallis statistical test was then conducted to determine whether there was a significant difference in the transconjugation efficiency of the transconjugants that arose after exposure to different drug conditions (LB, Bm, MERO and MMC).

4.3.7.4.   Sequencing

For short-read sequencing on the Illumina NextSeq 500 platform, the parent *E. coli* EC1 strain and the recipient *E. coli* J53 DNA was extracted using the Revolugen Fire Monkey kit. All extractions were done in triplicate from individual colonies, alongside 3 technical replicates. In parallel with this, the DNA from the *E. coli* J53 transconjugants from each treatment condition (LB, sub-MIC Bm, sub-MIC MERO and sub-MIC MMC) were also extracted using the Fire Monkey kit, each one done in triplicate. After extraction, the DNA was quantified using the Qubit dsDNA HS kit. The eluted DNA from Fraction A of the Fire Monkey kit was sent for Illumina sequencing at the QIB with David Baker and Steven Rudder after diluting with sterile distilled water to get a concentration of 0.5 ng/μL.

The Fraction B of the eluted DNA from the Fire Monkey kit which contains high molecular weight DNA was diluted with water or concentrated using AMPure beads (eluted in 20 μL of MinION buffer) to a concentration of 10 ng/μL before being sent to the QIB to be sequenced on the MinION platform using the Rapid Sequencing kit by David Baker and Steven Rudder.

To generate Hi-C libraries, the Phase Genomics ProxiMeta Hi-C kit (Microbe) was used. Three extractions using this kit was done with the *E. coli* EC1 and *E. coli* J53 parent strains and triplicates of each treatment condition (LB, sub-MIC Bm, sub-MIC MERO and sub-MIC MMC) conjugation mixes (a mixture of the *E. coli* EC1 donor and the *E. coli* J53 transconjugants that should carry the *bla*$_{NDM-4}$ gene after they were selected on MERO). The eluted Hi-C libraries were quantified using the Qubit dsDNA HS kit. The samples were diluted to a concentration of 0.5 ng/μL before being sent to the QIB to be sequenced on the Illumina NextSeq 500 platform by David Baker and Steven Rudder.

4.3.7.5.   Sequence analysis

All of the sequence analysis was conducted by Dr. Lisa Crossman. SAMTools (v 1.14) was used to detect the differences between the *E. coli* EC1 and J53 strain that were used as parents for the experiments. A file was generated with both the *E. coli* EC1 and J53 chromosomal DNA and our plasmid of interest in order to provide a reference file for alignments. For the *E. coli* J53 parent strain, a database reference file (accession GCA_003052645.1) was used as it was a single contig and easier to use for downstream analysis (4 SNP different to our *E. coli* J53 strain). All of the transconjugants from all of the different conditions were then mapped to the reference *E. coli* J53 file, and all the reads that didn't map to this sequence were assembled into the plasmid of interest. QC reports were then generated from this using the Phase Genomics QC pipeline 'hic_qc.py pipeline' and FitHiC significance files. Alongside this, the SAMTools (v 1.14) and

FreeBayes (v 1.3.2) with a ploidy of 1 (=p 1) was used to determine if there were any SNPs differences seen in our transconjugants when they were treated with different compounds (LB, Bm, MERO and MMC).

To demonstrate that the plasmid had transferred from the *E. coli* EC1 strain to the recipient *E. coli* J53 strain, the Hi-C library generated for each of the transconjugants was sequenced on the Illumina NextSeq 500 platform to generate reads. These reads were aligned using bowtie2 on Galaxy (Galaxy version 2.4.2+galaxy0) to the reference plasmid sequence using paired end reads and the default user settings: write aligned reads (in fastq format) to separate file(s), use a genome from the history and build index, analysis mode was set to 'default setting only/simple' and 'defaults', and 'use default job resource parameters'.

4.4. Results

4.4.1. Reducing the time taken to conduct the Hi-C method

4.4.1.1.   Phase Genomics Hi-C kit for Illumina sequencing

The Phase Genomics Hi-C kit was used to determine its effectiveness with our organisms of interest and also as a baseline for our optimisation work. Following the Phase Genomics Hi-C kit protocol, at the proximity ligation stage the MDR *E. coli* sample had a Qubit dsDNA BR value of 58 ng/µL. In terms of purity, the NanoDrop gave a A260/280 value of 1.24 and a A260/230 value of 0.43 which indicated at this stage that the DNA was of low quality. After purifying the sample DNA, the MDR *E. coli* sample had a Qubit dsDNA BR value of 4.85 ng/µL, which was unexpectedly low but was still sufficient for downstream methods. The sample was then split so that half of the sample could be processed for MinION sequencing. From the TapeStation results, there was an average DNA peak at 10,661 bp (range between 3,621 bp to >60,000 bp) with an approximate calibrated concentration of 1.01 ng/µL) which was considered to be good with the exception of the low DNA concentration for long-read sequencing.

After library preparation (following the Phase Genomics Hi-C kit protocol), the MDR *E. coli* sample before the PCR stage had a DNA concentration of 6.01 ng/µL, which was an improvement to the low concentration seen previously. The average DNA size on TapeStation was 208 bp (range of 149 bp to 694 bp), which was deemed suitable for the purposes of Illumina sequencing. Following the PCR steps, the MDR *E. coli* sample had a DNA concentration of 54.8 ng/µL, which was unexpectedly low given that the sample had been amplified by PCR. There were two DNA peaks that appeared for this sample after running TapeStation, one had an average size of 234 bp (range of 155 bp to 293 bp) and one at 934 bp (range of 293 bp to 4,411 bp). The water control that was set up alongside this had no detectable DNA using the Qubit dsDNA BR kit and assured us that there was no contaminating DNA that had been introduced while the method

was carried out. Finally, after DNA purification, the MDR *E. coli* Hi-C library for Illumina sequencing had a DNA concentration of 43.8 ng/µL. On the TapeStation results, there was a DNA peak at 630 bp (with a range of 141 bp to 3,480 bp). According to the ProxiMeta Hi-C kit instructions, library yields that are over 0.5 ng/µL indicates a successful library, but no comment is made on the target length of DNA for a successful library. From the indicators from the ProxiMeta Hi-C kit instructions at this stage, we were satisfied with the Hi-C library we had produced.

4.4.1.2. Phase Genomics Hi-C kit for MinION sequencing

The MDR *E. coli* sample was used here to determine whether the Phase Genomics ProxiMeta kit could be used to prepare a Hi-C library that is suitable for long-read sequencing. The DNA sample was prepared through the MinION rapid barcode sequencing kit and had a resulting Qubit (BR) value of 1.22 ng/uL, which was unexpectedly low but was still sufficient for downstream methods. The total elution volume for this Hi-C library was approximately 10 µL, the total DNA present was 12.2 ng and this was sequenced on a MinION device.

Using the Epi2Me sequence analysis workflow provided by ONT, a range of resistance genes were flagged in the MDR *E. coli* sample that were primarily involved in resistance to aminoglycosides, fluoroquinolones, TET, fosfomycin, CHL and cationic antimicrobial peptides (Table 30). The Basecalling with QScore filter (rev. 3.8.0) analysed 44,176 reads with an average quality score of 10.77, an average sequence length of 2,377 bp and a total yield of 105.0 Mbases. The WIMP Classification (rev. 3.1.0) determined that the species of bacteria in the sample was *Escherichia coli*.

Table 30: A summary of the Oxford Nanopore Technologies Epi2Me sequence analysis output for the multi-drug resistant (MDR) *Escherichia coli* strain. Listed below are the resistance determinants detected in the MDR *E. coli* sequence, with their number of alignments (which refers to the number of reads detected that report this gene sequence as the top alignment) and average accuracy of the alignments generated against this gene sequence detected, referring only to single-read level accuracy. Single-read accuracy is calculated by the proportion of bases that identically match over the number of alignment columns within an alignment of a read to a reference sequence, given as a percentage.

Gene	Alignments	Average Accuracy (%)
16S rRNA mutation in the *rrsB* gene conferring resistance to G418	9	88.9
16S rRNA mutation in the *rrsB* gene conferring resistance to paromomycin	9	88.2
16S rRNA mutation in the *rrsB* gene conferring resistance to streptomycin	9	89.7
16S rRNA mutation in the *rrsC* gene conferring resistance to kasugamicin	28	87.3
16S rRNA mutation in the *rrsD* gene conferring resistance to spectinomycin	10	90.9
AAC(3)lla	33	87.6
AAC(3)llc	47	88.1
AAC(6')-lb7	32	90.3
aadA2	12	91.5
aadA5	37	89.5
acrB	38	79.3
acrD	45	90.2
acrE	15	91.5
acrR	22	90.2
acrS	18	91.7
adiY	18	91.6
cysB conferring resistance to aminocoumarin	31	90.5
APH(6)-ld	31	90.9
arnA	41	88.8
bacA	25	89.8
baeS	12	88.4
catB3	14	92.4
bla$_{CMY-59}$	8	91.3
cpxA	31	89.3
cpxR	17	91.2
crp	26	90.7
bla$_{CTX-M-15}$	14	92.8
dfrA12	14	90.4
dfrA17	21	93.1
EF-Tu mutants conferring resistance to kirromycin	8	91.5
EF-Tu mutants conferring to resistance to encyloxin lla	14	89.9
emrA	9	89.4
emrB	23	91.3
emrD	16	89.1

emrE	16	85.5
emrK	18	90.3
emrR	17	91.2
emrY	35	91.2
Fosfomycin sensitivity pyruvyl transferase (*murA*)	9	88.2
gadW	8	86.6
gadX	15	89.9
GlpT mutant conferring resistance to fosfomycin	28	89.0
gyrA conferring resistance to fluoroquinolones	30	91.0
gyrB conferring resistance to aminocourmarin	36	89.4
H-NS	20	90.3
kdpE	18	87.9
leuO	22	91.3
marA	7	92.1
marR	15	89.9
mdfA	24	88.9
mdtA	21	88.1
mdtB	30	89.4
mdtD	12	89.8
mdtE	13	90.5
mdtG	41	90.4
mdtH	26	90.1
mdtL	27	88.8
mdtM	26	88.4
mdtN	18	89.6
mdtO	21	88.7
mdtP	29	88.5
mfd	34	90.1
mgrB	26	94.3
msbA	37	91.3
murA mutant conferring resistance to fosfomycin	37	89.1
bla_{NDM-4}	13	88.6
nfsA	23	91.7
omp36 mutants	15	75.9
ompF mutants	32	90.0
OmpK36 conferring resistance to beta-lactam	8	78.5
bla_{OXA-1}	18	92.4
parC conferring resistance to fluoroquinolone	32	90.1
parE conferring resistance to fluoroquinolones	47	89.3
patA	26	88.1
pmrC	27	90.0
pmrE	25	86.4
pmrF	24	90.2
QnrS1	24	91.5
QnrS7	8	92.4
rmtB	16	89.4
soxR mutants	18	91.6
sul2	12	89.9
Sulfonamide resistant mutant *folP*	20	89.8
tetA	39	90.2

tetR	25	91.3
tolC	26	90.7
yojI	27	89.3

4.4.1.3. Bioinformatics analysis

From the initial analysis of the MinION sequence data it was calculated computationally that the mean fragment size of the DNA would be approximately 230.97 ± 272 bp (standard deviation) following restriction enzyme digestion. The MinION reads were assembled into 42 contigs and a Bandage assembly graph was generated (Figure 74). From the Bandage assembly graph, it was concluded that the plasmid could be detected in our MinION reads but also that the plasmid was large and potentially a low copy number in the cell with multiple repeats within the structure. When the Illumina generated reads were assembled and visualised in a Bandage assembly graph, it was clear again that we were able to detect plasmid DNA alongside the chromosomal DNA, where the plasmid is highlighted below in colour (Figure 75). The Bandage graph shows that the plasmid (highlighted) is embedded within the rest of the chromosomal reads and demonstrates that the Hi-C method has successfully linked the chromosome and the plasmid together.

From the analysis of the Hi-C library on the Phase Genomics software platform, it was determined that the Hi-C library that was created was sufficient and of high quality in terms of the same strand high quality read pairs (7.13%) and the informative read pairs was estimated to be 38.40%. From the QC reports, it was determined that the fraction of high quality read pairs that were more than 10 kb apart was good at 12.16%. Clustering of usable high-quality reads per contig (CTGs >5 kb) was low at 428.42. The percentage of non-informative read pairs was low at 25.47%. The final assembly was 5,140,867 bp with a contig N50 of 652,171 bp.
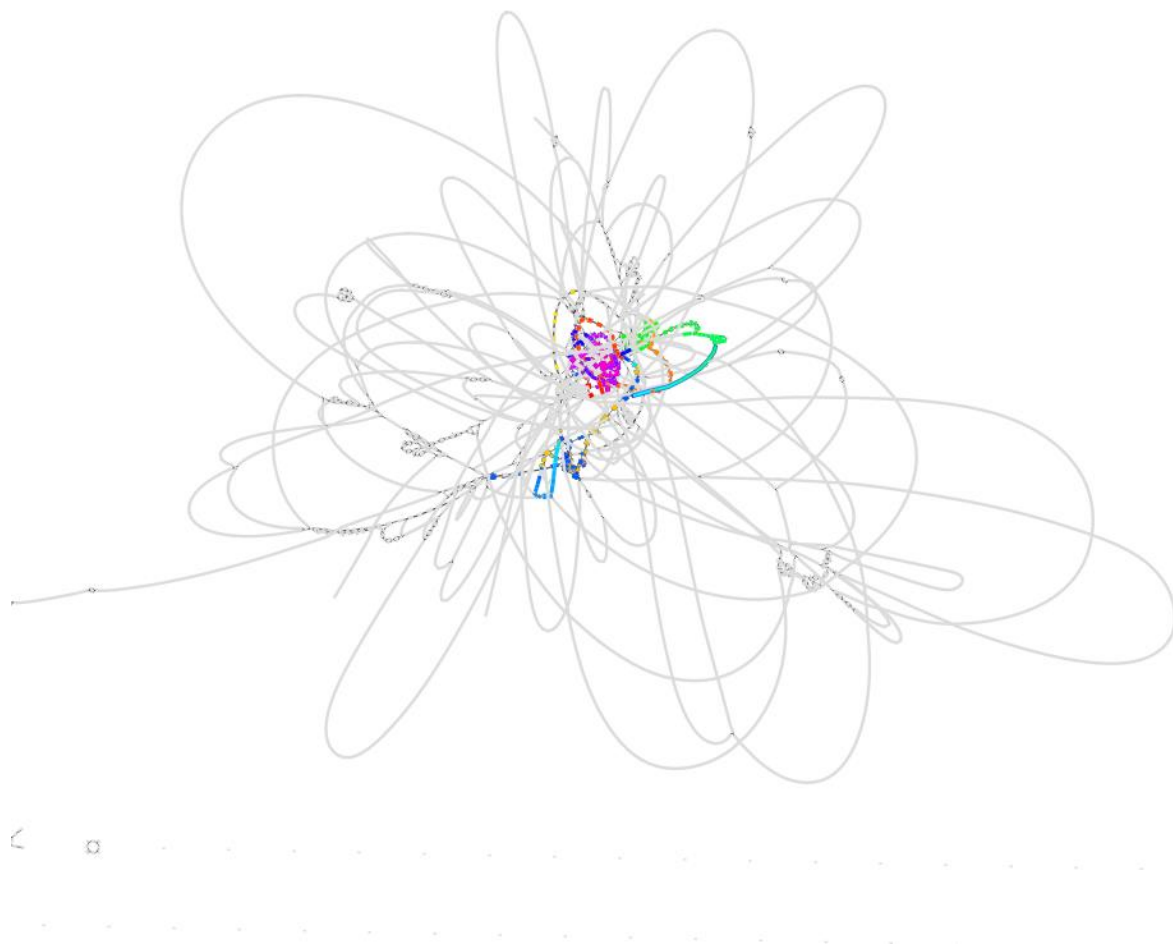
Figure 74: Bandage assembly graph from MinION sequencing that demonstrates the assembled plasmid sequence in different rainbow colours and the chromosomal DNA in grey from the Hi-C library created from a multi-drug resistant *Escherichia coli* strain.
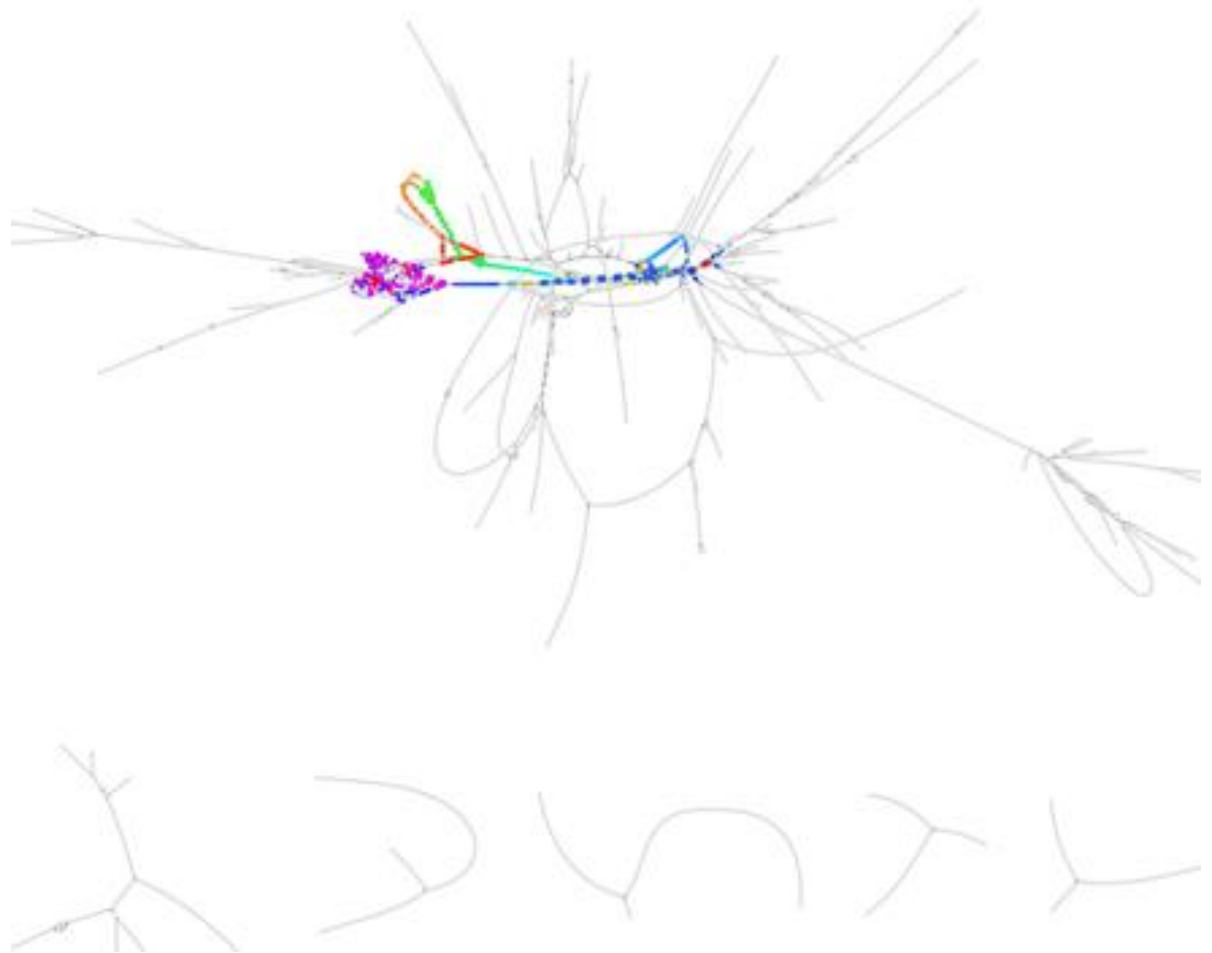
Figure 75: Bandage assembly graph from Illumina sequencing that demonstrates the assembled plasmid sequence in different rainbow colours and the chromosomal DNA in grey from the Hi-C library created from an multi-drug resistant *Escherichia coli* strain.

4.4.1.4. Simulating Hi-C restriction digestion to determine feasible contacts

When the Hi-C restriction digestion step was simulated using a small *S. aureus* plasmid and *E. coli* K12 chromosomal DNA, we see that when the simulation was supplied with 10% of the plasmid and 90% of the *E. coli* K12 chromosomal DNA, the plasmid assembled separately and couldn't be detected with contacts to the chromosome. When 20% of the plasmid was supplied with 80% of the *E. coli* K12 chromosomal DNA, we saw the plasmid assemble within the *E. coli* K12 DNA. When the *S. aureus* plasmid was supplied at a higher percentage (20%+) the plasmid assembled with the *E. coli* K12 chromosome. The Hi-C reads produced from MinION sequencing were then mapped to the MinION reference scaffold that was made up of 4 contigs. Heat map/contact maps were then generated to a resolution of 25,000 bp and visualised using HiGlass. A summary of how to read the contact maps is summarised in Figure 76 below. The bacterial genome reads are plotted on each axis, and where there is contact in the genome to

another part of the genome, it is coloured below in orange (Figure 77). The frequency of the contact detected from sequencing informs the intensity of the colour in the heat map. This work was conducted as proof of principle to demonstrate the contacts we'd expect from our samples using the REs used from the ProxiMeta kit. Each restriction enzyme was visualised separately, as at the time this work was conducted, the program used could only work with the input of one restriction enzyme, thus generating two outputs below.
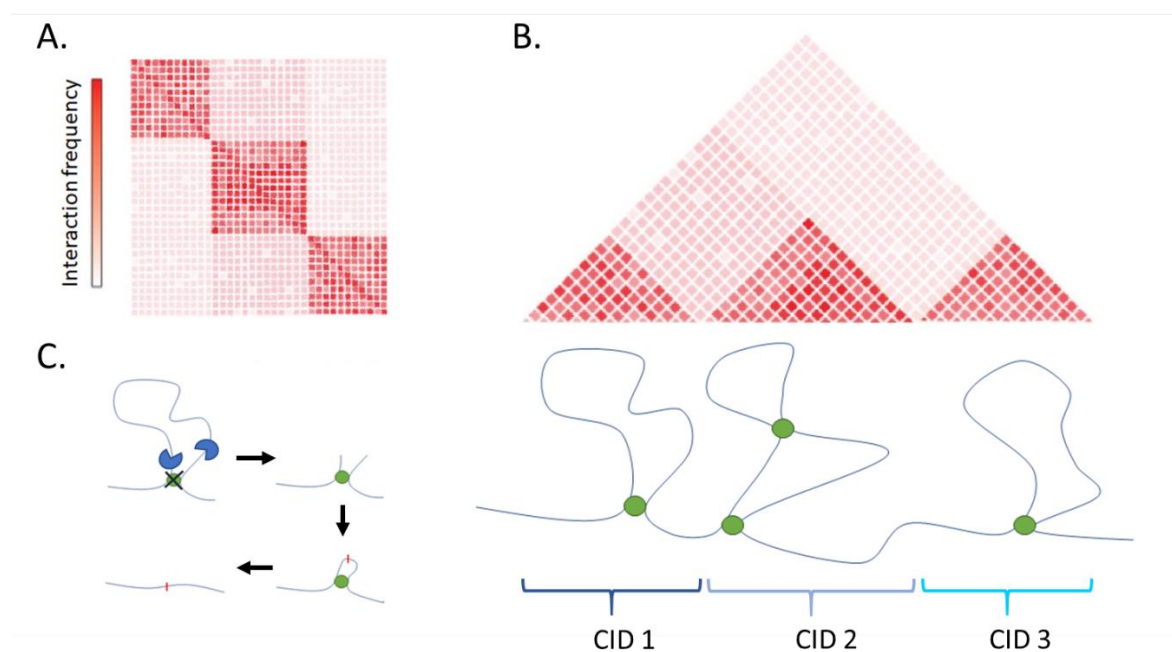
Figure 76: Chromosome conformation mapping using Hi-C. Mock data is displayed in this figure to aid the interpretation of subsequent Hi-C chromosome conformation figures. A:Chromosome contact map showing chromosome interaction frequency, with x- and y-axes representing the linear chromosome plotted against itself. Darker colours show a greater degree of interaction. B: The contact map indicates the chromatin structure (blue wavey line) and defines the boundaries between chromosome interacting domains (CIDs), maintained by various DNA-binding proteins (green circles). C: In Hi-C, following crosslinking of DNA-binding proteins, restriction enzymes (blue partial circles) cut the DNA, followed by ligation under dilute conditions resulting in chimeric DNA fragments that can be sequenced to identify regions of DNA that are co-localised in 3-dimensional space. Adapted from Mota-Gómez and Lupiáñez (2019) by Dr. Benjamin Evans.
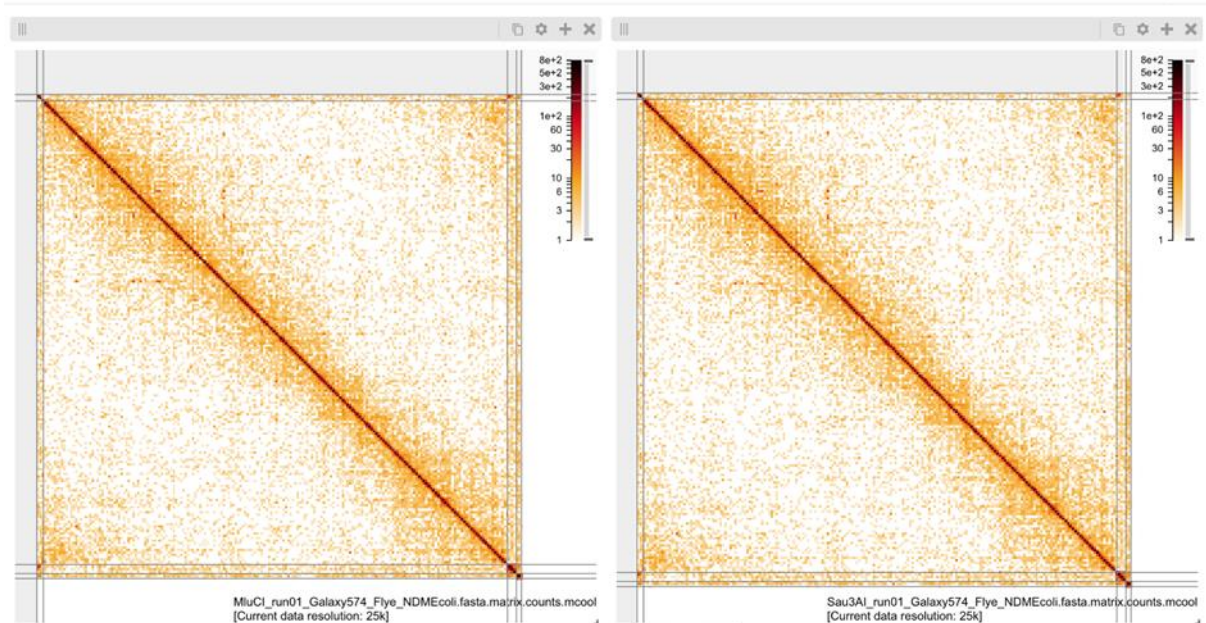
Figure 77: Simulated Hi-C digestion. The left panel demonstrates the contacts with the MluCI virtual digestion scaffold and on the right panel is the contacts with the Sau3AI virtual digestion scaffold. The contacts that we see demonstrated in the two panels is what we would expect to see from the MDR *E. coli* bacterial sample used in this study.

4.4.2. ProxiMeta Hi-C protocol with reagents substituted

This experiment was conducted to determine whether the Phase Genomics Hi-C protocol could be substituted with our own reagents and DNA extraction methods, as well as determine where DNA was being lost in the Phase Genomics Hi-C kit method. After the initial crosslinking step with formaldehyde and subsequent quenching with glycine, the MDR *E. coli* cells were not lysed at this stage but had a Qubit dsDNA BR reading of 92.8 ng/μL which indicated the presence of extracellular DNA that was not of interest for the current study. The DNA concentration was 10.2 ng/μL after the cells were lysed and run on the MagNA Pure Compact system which was concerning as the DNA concentration is considered to be low at this stage. As the Hi-C method continues we expect to lose more DNA which is needed at a suitable concentration in order to sequence the sample. From the fragmentation step where the DNA sample underwent restriction digestion, the sample DNA was out of range/too low which indicates that the levels of DNA at this stage are too low to sequence. All of the steps following this stage (proximity ligation and DNA purification) had no detectable DNA using the Qubit dsDNA BR kit. Supernatants that were saved throughout the process also reported a low DNA content that couldn't be detected using the Qubit dsDNA BR kit, with the exception of the supernatant taken after the restriction digestion step in the protocol, which had a DNA concentration of 3.56 ng/μL. Through testing the DNA concentration at different stages of the method and also testing the

DNA concentration in the supernatants that are usually disposed of, it was not clear whereabouts in the process we were losing DNA. It was considered that the DNA extraction method wasn't suitable for the extraction of crosslinked DNA due to the unexplained loss of almost all of the detectable DNA, so different DNA extraction kits and systems were tested. Furthermore, for the next stages of optimising this method, a DNase treatment inserted to the beginning of the Hi-C method was tested as we detected DNA before the cells of interest were lysed. We assumed this is extracellular DNA released by natural cell lysis, which we wanted to remove so that it wouldn't be picked up in the downstream analyses.

4.4.2.1. Testing DNase treatment in the Hi-C method

In this experiment, the effect of a DNase initial treatment on the extracted DNA sample was tested to see if the addition of the step would be detrimental to the Hi-C method and how well the sample ran on agarose gels. The results are summarised in Table 31 below. From this experiment, it appears as if using 1 mL of the overnight culture with DNase treatment was acceptable to use, especially as we can see that we are able to extract long sequences of DNA. In this sample, the largest DNA size on average was 55,390 bp using the 1 mL culture. Using a 10 mL overnight culture gave the highest quantity of DNA, but we can see that after DNase treatment, a huge proportion of this can probably attributed to extracellular DNA present in the media. To determine the quality of the extracted DNA, the A260/280 and A260/230 ratio from the NanoDrop is used, where values around 1.8 indicates low protein contamination and organic contaminants, respectively. The higher values that we see in the A260/280 and A260/230 ratios (2.00+) usually indicate that there is a contaminant present in the sample that absorbs light at the same wavelength as the DNA, or the wrong solution was used to blank the NanoDrop instrument.

Table 31: Testing bacterial input volumes for Hi-C. Different starting volumes of the overnight MDR *E. coli* strain (1 mL vs 10 mL) and treatment with DNase or without. After the DNA from the cells was extracted using the MagNA Pure compact system, the DNA was quantified using Qubit and the size of the DNA determined using TapeStation. To determine the purity of the DNA, NanoDrop readings were used. Multiple DNA bands can be seen in a few of the samples tested and indicate that the DNA has been sheared (n = 1).

	1 mL sample + DNase	1 mL sample	10 mL sample + DNase	10 mL sample
DNA concentration (ng/μL)	30.5	35.1	1.94	138
Average DNA size (bp)	2,502 (2,176 to 2,688 range)	2,440 (2,073 to 2,777 range)	>60,000 (10,246 to >60,000 range)	2,378 (1,979 to 2,679 range)
	2,923 (2,688 to 3,601 range)	3,127 (2,777 to 4,232 range)	-	3,047 (2,679 to 3,788 range)
	55,390 (5,916 to >60,000 range)	>60,000 (6,126 to >60,000 range)	-	>60,000 (6,433 to >60,000 range)
NanoDrop 260/280 ratio	2.10	2.10	2.32	2.02
NanoDrop 260/230 ratio	2.12	2.21	1.00	1.93

4.4.3. Testing different DNA extraction methods

To conduct the DNA extraction experiments, 6 conditions were always set up when testing each DNA extraction kit: 1A (DNase treatment pre-extraction and crosslinks reversed post-extraction), 1B (DNase treatment pre-extraction, DNA crosslinked pre-extraction and crosslinks reversed post-extraction), 1C (DNA crosslinked pre-extraction and then reversed post-extraction), 2A (DNase treatment pre-extraction), 2B (DNase treatment and DNA crosslinked, both pre-extraction), 2C (DNA crosslinked pre-extraction). A summary of the DNA per colony forming unit (CFU) for each of the sample conditions and DNA extraction methods tested is shown in Table 32 below. In the 1B condition (where the samples are treated with DNase pre-extraction, crosslinked and then the crosslinks reversed post-extraction), we can see that the Fire Monkey kit fraction A appears to produce the most DNA, followed by fraction B of the same kit, the DNeasy Blood and Tissue kit, the Promega Wizard® Genomic DNA Purification kit, and then finally the bead beating method that yielded no detectable DNA. It appears as if the spin column DNA extraction kits (Fire Monkey and DNeasy Blood and Tissue kit) are better at extracting the crosslinked DNA than any of the other kits tested.

Table 32: Average DNA concentration in ng/µL per colony forming unit (CFU) (ng/µL/CFU) for each of the sample conditions: 1A (DNase treatment and crosslinks reversed at the end), 1B (DNase treatment and crosslinks present before being reversed at the end of the experiment), 1C (DNA crosslinked and crosslinks removed at the end), 2A (DNase treatment), 2B (DNase treatment and DNA crosslinked) and 2C (DNA crosslinked). Entries that are marked as 'BDL' were Below the Detection Limit of the Qubit kit, and so the DNA concentration could not be quantified for those samples. All of the samples were extracted using the Fire Monkey kit (Revolugen), DNeasy Blood and Tissue kit (QIAGEN), Promega Wizard® Genomic Purification kit and a bead beating method (n = 3).

Condition description	Average Concentration of DNA per CFU (ng/µL/CFU)					
	1A	**1B**	**1C**	**2A**	**2B**	**2C**
	DNase treatment pre-extraction	DNase treatment pre-extraction		DNase treatment pre-extraction	DNase treatment pre-extraction	
		DNA cross-linked pre-extraction	DNA cross-linked pre-extraction		DNA cross-linked pre-extraction	DNA cross-linked pre-extraction
	Cross-links reversed post-extraction	Cross-links reversed post-extraction	Cross-links reversed post-extraction			
Fire Monkey kit Fraction A	2.49×10^{-10}	1.93×10^{-10}	4.26×10^{-10}	2.76×10^{-10}	2.98×10^{-10}	5.01×10^{-10}
Fire Monkey kit Fraction B	1.24×10^{-10}	9.41×10^{-11}	1.61×10^{-10}	1.53×10^{-10}	1.82×10^{-10}	1.97×10^{-10}
DNeasy Blood and Tissue kit	2.90×10^{-10}	3.55×10^{-11}	1.28×10^{-10}	3.87×10^{-10}	3.70×10^{-11}	1.01×10^{-10}
Promega Wizard	7.93×10^{-10}	9.17×10^{-12}	8.43×10^{-12}	8.61×10^{-10}	4.37×10^{-12}	3.2×10^{-12}
Bead Beating method	2.50×10^{-10}	BDL	BDL	1.47×10^{-10}	BDL	BDL

A Kruskal-Wallis test provided evidence of a statistically significant difference between DNA extraction kits used and the DNA extracted per CFU ($\chi(4) = 31.06$, $P <0.001$). Dunn's pairwise tests were carried out and determined that there was a statistical difference between the bead beating method and the DNeasy Blood and Tissue kit ($P= 0.03$, where the DNeasy Blood and Tissue kit performed better in terms of DNA extracted), the bead beating method and the Fire Monkey kit Fraction B ($P= 0.02$, where the Fire Monkey kit performed better), the bead beating method and the Fire Monkey kit Faction A ($P <0.001$, where the Fire Monkey kit performed better) and the Promega Wizard® Genomic DNA Purification kit and the Fire Monkey kit Fraction A ($P < 0.005$, where the Fire Monkey kit performed better).

An independent Kruskal-Wallis test was used to determine whether the presence of crosslinks affected the DNA concentration yield, as we suspected that the issues with extracting a high DNA yield was due to the ability of the DNA extraction kits and methods to deal with crosslinked DNA. For each of the DNA extraction methods tested, each of the sample conditions (1A, 1B, 1C, 2A, 2B, and 2C) were compared to each other using an independent Kruskal-Wallis test. From the statistical analysis, we find that the Fire Monkey kit Fractions A and B had no significant difference between the sample treatments ($P= 0.206$ and 0.243, respectively). For the Promega Wizard® Genomic DNA Purification kit and the bead beating method, the independent Kruskal-Wallis test found a significant difference between the groups where the Promega Wizard® kit produced a higher concentration of DNA, but when a Dunn's pairwise comparison was conducted and the adjusted P-value used, we found no significant difference between the groups. The DNeasy Blood and Tissue kit had a significant difference between the sample groups ($P <0.01$), and when we use a post-hoc Dunn's pairwise comparison, we see that there is a significant difference between the 1B and 2A treatments ($P= 0.026$, where more DNA was produced in the 2A treatment). However, when we look at these two treatments (1B and 2A), this doesn't answer the question directly of whether the presence of crosslinks affects DNA yield as 2A was only pre-treated with DNase to remove any extracellular DNA. To summarise, it appears as if crosslinking the samples during extraction and the addition of a DNase pre-treatment had no effect on the final DNA yield from the different extraction systems.

Finally, in the 1B condition (where the sample was treated following a normal Hi-C protocol with a DNase initial treatment, crosslinked and then the crosslinks reversed at the end) was analysed in more depth. A Kruskal-Wallis test provided evidence of a statistically significant difference between DNA extraction kits used and the DNA extracted per CFU ($\chi^2(4) = 13.24$, $P= 0.01$). Dunn's pairwise tests were carried out and there was evidence of a significant difference between the

bead beating method and the Fire Monkey kit Fraction A (*P*= 0.013) where the Fire Monkey kit Fraction A performed better. However, there was no evidence of a significant difference between the other pairs of kits/methods, all of the kits tested performed in a similar way, with the exception of the bead beating method.

4.4.3.1. Hi-C DNA extraction using the MagNA Pure extraction system

The MagNA Pure Extraction system was re-visited for DNA extraction as it is a magnetic bead system and we thought this would have the least amount of DNA lost during extraction so that it can be taken through the rest of the Hi-C method. In the previous experiment using different DNA extraction kits, spin columns that trap DNA performed better than methods involving evaporation to leave a DNA pellet. For each of the samples, the DNA was quantified, the size of the DNA was estimated and the purity of the DNA was determined which is summarised in Table 33 below. The action of a DNase treatment and the reversal of the crosslinks at the end of the experiment was also tested as conducted previously. From condition 1B (the condition that is most reflective of the Hi-C method) we can see that the MagNA Pure extraction system performed well as the range across the three replicates of the DNA concentration was 41.30-122 ng/µL. The DIN (DNA Integrity Number) generated by TapeStation was consistent at 6. The DNA extracted in condition 1B also generated consistent lengths of DNA in the range of 17,576->60,000 bp. When we look at condition 1C (where the cells were initially not treated with DNase), we can see that the DNA concentration is generally lower in condition 1B which indicates that we have removed any DNA that is not of interest to us and is more likely to be extracellular DNA. What was interesting to note was the purity of all of the samples in the conditions were low with the exception of condition 2A and a replicate in the 2C condition (where the DNA was just crosslinked).

Table 33: Using the MagNA Pure Extraction System for Hi-C. A summary of the DNA concentration, the DNA Integrity Number (DIN), the average DNA size and the purity of the different samples tested on the MagNA Pure Extraction system. The different samples tested were conducted in triplicate, and where: 1A (DNase treatment and the DNA crosslinks are reversed), 1B (DNase treatment, DNA is crosslinked and the crosslinks are reversed at the end), 1C (DNA crosslinked and the crosslinks are reversed at the end), 2A (DNase treatment), 2B (DNase treatment and DNA crosslinked), and 2C (DNA crosslinked) (n = 3).

	1A.1	1A.2	1A.3	1B.1	1B.2	1B.3	1C.1	1C.2	1C.3	2A.1	2A.2	2A.3	2B.1	2B.2	2B.3	2C.1	2C.2	2C.3
DNA concentration (ng/µL)	14.10	0.08	30.20	122.00	44.30	41.30	181.00	42.40	47.80	16.50	0.05	32.10	81.70	31.20	36.70	68.10	33.20	41.70
TapeStation DIN	3	-	5	6	6	6	5	6	6	6	-	3	6	6	6	5	5	6
Average DNA size (bp)	3,624	>60,000	3,843 >60,000	>60,000	17,576 >60,000	21,015	2,693 >60,000	2,912 >60,000	19,824 >60,000	2,056 3,414 35,512 >60,000	100	1,162 2,012 3,512 >60,000	10,261 >60,000	12,940 >60,000	11,522 >60,000	2,284 >60,000	2,273 >60,000	2,328 12,789 >60,000
NanoDrop 260/280 ratio	1.19	0.57	1.15	1.14	1.28	1.08	1.45	1.28	1.16	2.12	1.83	2.16	1.71	1.83	1.86	1.73	2.23	1.88
NanoDrop 260/230 ratio	0.41	0.41	0.39	0.41	0.55	0.35	0.65	0.51	0.41	2.11	0.27	2.21	1.54	1.72	1.81	1.71	2.55	1.82

The MagNA Pure extraction data was added to the data from the other extraction methods and kits that were tested. A Kruskal-Wallis test provided evidence of a significant difference between the mean ranks of at least one pair of groups tested in the concentration of DNA that was extracted ($\chi^2(5) = 54.63$, $P <0.001$). A Dunn's pairwise test was carried out and determined there was a significant difference between the bead beating method and the Fire Monkey Kit Fraction A where the Fire Monkey Kit Fraction A performed better ($P <0.01$), the bead beating method and the MagNA Pure extraction system, where the MagNA Pure system performed better ($P<0.01$), the Promega Wizard® Genomic DNA Purification kit and the Fire Monkey kit Fraction A, where the Fire Monkey kit Fraction A performed better ($P<0.05$), the Promega Wizard® Genomic DNA Purification kit and the MagNA Pure extraction system where the MagNA Pure extraction system performed better ($P<0.05$), the DNeasy Blood and Tissue kit and the MagNA Pure extraction system, where the MagNA Pure extraction system performed better ($P<0.01$) and the Fire Monkey kit Fraction B and the MagNA Pure extraction system, where the MagNA Pure Extraction system performed better ($P<0.05$). The summary output generated from the statistical analysis conducted in SPSS is below in Table 34. However, there was no evidence of a significant difference between the other pairs, so it is difficult to assess how each kit or method performed in a ranked order, although it appears as if the MagNA Pure extraction system performed the best. The bead beating method appears to have performed the worst out of all the kits and methods, but it was only statistically different to the MagNA Pure extraction system and Fire Monkey kit Fraction A.

Table 34: Statistical analysis of the DNA extraction methods for Hi-C. A summary of the Dunn's pairwise statistical test for the different DNA extraction methods tested. DNA extraction kits that were tested were: Fire Monkey kit (Revolugen), Promega Wizard® Genomic DNA Purification kit, DNeasy Blood and Tissue kit (QIAGEN), bead beating method, and the MagNA Pure extraction system (Roche). The significance values were adjusted by the Bonferroni correction for multiple tests ($n = 3$).

Sample1–Sample2	Test Statistic	Std. Error	Std. Test Statistic	Sig.	Adj.Sig.
Bead Beating–Promega Wizard	10.556	10.431	1.012	.312	1.000
Bead Beating–DNeasy Blood and Tissue	27.000	10.431	2.588	.010	.145
Bead Beating–Fire Monkey Fraction B	28.222	10.431	2.706	.007	.102
Bead Beating–Fire Monkey Fraction A	46.222	10.431	4.431	.000	.000
Bead Beating–MagNA Pure	−67.667	10.431	−6.487	.000	.000
Promega Wizard–DNeasy Blood and Tissue	−16.444	10.431	−1.576	.115	1.000
Promega Wizard–Fire Monkey Fraction B	17.667	10.431	1.694	.090	1.000
Promega Wizard–Fire Monkey Fraction A	35.667	10.431	3.419	.001	.009
Promega Wizard–MagNA Pure	−57.111	10.431	−5.475	.000	.000
DNeasy Blood and Tissue–Fire Monkey Fraction B	1.222	10.431	.117	.907	1.000
DNeasy Blood and Tissue–Fire Monkey Fraction A	19.222	10.431	1.843	.065	.980
DNeasy Blood and Tissue–MagNA Pure	−40.667	10.431	−3.899	.000	.001
Fire Monkey Fraction B–Fire Monkey Fraction A	18.000	10.431	1.726	.084	1.000
Fire Monkey Fraction B–MagNA Pure	−39.444	10.431	−3.781	.000	.002
Fire Monkey Fraction A–MagNA Pure	−21.444	10.431	−2.056	.040	.597

Each row tests the null hypothesis that the Sample 1 and Sample 2 distributions are the same.
Asymptotic significances (2–sided tests) are displayed. The significance level is .05.
Significance values have been adjusted by the Bonferroni correction for multiple tests.

We previously saw in section 4.4.3.1 that the crosslinking of the samples before extraction and the addition of a DNase pre-treatment had no effect on the DNA yield, as determined through the use of a Kruskal-Wallis statistical test. For the MagNA Pure extraction system, we see that there was a significant difference between all of the conditions (1A, 1B, 1C, 2A, 2B and 2C) in terms of the DNA concentration extracted. When a Dunn's pairwise test was conducted, there was no significant difference between the conditions which indicates that the presence of crosslinks when the samples were extracted and the use of a DNase pre-treatment had no effect on the DNA yield ($\chi^2(5) = 11.97$, $P= 0.035$).

Finally, condition 1B (where the cells were initially treated with DNase, the DNA was crosslinked and then post-DNA extraction the crosslinks were reversed) was looked at specifically across all the kits used to determine if there was a significant difference, as condition 1B is more reflective of the Hi-C method as a whole. A Kruskal-Wallis test provided evidence of a statistically significant difference between DNA extraction kits used and the DNA extracted per colony forming unit ($\chi^2(5) = 16.460$, $P= 0.006$). A Dunn's pairwise test was carried out and there was evidence that there was a significant difference between the bead beating method and the MagNA Pure extraction system ($P= 0.008$) where there was a higher DNA concentration per CFU when the DNA was extracted using the MagNA Pure DNA extraction system, but nowhere else. The bead beating method appears to have performed poorly out of all the kits tested in the 1B condition, with the MagNA Pure extraction system appearing to be the best.

4.4.3.2.   Zymo HMW bead extraction

The MDR *E. coli* samples that were extracted using the Zymo HMW Bead extraction kit had their DNA quantified. The Zymo HMW Bead extraction was tested as it is a magnetic bead method and was created to extract longer lengths of DNA for long-read sequencing. Each condition was conducted in triplicate, and the conditions were as followed: A (positive control that was not crosslinked), B (the test sample, which follows the normal Hi-C protocol where the DNA is crosslinked and then reversed at the end) and, C (the DNase negative sample). The conditions that are labelled with a 1 following the letter were treated before purification to remove any crosslinks (e.g. A1), and conditions that are labelled with a 2 following the letter were not treated to remove any crosslinks present before DNA purification (e.g. A2). The results of this experiment is displayed below in Table 35. From looking at the DNA concentrations produced in condition B1 (the condition that reflects the Hi-C method the most), the average DNA concentration across the three replicates was 0.1 ng/µL which is not sufficient for long-read sequencing. Looking at the DNA bands produced when the samples were run on TapeStation,

the lengths of the DNA was not long enough to qualify for long-read sequencing, and the purity of the DNA was spurious and not of good quality. From the results, we could see that the only condition that provided a suitable quantity of DNA for our downstream methods were the conditions where the DNA was not crosslinked and would not be suitable for the purposes of our experiments using the Hi-C method.

Table 35: Multi-drug resistant (MDR) *Escherichia coli* strain treated under different conditions before DNA was extracted using the Zymo Research *Quick*-DNA HMW MagBead Kit. The conditions were set up in triplicate (*n* = 3), where: A1 (treated with DNase and DNA not crosslinked but treated with proteinase K to remove crosslinks), B1 (DNase treatment and DNA crosslinked and reversed at the end), C1 (no DNase treatment, DNA crosslinked and reversed at the end), A2 (treated with DNase and DNA not crosslinked), B2 (DNase treatment and DNA crosslinked), and C2 (no DNase treatment, DNA crosslinked). A '*' indicates that the DNA concentration was too low to be detected by Qubit. The final DNA concentration is presented, alongside the 260/280 and 26/230 ratios generated by NanoDrop, as well as the TapeStation DNA Integrity Number (DIN).

MDR *E. coli* condition	DNA concentration (ng/µL)	260/280 ratio	260/230 ratio	TapeStation DIN	Average DNA size (bp)	
1A1	7.05	0.52	0.15	1.8	537	
2A1	3.12	0.70	0.34	2.4	659	
3A1	7.35	0.76	0.32	4.3	2,904	
1B1	0.091	-2.75	-0.40	1.3	557	
2B1	0.128	0.54	0.14	2.5	-	
3B1	0.085	0.55	0.15	1.8	-	
1C1	0.195	-0.73	-0.12	-	848	
2C1	0.242	0.52	0.15	1.9	518	
3C1	0.146	0.21	0.06	1.6	-	
1A2	11.8	2.85	4.39	6.8	3,303	>60,000
2A2	6.66	2.75	3.00	6.9	3,274	>60,000
3A2	14.8	3.30	7.32	-	3,396	>60,000
1B2	0.074	0.57	0.40	-	-	
2B2	0.132	0.59	0.52	-	-	
3B2	*	0.59	0.45	-	-	
1C2	0.088	1.13	0.52	-	-	
2C2	0.488	0.54	0.37	-	815	
3C2	0.425	0.54	0.45	-	-	

4.4.4. Optimised Hi-C method trials

4.4.4.1.   Digestion inside cells

The purpose of these experiments was to determine whether *E. coli* DNA could be digested within the crosslinked cells before lysing the cells. This was attempted to streamline the Hi-C method and remove the need for extra purification steps before acquiring the final Hi-C library. To this end, PMBN was used to permeabilise the cell membranes. In the *E. coli* ATCC 25922 sample that was tested under different conditions: condition A (just bacteria), condition B (with bacteria and REs added, condition C (where the bacteria were restriction digested in the presence of PMBN before the DNA was extracted), and condition D (where the DNA was extracted before it was incubated with REs). A summary of the results of the DNA quantification and size determination of the extracted DNA is presented in Table 36 below. It is difficult to determine from the results whether restriction digestion worked by permeabilising the membrane as the results from each of the conditions that acted as controls (B and D) were unexpected. From condition D where the DNA was extracted before it was digested, we expected to see fragmented DNA of different sizes but TapeStation detected no DNA bands. For condition B where the bacterial cells were incubated with the REs, we see two different bands (2,495 bp and 59,300 bp), but the treatment condition (C) which had PMBN added had similar DNA band sizes (2,259 bp and 39,630 bp) which indicates that permeabilising the cell membrane using PMBN didn't work as expected in the *E. coli* ATCC 25922 strain, as if PMBN aids the access of the REs to the DNA inside the cell, we'd expect to see multiple bands in the gel as smaller fragments of DNA should be present.

Table 36*: Polymyxin B nonapeptide cell permeabilisation in *Escherichia coli*. The *E. coli* ATCC 25922 strain was tested under a variety of conditions in order to determine whether treatment with polymyxin B nonapeptide (PMBN) was able to permeabilise the cell membrane to allow restriction enzymes (REs) access to the cellular DNA and digest the DNA without lysing the cells. Condition A contained just bacterial cells with no treatment, condition B had bacterial cells and restriction enzymes added, condition C had the bacterial cells with the addition of PMBN and the REs and condition D had DNA with the REs added (*n* = 1).

	E. coli ATCC 25922 condition			
	Bacteria (A)	Bacteria + REs (B)	Bacteria + PMBN (C)	DNA + REs (D)
DNA concentration (ng/µL)	13.70	11.20	8.80	6.59
TapeStation DIN	7.00	7.20	7.60	1.20
Average DNA size (bp)	2,282	2,495	2,259	-
		59,300	39,630	

A *S. aureus* strain was included in the experiments to determine whether the action of PMBN was affected by the thickness of the cell wall. The same conditions were set up for the *S. aureus* ATCC 25923 strain as conducted in the *E. coli* ATCC 25922 strain. From looking at the results from the experiments, it looks as if the addition of PMBN had no effect on the permeability of the cell membrane of the *S. aureus* cells, so the DNA inside the cells were not digested by the REs (condition C). A summary of the DNA concentration and size of the DNA is shown for all of the conditions in Table 37 below.

Table 37: Polymyxin B nonapeptide cell permeabilisation in *Staphylococcus aureus*. The *S. aureus* ATCC 25923 strain was tested under a variety of conditions in order to determine whether treatment with polymyxin B nonapeptide (PMBN) was able to permeabilise the cell membrane to allow restriction enzymes (REs) access to the cellular without lysing the cells. Condition A contained just bacterial cells with no further treatment, condition B had bacterial cells and REs added, condition C had the bacterial cells with the addition of PMBN and the REs and condition D had DNA with the REs added (*n* = 1).

	S. aureus ATCC 25923 condition			
	Bacteria (A)	Bacteria + REs (B)	Bacteria + PMBN (C)	DNA + REs (D)
DNA concentration (ng/µL)	28.20	30.10	31.70	14.70
TapeStation DIN	8.90	9.40	9.30	-
Average DNA size (bp)	2,296	2,543	56,618	3,908
	47,957	4,931		
		57,150		

4.4.4.2. Polymyxin B nonapeptide permeabilisation

From the previous experiment, it was hypothesised that the issue with cell membrane permeabilisation was the concentration of PMBN used, so the purpose of these experiments was to determine whether different concentrations of PMBN and the REs were able to digest the DNA inside the bacterial cells. In these experiments the *E. coli* ATCC 25922 strain was used in the conditions: A (just bacteria with DNA extracted normally), B (where the bacteria were treated with REs before the DNA was extracted), C (where the bacteria were treated with REs and PBMN at 20 µg/mL before the DNA was extracted), D (where the bacteria were treated with REs and PMBN at 40 µg/mL before the DNA was extracted), E (bacteria treated with REs and PMBN at 60 µg/mL before DNA extraction), F (bacteria treated with REs and 80 µg/mL PMBN before the DNA was extracted), G (bacteria treated with REs and 100 µg/mL PMBN before the DNA was extracted), and H where the DNA was extracted as normal before being incubated with the REs. The results of the DNA concentration and DNA sizes for each condition is summarised in Table 38 below. From the results, it is difficult to determine whether a higher concentration of PMBN allowed for the permeabilisation of the cell membrane to allow the REs access to the DNA inside the cells. Generally, from the results it appears as if the average DNA band size on the TapeStation decreases with PMBN concentration as in condition G (with 100 µg/mL PMBN) the average band size was 28,125 bp long whereas in condition C where 20 µg/mL PMBN was added, the largest DNA band was 48,500. However, it is interesting that also seen in condition C that there is a smaller DNA band that is approximately 179 bp long which is not seen in any of the other PMBN treatments which may indicate that REs are able to penetrate into the cell, but this cannot be firmly concluded without further experimentation.

Table 38: Polymyxin B nonapeptide cell permeabilisation in *Escherichia coli* at different concentrations. The *E. coli* ATCC 25922 strain was tested under a variety of conditions in order to determine whether treatment with polymyxin B nonapeptide (PMBN) was able to permeabilise the cell membrane to allow restriction enzymes (REs) access to the cellular without lysing the cells. Condition A contained just bacterial cells with no further treatment, condition B had bacterial cells and REs added, condition C had the bacterial cells with the addition of 20 µg/mL PMBN and the REs, condition D had the bacterial cells and 40 µg/mL PMBN and REs, condition E had the bacterial cells and 60 µg/mL PMBN and REs, condition F had bacterial cells and 80 µg/mL PMBN and REs, condition G had bacterial cells and 100 µg/mL PMBN and REs, and condition H had extracted DNA and REs added (n = 1).

	Bacteria (A)	Bacteria + RE (B)	Bacteria + 20 µg/mL PMBN + REs (C)	Bacteria + 40 µg/mL PMBN + REs (D)	Bacteria + 60 µg/mL PMBN + REs (E)	Bacteria + 80 µg/mL PMBN + REs (F)	Bacteria + 100 µg/mL PMBN + REs (G)	DNA + REs (H)
DNA concentration (ng/µL)	7.19	8.23	5.59	9.02	9.27	8.83	9.18	4.53
TapeStation DIN	8.00	7.10	8.80	7.60	7.60	8.90	-	-
Average DNA size (bp)	50,124	38,682	179 48,500	52,967	44,660	51,889	28,125	-

4.4.4.3. DNA extraction using phenol-chloroform

The MDR *E. coli* strain was extracted using a phenol-chloroform method, as it is considered the gold standard for DNA extractions and would offer insight into how well crosslinked DNA could be extracted using this method. Triplicates were set up for each condition: A (positive control that was not crosslinked), B (the test sample, which follows the normal Hi-C protocol where the DNA is crosslinked and then reversed following extraction) and, C (the DNase negative sample with no prior crosslinking). The conditions that are labelled with a 1 had the DNA crosslinks reversed before the DNA was quantified whereas the conditions that are labelled with a 2 did not have the DNA crosslinks reversed e.g. A1 and A2, respectively. The DNA concentration for each of the samples is summarised in Table 39 below. On average across the three replicates, the most DNA extracted was from the condition where the samples were treated with DNase before extraction and the samples were treated to remove any crosslinks post-extraction (condition A1 with an average DNA concentration of 16.42 ng/µL). The conditions where crosslinks were present during the extraction (conditions B and C) had low average DNA concentrations. These results suggest that crosslinked DNA is not purified effectively in our study by using the phenol-chloroform method and may not be suitable in our attempts to combine the Hi-C method with long-read sequencing.

Table 39: Multi-drug resistant (MDR) *Escherichia coli* strain treated under different conditions before DNA was extracted using a phenol-chloroform method. The conditions were set up in triplicate (*n* = 3), where: A1 (treated with DNase and DNA not crosslinked but treated with proteinase K to remove crosslinks), B1 (DNase treatment and DNA crosslinked and reversed at the end), C1 (no DNase treatment, DNA crosslinked and reversed at the end), A2 (treated with DNase and DNA not crosslinked), B2 (DNase treatment and DNA crosslinked), and C2 (no DNase treatment, DNA crosslinked). A '*' indicates that the DNA concentration was too low to be detected by Qubit.

MDR *E. coli* condition	Condition description	DNA concentration (ng/µL)
1A1	DNase treatment pre-extraction	0.36
2A1		20.30
3A1	Crosslinks reversed post-extraction	21.90
1B1	DNase treatment pre-extraction	0.31
2B1	DNA crosslinked pre-extraction	0.08
3B1	Crosslinks reversed post-extraction	0.08
1C1		0.09
2C1	DNA crosslinked pre-extraction	0.07
3C1	Crosslinks reversed post-extraction	0.29
1A2	DNase treatment pre-extraction	0.58
2A2		17.60
3A2		12.50
1B2	DNase treatment pre-extraction	*
2B2	DNA crosslinked pre-extraction	*
3B2		*
1C2		*
2C2	DNA crosslinked pre-extraction	*

3C2	0.22

4.4.4.4. Hi-C method with wash step and Fire Monkey DNA extraction

The Hi-C method coupled with the Fire Monkey extraction kit was compared to the Hi-C method with a wash step before adding the sample to the Fire Monkey extraction kit. A wash step was included because we hypothesised that the different reagents we used for the Hi-C portion of the experiment was interfering with the ability of the Fire Monkey extraction kit to extract DNA as the different reagents could be reacting with the buffers in the kit. The results are summarised below in Table 40. On average, we previously saw that the Fraction A from the Fire Monkey kit extracted 3.47 ng/μL of DNA and Fraction B extracted 1.69 ng/μL without the addition of the wash step. With the introduction of a wash step, on average Fraction A had 9.27 ng/μL of DNA whereas Fraction B had an average concentration of 6.89 ng/μL which indicates that the addition of the wash step has improved the DNA yield. As seen with the other extraction methods tested, the purity of the DNA samples is still low and it is unusual that in Fraction B, the TapeStation could not detect any DNA bands.

Table 40: Multi-drug resistant (MDR) *Escherichia coli* extracted using the Hi-C method, a wash step and the Fire Monkey DNA extraction kit. The extraction was conducted using two replicates (*n* = 2), and the Fire Monkey kit elutes into two fractions, Fraction A and Fraction B. The DNA concentration is presented in ng/μL, as well as the NanoDrop purity ratios, the TapeStation DNA Integrity Number (DIN) and the average DNA size (bp). Where no value was generated, a '-' is marked.

	Fraction A replicate 1	Fraction A replicate 2	Fraction B replicate 1	Fraction B replicate 2
DNA concentration (ng/μL)	10.1	8.43	4.44	9.33
260/280 ratio	1.26	0.57	1.52	0.59
260/230 ratio	0.88	0.16	0.9	0.27
TapeStation DIN	7.8	1	-	-
Average DNA size (bp)	5,669	862	-	-
	>60,000	>60,000	-	-

4.4.4.5.   Substituted Reagents Hi-C test with DNA Loss

This experiment was run using the MDR *E. coli* strain to determine where DNA was being lost in the Hi-C method we were testing using substituted reagents instead of the ProxiMeta kit reagents. As we showed above there was not one final method that significantly outperformed the others. So, the MagNA Pure Compact system was used and the Promega Wizard® Genomic DNA Purification kit (for final purification) was used as there are no spin columns involved in the method. We wanted to avoid the use of spin columns as we hypothesised that the crosslinked DNA was potentially getting stuck in the spin column, as many DNA extraction kits available commercially aren't used for fixed DNA samples and require the samples to be treated to remove the fixative agent before DNA extraction can be done. The results of the experiment are summarised below in Table 41. In general, the DNA concentration of the sample decreases as you progress through the Hi-C method, and the supernatants at different stages had little DNA present that may not have been detectable by the Qubit kit. Similarly, to the DNA concentration, the size of the extracted DNA decreases as you progress through the Hi-C method, with a variety of different sizes of DNA present after the MagNA Pure DNA extraction step.

Table 41: A summary of the DNA concentration and the average DNA band sizes for the multi-drug resistant (MDR) *Escherichia coli* strain at different stages of the Hi-C method to determine where DNA was being lost (*n* = 1). Cells marked with '‡' indicate that the test sample produced no bands, but the supernatant produced a DNA band on TapeStation and is presented in instead.

	DNA concentration of sample (ng/µL)	DNA concentration of supernatant (ng/µL)	Average DNA size (bp)
After DNA crosslinking	92.8	N/A	14,606 >60,000
After MagNA Pure extraction	10.2	N/A	228 1,931 2,878 9,604 >60,000
After restriction digestion	*	N/A	>60,000
After centrifugation	*	3.56	‡16,346
Crosslinks reversed	*	N/A	-
Proximity ligation	*	N/A	-
Promega Wizard purification	*	-	‡184
Final Promega Wizard purification	*	-	‡855

4.4.4.6. Hi-C method with Fire Monkey extraction and bead purification

To improve on the DNA extraction methods we tested, we tried to combine the use of the Fire Monkey extraction kit and AMPure beads (to imitate the purification system used in the MagNA Pure extraction system). We wanted to extract DNA in sizes as long as possible without continually losing significant amounts of DNA in the process. The results are summarised in Table 42 below. For long-read sequencing using MinION using the rapid sequencing kit, we want an average DNA concentration of at least 50 ng/µL which was not achieved in these tests. For the Rapid PCR Sequencing kit (ONT) a minimum of 10 ng of DNA is required which could potentially still be used for these samples if the DNA is concentrated. On average, more DNA was extracted from the MDR *E. coli* sample (average of 5.18 ng/µL across the three replicates) than the *A. baumannii* A21 strain (3.30 ng/µL average). What was interesting to see was the MDR *E. coli* strain had a lot of DNA lost in the supernatant after the bead washing step, compared to the *A. baumannii* A21 strain.

Table 42: Summary of the DNA concentration of the *Acinetobacter baumannii* A21 and multi-drug resistant (MDR) *Escherichia coli* strains at different stages in the Hi-C method. Three replicates of each strain were tested (*n* = 3). No data is available in cells marked with a '-'.

| | | DNA concentration (ng/µL) | | | |
		Cells crosslinked and DNase treatment	After Fire Monkey DNA extraction	After bead washing steps	Final Hi-C library
A. baumannii A21	Sample Replicate 1	0.218	1.07	-	2.32
	Sample Replicate 2	0.249	1.83	-	2.45
	Sample Replicate 3	0.422	2.25	-	5.13
	Supernatant Replicate 1	-	-	0.214	-
	Supernatant Replicate 2	-	-	0.328	-
	Supernatant Replicate 3	-	-	0.504	-
MDR *E. coli*	Sample Replicate 1	0.341	4.66	-	3.74
	Sample Replicate 2	0.322	4.31	-	6.53
	Sample Replicate 3	0.348	6.66	-	5.28
	Supernatant Replicate 1	-	-	4.91	-
	Supernatant Replicate 2	-	-	3.52	-
	Supernatant Replicate 3	-	-	3.9	-

4.4.4.7. Full Hi-C method run through with bead purification and centrifugation steps

As it was clear that we were losing DNA from the purification step of the methods we were trying, we attempted to combine the use of bead purification to capture as much of the DNA as possible, and centrifugation to pull down as much of the DNA as possible. For the first full run through of the Hi-C method with the reagents substituted and bead purification used, the final MDR *E. coli* Hi-C libraries had low DNA content that couldn't be detected by the Qubit dsDNA HS kit. Figure 78 below highlights at which point in the Hi-C method the samples and supernatants were tested for their DNA concentration in order to determine where most of the DNA was being lost. In this iteration of the method, the most DNA appears to have been lost after the ligation step, which is the step in the method where the most volume is removed and disposed of. The biotin purification step doesn't appear to be working as it should, as the previous step after the DNA crosslinks were reversed had an average DNA concentration of 19.73 ng/μL but after the biotin pull down, the average DNA concentration was 0.07 ng/μL.
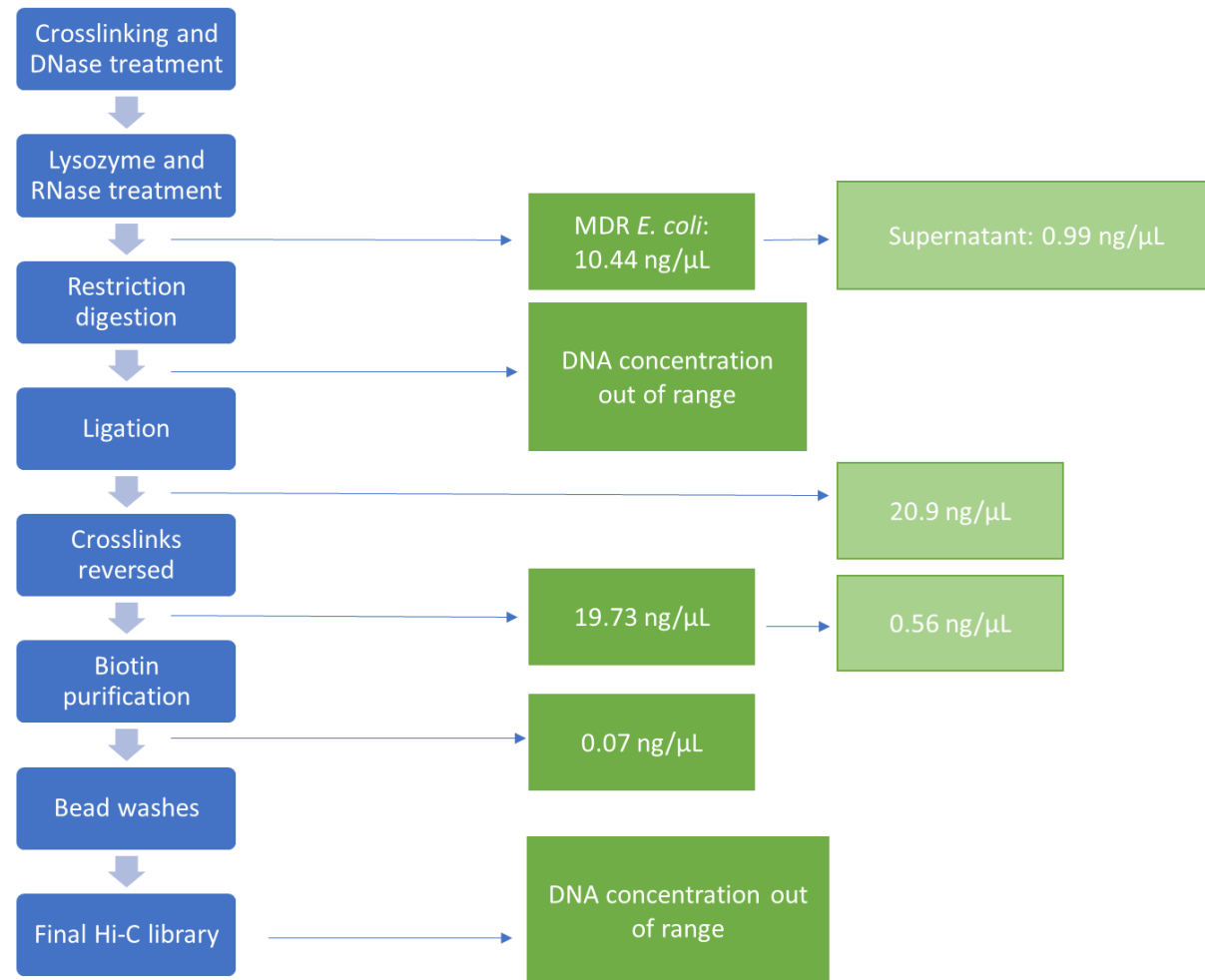
Figure 78: A summary of the Hi-C method conducted with bead purification and centrifugation. At various stages throughout the process (highlighted in blue boxes), the DNA was quantified for the multi-drug resistant (MDR) *Escherichia coli* sample (dark green boxes) and for the supernatant (light green boxes) that is usually disposed of (*n* = 3). Presented are the DNA quantification averages.

235

In the second run through of this method, it was conducted with both the MDR *E. coli* and *A. baumannii* strains. A summary of the DNA concentration at different stages of the Hi-C method is in Figure 79. The results from the TapeStation indicated that many of the samples had DNA that had accumulated in the well of the gel, and had not moved, which could indicate long DNA sequences, however this cannot be determined to be the case for sure. While trying to determine the DNA sizes using TapeStation, there were many internal marker issues and due to our limited sample saved and reagents, they could not be re-done. The final Hi-C library DNA sizes couldn't be determined in either of the bacterial strains tested due to ladder peak detection issues. For the MDR *E. coli* sample, the DNA concentration generally decreases as you progress through the Hi-C method, with the exception of the sample when it was taken straight after the restriction digestion step. It appears that there was a problem with the biotin purification step as most of the DNA was detected in the supernatant at this step (the supernatant is usually disposed of). We see a similar pattern in the *A. baumannii* A21 samples, where the DNA concentration gradually decreases as you progress through the Hi-C method, with the most DNA lost in the supernatant after the restriction digestion step.
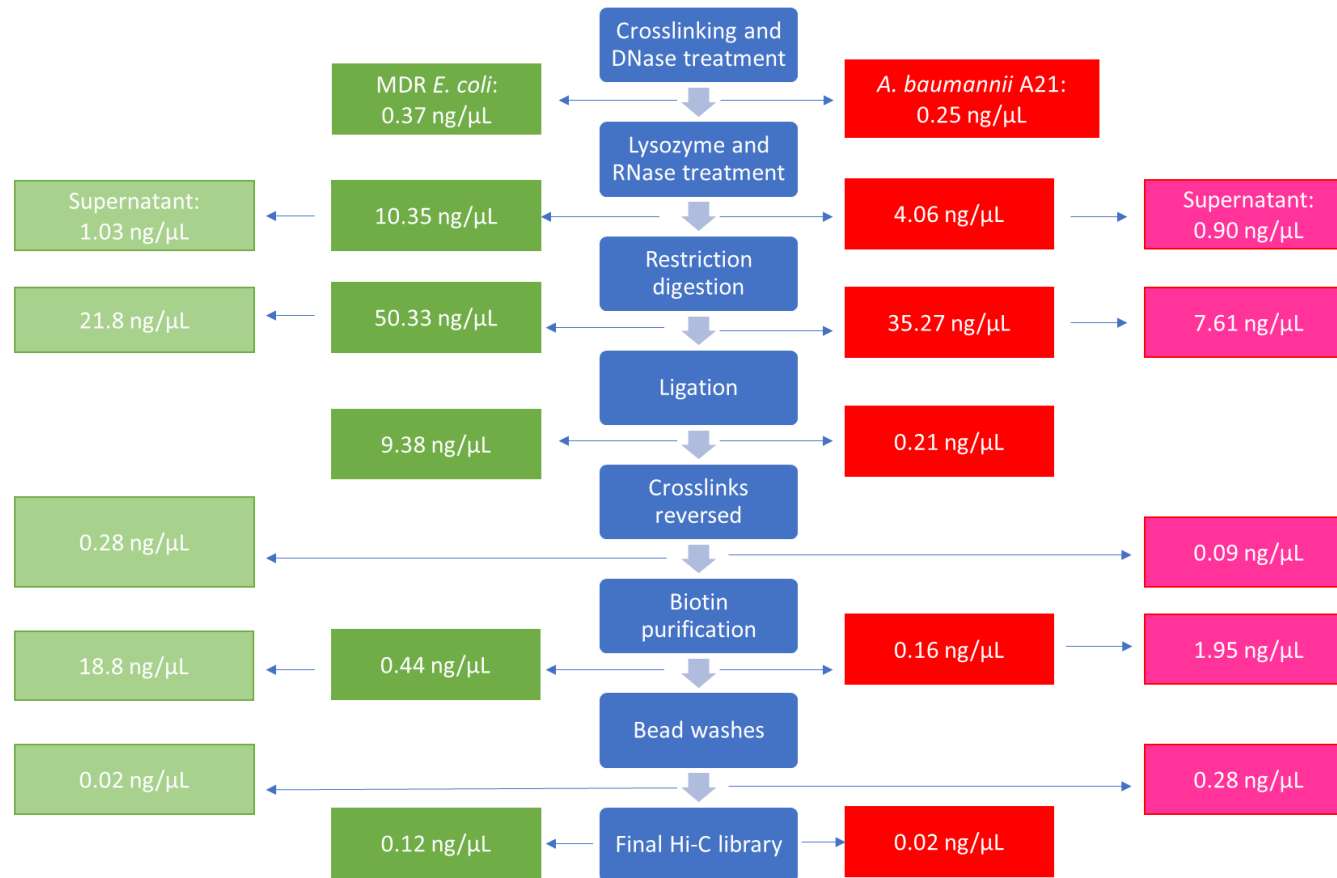
Figure 79: A summary of the Hi-C method conducted using bead purification and centrifugation with two bacterial organisms. At various stages throughout the process (highlighted in blue), the DNA was quantified for the multi-drug resistant (MDR) *Escherichia coli* sample (dark green boxes) and for the supernatant (light green boxes) that is usually disposed of. The *Acinetobacter baumannii* A21 strain was also tested, with the DNA concentration of the sample highlighted in red boxes, and the corresponding supernatant in pink boxes (*n* = 3). Presented are the DNA quantification averages.

237

4.4.4.8. Whole method run through with bead purification and no centrifugation steps

From the results of the previous whole method run through, it appears that most of the DNA was being lost in the centrifugation steps, so we hypothesised that removing the centrifugation steps and replacing them with magnetic bead washes would be better. The results are summarised in Figure 80 below. As we have seen previously, extraction of *A. baumannii* A21 DNA is not as efficient as extraction from the MDR *E. coli* strain, and most of the DNA seems to be lost following the ligation step in the method. The amount of DNA we are detecting in the supernatants do not account for this loss of DNA, but the question of where the DNA is going remains unknown. The final Hi-C libraries generated had no detectable DNA for either of the strains and is therefore not suitable for long-read sequencing.
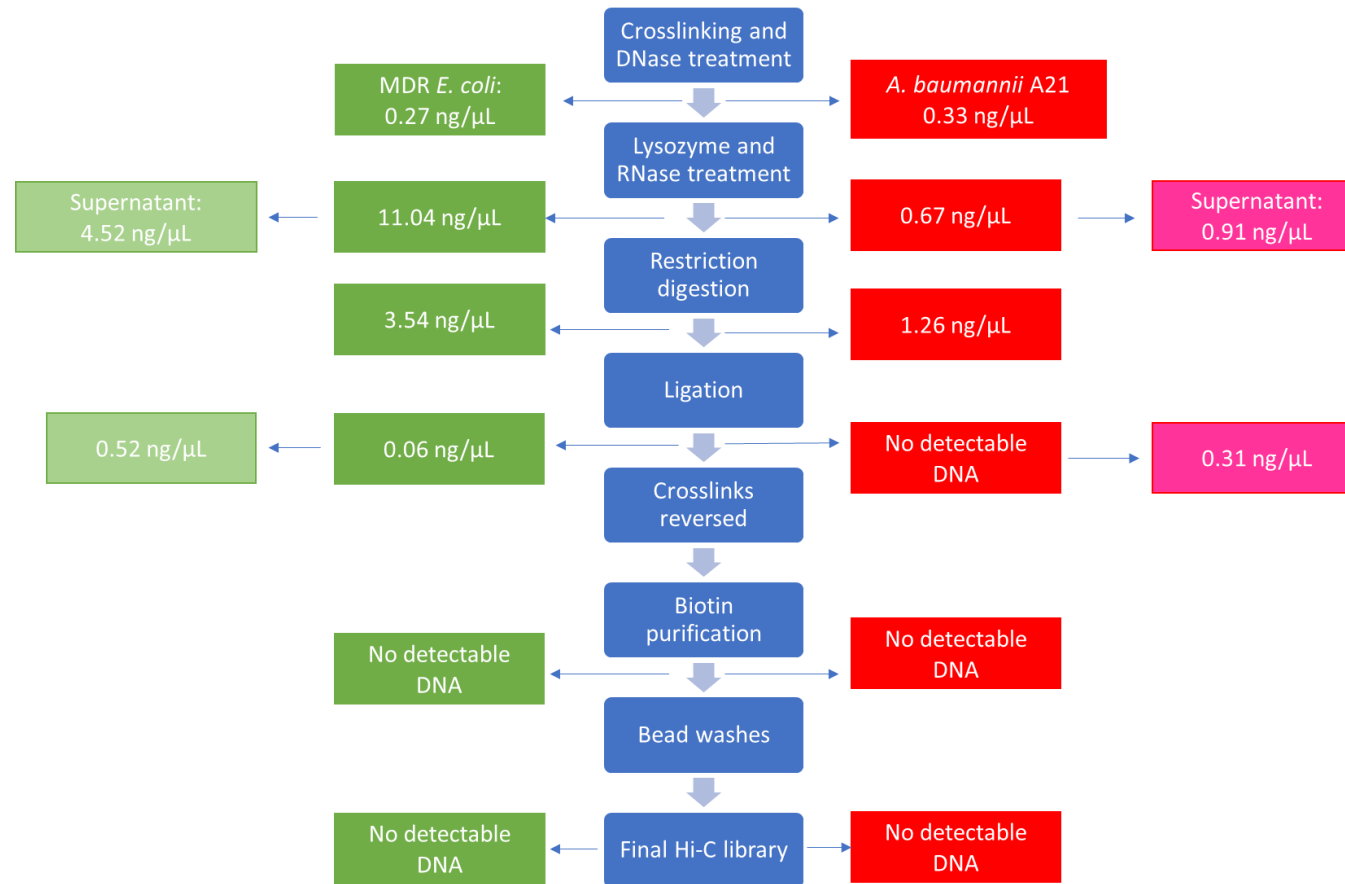
Figure 80: A summary of the Hi-C method with bead purification. At various stages throughout the process (highlighted in blue boxes), the DNA was quantified for the multi-drug resistant (MDR) *Escherichia coli* sample (dark green boxes) and for the supernatant (light green boxes) that is usually disposed of. The *Acinetobacter baumannii* A21 strain was also tested, with the DNA concentration of the sample highlighted in red boxes, and the corresponding supernatant in pink boxes (*n* = 3).

4.4.5. Summary of Hi-C method optimisations

Through many different trials in our attempt to streamline the Hi-C method at a reasonable cost, we have not yet been able to extract and purify substantial amounts of DNA following the Hi-C method for long-read sequencing. After exploring different extraction kits and trying to determine the effects of crosslinks being present in the sample, we have not yet found a suitable extraction system and a way to keep a good, high concentration of DNA in our versions of the Hi-C method that also provide DNA at a length that is suitable for long-read sequencing. In these experiments, we introduced a DNase treatment step, which doesn't contribute to the final Hi-C library (in terms of quantity, quality and length) but removes extracellular DNA that may affect the downstream analyses where we want to track the movement of MGEs between different bacteria. In future experiments, we would continue to use the DNase treatment step. In the interests of time to complete this PhD thesis, we decided to focus on whether or not Hi-C coupled with long-read sequencing is suitable to track the movement of MGEs in a population. To do this, we moved on to conducting relatively simple conjugation experiments, followed by the ProxiMeta Hi-C commercial kit in order to track the movement of a MGE

4.4.6. Conjugation experiments

Conjugation experiments were set up to determine simply whether we could track the movement of a MGE, in this case a plasmid, from one bacterial strain to another using phenotypic data generated from selective agar plates. We then used the Hi-C method (specifically the Hi-C kit from Phase Genomics) and long-read sequencing to see if we could track the movement of the plasmid without the need for selective agar plates.

4.4.6.1. MIC testing

MIC testing of the donor and recipient strains was conducted to determine which strains could be used in the conjugation experiments and could be distinguished from each other after conjugation, on selective agar plates. A summary of the MICs in displayed in Table 43. Three possible donor strains were selected based upon their known carriage of the carbapenemase gene bla_{NDM} as the sole acquired carbapenem resistance mechanism. The results of this experiment show that all of the donors could be used for the conjugation experiments as they have different MICs to the recipient *E. coli* J53 strain in terms of their susceptibility to Bm, MERO and MMC and their inability to grow on sodium azide at 100 µg/mL.

Table 43: Minimum inhibitory concentration testing before conjugation. The minimum inhibitory concentrations (MICs) of the antimicrobial agents bleomycin (Bm), meropenem (MERO), mitomycin C (MMC) and sodium azide for the bacterial strains: *Klebsiella pneumoniae* K9 (a *bla*$_{NDM-1}$ donor), *Escherichia coli* strains EC1 and EC4 (*bla*$_{NDM-4}$ donors) and *E. coli* J53 (recipient that is able to grow on sodium azide). The MIC tests were conducted in triplicate (*n* = 3).

Organism	Bm MIC (µg/mL)	MERO MIC (µg/mL)	MMC MIC (µg/mL)	Sodium azide (100 µg/mL)
K. pneumoniae K9 (donor)	>64	8	16	No growth
E. coli EC1 (donor)	>64	8	4	No growth
E. coli EC4 (donor)	>64	8	4	No growth
E. coli J53 (recipient)	0.45	0.03	2	Growth

4.4.6.2. Conjugation

Conjugation experiments were carried out using all three of the donor strains (*K. pneumoniae* K9, *E. coli* EC1 and EC4) with the recipient *E. coli* J53 strain. Three donor strains were used to determine whether they had a *bla*$_{NDM}$ gene on a plasmid and whether it was transferable. The resulting cultures were plated on MERO and sodium azide LB plates and plain sodium azide plates to determine whether transconjugants existed that were *E. coli* J53 and had a *bla*$_{NDM}$ gene present. No colonies grew on the MERO and sodium azide selective plates when the donor *K. pneumoniae* K9 was used. In the *E. coli* EC1 strain, one of the three replicates demonstrated growth on the MERO and sodium azide selective plate. In the *E. coli* EC4 strain, all three of the replicate plates demonstrated growth on MERO and sodium azide LB plates. However, the growth demonstrated (seen in both *E. coli* donor strains) was not clear enough to determine whether conjugation was successful. The control sodium azide plates demonstrated that there was growth and the presence of the *E. coli* J53 strain in all of the experiments. To determine whether true transconjugants existed on the selective MERO and sodium azide plates, the concentration of MERO on the plates was lowered from 4 µg/mL to 1 µg/mL and transconjugants were streaked onto new selective MERO and sodium azide plates. For one replicate of the *E. coli* EC1 donor cells mixed with the *E. coli* J53 recipient cells, the overnight culture for DNA extraction failed to grow and so was not included in the rest of the experiment. The phenotypic data suggested that the plasmid had been successfully transferred, which we then took forward to be confirmed by Hi-C sequencing (section 4.4.6.4 below).

4.4.6.3. Colony counts

Following the previous experiments where we determined whether the donor strains were carrying a *bla*$_{NDM}$ gene, the *E. coli* EC1 strain was taken forward for the conjugation experiments. We then investigated the effect of different drugs on the conjugation efficiency between the *E. coli* strains EC1 (donor) and J53 (recipient). Exposure to different drug conditions during conjugation affects the percentage of cells that are transformed. The *E. coli* EC1 donor strain and *E. coli* J53 recipient strain, when exposed to plain LB broth, had an average of 0.01% (2 d.p.) of cells that were transconjugants whereas when the cells were exposed to Mero, Bm and MMC the average percentage of transconjugants increased (0.02%, 0.06% and 5.21% (2 d.p.), respectively). The conjugation efficiency for each of the different drug conditions plotted in Figure 81, where it is clear that treatment with sub-MIC MMC had a higher conjugation efficiency when compared to LB, sub-MIC Bm and MERO treatments ($\chi^2(2)$= 251, *P*= 3.13 x 10^{-55}). The result of this experiment indicates that the genotoxic agent MMC stimulates a higher conjugation efficiency.
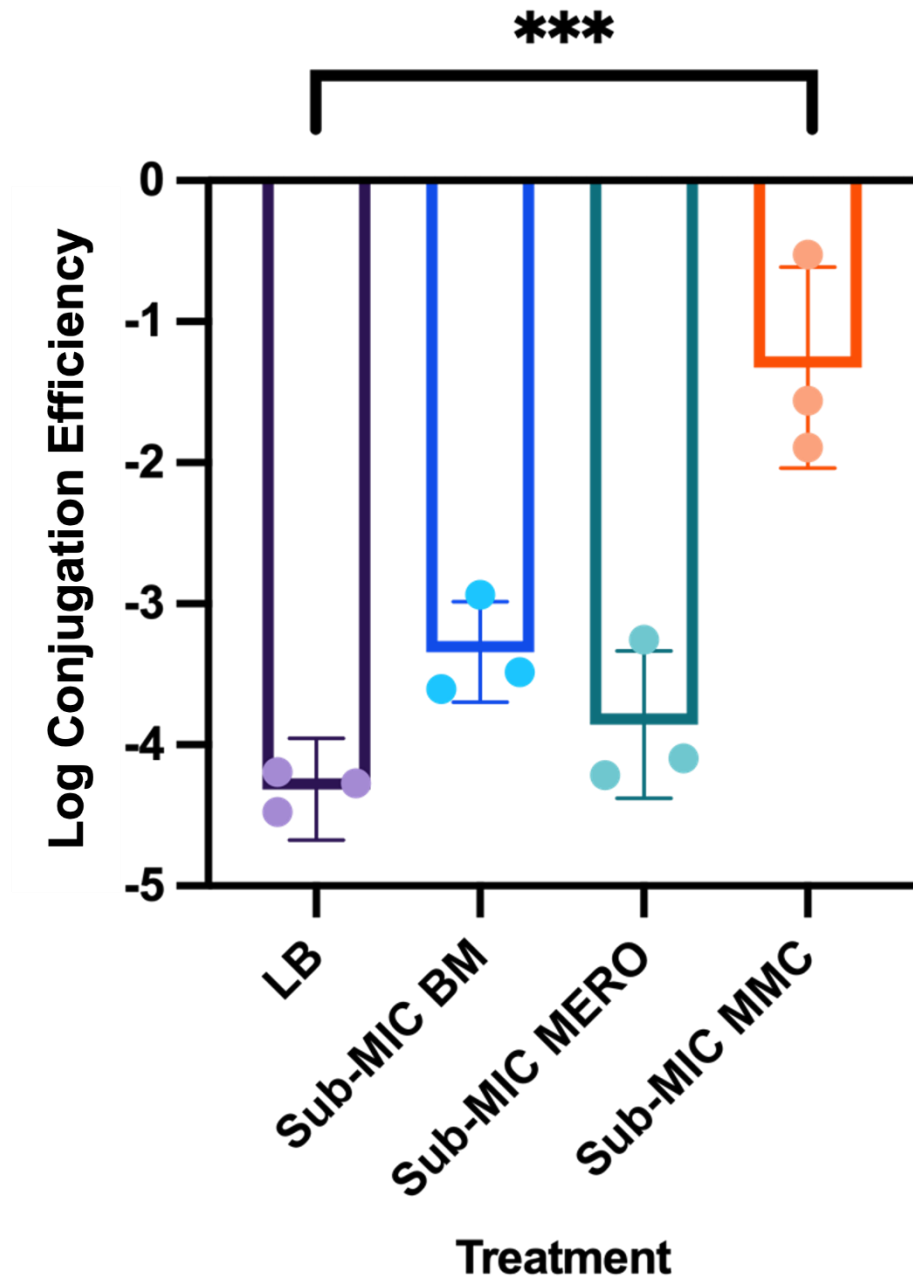
Figure 81: The conjugation efficiency for the *Escherichia coli* J53 strain in the presence of LB (purple), sub-MIC bleomycin (Bm, blue), meropenem (MERO, green) and mitomycin C (MMC, orange). The donor plasmid carrying the bla_{NDM-4} originates from the *E. coli* EC1 strain isolate from Kuwait. The 95% confidence interval is plotted alongside the conjugation efficiency. Significance of $P<0.001$ is indicated by '***' calculated using a Kruskal-Wallis test ($n = 3$).

4.4.6.4. Sequencing and analysis

E. coli J53 transconjugants that were present on MERO and sodium azide selective plates after treatment with either LB, Bm, MERO or MMC were sequenced on the Illumina and MinION platforms, as well as the parent *E. coli* EC1 and *E. coli* J53 parental strains. For each treatment, three replicates were conducted, as well as three technical replicates within each replicate (each treatment had 9 DNA extractions for sequencing). The transconjugants that had their DNA extracted using the Phase Genomics Hi-C kit to generate Hi-C libraries were sequenced on the Illumina platform. Using the Phase Genomics QC software, we can see that the donor and recipient *E. coli* strains (EC1 and J53, respectively) produced sufficient Hi-C libraries, but the *E. coli* J53 transconjugants that were exposed to LB, sub-MIC Bm and MERO during conjugation didn't produce sufficient Hi-C libraries. The conjugation experiments that were conducted in the presence of sub-MIC MMC, produced sufficient Hi-C libraries. A summary of the QC reports is presented below in Table 44. The QC reports indicate that we have to be careful with the conclusions we draw from these experiments as our library doesn't appear to be good quality or as informative as it could be, with the exception of the parental strains and one of the MMC exposed replicates.

Table 44: A summary of the parental *Escherichia coli* EC1 (donor), J53 (recipient) and the transconjugant J53 strains Hi-C library QC reports generated using the Phase Genomics software. The different conditions used to generate the transconjugants included LB, sub-minimum inhibitory concentration (MIC) bleomycin (Bm), sub-MIC meropenem (MERO) and sub-MIC MMC. To determine if a criterion was met for a sufficient or insufficient Hi-C library for downstream analysis, the cut-off values were as follows: Same strand high quality (HQ) read pairs (RPs) = >1.5%, informative RPs = >5.0%, fraction of HQ RPs >10 kb apart = >3.0%, clustering of usable HQ reads per contig = >600.000 and non-informative RPs = ≤ 50.00% (n = 3).

Sample	Condition	Replicate	Same strand HQ RPs	Informative RPs	Fraction of HQ RPs >10 kb apart	Clustering of usable HQ reads per contig	Non-informative read pairs
Parental *E. coli* EC1 and J53 mixture		1	17.36%	30.06%	33.63%	1406.50	30.43%
		2	25.69%	45.19%	49.91%	1774.00	22.87%
		3	23.83%	41.05%	46.11%	2333.50	26.01%
E. coli J53 Transconjugant	LB	1	0.28%	0.46%	0.49%	60.00	62.26%
		2	0.13%	0.21%	0.19%	26.50	65.79%
		3	0.12%	0.19%	0.17%	23.50	60.34%
	Bm	1	0.25%	0.34%	0.36%	47.00	62.22%
		2	0.13%	0.22%	0.19%	22.50	61.47%
		3	0.16%	0.26%	0.24%	25.50	60.96%
	MERO	1	0.28%	0.40%	0.42%	49.50	49.80%
		2	0.16%	0.23%	0.21%	19.50	56.89%

	3	5.49%	8.84%	10.23%	1129.00	68.35%
MMC	1	8.95%	14.21%	16.87%	2258.50	47.39%
	2	8.32%	12.96%	15.67%	2014.00	52.95%
	3	9.93%	15.53%	18.38%	2215.00	54.20%

The Cooler output files appeared to reflect the Phase Genomic QC reports to an extent, where we can see good contacts in the parental *E. coli* strains (control). However, according to the QC reports one of the MERO replicates was good quality, but when we look at the Cooler contact maps, all of the MERO replicates looked usable. When we look at the MMC replicates, the QC report looks positive but then when we produce the Cooler contact map we don't see strong signals from the donor *E. coli* J53 strain. The *E. coli* J53 transconjugants that were exposed to LB and sub-MIC Bm had fewer chromosomal contacts present in the contact map (see Appendix Section A).

FitHi-C was used to determine the statistical confidence estimates for the chromosomal contact maps generated from the Hi-C data for the *E. coli* parental controls and the MERO treated cells as they produced the best contact data when we looked at the QC report and Cooler outputs. A summary is presented in Table 45 below that outlines the number of significant contacts we see for each sample tested. From the control samples that were just the *E. coli* EC1 and *E. coli* J53 strains mixed together, there are many significant contacts (*p*-value <0.05) seen within the *E. coli* strains EC1 and J53 chromosomes, and a few instances where there are significant contacts between the chromosomal fragments of *E. coli* EC1 and J53. There are no significant contacts between the recipient *E. coli* J53 strain and the plasmid of interest. For the conjugation experiments conducted in the presence of MERO, we see lots of significant contacts (*p*-value <0.05) within the *E. coli* EC1 strain, within the *E. coli* J53 strain and some instances where we see significant contacts between *E. coli* EC1 and *E. coli* J53 chromosomal DNA. As expected, we also see significant contacts between the *E. coli* EC1 chromosome and the plasmid of interest. We also see a small number of *E. coli* J53 chromosomal contacts with the plasmid of interest (*p*-value <0.05), but in the FitHi-C output, a *q*-value is also calculated where Benjamini-Hochberg correction is conducted on the *p*-value, and we see that none of these contacts after correction are significant (*q*-value >0.05). In general, we can see that when the conjugation was conducted in the presence of MERO, the number of contacts seen (within or between strains and the plasmid of interest) decreases compared to the parental control strains. The results of the FitHi-C analysis demonstrate that the use of the Hi-C method coupled with short- and long-read sequencing allows us to detect intra-chromosomal contacts and inter-chromosomal contacts and determine whether these contacts are significant. The QC data demonstrated previously that the quality of our Hi-C libraries can be low, and so any conclusions we draw will need to be tentative until further experimentation can be done. However, this work gives a good indication that the Hi-C method (in this scenario, the kit) can be used to detect the movement of plasmids as demonstrated by the detection of significant contacts (*p*-value <0.05) in replicate 1 and 2 in the MERO condition that were not present in the control strains.

Table 45: FitHi-C significant contacts detected. A summary of table of the number of significant contacts (*p*-value <0.05) that we see after running FitHi-C on our parental strain mix (*Escherichia coli* EC1 and J53) and the transconjugants (*E. coli* J53) that were treated with meropenem (MERO). The *q*-value is also presented, where Benjamini-Hochberg correction is applied to the *p*-values generated (*n* = 3).

Sample	Replicate	Contacts Seen	Number of Significant Contacts (*p*-value)	Number of Significant Contacts (*q*-value)
Parental *E. coli* EC1 and J53	1	*E. coli* EC1-EC1 chromosome	16,067	9,751
		E. coli J53-J53 chromosome	391	73
		E. coli EC1-J53 chromosome	4	2
		E. coli EC1-plasmid	942	827
		E. coli J53-plasmid	0	0
		Plasmid-plasmid	1	0
	2	*E. coli* EC1-EC1 chromosome	20,798	17,678
		E. coli J53-J53 chromosome	425	206
		E. coli EC1-J53 chromosome	3	2
		E. coli EC1-plasmid	989	969
		E. coli J53-plasmid	0	0
		Plasmid-plasmid	1	1
	3	*E. coli* EC1-EC1 chromosome	19,559	15,024
		E. coli J53-J53 chromosome	861	232
		E. coli EC1-J53 chromosome	1	1

		E. coli EC1-plasmid	987	946
		E. coli J53-plasmid	0	0
		Plasmid-plasmid	2	1
Transconjugant treated with MERO	1	*E. coli* EC1-EC1 chromosome	1,573	9
		E. coli J53-J53 chromosome	749	3
		E. coli EC1-J53 chromosome	102	4
		E. coli EC1-plasmid	50	1
		E. coli J53-plasmid	20	0
		Plasmid-plasmid	1	0
	2	*E. coli* EC1-EC1 chromosome	1,203	5
		E. coli J53-J53 chromosome	294	3
		E. coli EC1-J53 chromosome	148	16
		E. coli EC1-plasmid	64	1
		E. coli J53-plasmid	4	0
		Plasmid-plasmid	0	0
	3	*E. coli* EC1-EC1 chromosome	6,190	850
		E. coli J53-J53 chromosome	1,212	33
		E. coli EC1-J53 chromosome	8	0
		E. coli EC1-plasmid	22	17
		E. coli J53-plasmid	0	0

| Plasmid-plasmid | 0 | 0 |

4.4.6.5. SNPs detected in the transconjugants

From the FreeBayes analysis conducted, there were SNPs seen in the majority of the transconjugants in genes responsible for the elongation factor Tu, DNA repair, acetate kinase, the 30S ribosomal protein S9, the BenE family transporter and phosphate acetyltransferase (a summary of the results is presented in Table 46). Any mutations that were present in the absence of selective pressure (*E. coli* J53 transconjugant in LB, control) were removed from the final analysis if they were present in the other transconjugants when exposed to selective pressure (Bm, MERO or MMC). We were interested in the SNP data generated from the transconjugant sequences as they were mapped back to the parental *E. coli* J53 sequences in order to determine whether the different drug treatments introduced any changes to the *E. coli* J53 strain that could account for its ability to grow on the selective plates after conjugation. From the SNP data, it appears that the change in the *E. coli* J53 transconjugants phenotype wasn't attributed to any spontaneous mutations.

Table 46: A summary of the single nucleotide polymorphisms (SNPs) detected in the *Escherichia coli* transconjugants that were created in different conditions where the cells were either exposed to: LB (control), sub-minimum inhibitory concentration (MIC) of bleomycin (Bm), sub-MIC meropenem (MERO) and sub-MIC mitomycin C (MMC). Each condition had three replicates plus three technical replicates conducted. Presented first (*E. coli* J53 transconjugant in LB) are the SNPs present in the control, followed by SNPs that were not present in the LB control that appeared under selection (Bm, MERO and MMC).

Sample	Condition	Replicate	SNP in Gene	Predicted Protein Product
E. coli J53 transconjugant	LB	1.1	*tuf*	Elongation factor Tu
		1.2	rRNA	Ribosomal RNA
		3.1	*radA*	DNA repair protein
			Repeat region	-
		3.2	*radA*	DNA repair protein
			ackA	Acetate kinase
		3.3	*radA*	DNA repair protein
			ackA	Acetate kinase
			tuf	Elongation factor Tu
	Bm	1.1	DBB46_19845	30S ribosomal protein S9
		1.2	*ydcO*	BenE family transporter
			DBB46_14930	Phosphate acetyltransferase
	MERO	2.2	DBB46_16720	DUF945 domain protein
		2.3	*rimM*	Ribosome maturation
	MMC	-	-	-

To confirm that the plasmid had transferred from the *E. coli* EC1 donor to the *E. coli* J53 recipient, the Hi-C library sequencing generated from the transconjugants using the ProxiMeta Hi-C kit were aligned to the reference plasmid using bowtie2 on Galaxy. The parent *E. coli* J53 recipient strain (prior to conjugation) Illumina reads were also aligned to the reference plasmid using bowtie2 on Galaxy. From these sequencing reads, we can see that the plasmid DNA is detected in the transconjugants in all of the experimental conditions and is not present in the *E. coli* J53 recipient strain. The results of this analysis is presented in Table 47 below. A pair of reads that aligns to the reference sequence (in this case, our plasmid of interest) within an expected range of distances and in the expected orientation it is defined as aligning 'concordantly', If the paired reads aren't in the expected orientation and/or aren't within an expected range of distance, it is defined as aligning 'discordantly'. If the plasmid is indeed in the recipient strain, we would expect to see reads from the Hi-C library that align concordantly to the plasmid. We would expect a low percentage of the reads to align to the reference plasmid (approximately 5% of reads from our data), as the majority of the Hi-C library will be chromosomal DNA (approximately 95% of our reads) and will not align to our reference plasmid. Some reads that align discordantly may be because they are Hi-C library generated lengths of sequence (so a hybrid of chromosomal DNA and plasmid DNA), but it can also be repetitive DNA.

Table 47: bowtie2 alignment of the transconjugant Hi-C libraries to the reference plasmid. The *E. coli* J53 parent strain (prior to conjugation) Illumina sequencing reads were also aligned to the reference plasmid as a control. The *E. coli* J53 transconjugants that were exposed to different experimental conditions (sub-minimum inhibitory concentration (sub-MIC) bleomycin (Bm), LB broth, sub-MIC meropenem (MERO), sub-MIC mitomycin C (MMC)). Presented is the number of reads generated, how many of the reads aligned concordantly to the plasmid (either once or more than once) and as a percentage of the number of reads, the number of reads aligned discordantly and as a percentage of the number of reads. In the final column the overall alignment rate to the reference plasmid is presented, calculated as the total percentage of reads that mapped to the reference plasmid sequence.

E. coli J53 transconjugant condition	Number of reads	Aligned concordantly 1 time to plasmid	% of reads	Aligned concordantly >1 times to plasmid	% of reads	Aligned discordantly 1 time to plasmid	% of reads	Overall alignment rate to plasmid
E. coli J53 parent (control) replicate 1	889,598	2	<0.01%	0	0.00%	0	0.00%	0.00%
E. coli J53 parent (control) replicate 2	733,233	0	0.00%	0	0.00%	0	0.00%	0.00%
E. coli J53 parent (control) replicate 3	997,154	0	0.00%	0	0.00%	0	0.00%	0.00%
Bm replicate 1	6,673,050	289,328	4.34%	37,778	0.57%	13,827	0.22%	5.31%
Bm replicate 2	12,910,015	683,245	5.29%	95,957	0.74%	22,226	0.18%	6.46%
Bm replicate 3	15,009,982	804,136	5.36%	113,089	0.75%	28,311	0.20%	6.56%
LB replicate 1	2,560,840	90,589	3.54%	12,397	0.48%	5,618	0.23%	4.43%
LB replicate 2	7,769,217	336,025	4.33%	45,452	0.59%	12,039	0.16%	5.28%
LB replicate 3	6,959,479	291,661	4.19%	39,158	0.56%	10,978	0.17%	5.10%
MERO replicate 1	5,785,428	239,864	4.15%	31,968	0.55%	7,173	0.13%	4.98%
MERO replicate 2	10,483,979	518,138	4.94%	71,973	0.69%	16,444	0.17%	6.03%
MERO replicate 3	6,312,683	207,300	3.28%	27,230	0.43%	8,324	0.14%	4.11%

MMC replicate 1	5,092,711	196,548	3.86%	27,015	0.53%	8,392	0.17%	4.99%
MMC replicate 2	6,786,202	222,446	3.28%	30,554	0.45%	8,006	0.12%	4.22%
MMC replicate 3	7,691,511	245,257	3.19%	33,000	0.43%	9,638	0.13%	4.13%

Overall, the results of the conjugation experiments have demonstrated that we have transferred the plasmid containing the bla_{NDM-4} gene to the recipient *E. coli* J53 strain through the use of MERO and sodium azide selective agar plates, as well as sequencing of the transconjugant Hi-C libraries generated using Illumina sequencing. We have also demonstrated that the transconjugation efficiency was higher when the conjugation experiments were conducted in the presence of sub-MIC MMC. We can see that the Hi-C method can be used in order to track the movement of MGEs (for instance, a plasmid) from one bacterial strain to another without relying on culturing techniques on selective media, although more work needs to be conducted to improve the quality of the data and the subsequent conclusions that we can draw from this.

4.5 Discussion

4.5.1. Optimising the Hi-C method

From the results of this study, it is clear that obtaining long fragments of DNA that are suitable for Hi-C sequencing is difficult. In this particular study, the concentrations of DNA in the final Hi-C libraries were not sufficient for MinION sequencing without the use of an amplification step. Ideally, amplification steps would be avoided so that in future studies, it is possible to look more in depth at the DNA methylation patterns which can give more information on the transcription of genes that may be involved in important processes like biofilm formation and DNA repair (Shin *et al.*, 2016). A study conducted by Niu *et al.* (2019) highlights that the PCR amplification step in the normal Hi-C method can introduce a more biased view of the chromatin interactions and the authors have developed a method called SAFE Hi-C that was tested on *Drosophila* cells to be a simplified Hi-C method without the amplification step. The actual method that Niu *et al.* (2019) based their SAFE Hi-C method on was the *in situ* Hi-C method developed by Rao *et al.* (2014) for the human genome. Their method takes at least 12 hours to get a Hi-C library ready for sequencing, as opposed to the Lieberman-Aiden *et al.* (2009) original Hi-C method that takes approximately 60 hours to create a Hi-C library for sequencing.

Many different variations of the Hi-C method exist, each with their own slight alterations that can make it difficult to determine what the best steps should be to consistently generate a good Hi-C library for sequencing. A paper by Cremazy *et al.* (2018) makes helpful suggestions and points to consider, such as introducing a wash step before formaldehyde fixation to avoid introducing compounds that may affect DNA crosslinking and being mindful of DNA methylation that may impact restriction digestion. An in-depth look at different variables and steps in the Hi-C method needs to be conducted in order to determine what changes benefit the method and

can streamline the method, and what changes are actually detrimental to the method. Furthermore, the intended use of the Hi-C method should also be taken into account (for instance, if the study is looking at chromosome conformation or the ability to track MGEs).

A step that was added to our version of the Hi-C method was the inclusion of a DNase step before the cells were lysed. This was introduced because we were able to detect DNA before the cells were lysed when we were trying to determine where DNA was being lost. Studies in the past have demonstrated that DNA can be detected outside of cells, and in the context of clinical samples where the detection of pathogens is important, it can be crucial that this DNA is removed. It would not be unusual in this case that there is extracellular DNA present in the overnight cultures we used for our Hi-C experiments. A study conducted by Burnham *et al*. (2020) demonstrated that cell-free DNA could be detected in blood and urine samples and could be utilised in screens for pathogens, and environmental contamination of a DNA sample could impact any interpretation of metagenomic sequencing results. Another study conducted by Woegerbauer *et al*. (2020) looked at the possible reservoir of antibiotic resistance genes in wastewater that can be found in cell free/extracellular DNA. The researchers brought attention to this potential resistance gene reservoir as they detected antibiotic resistance genes in purified effluent from wastewater treatment plants, and were concerned about HGT. This is an issue that needs to be addressed as antimicrobial agents can be detected in wastewater treatment samples, and the exposure of bacteria to sub-lethal concentrations of these agents, as well as the amount of extracellular DNA released into the environment, can stimulate HGT. This highlights why a DNase treatment is important at the beginning of the Hi-C method, as it removes any background signal of resistance genes that are not interesting in terms of the direct transfer of resistance genes between organisms (tracking the movement of MGEs). While looking at resistance genes and the spread of those resistance genes in a more holistic way in terms of what is present in the environment is also important, this is not the focus of this project.

4.5.1.1. Sample preparation

From the experiments where we tried to determine where DNA was being lost in the Hi-C method, it became apparent that the original Hi-C method requires a high starting quantity of DNA to be used, as during processing DNA is continually lost. For the application of our work where we see the Hi-C method being used in metagenomic studies, having a high quantity of DNA to begin with can be difficult. A study conducted by Díaz *et al*. (2018) tried to overcome this issue by developing a version of the Hi-C method (called Low-C) that only requires a low quantity of starting material. The Low-C method differs from the Hi-C method by using a different method

of lysing the cells, altering the restriction digestion incubation period, and generally using smaller reagent volumes.

A factor that could have influenced the DNA yield after extraction was the effect of freezing on the *E. coli* and *A. baumannii* samples before they were prepared for Hi-C and DNA extraction. In this study freeze-thaw cycles were avoided, and all of the samples were treated in the same way before and after freezing and therefore any effects of freeze-thawing should be minimal and broadly consistent across all of the samples. However, in a study conducted by Zheng *et al*. (2020), they highlighted that in Hi-C experiments the ideal sample input would be fresh in order to maintain the natural chromatin conformation as the effects of freezing are not clear. This presents issues in the future in terms of the practicality of maintaining fresh samples when they are taken from different environments and especially if they are patient samples collected to characterise dynamics of a microbiome.

A difficulty with this project was determining where problems were occurring when we tried to combine the Hi-C method with a commercial DNA extraction kit. As the DNA extraction methods that were tested were commercial kits, it is unlikely that the issues with DNA yield and quality are due solely to the extraction kits because these are usually robust and reliable for DNA extraction. It is more likely that the issues with DNA yield arise when the Hi-C kit preparation method is coupled with the extraction kits. In order to confirm that this is the case, the *E. coli* and *A. baumannii* samples should have their DNA extracted using the different extraction kits without the Hi-C initial steps to demonstrate that the issues with DNA extraction aren't due to the kits and the organisms that we are using.

4.5.1.2.   Crosslinking

To eliminate the possibility that crosslinking the DNA in the bacteria is causing problems with the extraction process and the final DNA yield for the Hi-C library, it would be useful to find a method or develop a way to detect and/or quantify the presence of crosslinks and ensure that they are reversed before the DNA from the cells is extracted. Alternatively, the reverse crosslinking step could be left overnight to incubate, which is what has been done traditionally and would extend the length of the whole Hi-C method. A study conducted by Kennedy-Darling and Smith (2014) investigated the reversal rate of protein-DNA crosslinks that were formed under the influence of formaldehyde treatment. Using a yeast lysate, they found that at 47˚C (the highest temperature they tested), the half-life of the crosslinks were on average 11.3 hours, which for the traditional Hi-C method is not suitable due to the extended incubation times needed for certain steps. This may also indicate a problem in the methods we used, as to inactivate enzymes used at different steps, high temperatures are used often, and the rate of

crosslink reversal increases with increasing temperature (Kennedy-Darling and Smith, 2014). For the enzymes used in our experiments (for instance, TURBO DNase) the most common methods used to deactivate the enzyme is incubating the samples at high temperatures, but usually phenol-chloroform extraction is suggested as an alternative. However, in the interest of time for our experiments, we did not attempt to inactivate the enzymes by phenol-chloroform as it would be very time consuming due to the number of enzymes used, which made the Phase Genomics Hi-C kit more appealing to use.

4.5.1.3.   DNA extraction

From the experiments conducted in this study, it is difficult to determine where DNA is being lost in the Hi-C method we developed. It is possible that combining the Hi-C method with other extraction protocols impacts on the chemistry of the buffers and reagents in the kits/protocols which is impeding extraction of good quality DNA in sufficient concentrations. This is possible, as DNA extracted using commercially bought kits produced sufficient quantities and quality of DNA for sequencing (typically short-read sequencing platforms like Illumina), but once the Hi-C method was introduced, the kit protocols didn't perform as well. Although there may be compatibility issues between the commercially bought kits and the Hi-C method, it is difficult to determine the problems seen with the DNA extractions that were conducted using a normal phenol-chloroform extraction method. Other studies looking at bacterial chromosome conformation capture that used phenol-chloroform to purify the DNA had no issues with DNA concentrations for sequencing (Beitel *et al.*, 2014; Burton *et al.*, 2014; Marbouty *et al.*, 2014; Trussart *et al.*, 2017). It is possible that the differences between concentrations of DNA is due to the method used for lysis of the cells. In the paper by Marbouty *et al.* (2014) where a meta3C library was being created, *Bacillus subtilis*, *E. coli* and *Vibrio cholerae* were the organisms of interest and Ready-Lyse lysozyme and SDS was used to lyse the cells. In the paper by Beitel *et al.* (2014), fresh lysozyme was used to lyse a mixed population of bacteria and then SDS was also added to the lysed cells. In the paper by Burton *et al.* (2014), the mixture of bacterial cells and yeast were lysed using 0.5 mm diameter glass beads. Although this study primarily worked on *E. coli* and *A. baumannii* cells, it is possible that the initial cell lysis method is not appropriate to release all of the DNA from the cells to then purify later on in the Hi-C method. In the future, small experiments could be conducted to determine whether the use of detergents such as SDS and Triton X-100 would benefit the overall extraction of DNA for Hi-C long-read sequencing. A paper by Jacobs *et al.* (2013) demonstrated the use of adenylate kinase release to report bacterial lysis in the context of discovering new antibacterial agents. In a similar way, the adenylate kinase assay could be utilised in these Hi-C optimisation methods to indicate whether the bacterial cells are lysing sufficiently to release DNA for purification and sequencing.

In a study conducted by Trigodet *et al.* (2021), where they tested different commercial kits, phenol-chloroform extraction and an agarose plug for DNA extraction for long-read sequencing, they highlighted that steps that involved vortexing or mixing by pipetting should be avoided. They suggested that the tubes should be inverted to mix the sample and to avoid velocity gradients and to reduce DNA breakage. They also suggested that freeze-thaw cycles should be avoided, and before sequence analysis the DNA should be stored at 4˚C instead of in a -20˚C freezer. What was also mentioned in the Trigodet *et al.* (2021) study that should be tested in our own study is whether steps that involve AMPure beads should have an extended incubation before eluting the DNA to allow the long fragments of DNA to release from the beads. This could potentially be where we appear to be losing DNA, as we aren't detecting high concentrations in our supernatants that could account for the extent of DNA loss we see.

The results of our phenol-chloroform extraction experiment were surprising as it appeared as if we had barely any DNA to work with for the Hi-C library. This is concerning as many (if not all) of the existing Hi-C methods, or variations of this method, use phenol-chloroform extraction and ethanol purification at some point in the method regardless of if the study uses bacterial or mammalian cells (Beitel *et al.*, 2014; Belaghzal *et al.*, 2017; Belton *et al.*, 2012; Belton and Dekker, 2015; Burton *et al.*, 2014; Cremazy *et al.*, 2018; Gabdank *et al.*, 2016; Harewood *et al.*, 2017; Jäger *et al.*, 2015; Le *et al.*, 2013; Lieberman-Aiden *et al.*, 2009; Lin *et al.*, 2018; Lu *et al.*, 2016; Marbouty *et al.*, 2014; Nagano *et al.*, 2015; Naumova *et al.*, 2012; Rao *et al.*, 2014; Trussart *et al.*, 2017; van Berkum *et al.*, 2010). The only obvious difference between the method we used, and the Lieberman-Aiden *et al.* (2009) method is the fact that we didn't complete the full method to get the Hi-C library (we didn't attempt restriction digestion, biotinylation or biotin pull-down) and our crosslinks in our DNA were reversed after phenol-chloroform extraction. In the future, it may be worth seeing our whole method to completion, although with the steps that we did take, it was not promising to see such little DNA at that point, and it is not clear what we did differently to the existing papers that have successfully used the Hi-C method.

4.5.1.4. Amplification and purification

In existing Hi-C methods and derivatives of the Hi-C method, it is very unusual to find a method that doesn't contain an amplification step using PCR (Beitel *et al.*, 2014; Belaghzal *et al.*, 2017; Belton *et al.*, 2012; Belton and Dekker, 2015; Gabdank *et al.*, 2016; Jäger *et al.*, 2015; Lieberman-Aiden *et al.*, 2009; Lu *et al.*, 2018; Nagano *et al.*, 2013; Press *et al.*, 2017; Trussart *et al.*, 2017). It is possible that in the method that we tried to develop in this project where we avoid the additional amplification steps to conserve the methylation pattern of the DNA needs more optimisation than we initially thought. It is possible that the Hi-C method in itself is not an

efficient method. Its ability to extract DNA at high concentrations is severely limited, potentially due to the way the DNA is treated and fixed, and the compatibility of the chemicals and buffers used in the method that interfere with DNA extraction. During the course of these experiments, a few papers were published that used a variation of the Hi-C method without an amplification step. We wondered whether these studies were able to remove the amplification step as they had a higher initial input of cells/DNA. In a study conducted by Niu *et al*. (2019) where they used the *Drosophila melanogaster* S2 cell line, around 30 million cells were crosslinked and used as the input for the Hi-C library. Another study in eukaryotic cells by Ulahannan *et al*. (2019) used human B lymphocytes and HG002 cells, with around 10 million cells crosslinked as the input for the Hi-C library. What was also interesting was the study conducted by Yaffe and Relman (2020) where the researchers used human stool samples as their input material for Hi-C. Typically, extracting DNA from human stool samples is difficult due to the variation of microbes present and the low volume of DNA detected in them. However, by using between 50-100 mg of stool sample, the researchers were able to produce 1.4 billion Hi-C read pairs for one of their participant samples. In our experiments, we used approximately an input of 1×10^9 bacterial cells which should have been sufficient. It is worth following our method using the Fire Monkey kit with a few changes and then running a PCR on the sample and sequencing it to determine whether the Hi-C portion of the method is working as it should be before trying to optimise the extraction method.

Throughout the Hi-C library preparation process, this study has demonstrated that DNA is being constantly lost, especially between steps that involve centrifugation and the disposal of a supernatant. To overcome this problem, SPRI beads were used to immobilise the DNA in solution before the supernatant was disposed of. However, the end results of this study demonstrated that DNA was still being lost and was not at sufficient concentrations for long-read sequencing. It is not clear here what these issues may be, as the DNA should no longer be crosslinked which may have posed a problem with purification. The state of the DNA (if the DNA is crosslinked or not) could be tested at different stages of the Hi-C method by conducting a DNA crosslinking assay, similar to the assay conducted in Burby and Simmons (2018), although a method to quantify the number of crosslinks in a sample would be more useful. The different forms of DNA could then be purified with SPRI to see whether the presence of crosslinks impacted the immobilisation capacity of the SPRI beads. However, the presence of crosslinks should not be a problem for SPRI bead binding, as they have been used in the past for DNA, RNA, intact nuclei and chromatin complexes (Ma *et al*., 2018). The cell wall thickness of a bacterium can affect the ability of formaldehyde to crosslink the DNA and further down the Hi-C method, high concentrations of formalin can impact DNA recovery, although this may not be the source of the issues seen in this study (Liu and Darling, 2015).

When the kits were evaluated in terms of the DNA yield in the test condition that is the most representative of the Hi-C method as a whole, it was difficult to determine which kit or method performed the best. In order to determine which kit or method performed the best overall, it would be useful to include more replicates for each method to increase the accuracy of the results. It appears that the worst performing method was the bead beating method. This could be because *E. coli* isn't an especially difficult organism to extract DNA from, unlike bacteria like some strains of *S. aureus* and *A. baumannii*. Extracting DNA from Gram-positive and Gram-negative bacteria can be different and especially more difficult in Gram-positive bacteria due to thick cell walls that they possess (Li *et al.*, 2020). The bead beating method itself may be detrimental as the beads can shear any DNA that is released into the solution. If we put this into context of the type of samples we'd be interested in future work (for example in environmental soil samples), organisms that are more easily lysed will have shorter DNA that is sheared and this will introduce bias against them in downstream analyses (Maghini *et al.*, 2021). In the context of this study where we looked at DNA from a pure culture of *E. coli*, the results suggest that a bead beating method shouldn't be used as it is too abrasive and negatively impacts the size of the DNA for long-read sequencing. However, a study conducted by Ketchum *et al*. (2018) that was looking at the microbiome in the marine invertebrate *Echinometra mathaei* demonstrated that the use of a bead beating method and the addition of a lysozyme step was able to provide a better estimate of the bacterial diversity of the sample as organisms that are more difficult to extract DNA from were detected and represented. The study by Ketchum *et al*. (2018) also highlighted the importance of establishing standard protocols in order to accurately capture a representative bacterial community. It is also possible that crosslinked DNA is more susceptible to damage and fragmenting as crosslinked may be more rigid and inflexible (Gavrilov *et al*., 2015). A paper written by Gavrilov *et al*. (2015) highlights that a lot of methods that utilise formaldehyde crosslinking are not well understood, especially in *in vivo* experiments and factors such as temperature and pH can affect the crosslinking reaction and can even reverse the crosslinks that are formed.

4.5.1.5. Polymyxin B nonapeptide

In an effort to streamline the Hi-C method and reduce the time taken to prepare a Hi-C library, we attempted to conduct the restriction digestion step inside the cells before they were lysed. From this study, PMBN was used and it didn't seem to be effective in allowing the REs to pass through the cell membrane and digest the DNA. A paper published by Diebold *et al*. (2021), has the potential to streamline the Hi-C method by utilising their One-step Isolation and Lysis PCR

(OIL-PCR) method. The OIL-PCR method uses amplification of the target genes to attach a universal 16S primer sequence and the target amplicon within an oil emulsion. The oil component of the method provides an environment where one cell is encapsulated in one droplet and can allow the addition of other reagents e.g. PCR master mix and lysozyme.

A study conducted by Vaara and Viljanen (1985) found that administering PMBN was able to sensitise bacteria such as *S. typhimurium*, *E. coli*, *P. aeruginosa* and *Haemophilus influenzae* to the action of hydrophobic antibiotics (for example, clindamycin). Another study by Ofek *et al*. (1994) also demonstrated the ability of PMBN to sensitise Gram-negative bacteria to hydrophobic antibiotics (the antibiotic they tested was novobiocin) and attribute this to PMBN's ability to disorganise the bacterial outer membrane. A study by Duwe *et al*. (1986) also showed the ability of PMBN to sensitise Gram-negative bacteria (and to a lesser degree in Gram-positive bacteria) to hydrophobic antibiotics but also serum complement proteins. From the conditions we tested, it was not possible to digest the DNA within the cells, and further testing under different conditions may improve the ability of PMBN to permeabilise the cell to allow the REs access to the DNA. It may also be that using PMBN to permeabilise the cell membrane is not a viable option to get REs into the bacterial cell to digest DNA. There are other substances that can be used instead of PMBN to permeabilise the cell membrane to allow the entry of REs that have been reported in the literature that could be tested. For instance bacterial defensins (such as NaD1), Crecopin A, Magainin 2, Melittin, Nisin and Tris (Agrawal *et al*., 2019; Imura *et al*., 2008; Irvin *et al*., 1981; Poon *et al*., 2014; Rangarajan *et al*., 2013; Singh *et al*., 2014).

Optimising the Hi-C method and combining the consequent Hi-C library with long-read sequencing can be beneficial for a wide range of research areas, from environmental studies looking at wastewater treatment plants, to human health and looking at the interactions of pathogens or the normal microbiota with the host. The benefits that long-read sequencing can provide include combining the reads with short-read sequencing for hybrid assemblies that can provide more accurate genomes and discern between different bacterial species (Bertrand *et al*., 2019). What makes combining Hi-C with long-read sequencing difficult is that existing protocols for Hi-C that have been shown to work were only suitable for short-read sequencing platforms, and the way that the DNA is treated in the Hi-C method can make it easy to generate small DNA fragments. The next steps for this Hi-C optimisation project would be to attempt Hi-C method derivatives that are optimised for low-input samples and aim to reduce the time taken to generate a Hi-C method and take into consideration other steps to help preserve crosslinks and improve the resolution of chromosome contacts. A method that might be good to test on bacterial cells is the method developed by Lafontaine *et al*. (2021) called Hi-C 3.0 that uses

disuccinimidyl glutarate (DSG) as well as formaldehyde during the fixation of the cells and provides explanations for certain steps in the Hi-C method that might help the generation of a good Hi-C library. Another paper that came out towards the end of this project was the paper by Ulahannan *et al.* (2019) that uses a method they called Pore-C to directly sequence a Hi-C library without the need for amplification and has the added benefit of using ONT long-read sequencing. It would be interesting to see how our pure bacterial lab cultures perform using this method as the Ulahannan *et al*. (2019) study uses human B lymphocytes and breast cancer cells.

As the project needed to advance given the time restraints we had, we decided to use the Phase Genomics ProxiMeta kit, as it is a commercially bought kit that has been shown in various papers to produce good Hi-C libraries where chromosomal contacts have been detected (Beyi *et al*., 2021; Beyi *et al*., 2021; Bickhart *et al*., 2022; Press *et al*., 2017; Stalder *et al*., 2019).

4.5.2. Conjugation experiments

4.5.2.1.   Conjugation and Hi-C

It is not unusual that as a DNA damaging agent, MMC has the potential to stimulate higher rates of HGT via conjugation, as we have seen in our study. A study conducted by Beaber *et al*. (2004) demonstrated that SXT (an integrating conjugative element) transferred more frequently after exposure to MMC. The Beaber *et al*. (2004) paper reasoned that the increased transfer frequency of SXT was due to the ability of MMC to induce the SOS response in *E. coli*. It would not be unreasonable to suggest that Bm has the ability to encourage HGT between different bacterial strains, as Bm can produce superoxide radicals that can damage DNA and may enhance conjugation (Wang *et al*., 2021).

Many studies have indicated that antibiotics can stimulate HGT. In a study conducted by Xia *et al*. (2008) they found that using a sub-MIC concentration of the antibiotics GENT and CHL together, increased the transfer of the pCVD442 plasmid from *E. coli* DH5α to *Sorangium cellulosum.* The researchers hypothesised that the presence of antibiotics interfered with the cells and potentially their metabolic pathways which made them more amenable to DNA transfer (Xia *et al*., 2008). A similar study conducted by Zhang *et al*. (2013) found that the use of kanamycin and streptomycin at sub-MIC promoted the conjugation of the plasmids pRK2013, pSU2007 and RP4 between two strains of *E. coli*. The authors of the paper suggested that the two antibiotics used were able to induce the SOS response in the donor *E. coli* strain and encouraged transfer of the plasmids (Zhang *et al*., 2013). A paper by Lopatkin *et al*. (2016) found

that antibiotics may not always encourage HGT via conjugation, and instead may depend on the selective pressure of the antibiotics which may also discourage HGT, depending on the concentration of antibiotic used. This work brings into focus the importance of understanding the antibiotics we use to treat secondary bacterial infections in cancer patients, as antibiotics can stimulate the movement of MGEs that may contain resistance determinant genes and stimulate the evolution towards more MDR infections in patients that are already immunocompromised.

Tracking the movement of plasmids using the Hi-C ProxiMeta kit appears to be promising in the conditions and samples we tested, as we were able to detect chromosomal contacts within each strain, contacts between the donor *E. coli* EC1 strain and the plasmid of interest, as well as contacts between the recipient *E. coli* J53 strain with the plasmid of interest. However, when the number of contacts seen between the *E. coli* J53 strain with the plasmid was adjusted using Benjamini-Hochberg correction on the *p*-value to generate a *q*-value, we saw no significant contacts. It is likely that our libraries were poor quality which impacted the significance of these results, but it was clear that between the parental strains (controls) and the MERO treated samples, there were fewer contacts seen in general after MERO treatment. It could be that the REs we used cut the plasmid too frequently, and so it wasn't being detected in the downstream analysis as a significant contact. The size of the plasmid was also not known, and it could also be that the plasmid was present at a low copy number in the cell. To investigate this further, the plasmid should be sequenced and assembled fully to determine its size and how frequently the plasmid may theoretically be cut. It is unexpected that we were unable to detect plasmid from pure cultures of the transconjugants, as many studies that have used this Hi-C kit have been able to detect bacteria and their associated plasmids from samples that are considered more difficult to work with, such as faecal samples and wastewater samples. These samples are more difficult to work with due to the presence of multiple bacterial species and a low concentration of bacteria (Beyi *et al*., 2021a; Beyi *et al*., 2021b; Press *et al*., 2017; Stalder *et al*., 2019).

5. <u>**Overall conclusions**</u>

The anti-cancer drug bleomycin has antibacterial effects and is commonly used in combination with other anti-cancer drugs. The main purpose of this project was to determine whether the use of bleomycin can stimulate evolution of antibiotic resistance. We hypothesised that when bacteria were exposed to bleomycin, we would see mutations that confer a resistance phenotype to bleomycin and cross-resistance to other antibiotics. When we looked in more depth at *Enterobacteriaceae*, we saw that there was a bleomycin resistance gene that is 3 bp downstream of a bla_{NDM} variant that encodes a metallo-β-lactamase which provides resistance to β-lactam antibiotics. The bleomycin resistance gene is prevalent in existing genome databases and we hypothesised that this may be due to a fitness advantage conferred to the organisms. One way through which antibiotic resistance can develop, is through the exchange of DNA between bacteria using mobile genetic elements when they are exposed to an antimicrobial (horizontal gene transfer). We hypothesised that the exposure of bacteria to bleomycin would stimulate the movement of antibiotic resistant genes that are present on mobile genetic elements. This would indicate the need for more care when treating cancer patients that may also experience a secondary bacterial infection that would need to be treated with antibiotics.

When we investigated the SNPs that appeared in *Escherichia coli* after bleomycin exposure, we found that bleomycin selected for mutations in a range of genes involved in different pathways that can provide general protection to antibiotics and external stressors. This suggested that bleomycin exposure may induce cross-resistance to other antibiotics. However, when we looked at the antibiotic susceptibility profiles of our mutant *E. coli* strains, we did not see clinically significant levels of antibiotic resistance and this may be due to the non-specific mechanism of action of bleomycin, so the mutations that we see may increase cell survival through various methods that may not be specific to the bleomycin drug. In this study we also used a sub-inhibitory concentration of bleomycin that may select for mutations of smaller effect. Nevertheless, this thesis showed that the exposure to bleomycin enabled bacterial strains to adapt and resist the effects of different antibiotics. This is an important result as the accumulation of further adaptations could lead to antibiotic susceptibility profiles that are clinically significant and would need to be addressed.

From our work looking at the carriage of the ble_{MBL} gene and bla_{NDM-1} gene, that encode the bleomycin resistance protein and a metallo-β-lactamase, respectively, we have seen that the

presence of the ble_{MBL} can confer a fitness advantage alongside the bla_{NDM-1} gene in normal LB media. However, more investigation is needed that looks into how carriage of the ble_{MBL} affects cells, whether it be by changing gene expression or by temporal differences due to transcript lengths in our study. The *E. coli* strains we used in this study attempt to reflect what would see in 'real' environments that are continually changing. The advantage that the ble_{MBL} gives to the bacteria may explain its prevalence in genome databases that mainly focus on the genomes of bacteria isolated from clinical labs. The advantage that the bleomycin resistance gene affords may also explain why we see in the literature different bleomycin resistance genes associated with other mobile genetic elements in other bacterial species, such as the Tn*5* transposon and pUB110 plasmid that were not explored in this study. When we delved further to determine how ble_{MBL} confers a fitness benefit to the host, we investigated the mutation frequency of our strains as a previous study by Dortet *et al*. (2012) demonstrated that the bleomycin resistance gene appeared to stabilise the genome and reduce the frequency of mutations. In our study, we did not find a change in the mutation frequency but more studies need to be conducted to determine the fitness benefit that the bleomycin resistance gene provides for bacteria that carry it.

Many papers in the literature have indicated the ability of some antimicrobials to activate the movement of mobile genetic elements. In this study we have seen this through a higher conjugation efficiency when cells were exposed to mitomycin C. We also hypothesise that exposure to bleomycin promotes the mobilisation of mobile genetic elements (e.g. a plasmid) but were unable to demonstrate this effectively through the use of the Hi-C method due to the generation of poor-quality libraries. What we were able to see was the movement of the plasmid in phenotypic data through the use of meropenem and sodium azide selective plates, and also the detection of plasmid DNA in the recipient *E. coli* strain when we conducted Illumina sequencing on the transconjugants that was aligned to our plasmid of interest. We hypothesise that bleomycin will encourage the movement of mobile genetic elements through generic mechanisms that are activated when the bacterial cells are under stress. Although it was not studied in this project, it would be interesting to see whether the presence of the bleomycin resistance gene impacts on this phenomenon where exposure to an antimicrobial stimulates mobile genetic element movement.

Overall, the findings in this project add to the growing picture that drugs other than antibiotics can select for bacteria that are less susceptible to antibiotic treatment, and this may be contributing to the spread of antibiotic resistance genes. This is of particular concern as these

drugs are typically given to patients that are already immunocompromised and are more susceptible to infections. Further investigations into the action of other drugs that can stimulate antibiotic resistance must be done to assess the impact this can have on clinical outcomes. To tackle this issue, a move toward drugs that have more specific, targeted mechanisms of action should be used. This is because we have demonstrated that bleomycin (an anti-cancer drug) acts in a non-specific way that damages DNA and encourages mutations that alter the ability of the bacteria to resist the effect of different antibiotics. The use of both anti-cancer drugs and antibiotics in combination should also be investigated in order to treat cancer patients that are affected by secondary bacterial infections. Ultimately, research should work towards minimising the potential impacts on the growing antibiotic resistance problem without exacerbating the problems and symptoms that the patient experiences.

References

Abdollahi, A., Hakimi, F., Doomanlou, M., Azadegan, A., 2016. Microbial and Antibiotic Susceptibility Profile among Clinical Samples of Patients with Acute Leukemia. Int. J. Hematol. Stem Cell Res. 10, 61–69.

Acharya, K.P., Pathak, S., 2019. Applied Research in Low-Income Countries: Why and How? Front. Res. Metrics Anal. 0, 3. https://doi.org/10.3389/FRMA.2019.00003

Adam, E., Volkert, M.R., Blot, M., 1998. Cytochrome c biogenesis is involved in the transposon Tn5-mediated bleomycin resistance and the associated fitness effect in Escherichia coli. Mol Microbiol 28, 15–24.

Adewale, B.A., 2020. Will long-read sequencing technologies replace short-read sequencing technologies in the next 10 years? Afr. J. Lab. Med. 9.

Aggarwal, D., Myers, R., Hamilton, W.L., Bharucha, T., Tumelty, N.M., Brown, C.S., Meader, E.J., Connor, T., Smith, D.L., Bradley, D.T., Robson, S., Bashton, M., Shallcross, L., Zambon, M., Goodfellow, I., Chand, M., O'Grady, J., Török, M.E., Peacock, S.J., Page, A.J., 2022. The role of viral genomics in understanding COVID-19 outbreaks in long-term care facilities. The Lancet Microbe 3, e151–e158. https://doi.org/10.1016/S2666-5247(21)00208-1/ATTACHMENT/C7581951-D524-4C44-8D28-74A1FFEA4276/MMC1.PDF

Agrawal, A., Rangarajan, N., Weisshaar, J.C., 2019. Resistance of early stationary phase E. coli to membrane permeabilization by the antimicrobial peptide Cecropin A. Biochim. Biophys. acta. Biomembr. 1861. https://doi.org/10.1016/J.BBAMEM.2019.05.012

Ahmad, N., Khalid, S., SM, A., AU, K., 2018. Occurrence of blaNDM Variants Among Enterobacteriaceae From a Neonatal Intensive Care Unit in a Northern India Hospital. Front Microbiol 9. https://doi.org/10.3389/fmicb.2018.00407

Amanatidou, E., Matthews, A.C., Kuhlicke, U., Neu, T.R., McEvoy, J.P., Raymond, B., 2019. Biofilms facilitate cheating and social exploitation of β-lactam resistance in Escherichia coli. NPJ biofilms microbiomes 5, 1–10. https://doi.org/doi:10.1038/s41522-019-0109-2

Amarasinghe, S.L., Su, S., Dong, X., Zappia, L., Ritchie, M.E., Gouil, Q., 2020. Opportunities and challenges in long-read sequencing data analysis. Genome Biol. 21, 1–16. https://doi.org/doi:10.1186/s13059-020-1935-5

Ashcroft, M.M., Forde, B.M., Phan, M.-D., Peters, K.M., Henderson, A., Hancock, S.J., Roberts, L.W., White, R.T., Chan, K.-G., Chong, T.M., Yin, W.-F., Paterson, D.L., Walsh, T.R., Schembri, M.A., Beatson, S.A., 2020. Genomic characterisation and context of the blaNDM-

1 carbapenemase in Escherichia coli ST101. https://doi.org/10.1101/860726

Ashour, H.M., el-Sharif, A., 2007. Microbial spectrum and antibiotic susceptibility profile of gram-positive aerobic bacteria isolated from cancer patients. J. Clin. Oncol. 25, 5763–5769. https://doi.org/10.1200/jco.2007.14.0947

Ashton, D., Hilton, M., Thomas, K. V, 2004. Investigating the environmental transport of human pharmaceuticals to streams in the United Kingdom - ScienceDirect. Sci. Total Environ. 333, 167–184. https://doi.org/10.1016/j.scitotenv.2004.04.062

Ashton, P.M., Nair, S., Dallman, T., Rubino, S., Rabsch, W., Mwaigwisya, S., Wain, J., O'Grady, J., 2015. MinION nanopore sequencing identifies the position and structure of a bacterial antibiotic resistance island. Nat. Biotechnol. https://doi.org/10.1038/nbt.3103

Auda, I.G., 2007. Cyclophosphamide and Doxorubicin but Not Methotrexate Responsible For Rapid Development of the Resistance to Ciprofloxacin in Uropathogenic Escherichia Coli in Vitro (PDF Download Available). https://doi.org/http://dx.doi.org/

Ay, F., Bailey, T.L., Noble, W.S., 2014. Statistical confidence estimation for Hi-C data reveals regulatory chromatin contacts. Genome Res. 24, 999–1011. https://doi.org/10.1101/GR.160374.113

Baharoglu, Z., Mazel, D., 2011. Vibrio cholerae triggers SOS and mutagenesis in response to a wide range of antibiotics: a route towards multiresistance. Antimicrob Agents Chemother 55, 2438–2441. https://doi.org/10.1128/aac.01549-10

Baquero, F., Levin, B.R., 2020. Proximate and ultimate causes of the bactericidal action of antibiotics | Nature Reviews Microbiology.

Bart, A., van Passel, M.W.J., van Amsterdam, K., van der Ende, A., 2005. Direct detection of methylation in genomic DNA. Nucleic Acids Res 33, e124.

Basu, S., 2020. Variants of the New Delhi metallo-β-lactamase: new kids on the block. https://doi.org/10.2217/fmb-2020-0035. https://doi.org/10.2217/fmb-2020-0035

Beaber W., J., Hochhut, B., Waldor K., M., 2004. SOS response promotes horizontal dissemination of antibiotic resistance genes | Nature. Nature 427.

Beitel, C.W., Froenicke, L., Lang, J.M., Korf, I.F., Michelmore, R.W., Eisen, J.A., Darling, A.E., 2014. Strain- and plasmid-level deconvolution of a synthetic metagenome by sequencing proximity ligation products. PeerJ 2014, 1–19. https://doi.org/10.7717/peerj.415

Belaghzal, H., Dekker, J., Gibcus, J.H., 2017. Hi-C 2.0: An optimized Hi-C procedure for high-resolution genome-wide mapping of chromosome conformation. Methods 123, 56–65.

https://doi.org/10.1016/j.ymeth.2017.04.004

Beloin, C., Michaelis, K., Lindner, K., Landini, P., Hacker, J., Ghigo, J.M., Dobrindt, U., 2006. The transcriptional antiterminator RfaH represses biofilm formation in Escherichia coli. J. Bacteriol. 188, 1316–1331. https://doi.org/10.1128/JB.188.4.1316-1331.2006

Belov, O. V, Krasavin, E.A., Parkhomenko, A.Y., 2009. Model of SOS-induced mutagenesis in bacteria Escherichia coli under ultraviolet irradiation. J. Theor. Biol. 261, 388–395. https://doi.org/10.1016/j.jtbi.2009.08.016

Belton, J.M., Dekker, J., 2015. Hi-C in budding yeast. Cold Spring Harb. Protoc. 2015, 649–662. https://doi.org/10.1101/pdb.prot085209

Belton, J.M., McCord, R.P., Gibcus, J.H., Naumova, N., Zhan, Y., Dekker, J., 2012. Hi-C: A comprehensive technique to capture the conformation of genomes. Methods 58, 268–276. https://doi.org/10.1016/j.ymeth.2012.05.001

Bertrand, D., Shaw, J., Kalathiyappan, M., Ng, A.H.Q., Kumar, M.S., Li, C., Dvornicic, M., Soldo, J.P., Koh, J.Y., Tong, C., Ng, O.T., Barkham, T., Young, B., Marimuthu, K., Chng, K.R., Sikic, M., Nagarajan, N., 2019. Hybrid metagenomic assembly enables high-resolution analysis of resistance determinants and mobile elements in human microbiomes. Nat. Biotechnol. 37, 937–944. https://doi.org/doi:10.1038/s41587-019-0191-2

Besse, J.P., Latour, J.F., Garric, J., 2012. Anticancer drugs in surface waters: what can we say about the occurrence and environmental significance of cytotoxic, cytostatic and endocrine therapy drugs? Env. Int 39, 73–86. https://doi.org/10.1016/j.envint.2011.10.002

Beyi, Ashenafi Feyisa, Brito-Goulart, D., Hawbecker, T., Slagel, C., Ruddell, B., Hassall, A., Dewell, R., Dewell, G., Sahin, O., Zhang, Q., Plummer, P.J., 2021. Danofloxacin Treatment Alters the Diversity and Resistome Profile of Gut Microbiota in Calves. Microorganisms 9. https://doi.org/10.3390/MICROORGANISMS9102023

Beyi, Ashenafi F., Hassall, A., Phillips, G.J., Plummer, P.J., 2021. Tracking Reservoirs of Antimicrobial Resistance Genes in a Complex Microbial Community Using Metagenomic Hi-C: The Case of Bovine Digital Dermatitis. Antibiot. 2021, Vol. 10, Page 221 10, 221. https://doi.org/10.3390/ANTIBIOTICS10020221

Bi, R., Kong, Z., Qian, H., Jiang, F., Kang, H., Gu, B., Ma, P., 2018. High Prevalence of blaNDM Variants Among Carbapenem-Resistant Escherichia coli in Northern Jiangsu Province, China. Front. Microbiol. 9. https://doi.org/10.3389/fmicb.2018.02704

Bickhart, D.M., Kolmogorov, M., Tseng, E., Portik, D.M., Korobeynikov, A., Tolstoganov, I., Uritskiy, G., Liachko, I., Sullivan, S.T., Shin, S.B., Zorea, A., Andreu, V.P., Panke-Buisse, K.,

Medema, M.H., Mizrahi, I., Pevzner, P.A., Smith, T.P.L., 2022. Generating lineage-resolved, complete metagenome-assembled genomes from complex microbial communities. Nat. Biotechnol. 2022 1–9. https://doi.org/10.1038/s41587-021-01130-z

Biel, S.W., Hartl, D.L., 1983. Evolution of transposons: natural selection for Tn5 in Escherichia coli K12. Genetics 103, 581–592.

Björkholm, B., Sjölund, M., Falk, P.G., Berg, O.G., Engstrand, L., Andersson, D.I., 2001. Mutation frequency and biological cost of antibiotic resistance in Helicobacter pylori. Proc Natl Acad Sci U S A 98, 14607–14612. https://doi.org/10.1073/pnas.241517298

Blaha, G.M., Wade, J.T., 2022. Transcription-Translation Coupling in Bacteria. https://doi.org/10.1146/annurev-genet-072220-033342 56, 187–205. https://doi.org/10.1146/ANNUREV-GENET-072220-033342

Blair, J.M., Bavro, V.N., Ricci, V., Modi, N., Cacciotto, P., Kleinekathfer, U., Ruggerone, P., Vargiu, A. V, Baylay, A.J., Smith, H.E., Brandon, Y., Galloway, D., Piddock, L.J., 2015. AcrB drug-binding pocket substitution confers clinically relevant resistance and altered substrate specificity. PNAS 112, 3511–3516. https://doi.org/10.1073/pnas.1419939112

Blot, M., Hauer, B., Monnet, G., 1994. The Tn5 bleomycin resistance gene confers improved survival and growth advantage on Escherichia coli. Mol. Gen. Genet. 242, 595–601. https://doi.org/10.1007/BF00285283

Blot, M., Heitman, J., Arber, W., 1993. Tn5-mediated bleomycin resistance in Escherichia coli requires the expression of host genes. Mol. Microbiol. 8, 1017–1024. https://doi.org/10.1111/j.1365-2958.1993.tb01646.x

Blot, M., Meyer, J., Arber, W., 1991. Bleomycin-resistance gene derived from the transposon Tn5 confers selective advantage to Escherichia coli K-12. Proc Natl Acad Sci U S A 88, 9112–9116.

Bodet, C.A., Jorgensen, J.H., Drutz, D.J., 1985. Antibacterial activities of antineoplastic agents. Antimicrob Agents Chemother 28, 437–439.

Bollenbach, T., Quan, S., Chait, R., Kishony, R., 2009. Nonoptimal microbial response to antibiotics underlies suppressive drug interactions. Cell 139, 707–718. https://doi.org/10.1016/J.CELL.2009.10.025

Booker, V., Halsall, C., Llewellyn, N., Johnson, A., Williams, R., 2014. Prioritising anticancer drugs for environmental monitoring and risk assessment purposes. Sci Total Env. 473–474, 159–170. https://doi.org/10.1016/j.scitotenv.2013.11.145

Bostock, J.M., Miller, K., O'Neill, A.J., Chopra, I., 2003. Zeocin resistance suppresses mutation in hypermutable Escherichia coli. Microbiology 149, 815–816. https://doi.org/10.1099/mic.0.C0111-0

Bound, J.P., Voulvoulis, N., 2005. Household Disposal of Pharmaceuticals as a Pathway for Aquatic Contamination in the United Kingdom. Environ. Health Perspect. 113, 1705–1711. https://doi.org/10.1289/ehp.8315

Brauner, A., Fridman, O., Gefen, O., Balaban, N.Q., 2016. Distinguishing between resistance, tolerance and persistence to antibiotic treatment. Nat. Rev. Microbiol. 2016 145 14, 320–330. https://doi.org/10.1038/nrmicro.2016.34

Brockhurst, M.A., Harrison, F., Veening, J.W., Harrison, E., Blackwell, G., Iqbal, Z., Maclean, C., 2019. Assessing evolutionary risks of resistance for new antimicrobial therapies. Nat. Ecol. Evol. 3, 515–517.

Brömme, D., Rossi, A.B., Smeekens, S.P., Anderson, D.C., Payan, D.G., 1996. Human Bleomycin Hydrolase: Molecular Cloning, Sequencing, Functional Expression, and Enzymatic Characterization 35. https://doi.org/S0006-2960(96)00092-X

Brown, C.L., Keenum, I.M., Dai, D., Zhang, L., Vikesland, P.J., Pruden, A., 2021. Critical evaluation of short, long, and hybrid assembly for contextual analysis of antibiotic resistance genes in complex environmental metagenomes. Sci. Reports 2021 111 11, 1–12. https://doi.org/10.1038/s41598-021-83081-8

Bundy, J.G., Willey, T.L., Castell, R.S., Ellar, D.J., Brindle, K.M., 2005. Discrimination of pathogenic clinical isolates and laboratory strains of Bacillus cereus by NMR-based metabolomic profiling. FEMS Microbiol. Lett. 242, 127–136. https://doi.org/10.1016/J.FEMSLE.2004.10.048

Burby, P.E., Simmons, L.A., 2018. A bacterial DNA repair pathway specific to a natural antibiotic - Burby - 2019 - Molecular Microbiology - Wiley Online Library. bioRxiv. https://doi.org/10.1111/mmi.14158

Burnham, P., Gomez-Lopez, N., Heyang, M., Cheng, A.P., Lenz, J.S., Dadhania, D.M., Lee, J.R., Suthanthiran, M., Romero, R., De Vlaminck, I., 2020. Separating the signal from the noise in metagenomic cell-free DNA sequencing. Microbiome 8, 1–9. https://doi.org/10.1186/S40168-020-0793-4/FIGURES/2

Burton, J.N., Liachko, I., Dunham, M.J., Shendure, J., 2014. Species-level deconvolution of metagenome assemblies with Hi-C-based contact probability maps. G3 4. https://doi.org/10.1534/g3.114.011825

Buser, G.L., Cassidy, P.M., Pfeiffer, C.D., Townes, J.M., Morey, K.E., Rayar, J., Kutumbaka, K.K., Han, S., Nadala, C., Samadpour, M., Weissman, S.J., Vega, R., Beldavs, Z.G., 2017. New Delhi metallo-β-lactamase-1 (NDM-1) Escherichia coli isolated from household vacuum cleaner—Oregon, 2013. IDCases 9, 56–58. https://doi.org/10.1016/j.idcr.2017.06.004

Calcutt, M.J., Schmidt, F.J., 1994. Gene organization in the bleomycin-resistance region of the producer organism Streptomyces verticillus 151, 17–21. https://doi.org/10.1016/0378-1119(94)90627-0

Card, K.J., Jordan, J.A., Lenski, R.E., 2020. Idiosyncratic variation in the fitness costs of tetracycline-resistance mutations in Escherichia coli. https://doi.org/10.1101/2020.09.12.294355

Carr, V.R., Shkoporov, A., Hill, C., Mullany, P., Moyes, D.L., 2020. Probing the Mobilome: Discoveries in the Dynamic Microbiome. Trends Microbiol. 0. https://doi.org/10.1016/j.tim.2020.05.003

Carvalho, G., Fouchet, D., Danesh, G., Godeux, A.-S., Laaberki, M.-H., Pontier, D., Charpentier, X., Venner, S., Koonin, E. V, Zhulin, I.B., 2020. Bacterial Transformation Buffers Environmental Fluctuations through the Reversible Integration of Mobile Genetic Elements. https://doi.org/10.1128/mBio.02443-19

Carver, T., Rutherford, K., Berriman, M., Rajandream, M., Barrell, B., Parkhill, J., 2005. ACT: the Artemis Comparison Tool. Bioinformatics 21, 3422–3423. https://doi.org/10.1093/BIOINFORMATICS/BTI553

Cepas, V., López, Y., Muñoz, E., Rolo, D., Ardanuy, C., Martí, S., Xercavins, M., Horcajada, J.P., Bosch, J., Soto, S.M., 2019. Relationship between Biofilm Formation and Antimicrobial Resistance in Gram-Negative Bacteria. Microb. Drug Resist. 25, 72–79. https://doi.org/10.1089/MDR.2018.0027/ASSET/IMAGES/LARGE/FIGURE3.JPEG

Cheng, G., Ning, J., Ahmed, S., Huang, J., Ullah, R., An, B., Hao, H., Dai, M., Huang, L., Wang, X., Yuan, Z., 2019. Selection and dissemination of antimicrobial resistance in Agri-food production. Antimicrob. Resist. Infect. Control 8, 1–13. https://doi.org/doi:10.1186/s13756-019-0623-2

Cheng, S., Liu, Y., Crowley, C., Yeates, T., Bobik, T., 2008. Bacterial microcompartments: their properties and paradoxes. Bioessays 30, 1084–1095. https://doi.org/10.1002/bies.20830

Cherny, S., Nevo, D., Baraz, A., Baruch, S., Lewin-Epstein, O., GY, S., Obolski, U., 2021. Revealing antibiotic cross-resistance patterns in hospitalized patients through Bayesian network modelling. J Antimicrob Chemother 76. https://doi.org/10.1093/jac/dkaa408

Chia, V.M., Quraishi, S.M., Devesa, S.S., Purdue, M.P., Cook, M.B., McGlynn, K.A., 2010. International trends in the incidence of testicular cancer, 1973–2002. Cancer Epidemiol Biomarkers Prev 19, 1151–1159. https://doi.org/10.1158/1055-9965.epi-10-0031

Ching, C., Zaman, M.H., 2020. Development and selection of low-level multi-drug resistance over an extended range of sub-inhibitory ciprofloxacin concentrations in Escherichia coli. Sci. Rep. 10, 1–9. https://doi.org/doi:10.1038/s41598-020-65602-z

Chitapanarux, I., Lorvidhaya, V., Sittitrai, P., Pattarasakulchai, T., Tharavichitkul, E., Sriuthaisiriwong, P., Kamnerdsupaphon, P., Sukthomya, V., 2006. Oral cavity cancers at a young age: analysis of patient, tumor and treatment characteristics in Chiang Mai University Hospital. Oral Oncol. 42, 83–88. https://doi.org/10.1016/j.oraloncology.2005.06.015

Chu, D., Wei, L., 2019. Nonsynonymous, synonymous and nonsense mutations in human cancer-related genes undergo stronger purifying selections than expectation. BMC Cancer 19, 1–12. https://doi.org/10.1186/S12885-019-5572-X/FIGURES/5

Chuanchuen, R., Beinlich, K., Hoang, T.T., Becher, A., Karkhoff-Schweizer, R.R., Schweizer, H.P., 2001. Cross-resistance between triclosan and antibiotics in Pseudomonas aeruginosa is mediated by multidrug efflux pumps: exposure of a susceptible mutant strain to triclosan selects nfxB mutants overexpressing MexCD-OprJ. Antimicrob. Agents Chemother. 45, 428–432. https://doi.org/10.1128/AAC.45.2.428-432.2001

Colclough, A., Corander, J., Sheppard, S.K., Bayliss, S.C., Vos, M., 2019. Patterns of cross-resistance and collateral sensitivity between clinical antibiotics and natural antimicrobials. Evol. Appl. 12, 878. https://doi.org/10.1111/EVA.12762

Collis, C.M., Hall, R.M., 1985. Identification of a Tn5 determinant conferring resistance to phleomycins, bleomycins, and tallysomycins. Plasmid 14, 143–151.

Courcelle, J., Khodursky, A., Peter, B., Brown, P.O., Hanawalt, P.C., 2001. Comparative gene expression profiles following UV exposure in wild-type and SOS-deficient Escherichia coli. Genetics 158, 41–64.

Cremazy, F.G., Rashid, F.M., Haycocks, J.R., Lamberte, L.E., Grainger, D.C., Dame, R.T., 2018. Determination of the 3D Genome Organization of Bacteria Using Hi-C, in: Methods Mol Biol. pp. 3–18. https://doi.org/10.1007/978-1-4939-8675-0_1

Crnovcic, I., Gan, F., Yang, D., Dong, L.-B., Schultz, P.G., Shen, B., 2018. Activities of recombinant human bleomycin hydrolase on bleomycins and engineered analogues revealing new opportunities to overcome bleomycin-induced pulmonary toxicity. Bioorg. Med. Chem.

Lett. https://doi.org/https://doi.org/10.1016/j.bmcl.2018.04.065

Dallo, S.F., Weitao, T., 2010. Bacteria under SOS evolve anticancer phenotypes, in: Infect Agent Cancer. p. 3. https://doi.org/10.1186/1750-9378-5-3

Danshiitsoodol, N., de Pinho, C.A., Matoba, Y., Kumagai, T., Sugiyama, M., 2006. The mitomycin C (MMC)-binding protein from MMC-producing microorganisms protects from the lethal effect of bleomycin: crystallographic analysis to elucidate the binding mode of the antibiotic to the protein. J Mol Biol 360, 398–408. https://doi.org/10.1016/j.jmb.2006.05.017

Davis, S.Z., Hollin, T., Lenz, T., Le Roch, K.G., 2021. Three-dimensional chromatin in infectious disease—A role for gene regulation and pathogenicity? https://doi.org/10.1371/journal.ppat.1009207

Díaz, N., Kruse, K., Erdmann, T., Staiger, A.M., Ott, G., Lenz, G., Vaquerizas, J.M., 2018. Chromatin conformation analysis of primary patient tissue using a low input Hi-C method. Nat. Commun. 2018 91 9, 1–13. https://doi.org/10.1038/s41467-018-06961-0

Diebold, P.J., New, F.N., Hovan, M., Satlin, M.J., Brito, I.L., 2021. Linking plasmid-based beta-lactamases to their bacterial hosts using single-cell fusion PCR. https://doi.org/10.1101/2021.01.22.427834

Dieltjens, L., Appermans, K., Lissens, M., Lories, B., Kim, W., Van der Eycken, E. V., Foster, K.R., Steenackers, H.P., 2020. Inhibiting bacterial cooperation is an evolutionarily robust anti-biofilm strategy. Nat. Commun. 2020 111 11, 1–11. https://doi.org/10.1038/s41467-019-13660-x

Djordjevic, D., Wiedmann, M., McLandsborough, L., 2002. Microtiter plate assay for assessment of Listeria monocytogenes biofilm formation. Appl. Environ. Microbiol. 68, 2950–2958. https://doi.org/10.1128/AEM.68.6.2950-2958.2002

Dombach, J.L., Quintana, J.L.J., Nagy, T.A., Wan, C., Crooks, A.L., Yu, H., Su, C.C., Yu, E.W., Shen, J., Detweiler, C.S., 2020. A small molecule that mitigates bacterial infection disrupts Gram-negative cell membranes and is inhibited by cholesterol and neutral lipids. PLoS Pathog. 16. https://doi.org/10.1371/journal.ppat.1009119

Dörr, T., Lewis, K., Vulić, M., 2009. SOS Response Induces Persistence to Fluoroquinolones in Escherichia coli. PLoS Genet. 5.

Dortet, L., Girlich, D., Virlouvet, A.-L., Poirel, L., Nordmann, P., Iorga, B.I., Naas, T., 2017. Characterization of BRPMBL, the Bleomycin Resistance Protein Associated with the Carbapenemase NDM. https://doi.org/10.1128/AAC.02413-16

Dortet, L., Nordmann, P., Poirel, L., 2012. Association of the Emerging Carbapenemase NDM-1 with a Bleomycin Resistance Protein in Enterobacteriaceae and Acinetobacter baumannii, in: Antimicrob Agents Chemother. pp. 1693–1697. https://doi.org/10.1128/aac.05583-11

Dumas, P., Bergdoll, M., Cagnon, C., Masson, J.-M., 1994. Crystal structure and site-directed mutagenesis of a bleomycin resistance protein and their significance for drug sequestering. EMBO J 13, 2483–2492.

Dupont, M., James, C.E., Chevalier, J., Pages, J.M., 2007. An early response to environmental stress involves regulation of OmpX and OmpF, two enterobacterial outer membrane pore-forming proteins. Antimicrob Agents Chemother 51, 3190–3198. https://doi.org/10.1128/aac.01481-06

Duwe, A.K., Rupar, C.A., Horsman, G.B., Vas, S.I., 1986. In vitro cytotoxicity and antibiotic activity of polymyxin B nonapeptide. Antimicrob Agents Chemother 30, 340–341.

Dyrda, G., Boniewska-Bernacka, E., Man, D., Barchiewicz, K., Słota, R., 2019. The effect of organic solvents on selected microorganisms and model liposome membrane. Mol. Biol. Reports 2019 463 46, 3225–3232. https://doi.org/10.1007/S11033-019-04782-Y

Enenkel, C., Wolf, D.H., 1993. BLH1 Codes for a Yeast Thiol Aminopeptidase, the Equivalent of Mammalian Bleomycin Hydrolase. J. Biol. Chem. 268.

Enne, V.I., Delsol, A.A., Davis, G.R., Hayward, S.L., Roe, J.M., Bennett, P.M., 2005. Assessment of the fitness impacts on Escherichia coli of acquisition of antibiotic resistance genes encoded by different types of genetic element. J Antimicrob Chemother 56, 544–551. https://doi.org/10.1093/jac/dki255

Faber, F., Thiennimitr, P., Spiga, L., Byndloss, M.X., Litvak, Y., Lawhon, S., Andrews-Polymenis, H.L., Winter, S.E., Bäumler, A.J., 2017. Respiration of Microbiota-Derived 1,2-propanediol Drives Salmonella Expansion during Colitis. PLOS Pathog. 13, e1006129. https://doi.org/10.1371/JOURNAL.PPAT.1006129

Farhat, N., Khan, A.U., 2020. Evolving trends of New Delhi Metallo-betalactamse (NDM) variants: A threat to antimicrobial resistance. Infect. Genet. Evol. 86, 104588. https://doi.org/10.1016/J.MEEGID.2020.104588

Ferrando-Climent, L., Rodriguez-Mozaz, S., Barceló, D., 2014. Incidence of anticancer drugs in an aquatic urban system: From hospital effluents through urban wastewater to natural environment. Environ. Pollut. 193, 216–223. https://doi.org/https://doi.org/10.1016/j.envpol.2014.07.002

Friedman, N., Vardi, S., Ronen, M., Alon, U., Stavans, J., 2005. Precise Temporal Modulation in

teh Response of the SOS DNA Repair Network in Individual Bacteria. PLoS Biol. 3.

Frost, I., Smith, W.P.J., Mitri, S., Millan, A.S., Davit, Y., Osborne, J.M., Pitt-Francis, J.M., MacLean, R.C., Foster, K.R., 2018. Cooperation, competition and antibiotic resistance in bacterial colonies. ISME J. 12, 1582–1593. https://doi.org/10.1038/s41396-018-0090-4

Gabdank, I., Ramakrishnan, S., Villeneuve, A.M., Fire, A.Z., 2016. A streamlined tethered chromosome conformation capture protocol. BMC Genomics 17, 1–13. https://doi.org/10.1186/s12864-016-2596-3

Galba, J., Veizerová, L., Piešťanský, J., Mego, M., Novotný, L., Dokupilová, S., Maráková, K., Havránek, E., Mikuš, P., 2014. HPLC-QTOF-MS Method for Identification and Determination of Bleomycin A2 and B2 Fractions. J. Liq. Chromatogr. Relat. Technol. 38, 294–302. https://doi.org/Journal of Liquid Chromatography & Related Technologies, Vol. 38, No. 2, pp. 294–302

Galvan, L., Huang, C.H., Prestayko, A.W., Stout, J.T., Evans, J.E., Crooke, S.T., 1981. Inhibition of Bleomycin-induced DNA Breakage by Superoxide Dismutase.

Gasparrini, A.J., Markley, J.L., Kumar, H., Wang, B., Fang, L., Irum, S., Symister, C.T., Wallace, M., Burnham, C.-A.D., Andleeb, S., Tolia, N.H., Wencewicz, T.A., Dantas, G., 2020. Tetracycline-inactivating enzymes from environmental, human commensal, and pathogenic bacteria cause broad-spectrum tetracycline resistance. Commun. Biol. 3, 1–12. https://doi.org/doi:10.1038/s42003-020-0966-5

Gavrilov, A., Razin, S. V., Cavalli, G., 2015. In vivo formaldehyde cross-linking: it is time for black box analysis. Brief. Funct. Genomics 14, 163. https://doi.org/10.1093/BFGP/ELU037

Gefen, O., Chekol, B., Strahilevitz, J., Balaban, N.Q., 2017. TDtest: easy detection of bacterial tolerance and persistence in clinical isolates by a modified disk-diffusion assay, in: Sci Rep. https://doi.org/10.1038/srep41284

Genilloud, O., Garrido, M.C., Moreno, F., 1984. The transposon Tn5 carries a bleomycin-resistance determinant. Gene 32, 225–233.

Gennimata, D., Davies, J., Tsiftsoglou, A.S., 1996. Bleomycin resistance in Staphylococcus aureus clinical isolates. J Antimicrob Chemother 37, 65–75.

Gingold, H., Pilpel, Y., 2011. Determinants of translation efficiency and accuracy. Mol. Syst. Biol. 7, 1–13. https://doi.org/10.1038/msb.2011.14

GitHub - open2c/pairtools: CLI tools to process mapped Hi-C data [WWW Document], n.d. URL https://github.com/open2c/pairtools (accessed 12.20.21).

González, L., Bahr, G., Nakashige, T., Nolan, E., Bonomo, R., Vila, A., 2016. Membrane anchoring stabilizes and favors secretion of New Delhi metallo-β-lactamase. Nat. Chem. Biol. 12, 516–522. https://doi.org/10.1038/NCHEMBIO.2083

Göttig, S., Hamprecht, A.G., Christ, S., Kempf, V.A.J., Wichelhaus, T.A., 2013. Detection of NDM-7 in Germany, a new variant of the New Delhi metallo-β-lactamase with increased carbapenemase activity. J. Antimicrob. Chemother. 68. https://doi.org/10.1093/jac/dkt088

Grollman, A.P., Takeshita, M., 1980. Interactions of bleomycin with DNA - ScienceDirect. Adv. Enzyme Regul. 18, 67–72. https://doi.org/10.1016/0065-2571(80)90009-6

Guðmundsdóttir, J.S., Fredheim, E.G.A., Koumans, C.I.M., Hegstad, J., Tang, P.-C., Andersson, D.I., Samuelsen, Ø., Johnsen, P.J., 2021. The chemotherapeutic drug methotrexate selects for antibiotic resistance. https://doi.org/10.1101/2020.11.12.378059

Guo, Y., Liu, G., Shui, W., Sun, Y., Zhou, H., Zhang, Y., Yang, C., Lou, Z., Rao, Z., 2011. A structural view of the antibiotic degradation enzyme NDM-1 from a superbug | SpringerLink. Protein Cell 2. https://doi.org/10.1007/s13238-011-1055-9

Gurtovenko, A.A., Anwar, J., 2007. Modulating the Structure and Properties of Cell Membranes: The Molecular Mechanism of Action of Dimethyl Sulfoxide. J. Phys. Chem. B 111, 10453–10460.

Haidle, C.W., Weiss, K.K., Kuo, M.T., 1972a. Release of Free Bases from Deoxyribonucleic Acid after Reaction with Bleomycin.

Haidle, C.W., Weiss, K.K., Mace Myles L., J., 1972b. Induction of bacteriophage by bleomycin. https://doi.org/http://dx.doi.org/10.1016/0006-291X(72)90835-2

Hamilton-Miller, J.M., 1984. Antimicrobial activity of 21 anti-neoplastic agents. Br J Cancer 49, 367–369.

Hannan, M.A., Nasim, A., 1978. Genetic activity of bleomycin: Differential effects on mitotic recombination and mutations in yeast - ScienceDirect. Mutat. Res. 53, 309–316. https://doi.org/10.1016/0165-1161(78)90003-1

Harewood, L., Kishore, K., Eldridge, M.D., Wingett, S., Pearson, D., Schoenfelder, S., Collins, V.P., Fraser, P., 2017. Hi-C as a tool for precise detection and characterisation of chromosomal rearrangements and copy number variation in human tumours. Genome Biol. 18, 1–11. https://doi.org/10.1186/s13059-017-1253-8

Hartmann, M., Berditsch, M., Hawecker, J., MF, A., Gerthsen, D., AS, U., 2010. Damage of the bacterial cell envelope by antimicrobial peptides gramicidin S and PGLa as revealed by

transmission and scanning electron microscopy. Antimicrob. Agents Chemother. 54. https://doi.org/10.1128/AAC.00124-10

Harwani, D., Zangoui, P., Mahadevan, S., 2012. The β-Glucoside (bgl) Operon of Escherichia coli Is Involved in the Regulation of oppA, Encoding an Oligopeptide Transporter. J Bacteriol 194, 90–99. https://doi.org/10.1128/jb.05837-11

Hasman, H., Chakraborty, T., Klemm, P., 1999. Antigen-43-Mediated Autoaggregation of Escherichia coli Is Blocked by Fimbriation. J Bacteriol 181, 4834–4841.

Herencias, C., Rodríguez-Beltrán, J., León-Sampedro, R., Valle, A.A., Palkovičová, J., Cantón, R., Millán, Á.S., 2021. Collateral sensitivity associated with antibiotic resistance plasmids. https://doi.org/doi:10.7554/eLife.65130

Herren, C.M., Baym, M., 2021. Decreased thermal tolerance as a trade-off of antibiotic resistance. https://doi.org/10.1101/2021.04.05.438396

Hetu, M., Koutouki, K., Joly, Y., 2019. Genomics for All: International open science projects and cpacity building in the developing world. Front. Genet. 10, 95. https://doi.org/10.3389/FGENE.2019.00095/BIBTEX

Heydari-Bafrooei, E., Amini, M., Saeednia, S., 2017. Electrochemical detection of DNA damage induced by Bleomycin in the presence of metal ions - ScienceDirect. https://doi.org/10.1016/j.jelechem.2017.09.031

Hines, K.M., Shen, T., Ashford, N.K., Waalkes, A., Penewit, K., Holmes, E.A., McLean, K., Salipante, S.J., Werth, B.J., Xu, L., 2019. Occurrence of cross-resistance and beta-lactam seesaw effect in glycopeptide, lipopeptide, and lipoglycopeptide-resistant MRSA correlates with membrane phosphatidylglycerol levels. J. Antimicrob. Chemother. 75. https://doi.org/10.1101/671438

Holmes, C.E., Abraham, A.T., Hecht, S.M., Florentz, C., Giege, R., 1996. Fe.bleomycin as a probe of RNA conformation. Nucleic Acids Res 24, 3399–3406.

Imai, Y., Meyer, K.J., Iinishi, A., Favre-Godal, Q., Green, R., Manuse, S., Caboni, M., Mori, M., Niles, S., Ghiglieri, M., Honrao, C., Ma, X., Guo, J.J., Makriyannis, A., Linares-Otoya, L., Böhringer, N., Wuisan, Z.G., Kaur, H., Wu, R., Mateus, A., Typas, A., Savitski, M.M., Espinoza, J.L., O'Rourke, A., Nelson, K.E., Hiller, S., Noinaj, N., Schäberle, T.F., D'Onofrio, A., Lewis, K., 2019. A new antibiotic selectively kills Gram-negative pathogens. Nature 576, 459–464. https://doi.org/doi:10.1038/s41586-019-1791-1

Imura, Y., Choda, N., Matsuzaki, K., 2008. Magainin 2 in action: distinct modes of membrane permeabilization in living bacterial and mammalian cells. Biophys. J. 95, 5757–5765.

https://doi.org/10.1529/BIOPHYSJ.108.133488

Irvin, R.T., MacAlister, T.J., Costerton, J.W., 1981. Tris(hydroxymethyl)aminomethane buffer modification of Escherichia coli outer membrane permeability. J. Bacteriol. 145, 1397–1403. https://doi.org/10.1128/JB.145.3.1397-1403.1981

Jacobs, A.C., Didone, L., Jobson, J., Sofia, M.K., Krysan, D., Dunman, P.M., 2013. Adenylate kinase release as a high-throughput-screening-compatible reporter of bacterial lysis for identification of antibacterial agents. Antimicrob Agents Chemother 57, 26–36. https://doi.org/10.1128/aac.01640-12

Jäger, R., Migliorini, G., Henrion, M., Kandaswamy, R., Speedy, H.E., Heindl, A., Whiffin, N., Carnicer, M.J., Broome, L., Dryden, N., Nagano, T., Schoenfelder, S., Enge, M., Yuan, Y., Taipale, J., Fraser, P., Fletcher, O., Houlston, R.S., 2015. Capture Hi-C identifies the chromatin interactome of colorectal cancer risk loci. Nat. Commun. 6, 1–9. https://doi.org/10.1038/ncomms7178

Jamal, W.Y., Albert, M.J., Rotimi, V.O., 2016. High Prevalence of New Delhi Metallo-β-Lactamase-1 (NDM-1) Producers among Carbapenem-Resistant Enterobacteriaceae in Kuwait. PLoS One 11. https://doi.org/10.1371/journal.pone.0152638

Janvier, F., Jeannot, K., Tessé, S., Robert-Nicoud, M., Delacour, H., Rapp, C., Mérens, A., 2013. Molecular Characterization of blaNDM-1 in a Sequence Type 235 Pseudomonas aeruginosa Isolate from France, in: Antimicrob Agents Chemother. pp. 3408–3411. https://doi.org/10.1128/aac.02334-12

Jara, L.M., Cortés, P., Bou, G., Barbé, J., Aranda, J., 2015. Differential Roles of Antimicrobials in the Acquisition of Drug Resistance through Activation of the SOS Response in Acinetobacter baumannii. Antimicrob. Agents Chemother. 59, 4318–4320. https://doi.org/10.1128/AAC.04918-14

Jesse, T., Englen, M., Pittenger-Alley, L., Fedorka-Cray, P., 2006. Two distinct mutations in gyrA lead to ciprofloxacin and nalidixic acid resistance in Campylobacter coli and Campylobacter jejuni isolated from chickens and beef cattle. J. Appl. Microbiol. 100, 682–688. https://doi.org/10.1111/J.1365-2672.2005.02796.X

Jilk, R.A., York, D., Reznikoff, W.S., 1996. The organization of the outside end of transposon Tn5. J. Bacteriol. 178, 1671–1679. https://doi.org/10.1128/JB.178.6.1671-1679.1996

Jóna, Á., Miltenyi, Z., Poliska, S., Balint, B.L., Illes, A., 2016. Effect of Bleomycin Hydrolase Gene Polymorphism on Late Pulmonary Complications of Treatment for Hodgkin Lymphoma. PLoS One 11, e0157651. https://doi.org/10.1371/journal.pone.0157651

Jutkina, J., Marathe, N.P., Flach, C.F., Larsson, D.G.J., 2018. Antibiotics and common antibacterial biocides stimulate horizontal transfer of resistance at low concentrations. Sci Total Env. 616–617, 172–178. https://doi.org/10.1016/j.scitotenv.2017.10.312

Jutkina, J., Rutgersson, C., Flach, C.F., Larsson, D.G., 2016. An assay for determining minimal concentrations of antibiotics that drive horizontal transfer of resistance. Sci Total Env. 548–549, 131–138. https://doi.org/10.1016/j.scitotenv.2016.01.044

Kawano, Y., Kumagai, T., Muta, K., Matoboa, Y., Davies, J., Sugiyama, M., 2000. The 1.5 A crystal structure of a bleomycin resistance determinant from bleomycin-producing... - Abstract - Europe PMC. https://doi.org/https://doi.org/10.1006/jmbi.1999.3404

Ke, X., Shen, L., 2017. Molecular targeted therapy of cancer: The progress and future prospect - ScienceDirect. Front. Lab. Med. 1. https://doi.org/10.1016/j.flm.2017.06.001

Kennedy-Darling, J., Smith, L.M., 2014. Measuring the formaldehyde protein-DNA cross-link reversal rate. Anal. Chem. 86, 5678–5681. https://doi.org/10.1021/AC501354Y/SUPPL_FILE/AC501354Y_SI_001.PDF

Kent, A.G., Vill, A.C., Shi, Q., Satlin, M.J., Brito, I.L., 2020. Widespread transfer of mobile antibiotic resistance genes within individual gut microbiomes revealed through bacterial Hi-C. Nat. Commun. 11. https://doi.org/10.1038/s41467-020-18164-7

Kerpedjiev, P., Abdennur, N., Lekschas, F., McCallum, C., Dinkla, K., Strobelt, H., Luber, J.M., Ouellette, S.B., Azhir, A., Kumar, N., Hwang, J., Lee, S., Alver, B.H., Pfister, H., Mirny, L.A., Park, P.J., Gehlenborg, N., 2018. HiGlass: Web-based visual exploration and analysis of genome interaction maps. Genome Biol. 19, 1–12. https://doi.org/10.1186/S13059-018-1486-1/FIGURES/6

Ketchum, R.N., Smith, E.G., Vaughan, G.O., Phippen, B.L., McParland, D., Al-Mansoori, N., Carrier, T.J., Burt, J.A., Reitzel, A.M., 2018. DNA Extraction Method Plays a Significant Role When Defining Bacterial Community Composition in the Marine Invertebrate Echinometra mathaei. Front. Mar. Sci. 5, 255. https://doi.org/10.3389/FMARS.2018.00255/BIBTEX

Kier, M.G., Lauritsen, J., Mortensen, M.S., Bandak, M., Andersen, K.K., Hansen, M.K., Agerbaek, M., Holm, N. V, Dalton, S.O., Johansen, C., Daugaard, G., 2017. Prognostic Factors and Treatment Results After Bleomycin, Etoposide, and Cisplatin in Germ Cell Cancer: A Population-based Study. Eur Urol 71, 290–298. https://doi.org/10.1016/j.eururo.2016.09.015

Kimura, I., Onoshi, T., Kunimasa, I., Takano, J., 1972. Treatment of malignant lymphomas with bleomycin. Cancer 29, 58–60. https://doi.org/10.1002/1097-0142(197201)29:1<58::AID-

CNCR2820290110>3.0.CO;2-R

Kohanski, M.A., DePristo, M.A., Collins, J.J., 2010. Sub-lethal antibiotic treatment leads to multidrug resistance via radical-induced mutagenesis. Mol Cell 37, 311–320. https://doi.org/10.1016/j.molcel.2010.01.003

Kousathanas, A., Pairo-Castineira, E., Rawlik, K., Stuckey, A., Odhams, C.A., Walker, Susan, Russell, C.D., Malinauskas, T., Wu, Y., Millar, Jonathan, Shen, X., Elliott, K.S., Griffiths, F., Oosthuyzen, W., Morrice, K., Keating, S., Wang, B., Rhodes, D., Klaric, L., Zechner, M., Parkinson, N., Siddiq, A., Goddard, P., Donovan, S., Maslove, D., Nichol, Alistair, Semple, M.G., Zainy, T., Maleady-Crowe, F., Todd, L., Salehi, S., Knight, J., Elgar, G., Chan, G., Arumugam, P., Patch, C., Rendon, A., Bentley, D., Kingsley, C., Kosmicki, J.A., Horowitz, J.E., Baras, A., Abecasis, G.R., Ferreira, M.A.R., Justice, A., Mirshahi, T., Oetjens, M., Rader, D.J., Ritchie, M.D., Verma, A., Fowler, T.A., Shankar-Hari, M., Summers, C., Hinds, C., Horby, P., Ling, L., McAuley, D., Montgomery, H., Openshaw, P.J.M., Elliott, P., Walsh, T., Tenesa, A., Baillie, J.K., Begg, C., Clohisey Hendry, S., Hinds, C., Horby, P., Knight, J., Ling, L., Maslove, D., McAuley, D., Millar, Johnny, Montgomery, H., Nichol, Alistair, Openshaw, P.J.M., Pereira, A.C., Ponting, C.P., Rowan, K., Semple, M.G., Shankar-Hari, M., Summers, C., Walsh, T., Aravindan, L., Armstrong, R., Biggs, H., Boz, C., Brown, Adam, Clark, R., Coutts, A., Coyle, J., Cullum, L., Das, S., Day, N., Donnelly, L., Duncan, Esther, Fawkes, A., Finernan, P., Fourman, M.H., Furlong, A., Furniss, J., Gallagher, B., Gilchrist, T., Golightly, A., Griffiths, F., Hafezi, K., Hamilton, D., Hendry, R., Law, A., Law, D., Law, R., Law, S., Lidstone-Scott, R., Macgillivray, L., Maclean, A., Mal, H., McCafferty, S., Mcmaster, E., Meikle, J., Moore, S.C., Morrice, K., Murphy, Lee, Murphy, S., Hellen, M., Oosthuyzen, W., Zheng, C., Chen, J., Parkinson, N., Paterson, T., Schon, K., Stenhouse, A., Das, M., Swets, M., Szoor-McElhinney, H., Taneski, F., Turtle, L., Wackett, T., Ward, M., Weaver, J., Wrobel, N., Zechner, M., Arbane, G., Bociek, A., Campos, S., Grau, N., Jones, T.O., Lim, R., Marotti, M., Ostermann, M., Shankar-Hari, M., Whitton, C., Alldis, Z., Astin-Chamberlain, R., Bibi, F., Biddle, J., Blow, S., Bolton, M., Borra, C., Bowles, R., Burton, M., Choudhury, Y., Collier, David, Cox, A., Easthope, A., Ebano, P., Fotiadis, S., Gurasashvili, J., Halls, R., Hartridge, P., Kallon, D., Kassam, J., Lancoma-Malcolm, I., Matharu, M., May, P., Mitchelmore, O., Newman, T., Patel, M., Pheby, J., Pinzuti, I., Prime, Z., Prysyazhna, O., Shiel, J., Taylor, Melanie, Tierney, C., Wood, S., Zak, A., Zongo, O., Bonner, S., Hugill, K., Jones, Jessica, Liggett, S., Headlam, E., Bandla, N., Gellamucho, M., Davies, M., Thompson, C., Abdelrazik, M., Bakthavatsalam, D., Elhassan, M., Ganesan, A., Haldeos, A., Moreno-Cuesta, J., Purohit, D., Vincent, R., Xavier, K., Kumar, Rohit, Frater, A., Saleem, M., Carter, D., Jenkins, Samuel, Lamond, Z., Wall, A., Fernandez-Roman, J., Hamilton, D.O., Johnson, E., Johnston, B., Martinez, M.L., Mulla, S., Shaw, D., Waite, A.A.C., Waugh, V., Welters, I.D., Williams, K., Cavazza, A., Cockrell, M.,

Corcoran, E., Depante, M., Finney, C., Jerome, E., McPhail, M., Nayak, M., Noble, H., O'Reilly, K., Pappa, E., Saha, Rohit, Saha, S., Smith, John, Knighton, A., Antcliffe, D., Banach, D., Brett, S., Coghlan, P., Fernandez, Z., Gordon, A., Rojo, R., Arias, S.S., Templeton, M., Meredith, M., Morris, L., Ryan, L., Clark, A., Sampson, J., Peters, C., Dent, M., Langley, M., Ashraf, S., Wei, S., Andrew, A., Bashyal, A., Davidson, N., Hutton, P., McKechnie, S., Wilson, J., Baptista, D., Crowe, R., Fernandes, R., Herdman-Grant, R., Joseph, A., O'Connor, D., Allen, M., Loveridge, A., McKenley, I., Morino, E., Naranjo, A., Simms, R., Sollesta, K., Swain, A., Venkatesh, H., Khera, J., Fox, J., Andrew, G., Baillie, J.K., Barclay, L., Callaghan, M., Campbell, R., Clark, S., Hope, D., Marshall, L., McCulloch, C., Briton, K., Singleton, J., Birch, S., Brimfield, L., Daly, Z., Pogson, D., Rose, S., Nown, A., Battle, C., Brinkworth, E., Harford, R., Murphy, C., Newey, L., Rees, T., Williams, M., Arnold, S., Polgarova, P., Stroud, K., Summers, C., Meaney, E., Jones, M., Ng, A., Agrawal, S., Pathan, N., White, D., Daubney, E., Elston, K., Grauslyte, L., Hussain, M., Phull, M., Pogreban, T., Rosaroso, L., Salciute, E., Franke, G., Wong, J., George, A., de Gordoa, L.O.-R., Peasgood, E., Phillips, C., Bates, M., Dasgin, J., Gill, J., Nilsson, A., Scriven, J., Collins, A., Khaliq, W., Gude, E.T., Delgado, C.C., Dawson, D., Ding, L., Durrant, G., Ezeobu, O., Farnell-Ward, S., Harrison, Abiola, Kanu, R., Leaver, S., Maccacari, E., Manna, S., Saluzzio, R.P., Queiroz, J., Samakomva, T., Sicat, C., Texeira, J., Da Gloria, E.F., Lisboa, A., Rawlins, J., Mathew, J., Kinch, A., Hurt, W.J., Shah, N., Clark, V., Thanasi, M., Yun, N., Patel, K., Bennett, S., Goodwin, E., Jackson, M., Kent, A., Tibke, C., Woodyatt, W., Zaki, A., Abraheem, A., Bamford, P., Cawley, K., Dunmore, C., Faulkner, M., Girach, R., Jeffrey, H., Jones, R., London, E., Nagra, I., Nasir, F., Sainsbury, H., Smedley, C., Patel, T., Smith, M., Chukkambotla, S., Kazi, A., Hartley, J., Dykes, J., Hijazi, M., Keith, S., Khan, M., Ryan-Smith, J., Springle, P., Thomas, J., Truman, N., Saad, S., Coleman, D., Fine, C., Matt, R., Gay, B., Dalziel, J., Ali, S., Goodchild, D., Harling, R., Bhatterjee, R., Goddard, W., Davison, C., Duberly, S., Hargreaves, J., Bolton, R., Davey, M., Golden, D., Seaman, R., Cherian, S., Cutler, S., Heron, A.E., Roynon-Reed, A., Szakmany, T., Williams, G., Richards, O., Cheema, Y., Brooke, H., Buckley, S., Suarez, J.C., Charlesworth, R., Hansson, K., Norris, J., Poole, A., Rose, A., Sandhu, R., Sloan, B., Smithson, E., Thirumaran, M., Wagstaff, V., Metcalfe, A., Brunton, M., Caterson, J., Coles, H., Frise, M., Rai, S.G., Jacques, N., Keating, L., Tilney, E., Bartley, S., Bhuie, P., Gibson, S., Lyle, A., McNeela, F., Radhakrishnan, J., Hughes, A., Yates, B., Reynolds, J., Campbell, H., Thompsom, M., Dodds, S., Duffy, S., Greer, S., Shuker, K., Tridente, A., Khade, R., Sundar, A., Tsinaslanidis, G., Birkinshaw, I., Carter, J., Howard, K., Ingham, J., Joy, R., Pearson, H., Roche, S., Scott, Z., Bancroft, H., Bellamy, M., Carmody, M., Daglish, J., Moore, F., Rhodes, J., Sangombe, M., Kadiri, S., Scriven, J., Croft, M., White, I., Frost, V., Aquino, M., Jha, R., Krishnamurthy, V., Lim, Lai, Lim, Li, Combes, E., Joefield, T., Monnery, S., Beech, V., Trotman, S., Almaden-Boyle, C., Austin, P., Cabrelli, L., Cole, S., Casey, M., Chapman, S., Whyte, C., Baird, Y., Butler, A.,

Chadbourn, I., Folkes, L., Fox, H., Gardner, A., Gomez, R., Hobden, G., Hodgson, L., King, K., Margarson, M., Martindale, T., Meadows, E., Raynard, D., Thirlwall, Y., Helm, D., Margalef, J., Criste, K., Cusack, R., Golder, K., Golding, H., Jones, O., Leggett, S., Male, M., Marani, M., Prager, K., Williams, T., Roberts, B., Salmon, K., Anderson, P., Archer, K., Austin, K., Davis, C., Durie, A., Kelsall, O., Thrush, J., Vigurs, C., Wild, L., Wood, H.-L., Tranter, H., Harrison, Alison, Cowley, N., McAlindon, M., Burtenshaw, A., Digby, S., Low, E., Morgan, A., Cother, N., Rankin, T., Clayton, S., McCurdy, A., Ahmed, C., Baines, B., Clamp, S., Colley, J., Haq, R., Hayes, A., Hulme, J., Hussain, S., Joseph, S., Kumar, Rita, Maqsood, Z., Purewal, M., Benham, L., Bradshaw, Z., Brown, J., Caswell, M., Cupitt, J., Melling, S., Preston, S., Slawson, N., Stoddard, E., Warden, S., Deacon, B., Lynch, C., Pothecary, C., Roche, L., Howe, G.S., Singh, J., Turner, K., Ellis, H., Stroud, N., Hunt, Jodie, Dearden, J., Dobson, E., Drummond, A., Mulcahy, M., Munt, S., O'Connor, G., Philbin, J., Rishton, C., Tully, R., Winnard, S., Cathcart, S., Duffy, K., Puxty, A., Puxty, K., Turner, L., Ireland, J., Semple, G., Long, K., Whiteley, S., Wilby, E., Ogg, B., Cowton, A., Kay, A., Kent, M., Potts, K., Wilkinson, A., Campbell, S., Brown, E., Melville, J., Naisbitt, J., Joseph, R., Lazo, M., Walton, O., Neal, A., Alexander, P., Allen, S., Bradley-Potts, J., Brantwood, C., Egan, J., Felton, T., Padden, G., Ward, L., Moss, S., Glasgow, S., Abel, L., Brett, M., Digby, B., Gemmell, L., Hornsby, J., MacGoey, P., O'Neil, P., Price, R., Rodden, N., Rooney, K., Sundaram, R., Thomson, N., Hopkins, B., Scriven, J., Thrasyvoulou, L., Willis, H., Clark, Martyn, Coulding, M., Jude, E., McCormick, J., Mercer, O., Potla, D., Rehman, H., Savill, H., Turner, V., Downes, C., Holding, K., Riches, K., Hilton, M., Hayman, M., Subramanian, D., Daniel, P., Adanini, O., Bhatia, N., Msiska, M., Collins, R., Clement, I., Patel, Bijal, Gulati, A., Hays, C., Webster, K., Hudson, A., Webster, A., Stephenson, E., McCormack, L., Slater, V., Nixon, R., Hanson, H., Fearby, M., Kelly, S., Bridgett, V., Robinson, P., Camsooksai, J., Humphrey, C., Jenkins, Sarah, Reschreiter, H., Wadams, B., Death, Y., Bastion, V., Clarke, D., David, B., Kent, H., Lorusso, R., Lubimbi, G., Murdoch, S., Penacerrada, M., Thomas, Alastair, Valentine, J., Vochin, A., Wulandari, R., Djeugam, B., Bell, G., English, K., Katary, A., Wilcox, L., Bruce, M., Connolly, K., Duncan, T., Michael, H.T., Lindergard, G., Hey, S., Fox, C., Alfonso, J., Durrans, L.J., Guerin, J., Blackledge, B., Harris, J., Hruska, M., Eltayeb, A., Lamb, T., Hodgkiss, T., Cooper, L., Rothwell, J., Allan, A., Anderson, F., Kaye, C., Liew, J., Medhora, J., Scott, T., Trumper, E., Botello, A., Lankester, L., Nikitas, N., Wells, C., Stowe, B., Spencer, K., Brandwood, C., Smith, L., Clark, R., Birchall, Katie, Kolakaluri, L., Baines, D., Sukumaran, A., Apetri, E., Basikolo, C., Blackledge, B., Catlow, L., Charles, B., Dark, P., Doonan, R., Harris, J., Harvey, A., Horner, D., Knowles, K., Lee, S., Lomas, D., Lyons, C., Marsden, T., McLaughlan, D., McMorrow, L., Pendlebury, J., Perez, J., Poulaka, M., Proudfoot, N., Slaughter, M., Slevin, K., Taylor, Melanie, Thomas, V., Walker, D., Michael, A., Collis, M., Cosier, T., Millen, G., Richardson, N., Schumacher, N., Weston, H., Rand, J., Baxter, N., Henderson, S., Kennedy-

Hay, S., McParland, Christopher, Rooney, L., Sim, M., McCreath, G., Akeroyd, L., Bano, S., Bromley, M., Gurr, L., Lawton, T., Morgan, J., Sellick, K., Warren, D., Wilkinson, B., McGowan, J., Ledgard, C., Stacey, A., Pye, K., Bellwood, R., Bentley, M., Bewley, J., Garland, Z., Grimmer, L., Gumbrill, B., Johnson, R., Sweet, K., Webster, D., Efford, G., Convery, K., Fottrell-Gould, D., Hudig, L., Keshet-Price, J., Randell, G., Stammers, K., Bokhari, M., Linnett, V., Lucas, R., McCormick, W., Ritzema, J., Sanderson, A., Wild, H., Rostron, A., Roy, A., Woods, L., Cornell, S., Wakinshaw, F., Rogerson, K., Jarmain, J., Parker, R., Reddy, A., Turner-Bone, I., Wilding, L., Harding, P., Abernathy, C., Foster, L., Gratrix, A., Martinson, V., Parkinson, P., Stones, E., Carbral-Ortega, L., Bercades, G., Brealey, D., Hass, I., MacCallum, N., Martir, G., Raith, E., Reyes, A., Smyth, D., Zitter, L., Benyon, S., Marriott, S., Park, L., Keenan, S., Gordon, E., Quinn, H., Baines, K., Cagova, L., Fofano, A., Garner, L., Holcombe, H., Mepham, S., Mitchell, A.M., Mwaura, L., Praman, K., Vuylsteke, A., Zamikula, J., Purewal, B., Rivers, V., Bell, S., Blakemore, H., Borislavova, B., Faulkner, B., Gendall, E., Goff, E., Hayes, K., Thomas, M., Worner, R., Smith, K., Stephens, D., Mew, L., Mwaura, E., Stewart, R., Williams, F., Wren, L., Sutherland, S.-B., Bevan, E., Martin, J., Trodd, D., Watson, G., Wrey Brown, C., Akinkugbe, O., Bamford, A., Beech, E., Belfield, H., Bell, M., Davies, C., Jones, G.A.L., McHugh, T., Meghari, H., O'Neill, L., Peters, M.J., Ray, S., Tomas, A.L., Burn, I., Hambrook, G., Manso, K., Penn, R., Shanmugasundaram, P., Tebbutt, J., Thornton, D., Cole, Jade, Davies, M., Davies, R., Duffin, D., Hill, H., Player, B., Thomas, E., Williams, Angharad, Griffin, D., Muchenje, N., Mupudzi, M., Partridge, R., Conyngham, J.-A., Thomas, R., Wright, M., Corral, M.A., Jacob, R., Jones, C., Denmade, C., Beavis, S., Dale, K., Gascoyne, R., Hawes, J., Pritchard, K., Stevenson, L., Whileman, A., Doble, P., Hutter, J., Pawley, C., Shovelton, C., Vaida, M., Butcher, D., O'Sullivan, S., Butterworth-Cowin, N., Ahmad, N., Barker, J., Bauchmuller, K., Bird, S., Cawthron, K., Harrington, K., Jackson, Y., Kibutu, F., Lenagh, B., Masuko, S., Mills, G.H., Raithatha, A., Wiles, M., Willson, J., Newell, H., Lye, A., Nwafor, L., Jarman, C., Rowland-Jones, S., Foote, D., Cole, Joby, Thompson, R., Watson, J., Hesseldon, L., Macharia, I., Chetam, L., Smith, Jacqui, Ford, A., Anderson, Samantha, Birchall, Kathryn, Housley, K., Walker, Sara, Milner, L., Hanratty, H., Trower, H., Phillips, P., Oxspring, S., Donne, B., Jardine, C., Williams, D., Hay, A., Flanagan, R., Hughes, G., Latham, S., McKenna, E., Anderson, J., Hull, R., Rhead, K., Cruz, C., Pattison, N., Charnock, R., McFarland, D., Cosgrove, D., Ahmed, A., Morris, A., Jakkula, S., Nune, A., Ali, Asifa, Brady, M., Dale, S., Dance, A., Gledhill, L., Greig, J., Hanson, K., Holdroyd, K., Home, M., Kelly, D., Kitson, R., Matapure, L., Melia, D., Mellor, S., Nortcliffe, T., Pinnell, J., Robinson, M., Shaw, L., Shaw, R., Thomis, L., Wilson, A., Wood, T., Bayo, L.-A., Merwaha, E., Ishaq, T., Hanley, S., Deacon, B., Hibbert, M., Pothecary, C., Tetla, D., Woodford, C., Durga, L., Kennard-Holden, G., Branney, D., Frankham, J., Pitts, S., White, Nigel, Laha, S., Verlander, M., Williams, Alexandra, Altabaibeh, A., Alvaro, A., Gilbert, K., Ma, L., Mostoles,

L., Parmar, C., Simpson, Kathryn, Jetha, C., Booker, L., Pratley, A., Adams, C., Agasou, A., Arden, T., Bowes, A., Boyle, P., Beekes, M., Button, H., Capps, N., Carnahan, M., Carter, A., Childs, D., Donaldson, D., Hard, K., Hurford, F., Hussain, Y., Javaid, A., Jones, James, Jose, S., Leigh, M., Martin, T., Millward, H., Motherwell, N., Rikunenko, R., Stickley, J., Summers, J., Ting, L., Tivenan, H., Tonks, L., Wilcox, R., Skinner, D., Gaylard, J., Mullan, D., Newman, J., Holland, M., Keenan, N., Lyons, M., Wassall, H., Marsh, C., Mahenthran, M., Carter, E., Kong, T., Blackman, H., Creagh-Brown, B., Donlon, S., Michalak-Glinska, N., Mtuwa, S., Pristopan, V., Salberg, A., Smith, E., Stone, S., Piercy, C., Verula, J., Burda, D., Montaser, R., Harden, L., Mayangao, I., Marriott, C., Bradley, P., Harris, C., Anderson, Susan, Andrews, E., Birch, Janine, Collins, Emma, Hammerton, K., O'Leary, R., Clark, Michele, Purvis, S., Barber, R., Hewitt, C., Hilldrith, A., Jackson-Lawrence, K., Shepardson, S., Wills, M., Butler, S., Tavares, S., Cunningham, A., Hindale, J., Arif, S., Bean, S., Burt, K., Spivey, M., Demetriou, C., Eckbad, C., Hierons, S., Howie, L., Mitchard, S., Ramos, L., Serrano-Ruiz, A., White, K., Kelly, F., Cristiano, D., Dormand, N., Farzad, Z., Gummadi, M., Liyanage, K., Patel, Brijesh, Salmi, S., Sloane, G., Thwaites, V., Varghese, M., Zborowski, A.C., Allan, J., Geary, T., Houston, G., Meikle, A., O'Brien, P., Forsey, M., Kaliappan, A., Nicholson, Anne, Riches, J., Vertue, M., Allan, E., Darlington, K., Davies, F., Easton, J., Kumar, S., Lean, R., Menzies, D., Pugh, R., Qiu, X., Davies, L., Williams, H., Scanlon, J., Davies, G., Mackay, C., Lewis, J., Rees, S., Oblak, M., Popescu, M., Thankachen, M., Higham, A., Simpson, Kerry, Craig, J., Baruah, R., Morris, S., Ferguson, S., Shepherd, A., Moore, L.S.P., Vizcaychipi, M.P., de Almeida Martins, L.G., Carungcong, J., Ali, I.A.M., Beaumont, K., Blunt, M., Coton, Z., Curgenven, H., Elsaadany, M., Fernandes, K., Mohamed Ally, S., Rangarajan, H., Sarathy, V., Selvanayagam, S., Vedage, D., White, M., Gill, M., Paul, P., Ratnam, V., Shelton, S., Wynter, I., Carmody, S., Page, V.J., Beith, C.M., Black, K., Clements, S., Morrison, A., Strachan, D., Taylor, Margaret, Clarkson, M., D'Sylva, S., Norman, K., Auld, F., Donnachie, J., Edmond, I., Prentice, L., Runciman, N., Salutous, D., Symon, L., Todd, A., Turner, P., Short, A., Sweeney, L., Murdoch, E., Senaratne, D., Hill, M., Kannan, T., Wild, L., Crawley, R., Crew, A., Cunningham, M., Daniels, A., Harrison, L., Hope, S., Inweregbu, K., Jones, S., Lancaster, N., Matthews, J., Nicholson, Alice, Wray, G., Langton, H., Prout, R., Watters, M., Novis, C., Barron, A., Collins, C., Kaul, S., Passmore, H., Prendergast, C., Reed, A., Rogers, P., Shokkar, R., Woodruff, M., Middleton, H., Polgar, O., Nolan, C., Thwaites, V., Mahay, K., Collier, Dawn, Hormis, A., Maynard, V., Graham, C., Walker, R., Knights, E., Price, A., Thomas, Alice, Thorpe, C., Behan, T., Burnett, C., Hatton, J., Heeney, E., Mitra, A., Newton, M., Pollard, R., Stead, R., Amin, V., Anastasescu, E., Anumakonda, V., Karthik, K., Kausar, R., Reid, K., Smith, Jacqueline, Imeson-Wood, J., Brown, Alison, Crickmore, V., Debreceni, G., Wilkins, J., Nicol, L., Khaliq, W., Reece-Anthony, R., Birt, M., Ghosh, A., Williams, E., Allen, L., Beranova, E., Crisp, N., Deery, J., Hazelton, T., Knight, A., Price, C., Tilbey, S., Turki, S., Turney, S., Cooper,

J., Finch, C., Liderth, S., Quinn, A., Waddington, N., Coventry, T., Fowler, S., MacMahon, M., McGregor, Amanda, Cowley, A., Highgate, J., Brown, Alison, Gregory, J., O'Connell, S., Smith, T., Barberis, L., Gopal, S., Harris, N., Lake, V., Metherell, S., Radford, E., Daniel, A., Finn, J., Saha, Rajnish, White, Nikki, Easthope, A., Donnison, P., Trim, F., Eapen, B., Birch, Jenny, Bough, L., Goodsell, J., Tutton, R., Williams, P., Williams, S., Winter-Goodwin, B., Nichol, Ailstair, Brickell, K., Smyth, M., Murphy, Lorna, Coetzee, S., Gales, A., Otahal, I., Raj, M., Sell, C., Hilltout, P., Evitts, J., Tyler, A., Waldron, J., Beesley, K., Board, S., Kubisz-Pudelko, A., Lewis, A., Perry, J., Pippard, L., Wood, D., Buckley, C., Barry, P., Flint, N., Rekha, P., Hales, D., Bunni, L., Jennings, C., Latif, M., Marshall, R., Subramanian, G., McGuigan, P.J., Wasson, C., Finn, S., Green, J., Collins, Erin, King, B., Campbell, Andy, Smuts, S., Duffield, J., Smith, O., Mallon, L., Watkins, C., Botfield, L., Butler, J., Dexter, C., Fletcher, J., Garg, A., Kuravi, A., Ranga, P., Virgilio, E., Belagodu, Z., Fuller, B., Gherman, A., Olufuwa, O., Paramsothy, R., Stuart, C., Oakley, N., Kamundi, C., Tyl, D., Collins, K., Silva, P., Taylor, J., King, L., Coates, C., Crowley, M., Wakefield, P., Beadle, J., Johnson, L., Sargeant, J., Anderson, M., Brady, A., Chan, R., Little, J., McIvor, S., Prady, H., Whittle, H., Mathew, B., Attwood, B., Parsons, P., Ward, G., Bremner, P., Joe, W., Tracy, B., Jim, R., Davies, E., Roche, L., Sathe, S., Dennis, C., McGregor, Alastair, Parris, V., Srikaran, S., Sukha, A., Campbell, R., Clarke, N., Whiteside, J., Mascarenhas, M., Donaldson, A., Matheson, J., Barrett, F., O'Hara, M., Okeefe, L., Bradley, C., Eastgate-Jackson, C., Filipe, H., Martin, D., Maharajh, A., Garcia, S.M., Pakou, G., De Neef, M., Dent, K., Horsley, E., Akhtar, M.N., Pearson, S., Potoczna, D., Spencer, S., Clapham, M., Harper, R., Poultney, U., Rice, P., Smith, T., Mutch, R., Barberis, L., Armstrong, L., Bates, H., Dooks, E., Farquhar, F., Hairsine, B., McParland, Chantal, Packham, S., Bi, R., Scholefield, B., Ashton, L., George, L., Twiss, S., Wright, D., Chablani, M., Kirkby, A., Netherton, K., Davies, K., O'Brien, L., Omar, Z., Otahal, I., Perkins, E., Lewis, T., Sutherland, I., Burns, K., Higham, A., Chandler, B., Elliott, K., Mallinson, J., Turnbull, A., Gondo, P., Hadebe, B., Kayani, A., Masunda, B., Anderson, T., Hawcutt, D., O'Malley, L., Rad, L., Rogers, N., Saunderson, P., Allison, K.S., Afolabi, D., Whitbread, J., Jones, D., Dore, R., Halkes, M., Mercer, P., Thornton, L., Dawson, J., Garrioch, S., Tolson, M., Aldridge, J., Kapoor, R., Loader, D., Castle, K., Humphreys, S., Tampsett, R., Mackintosh, K., Ayers, A., Harrison, W., North, J., Allibone, S., Genetu, R., Kasipandian, V., Patel, A., Mac, A., Murphy, A., Mahjoob, P., Nazari, R., Worsley, L., Fagan, A., Bemand, T., Black, E., Dela Rosa, A., Howle, R., Jhanji, S., Baikady, R.R., Tatham, K.C., Thomas, B., Bell, D., Boyle, R., Douglas, K., Glass, L., Lee, E., Lennon, L., Rattray, A., Taylor, A., Hughes, R.A., Thomas, H., Rees, A., Duskova, M., Phipps, J., Brooks, S., Edwards, M., Parris, V., Quaid, S., Watson, E., Brayne, A., Fisher, E., Hunt, Jane, Jackson, P., Kaye, D., Love, N., Parkin, J., Tuckey, V., van Koutrik, L., Carter, S., Andrew, B., Findlay, L., Adams, K., Service, J., Williams, Alison, Cheyne, C., Saunderson, A., Moultrie, S., Odam, M., Hall, K., Mapfunde, I.,

Willis, C., Lyon, A., Sri-Chandana, C., Scherewode, J., Stephenson, L., Marsh, S., Brealey, D., Hardy, J., Houlden, H., Moncur, E., Raith, E., Tariq, A., Tucci, A., Hobrok, M., Loosley, R., McGuinness, H., Tench, H., Wolf-Roberts, R., Irvine, V., Shelley, B., Easthope, A., Gorman, C., Gupta, A., Timlick, E., Brady, R., Milligan, B., Bellini, A., Bryant, J., Mayer, A., Pickard, A., Roe, N., Sowter, J., Howlett, A., Fidler, K., Tagliavini, E., Donnelly, K., Shelton, J.F., Shastri, A.J., Ye, C., Weldon, C.H., Filshtein-Sonmez, T., Coker, D., Symons, A., Esparza-Gordillo, J., Aslibekyan, S., Auton, A., Pathak, G.A., Karjalainen, J., Stevens, C., Andrews, S.J., Kanai, M., Cordioli, M., Polimanti, R., Pirinen, M., Harerimana, N., Veerapen, K., Wolford, B., Nguyen, H., Solomonson, M., Liao, R.G., Chwialkowska, K., Trankiem, A., Balaconis, M.K., Hayward, C., Richmond, A., Campbell, Archie, Morris, M., Fawns-Ritchie, C., Glessner, J.T., Shaw, D.M., Chang, X., Polikowski, H., Petty, L.E., Chen, H.-H., Wanying, Z., Hakonarson, H., Porteous, D.J., Below, J., North, K., McCormick, J.B., Timmers, P.R.H.J., Wilson, J.F., Tenesa, A., D'Mellow, K., Kerr, S.M., Niemi, M.E.K., Nkambul, Lindokuhle, von Hohenstaufen, K.A., Sobh, A., Eltoukhy, M.M., Yassen, A.M., Hegazy, M.A.F., Okasha, K., Eid, M.A., Moahmed, H.S., Shahin, D., El-Sherbiny, Y.M., Elhadidy, T.A., Abd Elghafar, M.S., El-Jawhari, J.J., Mohamed, A.A.S., Elnagdy, M.H., Samir, A., Abdel-Aziz, M., Khafaga, W.T., El-Lawaty, W.M., Torky, M.S., El-shanshory, M.R., Batini, C., Lee, P.H., Shrine, N., Williams, A.T., Tobin, M.D., Guyatt, A.L., John, C., Packer, R.J., Ali, Altaf, Free, R.C., Wang, X., Wain, L. V., Hollox, E.J., Venn, L.D., Bee, C.E., Adams, E.L., Niavarani, A., Sharififard, B., Aliannejad, R., Amirsavadkouhi, A., Naderpour, Z., Tadi, H.A., Aleagha, A.E., Ahmadi, S., Moghaddam, S.B.M., Adamsara, A., Saeedi, M., Abdollahi, H., Hosseini, A., Chariyavilaskul, P., Chamnanphon, M., Suttichet, T.B., Shotelersuk, V., Pongpanich, M., Phokaew, C., Chetruengchai, W., Jantarabenjakul, W., Putchareon, O., Torvorapanit, P., Puthanakit, T., Suchartlikitwong, P., Hirankarn, N., Nilaratanakul, V., Sodsai, P., Brumpton, B.M., Hveem, K., Willer, C., Zhou, W., Rogne, T., Solligard, E., Åsvold, B.O., Abedalthagafi, M., Alaamery, M., Alqahtani, S., Barakeh, D., Al Harthi, F., Alsolm, E., Safieh, L.A., Alowayn, A.M., Alqubaishi, F., Al Mutairi, A., Mangul, S., Alshareef, A., Sawaji, M., Almutairi, M., Aljawini, N., Albesher, N., Arabi, Y.M., Mahmoud, E.S., Khattab, A.K., Halawani, R.T., Alahmadey, Z.Z., Albakri, J.K., Felemban, W.A., Suliman, B.A., Hasanato, R., Al-Awdah, L., Alghamdi, J., AlZahrani, D., AlJohani, S., Al-Afghani, H., Alrashed, M., AlDhawi, N., AlBardis, H., Alkwai, S., Alswailm, M., Almalki, F., Albeladi, M., Almohammed, I., Barhoush, E., Albader, A., Massadeh, S., AlMalik, A., Alotaibi, S., Alghamdi, B., Jung, J., Fawzy, M.S., Lee, Y., Magnus, P., Trogstad, L.-I.S., Helgeland, Ø., Harris, J.R., Mangino, M., Spector, T.D., Duncan, Emma, Smieszek, S.P., Przychodzen, B.P., Polymeropoulos, C., Polymeropoulos, V., Polymeropoulos, M.H., Fernandez-Cadenas, I., Perez-Tur, J., Llucià-Carol, L., Cullell, N., Muiño, E., Cárcel-Márquez, J., DeDiego, M.L., Iglesias, L.L., Planas, A.M., Soriano, A., Rico, V., Agüero, D., Bedini, J.L., Lozano, F., Domingo, C., Robles, V., Ruiz-Jaén, F., Márquez, L.,

288

Gomez, J., Coto, E., Albaiceta, G.M., García-Clemente, M., Dalmau, D., Arranz, M.J., Dietl, B., Serra-Llovich, A., Soler, P., Colobrán, R., Martín-Nalda, A., Martínez, A.P., Bernardo, D., Rojo, S., Fiz-López, A., Arribas, E., de la Cal-Sabater, P., Segura, T., González-Villa, E., Serrano-Heras, G., Martí-Fàbregas, J., Jiménez-Xarrié, E., de Felipe Mimbrera, A., Masjuan, J., García-Madrona, S., Domínguez-Mayoral, A., Villalonga, J.M., Menéndez-Valladares, P., Chasman, D.I., Buring, J.E., Ridker, P.M., Franco, G., Sesso, H.D., Manson, J.E., Glessner, J.R., Hakonarson, H., Medina-Gomez, C., Uitterlinden, A.G., Ikram, M.A., Kristiansson, K., Koskelainen, S., Perola, M., Donner, K., Kivinen, K., Palotie, A., Ripatti, S., Ruotsalainen, S., Kaunisto, M., Nakanishi, T., Butler-Laporte, G., Forgetta, V., Morrison, D.R., Ghosh, B., Laurent, L., Belisle, A., Henry, D., Abdullah, T., Adeleye, O., Mamlouk, N., Kimchi, N., Afrasiabi, Z., Rezk, N., Vulesevic, B., Bouab, M., Guzman, C., Petitjean, L., Tselios, C., Xue, X., Schurr, E., Afilalo, J., Afilalo, M., Oliveira, M., Brenner, B., Lepage, P., Ragoussis, J., Auld, D., Brassard, N., Durand, M., Chassé, M., Kaufmann, D.E., Lathrop, G.M., Mooser, V., Richards, J.B., Li, R., Adra, D., Rahmouni, S., Georges, M., Moutschen, M., Misset, B., Darcis, G., Guiot, J., Guntz, J., Azarzar, S., Gofflot, S., Beguin, Y., Claassen, S., Malaise, O., Huynen, P., Meuris, C., Thys, M., Jacques, J., Léonard, P., Frippiat, F., Giot, J.-B., Sauvage, A.-S., von Frenckell, C., Belhaj, Y., Lambermont, B., Pigazzini, S., Nkambule, L., Daya, M., Shortt, J., Rafaels, N., Wicks, S.J., Crooks, K., Barnes, K.C., Gignoux, C.R., Chavan, S., Laisk, T., Läll, K., Lepamets, M., Mägi, R., Esko, T., Reimann, E., Milani, L., Alavere, H., Metsalu, K., Puusepp, M., Metspalu, A., Naaber, P., Laane, E., Pesukova, J., Peterson, P., Kisand, K., Tabri, J., Allos, R., Hensen, K., Starkopf, J., Ringmets, I., Tamm, A., Kallaste, A., Bochud, P.-Y., Rivolta, C., Bibert, S., Quinodoz, M., Kamdar, D., Boillat, N., Nussle, S.G., Albrich, W., Suh, N., Neofytos, D., Erard, V., Voide, C., de Cid, R., Galván-Femenía, I., Blay, N., Carreras, A., Cortés, B., Farré, X., Sumoy, L., Moreno, V., Mercader, J.M., Guindo-Martinez, M., Torrents, D., Kogevinas, M., Garcia-Aymerich, J., Castaño-Vinyals, G., Dobaño, C., Renieri, A., Mari, F., Fallerini, C., Daga, S., Benetti, E., Baldassarri, M., Fava, F., Frullanti, E., Valentino, F., Doddato, G., Giliberti, A., Tita, R., Amitrano, S., Bruttini, M., Croci, S., Meloni, I., Mencarelli, M.A., Rizzo, C. Lo, Pinto, A.M., Beligni, G., Tommasi, A., Di Sarno, L., Palmieri, M., Carriero, M.L., Alaverdian, D., Busani, S., Bruno, R., Vecchia, M., Belli, M.A., Picchiotti, N., Sanarico, M., Gori, M., Furini, S., Mantovani, S., Ludovisi, S., Mondelli, M.U., Castelli, F., Quiros-Roldan, E., Antoni, M.D., Zanella, I., Vaghi, M., Rusconi, S., Siano, M., Montagnani, F., Emiliozzi, A., Fabbiani, M., Rossetti, B., Bargagli, E., Bergantini, L., D'Alessandro, M., Cameli, P., Bennett, D., Anedda, F., Marcantonio, S., Scolletta, S., Franchi, F., Mazzei, M.A., Guerrini, S., Conticini, E., Cantarini, L., Frediani, B., Tacconi, D., Spertilli, C., Feri, M., Donati, A., Scala, R., Guidelli, L., Spargi, G., Corridi, M., Nencioni, C., Croci, L., Bandini, M., Caldarelli, G.P., Piacentini, P., Desanctis, E., Cappelli, S., Canaccini, A., Verzuri, A., Anemoli, V., Ognibene, A., Pancrazzi, A., Lorubbio, M., D'Arminio Monforte, A., Miraglia, F.G.,

Girardis, M., Venturelli, S., Cossarizza, A., Antinori, A., Vergori, A., Gabrieli, A., Riva, A., Francisci, D., Schiaroli, E., Paciosi, F., Scotton, P.G., Andretta, F., Panese, S., Scaggiante, R., Gatti, F., Parisi, S.G., Baratti, S., Della Monica, M., Piscopo, C., Capasso, M., Russo, R., Andolfo, I., Iolascon, A., Fiorentino, G., Carella, M., Castori, M., Merla, G., Squeo, G.M., Aucella, F., Raggi, P., Marciano, C., Perna, R., Bassetti, M., Di Biagio, A., Sanguinetti, M., Masucci, L., Valente, S., Mandalà, M., Giorli, A., Salerni, L., Zucchi, P., Parravicini, P., Menatti, E., Trotta, T., Giannattasio, F., Coiro, G., Lena, F., Coviello, D.A., Mussini, C., Martinelli, E., Mancarella, S., Tavecchia, L., Crotti, L., Gabbi, C., Rizzi, M., Maggiolo, F., Ripamonti, D., Bachetti, T., La Rovere, M.T., Sarzi-Braga, S., Bussotti, M., Ceri, S., Pinoli, P., Raimondi, F., Biscarini, F., Stella, A., Zguro, K., Capitani, K., Suardi, C., Dei, S., Parati, G., Ravaglia, S., Artuso, R., Bottà, G., Di Domenico, P., Rancan, I., Perrella, A., Bianchi, F., Romani, D., Bergomi, P., Catena, E., Colombo, R., Tanfoni, M., Vincenti, A., Ferri, C., Grassi, D., Pessina, G., Tumbarello, M., Di Pietro, M., Sabrina, R., Luchi, S., Barbieri, C., Acquilini, D., Andreucci, E., Segala, F.V., Tiseo, G., Falcone, M., Lista, M., Poscente, M., De Vivo, O., Petrocelli, P., Guarnaccia, A., Baroni, S., Smith, A. V., Boughton, A.P., Li, K.W., LeFaive, J., Annis, A., Justice, A.E., Mirshahi, T., Chittoor, G., Josyula, N.S., Kosmicki, J.A., Ferreira, M.A.R., Leader, J.B., Carey, D.J., Gass, M.C., Horowitz, J.E., Cantor, M.N., Yadav, A., Baras, A., Abecasis, G.R., van Heel, D.A., Hunt, K.A., Mason, D., Huang, Q.Q., Finer, S., Trivedi, B., Griffiths, C.J., Martin, H.C., Wright, J., Trembath, R.C., Soranzo, N., Zhao, J.H., Butterworth, A.S., Danesh, J., Di Angelantonio, E., Franke, L., Boezen, M., Deelen, P., Claringbould, A., Lopera, E., Warmerdam, R., Vonk, J.M., van Blokland, I., Lanting, P., Ori, A.P.S., Zöllner, S., Wang, J., Beck, A., Peloso, G., Ho, Y.-L., Sun, Y. V., Huffman, J.E., O'Donnell, C.J., Cho, K., Tsao, P., Gaziano, J.M., Nivard, M., de Geus, E., Bartels, M., Jan Hottenga, J., Weiss, S.T., Karlson, E.W., Smoller, J.W., Green, R.C., Feng, Y.-C.A., Mercader, J., Murphy, S.N., Meigs, J.B., Woolley, A.E., Perez, E.F., Rader, D., Verma, A., Ritchie, M.D., Li, B., Verma, S.S., Lucas, A., Bradford, Y., Zeberg, H., Frithiof, R., Hultström, M., Lipcsey, M., Nkambul, Lindo, Tardif, N., Rooyackers, O., Grip, J., Maricic, T., Karczewski, K.J., Atkinson, E.G., Tsuo, K., Baya, N., Turley, P., Gupta, R., Callier, S., Walters, R.K., Palmer, D.S., Sarma, G., Cheng, N., Lu, W., Bryant, S., Churchhouse, C., Cusick, C., Goldstein, J.I., King, D., Seed, C., Finucane, H., Martin, A.R., Satterstrom, F.K., Wilson, D.J., Armstrong, J., Rudkin, J.K., Band, G., Earle, S.G., Lin, S.-K., Arning, N., Crook, D.W., Wyllie, D.H., O'Connell, A.M., Spencer, C.C.A., Koelling, N., Caulfield, M.J., Scott, R.H., Fowler, T., Moutsianas, L., Kousathanas, A., Pasko, D., Walker, Susan, Rendon, A., Stuckey, A., Odhams, C.A., Rhodes, D., Chan, G., Arumugam, P., Ball, C.A., Hong, E.L., Rand, K., Girshick, A., Guturu, H., Baltzell, A.H., Roberts, G., Park, D., Coignet, M., McCurdy, S., Knight, S., Partha, R., Rhead, B., Zhang, M., Berkowitz, N., Gaddis, M., Noto, K., Ruiz, L., Pavlovic, M., Sloofman, L.G., Charney, A.W., Beckmann, N.D., Schadt, E.E., Jordan, D.M., Thompson, R.C., Gettler, K., Abul-Husn, N.S., Ascolillo, S., Buxbaum, J.D.,

Chaudhary, K., Cho, J.H., Itan, Y., Kenny, E.E., Belbin, G.M., Sealfon, S.C., Sebra, R.P., Salib, I., Collins, B.L., Levy, T., Britvan, B., Keller, K., Tang, L., Peruggia, M., Hiester, L.L., Niblo, K., Aksentijevich, A., Labkowsky, A., Karp, A., Zlatopolsky, M., Preuss, M., Loos, R.J.F., Nadkarni, G.N., Do, R., Hoggart, C., Choi, S., Underwood, S.J., O'Reilly, P., Huckins, L.M., Zyndorf, M., Daly, M.J., Neale, B.M., Ganna, A., Fawkes, A., Murphy, Lee, Rowan, K., Ponting, C.P., Vitart, V., Wilson, J.F., Yang, J., Bretherick, A.D., Scott, R.H., Hendry, S.C., Moutsianas, L., Law, A., Caulfield, M.J., Baillie, J.K., 2022. Whole-genome sequencing reveals host factors underlying critical COVID-19. Nat. 2022 6077917 607, 97–103. https://doi.org/10.1038/s41586-022-04576-6

Kovacs, R., Csenki, Z., Bakos, K., Urbanyi, B., Horvath, A., Garaj-Vrhovac, V., Gajski, G., Geric, M., Negreira, N., Lopez de Alda, M., Barcelo, D., Heath, E., Kosjek, T., Zegura, B., Novak, M., Zajc, I., Baebler, S., Rotter, A., Ramsak, Z., Filipic, M., 2015. Assessment of toxicity and genotoxicity of low doses of 5-fluorouracil in zebrafish (Danio rerio) two-generation study. Water Res 77, 201–212. https://doi.org/10.1016/j.watres.2015.03.025

Krašovec, R., Belavkin, R. V., Aston, J.A.D., Channon, A., Aston, E., Rash, B.M., Kadirvel, M., Forbes, S., Knight, C.G., 2014. Mutation rate plasticity in rifampicin resistance depends on Escherichia coli cell-cell interactions. Nat. Commun. 5. https://doi.org/10.1038/NCOMMS4742

Kumagai, T., Nakano, T., Maruyama, M., Mochizuki, H., Sugiyama, M., 1999. Characterization of the bleomycin resistance determinant encoded on the transposon Tn5 - ScienceDirect 442. https://doi.org/10.1016/S0014-5793(98)01613-5

Kurylo, C.M., Alexander, N., Dass, R.A., Parks, M.M., Altman, R.A., Vincent, C.T., Mason, C.E., Blanchard, S.C., 2016. Genome Sequence and Analysis of Escherichia coli MRE600, a Colicinogenic, Nonmotile Strain that Lacks RNase I and the Type I Methyltransferase, EcoKI. Genome Biol. Evol. 8, 742–752. https://doi.org/10.1093/GBE/EVW008

Kussell, E., Kishony, R., Balaban, N.Q., Leibler, S., 2005. Bacterial persistence: a model of survival in changing environments. Genetics 169, 1807–1814. https://doi.org/10.1534/genetics.104.035352

Kwong, J.C., Mccallum, N., Sintchenko, V., Howden, B.P., 2015. Whole genome sequencing in clinical and public health microbiology. Pathology 47, 199. https://doi.org/10.1097/PAT.0000000000000235

Lafontaine, D.L., Yang, L., Dekker, J., Gibcus, J.H., 2021. Hi-C 3.0: Improved Protocol for Genome-Wide Chromosome Conformation Capture. Curr. Protoc. 1, e198. https://doi.org/10.1002/CPZ1.198

Lagendijk, E.L., Validov, S., Lamers, G.E., de Weert, S., Bloemberg, G. V, 2010. Genetic tools for tagging Gram-negative bacteria with mCherry for visualization in vitro and in natural habitats, biofilm and pathogenicity studies. FEMS Microbiol Lett 305, 81–90. https://doi.org/10.1111/j.1574-6968.2010.01916.x

Lázár, V., Nagy, I., Spohn, R., Csörgő, B., Györkei, Á., Nyerges, Á., Horváth, B., Vörös, A., Busa-Fekete, R., Hrtyan, M., Bogos, B., Méhi, O., Fekete, G., Szappanos, B., Kégl, B., Papp, B., Pál, C., 2014. Genome-wide analysis captures the determinants of the antibiotic cross-resistance interaction network. Nat. Commun. 5. https://doi.org/10.1038/ncomms5352

Le, T.B.K., Imakaev, M. V., Mirny, L.A., Laub, M.T., 2013. High-resolution mapping of the spatial organization of a bacterial chromosome. Science (80-.). 342, 731–734. https://doi.org/10.1126/SCIENCE.1242059/SUPPL_FILE/LE.SM.PDF

Lee, H., Popodi, E., Tang, H., Foster, P.L., 2012. Rate and molecular spectrum of spontaneous mutations in the bacterium Escherichia coli as determined by whole-genome sequencing. Proc. Natl. Acad. Sci. 109, E2774–E2783. https://doi.org/10.1073/PNAS.1210309109

Lee, I., Razaghi, R., Gilpatrick, T., Molnar, M., Sadowski, N., Simpson, J.T., Sedlazeck J., F., Timp, W., 2018. Simultaneous profiling of chromatin accessibility and methylation on human cell lines with nanowire sequencing. bioRxiv.

Levin-Reisman, I., Ronin, I., Gefen, O., Braniss, I., Shoresh, N., Balaban, N.Q., 2017. Antibiotic tolerance facilitates the evolution of resistance. Science (80-.). 355, 826–830. https://doi.org/10.1126/science.aaj2191

Li, S., Li, T., Xu, Y., Zhang, Q., Zhang, W., Che, S., Liu, R., Wang, Y., Bartlam, M., 2015. Structural insights into YfiR sequestering by YfiB in Pseudomonas aeruginosa PAO1. Sci. Rep. 5. https://doi.org/10.1038/srep16915

Li, T., Garcia-Gutierrez, E., Yara, D.A., Scadden, J., Davies, J., Hutchins, C., Aydin, A., O'Grady, J., Narbad, A., Romano, S., Sayavedra, L., 2021. An optimised protocol for detection of SARS-CoV-2 in stool. BMC Microbiol. 21. https://doi.org/10.1186/S12866-021-02297-W

Li, X., Bosch-Tijhof, C.J., Wei, X., de Soet, J.J., Crielaard, W., Loveren, C. van, Deng, D.M., 2020. Efficiency of chemical versus mechanical disruption methods of DNA extraction for the identification of oral Gram-positive and Gram-negative bacteria. J. Int. Med. Res. 48, 1–12. https://doi.org/10.1177/0300060520925594

Lieberman-Aiden, E., Van Berkum, N.L., Williams, L., Imakaev, M., Ragoczy, T., Telling, A., Amit, I., Lajoie, B.R., Sabo, P.J., Dorschner, M.O., Sandstrom, R., Bernstein, B., Bender, M.A., Groudine, M., Gnirke, A., Stamatoyannopoulos, J., Mirny, L.A., Lander, E.S., Dekker, J.,

2009. Comprehensive mapping of long-range interactions reveals folding principles of the human genome. Science (80-.). 326, 289–293. https://doi.org/10.1126/science.1181369

Lin, D., Hong, P., Zhang, S., Xu, W., Jamal, M., Yan, K., Lei, Y., Li, L., Ruan, Y., Fu, Z.F., Li, G., Cao, G., 2018. Digestion-ligation-only Hi-C is an efficient and cost-effective method for chromosome conformation capture. Nat. Genet. 50, 754–763. https://doi.org/10.1038/s41588-018-0111-2

Lipworth, S., Pickford, H., Sanderson, N., Chau, K.K., Kavanagh, J., Barker, L., Vaughan, A., Swann, J., Andersson, M., Jeffery, K., Morgan, M., Peto, T.E.A., Crook, D.W., Stoesser, N., Walker, A.S., 2020. Optimized use of oxford nanopore flowcells for hybrid assemblies. Microb. Genomics 6, 1–12. https://doi.org/10.1099/mgen.0.000453

Liu, C., Qin, S., Xu, L., Xu, L., Zhao, D., Liu, X., Lang, S., Feng, X., Liu, H.M., 2015. New Delhi Metallo-β-Lactamase 1(NDM-1), the Dominant Carbapenemase Detected in Carbapenem-Resistant Enterobacter cloacae from Henan Province, China 10. https://doi.org/10.1371/journal.pone.0135044

Liu, M., Darling, A., 2015. Metagenomic Chromosome Conformation Capture (3C): Techniques, applications, and challenges. F1000Research 4, 1–9. https://doi.org/10.12688/f1000research.7281.1

Liu, Z., Li, W., Wang, J., Pan, J., Sun, S., Yu, Y., Zhao, B., Ma, Y., Zhang, T., Qi, J., Liu, G., Lu, F., 2013. Identification and Characterization of the First Escherichia Coli Strain Carrying NDM-1 Gene in China. PLoS One 8. https://doi.org/10.1371/journal.pone.0066666

Lopatkin, A.J., Huang, S., Smith, R.P., Srimani, J.K., Sysoeva, T.A., Bewick, S., Karig, D.K., You, L., 2016. Antibiotics as a selective driver for conjugation dynamics. Nat. Microbiol. 2016 16 1, 1–8. https://doi.org/10.1038/nmicrobiol.2016.44

López, C., Prunotto, A., Bahr, G., Bonomo, R.A., González, L.J., Peraro, M.D., Vila, A.J., 2021. Specific protein-membrane interactions promote the export of metallo-β-lactamases via outer membrane vesicles. bioRxiv 2021.03.18.436108. https://doi.org/10.1101/2021.03.18.436108

Lopez, E., Elez, M., Matic, I., Blazquez, J., 2007. Antibiotic-mediated recombination: ciprofloxacin stimulates SOS-independent recombination of divergent sequences in Escherichia coli. Mol Microbiol 64, 83–93. https://doi.org/10.1111/j.1365-2958.2007.05642.x

Lu, H., Giordano, F., Ning, Z., 2016. Oxford Nanopore MinION Sequencing and Genome Assembly. Genomics, Proteomics Bioinforma. 14, 265–279. https://doi.org/10.1016/j.gpb.2016.05.004

Lu, L., Liu, X., Peng, J., Li, Y., Jin, F., 2018. Easy Hi-C: A simple efficient protocol for 3D genome mapping in small cell populations. bioRxiv 245688. https://doi.org/10.1101/245688

Ma, D., Mandell, J.B., Donegan, N.P., Cheung, A.L., Ma, W., Rothenberger, S., Shanks, R.M.Q., Richardson, A.R., Urish, K.L., 2019. The Toxin-Antitoxin MazEF Drives Staphylococcus Aureus Biofilm Formation, Antibiotic Tolerance, and Chronic Infection. MBio 10. https://doi.org/10.1128/mBio.01658-19

Ma, W., Ay, F., Lee, C., Gulsoy, G., Deng, X., Cook, S., Hesson, J., Cavanaugh, C., Ware, C.B., Krumm, A., Shendure, J., Blau, C.A., Disteche, C.M., Noble, W.S., Duan, Z., 2018. Using DNase Hi-C techniques to map global and local three-dimensional genome architecture at high resolution. Methods 142, 59–73. https://doi.org/10.1016/j.ymeth.2018.01.014

Madan, R., Kolter, R., Mahadevan, S., 2005. Mutations that activate the silent bgl operon of Escherichia coli confer a growth advantage in stationary phase. J Bacteriol 187, 7912–7917. https://doi.org/10.1128/jb.187.23.7912-7917.2005

Maghini, D.G., Moss, E.L., Vance, S.E., Bhatt, A.S., 2021. Improved high-molecular-weight DNA extraction, nanopore sequencing and metagenomic assembly from the human gut microbiome. Nat. Protoc. 16, 458–471. https://doi.org/10.1038/S41596-020-00424-X

Mahnik, S.N., Lenz, K., Weissenbacher, N., Mader, R.M., Fuerhacker, M., 2007. Fate of 5-fluorouracil, doxorubicin, epirubicin, and daunorubicin in hospital wastewater and their elimination by activated sludge and treatment in a membrane-bio-reactor system - ScienceDirect 66. https://doi.org/10.1016/j.chemosphere.2006.05.051

Malone, J.G., Jaeger, T., Spangler, C., Ritz, D., Spang, A., Arrieumerlou, C., Kaever, V., Landmann, R., Jenal, U., 2010. YfiBNR mediates cyclic di-GMP dependent small colony variant formation and persistence in Pseudomonas aeruginosa. PLoS Pathog 6, e1000804. https://doi.org/10.1371/journal.ppat.1000804

Mangalappalli-Illathu, A.K., Korber, D.R., 2006. Adaptive Resistance and Differential Protein Expression of Salmonella enterica Serovar Enteritidis Biofilms Exposed to Benzalkonium Chloride. Antimicrob. Agents Chemother. 50, 3588. https://doi.org/10.1128/AAC.00573-06

Mantilla-Calderon, D., Jumat, M.R., Wang, T., Pugalenthi, G., Nada, A.-J., Hong, P.-Y., 2016. Isolation and Characterization of NDM-Positive Escherichia coli from Municipal Wastewater in Jeddah, Saudi Arabia. Antimicrob. Agents Chemother. 6, 5223–5231. https://doi.org/10.1128/AAC.00236-16

Marbouty, M., Cournac, A., Flot, J.F., Marie-Nelly, H., Mozziconacci, J., Koszul, R., 2014. Metagenomic chromosome conformation capture (meta3C) unveils the diversity of

chromosome organization in microorganisms. Elife 3, e03318. https://doi.org/10.7554/eLife.03318

Mattiuzzo, M., Bandiera, A., Gennaro, R., Benincasa, M., Pacor, S., Antcheva, N., Scocchi, M., 2007. Role of the Escherichia coli SbmA in the antimicrobial activity of proline-rich peptides. Mol Microbiol 66, 151–163. https://doi.org/10.1111/j.1365-2958.2007.05903.x

Maxmen, A., 2021. One million coronavirus sequences: popular genome site hits mega milestone. Nature 593, 21. https://doi.org/10.1038/D41586-021-01069-W

Mazodier, P., Cossart, P., Giraud, E., Gasser, F., 1985. Completion of the nucleotide sequence of the central region of Tn5 confirms the presence of three resistance genes. Nucleic Acids Res 13, 195–205.

McInnes, R.S., uz-Zaman, M.H., Alam, I.T., Ho, S.F.S., Moran, R.A., Clemens, J.D., Islam, M.S., Schaik, W. van, 2021. Microbiota analysis of rural and urban surface waters and sediments in Bangladesh identifies human waste as driver of antibiotic resistance. https://doi.org/10.1101/2021.02.04.429629

McVicker, G., Prajsnar, T.K., Williams, A., Wagner, N.L., Boots, M., Renshaw, S.A., Foster, S.J., 2014. Clonal Expansion during Staphylococcus aureus Infection Dynamics Reveals the Effect of Antibiotic Intervention. PLoS Pathog. 10. https://doi.org/10.1371/journal.ppat.1003959

Melnyk, A.H., Wong, A., Kassen, R., 2015. The fitness costs of antibiotic resistance mutations. Evol. Appl. 8, 273. https://doi.org/10.1111/EVA.12196

Meunier, A., Nerich, V., Fagoni-Legat, C., Richard, M., Mazel, D., Adotevi, O., Bertrand, X., Hocquet, D., 2019. Enhanced emergence of antibiotic-resistant pathogenic bacteria after in vitro induction with cancer chemotherapy drugs. J. Antimicrob. Chemother. 74, 1572–1577.

Miller, K., O'Neill, A.J., Chopra, I., 2002. Response of Escherichia coli hypermutators to selection pressure with antimicrobial agents from different classes. J. Antimicrob. Chemother. 49, 925–934. https://doi.org/10.1093/jac/dkf044

Minato, Y., Dawadi, S., Kordus, S.L., Sivanandam, A., Aldrich, C.C., Baughn, A.D., 2018. Mutual potentiation drives synergy between trimethoprim and sulfamethoxazole. Nat. Commun. 2018 91 9, 1–7. https://doi.org/10.1038/s41467-018-03447-x

Moore, C.W., 1978. Bleomycin-induced mutation and recombination in Saccharomyces cerevisiae. - Abstract - Europe PMC. Mutat. Res. 58, 41–49. https://doi.org/https://doi.org/10.1016/0165-1218(78)90094-0

Mori, T., Mizuta, S., Suenaga, H., Miyazaki, K., 2008. Metagenomic Screening for Bleomycin Resistance Genes. Appl. Environ. Microbiol. 74, 6803–6805. https://doi.org/10.1128/AEM.00873-08

Mota-Gómez, I., Lupiáñez, D.G., 2019. A (3D-Nuclear) Space Odyssey: Making Sense of Hi-C Maps. Genes (Basel). 10, 415. https://doi.org/10.3390/genes10060415

Murray, C.J., Ikuta, K.S., Sharara, F., Swetschinski, L., Robles Aguilar, G., Gray, A., Han, C., Bisignano, C., Rao, P., Wool, E., Johnson, S.C., Browne, A.J., Chipeta, M.G., Fell, F., Hackett, S., Haines-Woodhouse, G., Kashef Hamadani, B.H., Kumaran, E.A.P., McManigal, B., Agarwal, R., Akech, S., Albertson, S., Amuasi, J., Andrews, J., Aravkin, A., Ashley, E., Bailey, F., Baker, S., Basnyat, B., Bekker, A., Bender, R., Bethou, A., Bielicki, J., Boonkasidecha, S., Bukosia, J., Carvalheiro, C., Castañeda-Orjuela, C., Chansamouth, V., Chaurasia, S., Chiurchiù, S., Chowdhury, F., Cook, A.J., Cooper, B., Cressey, T.R., Criollo-Mora, E., Cunningham, M., Darboe, S., Day, N.P.J., De Luca, M., Dokova, K., Dramowski, A., Dunachie, S.J., Eckmanns, T., Eibach, D., Emami, A., Feasey, N., Fisher-Pearson, N., Forrest, K., Garrett, D., Gastmeier, P., Giref, A.Z., Greer, R.C., Gupta, V., Haller, S., Haselbeck, A., Hay, S.I., Holm, M., Hopkins, S., Iregbu, K.C., Jacobs, J., Jarovsky, D., Javanmardi, F., Khorana, M., Kissoon, N., Kobeissi, E., Kostyanev, T., Krapp, F., Krumkamp, R., Kumar, A., Kyu, H.H., Lim, C., Limmathurotsakul, D., Loftus, M.J., Lunn, M., Ma, J., Mturi, N., Munera-Huertas, T., Musicha, P., Mussi-Pinhata, M.M., Nakamura, T., Nanavati, R., Nangia, S., Newton, P., Ngoun, C., Novotney, A., Nwakanma, D., Obiero, C.W., Olivas-Martinez, A., Olliaro, P., Ooko, E., Ortiz-Brizuela, E., Peleg, A.Y., Perrone, C., Plakkal, N., Ponce-de-Leon, A., Raad, M., Ramdin, T., Riddell, A., Roberts, T., Robotham, J.V., Roca, A., Rudd, K.E., Russell, N., Schnall, J., Scott, J.A.G., Shivamallappa, M., Sifuentes-Osornio, J., Steenkeste, N., Stewardson, A.J., Stoeva, T., Tasak, N., Thaiprakong, A., Thwaites, G., Turner, C., Turner, P., van Doorn, H.R., Velaphi, S., Vongpradith, A., Vu, H., Walsh, T., Waner, S., Wangrangsimakul, T., Wozniak, T., Zheng, P., Sartorius, B., Lopez, A.D., Stergachis, A., Moore, C., Dolecek, C., Naghavi, M., 2022. Global burden of bacterial antimicrobial resistance in 2019: a systematic analysis. Lancet 399, 629–655. https://doi.org/10.1016/S0140-6736(21)02724-0/ATTACHMENT/B227DEB3-FF04-497F-82AC-637D8AB7F679/MMC1.PDF

Murugan, N., Malathi, J., Umashankar, V., Madhavan, H.N., 2016. Unraveling genomic and phenotypic nature of multidrug-resistant (MDR) Pseudomonas aeruginosa VRFPA04 isolated from keratitis patient. Microbiol. Res. 193, 140–149. https://doi.org/https://doi.org/10.1016/j.micres.2016.10.002

Nagano, T., Lubling, Y., Stevens, T.J., Schoenfelder, S., Yaffe, E., Dean, W., Laue, E.D., Tanay, A.,

Fraser, P., 2013. Single-cell Hi-C reveals cell-to-cell variability in chromosome structure. Nature 502, 59–64. https://doi.org/10.1038/nature12593

Nagano, T., Várnai, C., Schoenfelder, S., Javierre, B.M., Wingett, S.W., Fraser, P., 2015. Comparison of Hi-C results using in-solution versus in-nucleus ligation. Genome Biol. 16, 1–13. https://doi.org/10.1186/s13059-015-0753-7

Napolitano, R., Janel-Bintz, R., Wagner, J., Fuchs, R., 2000. All three SOS-inducible DNA polymerases (Pol II, Pol IV and Pol V) are involved in induced mutagenesis. EMBO J. 19, 6259–6265. https://doi.org/10.1093/emboj/19.22.6259

Narayanan, S., JK, M., CS, R., Garcia-Bustos, J., JK, D., Roujeinikova, A., 2014. Mechanism of Escherichia coli resistance to Pyrrhocoricin. Antimicrob. Agents Chemother. 58. https://doi.org/10.1128/AAC.02565-13

Naumova, N., Smith, E.M., Zhan, Y., Dekker, J., 2012. Analysis of long-range chromatin interactions using Chromosome Conformation Capture. Methods 58, 192–203. https://doi.org/10.1016/J.YMETH.2012.07.022

NICE, 2021. Bleomycin [WWW Document]. Natl. Inst. Heal. Care Excell. URL https://bnf.nice.org.uk/drug/bleomycin.html

Niu, L., Shen, W., Huang, Y., He, N., Zhang, Y., Sun, J., Wan, J., Jiang, D., Yang, M., Tse, Y.C., Li, L., Hou, C., 2019. Amplification-free library preparation with SAFE Hi-C uses ligation products for deep sequencing to improve traditional Hi-C analysis. Commun. Biol. 2019 21 2, 1–8. https://doi.org/10.1038/s42003-019-0519-y

Norton, M.D., Spilkia, A.J., Godoy, V.G., 2013. Antibiotic Resistance Acquired through a DNA Damage-Inducible Response in Acinetobacter baumannii. J. Bacteriol. 195. https://doi.org/10.1128/JB.02176-12

O'Farrell, P.A., Gonzalez, F., Zheng, W., Johnston, S.A., Joshua-Tor, L., 1999. Crystal structure of human bleomycin hydrolase, a self-compartmentalizing cysteine protease. Structure 7, 619–627. https://doi.org/https://doi.org/10.1016/S0969-2126(99)80083-5

O'Neill, J., 2016. TACKLING DRUG-RESISTANT INFECTIONS GLOBALLY: FINAL REPORT AND RECOMMENDATIONS THE REVIEW ON ANTIMICROBIAL RESISTANCE CHAIRED BY JIM O'NEILL.

Ochoa, S.A., Cruz-Córdova, A., Luna-Pineda, V.M., Reyes-Grajeda, J.P., Cázares-Domínguez, V., Escalona, G., Sepúlveda-González, M.E., López-Montiel, F., Arellano-Galindo, J., López-Martínez, B., Parra-Ortega, I., Giono-Cerezo, S., Hernández-Castro, R., de la Rosa-Zamboni, D., Xicohtencatl-Cortes, J., 2016. Multidrug- and Extensively Drug-Resistant Uropathogenic

Escherichia coli Clinical Strains: Phylogenetic Groups Widely Associated with Integrons Maintain High Genetic Diversity. Front Microbiol 7. https://doi.org/10.3389/fmicb.2016.02042

Ofek, I., Cohen, S., Rahmani, R., Kabha, K., Tamarkin, D., Herzig, Y., Rubinstein, E., 1994. Antibacterial synergism of polymyxin B nonapeptide and hydrophobic antibiotics in experimental gram-negative infections in mice. Antimicrob Agents Chemother 38, 374–377.

Omadjela, O., Narahari, A., Strumillo, J., Mélida, H., Mazur, O., Bulone, V., Zimmer, J., 2013. BcsA and BcsB form the catalytically active core of bacterial cellulose synthase sufficient for in vitro cellulose synthesis. https://doi.org/10.1073/pnas.1314063110

Otto, K., Hermansson, M., 2004. Inactivation of ompX causes increased interactions of type 1 fimbriated Escherichia coli with abiotic surfaces. J Bacteriol 186, 226–234. https://doi.org/10.1128/jb.186.1.226-234.2004

Ou, F., McGoverin, C., Swift, S., Vanholsbeeck, F., 2017. Absolute bacterial cell enumeration using flow cytometry. J. Appl. Microbiol. 123, 464–477. https://doi.org/10.1111/jam.13508

Pál, C., Papp, B., Lázár, V., 2015. Collateral sensitivity of antibiotic-resistant microbes. Trends Microbiol. 23, 401–407. https://doi.org/10.1016/J.TIM.2015.02.009

Pal, S., Misra, A., Banerjee, S., Dam, B., 2020. Adaptation of ethidium bromide fluorescence assay to monitor activity of efflux pumps in bacterial pure cultures or mixed population from environmental samples. J. King Saud Univ. - Sci. 32, 939–945. https://doi.org/10.1016/J.JKSUS.2019.06.002

Palkova, Z., 2004. Multicellular microorganisms: laboratory versus nature. EMBO Rep. 5, 470. https://doi.org/10.1038/SJ.EMBOR.7400145

Papanicolas, L.E., Gordon, D.L., Wesselingh, S.L., Rogers, G.B., 2018. Not Just Antibiotics: Is Cancer Chemotherapy Driving Antimicrobial Resistance? Trends Microbiol 26, 393–400. https://doi.org/10.1016/j.tim.2017.10.009

Pautier, P., Gutierrez-Bonnaire, M., Rey, A., Sillet-Bach, I., Chevreau, C., Kerbrat, P., Morice, P., Duvillard, P., Lhomme, C., 2008. Combination of bleomycin, etoposide, and cisplatin for the treatment of advanced ovarian granulosa cell tumors. Int J Gynecol Cancer 18, 446–452.

Penesyan, A., IT, P., MR, G., Kjelleberg, S., MJ, M., 2020. Secondary Effects of Antibiotics on Microbial Biofilms. Front Microbiol 11. https://doi.org/10.3389/fmicb.2020.02109

Poirel, L., Lagrutta, E., Taylor, P., Pham, J., Nordmann, P., 2010. Emergence of metallo-beta-

lactamase NDM-1-producing multidrug-resistant Escherichia coli in Australia. Antimicrob Agents Chemother 54, 4914–4916. https://doi.org/10.1128/aac.00878-10

Poon, I.K.H., Baxter, A.A., Lay, F.T., Mills, G.D., Adda, C.G., Payne, J.A.E., Phan, T.K., Ryan, G.F., White, J.A., Veneer, P.K., van der Weerden, N.L., Anderson, M.A., Kvansakul, M., Hulett, M.D., 2014. Phosphoinositide-mediated oligomerization of a defensin induces cell lysis. Elife 2014. https://doi.org/10.7554/ELIFE.01808

Pope, C.F., O'Sullivan, D.M., McHugh, T.D., Gillespie, S.H., 2008. A Practical Guide to Measuring Mutation Rates in Antibiotic Resistance. https://doi.org/10.1128/AAC.01152-07

Porse, A., Jahn, L.J., Ellabaan, M.M.H., Sommer, M.O.A., 2020. Dominant resistance and negative epistasis can limit the co-selection of de novo resistance mutations and antibiotic resistance genes. Nat. Commun. 11, 1–9. https://doi.org/doi:10.1038/s41467-020-15080-8

Press, M.O., Wiser, A.H., Kronenberg, Z.N., Langford, K.W., Shakya, M., Lo, C.-C., Mueller, K.A., Sullivan, S.T., Chain, P.S.G., Liachko, I., 2017. Hi-C deconvolution of a human gut microbiome yields high-quality draft genomes and reveals plasmid-genome interactions. bioRxiv 198713. https://doi.org/10.1101/198713

Quoc Tuc, D., Elodie, M.-G., Pierre, L., Fabrice, A., Marie-Jeanne, T., Martine, B., Joelle, E., Marc, C., 2017. Fate of antibiotics from hospital and domestic sources in a sewage network. Sci. Total Environ. 575, 758–766. https://doi.org/https://doi.org/10.1016/j.scitotenv.2016.09.118

Rahman, M., Mukhopadhyay, C., RP, R., Singh, S., Gupta, S., Singh, A., Pathak, A., KN, P., 2018. Novel variant NDM-11 and other NDM-1 variants in multidrug-resistant Escherichia coli from South India. J Glob Antimicrob Resist 14. https://doi.org/10.1016/j.jgar.2018.04.001

Rahman, M., SK, S., KN, P., CM, O., BK, P., Tripathi, A., Singh, A., AK, S., Gonzalez-Zorn, B., 2014. Prevalence and molecular characterisation of New Delhi metallo-β-lactamases NDM-1, NDM-5, NDM-6 and NDM-7 in multidrug-resistant Enterobacteriaceae from India. Int J Antimicrob Agents 44. https://doi.org/10.1016/j.ijantimicag.2014.03.003

Ramadan, H., SK, G., Sharma, P., Ahmed, M., LM, H., JB, B., TA, W., JG, F., CR, J., 2020. Circulation of emerging NDM-5-producing Escherichia coli among humans and dogs in Egypt. Zoonoses Public Health 67. https://doi.org/10.1111/zph.12676

Rangarajan, N., Bakshi, S., Weisshaar, J.C., 2013. Localized permeabilization of E. coli membranes by the antimicrobial peptide Cecropin A. Biochemistry 52, 6584–6594. https://doi.org/10.1021/BI400785J/SUPPL_FILE/BI400785J_SI_002.PDF

Rao, S.S.P., Huntley, M.H., Durand, N.C., Stamenova, E.K., Bochkov, I.D., Robinson, J.T., Sanborn,

A.L., Machol, I., Omer, A.D., Lander, E.S., Aiden, E.L., 2014. A 3D map of the human genome at kilobase resolution reveals principles of chromatin looping. Cell 159, 1665–1680. https://doi.org/10.1016/j.cell.2014.11.021

Raterman, E.L., Shapiro, D.D., Stevens, D.J., Schwartz, K.J., Welch, R.A., 2013. Genetic analysis of the role of yfiR in the ability of Escherichia coli CFT073 to control cellular cyclic dimeric GMP levels and to persist in the urinary tract. Infect Immun 81, 3089–3098. https://doi.org/10.1128/iai.01396-12

Reese, M.G., 2001. Application of a time-delay neural network to promoter annotation in the Drosophila melanogaster genome. Comput. Chem. 26, 51–56. https://doi.org/10.1016/S0097-8485(01)00099-7

Rodríguez-Beltrán, J., DelaFuente, J., León-Sampedro, R., RC, M., Á, S.M., 2021. Beyond horizontal gene transfer: the role of plasmids in bacterial evolution. Nat. Rev. Microbiol. https://doi.org/10.1038/s41579-020-00497-1

Rolain, J.M., François, P., Hernandez, D., Bitter, F., Richet, H., Fournous, G., Mattenberger, Y., Bosdure, E., Stremler, N., Dubud, J.C., Sarles, J., M., R.-G., Boniface, S., Schrenzel, J., Raoult, D., 2009. Genomic analysis of an emerging multiresistant Staphylococcus aureus strain rapidly spreading in cystic fibrosis patients revealed the presence of an antibiotic inducible bacteriophage. Biol. Direct 4, 1. https://doi.org/10.1186/1745-6150-4-1

Salgado, L., Blank, S., Esfahani, R.A.M., Strap, J.L., Bonetta, D., 2019. Missense mutations in a transmembrane domain of the Komagataeibacter xylinus BcsA lead to changes in cellulose synthesis. BMC Microbiol. 19, 1–13. https://doi.org/doi:10.1186/s12866-019-1577-5

Sana, T., Laubier, A., Bleves, S., 2014. Gene Transfer: Conjugation. Methods Mol Biol 1149. https://doi.org/10.1007/978-1-4939-0473-0_3

Santos-Lopez, A., Marshall, C.W., Scribner, M.R., Snyder, D.J., Cooper, V.S., 2019. Evolutionary pathways to antibiotic resistance are dependent upon environmental structure and bacterial lifestyle. Elife 8. https://doi.org/10.7554/ELIFE.47612

Sausville, E.A., Peisach, J., Horwitz, S.B., 1978. Effect of chelating agents and metal ions on the degradation of DNA by bleomycin. https://doi.org/10.1021/bi00607a007

Savage, V.J., Chopra, I., O'Neill, A.J., 2013. Staphylococcus aureus Biofilms Promote Horizontal Transfer of Antibiotic Resistance. Antimicrob. Agents Chemother. 57. https://doi.org/10.1128/AAC.02008-12

Schembri, M.A., Kjærgaard, K., Klemm, P., 2003. Global gene expression in Escherichia coli biofilms. Mol. Microbiol. 48, 253–267. https://doi.org/10.1046/J.1365-2958.2003.03432.X

Schmidt, K., Mwaigwisya, S., Crossman, L.C., Doumith, M., Munroe, D., Pires, C., M. Khan, A., Woodford, N., Saunders, N.J., Wain, J., O'Grady, J., Livermore, D.M., 2017. Identification of bacterial pathogens and antimicrobial resistance directly from clinical urines by nanopore-based metagenomic sequencing. J. Antimicrob. Chemother. 72, 104–114. https://doi.org/10.1093/JAC/DKW397

Schwartz, D.R., Homanics, G.E., Hoyt, D.G., Klein, E., Abernethy, J., Lazo, J.S., 1999. The neutral cysteine protease bleomycin hydrolase is essential for epidermal integrity and bleomycin resistance. Proc Natl Acad Sci U S A 96, 4680–4685.

Sebti, S.M., Jani, J.P., Mistry, J.S., Gorelik, E., Lazo, J.S., 1991. Metabolic inactivation: a mechanism of human tumor resistance to bleomycin. Cancer Res 51, 227–232.

Sebti, S.M., Mignano, J.E., Jani, J.P., Srimatkandada, S., Lazo, J.S., 1989. Bleomycin hydrolase: molecular cloning, sequencing, and biochemical studies reveal membership in the cysteine proteinase family. Biochemistry 28. https://doi.org/10.1021/bi00442a003

Semon, D., Movva, N.R., Smith, T.F., el Alama, M., Davies, J., 1987. Plasmid-determined bleomycin resistance in Staphylococcus aureus. Plasmid 17, 46–53.

Servant, N., Varoquaux, N., Lajoie, B.R., Viara, E., Chen, C.J., Vert, J.P., Heard, E., Dekker, J., Barillot, E., 2015. HiC-Pro: An optimized and flexible pipeline for Hi-C data processing. Genome Biol. 16, 1–11. https://doi.org/10.1186/S13059-015-0831-X/TABLES/4

Shah, Z., Mahbuba, R., Turcotte, B., 2013. The anticancer drug tirapazamine has antimicrobial activity against Escherichia coli, Staphylococcus aureus and Clostridium difficile. FEMS Microbiol Lett 347, 61–69. https://doi.org/10.1111/1574-6968.12223

Shiboski, C.H., Schmidt, B.L., Jordan, R.C., 2005. Tongue and tonsil carcinoma: increasing trends in the U.S. population ages 20-44 years. Cancer 103, 1843–1849. https://doi.org/10.1002/cncr.20998

Shin, J.-E., Lin, C., Lim, H.N., 2016. Horizontal transfer of DNA methylation patterns into bacteria chromosomes. Nucleic Acids Res 44.

Singh, A.P., Preet, S., Rishi, P., 2014. Nisin/β-lactam adjunct therapy against Salmonella enterica serovar Typhimurium: a mechanistic approach. J. Antimicrob. Chemother. 69, 1877–1887. https://doi.org/10.1093/JAC/DKU049

Smith, A., Crouch, S., Lax, S., Li, J., Painter, D., Howell, D., Patmore, R., Jack, A., Roman, E., 2015. Lymphoma incidence, survival and prevalence 2004-2014: sub-type analyses from the UK's Haematological Malignancy Research Network. Br. J. Cancer 112, 1575–1584. https://doi.org/10.1038/bjc.2015.94

Snitkin, E.S., Zelazny, A.M., Thomas, P.J., Stock, F., Program, N.C.S., Henderson, D.K., Palmore, T.N., Segre, J.A., 2013. Tracking a Hospital Outbreak of Carbapenem-Resistant Klebsiella pneumoniae with Whole-Genome Sequencing. Sci. Transl. Med. 4.

Spohn, R., Daruka, L., Lázár, V., Martins, A., Vidovics, F., Grézal, G., Méhi, O., Kintses, B., Számel, M., Jangir, P.K., Csörgő, B., Györkei, Á., Bódi, Z., Faragó, A., Bodai, L., Földesi, I., Kata, D., Maróti, G., Pap, B., Wirth, R., Papp, B., Pál, C., 2019. Integrated evolutionary analysis reveals antimicrobial peptides with limited resistance. Nat. Commun. 10, 1–13. https://doi.org/doi:10.1038/s41467-019-12364-6

Stalder, T., Press, M.O., Sullivan, S., Liachko, I., Top, E.M., 2019. Linking the resistome and plasmidome to the microbiome. Isme j.

Stecher, B., Denzler, R., Maier, L., Bernet, F., Sanders, M.J., Pickard, D.J., Barthel, M., Westendorf, A.M., Krogfelt, K.A., Walker, A.W., Ackermann, M., Dobrindt, U., Thomson, N.R., Hardt, W.-D., 2012. Gut inflammation can boost horizontal gene transfer between pathogenic and commensal Enterobacteriaceae. https://doi.org/10.1073/pnas.1113246109

Subramanian, R., Meares, C.F., 1986. Photosensitization of Cobalt Bleomycin. J. Am. Chem. Soc. 108, 6427–6429. https://doi.org/10.1021/ja00280a072

Sugiyama, M., Kumagai, T., Matsuo, H., Bhuiyan, M.Z., Ueda, K., Mochizuki, H., Nakamura, N., Davies, J.E., 1995. Overproduction of the bleomycin-binding proteins from bleomycin-producing Streptomyces verticillus and a methicillin-resistant Staphylococcus aureus in Escherichia coli and their immunological characterisation. FEBS Lett 362, 80–84.

Sugiyama, M., Thompson, C.J., Kumagai, T., Suzuki, K., Deblaere, R., Villarroel, R., Davies, J., 1994. Characterisation by molecular cloning of two genes from Streptomyces verticillus encoding resistance to bleomycin 151, 11–16. https://doi.org/10.1016/0378-1119(94)90626-2

Sullivan, G.J., Delgado, N.N., Maharjan, R., Cain, A.K., 2020. How antibiotics work together: molecular mechanisms behind combination therapy. Curr. Opin. Microbiol. 57, 31–40. https://doi.org/10.1016/J.MIB.2020.05.012

Sutherland, R., Slocombe, B., Rolinson, G.N., 1964. Development in vitro of Bacterial Cross-resistance involving Penicillins, Chloramphenicol and Tetracycline. Nat. 1964 2034944 203, 548–549. https://doi.org/10.1038/203548a0

Suzuki, S., Horinouchi, T., Furusawa, C., 2016. Phenotypic changes associated with the fitness cost in antibiotic resistant Escherichia coli strains 12. https://doi.org/10.1039/C5MB00590F

Tanner, W.D., Atkinson, R.M., Goel, R.K., Toleman, M.A., Benson, L.S., Porucznik, C.A., VanDerslice, J.A., 2017. Horizontal transfer of the blaNDM-1 gene to Pseudomonas aeruginosa and Acinetobacter baumannii in biofilms. FEMS Microbiol Lett 364. https://doi.org/10.1093/femsle/fnx048

Tempest, D.W., 1978. Dynamics of Microbial Growth, in: Essays in Microbiology.

Torres-Barceló, C., Kojadinovic, M., Moxon, R., MacLean, R.C., 2015. The SOS response increases bacterial fitness, but not evolvability, under a sublethal dose of antibiotic. https://doi.org/10.1098/rspb.2015.0885

Trampari, E., Holden, E.R., Wickham, G.J., Ravi, A., Martins, L. de O., Savva, G.M., Webber, M.A., 2021. Exposure of Salmonella biofilms to antibiotic concentrations rapidly selects resistance with collateral tradeoffs. NPJ biofilms microbiomes 7. https://doi.org/10.1038/s41522-020-00178-0

Tran, T.B., Wang, J., Doi, Y., Velkov, T., Bergen, P.J., Li, J., 2018. Novel Polymyxin Combination With Antineoplastic Mitotane Improved the Bacterial Killing Against Polymyxin-Resistant Multidrug-Resistant Gram-Negative Pathogens. Front Microbiol 9.

Trastoy, R., Manso, T., Fernández-García, L., Blasco, L., Ambroa, A., Pérez Del Molino, M.L., Bou, G., García-Contreras, R., Wood, T.K., Tomás, M., 2018. Mechanisms of bacterial tolerance and persistence in the gastrointestinal and respiratory environments. Clin. Microbiol. Rev. 31. https://doi.org/10.1128/CMR.00023-18

Trigodet, F., Lolans, K., Fogarty, E., Shaiber, A., Morrison, H.G., Barreiro, L., Jabri, B., Eren, A.M., 2021. High molecular weight DNA extraction strategies for long-read sequencing of complex metagenomes. https://doi.org/10.1101/2021.03.03.433801

Trussart, M., Yus, E., Martinez, S., Baù, D., Tahara, Y.O., Pengo, T., Widjaja, M., Kretschmer, S., Swoger, J., Djordjevic, S., Turnbull, L., Whitchurch, C., Miyata, M., Marti-Renom, M.A., Lluch-Senar, M., Serrano, L., 2017. Defined chromosome structure in the genome-reduced bacterium Mycoplasma pneumoniae. Nat. Commun. 8. https://doi.org/10.1038/ncomms14665

Twentyman, P.R., 1983. Bleomycin--mode of action with particular reference to the cell cycle. Pharmacol Ther 23, 417–441.

Ulahannan, N., Pendleton, M., Deshpande, A., Schwenk, S., Behr, J.M., Dai, X., Tyer, C., Rughani, P., Kudman, S., Adney, E., Tian, H., Wilkes, D., Mosquera, J.M., Stoddart, D., Turner, D.J., Juul, S., Harrington, E., Imielinski, M., 2019. Nanopore sequencing of DNA concatemers reveals higher-order features of chromatin structure. bioRxiv.

https://doi.org/10.1101/833590

Vaara, M., Viljanen, P., 1985. Binding of Polymyxin B Nonapeptide to Gram-Negative Bacteria. Antimicrob. Agents Chemother. 27, 548–554.

Vallejos, A.C., Socías, S.B., Cristóbal, R.E. de, Salomón, R.A., 2011. An Escherichia coli sbmA tolC double mutant displays a thermosensitive colony formation phenotype. Ann. Microbiol. 62, 709–714. https://doi.org/doi:10.1007/s13213-011-0310-x

van Berkum, N.L., Lieberman-Aiden, E., Williams, L., Imakaev, M., Gnirke, A., Mirny, L.A., Dekker, J., Lander, E.S., 2010. Hi-C: A method to study the three-dimensional architecture of genomes. J. Vis. Exp. 1–7. https://doi.org/10.3791/1869

van Peer, A.F., de Bekker, C., Vinck, A., Wösten, H.A.B., Lugones, L.G., 2009. Phleomycin Increases Transformation Efficiency and Promotes Single Integrations in Schizophyllum commune. https://doi.org/10.1128/AEM.02162-08

Vielva, L., de Toro, M., Lanza, V.F., de la Cruz, F., 2017. PLACNETw: a web-based tool for plasmid reconstruction from bacterial genomes. Bioinformatics 33, 3796–3798. https://doi.org/10.1093/bioinformatics/btx462

Viveiros, M., Dupont, M., Rodrigues, L., Couto, I., Davin-Regli, A., Martins, M., Pages, J.M., Amaral, L., 2007. Antibiotic stress, genetic response and altered permeability of E. coli. PLoS One 2, e365. https://doi.org/10.1371/journal.pone.0000365

Wang, K., Li, P., Li, J., Hu, X., Lin, Y., Yang, L., Qiu, S., Ma, H., Li, P., Song, H., 2020. An NDM-1-Producing Acinetobacter towneri Isolate from Hospital Sewage in China. Infect. Drug Resist. 13. https://doi.org/10.2147/IDR.S246697

Wang, M., Wang, W., Niu, Y., Liu, T., Li, L., Zhang, M., Li, Z., Su, W., Liu, F., Zhang, X., Xu, H., 2020. A Clinical Extensively-Drug Resistant (XDR) Escherichia coli and Role of Its β-Lactamase Genes. Front. Microbiol. 11, 3178. https://doi.org/10.3389/FMICB.2020.590357

Wang, W., Peng, Z., Baloch, Z., Hu, Y., Xu, J., Zhang, W., Fanning, S., Li, F., 2017. Genomic characterization of an extensively-drug resistance Salmonella enterica serotype Indiana strain harboring blaNDM-1 gene isolated from a chicken carcass in China - ScienceDirect. https://doi.org/10.1016/j.micres.2017.07.006

Wang, Y., Lu, J., Zhang, S., Li, J., Mao, L., Yuan, Z., Bond, P.L., Guo, J., 2021. Non-antibiotic pharmaceuticals promote the transmission of multidrug resistance plasmids through intra- and intergenera conjugation. ISME J. 2021 159 15, 2493–2508. https://doi.org/10.1038/s41396-021-00945-7

Wang, Y., Wang, A., Liu, Z., Thurman, A.L., Powers, L.S., Zou, M., Zhao, Y., Hefel, A., Li, Y., Zabner, J., Au, K.F., 2019. Single-molecule long-read sequencing reveals the chromatin basis of gene expression. Genome Res.

Wardell, S., Rehman, A., Martin, L., Winstanley, C., Patrick, W., Lamont, I., 2019. A large-scale whole-genome comparison shows that experimental evolution in response to antibiotics predicts changes in naturally evolved clinical Pseudomonas aeruginosa. Antimicrob. Agents Chemother. 63. https://doi.org/10.1128/AAC.01619-19

Webber, M.A., Whitehead, R.N., Mount, M., Loman, N.J., Pallen, M.J., Piddock, L.J., 2015. Parallel evolutionary pathways to antibiotic resistance selected by biocide exposure. J Antimicrob Chemother 70, 2241–2248. https://doi.org/10.1093/jac/dkv109

Wein, T., Hülter, N.F., Mizrahi, I., Dagan, T., 2019. Emergence of plasmid stability under non-selective conditions maintains antibiotic resistance. Nat. Commun. 10, 1–13. https://doi.org/10.1038/s41467-019-10600-7

Wendling, C.C., Refardt, D., Hall, A.R., 2021. Fitness benefits to bacteria of carrying prophages and prophage-encoded antibiotic-resistance genes peak in different environments. Evolution (N. Y). 75, 515–528. https://doi.org/10.1111/EVO.14153

Westman, E.L., Canova, M.J., Radhi, I.J., Koteva, K., Kireeva, I., Waglechner, N., Wright, G.D., 2012. Bacterial inactivation of the anticancer drug doxorubicin. Chem Biol 19, 1255–1264. https://doi.org/10.1016/j.chembiol.2012.08.011

White, M.C., Holman, D.M., Boehm, J.E., Peipins, L.A., Grossman, M., Henley, S.J., 2014. Age and Cancer Risk: A Potentially Modifiable Relationship. Am. J. Prev. Med. 46, S7-15. https://doi.org/10.1016/j.amepre.2013.10.029

Wilkinson, E., Giovanetti, M., Tegally, H., San, J.E., Lessells, R., Cuadros, D., Martin, D.P., Rasmussen, D.A., Zekri, A.R.N., Sangare, A.K., Ouedraogo, A.S., Sesay, A.K., Priscilla, A., Kemi, A.S., Olubusuyi, A.M., Oluwapelumi, A.O.O., Hammami, A., Amuri, A.A., Sayed, A., Ouma, A.E.O., Elargoubi, A., Ajayi, N.A., Victoria, A.F., Kazeem, A., George, A., Trotter, A.J., Yahaya, A.A., Keita, A.K., Diallo, A., Kone, A., Souissi, A., Chtourou, A., Gutierrez, A. V., Page, A.J., Vinze, A., Iranzadeh, A., Lambisia, A., Ismail, A., Rosemary, A., Sylverken, A., Femi, A., Ibrahimi, A., Marycelin, B., Oderinde, B.S., Bolajoko, B., Dhaala, B., Herring, B.L., Njanpop-Lafourcade, B.M., Kleinhans, B., McInnis, B., Tegomoh, B., Brook, C., Pratt, C.B., Scheepers, C., Akoua-Koffi, C.G., Agoti, C.N., Peyrefitte, C., Daubenberger, C., Morang'a, C.M., James Nokes, D., Amoako, D.G., Bugembe, D.L., Park, D., Baker, D., Doolabh, D., Ssemwanga, D., Tshiabuila, D., Bassirou, D., Amuzu, D.S.Y., Goedhals, D., Omuoyo, D.O., Maruapula, D., Foster-Nyarko, E., Lusamaki, E.K., Simulundu, E., Ong'era, E.M., Ngabana, E.N., Shumba, E.,

El Fahime, E., Lokilo, E., Mukantwari, E., Philomena, E., Belarbi, E., Simon-Loriere, E., Anoh, E.A., Leendertz, F., Ajili, F., Enoch, F.O., Wasfi, F., Abdelmoula, F., Mosha, F.S., Takawira, F.T., Derrar, F., Bouzid, F., Onikepe, F., Adeola, F., Muyembe, F.M., Tanser, F., Dratibi, F.A., Mbunsu, G.K., Thilliez, G., Kay, G.L., Githinji, G., van Zyl, G., Awandare, G.A., Schubert, G., Maphalala, G.P., Ranaivoson, H.C., Lemriss, H., Anise, H., Abe, H., Karray, H.H., Nansumba, H., Elgahzaly, H.A., Gumbo, H., Smeti, I., Ayed, I.B., Odia, I., Boubaker, I.B. Ben, Gaaloul, I., Gazy, I., Mudau, I., Ssewanyana, I., Konstantinus, I., Lekana-Douk, J.B., Makangara, J.C.C., Tamfum, J.J.M., Heraud, J.M., Shaffer, J.G., Giandhari, J., Li, J., Yasuda, J., Mends, J.Q., Kiconco, J., Morobe, J.M., Gyapong, J.O., Okolie, J.C., Kayiwa, J.T., Edwards, J.A., Gyamfi, J., Farah, J., Nakaseegu, J., Ngoi, J.M., Namulondo, J., Andeko, J.C., Lutwama, J.J., O'Grady, J., Siddle, K., Adeyemi, K.T., Tumedi, K.A., Said, K.M., Hae-Young, K., Duedu, K.O., Belyamani, L., Fki-Berrajah, L., Singh, L., Martins, L. de O., Tyers, L., Ramuth, M., Mastouri, M., Aouni, M., el Hefnawi, M., Matsheka, M.I., Kebabonye, M., Diop, M., Turki, M., Paye, M., Nyaga, M.M., Mareka, M., Damaris, M.M., Mburu, M.W., Mpina, M., Nwando, M., Owusu, M., Wiley, M.R., Youtchou, M.T., Ayekaba, M.O., Abouelhoda, M., Seadawy, M.G., Khalifa, M.K., Sekhele, M., Ouadghiri, M., Diagne, M.M., Mwenda, M., Allam, M., Phan, M.V.T., Abid, N., Touil, N., Rujeni, N., Kharrat, N., Ismael, N., Dia, N., Mabunda, N., Hsiao, N.Y., Silochi, N.B., Nsenga, N., Gumede, N., Mulder, N., Ndodo, N., Razanajatovo, N.H., Iguosadolo, N., Judith, O., Kingsley, O.C., Sylvanus, O., Peter, O., Femi, O., Idowu, O., Testimony, O., Chukwuma, O.E., Ogah, O.E., Onwuamah, C.K., Cyril, O., Faye, O., Tomori, O., Ondoa, P., Combe, P., Semanda, P., Oluniyi, P.E., Arnaldo, P., Quashie, P.K., Dussart, P., Bester, P.A., Mbala, P.K., Ayivor-Djanie, R., Njouom, R., Phillips, R.O., Gorman, R., Kingsley, R.A., Carr, R.A.A., El Kabbaj, S., Gargouri, S., Masmoudi, S., Sankhe, S., Lawal, S.B., Kassim, S., Trabelsi, S., Metha, S., Kammoun, S., Lemriss, S., Agwa, S.H.A., Calvignac-Spencer, S., Schaffner, S.F., Doumbia, S., Mandanda, S.M., Aryeetey, S., Ahmed, S.S., Elhamoumi, S., Andriamandimby, S., Tope, S., Lekana-Douki, S., Prosolek, S., Ouangraoua, S., Mundeke, S.A., Rudder, S., Panji, S., Pillay, S., Engelbrecht, S., Nabadda, S., Behillil, S., Budiaki, S.L., van der Werf, S., Mashe, T., Aanniz, T., Mohale, T., Le-Viet, T., Schindler, T., Anyaneji, U.J., Chinedu, U., Ramphal, U., Jessica, U., George, U., Fonseca, V., Enouf, V., Gorova, V., Roshdy, W.H., Ampofo, W.K., Preiser, W., Choga, W.T., Bediako, Y., Naidoo, Y., Butera, Y., de Laurent, Z.R., Sall, A.A., Rebai, A., von Gottberg, A., Kouriba, B., Williamson, C., Bridges, D.J., Chikwe, I., Bhiman, J.N., Mine, M., Cotten, M., Moyo, S., Gaseitsiwe, S., Saasa, N., Sabeti, P.C., Kaleebu, P., Tebeje, Y.K., Tessema, S.K., Happi, C., Nkengasong, J., de Oliveira, T., 2021. A year of genomic surveillance reveals how the SARS-CoV-2 pandemic unfolded in Africa. Science (80-.). 374, 423–431. https://doi.org/10.1126/SCIENCE.ABJ4336/SUPPL_FILE/SCIENCE.ABJ4336_MDAR_REPROD UCIBILITY_CHECKLIST.PDF

Wiser, M.J., Lenski, R.E., 2015. A comparison of methods to measure fitness in Escherichia coli. PLoS One 10, e0126210. https://doi.org/10.1371/journal.pone.0126210

Wisplinghoff, H., Seifert, H., Wenzel, R.P., Edmond, M.B., 2003. Current trends in the epidemiology of nosocomial bloodstream infections in patients with hematological malignancies and solid neoplasms in hospitals in the United States. Clin. Infect. Dis. 36, 1103–1110. https://doi.org/10.1086/374339

Woegerbauer, M., Bellanger, X., Merlin, C., 2020. Cell-Free DNA: An Underestimated Source of Antibiotic Resistance Gene Dissemination at the Interface Between Human Activities and Downstream Environments in the Context of Wastewater Reuse. Front. Microbiol. 11, 671. https://doi.org/10.3389/FMICB.2020.00671/BIBTEX

Xia, Z.J., Wang, J., Hu, W., Liu, H., Gao, X.Z., Wu, Z.H., Zhang, P.Y., Li, Y.Z., 2008. Improving conjugation efficacy of Sorangium cellulosum by the addition of dual selection antibiotics. J. Ind. Microbiol. Biotechnol. 35, 1157–1163. https://doi.org/10.1007/S10295-008-0395-9

Xu, L., Seki, M., 2019. Recent advances in the detection of base modifications using the Nanopore sequencer. J. Hum. Genet. 65, 25–33. https://doi.org/doi:10.1038/s10038-019-0679-0

Yaffe, E., Relman, D.A., 2020. Tracking microbial evolution in the human gut using Hi-C reveals extensive horizontal gene transfer, persistence and adaptation. Nat. Microbiol. 5, 343–353. https://doi.org/10.1038/s41564-019-0625-0

Yang, Q.E., MacLean, C., Papkou, A., Pritchard, M., Powell, L., Thomas, D., Andrey, D.O., Li, M., Spiller, B., Yang, W., Walsh, T.R., 2020. Compensatory mutations modulate the competitiveness and dynamics of plasmid-mediated colistin resistance in Escherichia coli clones. Isme j 14, 861–865. https://doi.org/doi:10.1038/s41396-019-0578-6

Yu, Y.A., Shabahang, S., Timiryasova, T.M., Zhang, Q., Beltz, R., Gentschev, I., Goebel, W., Szalay, A.A., 2004. Visualization of tumors and metastases in live animals with bacteria and vaccinia virus encoding light-emitting proteins. Nat. Biotechnol. 22, 313–320. https://doi.org/doi:10.1038/nbt937

Yuasa, K., Sugiyama, M., 1995. Bleomycin-induced beta-lactamase overexpression in Escherichia coli carrying a bleomycin-resistance gene from Streptomyces verticillus and its application to screen bleomycin analogues. FEMS Microbiol Lett 132, 61–66.

Zhang, P.Y., Xu, P.P., Xia, Z.J., Wang, J., Xiong, J., Li, Y.Z., 2013. Combined treatment with the antibiotics kanamycin and streptomycin promotes the conjugation of Escherichia coli. FEMS Microbiol. Lett. 348, 149–156. https://doi.org/10.1111/1574-6968.12282

Zheng, W., Yang, Z., Ge, X., Feng, Y., Wang, Y., Liu, C., Luan, Y., Cai, K., Vakal, S., You, F., Guo, W., Wang, W., Feng, Z., Li, F., 2020. Freeze substitution Hi-C, a convenient and cost-effective method for capturing the natural 3D chromatin conformation from frozen samples. J. Genet. Genomics. https://doi.org/10.1016/j.jgg.2020.11.002

Final word count: 61,064

Appendix

Appendix A- Cooler Files
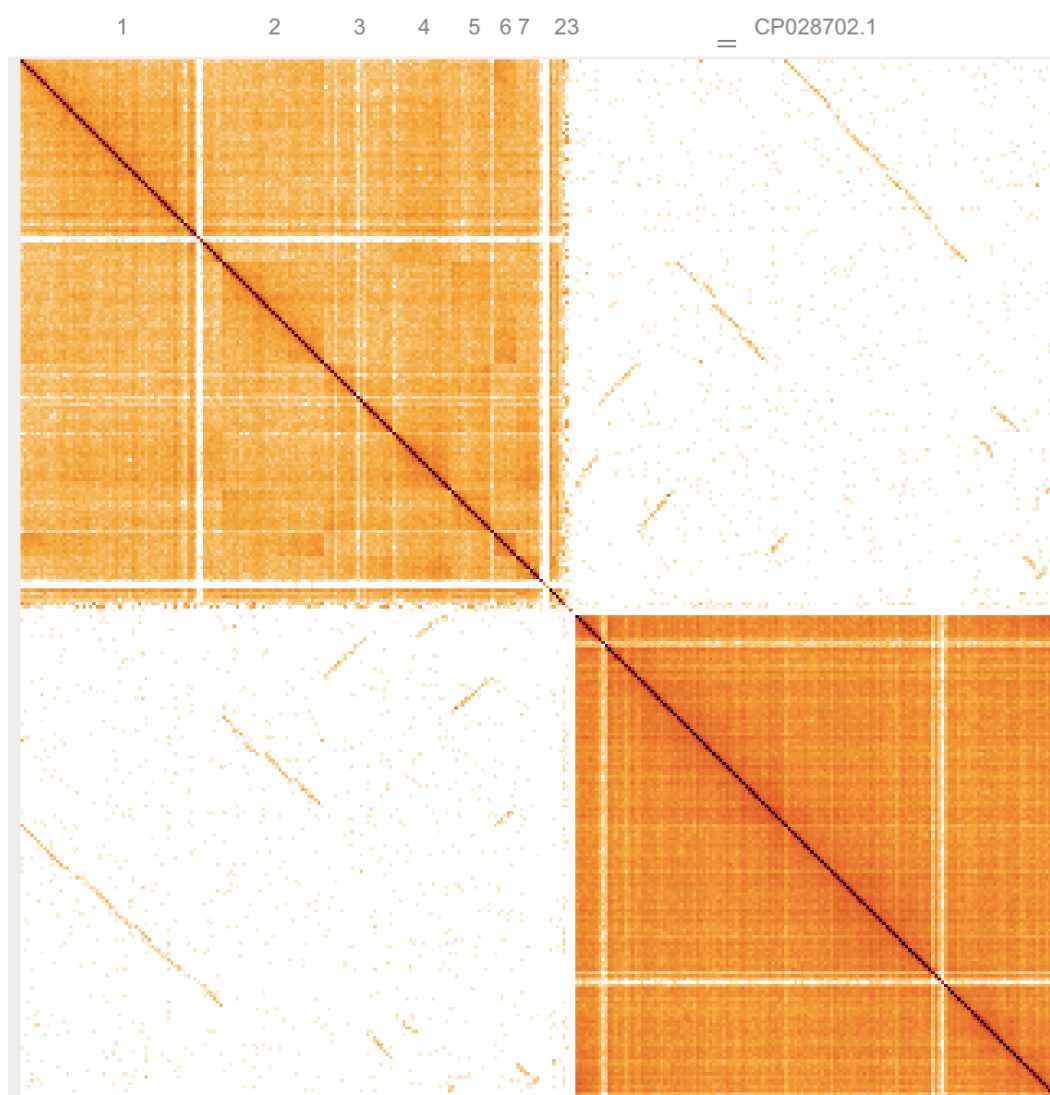
Figure A-1: A Cooler heatmap of the chromosomal contacts from the parental *Escherichia coli* EC1 (top left orange square) and J53 (bottom right orange square) strains that were used in the conjugation experiments as controls, replicate 1.
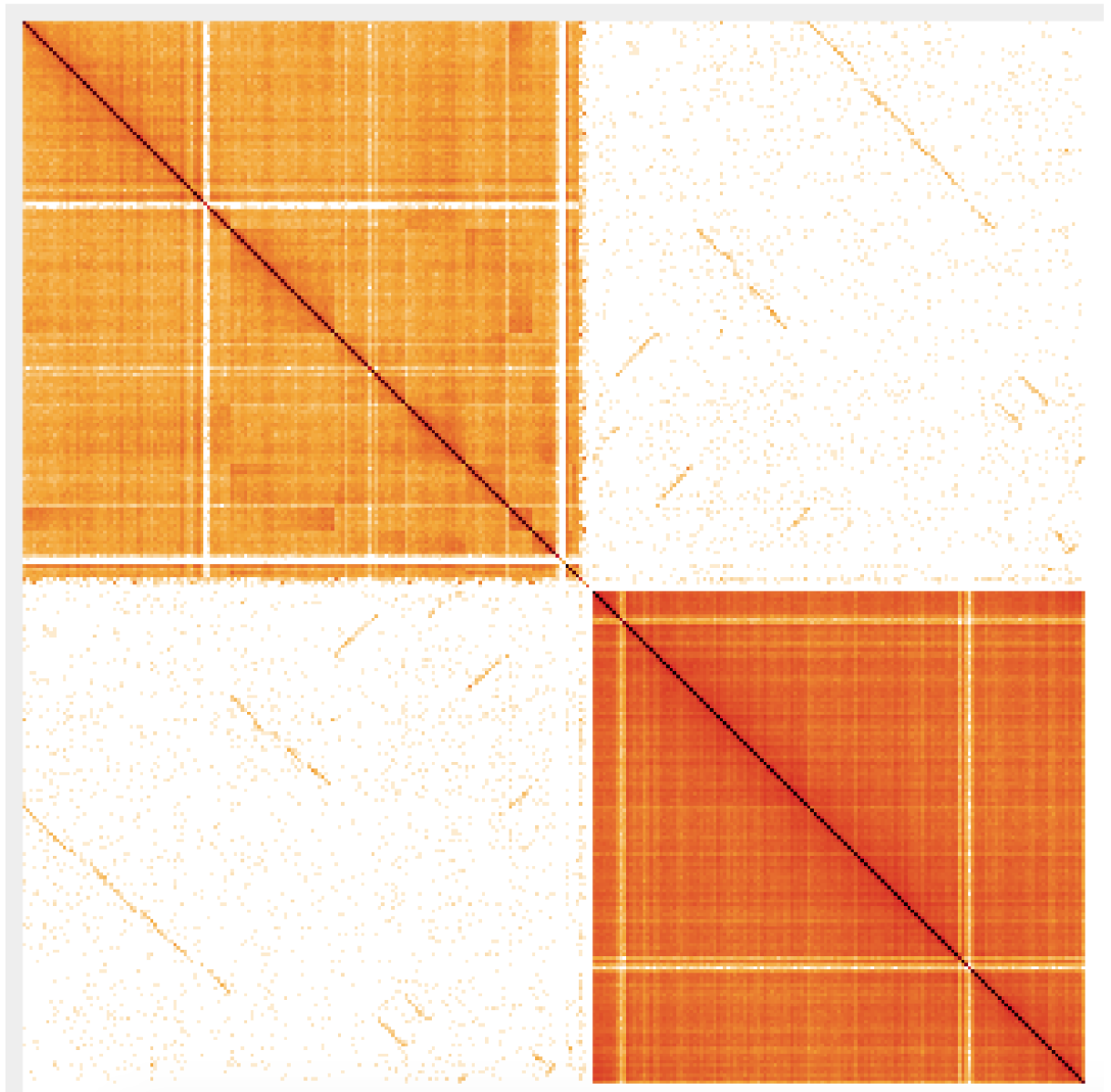
Figure A-2: A Cooler heatmap of the chromosomal contacts from the parental *Escherichia coli* EC1 (top left orange square) and J53 (bottom right orange square) strains that were used in the conjugation experiments as controls, replicate 2.
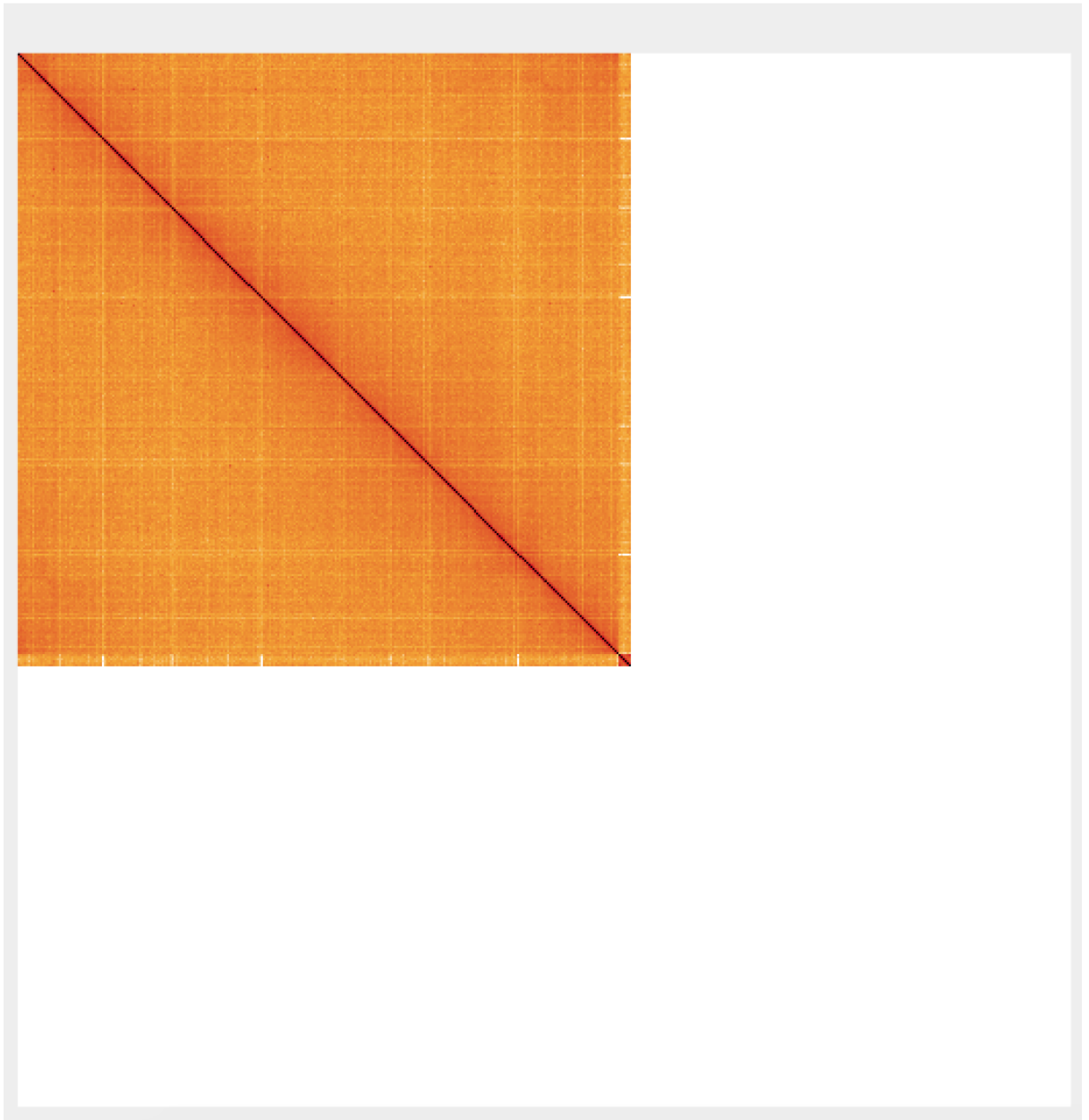
Figure A-3: A Cooler heatmap of the chromosomal contacts from the parental *Escherichia coli* EC1 (top left orange square) and J53 (bottom right orange square) strains that were used in the conjugation experiments as controls, replicate 3.
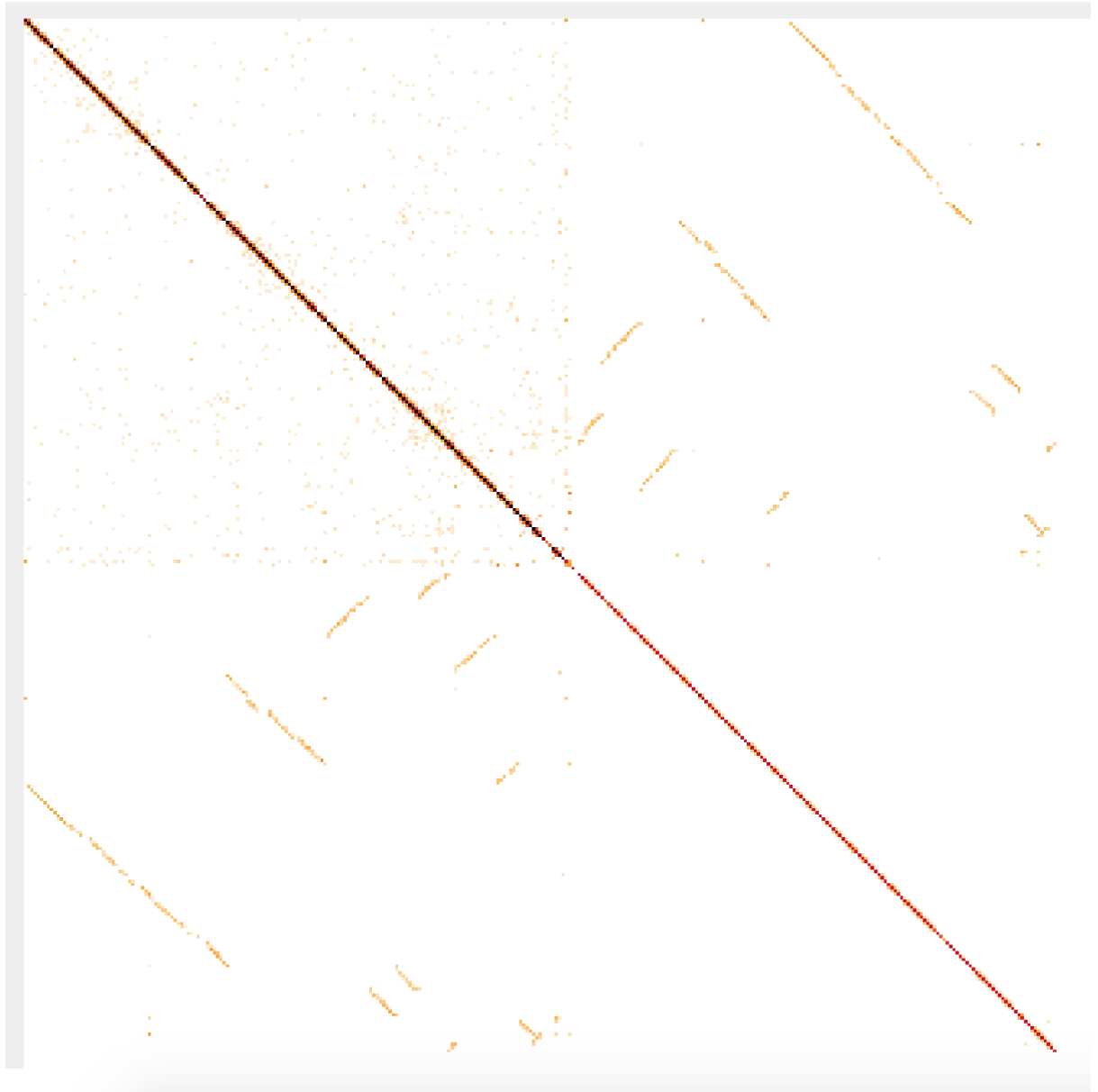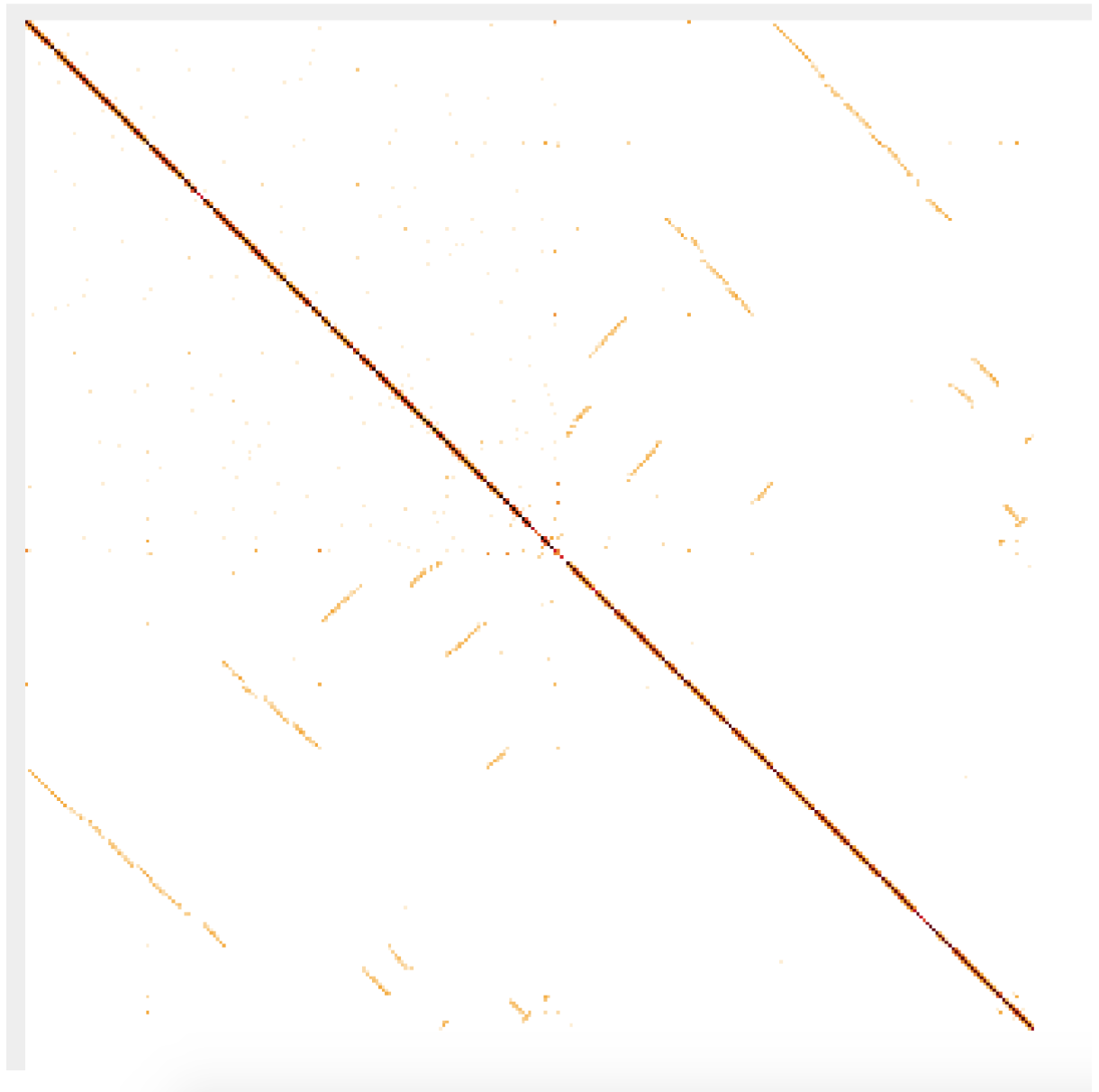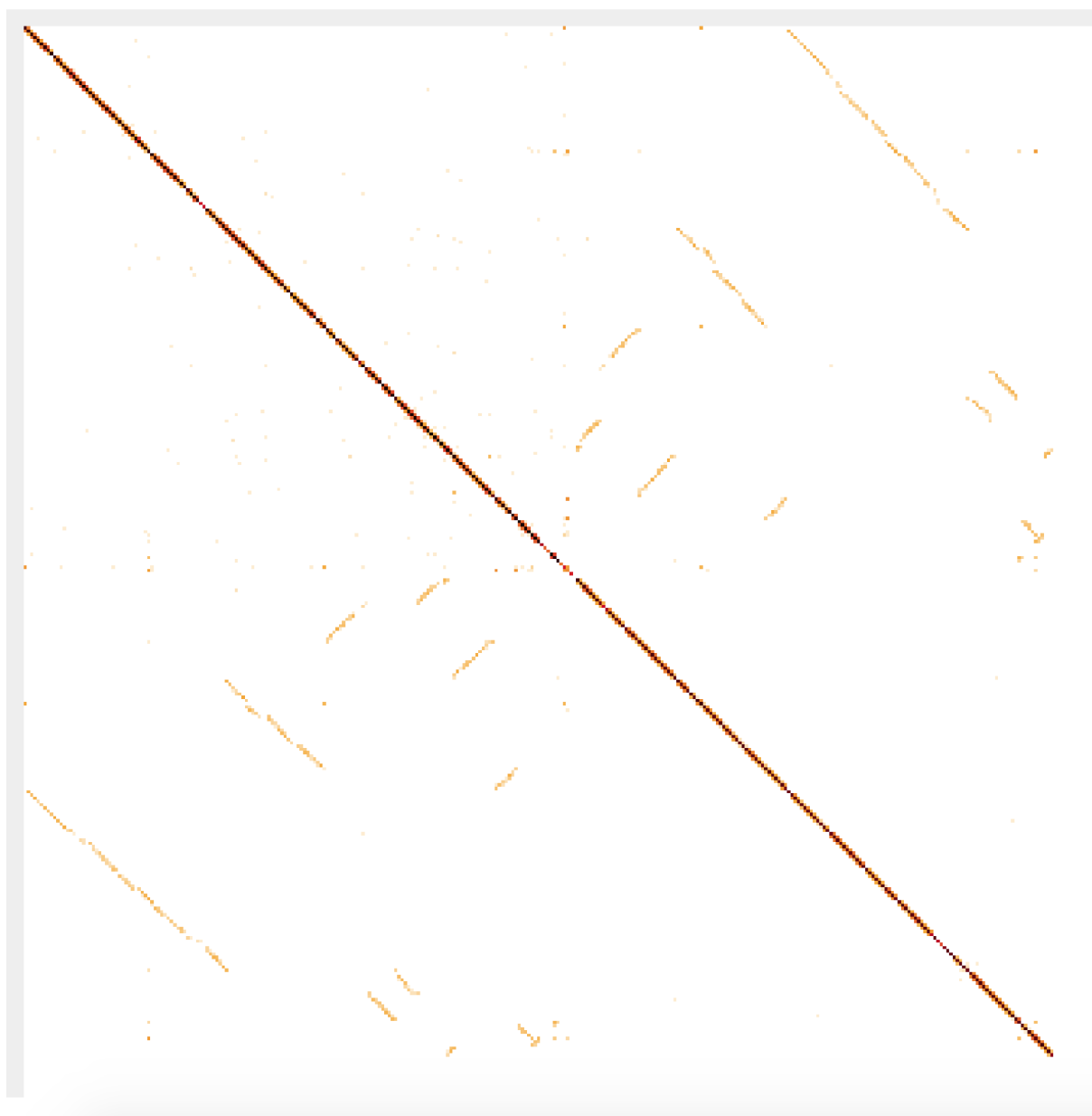
Figure A-4: A Cooler heatmap of the chromosomal contacts from the transconjugant *Escherichia coli* J53 strain from the conjugation experiments after exposure to sub-minimum inhibitory concentration of bleomycin, replicate 1.
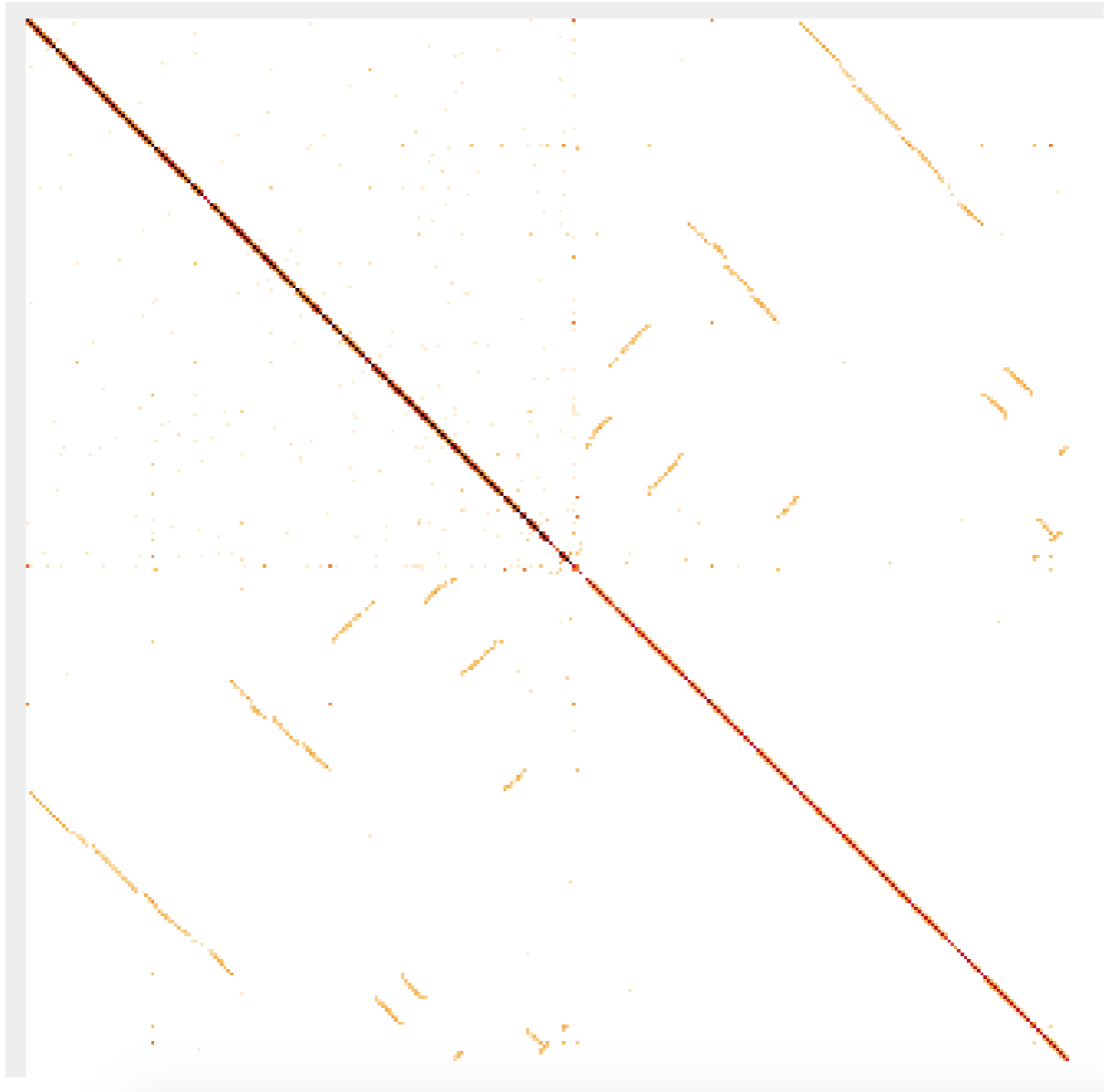
Figure A-5: A Cooler heatmap of the chromosomal contacts from the transconjugant *Escherichia coli* J53 strain from the conjugation experiments after exposure to sub-minimum inhibitory concentration of bleomycin, replicate 2.
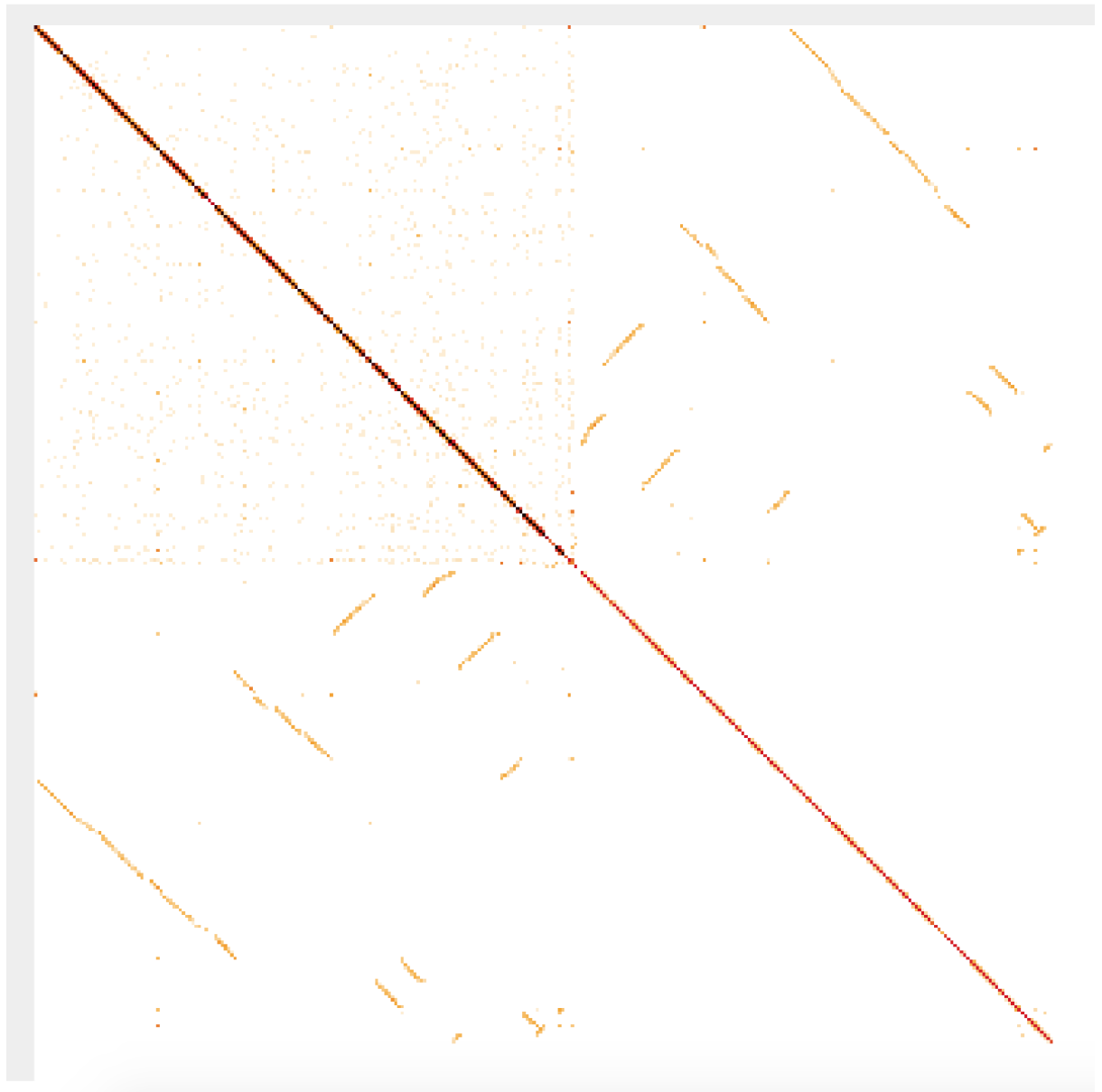
Figure A-6: A Cooler heatmap of the chromosomal contacts from the transconjugant *Escherichia coli* J53 strain from the conjugation experiments after exposure to sub-minimum inhibitory concentration of bleomycin, replicate 3.
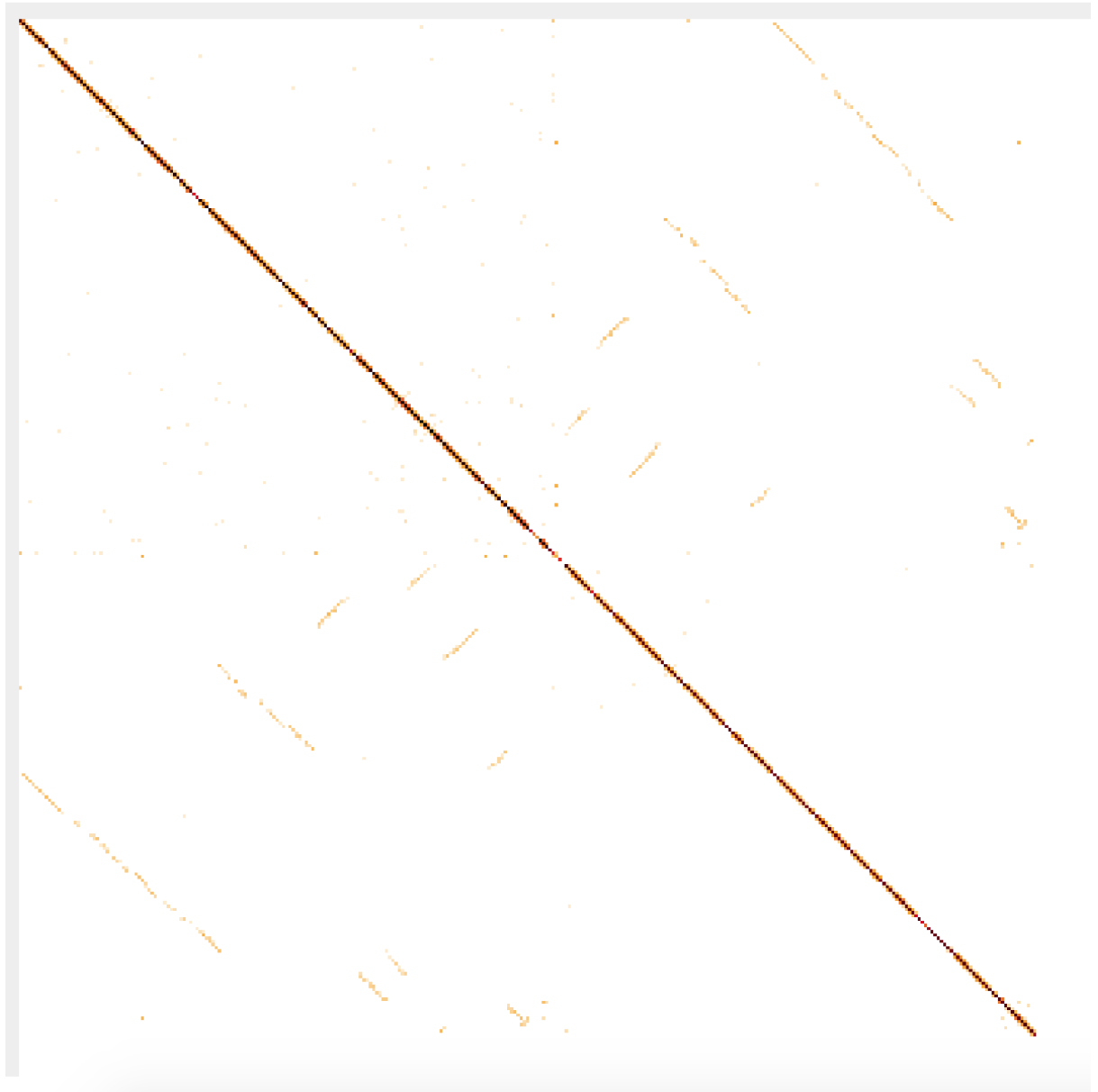
Figure A-7: A Cooler heatmap of the chromosomal contacts from the transconjugant *Escherichia coli* J53 strain from the conjugation experiments after exposure to LB media (control), replicate 1.
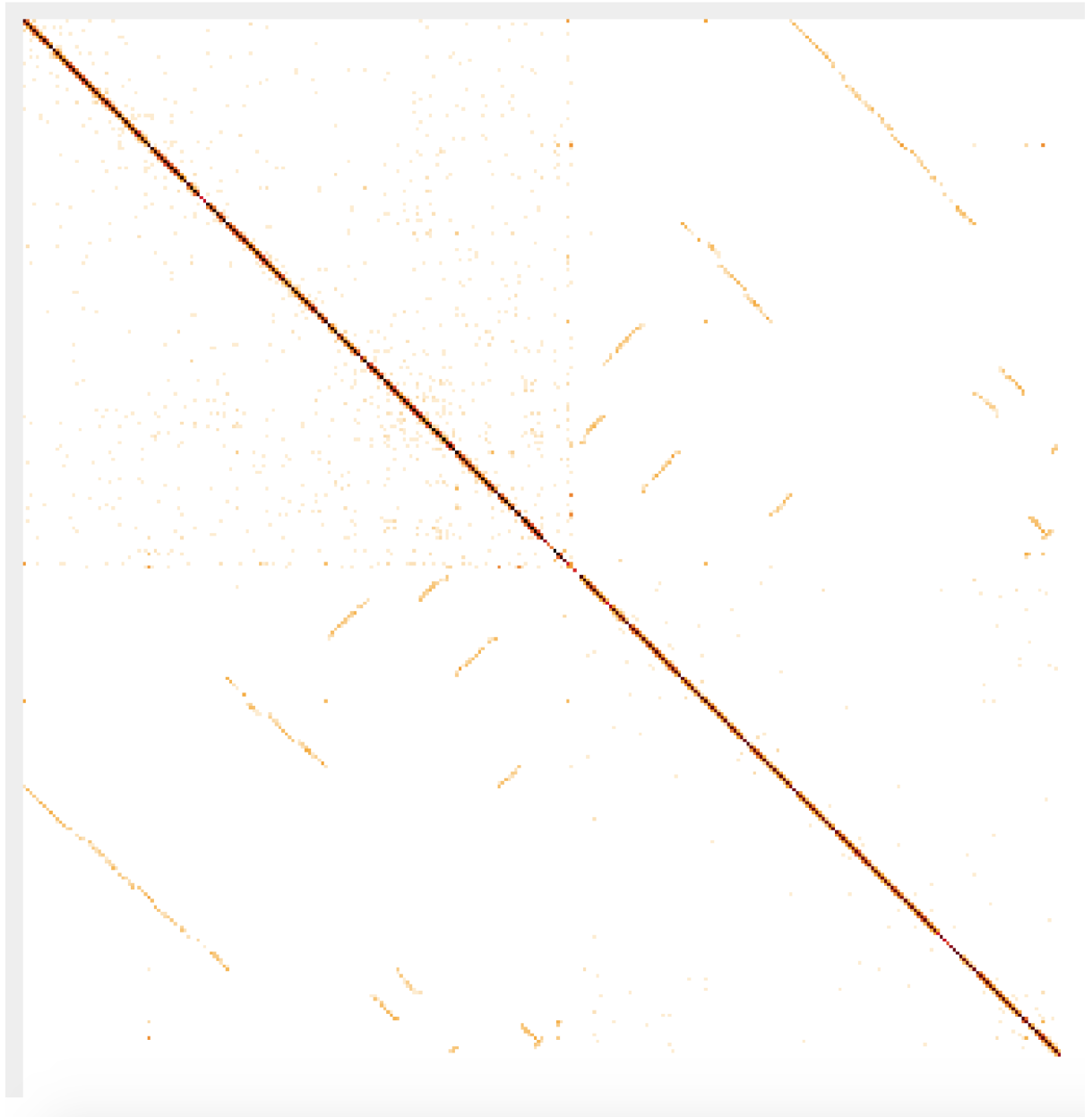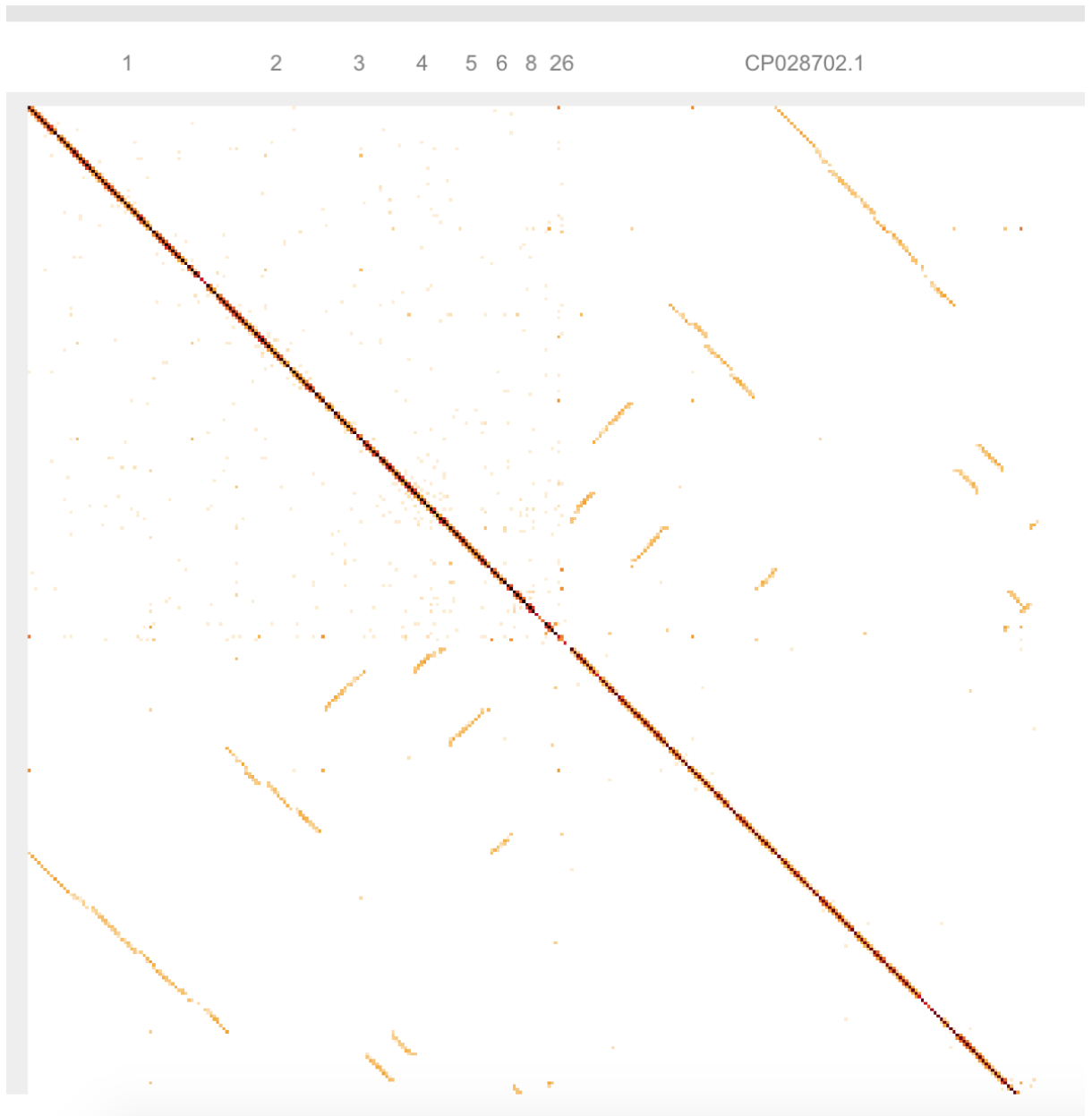
Figure A-8: A Cooler heatmap of the chromosomal contacts from the transconjugant *Escherichia coli* J53 strain from the conjugation experiments after exposure to LB media (control), replicate 2.

Figure A-9: A Cooler heatmap of the chromosomal contacts from the transconjugant *Escherichia coli* J53 strain from the conjugation experiments after exposure to LB media (control), replicate 3.
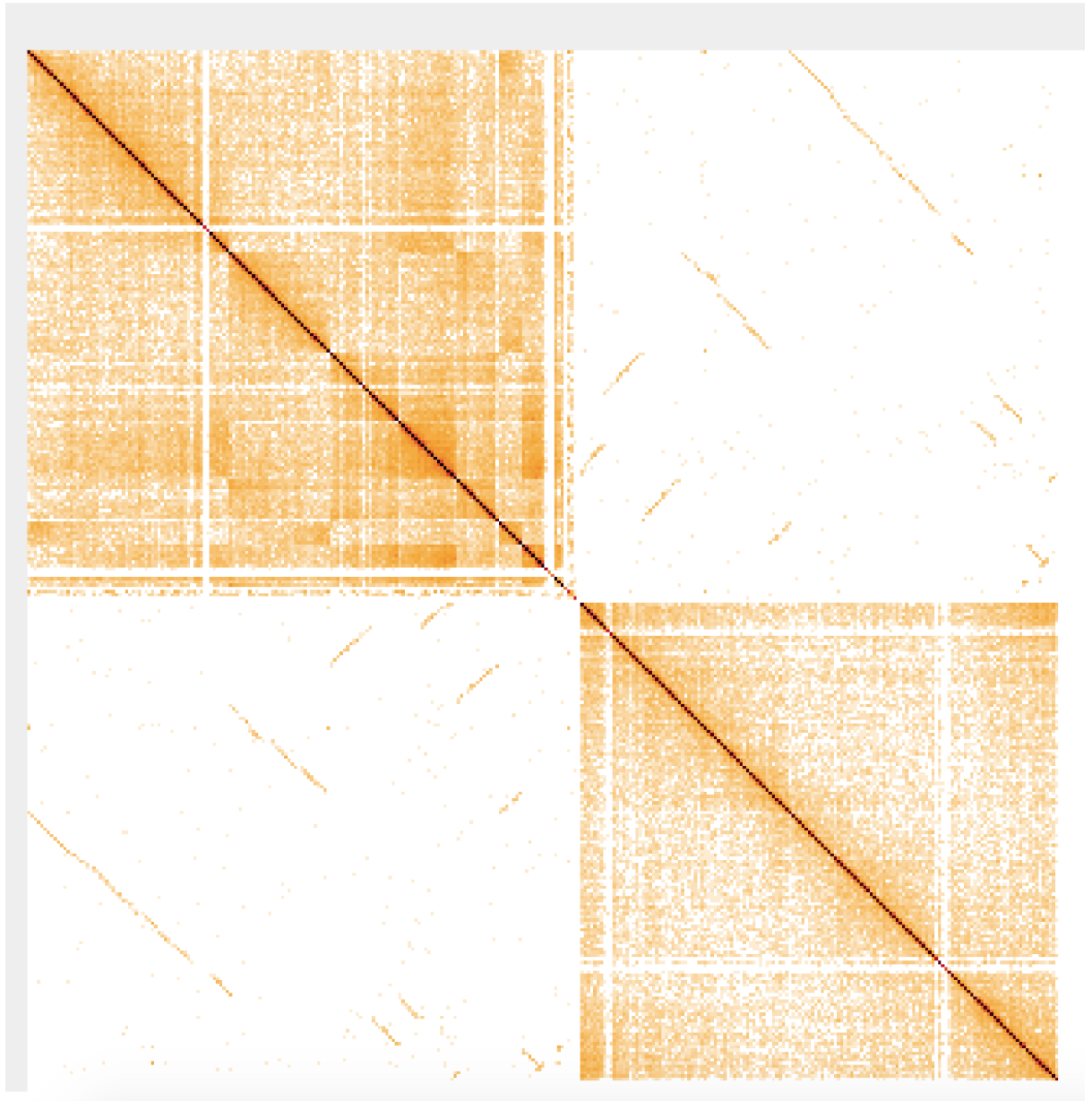
Figure A-10: A Cooler heatmap of the chromosomal contacts from the transconjugant *Escherichia coli* J53 strain from the conjugation experiments after exposure to sub-minimum inhibitory concentration of meropenem, replicate 1.
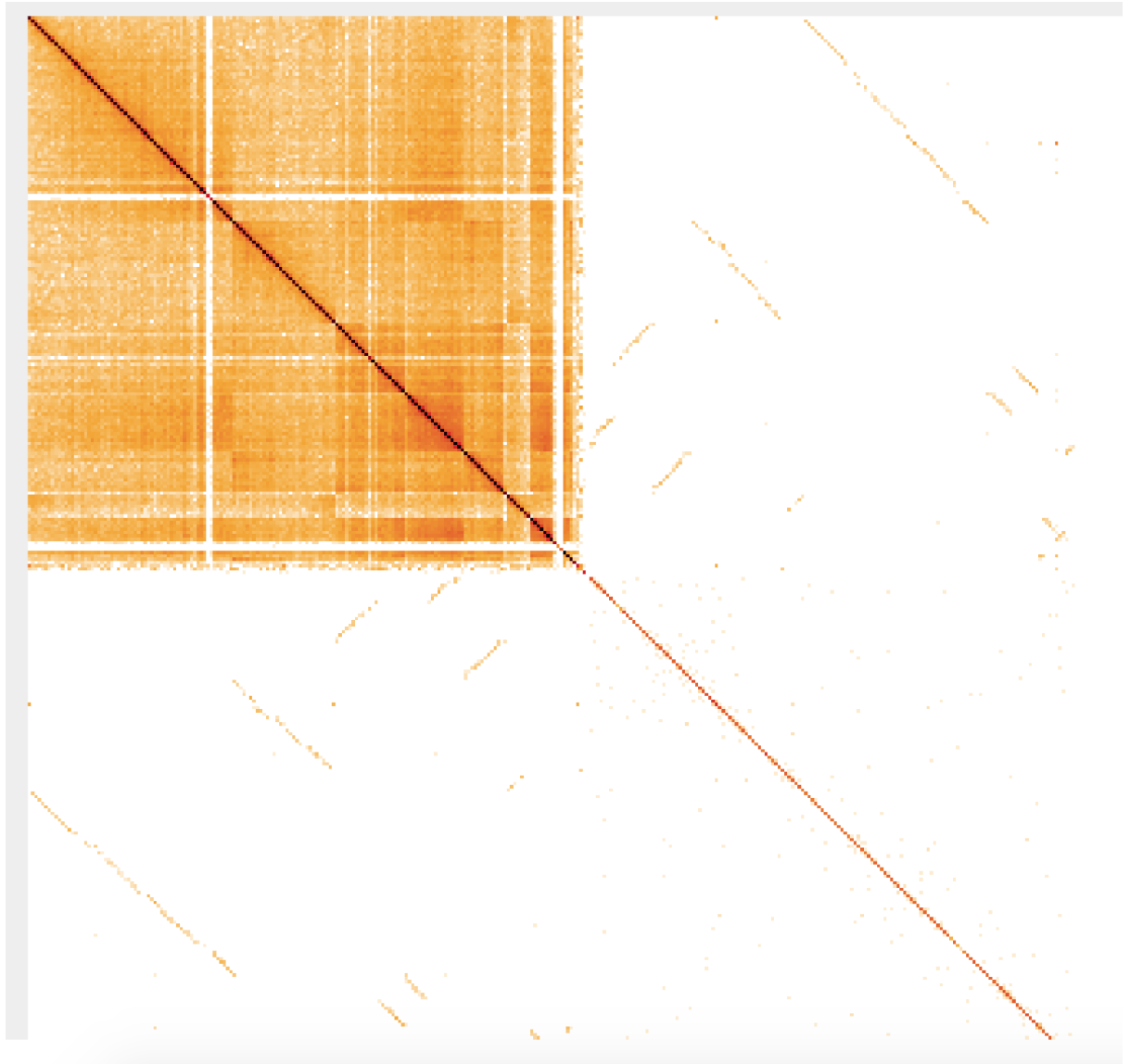
Figure A-11: A Cooler heatmap of the chromosomal contacts from the transconjugant *Escherichia coli* J53 strain from the conjugation experiments after exposure to sub-minimum inhibitory concentration of meropenem, replicate 2.

Figure A-12: A Cooler heatmap of the chromosomal contacts from the transconjugant *Escherichia coli* J53 strain from the conjugation experiments after exposure to sub-minimum inhibitory concentration of meropenem, replicate 3.

Figure A-13: A Cooler heatmap of the chromosomal contacts from the transconjugant *Escherichia coli* J53 strain from the conjugation experiments after exposure to sub-minimum inhibitory concentration of mitomycin C, replicate 1.
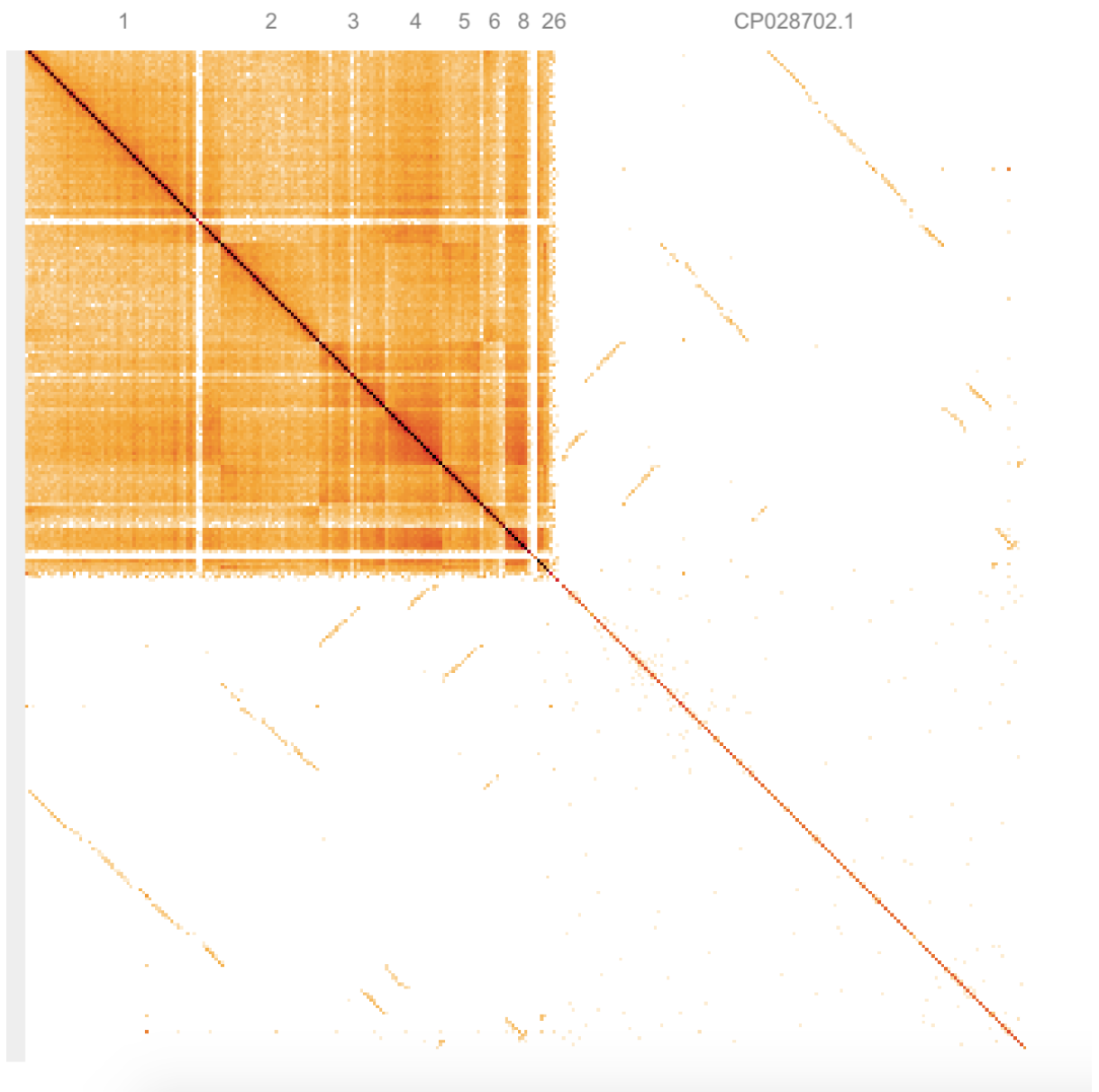
Figure A-14: A Cooler heatmap of the chromosomal contacts from the transconjugant *Escherichia coli* J53 strain from the conjugation experiments after exposure to sub-minimum inhibitory concentration of sub-minimum inhibitory concentration of mitomycin C, replicate 2.
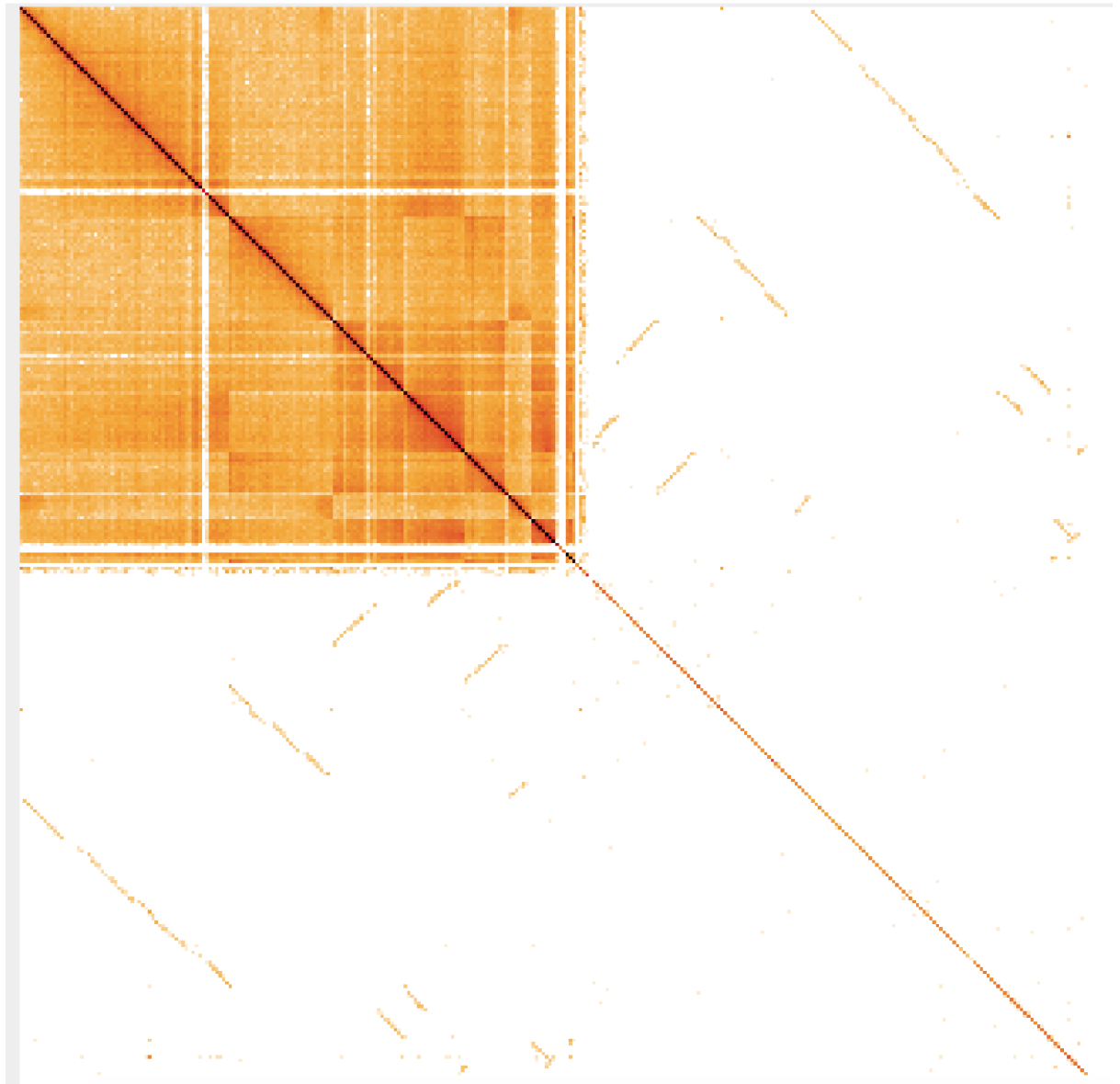
Figure A-15: A Cooler heatmap of the chromosomal contacts from the transconjugant *Escherichia coli* J53 strain from the conjugation experiments after exposure to sub-minimum inhibitory concentration of sub-minimum inhibitory concentration of mitomycin C, replicate 3.